

Zhen Fang
Richard L. Smith Jr.
Lujiang Xu *Editors*

Production of Biofuels and Chemicals from Sustainable Recycling of Organic Solid Waste

Biofuels and Biorefineries

Volume 11

Editor-in-Chief:

Zhen Fang, Nanjing Agricultural University, Nanjing, China

Editorial Board Members:

Jamal Chaouki, Polytechnique Montréal, Canada

Liang-shih Fan, Ohio State University, USA

John R. Grace[†], University of British Columbia, Canada

Vijaya Raghavan, McGill University, Canada

Yonghao Ni, University of New Brunswick, Canada

Norman R. Scott, Cornell University, USA

Richard L. Smith, Jr., Tohoku University, Japan

Ying Zheng, Western University, Canada

[†]passed away on May 26, 2021, during compilation of the text. <https://www.chbe.ubc.ca/2021/05/27/celebrating-the-life-of-dr-john-grace/>

Aims and Scope of the series

The Biofuels and Biorefineries Series aims at being a comprehensive and integrated reference for biomass, bioenergy, biofuels, and bioproducts. The Series provides leading global research advances and critical evaluations of methods for converting biomass into biofuels and chemicals. Scientific and engineering challenges in biomass production and conversion are covered that show technological advances and approaches for creating new bioeconomies in a format that is suitable for both industrialists and environmental policy decision-makers.

The Biofuels and Biorefineries Series provides readers with clear and concisely written chapters that are peer-reviewed on significant topics in biomass production, biofuels, bioproducts, chemicals, catalysts, energy policy, economics, thermochemical and processing technologies. The text covers major fields of plant science, green chemistry, economics and economy, biotechnology, microbiology, chemical engineering, mechanical engineering, and energy.

Series description

Annual global biomass production is about 220 billion dry tons or 4,500 EJ, equivalent to 8.1 times the world's energy consumption in 2020 (556 EJ). On the other hand, world-proven oil reserves at the end of 2020 reached 1732.4 billion barrels, which can only meet 51.5 years of global production. Therefore, alternative resources are needed to both supplement and replace fossil oils as the raw material for transportation fuels, chemicals and materials in petroleum-based industries. Renewable biomass is a likely candidate, because it is prevalent over the Earth and is readily converted to other products. Compared with coal, some of the advantages of biomass are: (i) its carbon-neutral and sustainable nature when properly managed; (ii) its reactivity in biological conversion processes; (iii) its potential to produce bio-oil (ca. yields of 75%) by fast pyrolysis because of its high oxygen content; (iv) its low sulphur and lack of undesirable contaminants (e.g. metals, nitrogen content) (v) its wide geographical distribution and (vi) its potential for creating jobs and industries in energy crop productions and conversion plants. Many researchers, governments, research institutions and industries are developing projects for converting biomass including forest woody and herbaceous biomass into chemicals, biofuels and materials and the race is on for creating new "biorefinery" processes needed for future economies. The development of biorefineries will create remarkable opportunities for the forestry sector, biotechnology, materials, chemical processing industry, and stimulate advances in agriculture. It will help to create a sustainable society and industries that use renewable and carbon-neutral resources.

Zhen Fang • Richard L. Smith Jr. • Lujiang Xu
Editors

Production of Biofuels and Chemicals from Sustainable Recycling of Organic Solid Waste



Editors

Zhen Fang
College of Engineering
Nanjing Agricultural University
Nanjing, China

Richard L. Smith Jr.
Graduate School of Environmental Studies
Tohoku University
Sendai, Japan

Luijiang Xu
College of Engineering
Nanjing Agricultural University
Nanjing, China

ISSN 2214-1537

Biofuels and Biorefineries
ISBN 978-981-16-6161-7
<https://doi.org/10.1007/978-981-16-6162-4>

ISSN 2214-1545 (electronic)

ISBN 978-981-16-6162-4 (eBook)

© The Editor(s) (if applicable) and The Author(s), under exclusive license to Springer Nature Singapore Pte Ltd. 2022

This work is subject to copyright. All rights are solely and exclusively licensed by the Publisher, whether the whole or part of the material is concerned, specifically the rights of translation, reprinting, reuse of illustrations, recitation, broadcasting, reproduction on microfilms or in any other physical way, and transmission or information storage and retrieval, electronic adaptation, computer software, or by similar or dissimilar methodology now known or hereafter developed.

The use of general descriptive names, registered names, trademarks, service marks, etc. in this publication does not imply, even in the absence of a specific statement, that such names are exempt from the relevant protective laws and regulations and therefore free for general use.

The publisher, the authors and the editors are safe to assume that the advice and information in this book are believed to be true and accurate at the date of publication. Neither the publisher nor the authors or the editors give a warranty, expressed or implied, with respect to the material contained herein or for any errors or omissions that may have been made. The publisher remains neutral with regard to jurisdictional claims in published maps and institutional affiliations.

This Springer imprint is published by the registered company Springer Nature Singapore Pte Ltd. The registered company address is: 152 Beach Road, #21-01/04 Gateway East, Singapore 189721, Singapore

Preface

World demand for polymers and their many related products has led to an explosive increase in the amount of plastic waste generated that is having serious consequences on the environment, nature, and human health. Sustainable recycling of organic solid waste (OSW), which includes municipal solid waste, organic sludge waste, polymer solid waste, and agricultural waste, will become of ever increasing importance, as world population increases and material recycle becomes a necessary characteristic of innovative technology. This text provides a compilation of state-of-the-art techniques for reducing, reusing, and recycling OSW and for converting these underutilized carbon resources into valuable chemicals and biofuels with sustainable methods. Chapter topics include manufacture of value-added products such as fuels, commodity chemicals, and bio-based functional materials from OSW feedstocks as well as methods for processing and handling many types of OSW. Aimed at improving conversion effectiveness and developing innovative techniques for new value-added products, this book was conceived as a collection of studies on state-of-the-art techniques and developed specifically for producing fuels and chemicals from multiple organic solid wastes via sustainable recycling methods. Discussion on related topics in terms of recent advances and their assessment and the promise and prospects of new methods or new technological strategies are provided to readers in a concise and informative format. Each individual chapter was contributed by globally selected experts or professionals and was peer-reviewed and edited for content and consistency in terminology.

This book is the eleventh book of the series entitled, *Biofuels and Biorefineries*, and contains 14 chapters contributed by leading experts in the field. The text is arranged into five key parts:

Part I. Introduction (Chap. 1)

Part II. Production of Biofuels and Chemicals by Thermo-Chemical Conversion Processes (Chaps. 2–4)

Part III. Production of Biofuels and Chemicals by Biodegradation (Chaps. 5–7)

Part IV. Production of Liquid Biofuels with New Technologies (Chaps. 8–12)**Part V. Techno-Economic Analysis (Chaps. 13 and 14)**

Chapter 1 provides an introduction to the types, sources, and properties of organic solid waste (OSW), and then outlines technologies including biological, chemical, thermo-chemical, and photo-chemical technologies for sustainable recycle or conversion of organic solid wastes into biofuels and chemicals. An overview of databases used in life cycle assessment and related topics is provided with example analyses. Chapter 2 presents a critical overview of the field of the catalytic co-pyrolysis of biomass with waste polymers in facilities ranging from bench and laboratory scale (thermogravimetric analysis and lab-scale reactors) to pilot scale, providing insights into the potential of this technology for the production of high quality bio-oils in a single-stage process, and discusses the most important of these results as reported in the literature obtained in facilities ranging from thermogravimetric reactors (technology readiness level (TRL 2) to pilot plants in a relevant environment (TRL 5). Chapter 3 presents an overview of low-cost catalytic processing of plastic wastes with a focus on biomass-derived activated carbons as low-cost catalysts, and summarizes the co-processing of plastic wastes with lignocellulosic biomass into high quality liquid fuels. Chapter 4 focuses on the extraction of leaves with carbon dioxide (CO_2) in its supercritical state (sc- CO_2) for effective recovery of valuable compounds (e.g., terpenes, phenolics, and phytosterols) and proposes several extraction models to express the kinetics of extraction with sc- CO_2 process. Chapter 5 summarizes the fundamentals of H_2 and CH_4 fermentation in recirculated two-phase anaerobic digestion process, discusses its characteristics of hydraulic separation, and highlights the potential and recent applications of R-TPAD (recirculated two-phase anaerobic digestion) process in treating different types of organic solid waste. Chapter 6 presents a comprehensive review of the science underlying the anaerobic digestion (AD) process, different feedstock types, the diverse array of microorganisms involved, process variables crucial for AD efficiency, industrial scope of the different reactor modes, and the optimization and pretreatment methods to improve process efficiency. Chapter 7 demonstrates the utility of biodegradation to produce market-ready products from otherwise wasted resources and discusses selected types of biodegradation, factors affecting each type, how the composition of organic fractions affect the outcome of biodegradation products, and the mitigation potential for recycling the organic fraction of municipal solid waste via biodegradation. Chapter 8 discusses organic waste recovery through photobiocatalytic processes, including enzymatic systems, electron reservoirs, and final acceptors, and focuses on light-driven valorization of organic by-products involving whole-cell biotransformation approaches. Chapter 9 gives several approaches for obtaining defined monomers or other valuable chemicals from different polyesters with sufficient high purity through highly selective reactions. Chapter 10 introduces the historical development of mechanochemistry, types of mechanochemical equipment, the relationship between mechanochemistry and organic solid wastes (e.g., waste biomass) conversion into value-added products (chemicals, fuels, and carbon materials) and presents the role and mechanism of

mechanochemical technology on waste biomass transformation process. Chapter 11 gives an overview of methods for converting OSW into chemical products using either hydrothermal (water) or solvothermal (ammonia) processing, discusses the physical properties of solvent and mechanism of conversion process, and provides fundamental principles for applying hydrothermal and solvothermal methods to valorize organic solid wastes and concludes with potential research areas. Chapter 12 discusses cultivation, extraction, enzymatic hydrolysis, and fermentation strategies and provides an overview of micro- and macro-algae biomass conversion into biofuels and other high value-added compounds in terms of the biorefinery concept. Chapter 13 highlights important and state-of-the-art processes for exploring fruit wastes for conversion into biofuel and biochemical production on the laboratory scale and prospects for commercial scale industrial opportunities of bioeconomies. Chapter 14 reviews and assesses waste management technologies in terms of waste reduction, stabilization, material recycling, energy recycling, and GHG reduction and discusses methods and nanomaterials that have been studied for increasing process conversion efficiency, environmental sustainability, and the quality of products for recycling and valorizing wastes using pyrolysis, gasification, and anaerobic digestion technologies.

The text should be of interest to professionals in academia and industry who are working in the fields of natural renewable materials, biorefinery of lignocellulose, biofuels, and environmental engineering. It can also be used as comprehensive references for university students with backgrounds in chemical engineering, material science, and environmental engineering.

Nanjing, China
Sendai, Japan
Nanjing, China

Zhen Fang
Richard L. Smith Jr.
Lujiang Xu

Acknowledgements

First and foremost, we would like to cordially thank all the contributing authors for their great efforts in writing and revising the chapters and insuring the reliability of the information given in their chapters. Their contributions have really made this project realizable.

Apart from the efforts of authors, we would also like to acknowledge the individuals listed below for carefully reading the book chapters and giving many constructive comments that significantly improved the quality of the chapters:

- Dr. Teng Bao, Ohio State University, USA
Prof. Riccardo Basosi, University of Siena, Italy
Dr. Richard Blair, University of Central Florida, USA
Dr. Catherine Brewer, New Mexico State University, USA;
Dr. Christian Israel Aragón Briceño, University of Twente, the Netherlands
Prof. Tony Bridgwater, Aston University, UK
Dr. Federica Conti, Aalborg University, Denmark
Prof. Shuguang Deng, Arizona State University, USA
Dr. Bipro R. Dhar, University of Alberta, Canada
Dr. Salvatore Fusco, University of Verona, Italy
Prof. Clifford Hall, South Dakota State University, USA
Dr. Silvia Greses Huerta, IMDEA Energy, Spain
Ms. Ann-Christine Johansson, Rise Research Institutes of Sweden, Sweden
Dr. Yong Chae Jung, Korea Institute of Science and Technology (KIST), South Korea
Dr. Xuye Lang, University of California Riverside, USA
Dr. Enshi Liu, University of Nebraska Lincoln, USA
Dr. Jianming Liu, National Food Institute, Technical University of Denmark, Denmark
Dr. Antonella Marone, Italian National Agency for New Technologies, Energy and Sustainable Economic Development, Italy
Dr. Jose A. Mendiola, Institute of Food Science Research (CIAL-CSIC), Spain
Dr. Xianzhi Meng, University of Tennessee Knoxville, USA
Dr. Miguel Miranda, National Laboratory of Engineering and Geology, IP LNEG, Portugal

Prof. Igor Polikarpov, University of Sao Paulo, Brazil
 Prof. Florian Pradelle, the Pontifical Catholic University of Rio de Janeiro, (PUC-Rio), Brazil
 Prof. Eugenio Quaranta, University of Bari, Italy
 Dr. Jimmy Roussel, Luxembourg Institute of Science and Technology, Environmental Research and Innovation, Luxembourg
 Prof. Warren D. Seider, University of Pennsylvania, USA
 Dr. Devinder Singh, National Research Council Canada, Canada
 Prof. Lee Keat Teong, Universiti Sains Malaysia, Malaysia
 Dr. Rahul Ukey, Alabama A&M University, USA
 Dr. Jiawei Wang, Aston University, UK
 Dr. Kui Wang, Cornell University, USA
 Dr. Chunfei Wu, Queen's University Belfast, UK
 Dr. Ana M. R. B. Xavier, Universidade de Aveiro Univ Aveiro, Portugal
 Dr. Geetanjali Yadav, University of Pennsylvania, USA
 Dr. Yifeng Zhang, Technical University of Denmark, Denmark
 Dr. Yi Zheng, Kansas State University, USA

We are also grateful to Dr. Mei Hann Lee (Editor, Springer Nature) for her encouragement, assistance, and guidance during preparation of the book.

We would like to express our deepest gratitude towards our families for their love, understanding, and encouragement, which help us in completion of this project.

It is with great sadness that Professor John Ross Grace (born in 1943) passed away on 26 May 2021. He served as the board member since 2012. Prof. Grace was Professor Emeritus in the Department of Chemical and Biological Engineering at the University of British Columbia, Canada.

(Zhen Fang)

(Richard L. Smith, Jr.)

(Lujiang Xu)

Zhen Fang, July 28, 2021 in Nanjing
 Richard L. Smith, Jr., July 28, 2021 in Sendai
 Lujiang Xu, July 28, 2021 in Nanjing

Contents

Part I Introduction

- 1 Sustainable Technologies for Recycling Organic Solid Wastes 3
Lujiang Xu, Xianjun Zhou, Chengyu Dong, Zhen Fang,
and Richard L. SmithJr

Part II Production of Biofuels and Chemicals by Thermo-Chemical Conversion Processes

- 2 Recent Advances in the Catalytic Co-pyrolysis of Lignocellulosic Biomass and Different Polymer Wastes from Laboratory Scale to Pilot Plant 33
Olga Sanahuja Parejo, A. Veses, A. Sanchís, M. S. Callén, R. Murillo,
and T. García
- 3 Roadmap to Low-Cost Catalytic Pyrolysis of Plastic Wastes for Production of Liquid Fuels 75
Oraléou Sangué Djandja, Dabo Chen, Lin-Xin Yin, Zhi-Cong Wang,
and Pei-Gao Duan
- 4 Production of Valuable Compounds from Leaves by Supercritical CO₂ Extraction 101
Takafumi Sato

Part III Production of Biofuels and Chemicals by Biodegradation

- 5 Recovery of Biohydrogen and Biomethane by Anaerobic Fermentation of Organic Solid Waste 135
Yu Qin, Aijun Zhu, and Yu-You Li

6	Recycling of Multiple Organic Solid Wastes into Biogas via Anaerobic Digestion	173
	Nima Hajinajaf, Manali Das, Pradipta Patra, Amit Ghosh, and Arul M. Varman	
7	Recycling of Multiple Organic Solid Wastes into Chemicals via Biodegradation	205
	Trevor J. Shoaf and Abigail S. Engelberth	

Part IV Production of Liquid Biofuels with New Technologies

8	Producing Value-Added Products from Organic Bioresources via Photo-BioCatalytic Processes	245
	Silvia Magri and David Cannella	
9	Depolymerisation of Fossil Fuel and Biomass-derived Polyesters	283
	Guido Grause	
10	Producing Value-added Products from Organic Solid Wastes with Mechanochemical Processes	317
	Haixin Guo, Xiao Zhang, and Feng Shen	
11	Fundamentals of Hydrothermal Processing of Biomass-Related Molecules for Converting Organic Solid Wastes into Chemical Products	339
	Taku Michael Aida	
12	Third Generation Biorefineries Using Micro- and Macro-Algae	373
	Rohit Saxena, Gilver Rosero-Chasoy, Elizabeth Aparicio, Abraham Lara, Araceli Loredo, Armando Robledo, Emily T. Kostas, Rosa M. Rodríguez-Jasso, and Héctor A. Ruiz	

Part V Techno-Economic Analysis

13	Prospects and Perspectives for Producing Biodiesel, Bioethanol and Bio-Chemicals from Fruit Waste: Case Studies in Brazil and Serbia	415
	Danijela Stanisić, Marija Tasić, Olivera Stamenković, and Ljubica Tasić	
14	Sustainable Recycling and Valorization of Organic Solid Wastes for Fuels and Fertilizers	453
	Lijun Wang, Bahare Salehi, and Bo Zhang	

Index	487
------------------------	-----

Editors and Contributors

About the Editors



Zhen Fang is a Professor and Leader of the Biomass Group at Nanjing Agricultural University. He is the inventor of the “fast hydrolysis” process and the elected fellow of the Canadian Academy of Engineering. Professor Fang specializes in thermal/biochemical conversion of biomass, nanocatalyst synthesis and their applications, pretreatment of biomass for biorefineries, and supercritical fluid processes. He holds Ph.D.s from China Agricultural University and McGill University. Professor Fang is Associate Editor of international journals, such as *Biotechnology for Biofuels* and *Journal of Renewable Materials*. He has more than 20 years of research experience in the field of renewable energy and green technologies at top universities and institutes around the globe, including 1 year in Spain (University of Zaragoza), 3 years in Japan (Biomass Technology Research Center, AIST; Tohoku University), and more than 8 years in Canada (McGill).



Richard L. Smith Jr. is a Professor of Chemical Engineering at the Graduate School of Environmental Studies, Research Center of Supercritical Fluid Technology, Tohoku University, Japan. He has a strong background in physical properties and separations and holds a Ph.D. in Chemical Engineering from the Georgia Institute of Technology (USA). His research focuses on developing green chemical processes, especially those that use water and carbon dioxide as the solvents in their supercritical state. He is an expert on physical property measurements and separation techniques with ionic liquids and has published more than 270 scientific papers, patents, and reports in the field of chemical engineering. Professor Smith is the Asia regional editor for the *Journal of Supercritical Fluids* and has served on the editorial boards of major international journals.



Lujiang Xu is an associate professor in the Biomass Group at Nanjing Agricultural University. He holds a Ph.D. in Renewable and Clean Energy from the Department of Chemistry of the University of Science and Technology of China and a B.S. in Light Chemical Engineering from Nanjing Forestry University. His research focuses on the selective thermo-chemical conversion of biomass and derived compounds into value-added chemicals and liquid fuels.

Contributors

Taku Michael Aida Department of Chemical Engineering, Faculty of Engineering, Fukuoka University, Fukuoka, Japan

Research Institute of Composite Materials, Fukuoka University, Fukuoka, Japan

Elizabeth Aparicio Biorefinery Group, Food Research Department, Faculty of Chemistry Sciences, Autonomous University of Coahuila, Saltillo, Coahuila, Mexico

M. Soledad Callén Instituto de Carboquímica (ICB-CSIC), Zaragoza, Spain

David Cannella PhotoBioCatalysis Unit, Crop Nutrition and Biostimulation Lab (CPBL) and Biomass Transformation Lab (BTL), Université libre de Bruxelles (ULB), Bruxelles, Belgium

Dabo Chen New More Graphene Application Technology Co., Ltd., Jinhua, Zhejiang, People's Republic of China

Manali Das School of Bioscience, Indian Institute of Technology Kharagpur, Kharagpur, West Bengal, India

Oraléou Sangué Djandja Shaanxi Key Laboratory of Energy Chemical Process Intensification, School of Chemical Engineering and Technology, Xi'an Jiaotong University, Xi'an, Shaanxi, People's Republic of China

Chengyu Dong Biomass Group, College of Engineering, Nanjing Agricultural University, Nanjing, Jiangsu Province, China

Pei-Gao Duan Shaanxi Key Laboratory of Energy Chemical Process Intensification, School of Chemical Engineering and Technology, Xi'an Jiaotong University, Xi'an, Shaanxi, People's Republic of China

Abigail S. Engelberth Department of Agricultural & Biological Engineering, Purdue University, West Lafayette, IN, USA

Laboratory of Renewable Resources Engineering, Purdue University, West Lafayette, IN, USA

Environmental & Ecological Engineering, Purdue University, West Lafayette, IN, USA

Center for the Environment, Purdue University, West Lafayette, IN, USA

Zhen Fang Biomass Group, Nanjing Agricultural University, Nanjing, Jiangsu Province, China

Alberto Sanchis García Instituto de Carboquímica (ICB-CSIC), Zaragoza, Spain

Amit Ghosh School of Energy Science and Engineering, Indian Institute of Technology Kharagpur, Kharagpur, West Bengal, India

P.K. Sinha Centre for Bioenergy and Renewables, Indian Institute of Technology Kharagpur, Kharagpur, West Bengal, India

Guido Grause Graduate School of Environmental Studies, Tohoku University, Sendai, Japan

Haixin Guo Graduate School of Environmental Studies, Tohoku University, Sendai, Japan

Nima Hajinajaf Chemical Engineering, School for Engineering of Matter, Transport, and Energy, Arizona State University, Tempe, AZ, USA

Emily T. Kostas Department of Biochemical Engineering, The Advanced Centre of Biochemical Engineering, University College London, London, UK

Abraham Lara Biorefinery Group, Food Research Department, Faculty of Chemistry Sciences, Autonomous University of Coahuila, Saltillo, Coahuila, Mexico

Yu-You Li Laboratory of Environmental Protection Engineering, Department of Civil and Environmental Engineering, Graduate School of Engineering, Tohoku University, Sendai, Japan

Araceli Loredo Biorefinery Group, Food Research Department, Faculty of Chemistry Sciences, Autonomous University of Coahuila, Saltillo, Coahuila, Mexico

Silvia Magri PhotoBioCatalysis Unit, Crop Nutrition and Biostimulation Lab (CPBL) and Biomass Transformation Lab (BTL), Université libre de Bruxelles (ULB), Bruxelles, Belgium

Tomas García Martínez Instituto de Carboquímica (ICB-CSIC), Zaragoza, Spain

Pradipita Patra School of Energy Science and Engineering, Indian Institute of Technology Kharagpur, Kharagpur, West Bengal, India

Yu Qin Laboratory of Environmental Protection Engineering, Department of Civil and Environmental Engineering, Graduate School of Engineering, Tohoku University, Sendai, Japan

Armando Robledo Food Science and Technology Department, Universidad Autónoma Agraria Antonio Narro, Saltillo, Coahuila, México

Alberto Veses Roda Instituto de Carboquímica (ICB-CSIC), Zaragoza, Spain

Rosa M. Rodríguez-Jasso Biorefinery Group, Food Research Department, Faculty of Chemistry Sciences, Autonomous University of Coahuila, Saltillo, Coahuila, Mexico

Gilver Rosero-Chasoy Biorefinery Group, Food Research Department, Faculty of Chemistry Sciences, Autonomous University of Coahuila, Saltillo, Coahuila, Mexico

Héctor A. Ruiz Biorefinery Group, Food Research Department, Faculty of Chemistry Sciences, Autonomous University of Coahuila, Saltillo, Coahuila, Mexico

Bahare Salehi Department of Nanoengineering, North Carolina Agricultural and Technical State University, Greensboro, NC, USA

Olga Sanahuja Parejo Instituto de Carboquímica (ICB-CSIC), Zaragoza, Spain

Takafumi Sato Department of Fundamental Engineering, Utsunomiya University, Utsunomiya, Japan

Rohit Saxena Biorefinery Group, Food Research Department, Faculty of Chemistry Sciences, Autonomous University of Coahuila, Saltillo, Coahuila, Mexico

Feng Shen Agro-Environmental Protection Institute, Ministry of Agricultural and Rural Affairs, Tianjin, China

Trevor J. Shoaf Laboratory of Renewable Resources Engineering, Department of Agricultural & Biological Engineering, Purdue University, West Lafayette, IN, USA

Richard L. Smith Jr Graduate School of Environmental Studies, Research Center of Supercritical Fluid Technology, Tohoku University, Sendai, Japan

Olivera Stamenković Faculty of Technology, University of Nis, Leskovac, Serbia

Danijela Stanisić Department of Organic Chemistry, Institute of Chemistry, University of Campinas, Campinas, SP, Brazil

Ljubica Tasić Department of Organic Chemistry, Institute of Chemistry, University of Campinas, Campinas, SP, Brazil

Marija Tasić Faculty of Technology, University of Nis, Leskovac, Serbia

Arul M. Varman Chemical Engineering, School for Engineering of Matter, Transport, and Energy, Arizona State University, Tempe, AZ, USA

Ramón Murillo Villuendas Instituto de Carboquímica (ICB-CSIC), Zaragoza, Spain

Lijun Wang Department of Natural Resources and Environmental Design, North Carolina Agricultural and Technical State University, Greensboro, NC, USA

Zhi-Cong Wang New More Graphene Application Technology Co., Ltd., Jinhua, Zhejiang, China

Shaanxi Key Laboratory of Energy Chemical Process Intensification, School of Chemical Engineering and Technology, Xi'an Jiaotong University, Xi'an, Shaanxi, People's Republic of China

Lujiang Xu Biomass Group, College of Engineering, Nanjing Agricultural University, Nanjing, Jiangsu Province, China

Lin-Xin Yin Shaanxi Key Laboratory of Energy Chemical Process Intensification, School of Chemical Engineering and Technology, Xi'an Jiaotong University, Xi'an, Shaanxi, China

Bo Zhang Department of Natural Resources and Environmental Design, North Carolina Agricultural and Technical State University, Greensboro, NC, USA

Xiao Zhang School of Energy and Environmental Engineering, Hebei University of Technology, Tianjin, China

Xianjun Zhou Biomass Group, College of Engineering, Nanjing Agricultural University, Nanjing, Jiangsu Province, China

Aijun Zhu Laboratory of Environmental Protection Engineering, Department of Civil and Environmental Engineering, Graduate School of Engineering, Tohoku University, Sendai, Japan

Part I

Introduction

Chapter 1

Sustainable Technologies for Recycling Organic Solid Wastes



**Lujiang Xu, Xianjun Zhou, Chengyu Dong, Zhen Fang,
and Richard L. Smith Jr**

Abstract Sustainable management of organic solid wastes (OSW) within environmental, economic, and social standards is becoming an increasingly important and hot topic. This chapter gives a brief introduction to the types, sources and properties of OSW and then outlines technologies for sustainable recycle or conversion of OSW into biofuels and chemicals. In this chapter, features of biological, chemical, thermochemical, and photo-chemical technologies are described. An overview of databases used in life cycle assessment (LCA) of OSW and related topics are given. Advantages and scope of each technology are given for converting OSW into valuable products.

Keywords Organic solid wastes · Recovery · Technologies · Life cycle assessment · Advantages

1.1 Introduction

Since the industrial revolution, world population and economic development have entered a period of rapid development. By 2030, the world's population will increase to 8.6×10^9 people [1] and with the bloom of modern science and technology, large percentages of society will have migrated from rural areas to urban areas, which now account for more than 55% of the population ($>4 \times 10^9$ persons) in 2017 [2]. The GDP of the world economy has been increasing at an annual rate of about 2% [3] such that world health and prosperity depend on large amounts of basic materials

L. Xu · X. Zhou · C. Dong · Z. Fang (✉)

Biomass Group, College of Engineering, Nanjing Agricultural University, Nanjing, Jiangsu Province, China

e-mail: zhenfang@njau.edu.cn

R. L. Smith Jr

Graduate School of Environmental Studies, Research Center of Supercritical Fluid Technology, Tohoku University, Aoba-ku, Sendai, Japan

needed for survival, such as food, clean water, air, shelter, clothing, clean cooking facilities and energy [4]. The World Bank (2020) reported that an average individual generates nearly 0.74 kg of solid waste per day and that generation of solid waste in 2025 can be expected to increase to 2.2×10^9 tons per year [5]. Hence, appropriate methods for processing solid waste with the aim of reducing and conserving resources are requirements for achieving sustainable society.

A considerable part of solid waste contains carbon compounds and is referred to as organic solid waste (OSW) in this book. According to the source and characteristics of OSW, it can be divided into municipal solid waste (MSW), organic sludge, polymer solid waste and agricultural waste [6, 7]. OSW has a complex composition and creates environmental pollution due to its wide variety, changeable shape, and properties. However, OSW still has some common characteristics, such as being mainly composed of elements, C, H, and O and containing highly volatile compounds and having high calorific value [8, 9]. Therefore, OSW cannot simply be regarded as another type of polluting waste, but rather as an under-utilized resource. In other words, OSW should be regarded as a new type of renewable resource that contains large amounts of carbon and hydrogen. OSW has the potential to be used as a renewable carbon source for producing energy and chemicals provided that efficient and sustainable methods can be developed for its conversion. The concept of OSW as a renewable resource for sustainable development should become an essential element necessary for achieving ecological harmony.

Waste-to-energy and chemicals (WTEC) strategy is an economically viable and environmentally sustainable proposal for recovering carbon from waste resources through production of fuel, chemical, heat, and electricity [10, 11]. WTEC strategy has a vital role for sustainable waste management and mitigation of environmental issues and can also address global warming and climate change [12]. To date, many techniques have been proposed and applied for the recovery of OSW. According to the strategy, processing conditions, technology maturity, product, recycle methods can be divided into conventional treatment and advanced treatment categories. Conventional technologies are incineration, gasification, pyrolysis, hydrothermal treatment [13–16] and bio-chemical methods (*e.g.*, anaerobic fermentation, aerobic fermentation, and enzymatic hydrolysis) [7, 17, 18]. Advanced technologies include chemolysis, mechanochemical degradation, photodegradation and microbial fuel cells [19–22].

This chapter provides a brief introduction to multiple solid wastes (type, sources, and properties) and introduces conventional and advanced strategies for sustainable recycle of OSW into biofuels and chemicals.

1.2 Classification, Properties of Organic Solid Waste

The origin and characteristics of OSW can be divided into four categories: (i) MSW, (ii) organic sludge, (iii) polymer solid waste and (iv) agricultural wastes. OSW has complex composition, wide variability and consists of an aggregate of many kinds of

materials that can have very different physical properties which means that much more attention needs to be given to its source for effective reuse and recycle. Properties and characteristics of four typical OSW along with their variations according to source will be introduced in the following sections.

1.2.1 *Multiple Solid Wastes (MSW)*

MSW refers to the materials that are discarded as a result of urban daily life or activities, mainly coming from urban households, urban commerce, catering industry, hotel industry, tourism, service industry, municipal sanitation, transportation, industrial enterprises, water supply and drainage treatment sludge activities [23–25]. MSW has the characteristics of being huge in quantity, wide in variety, and complex in composition. Annual MSW generation can be expected to continue to increase with changing lifestyles and increasing population [5]. As shown in Fig. 1.1, 2.01×10^9 tons of MSW were generated in 2016, and 2.59×10^9 tons of global MSW are expected to be generated annually by 2030. Moreover, MSW generation across the world is expected to reach 3.40×10^9 tons in 2050.

Typical MSW includes organic wastes (kitchen discards, yard, or garden related, paper, plastic) and inorganic wastes (glass, metal, electronics, construction) [26, 27]. The composition of MSW not only depends on its region of generation, but also on socioeconomic status and stage of human development (infancy, adolescence, adulthood). Table 1.1 illustrates the composition of MSW collected from different regions according to income level. Global food loss and green waste

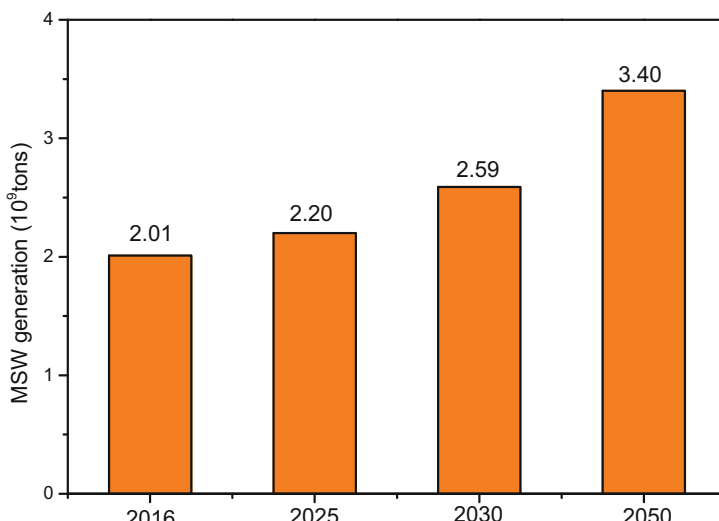


Fig. 1.1 Forecast of global MSW generation based on historical trends [5]

Table 1.1 Category and composition of MSW (dry basis) according to different levels of household income levels. Income levels are relative according to country development

Category (%)	Household income level			
	High	Up-middle	Lower-middle	Low
OSW	78	79	77	69
Food & green	32	54	53	56
Paper & cardboard	25	12	12	7
Plastics	13	11	11	6
Rubber & leather	4	1	1	–
Wood	4	1	1	<1
Inorganic solid waste (ISW)	11	6	5	3
Metal	6	2	2	2
Glass	5	4	3	1
Other	11	15	17	27

Data based on Ref. [5]

(weeds, leaves, and grass cuttings) account for a large proportion of wastes for middle- and low-income level households with the percentage of food and green waste being over 50% [5]. The percentage of OSW in MSW decreases as income levels increase. Compared with low-income countries, consumption waste, such as paper and plastic, has higher percentage in MSW collected from high-income level households. Moreover, the granularity of waste composition, such as detailed rubber and wood waste, increases as household income levels increase. The percentage of “Other” in MSW from low-income level households is up to 27%, which is much higher than high-income level households, and implies that MSW from low-income level households is less-defined than MSW from higher-income level households. Nevertheless, MSW has value as a resource and it could be used to produce useful chemical products within a certain scope, time, and conditions, rather than being treated as something to be discarded.

1.2.2 *Organic Sludge*

Organic sludge is a solid residue generated from wastewater treatment operations. Sources of organic sludge can be divided into three major categories: (i) sewage, (ii) paper, and (iii) dye [28]. Sewage sludge, which is the largest source of solids, is generated in quantities of more than 1.50×10^8 tons each year [29]. The main component of sewage sludge is functional microbes and secreted extracellular polymeric substances (EPS) that are suspended in wastewater [30]. Paper sludge is derived from wastewater treatment operations in the pulp and paper industry for which approximately (40–50) kg of paper sludge is generated per 1000 kg paper produced in typical mills [31]. Paper sludge is rich in cellulose with low lignin content, which makes it a useful raw material for renewable production of hydrogen,

Table 1.2 Proximate analysis (dry basis) of major categories of organic sludge

Category of sludge (%)	Moisture	Volatile	Ash	Fixed carbon	HHV (MJ/kg)	Ref.
Sewage	6.0	64.1	11.2	6.6	7.6	30
Paper	3.6	60.6	32.3	3.4	7.1	31
Dye	6.9	66.9	12.4	13.7	16.8	32

bio-fuels and chemicals. Dye sludge is a waste stream generated by wastewater treatment plants of the textile industry [32]. Currently, more than 2.1×10^7 tons of dye sludge are generated each year in China, and its quantity continues to increase annually [33]. In addition, many toxic components (dyes, pathogens, additives, and heavy metals) are contained in dye sludge, which makes it a high priority to properly dispose and treat the waste to prevent serious hazards to the natural environment and public health [34]. The main characteristics of dye sludge are high water content, high organic content, and low calorific value. Dye sludge is rich in nitrogen, phosphorus, and other nutrients, but it can contain heavy metals ions. Table 1.2 shows the proximate analysis of organic sludge derived from three major sources. Considerable opportunities exist for developing suitable recycle and reuse technologies for organic sludge.

1.2.3 Polymer Solid Waste

Polymer solid waste is generated from human daily life and industrial production for which the source materials are mainly derived from petroleum [35, 36]. Polymer solid waste can be divided into two categories, (i) plastics and (ii) rubber [37] and they are mainly composed of carbon, hydrogen, oxygen (C, H and O) and some metals. Polymer solid waste is difficult to degrade by nature according to its design for durability in the environment, thus it causes environmental pollution, including ecosystem disturbance and toxic substance release, with common examples being microplastics and heavy metals [38, 39].

Waste plastic is a general term for plastics that have been used and eventually eliminated or replaced in civil, industrial, and other applications. Due to their favorable properties (e.g., lightweight, good processing characteristics, easy application, chemical stability), plastics are widely used in consumer products [40–42]. Plastic products are an indispensable part of daily life and are widely applied in construction, healthcare, electronic components, agriculture, automotive, and packaging industries. From 1950 to 2015, it is estimated that over 9×10^9 tons of virgin plastic have been produced all over the world [43]. In 2018, approximately 3.60×10^8 tons of plastics were produced globally with increasing trends so that production can be expected to increase to 5×10^8 tons in 2025 at an annual global production growth rate of 8.4% [44]. Demand for plastics is mainly for polyethylene (PE), polypropylene (PP), polyvinyl chloride (PVC), polyurethane (PUR), polyethylene terephthalate (PET), and polystyrene (PS) [43]. Correspondingly, generated

plastic waste is proportional to the above major plastic products. Waste plastics that do not easily degrade in nature can persist in the environment for decades or hundreds of years and can cause problems that affect the ecosystem and living creatures [45–47].

Rubber is widely used as a raw material for producing many flexible polymeric products that are widely used in transportation, industrial, agricultural, medical treatment, and construction [48–50]. Rubber has become the second most used polymer after plastics. In 2018, global rubber consumption reached 2.94×10^7 tons and has an annual growth rate of 3.4% which means that much waste rubber will continue to be generated in the future [51]. Rubber differs from polymers in that a vulcanization step or curing step is needed to make the product useful. Over 60% of rubber is used as a raw material for producing tires, with more than 2×10^7 tons of waste tires being generated in 2020, such that rubber has an annual growth rate of 8% [52, 53]. Waste tires are challenging to recycle because of their complex ingredients and additives that make them non-biodegradable by design, and furthermore, they have lead to the phrase, “black pollution” that has become a global scale environmental, public health and safety issue [54]. Waste rubber has high volatile content, low ash content, high calorific value with a higher heating value (HHV) of (26–36) MJ/kg that is similar to high rank coals, so that waste rubber can be considered as a rich source of fuel and chemicals through technologies such as pyrolysis and combustion [48].

1.2.4 Agricultural and Forestry Solid Waste

Agricultural and forestry solid waste refers to unwanted materials generated in farming, forest management and animal husbandry that are required to maintain the life of about 7×10^9 people all over the world [55–57]. Agricultural and forestry solid waste can be divided into two categories: (i) lignocellulosic waste, such as straw, bagasse, discarded branches and palm kernel shells, and (ii) animal manure waste, such as that generated from the production of poultry, dairy, or pig farming. The properties and characteristics of lignocellulosic waste and animal manure waste will be introduced next.

Lignocellulosic waste refers to biomass-like solid wastes such as rice straw, wheat straw, bagasse, or wood sawdust some of which are also generated in agricultural and forestry production processes [58]. Lignocellulosic waste is the most abundant form of OSW and is composed of carbon, hydrogen, and oxygen, but it can also include inorganics such as silica, potassium, calcium, sodium, magnesium, and aluminum oxides [59]. Every year, more than 2×10^9 tons of lignocellulose solid waste are generated worldwide [60]. Lignocellulosic waste is composed of cellulose, hemicellulose, and lignin [61]. Cellulose is composed of D-glucose monomers through the linear polymerization of $\beta(1\cdot4)$ glycoside bonds and makes up about 40–80% of the content of lignocellulosic waste [62]. Hemicellulose is composed of sugar monomers (C5 and C6) including glucose, galactose,

mannose, xylose, arabinose, with xylose (C5) monomers or mannose (C5) monomers being in larger proportions than C6 monomeric units with the content of hemicellulose being about 25–35% in lignocellulosic biomass [63]. Lignin is a complex three-dimensional polymer of propyl-phenol groups bound together by C-O (β -O-4, α -O-4, 4-O-5 linkage) and C-C (β -5, 5-5, β -1, β - β linkage) bonds with its content in lignocellulosic biomass being about 10–36% [64]. More than 5×10^7 tons of industrial lignin are generated annually in the paper and pulp industry [65]. Lignocellulosic waste has the characteristics of being renewable, having low pollution potential, being widely distributed and being available in large amounts as a carbon neutral resource. Valorization of lignocellulosic waste into high value-added, eco-friendly, eco-efficient, and recyclable products (*e.g.*, biofuels, biochemical, materials) with sustainable methods is an important goal for realizing renewable carbon circulation for a zero-waste society [66–68].

Animal manure is a solid waste obtained from livestock farming that has a wide range of applications [69]. In 2014, the total mass of animal manure waste was 3.9×10^9 tons, and this amount will continue to grow at a rate of about 2% per year [70]. By 2030, generation of animal manure is expected to reach at least 4.6×10^9 tons. Unlike lignocellulosic wastes, animal manure waste has high nitrogen content and intrinsic metal content, which makes it highly recyclable as a source of organic fertilizer or nutrients or as a source of energy and metals [71]. The carbon/nitrogen (C/N) ratio, which is a key organic fertilizer quality parameter, is inversely proportional to nitrogen immobilization in soil and favorable for animal manure waste. The overall C/N ratio in the composting process is in the range of 10–30, but the appropriate C/N ratio for different substrates is different and requires further research [72]. Apart from its use as an organic fertilizer, animal manure can be used as an energy resource in the production of biogas. However, there are risks in animal manure waste processing due to its potential as a biohazard, so that management technologies are needed to realize its effective use [73].

1.3 Thermochemical Recycling Technology

Technologies for recovery of OSW are highly dependent on factors related to technological, social, environmental, and economic impact. Moreover, properties of OSW, such as type, composition, volume, and energy content, also depend on region, population, and economy [5]. Thermochemical recycle technology, which includes incineration, gasification, pyrolysis, and liquefaction, is widely applicable for converting OSW into valuable products (*e.g.*, biofuels, chemicals, biochar, and heat) under appropriate conditions [74–76]. Figure 1.2 summarizes selected thermochemical conversion technologies for recycling OSW along with their corresponding products that will be discussed in detail below.

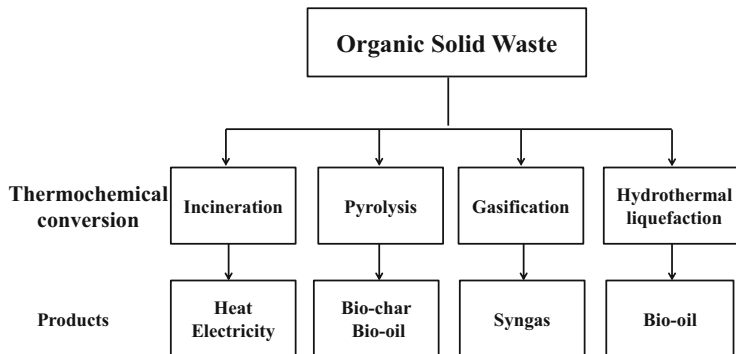


Fig. 1.2 Thermochemical technologies for recycling OSW into valuable products

1.3.1 *Incineration/Combustion*

Incineration or combustion is a treatment technology that can convert OSW into heat and electricity through oxidation in air at short reaction times [77]. Due to the many advantages of the technology, such as large processing capacity, small space requirements, low labor requirements, low time consumption and low investment and operating costs, incineration or combustion is the most common recycling method for converting waste into energy and preferred in many cases over landfilling wastes [78, 79]. During incineration, OSW is completely converted into flue gas, bottom ash, fly ash, and slag that are accompanied with the release of a large amount of heat at high temperatures that can be further used for generating electrical power. Two types of incineration systems in general use are: (i) mass incineration and (ii) modular incineration and they depend on process scale [26]. Mass incineration systems are the most widely applied thermal treatment, in which unprocessed or unsorted MSW is burned in large furnaces in the presence of excess air, which is coupled to a boiler and a generator for producing electricity [80]. Modular incineration systems are mainly composed of a rotary kiln and fluidized bed, which are an important supplement to mass incineration [81]. The compact nature of modular systems makes it easier to transport and act as a mobile solid waste treatment device than mass incineration systems.

Compared with landfilling, incineration has several important merits: (i) direct treatment of virtually any waste without pretreatment, (ii) weight reduction by 80–85%, and (iii) volume reduction by 95–96%, thereby realizing low amounts and volumes of solid waste while generating energy [82, 83]. Moreover, incineration reduces maintenance and eliminates biohazards due to rodents, pests, flies, and foul odors from microbial decomposition, and thereby increasing safety and health for much of the surroundings. However, incineration also generates fly ash (solid residue) or potentially releases dioxins (extremely harmful exhaust gases) depending on the constituents of the substrates which can cause serious health problems to humans and living creatures [84]. Therefore, the tail gas and tailings generated by

incineration must be treated with effective techniques to remove solid and gaseous pollutants. Incineration process generates large amounts of CO₂ [85], so that carbon capture and storage (CCS) or carbon capture and utilization (CCU) strategies must be implemented.

1.3.2 Pyrolysis

Pyrolysis is a thermochemical transformation technology that depolymerizes OSW into solid, liquid and gas products in an inert atmosphere [86]. Pyrolysis is one of the main thermochemical technologies for converting OSW into energy-dense bio-oils [87]. Transformation of OSW to bio-oils under pyrolysis conditions occurs via free radical mechanisms, concerted mechanisms, and ionic mechanisms [88]. During the pyrolysis process, many chemical reactions occur simultaneously, such as decomposition, dehydration, cracking, isomerization, and hydrothermal reforming [89]. Although pyrolysis is a complex thermodynamic degradation process and the detailed pyrolysis product distributions are also complicated, much progress has been made in elucidating its reaction schemes [90].

The main products produced via pyrolysis processes are bio-oil (liquid product), bio-char (solid product), and gases [88]. The product distribution is greatly influenced by catalyst, temperature, heating rate, vapor residence time, inert gas flow rate, reactor geometry, feedstock type and properties such as moisture, particle size, and elemental composition [91]. According to the heating rate and vapor residence time, pyrolysis can be divided into several main types: (i) slow pyrolysis, (ii) fast pyrolysis, (iii) intermediate pyrolysis and (iv) flash pyrolysis [92]. Slow pyrolysis is distinguished by its moderate temperature, low heating rate and longer residence time compared with other types of pyrolysis, thus increasing the yield of bio-char. Fast and flash pyrolysis processes are characterized by high temperatures, high heating rates, and short residence times, which promote higher yields of bio-oil than the other pyrolysis types. Pyrolysis can also be applied as a catalytic or non-catalytic process [93]. Catalysts used in the pyrolysis process can improve bio-oil quality and reduce costs [94]. Moreover, product distribution of bio-oil can also be simplified with catalytic pyrolysis processes. Catalytic pyrolysis can be applied as an in-situ or ex-situ process [95]. When the catalyst is mixed directly with the feedstock in the pyrolysis reactor, the process is referred to as in-situ catalytic fast pyrolysis (in-situ CFP), whereas when the catalysts are only contacted with pyrolysis gases, the process is referred to as ex-situ catalytic fast pyrolysis (ex-situ CFP). Many reactor types are used in pyrolysis processes, including fixed-bed, rotary kiln, fluidized-bed, and tubular, which depend on the properties of the raw materials and target products [96].

Pyrolysis has several advantages and disadvantages in its application [97, 98]. Pyrolysis processes are applicable to a variety of OSW, such as waste biomass, waste plastics, waste rubber, or MSW in which different targeted products (*e.g.*, bio-char, bio-oil and biogas) can be selectively produced by optimizing

pyrolysis conditions. Pyrolysis processes have low operating cost and high flexibility making them simple and reliable for large-scale commercial applications. On the other hand, pyrolysis processes tend to have complicated reactions, especially for the case of non-catalytic pyrolysis, which results in a complex distribution of liquid products along with a large amount of coke being formed, such that if catalysts are used, they are prone to deactivation. Since the price of catalysts used in pyrolysis processes tend to be relatively expensive, developing stable and inexpensive catalysts are necessary for future development. Furthermore, the obtained bio-char and pyrolysis gas can contain toxic components, which require further treatment before use.

1.3.3 Gasification

Gasification technology is a thermal conversion process that can break OSW into gaseous products such as syngas [99, 100]. Compared with pyrolysis processes, the products of gasification process are much simpler with the main components being CO, H₂, CH₄ and CO₂ [101]. Syngas products can be further processed to produce green diesel, higher alcohols, long-chain hydrocarbons, and gasoline-like products via Fischer-Tropsch reaction [102].

According to the operating conditions, gasification processes can be divided into two main types: (i) high temperature thermo-gasification and (ii) hydrothermal gasification [26]. High temperature thermo-gasification involves partial or incomplete oxidation in presence of controlled amounts of oxidants (air, oxygen, steam) at very high temperatures (550 °C–1200 °C) [103]. Hydrothermal gasification involves cracking reactions under subcritical or supercritical water conditions [104]. For hydrothermal gasification, water not only serves as reaction medium but also as reactant. In hydrothermal gasification, water can be in a supercritical thermodynamic state or a subcritical thermodynamic state [105, 106]. Water in a thermodynamic state that is higher than its critical temperature ($T_c \geq 374.1\text{ }^\circ\text{C}$) and critical pressure ($P_c \geq 22.1\text{ MPa}$) is referred to as supercritical water; water in a thermodynamic liquid state below its critical temperature ($T_c < 374.1\text{ }^\circ\text{C}$) and critical pressure ($P_c < 22.1\text{ MPa}$) is referred to as subcritical water. Gasification processes can be catalytic or non-catalytic depending on the product requirements. Catalysts used in gasification processes are generally nickel-based, because conditions can be mild and reaction pathways can be regulated to form more H₂ and CO than other products [107]. Gasification processes can be implemented as downdraft or updraft fixed bed, fluidized bed, entrained flow, or twin bed reactors depending on the product requirements [108]. Among the above gasification processes, fluidized bed reactors and twin bed reactors have great potential for application to form syngas of high-quality in scale-up.

Gasification processes are applicable to the same types of OSW as those used in incineration and pyrolysis processes [13, 99, 100, 108], but they are much cleaner than incineration and moreover, purification steps used for syngas products can be

designed to eliminate emissions of poisonous gaseous impurities such as dioxins, allowing gasification processes to be much simpler than those of pyrolysis. Furthermore, in gasification of OSW, there is less liquid and coke produced than either pyrolysis or incineration, which make the technology easy to scale-up and to operate on a continuous basis. On the other hand, operating conditions for gasification processes are more severe regarding high temperatures for thermo-gasification and high pressures for hydrothermal gasification and some preprocessing steps (shredding, torrefaction, pelletization) are necessary to ensure uniform heat transfer and product quality. Catalysts, purification steps instruments, and high standard gasification reactors make the costs of gasification processes much higher than the other methods, such that further technology development is still needed.

1.3.4 Liquefaction

Liquefaction is a thermochemical technology for producing high energy-density liquid bio-oil from OSW by liquid phase decomposition of organic compounds under high-temperatures and high-pressure [109]. In addition to bio-oil, adhesives or epoxy resins may also be produced in the liquefaction process. Operating conditions for liquefaction are usually in the range of (200–370) °C and (4–20) MPa, which are milder than hydrothermal gasification processes [26]. Typical liquid phase mediums used in liquefaction are water or organic solvents, such as methanol, ether, butanol, or octanol [110]. Processes that use water as medium are referred to as hydrothermal liquefaction, while those that use organic solvents as medium are referred to as solvothermal liquefaction. Decomposition mechanisms in liquefaction are complicated and involve a series of chemical reactions that may include degradation, hydrolysis, cracking, steam reforming and isomerization [111]. Liquefaction processes can be operated with or without catalyst depending on the target products. Introducing catalysts into the liquefaction process can lower reaction temperature, increase product selectivity, enhance reaction kinetics, reduce reaction time, and improve bio-oil yields.

Liquefaction processes are suitable to treat high-moisture substrates, such as algae, sewage sludge, kitchen waste, animal manure, and aquatic biomass when water medium is used [110, 111]. When using water medium, raw materials do not need to be dried, which lowers operating cost and saves much energy. Bio-oil yields obtained from liquefaction processes are higher than those obtained from pyrolysis processes, and OSW can be transformed into energy at nearly complete conversion. On the other hand, liquefaction processes require somewhat harsh operating conditions, which means that high standards for liquefaction reactors must be used resulting in high equipment costs. The harsh conditions of high-pressure liquefaction make scale-up less certain than other methods and for continuous production, solid formation may limit OSW throughput.

1.4 Biochemical Recycling Technology

Biochemical recycling technology is a process that can convert OSW into chemical products through the presence of microorganisms or active enzymes, including anaerobic fermentation, aerobic fermentation, and enzymatic hydrolysis [6, 9, 10, 12]. Figure 1.3 summarizes OSW biochemical recycle technologies and their corresponding products. The processes shown in Fig. 1.3 will be discussed in detail in the following sections.

1.4.1 Anaerobic Digestion (*Biomethanation*)

Anaerobic digestion, which is also referred to as biomethanation, is one of the most important methods for converting OSW into energy [16]. In anaerobic digestion, microorganisms degrade OSW into dissolved organic matter and produce gaseous products such as CH_4 , H_2 and CO_2 in the absence of free oxygen [17, 26]. MSW, animal manure, sewage sludge, food processing waste, fats, grease, agricultural crop residues are among the wide ranges of biodegradable substrates that can be treated with anaerobic digestion.

Anaerobic digestion process is mainly composed of four stages: (i) hydrolysis, (ii) acidogenesis, (iii) acetogenesis, and (iv) methanogenesis [112]. In the hydrolysis stage, OSW is hydrolyzed to form simple soluble monomers or oligomers (e.g., glucose, amino acids, glycerol, fatty acids) via promotion by a diverse population of bacteria. In the acidogenesis stage, volatile fatty acids (e.g., acetic acid, propionic acid, butyric acid, and other minor products) are produced by fermentative bacteria that promote formation of small water-soluble molecules. In the acetogenesis stage, volatile fatty acids are transformed into acetate, CO_2 and H_2 by acetogenic bacteria. In the methanogenesis stage, acetic acid, H_2 and CO_2 are converted into CH_4 and CO_2 by strictly anaerobic methanogenic bacteria. Biogas yield is highly affected by

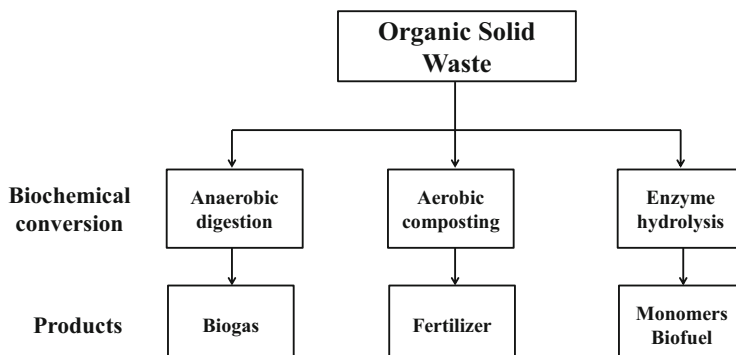


Fig. 1.3 Biochemical recycling technologies for conversion of OSW into value-added products

factors, such as substrate composition, microbial loading, and operating parameters (temperature, pH, C/N ratio, water content, oxygen content, nutrition elements).

Anaerobic digestion has many advantages such as being able to: (i) treat many types of OSW, especially those with high-moisture or high nitrogen content, (ii) prevent manure and odor missions and (iii) improve air and water quality [113, 114]. Biogas from anaerobic digestion can be harvested to generate energy and thus reduce greenhouse-gas emissions, while solid residues can be used as fertilizer to improve soil nutrient content and to reduce the use of chemical fertilizers. Anaerobic digestion uses mild conditions and is a very simple process, which allows the technology to be readily implemented on a large scale with low treatment cost. However, anaerobic digestion has some weak points as a conversion technology [115]. In anaerobic digestion, the proliferation of anaerobic microorganisms is slow, making the entire treatment process require several weeks or even months. In the anaerobic digestion process, much wastewater is generated, which must be treated and so this increases the cost. Finally, the content of methane in the gas mixtures produced by anaerobic digestion is typically below 70%, thus making the methane gas purity very low. Moreover, because methane is an explosive gas, the reactor needs to be explosion-proof and to have subsequent gas purification steps [116].

1.4.2 Aerobic Composting

Aerobic composting uses the natural decomposition of organic matter in the presence of air to form a semi-solid product with the help of living microorganisms, worms and insects and their derived enzymes [42, 117]. Composting is a traditional, widely used, cheap and simple technology that can effectively treat and valorize OSW into useful products. Aerobic composting should be carried out in the presence of sufficient oxygen, and good ventilation should be maintained [118]. The semi-solid product formed is a type of organic fertilizer that typically has rich plant-available nutrients and is widely applicable to agriculture, horticulture, landscape, and other fields. In aerobic digestion processes, many types of substrates can be used such as MSW, animal manure, sewage sludge, food processing waste, fats, grease, and agricultural crop residues, showing that it has many similarities with anaerobic digestion [119].

Aerobic composting process is regarded as a biological and chemical coupling process that relies on aerobic bacteria to degrade organic matter [117, 120, 121]. In the process of aerobic composting, small water-soluble organic molecules penetrate microorganism cell walls and are absorbed, and then utilized by the microorganisms. Insoluble macromolecular organic substances become attached to the microorganism and are decomposed into small water-soluble molecules that further support microorganism bioactivity through the secretion of extracellular enzymes. Aerobic composting is affected by many parameters, including organisms, use of cultures, nutrients (C/N ratio), aeration, addition of sewage, characteristics of sewage sludge

and operating parameters, such as temperature, pH, moisture, oxygen content, and compost (container or pile) flip frequency [122].

Aerobic composting is a mature technology that can reduce the amount of waste on a large scale, save much space, produce fertilizers, recycle humus and nutrients into the soil, protect and improve microbiological diversity and generally improve the quality of cultivated soils [26, 123]. Aerobic composting is an easily used technology that has minimal equipment requirements and low operating costs, however it carries the risk of secondary pollution, such as odor and potential contamination [117]. Moreover, greenhouse gas emissions (CH_4 , CO_2) can be large for aerobic composting and if the OSW contains heavy metals or antibiotics, there is risk for soil and groundwater pollution along with the transfer of pathogens or chemicals into the life cycle [117]. Treatment of waste plastics and rubber is generally ineffective with aerobic composting.

1.4.3 Enzyme Hydrolysis

Enzymatic hydrolysis breaks down macromolecules into small molecules or monomeric compounds via biocatalysts (enzymes) that become active in water [124, 125]. In enzymatic hydrolysis, enzymes act on specific chemical bonds of macromolecules [126] to achieve high selectivity at mild operating conditions that can be under continuous reaction conditions. Enzymatic hydrolysis is widely used to produce ethanol from lignocellulosic materials, in which lignocellulose undergoes saccharification to form soluble monosaccharides with the help of cellulases. Enzymatic hydrolysis involves the following key steps [127, 128]: (i) enzymes transfer from aqueous phase to substrate surface; (ii) enzymes adsorb onto substrate to form enzyme-substrate complexes, (iii) substrate undergoes hydrolysis, (iv) hydrolysis products transfer from substrate surface to aqueous phase. For the case of cellulose, celldextrin, and cellobiose are further hydrolyzed into glucose in the aqueous phase. Enzymatic hydrolysis rates are sensitive to substrate type, substrate chemical structure, enzyme type, enzyme loading and operating conditions such as pH, temperature, substrate concentration, product concentration and oxygen content [128].

Enzymatic hydrolysis shows high conversion rates for specific substrates, high selectivity for product compounds and little undesirable by-product formation, so that it generates low amounts of aqueous waste [126, 128, 129]. Mild reaction conditions make enzymatic hydrolysis possible to be performed in commonly available equipment, thereby reducing equipment costs. However, reaction rates obtainable with enzymatic hydrolysis are relatively low (hours to days) compared with synthetic reactions and along with their low catalytic activity, there are few types hydrolytic enzymes making their cost high and their recycle necessary which is difficult for general OSW. Presently, enzymatic hydrolysis is limited to specific feedstocks such as lignocellulosic-based waste or polyesters (e.g., PET, PLA).

1.5 Advanced Technologies

1.5.1 Chemolysis

Chemolysis, which is also referred to as solvolysis or chemical depolymerization, is a recovery method following the principles of sustainable development [130]. Chemolysis is a process in which OSW can be treated to form chemical compounds or OSW can be depolymerized into monomeric compounds via selective breakage of C–O and C–N bonds [131]. Chemolysis is presently applicable to natural polymers (cellulose, chitin), petro-based polyesters, polyamides, polycarbonates, polylactides, polyethylenes terephthalates, polyurethanes, and nylons [131, 132]. Chemolysis processes can be placed into categories of (i) hydrolysis, (ii) alcoholysis (*e.g.*, methanolysis, glycolysis) or (iii) aminolysis as appropriate to the required degradation processes and desired chemical products [132]. Hydrolysis depolymerizes macromolecules in the aqueous phase using catalysts. Alcoholysis degrades polymers into suitable monomers in alcohol medium [133]. For example, when methanol is used as solvent, the process is called methanolysis; when polyols such as ethylene glycol, glycerol are used, the process is called glycolysis. Aminolysis uses nitrogen-containing solvents (*e.g.*, ammonia, ammonium formate) to catalyze the depolymerization of polymers to form nitrogen-containing compounds [134]. Chemolysis is affected by substrate type and substrate chemical structure, reaction chemistry and reaction conditions [20, 135, 136]. In chemolysis processes, the type of catalyst is important for achieving desired product selectivity, for reducing reaction time and reaction temperatures and for improving reaction efficiency [20, 136]. Comparing with traditional thermochemical recovery processes, chemolysis has advantages of high selectivity, high product value, and high recovery rate [132]. Compared with traditional biochemical recovery process, chemolysis has advantages of high efficiency, high recovery rate and high selectivity. However, low substrate concentration is necessary to reduce side reactions that may occur during chemolysis processes, because byproducts complicate product recovery and solvent recycle. Therefore, classification of OSW prior to application of chemolysis is required. Development of robust chemolysis processes is required for future applications to paraffin waxes and thermoplastic polymers.

1.5.2 Mechanochemical Treatment

Mechanochemical treatment is a method that can convert OSW into small molecular compounds through coupling mechanical (shearing, grinding, compression, impaction) and chemical reactions that can be promoted by homogeneous or heterogeneous catalysts [137]. During the mechanochemical treatment process, mechanical stress changes the substrate physical structure by breaking weak chemical bonds, lowering crystallinity, and increasing specific surface area while chemical reactions

occur simultaneously [138]. In addition, oxygen atmospheres can assist mechanochemical conversion reactions by promoting the generation of free radicals that accelerate degradation [139]. Therefore, mechanochemical treatment is applicable to the degradation of some types of OSW [137]. Mechanochemical treatment does not necessarily require solvent, which allows reduction of reagents and solvents and avoids post-processing separation or solvent recycle steps [138]. Compared with traditional recovery processes, mechanochemical treatment has advantages of simple processing steps, mild reaction conditions, short processing time and ecological safety [140]. Mechanochemistry has been regarded by the International Union of Pure and Applied Chemistry (IUPAC) as one of the ten world-changing technologies [141]. Although mechanochemistry has high potential for OSW valorization, energy consumption limits its application for large-scale industrialization. Thus, protocols that are both energy efficient and selective will be important for future development of mechanochemical treatment as a recycling technology.

1.5.3 Photodegradation

Photodegradation, which is also referred to as photooxidative degradation, is the process of decomposing polymers by absorbing energy from light to generate free radicals in the presence of oxygen [142]. Generally, light sources that promote photodegradation have near-ultraviolet wavelengths in the range of 290–400 nm [132, 139]. In photodegradation processes, polymer decomposition reactions include chain scission, crosslinking and secondary oxidative reactions, which are promoted via generation and transfer of free radicals [143]. There are two methods for generating free radicals in photodegradation: (i) irradiation of samples with ultraviolet light directly without catalyst and (ii) irradiation of samples with ultraviolet light with catalyst. Compared with other degradation technologies, photodegradation has the unique advantage of being spatiotemporally local, so that reactions can be controlled in a facile, green, and independent way [144]. Photodegradation can make use of sunlight in nature to degrade plastics for reducing time required for subsequent biodegradation or to completely degrade plastics [46]. On the other hand, photodegradation lacks product control and typically has low degradation rates along with low catalyst stability, making development of effective photodegradation systems a hot research topic.

1.5.4 Other Advanced Technologies

There are several other advanced technologies applicable to conversion of OSW that should be mentioned: (i) microbial fuel cells, (ii) ozonation, and (iii) Fenton oxidation. Microbial fuel cells are bio-electrochemical processes that can produce electricity through oxidizing organic compounds into adenosine triphosphate (ATP) in a

series of continuous biochemical reactions [145, 146]. Ozonation and Fenton oxidation (H_2O_2 with ferrous iron) generate oxygen species to degrade OSW into chemical compounds [132, 147–149]. Although the number of research reports is still relatively few, the unique attributes of these methods are bound to spark the curiosity of scientists and engineers interested in developing new methods.

1.6 Life Cycle Assessment

To evaluate environmental impact, economic costs, and energy benefits in the scale-up of recycling technologies, life cycle assessment (LCA) models are used to analyze incineration, gasification, pyrolysis, anaerobic digestion and composting with energy recovery. In LCA, all material and energy inputs and outputs (e.g., emissions to air, water, land and products like power, heat, chemicals, biofuels, and fertilizers) are identified and quantified [150]. The quality of the database used in LCA is important, which can govern the impact and validity of the model's output, and can even bias the conclusions [151]. Currently, databases used for LCA include Ecoinvent, GaBi, Easewaste, Easetech, Triangle Institute (RTI) and GEMIS [152]. Among them, Ecoinvent database is widely used and contains more than more than 2500 processes. In addition to databases, software is also essential for LCA. More than 20 kinds of LCA software have been used to conduct studies, including SimaPro, GaBi, OpenLCA, and Easewaste. SimaPro is one of the most popular LCA software platforms, as it has been employed in more than 30% of the surveyed studies [152]. These LCA software tools allow estimation of mass and energy flows and contain modules to include different waste treatment processes. For waste to energy, the inputs and outputs of OSW and energy are used to estimate the cost of energy and related processes, raw materials, pumps, pipes, transportation, and construction of the processing plants. Emissions from processes are also accounted for in the LCA analysis software. Table 1.3 shows some LCA results on the energy generation potential and greenhouse gas (GHG) emissions due to scale-up.

Table 1.3 Energy generation and GHG emissions from technologies that treat municipal solid waste (MSW), organic solid waste (OSW) and food waste (FW) on dry food waste (dfw) basis

Technology	Feed	Energy generation kWh/t of waste	GHG emissions kg CO ₂ -eq/t of waste	Ref.
Anaerobic Digestion	OSW	404	370	[153]
Gasification	MSW	466	271	[154]
Incineration	MSW	400	285	[155]
Pyrolysis	MSW	411	—	[156]
Composting	FW	34	−30	[157]
Ethanol Fermentation	FW	6.9 (Ethanol) GJ /t dfw	430	[158]

1.7 Conclusions and Outlook

Large amounts of organic solid waste (OSW) are generated every year which will lead to serious environmental and energy consequences if not properly recycled. Therefore, taking Reduce, Recycle and Reuse (3R's) as important criteria, conversion of OSW into raw materials for energy and chemicals will not only reduce world dependence on fossil fuels, but also provide new avenues to eco-friendly restoration of the Earth. This chapter has provided a brief overview of the types and characteristics of substrates of OSW and introduced relevant technologies including thermochemical (*e.g.*, incineration, gasification, pyrolysis, and hydrothermal treating), bio-chemical (*e.g.*, anaerobic fermentation, aerobic fermentation, and enzymatic hydrolysis) and several advanced methods (*e.g.*, chemolysis, mechanochemical degradation, photodegradation, microbial fuel cell, and Fenton oxidation) for processing of OSW.

Recovery of OSW still faces many challenges: types of raw materials, collection and transportation, land use, environmental and economic impact. In terms of types of raw materials, the physical properties, chemical composition, and prices vary greatly according to the source, type, and collection location of the raw materials. It is difficult to establish a reproducible supply framework that has specific transformation methods for different types of raw materials for biological control or biofuels with such a wide variation of material feedstocks. One possible solution is improved consumer segregation or classification of materials that is being practiced at some level in virtually every country. In terms of collection and transportation of OSW, combined recovery technologies that require large amounts of OSW typically need to be far away from the source in current methodology. The cost for collecting and transporting large amounts of OSW is still high and challenging, such that local type of processing systems need to be extensively developed. Furthermore, there are increasing restrictions on land use: large areas of land would be required to completely replace chemicals and petroleum-derived fuels with OSW. In terms of sustainability aspects of each technology, appropriate monitoring and life cycle assessments must be modeled to investigate detailed social, environmental, and economic impact of OSW recovery methods. Finally, in developing new methods and technologies for OSW, it is necessary to assess environment risks to society, nature and the Earth.

References

1. McNabb DE. The population growth barrier. In: Global pathways to water sustainability. Palgrave Macmillan, Champions; 2019. https://doi.org/10.1007/978-3-030-04085-7_5.
2. Hedblom M, Knez I, Ode Sang Å, Gunnarsson B. Evaluation of natural sounds in urban greenery: potential impact for urban nature preservation. R Soc Open Sci. 2017;4:170037. <https://doi.org/10.1098/rsos.170037>.

3. Jean F, Agnes BQ, Lionel F. The great shift: macroeconomic projections for the world economy at the 2050 Horizon (February 10, 2012). CEPPI Working Paper No. (2012), 3: Available at SSRN: <https://ssrn.com/abstract=2004332>
4. De Medina-Salas L, Castillo-González E, Giraldi-Díaz MR, Jamed-Boza LO. Valorisation of the organic fraction of municipal solid waste. *Waste Manag Res.* 2019;37(1):59–73. <https://doi.org/10.1177/0734242X18812651>.
5. Kaza S, Yao LC, Bhada-Tata P, Van Woerden F. What a waste 2.0: a global snapshot of solid waste management to 2050. Urban development, 2018. World Bank. <https://openknowledge.worldbank.org/handle/10986/30317>
6. Kumar A, Samadder SR. A review on technological options of waste to energy for effective management of municipal solid waste. *Waste Manage.* 2017;69:407–22. <https://doi.org/10.1016/j.wasman.2017.08.046>.
7. Wainaina S, Awasthi MK, Sarsaiya S, Chen H, Singh E, Kumar A, Ravindran B, Awasthi SK, Liu T, Duan Y, Kumar S, Zhang Z, Taherzadeh MJ. Resource recovery and circular economy from organic solid waste using aerobic and anaerobic digestion technologies. *Bioresour Technol.* 2020;301:122778. <https://doi.org/10.1016/j.biortech.2020.122778>.
8. Ortiz FJG, Kruse A, Ramos F, Ollero P. Integral energy valorization of municipal solid waste reject fraction to biofuels. *Energy Convers Manag.* 2019;180:1167–84. <https://doi.org/10.1016/j.enconman.2018.10.085>.
9. Dixon N, Jones DRV. Engineering properties of municipal solid waste. *Geotext Geomembr.* 2005;23(3):205–33. <https://doi.org/10.1016/j.geotexmem.2004.11.002>.
10. Stehlík P. Contribution to advances in waste-to-energy technologies. *J Clean Prod.* 2009;17(10):919–31. <https://doi.org/10.1016/j.jclepro.2009.02.011>.
11. Kothari R, Tyagi VV, Pathak A. Waste-to-energy: a way from renewable energy sources to sustainable development. *Renew Sust Energ Rev.* 2010;14(9):3164–70. <https://doi.org/10.1016/j.rser.2010.05.005>.
12. Sharma S, Basu S, Shetti NP, Kamali M, Walvekar P, Aminabhavi TM. Waste-to-energy nexus: a sustainable development. *Environ Pollut.* 2020;115501 <https://doi.org/10.1016/j.envpol.2020.115501>.
13. Assi A, Bilo F, Zanoletti A, Pontiet J, Valsesia A, Spina R, Zacco A, Bontempi E. Zero-waste approach in municipal solid waste incineration: reuse of bottom ash to stabilize fly ash. *J Clean Prod.* 2020;245:118779. <https://doi.org/10.1016/j.jclepro.2019.118779>.
14. Morris M, Waldheim L. Energy recovery from solid waste fuels using advanced gasification technology. *Waste Manag.* 1998;18(6–8):557–64. [https://doi.org/10.1016/S0956-053X\(98\)00146-9](https://doi.org/10.1016/S0956-053X(98)00146-9).
15. Chen D, Yin L, Wang H, He P. Pyrolysis technologies for municipal solid waste: a review. *Waste Manag.* 2014;34(12):2466–86. <https://doi.org/10.1016/j.wasman.2014.08.004>.
16. Zhan L, Jiang L, Zhang Y, Gao B, Xu Z. Reduction, detoxification and recycling of solid waste by hydrothermal technology: a review. *Chem Eng J.* 2020;390:124651. <https://doi.org/10.1016/j.cej.2020.124651>.
17. Zamri M, Hasmady S, Akhiar A, Ideris F, Shamsuddin AH, Mofijur M, Fattah IMR, Mahlia TMI. A comprehensive review on anaerobic digestion of organic fraction of municipal solid waste. *Renew Sust Energ Rev.* 2021;137:110637. <https://doi.org/10.1016/j.rser.2020.110637>.
18. Jensen JW, Felby C, Jørgensen H, Nørholm ND, Rønsch G. Enzymatic processing of municipal solid waste. *Waste Manag.* 2010;30(12):2497–503. <https://doi.org/10.1016/j.wasman.2010.07.009>.
19. Kumar S, Panda AK, Singh RK. A review on tertiary recycling of high-density polyethylene to fuel. *Resource Conserv Recycl.* 2011;55(11):893–910. <https://doi.org/10.1016/j.resconrec.2011.05.005>.
20. Ragaert K, Delva L, Van Geem K, Laurenti E, Montoneri E, Arques A, Carlos L. Mechanical and chemical recycling of solid plastic waste. *Waste Manag.* 2017;69:24–58. <https://doi.org/10.1016/j.wasman.2017.07.044>.

21. Avetta P, Bella F, Prevot AB, Laurenti E, Montoneri E, Arques A, Carlos L. Waste cleaning waste: photodegradation of monochlorophenols in the presence of waste-derived photosensitizer. *ACS Sustain Chem Eng.* 2013;1(12):1545–50. <https://doi.org/10.1021/sc400294z>.
22. Lee Y, Nirmalakhandan N. Electricity production in membrane-less microbial fuel cell fed with livestock organic solid waste. *Bioresour Technol.* 2011;102(10):5831–5. <https://doi.org/10.1016/j.biortech.2011.02.090>.
23. Singh RP, Tyagi VV, Allen T, Ibrahim MH, Kothari R. An overview for exploring the possibilities of energy generation from municipal solid waste (MSW) in Indian scenario. *Renew Sust Energ Rev.* 2011;15(9):4797–808. <https://doi.org/10.1016/j.rser.2011.07.071>.
24. Baawain M, Al-Mamun A, Omidvarborna H, Al-Amri W. Ultimate composition analysis of municipal solid waste in Muscat. *J Clean Prod.* 2017;148:355–62. <https://doi.org/10.1016/j.jclepro.2017.02.013>.
25. Colon J, Cadena E, Colazo AB, Quiros R, Sanchez A, Font X, Artola A. Toward the implementation of new regional biowaste management plans: environmental assessment of different waste management scenarios in Catalonia. *Resources Conserv Recycl.* 2015;95:143–55. <https://doi.org/10.1016/j.resconrec.2014.12.012>.
26. Mukherjee C, Denney J, Mbomimpa EG, Slagley J, Bhowmik R. A review on municipal solid waste-to-energy trends in the USA. *Renew Sust Energ Rev.* 2020;119:109512. <https://doi.org/10.1016/j.rser.2019.109512>.
27. Mou Z, Scheutz C, Kjedsen P. Evaluating the biochemical methane potential (BMP) of low-organic waste at Danish landfills. *Waste Manag.* 2014;34:2251–9. <https://doi.org/10.1016/j.wasman.2014.06.025>.
28. Hao Z, Yang B, Jahng D. Combustion characteristics of biodried sewage sludge. *Waste Manag.* 2018;72:296–305. <https://doi.org/10.1016/j.wasman.2017.11.008>.
29. Zhang Q, Hu J, Lee D-J, Chang Y, Lee Y-J. Sludge treatment: current research trends. *Bioresour Technol.* 2017;243:1159–72. <https://doi.org/10.1016/j.biortech.2017.07.070>.
30. Wu RM, Lee DJ. Hydrodynamic drag force exerted on a moving floc and its implication to free-settling tests. *Water Res.* 1998;32:760–8. [https://doi.org/10.1016/S0043-1354\(97\)00320-5](https://doi.org/10.1016/S0043-1354(97)00320-5).
31. Gottumukkala L D, Haigh K, Collard F X, Rensburg Van R E, Görgens J. Opportunities and prospects of biorefinery-based valorisation of pulp and paper sludge. *Bioresour Technol.* (2016) 215: 37–49. doi: <https://doi.org/10.1016/j.biortech.2016.04.015>
32. Xu G, Yang X, Spinosa L. Development of sludge-based adsorbents: preparation, characterization, utilization and its feasibility assessment. *J Environ Manage.* 2015;151:221–32. <https://doi.org/10.1016/j.jenvman.2014.08.001>.
33. Xie C, Liu J, Zhang X, Xie W, Sun J, Chang K, Kuo J, Xie W, Liu C, Sun S. Co-combustion thermal conversion characteristics of textile dyeing sludge and pomelo peel using TGA and artificial neural networks. *Appl Energy.* 2018;212:786–95. <https://doi.org/10.1016/j.apenergy.2017.12.084>.
34. Zhang H, Gao Z, Liu Y, Ran C, Mao X, Kang Q, Ao W, Fu J, Li J, Liu G, Dai J. Microwave-assisted pyrolysis of textile dyeing sludge, and migration and distribution of heavy metals. *J Hazard Mater.* 2018;355:128–35. <https://doi.org/10.1016/j.jhazmat.2018.04.080>.
35. Al-Salem SM, Lettieri P, Baeyens J. Recycling and recovery routes of plastic solid waste (PSW): a review. *Waste Manag.* 2009;29(10):2625–43. <https://doi.org/10.1016/j.wasman.2009.06.004>.
36. Al-Salem SM, Lettieri P, Baeyens J. The valorization of plastic solid waste (PSW) by primary to quaternary routes: from re-use to energy and chemicals. *Prog Energy Combust Sci.* 2010;36 (1):103–29. <https://doi.org/10.1016/j.pecs.2009.09.001>.
37. Liu H, Wang Y, Zhao S, Hu H, Cao C, Li A, Yu Y, Yao H. Review on the current status of the co-combustion technology of Organic Solid Waste (OSW) and coal in China. *Energy Fuel.* 2020;34(12):15448–87. <https://doi.org/10.1021/acs.energyfuels.0c02177>.

38. Okan M, Aydin HM, Barsbay M. Current approaches to waste polymer utilization and minimization: a review. *J Chem Technol Biotechnol.* 2019;94(1):8–21. <https://doi.org/10.1002/jctb.5778>.
39. Coates GW, Getzler YDYL. Chemical recycling to monomer for an ideal, circular polymer economy. *Nat Rev Mater.* 2020;5(7):501–16. <https://doi.org/10.1038/s41578-020-0190-4>.
40. Silvarrey LSD, Phan AN. Kinetic study of municipal plastic waste. *Int J Hydrg Energy.* 2016;41(37):16352–64. <https://doi.org/10.1016/j.ijhydene.2016.05.202>.
41. Miskolczi N, Bartha L, Deak G, Jover B. Thermal degradation of municipal plastic waste for production of fuel-like hydrocarbons. *Polym Degrad Stab.* 2004;86(2):357–66. <https://doi.org/10.1016/j.polymdegradstab.2004.04.025>.
42. Quecholac-Piña X, García-Rivera MA, Espinosa-Valdemar RM, Vázquez-Morillas A, Beltrán-Villavicencio M, de la Luz Cisneros-Ramos A. Biodegradation of compostable and oxodegradable plastic films by backyard composting and bioaugmentation. *Environ Sci Pollut Res.* 2017;24(33):25725–30. <https://doi.org/10.1007/s11356-016-6553-0>.
43. Geyer R, Jambeck JR, Law KL. Production, use, and fate of all plastics ever made. *Sci Adv.* 2017;3(7):e1700782. <https://doi.org/10.1126/sciadv.1700782>.
44. Jambeck JR, Geyer R, Wilcox C, Siegler TR, Perryman M, Andrady A, Narayan R, Law KL. Plastic waste inputs from land into the ocean. *Science.* 2015;347(6223):768–71. <https://doi.org/10.1126/science.1260352>.
45. Zhao YB, Lv XD, Ni HG. Solvent-based separation and recycling of waste plastics: A review. *Chemosphere.* 2018;209:707–20. <https://doi.org/10.1016/j.chemosphere.2018.06.095>.
46. Jiao X, Zheng K, Chen Q, Li X, Li Y, Shao W, Xu J, Zhu J, Pan Y, Sun Y, Xie Y. Photocatalytic conversion of waste plastics into C2 fuels under simulated natural environment conditions. *Angew Chem Int Ed.* 2020;59(36):15497–501. <https://doi.org/10.1002/anie.201915766>.
47. Barnes SJ. Understanding plastics pollution: the role of economic development and technological research. *Environ Pollut.* 2019;249:812–21. <https://doi.org/10.1016/j.envpol.2019.03.108>.
48. Larsen MB, Schultz L, Glarborg P, Skaarup-Jensen L, Dam-Johansen K, Frandsen F, Henriksen U. Devolatilization characteristics of large particles of tyre rubber under combustion conditions. *Fuel.* 2006;85(10–11):1335–45. <https://doi.org/10.1016/j.fuel.2005.12.014>.
49. Fazli A, Rodrigue D. Waste rubber recycling: a review on the evolution and properties of thermoplastic elastomers. *Materials.* 2020;13(3):782. <https://doi.org/10.3390/ma13030782>.
50. Tang X, Chen Z, Liu J, Chen Z, Xie W, Evrendilek F, Buyukada M. Dynamic pyrolysis behaviors, products, and mechanisms of waste rubber and polyurethane bicycle tires. *J Hazard Mater.* 2021;402:123516. <https://doi.org/10.1016/j.jhazmat.2020.123516>.
51. Chen R, Li Q, Zhang Y, Xu X, Zhang D. Pyrolysis kinetics and mechanism of typical industrial non-tyre rubber wastes by peak-differentiating analysis and multi kinetics methods. *Fuel.* 2019;235:1224–37. <https://doi.org/10.1016/j.fuel.2018.08.121>.
52. Thomas BS, Gupta RC. A comprehensive review on the applications of waste tire rubber in cement concrete. *Renew Sust Energ Rev.* 2016;54:1323–33. <https://doi.org/10.1016/j.rser.2015.10.092>.
53. Ramarad S, Khalid M, Ratnam CT, Chuah AL, Rashmi W. Waste tire rubber in polymer blends: a review on the evolution, properties and future. *Prog Mater Sci.* 2015;72:100–40. <https://doi.org/10.1016/j.pmatsci.2015.02.004>.
54. Miranda M, Pinto F, Gulyurtlu I, Cabrita I. Pyrolysis of rubber tyre wastes: a kinetic study. *Fuel.* 2013;103:542–52. <https://doi.org/10.1016/j.fuel.2012.06.114>.
55. Chen W, Lin B, Lin Y, Chu Y, Ubando AT, Show PL, Ong HC, Chang J, Ho S, Culaba AB, Petrisans A, Petrisans M. Progress in biomass torrefaction: Principles, applications and challenges. *Prog Energy Combust Sci.* 2021;82:100887. <https://doi.org/10.1016/j.pecs.2020.100887>.

56. Nowak DJ, Greenfield EJ, Ash RM. Annual biomass loss and potential value of urban tree waste in the United States. *Urban For Urban Green*. 2019;46:126469. <https://doi.org/10.1016/j.ufug.2019.126469>.
57. Sayed ET, Wilberforce T, Elsaied K, Rabaia MKH, Abdelkareem MA, Chae KJ, Olabi AG. A critical review on environmental impacts of renewable energy systems and mitigation strategies: wind, hydro, biomass and geothermal. *Sci Total Environ*. 2020;144505. <https://doi.org/10.1016/j.scitotenv.2020.144505>.
58. Arevalo-Gallegos A, Ahmad Z, Asgher M, Parra-Saldivar R, Iqbal HMN. Lignocellulose: a sustainable material to produce value-added products with a zero waste approach-a review. *Int J Biol Macromol*. 2017;99:308–18. <https://doi.org/10.1016/j.ijbiomac.2017.02.097>.
59. Vassilev SV, Baxter D, Andersen LK, Vassileva CG. An overview of the chemical composition of biomass. *Fuel*. 2010;89(5):913–33. <https://doi.org/10.1016/j.fuel.2009.10.022>.
60. Bar-On YM, Phillips R, Milo R. The biomass distribution on Earth. *Proc Natl Acad Sci*. 2018;115(25):6506–11. <https://doi.org/10.1073/pnas.1711842115>.
61. Yang H, Yan R, Chen H, Zheng C, Lee D, Liang D. In-depth investigation of biomass pyrolysis based on three major components: hemicellulose, cellulose and lignin. *Energy Fuel*. 2006;20(1):388–93. <https://doi.org/10.1021/ef0580117>.
62. Brinch L, Cotana F, Fortunati E, Kenny JM. Production of nanocrystalline cellulose from lignocellulosic biomass: technology and applications. *Carbohydr Polym*. 2013;94(1):154–69. <https://doi.org/10.1016/j.carbpol.2013.01.033>.
63. Luo Y, Li Z, Li X, Liu X, Fan J, Clark JH, Hu C. The production of furfural directly from hemicellulose in lignocellulosic biomass: a review. *Catal Today*. 2019;319:14–24. <https://doi.org/10.1016/j.cattod.2018.06.042>.
64. Gani A, Naruse I. Effect of cellulose and lignin content on pyrolysis and combustion characteristics for several types of biomass. *Renew Energy*. 2007;32(4):649–61. <https://doi.org/10.1016/j.renene.2006.02.017>.
65. Hu J, Zhang Q, Lee DJ. Kraft lignin biorefinery: a perspective. *Bioresour Technol*. 2018;247: 1181–3. <https://doi.org/10.1016/j.biortech.2017.08.169>.
66. Haq I, Qaisar K, Nawaz A, Akram F, Mukhtar H, Zohu X, Xu Y, Mumtaz MW, Rashid U, Ghani WAWAK, Choong TSY. Advances in valorization of lignocellulosic biomass towards energy generation. *Catalysts*. 2021;11(3):309. <https://doi.org/10.3390/catal11030309>.
67. Ji H, Dong C, Yang G, Pang Z. Valorization of lignocellulosic biomass toward multipurpose fractionation: furfural, phenolic compounds, and ethanol. *ACS Sustain Chem Eng*. 2018;6 (11):15306–15. <https://doi.org/10.1021/acssuschemeng.8b03766>.
68. Tuck CO, Pérez E, Horváth IT, Sheldon RA, Poliakoff M. Valorization of biomass: deriving more value from waste. *Science*. 2012;337(6095):695–9. <https://doi.org/10.1126/science.1218930>.
69. Esteves EMM, Herrera AMN, Esteves VPP, Morgado CDRV. Life cycle assessment of manure biogas production: a review. *J Clean Prod*. 2019;219:411–23. <https://doi.org/10.1016/j.jclepro.2019.02.091>.
70. Berendes DM, Yang PJ, Lai A, Hu D, Brown J. Estimation of global recoverable human and animal faecal biomass. *Nat Sustain*. 2018;1(11):679–85. <https://doi.org/10.1038/s41893-018-0167-0>.
71. Mihelcic JR, Fry LM, Shaw R. Global potential of phosphorus recovery from human urine and feces. *Chemosphere*. 2011;84(6):832–9. <https://doi.org/10.1016/j.chemosphere.2011.02.046>.
72. Hamoda MF, Abu Qdais HA, Newham J. Evaluation of municipal solid waste composting kinetics. *Resources Conserv Recycl*. 1998;23:209–23. [https://doi.org/10.1016/S0921-3449\(98\)00021-4](https://doi.org/10.1016/S0921-3449(98)00021-4).
73. Vermeulen LC, Benders J, Medema G, Hofstra N. Global Cryptosporidium loads from livestock manure. *Environ Sci Technol*. 2017;51(15):8663–71. <https://doi.org/10.1021/acs.est.7b00452>.

74. Zhang L, Xu CC, Champagne P. Overview of recent advances in thermo-chemical conversion of biomass. *Energy Convers Manag.* 2010;51(5):969–82. <https://doi.org/10.1016/j.enconman.2009.11.038>.
75. Xu L, Shi C, He Z, Zhang H, Chen M, Fang Z, Zhang Y. Recent advances of producing biobased N-containing compounds via thermo-chemical conversion with ammonia process. *Energy Fuel.* 2020;34(9):10441–58. <https://doi.org/10.1021/acs.energyfuels.0c01993>.
76. Lopez G, Artetxe M, Amutio M, Bilbao J, Olazar M. Thermochemical routes for the valorization of waste polyolefinic plastics to produce fuels and chemicals. a review. *Renew Sust Energ Rev.* 2017;73:346–68. <https://doi.org/10.1016/j.rser.2017.01.142>.
77. Sabbas T, Polettini A, Pomi R, Astrup T, Hjelmar O, Mostbauer P, Cappai G, Magel G, Salhofer S, Speiser C, Heuss-Assbichler S, Klein R, Lechner P. Management of municipal solid waste incineration residues. *Waste Manag.* 2003;23(1):61–88. [https://doi.org/10.1016/S0956-053X\(02\)00161-7](https://doi.org/10.1016/S0956-053X(02)00161-7).
78. Lu J, Zhang S, Hai J, Lei M. Status and perspectives of municipal solid waste incineration in China: a comparison with developed regions. *Waste Manag.* 2017;69:170–86. <https://doi.org/10.1016/j.wasman.2017.04.014>.
79. Wang P, Hu Y, Cheng H. Municipal solid waste (MSW) incineration fly ash as an important source of heavy metal pollution in China. *Environ Pollut.* 2019;252:461–75. <https://doi.org/10.1016/j.envpol.2019.04.082>.
80. Psaltis P, Komilis D. Environmental and economic assessment of the use of biodrying before thermal treatment of municipal solid waste. *Waste Manag.* 2019;83:95–103. <https://doi.org/10.1016/j.wasman.2018.11.007>.
81. Makarichi L, Jutidamrongphan W, Techato K. The evolution of waste-to-energy incineration: a review. *Renew Sust Energ Rev.* 2018;91:812–21. <https://doi.org/10.1016/j.rser.2018.04.088>.
82. Panepinto D, Zanetti MC. Municipal solid waste incineration plant: a multi-step approach to the evaluation of an energy-recovery configuration. *Waste Manag.* 2018;73:332–41. <https://doi.org/10.1016/j.wasman.2017.07.036>.
83. Nyashina GS, Vershinina KY, Shlegel NE, Strizhak PA. Effective incineration of fuel-waste slurries from several related industries. *Environ Res.* 2019;176:108559. <https://doi.org/10.1016/j.envres.2019.108559>.
84. Zhang Y, Ma Z, Fang Z, Qian Y, Zhong P, Yan J. Review of harmless treatment of municipal solid waste incineration fly ash. *Waste Disposal Sustain Energy.* 2020;2(1):1–25. <https://doi.org/10.1007/s42768-020-00033-0>.
85. Eriksson O, Finnveden G. Energy recovery from waste incineration—the importance of technology data and system boundaries on CO₂ emissions. *Energies.* 2017;10(4):539. <https://doi.org/10.3390/en10040539>.
86. Martínez JD, Puy N, Murillo R, Garcia T, Victoria Navarro M, Mastral MA. Waste tyre pyrolysis—a review. *Renew Sust Energ Rev.* 2013;23:179–213. <https://doi.org/10.1016/j.rser.2013.02.038>.
87. Sharuddin SDA, Abnisa F, Daud WMAW, Aroua MK. A review on pyrolysis of plastic wastes. *Energy Convers Manag.* 2016;115:308–26. <https://doi.org/10.1016/j.enconman.2016.02.037>.
88. Kan T, Strezov V, Evans TJ. Lignocellulosic biomass pyrolysis: a review of product properties and effects of pyrolysis parameters. *Renew Sust Energ Rev.* 2016;57:1126–40. <https://doi.org/10.1016/j.rser.2015.12.185>.
89. Liu C, Wang H, Karim AM, Sun J, Wang Y. Catalytic fast pyrolysis of lignocellulosic biomass. *Chem Soc Rev.* 2014;43(22):7594–623. <https://doi.org/10.1039/C3CS60414D>.
90. Kumar R, Strezov V, Weldekidan H, He J, Singh S, Kan T, Dastjerdi B. Lignocellulose biomass pyrolysis for bio-oil production: a review of biomass pre-treatment methods for production of drop-in fuels. *Renew Sust Energ Rev.* 2020;123:109763. <https://doi.org/10.1016/j.rser.2020.109763>.

91. Perkins G, Bhaskar T, Konarova M. Process development status of fast pyrolysis technologies for the manufacture of renewable transport fuels from biomass. *Renew Sust Energ Rev*. 2018;90:292–315. <https://doi.org/10.1016/j.rser.2018.03.048>.
92. Kumar V, Nanda M. Biomass pyrolysis-current status and future directions. *Energy Sources Part A: Recov Util Environ Effects*. 2016;38(19):2914–21. <https://doi.org/10.1080/15567036.2015.1098751>.
93. Dickerson T, Soria J. Catalytic fast pyrolysis: a review. *Energies*. 2013;6(1):514–38. <https://doi.org/10.3390/en6010514>.
94. Venderbosch RH. A critical view on catalytic pyrolysis of biomass. *ChemSusChem*. 2015;8(8):1306–16. <https://doi.org/10.1002/cssc.201500115>.
95. Li B, Ou L, Dang Q, Meyer P, Jones S, Brown R, Wright M. Techno-economic and uncertainty analysis of in situ and ex situ fast pyrolysis for biofuel production. *Bioresour Technol*. 2015;196:49–56. <https://doi.org/10.1016/j.biortech.2015.07.073>.
96. Wan S, Wang Y. A review on ex situ catalytic fast pyrolysis of biomass. *Front Chem Sci Eng*. 2014;8(3):280–94. <https://doi.org/10.1007/s11705-014-1436-8>.
97. Cai R, Pei X, Pan H, Wan K, Chen H, Zhang Z, Zhang Y. Biomass catalytic pyrolysis over zeolite catalysts with an emphasis on porosity and acidity: a state-of-the-art review. *Energy Fuel*. 2020;34(10):11771–90. <https://doi.org/10.1021/acs.energyfuels.0c02147>.
98. Hameed S, Sharma A, Pareek V, Wu H, Yu Y. A review on biomass pyrolysis models: kinetic, network and mechanistic models. *Biomass Bioenergy*. 2019;123:104–22. <https://doi.org/10.1016/j.biombioe.2019.02.008>.
99. Sansaniwal SK, Pal K, Rosen MA, Tyagi SK. Recent advances in the development of biomass gasification technology: a comprehensive review. *Renew Sust Energ Rev*. 2017;72:363–84. <https://doi.org/10.1016/j.rser.2017.01.038>.
100. Molino A, Chianese S, Musimarra D. Biomass gasification technology: the state of the art overview. *J Energy Chem*. 2016;25(1):10–25. <https://doi.org/10.1016/j.jechem.2015.11.005>.
101. Belgiorno V, De Feo G, Della Rocca C, Napoli RMA. Energy from gasification of solid wastes. *Waste Manag*. 2003;23(1):1–15. [https://doi.org/10.1016/S0956-053X\(02\)00149-6](https://doi.org/10.1016/S0956-053X(02)00149-6).
102. Wilhelm DJ, Simbeck DR, Karp AD, Dickenson RL. Syngas production for gas-to-liquids applications: technologies, issues and outlook. *Fuel Process Technol*. 2001;71(1–3):139–48. [https://doi.org/10.1016/S0378-3820\(01\)00140-0](https://doi.org/10.1016/S0378-3820(01)00140-0).
103. Werle S, Wilk RK. A review of methods for the thermal utilization of sewage sludge: the Polish perspective. *Renew Energy*. 2010;35(9):1914–9. <https://doi.org/10.1016/j.renene.2010.01.019>.
104. Schmieder H, Abeln J, Boukis N, Dinjus E, Kruse A, Kluth M, Petrich G, Sadri E, Schacht M. Hydrothermal gasification of biomass and organic wastes. *J Supercrit Fluids*. 2000;17(2):145–53. [https://doi.org/10.1016/S0896-8446\(99\)00051-0](https://doi.org/10.1016/S0896-8446(99)00051-0).
105. Guo L, Jin H, Lu Y. Supercritical water gasification research and development in China. *J Supercrit Fluids*. 2015;96:144–50. <https://doi.org/10.1016/j.supflu.2014.09.023>.
106. Nanda S, Gong M, Hunter HN, Dalai AK, Gokalp I, Kozinski JA. An assessment of pinecone gasification in subcritical, near-critical and supercritical water. *Fuel Process Technol*. 2017;168:84–96. <https://doi.org/10.1016/j.fuproc.2017.08.017>.
107. Wang D, Yuan W, Ji W. Char and char-supported nickel catalysts for secondary syngas cleanup and conditioning. *Appl Energy*. 2011;88(5):1656–63. <https://doi.org/10.1016/j.apenergy.2010.11.041>.
108. Xiang X, Gong G, Wang C, Cai N, Zhou X, Li Y. Exergy analysis of updraft and downdraft fixed bed gasification of village-level solid waste. *Int J Hydrom Energy*. 2021;46(1):221–33. <https://doi.org/10.1016/j.ijhydene.2020.09.247>.
109. Minowa T, Murakami M, Dote Y, Ogi T, Yokoyama SY. Oil production from garbage by thermochemical liquefaction. *Biomass Bioenergy*. 1995;8(2):117–20. [https://doi.org/10.1016/0961-9534\(95\)00017-2](https://doi.org/10.1016/0961-9534(95)00017-2).
110. Gollakota ARK, Kishore N, Gu S. A review on hydrothermal liquefaction of biomass. *Renew Sust Energ Rev*. 2018;81:1378–92. <https://doi.org/10.1016/j.rser.2017.05.178>.

111. Dimitriadis A, Bezergianni S. Hydrothermal liquefaction of various biomass and waste feedstocks for biocrude production: a state of the art review. *Renew Sust Energ Rev.* 2017;68:113–25. <https://doi.org/10.1016/j.rser.2016.09.120>.
112. Meegoda JN, Li B, Patel K, Wang LB. A review of the processes, parameters, and optimization of anaerobic digestion. *Int J Environ Res Public Health.* 2018;15(10):2224. <https://doi.org/10.3390/ijerph15102224>.
113. Jenicek P, Koubova J, Bindzar J, Zabranska J. Advantages of anaerobic digestion of sludge in microaerobic conditions. *Water Sci Technol.* 2010;62(2):427–34. <https://doi.org/10.2166/wst.2010.305>.
114. Angelidaki I, Ellegaard L, Ahring BK. Applications of the anaerobic digestion process. *Biomethanation II.* 2003:1–33. https://doi.org/10.1007/3-540-45838-7_1.
115. Neves NG, Berni M, Dragone G, Mussatto SI, Carneiro FT. Anaerobic digestion process: technological aspects and recent developments. *Int J Environ Sci Technol.* 2018;15(9):2033–46. <https://doi.org/10.1007/s13762-018-1682-2>.
116. Mao C, Feng Y, Wang X, Ren G. Review on research achievements of biogas from anaerobic digestion. *Renew Sust Energ Rev.* 2015;45:540–55. <https://doi.org/10.1016/j.rser.2015.02.032>.
117. Tran HT, Lin C, Bui XT, Ngo HH, Cheruiyot NK, Hoang HG, Vu CT. Aerobic composting remediation of petroleum hydrocarbon-contaminated soil. *Curr Future Perspect Sci Total Environ.* 2021;753:142250. <https://doi.org/10.1016/j.scitotenv.2020.142250>.
118. Gómez RB, Lima FV, Ferrer AS. The use of respiration indices in the composting process: a review. *Waste Manag Res.* 2006;24(1):37–47. <https://doi.org/10.1177/0734242X06062385>.
119. Himanen M, Hänninen K. Composting of bio-waste, aerobic and anaerobic sludges – effect of feedstock on the process and quality of compost. *Bioresour Technol.* 2011;102(3):2842–52. <https://doi.org/10.1016/j.biortech.2010.10.059>.
120. Sánchez ÓJ, Ospina DA, Montoya S. Compost supplementation with nutrients and microorganisms in composting process. *Waste Manag.* 2017;69:136–53. <https://doi.org/10.1016/j.wasman.2017.08.012>.
121. Singh S, Nain L. Microorganisms in the conversion of agricultural wastes to compost. *Process Indian Natl Sci Acad.* 2014;80(2):473–81. <https://doi.org/10.16943/ptinsa/2014/v80i2/7>.
122. Azim K, Soudi B, Boukhari S, Perissol C, Roussos S, Thami AI. Composting parameters and compost quality: a literature review. *Org Agric.* 2018;8(2):141–58. <https://doi.org/10.1007/s13165-017-0180-z>.
123. Hungría J, Gutiérrez MC, Siles JA, Martin MA. Advantages and drawbacks of OFMSW and winery waste co-composting at pilot scale. *J Clean Prod.* 2017;164:1050–7. <https://doi.org/10.1016/j.jclepro.2017.07.029>.
124. Houfani AA, Anders N, Spiess AC, Baldrian P, Benallaoua S. Insights from enzymatic degradation of cellulose and hemicellulose to fermentable sugars – a review. *Biomass Bioenergy.* 2020;134:105481. <https://doi.org/10.1016/j.biombioe.2020.105481>.
125. Radenkova V, Juhnevica-Radenkova K, Górnáš P, Seglina D. Non-waste technology through the enzymatic hydrolysis of agro-industrial by-products. *Trends Food Sci Technol.* 2018;77:64–76. <https://doi.org/10.1016/j.tifs.2018.05.013>.
126. Arfi Y, Shamshoum M, Rogachev I, Peleg Y, Bayer EA. Integration of bacterial lytic polysaccharide monooxygenases into designer cellulosomes promotes enhanced cellulose degradation. *Proc Natl Acad Sci.* 2014;111(25):9109–14. <https://doi.org/10.1073/pnas.1404148111>.
127. Levine SE, Fox JM, Blanch HW, Clark DS. A mechanistic model of the enzymatic hydrolysis of cellulose. *Biotechnol Bioeng.* 2010;107(1):37–51. <https://doi.org/10.1002/bit.22789>.
128. Modenbach AA, Nokes SE. Enzymatic hydrolysis of biomass at high-solids loadings – a review. *Biomass Bioenergy.* 2013;56:526–44. <https://doi.org/10.1016/j.biombioe.2013.05.031>.

129. Yu Y, Lou X, Wu H. Some recent advances in hydrolysis of biomass in hot-compressed water and its comparisons with other hydrolysis methods. *Energy Fuel*. 2008;22(1):46–60. <https://doi.org/10.1021/ef700292p>.
130. Kumar S, Panda AK, Singh RK. A review on tertiary recycling of high-density polyethylene to fuel. *Resour Conserv Recycl*. 2011;55(11):893–910. <https://doi.org/10.1016/j.resconrec.2011.05.005>.
131. Oliveux G, Dandy LO, Leeke GA. Current status of recycling of fibre reinforced polymers: review of technologies, reuse and resulting properties. *Prog Mater Sci*. 2015;72:61–99. <https://doi.org/10.1016/j.pmatsci.2015.01.004>.
132. Zhang F, Zhao Y, Wang D, Yan M, Zhang J, Zhang P, Ding T, Chen L, Chen C. Current technologies for plastic waste treatment: a review. *J Clean Prod*. 2020;124523 <https://doi.org/10.1016/j.jclepro.2020.124523>.
133. Pardal F, Tersac G. Comparative reactivity of glycols in PET glycolysis. *Polym Degrad Stab*. 2006;91(11):2567–78. <https://doi.org/10.1016/j.polymdegradstab.2006.05.016>.
134. Demarteau J, Olazabal I, Jehanno C, Sardon H. Aminolytic upcycling of poly (ethylene terephthalate) wastes using a thermally-stable organocatalyst. *Polym Chem*. 2020;11(30):4875–82. <https://doi.org/10.1039/DOPY00067A>.
135. Singh N, Hui D, Singh R, Ahuja IPS, Feo L, Fraternali F. Recycling of plastic solid waste: a state of art review and future applications. *Compos Part B*. 2017;115:409–22. <https://doi.org/10.1016/j.compositesb.2016.09.013>.
136. Payne J, McKeown P, Jones MD. A circular economy approach to plastic waste. *Polym Degrad Stab*. 2019;165:170–81. <https://doi.org/10.1016/j.polymdegradstab.2019.05.014>.
137. Gaudino EC, Cravotto G, Manzoli M, Tabasso S. Sono-and mechanochemical technologies in the catalytic conversion of biomass. *Chem Soc Rev*. 2021;50:1785–812. <https://doi.org/10.1039/DOSR01152E>.
138. Shen F, Xiong X, Fu J, Yang J, Qiu M, Qi X, Tsang DCW. Recent advances in mechanochemical production of chemicals and carbon materials from sustainable biomass resources. *Renew Sust Energ Rev*. 2020;130:109944. <https://doi.org/10.1016/j.rser.2020.109944>.
139. Singh B, Sharma N. Mechanistic implications of plastic degradation. *Polym Degrad Stab*. 2008;93(3):561–84. <https://doi.org/10.1016/j.polymdegradstab.2007.11.008>.
140. Bychkov A, Podgorbunskikh E, Bychkova E, Lomovsky O. Current achievements in the mechanically pretreated conversion of plant biomass. *Biotechnol Bioeng*. 2019;116(5):1231–44. <https://doi.org/10.1002/bit.26925>.
141. Ten G-BF. Chemical innovations that will change our world: IUPAC identifies emerging technologies in chemistry with potential to make our planet more sustainable. *Chem Int*. 2019;41(2):12–7. <https://doi.org/10.1515/ci-2019-0203>.
142. Ravelli D, Protti S, Fagnoni M. Carbon–carbon bond forming reactions via photogenerated intermediates. *Chem Rev*. 2016;116(17):9850–913. <https://doi.org/10.1021/acs.chemrev.5b00662>.
143. Bracco P, Costa L, Luda MP, Billingham N. A review of experimental studies of the role of free-radicals in polyethylene oxidation. *Polym Degrad Stab*. 2018;155:67–83. <https://doi.org/10.1016/j.polymdegradstab.2018.07.011>.
144. Chatani S, Kloxin CJ, Bowman CN. The power of light in polymer science: photochemical processes to manipulate polymer formation, structure, and properties. *Polym Chem*. 2014;5(7):2187–201. <https://doi.org/10.1039/C3PY01334K>.
145. Santoro C, Arbizzani C, Erable B, Ieropoulos I. Microbial fuel cells: From fundamentals to applications. A review. *J Power Sources*. 2017;356:225–44. <https://doi.org/10.1016/j.jpowsour.2017.03.109>.
146. Zhao Q, Yu H, Zhang W, Kabutey FT, Jiang J, Zhang Y, Wang K, Ding J. Microbial fuel cell with high content solid wastes as substrates: a review. *Front Environ Sci Eng*. 2017;11(2):13. <https://doi.org/10.1007/s11783-017-0918-6>.

147. Cesaro A, Belgiorno V. Sonolysis and ozonation as pretreatment for anaerobic digestion of solid organic waste. *Ultrason Sonochem.* 2013;20(3):931–6. <https://doi.org/10.1016/j.ultsonch.2012.10.017>.
148. Li J, Zhao L, Qin L, Tian X, Wang A, Zhou Y, Meng L, Chen Y. Removal of refractory organics in nanofiltration concentrates of municipal solid waste leachate treatment plants by combined Fenton oxidative-coagulation with photo-Fenton processes. *Chemosphere.* 2016;146:442–9. <https://doi.org/10.1016/j.chemosphere.2015.12.069>.
149. Liu P, Qian L, Wang H, Zhan X, Lu K, Gu C, Gao S. New insights into the aging behavior of microplastics accelerated by advanced oxidation processes. *Environ Sci Technol.* 2019;53(7): 3579–88. <https://doi.org/10.1021/acs.est.9b00493>.
150. Khandelwal H, Dhar H, Thalla AK, Kumar S. Application of life cycle assessment in municipal solid waste management: a worldwide critical review. *J Clean Prod.* 2019;209: 630–54. <https://doi.org/10.1016/j.jclepro.2018.10.233>.
151. Winkler J, Bilitewski B. Comparative evaluation of life cycle assessment models for solid waste management. *Waste Manag.* 2007;27:1021–31. <https://doi.org/10.1016/j.wasman.2007.02.023>.
152. Dastjerdi B, Strezov V, Ali Rajaeifar M, Kumar R, Behnia M. A systematic review on life cycle assessment of different waste to energy valorization technologies. *J Clean Prod.* 2021;290:125747. <https://doi.org/10.1016/j.jclepro.2020.125747>.
153. El Hanandeh A, El Zein A. Are the aims of increasing the share of green electricity generation and reducing GHG emissions always compatible? *Renew Energy.* 2011;36:3031–6. <https://doi.org/10.1016/j.renene.2011.03.034>.
154. Fernandez-Gonzalez JM, Grindlay AL, Serrano-Bernardo F, Rodriguez-Rojas MI, Zamorano M. Economic and environmental review of Waste-to-Energy systems for municipal solid waste management in medium and small municipalities. *Waste Manag.* 2017;67:360–74. <https://doi.org/10.1016/j.wasman.2017.05.003>.
155. Leme MMV, Rocha MH, Lora EES, Venturini OJ, Lopes BM, Ferreira CH. Techno-economic analysis and environmental impact assessment of energy recovery from Municipal Solid Waste (MSW) in Brazil. *Resource Conserv Recycl.* 2014;87:8–20. <https://doi.org/10.1016/j.resconrec.2014.03.003>.
156. Di Maria F, Fantozzi F. Life cycle assessment of waste to energy micro-pyrolysis system: case study for an Italian town. *Int J Energy Res.* 2004;28:449–61. <https://doi.org/10.1002/er.977>.
157. Thyberg KL, Tonjes DJ. The environmental impacts of alternative food waste treatment technologies in the US. *J Clean Prod.* 2017;158:101–8. <https://doi.org/10.1016/j.jclepro.2017.04.169>.
158. Ebner J, Babbitt C, Winer M, Hilton B, Williamson A. Life cycle green-house gas (GHG) impacts of a novel process for converting food waste to ethanol and co-products. *Apply Energy.* 2014;130:86–93. <https://doi.org/10.1016/j.apenergy.2014.04.099>.

Part II

Production of Biofuels and Chemicals by

Thermo-Chemical Conversion Processes

Chapter 2

Recent Advances in the Catalytic Co-pyrolysis of Lignocellulosic Biomass and Different Polymer Wastes from Laboratory Scale to Pilot Plant



Olga Sanahuja Parejo, A. Veses, A. Sanchís, M. S. Callén, R. Murillo, and T. García

Abstract Nowadays, it is generally accepted that the production of biofuels through the pyrolysis of lignocellulosic biomass may be an interesting alternative to fossil fuels. The appeal of this renewable resource is due to its worldwide availability and its environmentally friendly nature. The liquid fraction obtained from pyrolysis processes, bio-oil, is the most valuable product given its further application as biofuel, although it contains many oxygenated compounds and has a low heating value and high acidity, which hinders its direct application or even storage. To improve its quality, a dual strategy combining the two well-known upgrading approaches of cracking catalyst addition and waste plastics co-feeding has recently emerged as a promising solution since positive synergistic effects are achieved that are more suited to the production of upgraded biofuels. The upgrading reaction mechanism has mainly been associated with the presence of plastic wastes, which serve as H₂ donors to promote hydrocracking and hydrodeoxygenation catalytic reactions, and accordingly, highly significant results have been achieved using this dual strategy. This chapter discusses the most important of these results as reported in the literature obtained in facilities ranging from thermogravimetric reactors (technology readiness level (TRL) 2) to pilot plants in a relevant environment (TRL 5).

Keywords Biomass · Polymer wastes · Catalytic co-pyrolysis · Thermogravimetry · Laboratory scale · Pilot plants

O. Sanahuja Parejo · A. Veses · A. Sanchís · M. S. Callén · R. Murillo · T. García (✉)
Instituto de Carboquímica (ICB-CSIC), Zaragoza, Spain
e-mail: osanahuja@icb.csic.es; a.veses@icb.csic.es; marisol@icb.csic.es;
ramon.murillo@csic.es; tomas@icb.csic.es

Abbreviations

CC	Catalytic Cracking
DAEM	Distribution activation energy model
FCC	Fluid Catalytic Cracking
GC-MS	Gas Chromatography –Mass Spectrometry
GS	Grape seeds
HDO	High Pressure Hydrodeoxygenation
HDPE	High Density Polyethylene
HHV	High Heating Value
LDPE	Low Density Polyethylene
PET	Polyethylene terephthalate
PLA	Polylactic acid
PP	Polypropylene
PS	Polystyrene
PUR	Polyurethane
PVC	Poly (vinyl chloride)
RSO	Rubber Seed Oil
TGA	Thermogravimetric Analysis
TRL	Technology readiness level
WT	Waste tire

2.1 Introduction

The use and extraction of fossil fuels, associated with high levels of greenhouse gas emissions [1, 2], come with a hugely negative environmental impact. They are the world's primary source of energy and owing to the high energy demand created by the economic and social development of contemporary society, fossil fuels are also becoming more costly. To counteract this, much scientific research is focused on the search for alternative fuels or energy sources that are more widely available, economic, and environmentally friendly. Great efforts have been made in recent decades to satisfy the need for a sustainable development strategy with the potential to reduce the environmental impact of energy production while favoring economic and social development. In this sense, the use of biomass as a feedstock is emerging as an attractive renewable energy resource [1, 3, 4]. Processing of biomass to produce fuels began in the late nineteenth century, although it was only at the end of the twentieth century that biomass started to be used as an energy resource. The growth, development, and expansion of these processes were closely related to the phenomenon of globalization. The surge in the use of biomass as an energy resource came after the oil crisis of 1973, a consequence of the global repercussions felt by the skyrocketing price of crude oil, particularly in countries without petroleum reserves. The use of lignocellulosic biomass has grown considerably in recent years as it

represents an opportunity to obtain value-added products from a renewable source, with a significant reduction in environmental impact compared with the processing of fossil fuels. Furthermore, the use of this renewable energy source can advance the energy independence of non-oil-producing countries [5]. In particular, the use of residual lignocellulosic biomass from forestry and agricultural residues, among others, is considered to be of interest because it can be used as a raw material at a local and regional level, thus providing a potential market for by-products, generating employment, and contributing to the sustainable forest management. Finally, from an environmental perspective and when compared to fossil fuels, the use of lignocellulosic biomass represents a reduction in greenhouse gas emissions, due to its almost neutral character in CO₂ emissions.

For all these reasons, the use of lignocellulosic biomass in thermochemical processes such as pyrolysis, combustion, and gasification has achieved great importance in recent years. In particular, not only does pyrolysis provide an opportunity to obtain biofuels (liquid, solid or gas) and chemical products of reasonable quality from a renewable source, but a number of authors have also demonstrated that this process is more environmentally friendly. Consequently, the pyrolysis of lignocellulosic biomass is receiving renewed interest as it has the potential to become a viable option for transforming a great variety of waste materials such as industrial, agricultural, and forestry residues into value-added products in a profitable and decentralized manner [1, 6, 7]. Interestingly, the development of small-scale production units capable of efficiently processing a few tons of biomass per day could reduce the costs associated with handling and transporting biomass to the end user. In a pyrolysis process, the biomass is treated in a non-oxidizing atmosphere, usually at temperatures between 400 °C and 700 °C [4, 8]. As a result, three fractions are obtained: a solid fraction, also called biochar; a gas fraction, and a liquid fraction, also called bio-oil [3, 9, 10]. A general schematic of the pyrolysis mechanism involving the different endothermic and exothermic reactions of its main structural components (cellulose, hemicellulose, and lignin) using grape seed as biomass is shown in Fig. 2.1.

The origin of the lignocellulosic biomass strongly determines its characteristics and composition, and in turn, its behavior under pyrolysis conditions. Structurally, the basic composition of biomass is 25–50% cellulose, 15–40% hemicellulose, 10–40% lignin, 0–15% extractives, and a small fraction of inorganic minerals [11]. The relationship between the organic and inorganic components of the biomass depends on the environment in which it develops and the time at which it is harvested. These main components of biomass can be seen in Fig. 2.1.

It should be also noted that the physicochemical properties of the biomass (fixed carbon, volatile matter, moisture, and ash content), the type of reactor and its operating conditions (temperature, pressure, gas and vapor residence time, and heating rate) would also be factors that strongly influence product distribution [8, 12] after pyrolysis. Accordingly, ultimate and proximate analyses are common methods used to study biomass composition for further thermal processing. An example of the composition of two representative lignocellulosic biomasses (derived from forestry residues and agricultural residues) can be seen in Table 2.1. Volatile

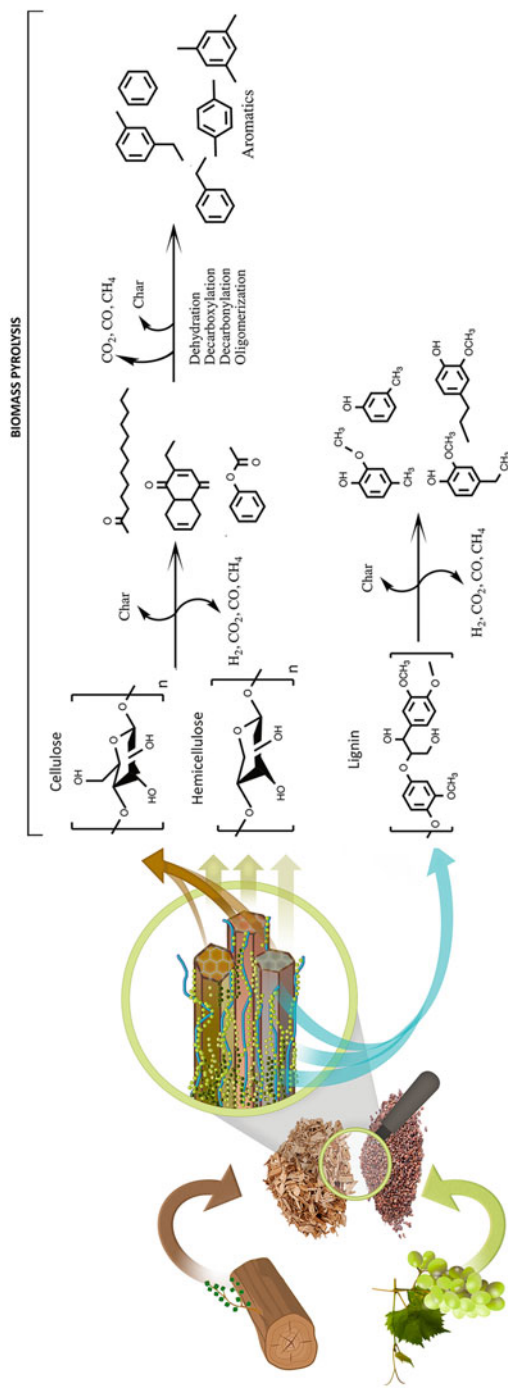


Fig. 2.1 Schematic of biomass pyrolysis

Table 2.1 Characterization of GS (grape seeds), Pine, PS (polystyrene), PP (polypropylene), HDPE (high density polyethylene), PET (polyethylene terephthalate), PLA (polylactic acid), and WT (waste tire) by ultimate and proximate analyses. All these samples came from waste sources (e.g., polystyrene from food packaging and polyethylene terephthalate from waste liquid containers) and were determined following standard methods

Properties	GS ^a	Pine ^a	PS ^a	PP ^a	HDPE ^a	PET ^a	PLA ^a	WT ^a
Proximate analysis (wt%)								
Moisture	6.3	6.3	0.5	0.2	0.1	0.4	0.4	1.1
Ash	4.6	0.5	0.1	0.1	0.0	0.1	0.0	3.8
Volatile matter	69.5	84.5	97.7	99.8	100.0	89.2	99.3	63.6
Fixed carbon	25.9	15.0	0.5	0.00	0.0	10.3	0.3	31.8
Ultimate analysis (wt%)								
C	57.6	52.5	90.3	85.4	85.5	62.7	51.1	87.9
H ^b	6.3	6.3	9.1	14.5	14.5	4.4	5.8	7.4
N	2.5	0.1	0.3	0.0	0.0	0.0	0.0	0.3
S	0.2	0.0	0.0	0.0	0.0	0.0	0.0	1.1
O ^c	33.4	41.2	0.3	0.0	0.0	32.8	44.0	3.3
HHV (MJ/kg)	23.5	20.6	42.1	43.1	43.1	22.2	17.2	38.6

Analyses performed at Instituto de Carboquímica

HHV Higher heating value

^a Air-dried basis

^b Hydrogen of moisture are contained

^c Calculated by difference

matter is the fraction that is released as condensable and non-condensable organic compounds under pyrolysis conditions. Moisture is associated with the presence of physically and chemically bound water. The amount of moisture is a parameter that must be controlled since is closely related to the final quality of the bio-oil (values lower than 10 wt% are commonly considered acceptable for pyrolysis processes). Therefore, drying units should be integrated into pyrolysis installations, which increases the energy requirements of the full process. Ash is the inorganic residue resulting from the complete combustion of the biomass, which mainly comprises Na, K, Ca, Mg, Si, and Fe. It should be noted that ashes can affect the pyrolysis process and product distribution, given that this inorganic matter can act as a catalyst to reduce the liquid yield [12]. Finally, fixed carbon is the organic matter that remains after the moisture and volatile matter from the biomass have been devolatilized [13], becoming the predominant component of the solid product.

In relation to pyrolysis conditions, a very important variable in the pyrolysis process is temperature. The highest liquid yields are normally obtained in the range of 400–600 °C. Above 600 °C, the liquid yield decreases because bio-oil is converted into gas by secondary cracking reactions. Additionally, temperatures higher than 700 °C further decrease the yield in liquid products since formation of heavy polycyclic aromatic hydrocarbons (tars), which are deposited on the biochar surface, is also promoted as a result of both decarboxylation and dehydration reactions [3, 7, 8, 10]. Likewise, biomass particle size strongly influences heat

transfer rate, and therefore the distribution of final products. Large particles lead to the presence of a large thermal gradient in the particle, so that longer solids residence times are needed to complete the devolatilization of biomass. Additionally, a slower devolatilization rate is achieved, decreasing vapor residence time, and therefore promoting secondary reactions through the increased contact time between primary vapors and hot char [12, 14]. Consequently, the use of biomass with large particle size reduces liquid production. Related to this, the residence time of volatiles inside the reactor is another parameter of considerable importance in a pyrolytic reaction. This parameter depends on the inert gas flow used to perform the pyrolysis process. A low inert gas flow leads to lower liquid yields caused by the promotion of cracking and retrogressive reactions, which increase the amount of both light gases and tars. Similarly, an increase in gas pressure could also lead to lower liquid yields since an increase occurs in the concentration of volatiles inside the reactor, favoring the presence of secondary reactions. A final key parameter in any pyrolysis process is heating rate. As in the case of large biomass particles, low heating rates increase the contact time between primary vapors and hot char, promoting secondary reactions and therefore leading to lower liquid yields. Both vapor residence time and heating rate also depend on the reactor design and will define the type of pyrolysis process. Generally, pyrolysis can be classified into three different types, referred to as slow pyrolysis, fast pyrolysis, and flash pyrolysis processes. The choice of the preferable option depends on the required product. Slow pyrolysis is focused on maximizing the solid product, whereas fast pyrolysis and flash pyrolysis maximize the liquid fraction, as can be seen in Table 2.2. At this point, it should be also highlighted that the liquids obtained from slow pyrolysis and fast/flash pyrolysis are remarkably different and cannot be processed in the same manner. For this reason, fast pyrolysis and bio-oil are carefully defined in standard specifications (ASTM D7544–12 (2017)).

The pyrolysis process has been studied in different types of reactors. At lower scales (TRL (technology readiness level) 2), the most widely used reactors are the thermogravimetric analyzer and the analytical pyrolyzer coupled with gas chromatography mass spectrometry (GC/MS) [16, 17]. At laboratory-scale (TRLs 3 and 4) the most prevalent are fixed-bed, autoclave, ablative, microwave, and entrained flow reactors. At higher scales, pilot plant or commercial plants, fluidized bed (circulating and bubbling), spouted bed, rotating cone, and auger reactors (single and twin) are the most prominent [7, 18]. In particular, fluidized bed, rotating cone, and auger

Table 2.2 Types of pyrolysis [3, 15]

	Slow	Fast	Flash
Yield	For biochar production. Low liquid yields (~30–35 wt%)	Liquid is the majority product (~50 wt%)	Higher liquid yields (up to 75 wt%)
Heating rate	0.1–1 °C/s	~100 °C/s	10–1000 °C/s
Residence time	>30 min	<2 s	>0.5 s
Temperature	300–700 °C	400–650 °C	800–1000 °C

reactors have the greatest commercial potential due to their robustness and attractiveness on the market [4]. Fluidized bed reactors have good temperature control and high heat transfer to biomass particles due to the high density of the solids [4]. However, biomass particles of small size are required for high heat transfer, necessitating additional pretreatment that significantly contributes to total operating costs. The system for operating rotating cone reactors can be considered similar, considering that the transport of sand and biomass is performed by means of centrifugal forces operating in a rotating cone. An advantage of their design is that intense mixing is possible without the use of an inert carrier gas, and the size of the equipment required downstream is minimal. On the other hand, auger reactors have a simple design, which allows their operation with low gas flows, and show high reproducibility and stability [19, 20]. A limiting factor for the scaling up the use of auger reactors is heat transfer owing to the use of external heating. Nevertheless, heating rates can be significantly improved by using sand, stainless steel beads, or even inexpensive minerals with catalytic properties, such as ilmenite, sepiolite, bentonite, attapulgite, calcite, and dolomite, as heat carrier materials [21, 22].

As previously explained, the pyrolysis of biomass produces three types of products: bio-oil, biochar and gas [3, 7]. The gas fraction has a low calorific value (8–9 MJ/m³) [23] because it is basically composed of H₂, CO, CO₂, and light hydrocarbons (e.g., methane (CH₄) and ethane (C₂H₆)). Although this fraction can be easily used for energy generation, its application is basically limited to meeting the energy requirements of the actual process. Biochar is essentially the fixed carbon and ashes (mineral fraction) derived from the biomass [3], although if the secondary mechanisms of pyrolysis (cracking and polymerization) were to take place, part of the volatile matter from the biomass would also contribute to increasing the char fraction. The char has a relatively high caloric value (~30 MJ/kg) [24, 25], which makes this product attractive for gasification and combustion applications, even replacing coal for the generation of electricity. This fraction has a heating value equivalent to that of coal, with the advantage that the SO_x and NO_x emissions produced by its application as a fuel (by combustion) are lower than those produced by conventional mineral carbons [26]. In addition, its textural properties give it the potential for use as both as a natural fertilizer [27], contributing to fixed CO₂, and as a precursor for activated carbons [28]. At the commercial scale, its most common use is to supply the energy required by the pyrolysis process. Finally, bio-oil is considered the most valuable product as it can be used as a fuel or as precursor for chemicals. The bio-oils obtained from fast pyrolysis processes are dark brown, corrosive liquids that consist of polar organic compounds (ca. 75–80 wt%) and water (ca. 15–30 wt%). The chemical composition of bio-oils is very complex as they are made up of a mixture of more than 400 compounds, including carboxylic acids, alcohols, aldehydes, esters, ketones and aromatic species, certain polymeric carbohydrates, and lignin-derivative compounds. In addition, lignocellulosic biomass-derived bio-oils usually have a high H₂O content (15–30 wt%) and high density (in the range of 1.15–1.25 kg/m³), and they may contain some solids in the form of fine char particles and ash (in the range of 0.1–1 wt%). Bio-oils have a high oxygen content (35–40 wt%), which, together with its acidity, (pH 2.5–3.5)

makes it corrosive and also accelerates its degradation (increased viscosity) by polymerization and oligomerization reactions, leading to difficulties during storage and transport [11]. Furthermore, its higher heating value (~15–20 MJ/kg) is generally less than half of that of mineral oils (~40 MJ/kg) [3, 29, 30] and, unfortunately, bio-oils and mineral oils are not miscible.

The point should be made at this stage that the application of bio-oils is basically limited to the substitution of heavy fuel oils in boilers [29, 31, 32]. It is of note, however, that very interesting research is underway focusing on long-duration experiments and accurate analytical test methods to allow the standardization of fast pyrolysis bio-oils as a fuel, paving the way towards the future marketing of this product. Nonetheless, the poor properties shown by bio-oil as a fuel and all the negative issues associated with its use have led to the conclusion that bio-oil quality should be improved by different upgrading strategies before it can be efficiently used as a transportation fuel or source of high-value chemical products. For this reason, a number of promising strategies have been postulated in recent decades to improve bio-oil properties. These upgrading strategies are generally based on physical treatments (such as the removal of light volatiles with acids, solvent addition, fractionation, and filtration of hot vapors) and chemical treatments (such as esterification, catalytic pyrolysis and co-pyrolysis, and co-processing of bio-oil in fluid catalytic cracking facilities). In general, chemical upgrading methods can be divided in two groups [15, 33, 34]: (i) ex situ (those produced after the pyrolysis process, where there is no contact between the biomass and catalyst), and (ii) in situ (those produced during the pyrolysis process itself, where the biomass and catalysts are in contact). Both strategies can be adapted to existing pyrolysis systems [11, 32, 34, 35]. Within the ex-situ strategies, we would highlight high pressure hydrodeoxygenation (HDO) [10, 36] and catalytic cracking (CC) [10, 36]. HDO is a complicated process that requires complex equipment, a high-performance catalyst, and pressurized H₂. This route leads to the partial deoxygenation of the bio-oil by the elimination of water molecules and the CO₂ generated by C–O bond breakage [12]. On the other hand, CC is a process in which high-molecular-weight molecules are broken down into low-molecular weight molecules, with the removal of the oxygen in the bio-oil components, such as water, CO, and CO₂. This upgrading process is usually performed in either fixed or fluidized bed reactors, and it also makes use of high-performance catalysts (usually tailor-made zeolites) [10]. This CC is based on the fluid catalytic cracking (FCC) process designed for the oil refining industry, which is an essential part of the refining process, transforming heavy crude oil into light compounds, including liquefied petroleum gas (LPG) and transportation fuels. In the FCC process, specific zeolite-based catalysts have demonstrated to be highly efficient. Unfortunately, FCC catalysts have shown a limited performance for the ex situ upgrading of bio-oils, mainly due to their fast deactivation and limited regeneration. Therefore, new tailor-made catalysts should be developed for bio-oil upgrading purposes [37, 38].

In-situ strategies require lower capital investment and offer better technical benefits than ex-situ ones, given that higher efficiencies can be achieved. The most popular in-situ upgrading strategy is catalytic pyrolysis, where the biomass

devolatilization process is performed in the presence of a catalyst [15, 32, 34]. A lower quantity of liquid product (~50 wt%) is usually obtained in a catalytic pyrolysis process, but a good choice of catalyst allows improved bio-oils to be obtained. A pyrolytic liquid obtained by catalytic upgrading usually has two differentiated phases: an aqueous phase, which comprises mainly water, polysaccharides, organic acids, hydroxyacetone, hydroxyacetaldehyde, furfural, and small amounts of guaiacols [39]; and an organic phase, which comprises oxygenated compounds (organic acids, aldehydes, ketones, alcohols, esters, furans, sugar derivatives, and phenols, among others) [28, 29] and aliphatic and aromatic hydrocarbons [40]. These two phases are easily separable, thus enabling valuable products to be obtained from both phases and the economy of the process to be improved. As an example, different industrial chemicals, including acids, levoglucosan, hydroxyacetaldehyde, and furfural, can be recovered by solvent extraction of the water phase. Moreover, catalytic steam reforming of the aqueous fraction is also considered a potential route for renewable H₂ production. As the different routes for application of the aqueous phase are not the aim of this work, more information can be found in the following references [41–43]. On the other hand, the organic phase could be used as a low-quality biofuel for boilers or as source of chemical products. However, as in the case of raw bio-oils from conventional fast pyrolysis processes, a significant amount of oxygenated compounds remain and cause many of its negative properties, such as low heating value, high corrosiveness, high viscosity, and instability. All these issues greatly limit its further application, particularly as a transportation fuel. Therefore, the introduction of further improvement processes is strongly advised.

The catalytic pyrolysis process is not only affected by the same factors that condition fast pyrolysis (reaction temperature, gas and solids residence time, heating rate, physicochemical properties of the biomass, type of reactor) but also by those of biomass-to-catalyst ratio and type of catalyst, which should be selected following certain guidelines [44]: high activity in the production of non-oxygenated compounds; resistance to deactivation due to coking, sintering, or fouling; stability and reusability; mechanical strength; low cost; and wide availability. As a result, current research is focused on the search for new catalysts that are able to meet these criteria. Despite this, the most widely studied catalysts for this process are zeolites, which are costly materials that present an important problem of deactivation resulting from coke deposition in the active sites [45]. Although a thermal regeneration of the zeolites can be postulated by ex-situ calcination together with biochar, as already performed in FCC processes, deactivation by ash deposition (from the inorganic content of biomass), in addition to their hydrothermal instability at high temperature, prevents the feasible regeneration of their catalytic properties. An interesting alternative to the use of zeolites could be readily available natural minerals or commercially available metal oxides. This line of research has studied different types of low-cost materials with relative success, including the use of different metal oxides, such as MgO, ZnO, NiO, Fe₂O₃, and TiO₂ [46–50], and different low-cost minerals, such as sepiolite, bentonite, attapulgite, ilmenite, calcite, and dolomite [22, 51–53]. While acid catalysts, such as bentonite, promote bio-oil deoxygenation

and aromatization through the Diels–Alder reaction and hydrocarbon pool mechanism, basic catalysts, such as MgO, calcite, and dolomite, can promote bio-oil deoxygenation through ketonization, aldol condensation, and hydrogen transfer reactions, thus minimizing acidity while enhancing light hydrocarbon components. In summary, the use of low-cost materials has also demonstrated notable improvements in the physicochemical properties of the organic fraction resulting in a bio-oil with lower acidity, lower O₂ content, and increased higher heating value, proving the potential of this type of materials. Finally, it should be added that the biomass-to-catalyst ratio is another important factor in a catalytic pyrolysis process because optimum contact between both materials must be ensured. While a high biomass-to-catalyst ratio could promote excessive cracking reactions that lead to the formation of heavy polycyclic aromatic compounds, an insufficient biomass-to-catalyst ratio would hardly improve the quality of the liquids [48, 50, 51].

Another in-situ upgrading strategy that has been receiving special attention in recent decades is the incorporation of oxygen-free materials, such as waste polymers, into the biomass pyrolysis process. It is well known that the demand for polymers is increasing every year owing to their use in different applications, such as toys, cars, packaging, electronics, and a wide variety of others. This demand has also led to an increase in the amount of waste leftover from these applications. Plastic waste consists mainly of high-density polyethylene (HDPE), low-density polyethylene (LDPE), polyethylene terephthalate (PET), polypropylene (PP), polystyrene (PS), polyurethane (PUR), and polyvinyl chloride (PVC). The structures of the different polymer repeating units can be seen in Fig. 2.2. The utilization of these type of waste materials is of great interest, for example, about 17.8 million metric tons of end-of-life plastics were collected for treatment in Europe in 2018, of which 42% were recycled, 39.5% were used for energy recovery, and 18.5% ended up in landfills [54, 55]. This represents a huge environmental problem because of their non-degradable nature; their potential health risks to water, land, and animals; and their impact on environmental pollution. Furthermore, it has recently been reported that end-of-life plastics that are not recycled will be subject to higher taxes. In response to this problem, different solutions have been proposed for the management of plastic waste, such as incineration and mechanical recycling [56]. Because incineration negatively contributes to pollution through harmful and toxic emissions, other alternatives need to be developed. On the other hand, the main drawbacks of mechanical recycling are its high economic costs and the low quality of the final products when pure streams are not used, emphasizing the key role to be played by advanced pretreatment sorting and cleaning processes for efficient mechanical recycling.

The global challenges for sustainable development in relation to plastic waste management, clean energy, and efficient use of resources can be simultaneously addressed by the production of high-value liquids by the pyrolysis of polymer wastes. Unlike biofuels, these liquids can have fuel properties similar to those of fossil fuels, particularly for the pyrolysis of polyolefins [57], where the absence of oxygen, together with their high carbon and hydrogen content, does away with the need for further improvement processes [58]. Compared to lignocellulosic biomass,

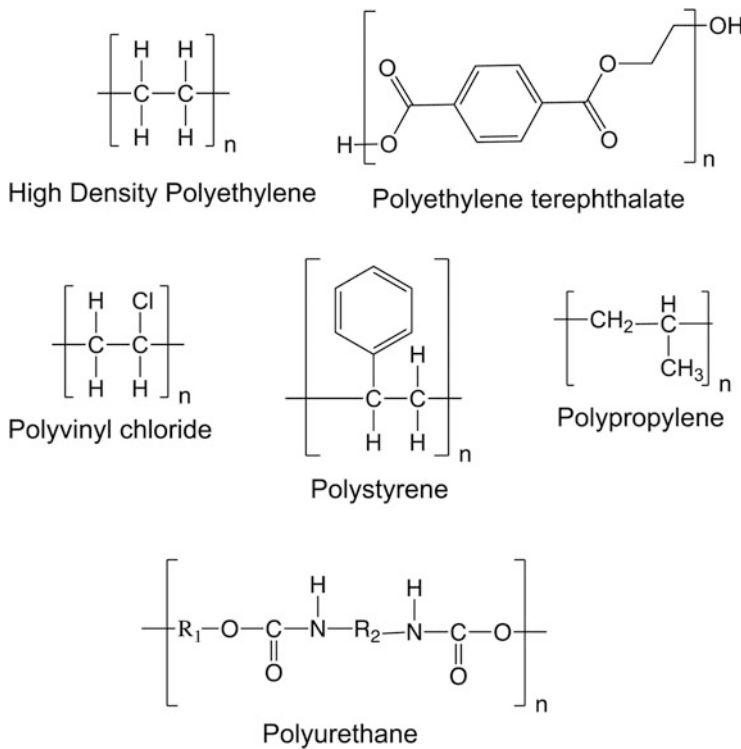


Fig. 2.2 Structures of the different polymer repeating units

see Table 2.1, the oxygen content in waste polymer materials can be considered negligible, with the exception of PET and biopolymers such as PLA. Additionally, synthetic waste polymers present a higher content in carbon (60–90 wt%) and hydrogen (4.5–14.5 wt%), achieving higher heating values (40 MJ/kg). Again as an exception, PLA and PET have a chemical composition similar to that of biomass. Therefore, there is potential to produce high-quality liquid oils with high calorific value and rich in compounds compatible with standard fuels by the pyrolysis of these polymers [57, 58]. In a similar way to biomass pyrolysis, waste plastics are heat-treated at temperatures ranging between 500 °C and 700 °C [59]. During the pyrolysis of waste plastics, devolatilization takes place through radical mechanisms (initiation, propagation, and termination), leading to a high liquid yield (higher than 80 wt% for PS and polyolefins). Obviously, catalytic pyrolysis processes have been also studied for waste polymers, for which zeolites are again the most commonly used catalysts. Under these pyrolysis conditions, higher yields to aromatic-rich oils are usually obtained, likely related to the fact that zeolites significantly promote the cracking of large aliphatic and olefin molecules and their further aromatization [60].

At this point, we would like to remark that liquids obtained from the pyrolysis of biomass and waste plastic are completely immiscible owing to their different polarity

(polar for biomass and nonpolar for polymer). Therefore, a simple blending strategy for the upgrading of bio-oil characteristics is not viable. However, a co-pyrolysis strategy for the formation of a new, upgraded bio-oil through the interaction of the radicals released by both feedstocks does seem to be a potential solution and can be seen as a promising in-situ upgrading approach to enhance both the efficiency of the process and the properties of bio-oil as fuel. At the same time, the addition of waste plastics to biomass pyrolysis processes would also not only contribute to mitigate their accumulation in the marine environment, or even in landfills, where they are a source of greenhouse gas emissions [10], but could also contribute to reducing processing costs and solve problems related to biomass availability. Interestingly, this initial hypothesis has been already demonstrated in several studies [61–63] that show the co-feeding of plastic wastes with biomass significantly improve the quality of pyrolytic oils. Bio-oil upgrading using this strategy was reflected in the formation of an organic fraction with improved properties (lower oxygen content and higher in value-added compounds, mainly cyclic hydrocarbons and aromatics) and a higher calorific value [57]. The upgrading mechanism was associated with the fact that waste plastics could act as hydrogen donors to enhance hydrodeoxygenation and hydrocracking reactions [61–63]. Accordingly, Brebu et al. [64] found that the addition of PS, LDPE, and PP to the pyrolysis of pine sawdust (1:1 weight ratio) in a fixed bed reactor at 500 °C produced a higher amount of bio-oil with lower oxygen content and a remarkable higher calorific value. Suriapparao et al. [65] recently studied the addition of PS to five different types of biomass (peanut shells, bagasse, rice husk, *Prosopis juliflora*, and mixed wood sawdust) in a microwave reactor. They found that a co-pyrolysis approach led to higher yields of an aromatic-rich bio-oil with a high calorific value (38–42 MJ /kg⁻¹), particularly when using sawdust and rice husk. They also found that bio-oil viscosity was remarkably lower than that obtained by the conventional fast pyrolysis of biomass. Finally, Akancha et al. [66] investigated the co-pyrolysis of rice bran wax and PP in a semi-batch reactor. They also found that not only higher liquid yields were obtained (using a 1:3 blend of PP and biomass) but also higher aliphatic compounds were found in the final liquid, thus improving its quality. Although different mixtures have been successfully studied in co-pyrolysis processes, as can be seen in Table 2.3, the selection of feedstock components is also an important factor as both raw materials should be devolatilized in the same temperature range under process conditions [10]. Further tools for the proper selection of feedstock components in a catalytic co-pyrolysis process will be provided in this chapter.

As could be expected, the use of a reasonable ratio of both feedstocks also plays a crucial role in the catalytic co-pyrolysis process from the sustainability and technical perspectives [67, 68], meaning that it is another parameter to be optimized. As an example of the importance of the biomass-to-plastic waste ratio, Stančin et al. [68] observed that although a high sawdust-to-PS ratio (25/75 wt%) led to higher liquid yields, these conditions generated a larger amount of polycyclic aromatic hydrocarbons (PAHs) [68]. These compounds are considered hazardous to health and harmful to the environment, thus limiting further bio-oil applications. Likewise, special attention should be paid to the use of high proportions of polymers with a significant

Table 2.3 Some representative studies of biomass/plastics co-pyrolysis

Biomass	Polymer	Biomass/polymer ratio	T (°C)	Scale	Reactor	Reference
Pine woodchips	WT	90/10 80/20	500	Laboratory Demonstration	Fixed bed Auger	[67]
Sawdust	PS	75/25 50/50 25/75	600	Laboratory	Stainless steel fixed reactor	[68]
Palm shells	PS	50/50	500	Laboratory	Fixed bed	[70]
Karanja and niger seeds	PS	50/50	500	Laboratory	Stainless steel semi-batch operation	[62]
Palm shells	Truck tires	25/75	500	Laboratory	Fixed bed	[63]

content in certain heteroatoms (e.g., sulfur and chlorine), since their thermal decomposition could lead to the formation of compounds that pose a risk to human health (dioxins formation from PVC pyrolysis) [69]. Therefore, although the quality of bio-oil could be remarkably improved by co-pyrolysis, there are still some crucial points to be resolved.

Against this background, a dual upgrading strategy involving the simultaneous incorporation of catalyst and waste plastics into the biomass pyrolysis process has recently emerged as a very promising approach for the production of upgraded bio-oils in a relatively simple one-step process, enabling some of the previously described problems observed in the conventional fast pyrolysis, catalytic pyrolysis, and co-pyrolysis processes to be solved. This statement is supported by the increasing number of articles regarding this process published in the last 10 years, as shown in Fig. 2.3, in which catalytic co-pyrolysis processes for the production of high-quality biofuels have been widely studied. The following sections of this chapter will present a critical overview of the field of the catalytic co-pyrolysis of biomass with waste polymers in facilities ranging from bench and laboratory scale (thermogravimetric analysis and lab-scale reactors) to pilot scale, providing insights into the potential of this technology for the production of high quality bio-oils in a single-stage process. We will show, with some representative examples carried out in our research group, how a proper selection of process conditions and feedstocks could facilitate the direct integration of catalytic co-pyrolysis bio-oils in the energy market as drop-in fuels. The use of drop-in fuels would increase the potential market for this product as a fuel that is fully interchangeable and compatible with conventional fossil fuels. This is advantageous because no costly adaptation of the fuel distribution network would be required.

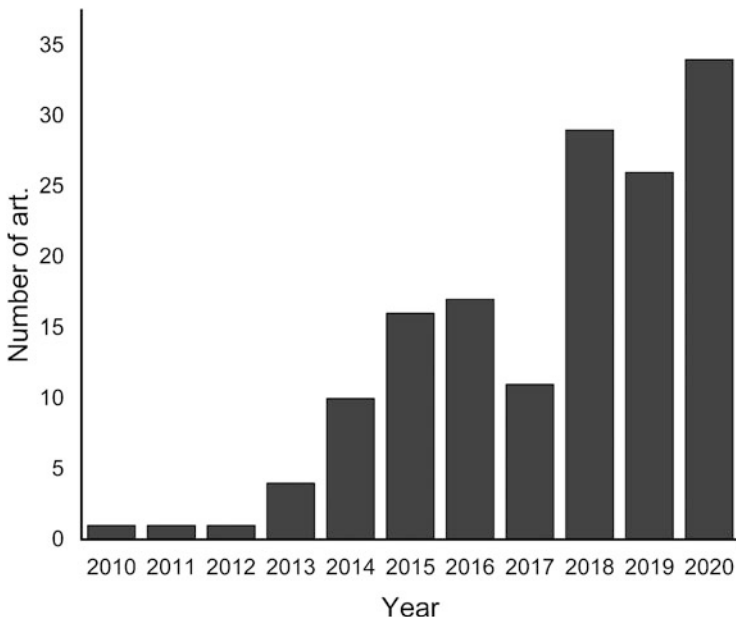


Fig. 2.3 Evolution of the number of articles on catalytic co-pyrolysis in the last 10 years. Articles found in Scopus using the keywords “catalytic co-pyrolysis biomass”

2.2 Recent Advances in the Catalytic Co-Pyrolysis Process

The potential of catalytic co-pyrolysis processes for the production of high-quality bio-oils has been addressed by several authors. It is generally accepted that the main process parameters, such as temperature, heating rate, and gas and vapor residence time, together with the selection of an optimum ratio between biomass, waste polymer and catalyst, are crucial and must be carefully studied from laboratory scale to pilot plant facilities, paving the way toward the development of commercial catalytic co-pyrolysis processes. In accordance, this overview has been divided into three different sections, depending on the technology readiness level (TRL) used [71–73], hopefully providing the reader with the appropriate tools for the development of catalytic co-pyrolysis processes able to produce high-quality bio-oils.

2.2.1 TRL 2: Bench-Scale Experiments in Microreactors

A useful tool for analyzing the first insights at TRL 2 of any catalytic co-pyrolysis process is thermogravimetric analysis (TGA), which is an effective study to identify the potential of any biomass/waste plastic/catalyst mixture. It should be pointed out,

that although this technique is limited to micro scales, it is a simple, inexpensive, and effective way to obtain useful data regarding the potential of the process. Accordingly, numerous research groups have conducted TGA studies to determine the thermal behavior of different materials, such as biomass, plastic wastes, and their mixtures [16, 74–76]. This characterization technique determines the percentage of mass loss of any material during heating and, in turn, its behavior during the pyrolysis (devolatilization) process. Additionally, TGA is a very useful system to determine the pyrolysis kinetic parameters under isothermal and non-isothermal conditions. It is interesting to highlight that the TGA of lignocellulosic biomass generally shows two ranges of decomposition that are linked with their main constituents: 150–350 °C for the decomposition of cellulose and hemicellulose, and 250–500 °C for lignin decomposition. However, this technique may present several limitations when using heterogeneous samples such as municipal solid waste [77], which contains numerous components including cellulose, hemicellulose, lignin, PE, PP, PVC, and PET, whose correct identification can be limited due to the overlapping of the devolatilization curves. As a guideline, however, it can be considered that in the form of individual components, cellulose degrades at the temperature range of 260–400 °C, lignin at 150–750 °C, PVC at 250–550 °C [77], PP at 400–500 °C [77], PET at 375–500 °C [77], PE at 450–550 °C [77], PLA at 315–375 °C [78], PS at 300–500 °C [79], and WT at 450–550 °C [80]. Interestingly, devolatilization profiles of the isolated components show that there is an operational window where some of these feedstocks are simultaneously devolatilized, and their devolatilization could therefore lead to interactions between the released compounds under co-pyrolysis conditions.

In line with this, as can be seen in Fig. 2.4, the first insights obtained by our group [81] using TGA studies applied to individual compounds already evidenced that the devolatilization of lignocellulosic biomass and waste polymers, such as HDPE, PP,

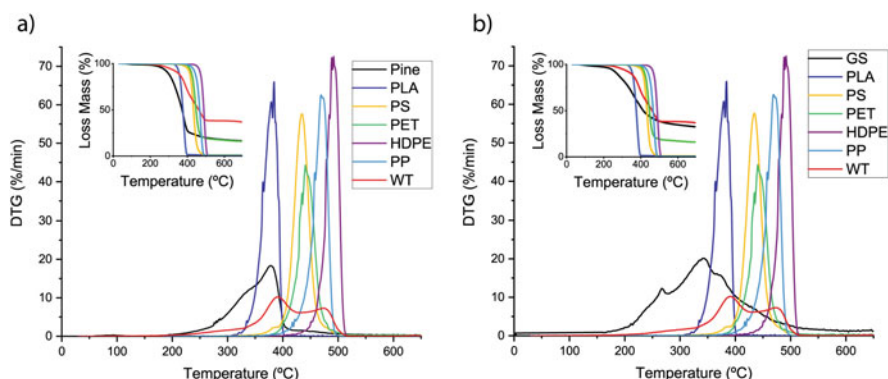


Fig. 2.4 Experimental TGA (insets) and derivative thermogravimetry (DTG) curves at 20 °C/min heating rate for (a) pine wood and plastic wastes (PLA (polylactic acid), PS (polystyrene), PET (polyethylene terephthalate), PP (polypropylene), HDPE (high-density polyethylene), WT (waste tire)), (b) grape seeds (GS) and plastic wastes

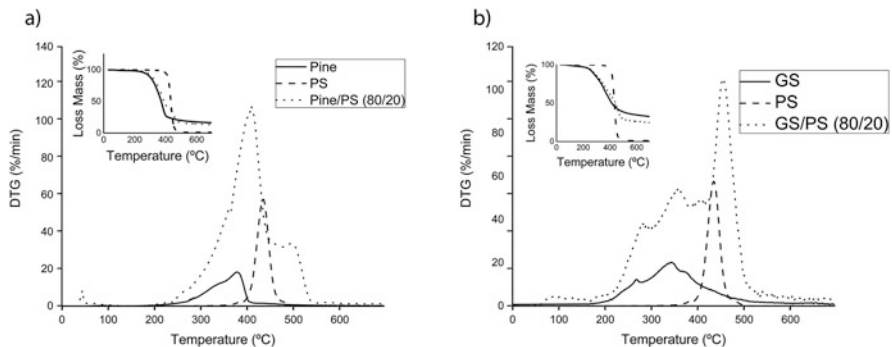


Fig. 2.5 TGA and DTG curves at 20 °C/min heating rate during co-pyrolysis of: (a) pine/PS (80/20), (b) TGA and DTG of co-pyrolysis of GS/PS (80/20)

PET, PS, PLA and WT, partially coincide within a common temperature range, and therefore potential interactions between the radicals released during the pyrolysis process could be taking place [16]. However, while a broad operational window is observed in the case of some waste plastics, such as WT, PLA, and PS, this zone is quite limited in the case of PET and polyolefins (Fig. 2.4). Very interesting results were found when experimental TGA profiles of lignocellulosic biomass/PS mixtures (Fig. 2.5) were compared to calculated profiles obtained from the sum of the individual components. Thus, it was observed that while the devolatilization of the biomass component in the mixture is highly comparable to that predicted by the individual samples, a slower decomposition rate was clearly observed for PS devolatilization, which seems to be related to the presence of biomass char preventing PS depolymerization while promoting intermolecular hydrogen-transfer reactions. Additionally, it was observed that a temperature about 600 °C could be adequate to achieve the full conversion of both feedstocks.

The co-pyrolysis of biomass with polymer-type residues using TGA has been also studied by other authors [62, 79, 80]. In line with our results, Hameed et al. [82] studied the thermal behavior of biomass and different feedstocks such as sludge, coal, and plastics. They also demonstrated that the presence of a common area where volatiles could coexist, eventually leading to interactions between the radicals released from these materials. Furthermore, Akancha et al. determined optimal reaction parameters by TGA in order to obtain maximum conversion in the co-pyrolysis of rice bran and PP [66]. Different reaction parameters were studied, such as temperature, heating rate, and the proportion of each material in the mixture, concluding that 550 °C and a biomass-to-waste plastic ratio of 1:3 were the optimum pyrolysis process conditions. Similarly, Alam et al. [83] studied the devolatilization of sawdust bamboo and LDPE. Significantly, they proposed that there could be radical interactions between those volatiles released from both feedstocks, and that the interactions would be enhanced at high waste plastic-to-biomass ratios. While cellulose and hemicellulose devolatilization was not significantly modified by the

presence of LDPE, it was observed that the radicals released during LDPE devolatilization could boost lignin decomposition at temperatures ranging between 380 °C and 520 °C. Finally, Önal et al. [84] also used TGA to define the optimum temperature for the co-pyrolysis of almond shells and HDPE, ensuring the full conversion of both feedstocks at 550 °C.

The downside of all those interesting works on TGA is that they were only able to provide data on devolatilization under slow or moderate pyrolysis conditions because heating rates higher than 200 °C/min are not feasible. Interestingly, this issue could be solved by applying a kinetic model to the TGA data. Kinetic parameters, such as activation energy (E_a) and the pre-exponential factor (A), can be obtained by means of different fitting models, including the one-step global model based on the model-fitting method, global model based on the model-free method, multi-step successive model, semi-global model, distribution activation energy model (DAEM), and molecular modeling [85]. Although kinetic modeling is beyond the scope of this chapter, detailed literature can be found in the following references [85–92]. Among them, DAEM is the most widely used method to determine the kinetics of the pyrolysis process as a first stage leading to the design of the pyrolysis reactor. In this regard, very interesting results were reported by our research group [81] when conducting a kinetic study of the co-pyrolysis of lignocellulosic and different polymer wastes. In particular, forestry (pine woodchips) and agricultural (grape seeds) residues were selected as lignocellulosic biomass samples. Additionally, six different polymers were introduced into the feed for their further analysis (PLA, PS, PET, PP, HDPE and WT). It was interesting to observe that a higher process temperature than that initially foreseen from the experimental TGA data (100 °C/min) should be used to ensure the full conversion of both feedstocks under realistic fast pyrolysis conditions (1000 °C/min). Therefore, it can be concluded that DAEM could be a very useful tool to predict the behavior of biomass/waste plastic mixtures under true fast co-pyrolysis process conditions, which cannot be experimentally obtained by TGA.

TGA was also used to identify the role of different catalysts in the devolatilization of single biomass [93–95] and plastic wastes, as a further step toward the study of biomass/waste plastic/catalyst mixtures [96, 97]. An interesting example of the biomass catalytic pyrolysis using TGA was shown by Nishu et al. [95], who studied the catalytic pyrolysis of cellulose extracted from rice straw using alkali-modified zeolite as the catalyst. The biomass-to-catalyst ratio used was 1:4. Remarkably, the use of catalysts slightly decreased the temperature needed for the full devolatilization of the rice straw. Along similar lines, Lei et al. [93] studied the thermal decomposition of cellulose in the presence of nickel dispersed on HZSM-5 zeolite. They concluded that the presence of nickel also reduced cellulose devolatilization temperature. However, they observed that the devolatilization rate was slowed down by the formation of coke on the catalyst surface. On the other hand, the catalytic pyrolysis of waste plastics was studied by Durmuş et al. [96], who studied the thermal decomposition of PP using Beta, Mordenite, and ZSM-5 zeolites as catalysts. As was found for cellulose, they demonstrated that the presence of zeolite in the process also decreased the temperature for PP devolatilization and that there was

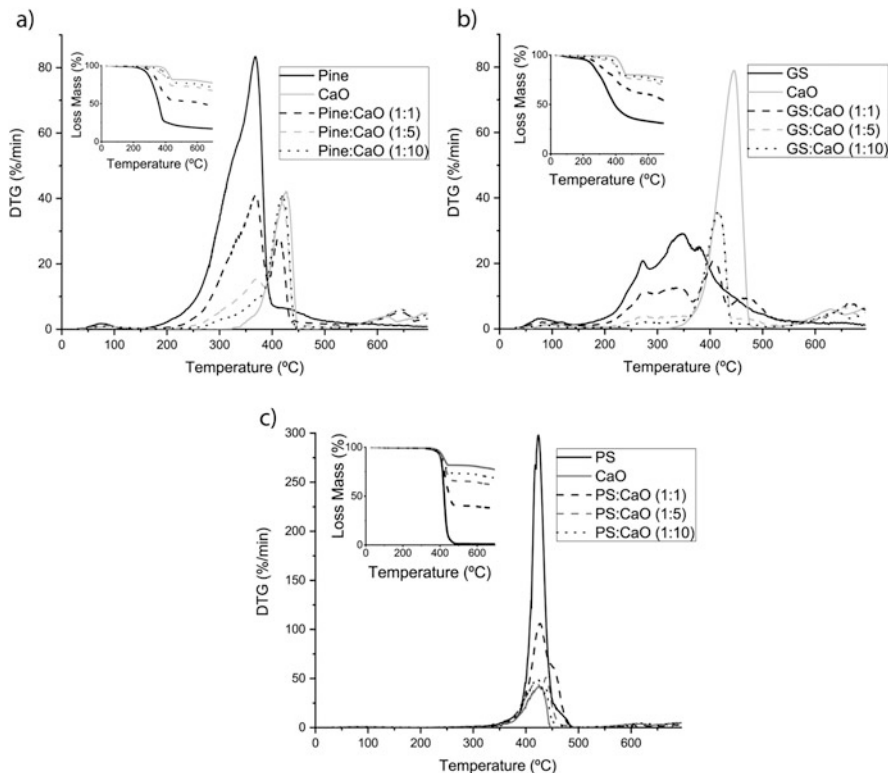


Fig. 2.6 TGA and DTG curves showing the effect of the catalyst amount on the catalytic pyrolysis of: (a) pine woodchips, (b) GS, (c) PS

a lower loss of mass resulting from the accumulation of coke on the surface and in the pores of the zeolites. Similarly, our research group studied the effect of CaO addition on the devolatilization of both lignocellulosic biomass and waste plastics. In this case, grape seeds and pine woodchips were selected as biomass representatives, while PS was chosen as the candidate for plastic waste. Fig. 2.6 shows the TGA and derivative thermogravimetric (DTG) curves. It can be observed that the dehydration and decarboxylation reactions of the biomass volatiles seem to have been promoted by CaO at temperatures higher than 350 °C. Interestingly, the catalytic role of CaO was not limited to these deoxygenation reactions since it was also observed that CaO could be also promoting the cracking of intermediate liquid tar to produce gas at high temperature, given that a decomposition rate higher than that theoretically expected is obtained at 400–450 °C and 450–550 °C for the pine woodchips and GS, respectively. As expected, both reactions were enhanced at a higher catalyst-to-biomass ratio. It is worth mentioning that catalyst-to-biomass ratio is a key parameter that also needs to be carefully evaluated at a higher TRL since an overbalanced cracking of the volatiles could lead to the formation of heavy tars and light gases instead of upgraded bio-oil. With this premise, we also performed TGA on PS/CaO

mixtures. We observed that CaO leads to a slight decrease in the PS decomposition rate, likely related to the addition of CaO promoting intermolecular hydrogen transfer reactions instead of supporting the PS depolymerization process through intramolecular hydrogen-transfer reactions.

Once the role of the different agents in the catalytic co-pyrolysis process was identified, the performance of biomass/waste plastic/catalyst mixtures could be studied by TGA. We would like to point out that the amount of data published in the literature is somewhat limited, although there are several works of interest to be found. As an example, Kim Y. M. et al. [98] studied two types of catalysts (microporous (HZSM-5) and mesoporous (Al-MCM-41)) in the catalytic co-pyrolysis of yellow poplar and HDPE. They showed that a large quantity of HZSM-5 catalyst (10/1) significantly reduced the temperature of HDPE decomposition so that yellow poplar and HDPE devolatilization overlapped at the range of 350–450 °C, whereas their simultaneous decomposition could not be observed without the catalyst. Similar results were found by Zhang et al. [75] for the catalytic co-pyrolysis of Douglas fir sawdust and LDPE using ZSM-5 as catalyst. These authors also observed that the addition of catalyst decreased the decomposition temperature of the biomass/plastic mixture, shifting the peak corresponding to LDPE devolatilization to lower temperatures [99]. Likewise, we recently studied the thermal devolatilization of different biomass/waste plastic mixtures using CaO as catalyst, where both pine woodchips or grape seeds were selected as lignocellulosic biomass samples and PS as waste plastic, the results of which can be found in Fig. 2.7. Regardless of the biomass/waste plastic mixture, TGA data showed that the addition of CaO only changed the devolatilization profile of those peaks related to biomass decomposition (either pine woodchips or grape seeds). At temperatures higher than 350 °C, CaO seemed to be promoting dehydration and decarboxylation reactions in the hemicellulose and cellulose components of the biomass. This effect was more apparent in the GS/PS/CaO mixtures. These results were in line with those found during biomass/CaO devolatilization, as previously mentioned. Nonetheless, it should be noted that there was only a marginal shift in the main peak to a lower

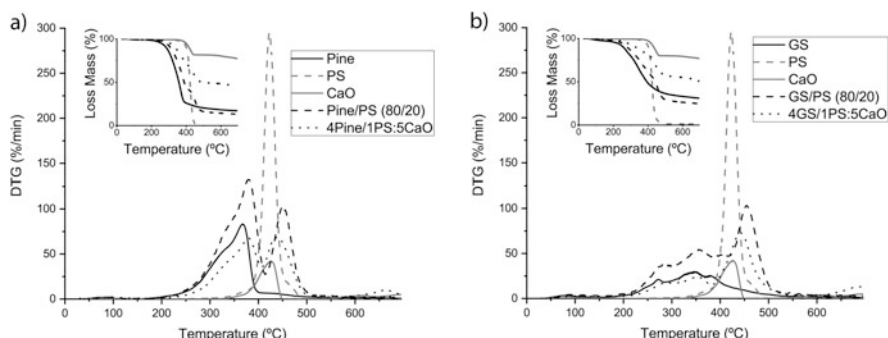


Fig. 2.7 Different catalytic co-pyrolysis experiments with: (a) pine/PS; (b) GS/PS CaO using the biomass/plastic-to-CaO ratio of 4/1:5

temperature, now involving both lignin and PS decomposition, likely pointing out that the tar cracking reactions previously observed for the devolatilization of biomass/CaO mixtures were not promoted under co-pyrolysis conditions. On the other hand, PS depolymerization seemed to be strongly affected by the presence of both CaO and biomass char, which may be explained by a significant decrease in the devolatilization rate observed at 450 °C, whereas a higher temperature is required for the full devolatilization of the PS component in the mixture. Again, it could be assumed that the presence of both CaO and biomass char could be promoting intermolecular hydrogen-transfer reactions instead of intramolecular ones, slowing down the PS depolymerization process while promoting interactions between the different volatiles in the mixture. This finding is quite important for the further design of a catalytic co-pyrolysis process involving a GS/PS/CaO mixture since it would require a higher temperature than that initially foreseen from the devolatilization of the individual components. Thus, it can be concluded that the use of TGA to study the depolymerization of biomass/waste plastic/catalyst mixtures should be established as a first step toward any scaling up of catalytic co-pyrolysis processes, given that the behavior of these complex mixtures cannot be extrapolated from the data obtained from the individual components.

Complementary to the use of TGA, analytical pyrolyzer coupled with gas chromatography mass spectrometry (GC/MS) allow information to be obtained on the composition of the volatiles. While this technique has been widely used for both the catalytic and fast pyrolysis of single biomass components [100–103], the number of works dealing with the catalytic co-pyrolysis of biomass/waste plastics is rather limited [16, 17]. An interesting example of this is the study by Sarker et al. [104], where a Pyroprobe-GC/MS was used to study the catalytic co-pyrolysis of poplar wood sawdust and HDPE using acid-modified ZSM-5 zeolites. A biomass/HDPE mixture (1:1) and a feedstock-to-catalyst ratio (1:1) were selected as experimental conditions. The catalyst was modified with an acidic solution (H_2SO_4) of different molarities (0.1, 0.3, 0.5, and 0.7 M). This treatment modified the amount and nature of the acidic sites and, in turn, the efficiency of the catalyst for the production of aromatic hydrocarbons. Interestingly, it was observed that catalytic co-pyrolysis with HDPE provided a higher relative olefin content than biomass catalytic pyrolysis, and the content of oxygenated compounds was significantly reduced, except for alcohols. The ZSM-5 sample treated with an acidic solution 0.5 M was the most selective catalyst for the formation of aromatic hydrocarbons. This behavior was linked to its higher content of Brønsted acidic sites. Another interesting example was reported by Xue et al. [105], who also used a Pyroprobe-GC/MS to assess the performance of MCM-41 silica for the catalytic co-pyrolysis of cellulose and PP mixtures. It was observed that the main products in the presence of catalyst were olefins and aromatics, whereas the main products without catalysts were oxygenated compounds. It can therefore be concluded that the use of an analytical pyrolyzer could be a very interesting alternative to assessing and optimizing the performance of different catalysts for the production of upgraded bio-oils since the composition of the volatiles could be promptly determined. Unfortunately, the use of a pyrolysis gas chromatography mass spectrometry (Py-GC/MS) is not a routine technique in most

laboratories. Additionally, microreactors can provide fast useful data but they present several limitations. These are mainly related to operational conditions, mass transfer, temperature profile...etc., than differs in a great extent from those conducted at higher or industrial scale [106].

2.2.2 TRL 3–4: Laboratory-Scale Catalytic Co-pyrolysis Processes

A further step toward the development of catalytic co-pyrolysis processes at industrial scale is based on the assessment of these types of processes in laboratory-scale reactors at TRLs 3 and 4. This scale allows information to be obtained on the influence of different process parameters, such as temperature, heating rate, solid and gas residence time, biomass-to-waste plastic ratio and feedstock-to-catalyst ratio, on both the yield and the composition of the pyrolysis products. Account should also be taken of the fact that these final results will be strongly dependent on the nature of the pyrolysis reactor. There are a large number of studies in the literature related to fast and catalytic pyrolysis of a single biomass or plastic, and very interesting information on the major aspects of these processes can be found in different reviews [58, 105–109], where it is generally accepted that further upgrading processes are needed to increase the quality of the liquid product and that the addition of waste plastics is one of the most interesting alternatives. In this respect, several interesting works can be found in the literature [59, 60, 63–65] at the scale of TRLs 3 and 4 for co-pyrolysis processes. In these studies, PP, HDPE, LDPE, PS, and WT are the most commonly used polymers. Interestingly, Brebu et al. [64] studied the co-pyrolysis of plastic polymers (PE, PP, and PS) and biomass (pine woodchips) mixtures (50/50) in a semi-batch reactor at 500 °C. They observed that the liquid product yields were always higher than 60 wt%, reaching 69.7 wt% in the case of the mixture with PS. Co-pyrolysis produced three different phases: aqueous, organic, and tars. In all cases, the calorific values of the organic phase were higher than 45 MJ/kg. While oxygenated polar compounds were distributed between the tar and aqueous phases, the organic phase was predominantly composed of hydrocarbons, their nature being dependent on the type of synthetic polyolefin. PE produced saturated and unsaturated hydrocarbons; PP produced branched hydrocarbons ranging from dimers to heptamers of PP; and PS produced styrene monomers, dimers, and trimers; all were similar to those obtained from the pyrolysis of the individual waste polymers. In line with the conclusions found in microreactor studies, it should be highlighted that unless process conditions are carefully selected, the formation of three different phases will take place simultaneously and, therefore, which will not favor interactions between the radicals released from the different components of the mixture, resulting in an immiscible liquid product similar to that obtained by mixing the individual components.

Conversely, a careful selection of both process conditions and feedstock components has demonstrated to be critical for the production of an upgraded bio-oil that does not only involve products coming from the pyrolysis of both feedstock components but also the compounds obtained through the interaction of radicals released by their devolatilization. In fact, it has been observed that plastic wastes can act as hydrogen donors, upgrading the pyrolytic oil through hydrogen transfer reactions [62, 67]. However, some drawbacks remain, mainly those associated with the plastic-to-biomass ratio. As previously explained, the choice of a reasonable ratio plays a crucial role in this process, from both the sustainability and technical points of view, given that the presence of significant amounts of bio-oil contaminants such as sulfur- and chloride-containing compounds or PAHs could be greatly increased [61, 65–67].

Progress toward the production of high-quality bio-oils at TRL 3–4 reactors has been also accomplished by the incorporation of catalysts to the co-pyrolysis process. Thus, different kinds of catalysts have been studied for this purpose: zeolites such as ZSM-5 [110–112]; mesoporous silicas, such as SBA-15 [113–115] and MCM-41 [116–118]; alkaline and alkaline earth metal oxides, such as CaO and MgO [17, 119]; different metal oxides of transition metals, such as Co, Ni, Cu, and Ga [9, 120]; and even mixtures of these catalysts [38, 121]. The most widely studied and used catalysts in catalytic upgrading processes at laboratory-scale facilities are ZSM-5 zeolites owing to their high specific surface and intrinsic acidity, adsorption capacity, ion-exchange capacity, and high hydrothermal stability. In addition, ZSM-5 zeolites have a precise balance of acidic strength, micropores with appropriate dimensions to inhibit the formation of large molecules that eventually lead to coke formation, and high porosity and pore connectivity, favoring the diffusion of reactives, products, and by-products to the internal acidic active sites. However, while the ZSM-5 deoxygenation rate may be successfully improved by the incorporation of different metal active sites such as Ni, Co, Ga, and Mg, among others [122] and/or the development of mesoporosity [38], the stability of ZSM-5-based materials has been demonstrated to be very limited [123], with some of the main issues commonly observed being coke formation under reaction conditions, and fouling and sintering during regeneration processes. Nonetheless, several attempts have been made to improve the stability of these very active materials. Zheng et al. [124] studied the catalytic pyrolysis of biomass/rubber seed oil (RSO) (1:1) over HZSM-5 at a feedstock-to-catalyst ratio of 1:2. They showed that RSO addition decreased coke formation, also leading to an aromatic-rich bio-oil with a lower PAH content. Interestingly, a similar effect was observed for the co-pyrolysis of poplar wood and HDPE (50/50) using HZSM-5 zeolite as catalyst (ratio 1:1) [125], pointing to the addition of plastics to the feedstock as a way of reducing coke formation. Another approach to deal with this issue was reported by Lin et al. [126], where lower coke formation during the catalytic co-pyrolysis of corn stover/HDPE (50/50) was also achieved by the impregnation of ZSM-5 with potassium. Interestingly, it was also observed that the addition of potassium promoted the formation of alkenes and monoaromatic hydrocarbons while inhibiting PAH formation as coke precursors. In this context, it should be noted that none of these works provided relevant

data on catalyst stability under cyclic operation involving catalyst regeneration, which should be carefully evaluated as coke formation was still observed, while fouling and sintering during regeneration stages could be very important during this stage. For this reason, it can be concluded that the future of zeolites in biomass catalytic pyrolysis processes seems to be quite limited unless novel materials and/or processes are developed that prevent these operational problems of paramount importance from taking place.

Therefore, novel strategies have been developed following the guidelines for the selection of new catalysts described in the introduction section [44]. Cao et al. [127] compared the performance of two mesoporous silica solids (SBA-15, MCM-41) versus acidic ZSM-5 zeolite for the co-pyrolysis of biomass/waste polymer mixtures in a fixed-bed reactor. Interestingly, they observed that mesoporous silica materials led to better results, particularly SBA-15, which enabled upgraded bio-oils with the lowest oxygen content, density, and viscosity to be obtained. The authors observed that mesoporous silicas could effectively decompose some of the large molecular compounds into smaller ones, which could not be upgraded with ZSM-5 due to limitations with their diffusion to internal acidic active sites. Another interesting alternative consisted of using alkaline and alkaline earth metal oxides as catalysts. In this respect, Ryu et al. [128] assessed the performance of MgO-supported catalysts in the co-pyrolysis of biomass/HDPE in a semi-batch reactor. Three different supports (activated charcoal, Al_2O_3 , ZrO_2) were selected for MgO impregnation, with activated charcoal being the support that obtained the highest yield in an aromatic-rich bio-oil. Positive effects were also found for CaO and BaO when these metal oxides were impregnated into red mud. Mohamed et al. [129] observed that these metal oxides significantly increased the deoxygenation rate of red mud. However, the catalytic co-pyrolysis of biomass/LDPE (1/4) mixtures led to lower aromatic yields. Again, we should note that there is a lack of data regarding the stability of these catalysts under process conditions. On the other hand, red mud is a highly available waste from the aluminum industry, which is likely to eliminate the need for a regeneration stage and can be of interest from a cost standpoint. Therefore, it can be concluded that although progress is being made on very interesting synthesis strategies for the development of more active and stable catalysts, relevant data regarding catalyst stability, cyclability, and operating costs are still required.

Against this background, we have recently reported [128, 129] some interesting results from the catalytic co-pyrolysis of different biomass/plastic waste mixtures in a TRL 3 fixed-bed reactor in which the influence of different relevant parameters of the catalytic co-pyrolysis process was assessed with regard to the yield and characteristics of the bio-oil produced. A comparison was made between the experimental and theoretical results obtained by the rule of mixtures in all cases, allowing the identification of possible synergetic effects. Initial insights into the stability of the catalysts under cyclic operating conditions were also provided. Owing to the interest of this approach, we proposed the use of several low-cost materials as potential catalysts for the catalytic co-pyrolysis of biomass/waste polymer mixtures. Grape seeds were selected as the sample for lignocellulosic biomass and PS and WT were used as waste plastics. The catalytic role of CaO in the pyrolysis of the individual

feedstock components was initially studied for comparative purposes. As expected, the catalytic upgrading process led to a lower yield in the organic phase, the most valuable product for further applications, and also resulted in a significantly lower gas yield. This issue was related to the partial absorption of CO₂ by the CaO material, simultaneously promoting H₂ formation through the CaO-enhanced water-gas shift reaction. This higher hydrogen content seemed to play a key role in the production of upgraded bio-oil since not only hydrodeoxygenation and hydrocracking reactions could be favored for the formation of aromatics from phenolic compounds, but also the production of olefins and cyclic hydrocarbons through hydrocracking and hydrogenation reactions. Finally, we cannot rule out an additional catalytic role of CaO given the slight increase in the number of ketones, which could be pointing to the simultaneous occurrence of a decarboxylation pathway via an acid ketonization reaction over CaO basic sites. On the other hand, the CaO addition had a minor influence on the pyrolysis of PS in terms of liquid yield. Similar results were found in the case of WT pyrolysis. However, it should be remarked that a higher hydrogen concentration was observed in the gas fraction for both waste plastics, likely associated with the promotion of light hydrocarbon cracking reactions as these compounds were simultaneously reduced. The promotion of cracking reactions was also observed in the composition of the liquid fraction, given the significant reduction in PS depolymerization molecules, styrene monomers, dimers, and trimers, which are the main oil components in non-catalytic fast pyrolysis processes, while an increase in the production of monoaromatic—mainly benzene, toluene, and xylenes—was observed. In contrast, the incorporation of CaO into the WT mainly promoted hydrocyclization reactions of linear paraffins, leading to the increase in cyclic hydrocarbons in the WT oils. These data were taken as a baseline from which the possible synergistic effects produced by a dual strategy based on the catalytic co-pyrolysis of plastic/biomass mixtures could be assessed.

In this light, in addition to CaO, our research group also assessed the applicability of other materials as economical, stable, and reusable catalysts for catalytic co-pyrolysis processes. Attapulgite [53], ilmenite [52], sepiolite [51], red mud [52], and dolomite were also evaluated. Experiments were carried out in a fixed-bed reactor using a GS/WT(80/20 wt%) mixture as the feedstock and a catalyst-to-feedstock ratio of 1:1 (except with sepiolite, for which the ratio was 5:1 due to the excessive cracking effect observed at higher ratios for biomass pyrolysis [22]). The results of these experiments were also compared with those obtained from the co-pyrolysis of grape seeds/WT (80/20 wt%). Table 2.4 provides a summary of some of the results obtained in these experiments. Significantly, the presence of the catalyst slightly increased the total liquid yield. An additional role of the catalyst as heat carrier could explain this fact since the GS/WT control experiment was carried out in absence of any inert material working as heat carrier. Additionally, some differences can be observed in the distribution between organic and aqueous phase. Thus, the organic phase yield was comparable for attapulgite, ilmenite and sepiolite, whilst this yield decreased for CaO and dolomite. This effect can be explained by the dehydrating effect of calcium-based catalysts, consequently increasing the aqueous phase yield in the liquid product. As regards the properties

Table 2.4 Yields of catalytic co-pyrolysis of GS/WT (80/20) with different low-cost catalysts and product liquid quality

Experiment	Yields (wt%)				Liquid phase distribution (wt.%)		Organic fraction quality			
	Liquid	Solid	Gas ^a	Total	Org.	Aq.	O ^a (wt %)	S (wt %)	HHV (MJ/kg)	pH
GS	39	33	24	96	61	39	14.3	0.0	36.6	6.4
WT	44	38	15	97	100	0	0.1	0.6	43.4	7.5
GS:CaO (1:1)	38	42	22	102	56	44	16.6	0.0	34.9	9.8
WT:CaO (1:1)	46	30	24	100	100	0	1.7	0.4	42.5	9.0
GS/WT (80/20)	40	33	26	99	69	31	10.6	0.2	38.8	6.7
<i>Catalytic Co-pyrolysis</i>										
GS/WT (80/20): CaO 1:1	44	40	16	100	55	45	5.3	<0.1	41.2	9.1
GS/WT (80/20): CaO.MgO 1:1	44	40	16	100	52	47	3.2	0.3	42.1	8.9
GS/WT (80/20): attapulgite 1:1	42	36	20	98	68	32	13.3	0.2	37.9	6.6
GS/WT (80/20): ilmenite 1:1	42	33	21	96	69	31	14.3	0.1	37.3	6.4
GS/WT (80/20): sepiolite 5:1	43	37	18	98	64	36	12.5	0.1	38.4	7.8
<i>Cyclic operation</i>										
GS/WT (80/20): CaO 1:1 C0	44	40	16	100	55	45	5.3	<0.1	41.2	9.1
GS/WT (80/20): CaO 1:1 C1	34	47	19	100	67	33	5.3	0.2	40.5	9.3
GS/WT (80/20): CaO 1:1 C2	38	45	17	100	60	40	5.2	0.3	40.5	9.0
GS/WT (80/20): CaO 1:1 C3	37	47	15	99	72	28	6.2	0.3	39.1	9.3

Adopted with permission from ref. [130]. Copyright © 2018, Elsevier

^aBy difference

of the organic phase, the oxygen content, heating value, and acidity of this phase were only remarkably improved after the addition of CaO or dolomite, with oxygen values remaining similar to those found in the non-catalytic experiments with the other catalysts. In addition, a reduction was achieved in the sulfur-containing compounds derived from the pyrolysis of WT, particularly when CaO was used, simultaneously increasing the calorific value of the bio-oil. In fact, HHVs were achieved close to those obtained for WTs (43.4 MJ/kg) and remarkably higher than those obtained from non-catalytic co-pyrolysis (38.8 MJ/kg). Finally, the chemical composition of this valuable fraction was also determined by GC/MS. Cyclic

hydrocarbons and single ring aromatics were observed to have been synergistically increased. Concurrently, there was a noticeably reduction in oxygenated compounds, mainly phenols, esters, and fatty acids. This behavior was associated with the additional promotion of hydrodeoxygenation, hydrocyclization, and aromatization reactions resulting from the availability of a significant amount of H₂ produced through both the catalytic cracking of light hydrocarbons and the CaO-enhanced water-gas shift reaction. Finally, calcium-based sorbents also promoted decarboxylation reactions, leading to a slight increase in the number of ketones. Therefore, a reaction mechanism comparable to those observed for the catalytic pyrolysis of the individual components was attained, although synergistic effects were observed in terms of fuel properties (lower oxygen and sulfur contents and higher calorific value), as shown in Table 2.4.

As previously stated, another important issue to be assessed is the performance of the catalyst under cyclic operation. In this case, the regeneration stage was carried out by combustion of the CaO/char mixture at 800 °C in air atmosphere. As a preliminary study, three consecutive cycles were performed involving pyrolysis + catalyst regeneration. We would highlight the fact that although the total liquid yields significantly decreased after the first cycle, the yield to the organic fractions were always close to that obtained in the initial experiment (about 25 wt%) since higher fraction of organic phase was attained. Positively, the CaO deoxygenation rate was maintained throughout the cyclic operation, leading to an upgraded bio-oil with comparable properties in terms of oxygen content, HHV, and acidity, see Table 2.4. Some significant differences were observed in the composition of the non-condensable gas since the CO₂ concentration increased while the H₂ content simultaneously decreased. As expected, this phenomenon could be associated to the well-known decline in the CO₂ absorption capacity of CaO natural sorbents, suppressing the CaO-assisted water-gas shift reaction. Fortunately, negligible differences were found in the composition of the bio-oil since cyclic hydrocarbons, aromatics, phenols, and ketones remained at similar values in this fraction during cyclic operation. These results corroborate the exceptional potential of CaO for use in catalytic co-pyrolysis processes, as already observed in biomass pyrolysis.

As the results from the catalytic co-pyrolysis of grape seeds/WT mixtures using CaO as catalyst were very encouraging, the applicability of this solid to other biomass/waste plastic mixtures was also evaluated. Thus, we modified either the nature of the polymer waste, using waste PS as biomass co-feedstock, or the type of lignocellulosic biomass, using pine woodchips as feedstock. Again, higher liquid yield was obtained in the upgrading process under catalytic co-pyrolysis conditions, although the organic phase yield was lower than that of the co-pyrolysis experiment (73.2 vs. 58.7 wt%). Regardless of the feedstock mixture, synergy between both upgrading strategies was similarly observed through this dual approach in the quality of the organic phase, leading to an upgraded bio-oil with a lower oxygen content and higher calorific value than theoretically expected, as can be appreciated in Table 2.5. On the other hand, GC-MS analysis of the liquid organic phase and chromatographic analysis of the gas fraction confirmed our positive results, demonstrating that the simultaneous addition of waste plastics and CaO to the biomass feedstock could lead

Table 2.5 Distribution of products and liquid quality of pyrolysis, catalytic pyrolysis, co-pyrolysis, and catalytic co-pyrolysis of GS, Pine, and PS

Experiment	Yield (wt%)			Liquid phase distribution (wt %)		Organic fraction quality		
	Liquid	Solid	Gas ^a	Org. phase	Aq. phase	Oxygen (wt%) ^a	HHV (MJ/Kg)	pH
GS	39	33	28	61	39	14.3	32.3	6.4
Pine	50	25	25	60	40	38.8	21.2	2.8
PS	82	1.0	17	100	0	2.3	40.8	3.8
GS:CaO (1:1)	38	43	19	56	44	14.4	35.8	6.6
PS:CaO(1:1)	52	28	20	61	39	0.0	40.7	4.0
Pine:CaO (1:1)	53	20	27	57	43	15.8	37.9	2.9
GS/PS (80/20)	51	27	22	80	20	5.3	39.0	5.6
Pine/PS (80/20)	62	18	20	73	26	31.5	37.9	3.0
GS/PS (80/20): CaO (1:1)	54	29	17	47	53	5.3	41.2	9.1
Pine/PS (80/20): CaO (1:1)	25	61	14	59	41	20.2	39.1	3.9

Adopted with permission from Refs. [131, 132]. Copyright © 2020, Elsevier. Copyright © 2019, Elsevier

^aBy difference

to synergetic effects since hydrodeoxygenation, hydrocracking and hydrocyclization reactions were promoted owing to the significant improvement in H₂ availability.

2.2.3 TRL 5: Pilot Plant Catalytic Co-pyrolysis Processes

The next step in the scale-up of the catalytic co-pyrolysis process would be its validation at TRL 5, where experiments in a relevant environment for further industrial application should be performed.

First, it should be pointed out that certain companies, such as KiOR (currently in bankruptcy proceedings), Anellotech [133], and the Gas Technology Institute (GTI) [134, 135] have already attempted to undertake projects involving the catalytic pyrolysis process at demonstration scale, and even commercial scale, with varying degrees of effectiveness. As to be expected at this magnitude, it is a difficult task to obtain specific information regarding product yields, bio-oil quality, and operational issues. In addition, companies such as ABRI-TECH (Canada), PYREG (Germany), and BIOGREEN-ETIA (France), and different research groups such as EBRI (University of Aston), IKFT-KIT (Germany), and ICB-CSIC (Spain) are developing biomass pyrolysis-based technologies at an industry-relevant scale, TRLs 5 and 7. The aim of these companies and research groups has been to demonstrate on a pilot scale level that pyrolysis, catalytic pyrolysis or even co-pyrolysis with different feedstocks can be profitable technologies for biomass valorization. Although these

results are not included in this chapter for the purpose of simplicity, relevant information can be attained elsewhere [21, 22, 67, 136–141]. Unfortunately, the degree of catalytic co-pyrolysis process development currently stands at lower TRLs, since scarce study has been given to the catalytic co-pyrolysis process at TRL 5 or higher. Nonetheless, some interesting results have been already reported by our research group using a single-screw auger reactor capable of processing up to a rate of approximately 20 kg/h., providing the first insights into the viability of this process in the relevant environment. Thus, we have assessed how process variables could influence the yield and quality of the final products, significantly leading to the production of an upgraded bio-oil fully compatible with conventional fuels. More information on this facility can be found elsewhere [131].

We highlight the fact that the experimental conditions reached in the auger reactor (temperature, heating rate and gas, vapor and solid residence time) can be considered close to the operating conditions of industrial-scale plants. Significantly, the incorporation of heat carriers with catalytic properties into the pyrolysis process in auger reactors, as first proposed by our research group, has demonstrated to be a key to the resolution of certain major issues associated with biomass pyrolysis since, first, heat transfer to the biomass particles is significantly increased and, second, the bio-oil is highly upgraded because the catalytic properties of the heat carriers are in close contact with the biomass and waste plastic particles. Based on the results found in the laboratory-scale reactor, we proposed the use of different calcium-based materials as heat carriers with catalytic properties, such as calcite and dolomite. As expected, lower organic phase yields were obtained compared to the non-catalytic experiment using sand as heat carrier without catalytic properties, but the oxygen content of the bio-oil greatly decreased. It should also be noted that both acidity and calorific value were also improved compared to the non-catalytic test, evidence that CaO materials are able to promote hydrodeoxygenation, decarboxylation, and ketonization reactions, as previously demonstrated in laboratory-scale reactors. Other low-cost minerals (sepiolite, bentonite, attapulgite and red mud) were also tested at TRL 5, but the performance of these heat carriers was again notably inferior to that shown by calcium-based sorbents. We would like to mention here that although calcium-based materials are low-cost minerals, their cyclability in a two-stage integrated process consisting of, first, biomass pyrolysis in the auger reactor and, second, char combustion in a fluidized bed reactor for heating and regeneration of the heat carrier was successfully demonstrated (Fig. 2.8), proving that biomass catalytic pyrolysis in an auger reactor is a self-sustaining process [21, 141].

Based on these encouraging results for biomass catalytic pyrolysis, we have recently tested the catalytic co-pyrolysis process at TRL 5 in order to see if the process performance in a more relevant environment was consistent with that achieved in the laboratory-scale fixed-bed reactor. These experiments were conducted at atmospheric pressure using N₂ as the inert carrier gas. The vapor residence time was fixed at 2–3 seconds. As in the fixed-bed reactor, grape seeds were selected as the lignocellulosic biomass, while PS and WT were the chosen plastic wastes. GS/WT and GS/PS mixtures were used at the ratio of 80:20 and 90:10, in both the co-pyrolysis and catalytic co-pyrolysis processes. In line with

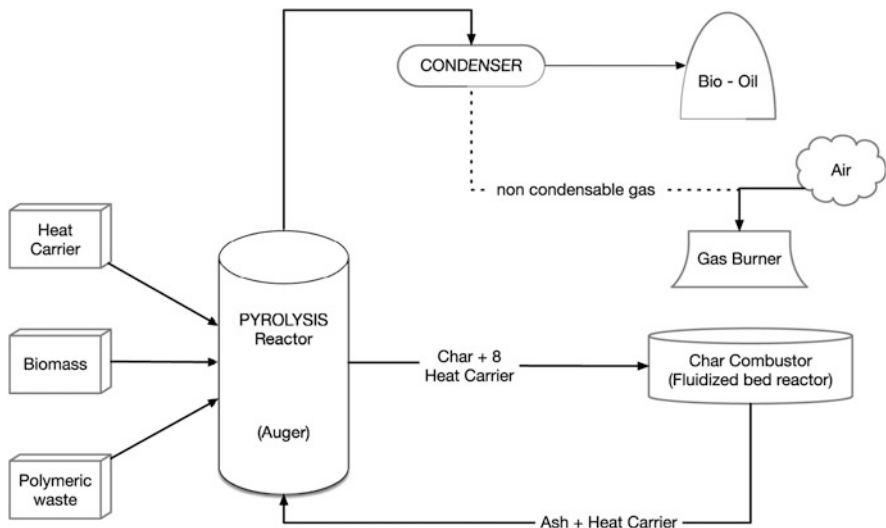


Fig. 2.8 Simple schematic of an integrated catalytic co-pyrolysis process using heat carriers

previous biomass catalytic pyrolysis results, CaO was selected as the catalyst and the feedstock-to-catalyst ratio was fixed at 2:1 since this heat carrier in recirculation was enough to meet the energy balance demand of the integrated process proposed in Fig. 2.8, while at the same time preventing the excessive cracking of volatiles observed at a higher ratio.

Fortunately, catalyst addition to the GS/PS co-pyrolysis process replicated or even enhanced those positive results observed at TRL 3 in the fixed-bed reactor. Thus, a lower organic fraction yield with upgraded properties was again obtained (Table 2.6). Significantly, the production of a fully deoxygenated organic phase with an oxygen content close to 1 wt% for the 80:20 grape seeds/PS:CaO mixture was achieved where the formation of a H₂-rich gas stream with low CO₂ concentration and high calorific value (32.2 MJ/m³), which was again linked to the promotion of both light HC cracking and Ca-enhanced water-gas shift reactions was observed. As the addition of CaO to the GS/PS co-pyrolysis generated very promising results, the use of WT as a waste polymer was also assessed. Very encouraging results were again achieved since a higher yield in upgraded bio-oils was also obtained (Table 2.7). As expected, the results from the single-screw auger reactor again reproduced the trends observed in the TRL 3 fixed bed reactor, proving that the addition of both CaO and WT to biomass pyrolysis can also promote synergistic effects on the upgrading of bio-oil in terms of both yield and quality. In line with this, the oxygen content achieved for the organic fraction was lower than 1 wt%, resulting in a bio-oil with a very high calorific value of more than 40 MJ/m³. Additionally, this upgraded bio-oil obtained at the TRL 5 auger facility showed very interesting physicochemical properties as a fuel since water content and acidity were significantly improved, and a high content in aromatics and hydrocarbons was obtained. It

Table 2.6 Yields, organic phase quality, and non-condensable gas composition of pyrolysis, catalytic pyrolysis, co-pyrolysis, and catalytic co-pyrolysis of GS and PS

Experiment	Yields (wt%)					Liquid phase distribution (wt%)			Organic phase quality (wt%)		Non-condensable gas composition (Vol%)			
	Liquid	Char	Gas	Total	Aq.	Org.	Oxygen ^a	HHV (MJ/Kg)	pH	H ₂	CO ₂	CO	CH ₄	
GS	42	31	23	96	62	38	11.8	35.5	8.0	15.6	34.9	16.0	17.5	
PS	94	0	2.5	96	0	100	0.0	42.0	8.1	33.7	8.4	3.9	19.0	
GS:CaO (2:1)	28	36	15	80	68	32	12.7	34.7	9.0	31.0	9.4	15.0	23.3	
PS:CaO (2:1)	92	0	2.4	95	0	100	0.0	42.0	7.8	41.1	8.6	4.3	19.4	
GS/PS (90/10)	44	30	25	99	45	55	9.2	36.9	7.4	16.0	35.2	15.9	17.5	
GS/PS (80/20)	51	25	23	99	30	70	2.2	40.4	7.3	16.7	36.0	15.3	17.4	
GS/PS (90/10):CaO	44	35	16	96	51	49	1.6	40.0	9.2	32.6	9.6	14.6	22.7	
GS/PS (80/20):CaO	46	33	16	95	41	59	1.0	40.9	8.7	33.2	8.7	14.9	22.7	

Adopted with permission from Ref. [131]. Copyright © 2020, Elsevier

^aBy difference

Table 2.7 Yields, organic phase quality, and non-condensable gas composition of pyrolysis, catalytic pyrolysis, co-pyrolysis, and catalytic co-pyrolysis of GS and WT using different Ca-based catalysts

Experiment	Yields (wt%)					Liquid phase distribution (wt%)			Organic phase quality		
	Liquid	Char	Gas	Total	Aq.	Org.	Oxygen ^a (wt%)	HHV (MJ/kg)	pH	Aromatics	Phenols
GS	43	31	23	97	62	38	11.8	36.8	8.0	31.6	17.1
WT	38	38	23	99	0	100	0.7	43.3	8.3	91.8	0.0
GS/WT (90/10)	33	37	29	99	61	39	7.8	34.8	9.6	63.3	6.4
GS/WT (80/20)	36	33	26	95	51	49	3.9	37.6	9.5	64.3	4.9
GS/WT (80/20):CaO	39	37	21	97	59	41	0.5	41.2	9.1	70.9	1.3

Adopted with permission from ref. [131]. Copyright © 2020, Elsevier
^aBy difference

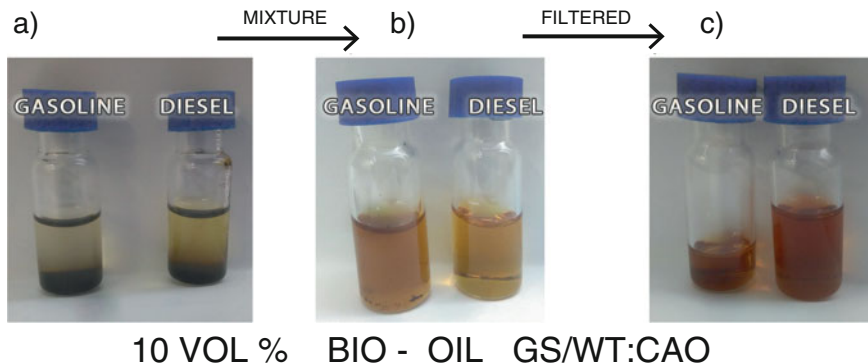


Fig. 2.9 Bio-oil with conventional fuels compatibility: (a) commercial gasoline and diesel mixture with bio-oil from catalytic co-pyrolysis (80 GSs/20 WTs/CaO). (b) Mechanical mixture of catalytic co-pyrolysis bio-oil with gasoline and diesel. (c) Mixture of catalytic co-pyrolysis bio-oil with gasoline and diesel after filtration process. Mixtures were prepared using a blend consisting of 90 vol% gasoline or diesel/10 vol % bio-oil. Adopted with permission from Ref. [130]. Copyright © 2018, Elsevier

should be highlighted that bio-oil upgrading process was actually more efficient in the TRL 5 auger facility compared to that performed in the TRL 3 fixed-bed reactor. Therefore, it can be concluded that although comparable upgrading routes were identified at both TRLs, better contact between volatiles and CaO active sites was promoted in the TRL 5 auger reactor, favoring the upgrading process.

Significantly, the bio-oils produced by catalytic co-pyrolysis of grape seeds with polymer wastes were highly compatible with conventional fuels, as can be observed in Fig. 2.9, showing the perfect blending achieved between this upgraded bio-oil and gasoline/diesel. Therefore, this technology could be identified as a simple and reliable solution for the production of drop-in biofuels.

2.3 Conclusions and Future Outlook

Insights into the potential of the catalytic pyrolysis of biomass and waste polymers at TRL 5 have been shown. Although further research is still necessary, focusing particularly on the optimizing of key parameters, such as i) the selection of an efficient and low-cost catalyst, ii) the biomass/waste polymer mixture, and iii) the optimization of the main operational parameters of the process (temperature and volatile residence time), the exceptional potential of this process for the production of transportation fuels in a single-stage process has been successfully revealed from laboratory scale to pilot plant scale. Significantly, this dual strategy has proven to be a robust and simple technology that enables high valuable liquids to be obtained for direct use as drop-in fuels. In fact, an almost fully deoxygenated liquid with a large proportion of valuable aromatics can be obtained using different types of biomass

(grape seeds or pine woodchips), waste plastic (polystyrene or waste tire), and catalyst (calcite or dolomite) mixtures. Hopefully, these positive results will not be limited to these mixtures, and the study of other mixtures will also lead to the efficient production of upgraded bio-oils. Therefore, the great versatility of this process, linked with the wide range of feedstocks that can be treated (both biomass and waste polymers) could enhance the potential of the catalytic co-pyrolysis process so that it can reach the commercial level.

References

1. Kumar R, Strezov V, Weldekidan H, He J, Singh S, Kan T, Dastjerdi B. Lignocellulose biomass pyrolysis for bio-oil production: a review of biomass pre-treatment methods for production of drop-in fuels. *Renew Sust Energ Rev.* 2020;123. <https://doi.org/10.1016/j.rser.2020.109763>.
2. Zhang X, Lei H, Chen S, Wu J. Catalytic co-pyrolysis of lignocellulosic biomass with polymers: a critical review. *Green Chem.* 2016;18:4145–69. <https://doi.org/10.1039/C6GC00911E>.
3. Kan T, Strezov V, Evans TJ. Lignocellulosic biomass pyrolysis: a review of product properties and effects of pyrolysis parameters. *Renew Sust Energ Rev.* 2016;57:1126–40. <https://doi.org/10.1016/j.rser.2015.12.185>.
4. Bridgwater AV. Review of fast pyrolysis of biomass and product upgrading. *Biomass Bioenergy.* 2012;38:68–94. <https://doi.org/10.1016/j.biombioe.2011.01.048>.
5. Secretary-General of the OECD. Energy for sustainable development OECD: Contribution to the United Nations Commission on Sustainable Development 15 (2007) Paris. 104 p.
6. Ryu HW, Kim DH, Jae J, Lam SS, Park ED, Park Y-K. Recent advances in catalytic co-pyrolysis of biomass and plastic waste for the production of petroleum-like hydrocarbons. *Bioresour Technol.* 2020;310:123473. <https://doi.org/10.1016/j.biortech.2020.123473>.
7. Dickerson T, Soria J. Catalytic fast pyrolysis: a review. *Energies.* 2013;6:514–38. <https://doi.org/10.3390/en6010514>.
8. Krutof A, Hawboldt KA. Upgrading of biomass sourced pyrolysis oil review: focus on co-pyrolysis and vapour upgrading during pyrolysis. *Biomass Conv Bioref.* 2018;8:775–87. <https://doi.org/10.1007/s13399-018-0326-6>.
9. Fermoso J, Pizarro P, Coronado JM, Serrano DP. Transportation biofuels via the pyrolysis pathway: status and prospects. New York: Encyclopedia of Sustainability Science and Technology; 2017. p. 1–33. https://doi.org/10.1007/978-1-4939-2493-6_963-1.
10. Abnisa F, Wan Daud WMA. A review on co-pyrolysis of biomass: an optional technique to obtain a high-grade pyrolysis oil. *Energy Convers Manag.* 2014;87:71–85. <https://doi.org/10.1016/j.enconman.2014.07.007>.
11. Fermoso J, Pizarro P, Coronado JM, Serrano DP. Advanced biofuels production by upgrading of pyrolysis bio-oil: Advanced biofuels production. *WIREs Energy Environ.* 2017;6:e245. <https://doi.org/10.1002/wene.245>.
12. Dabros TMH, Stummam MZ, Høj M, Jensen PA, Grunwaldt J-D, Gabrielsen J, Mortensen PM, Jensen AD. Transportation fuels from biomass fast pyrolysis, catalytic hydrodeoxygenation, and catalytic fast hydropyrolysis. *Prog Energy Combust Sci.* 2018;68:268–309. <https://doi.org/10.1016/j.pecs.2018.05.002>.
13. Montoya J, Chejne Janna F, Castillo E, Acero J, Gomez C, Sarmiento J, Valdés C, Garzón L, Osorio Velasco J, Tirado D, Blanco Leal L, Safra N, Marrugo G, Ospina E (2014) Pirólisis rápida de biomasa. National University of Colombia. 978-958-761-774-0.

14. Sharma A, Pareek V, Zhang D. Biomass pyrolysis—A review of modelling, process parameters and catalytic studies. *Renew Sust Energ Rev*. 2015;50:1081–96. <https://doi.org/10.1016/j.rser.2015.04.193>.
15. Yildiz G, Ronsse F, van Duren R, Prins W. Challenges in the design and operation of processes for catalytic fast pyrolysis of woody biomass. *Renew Sust Energ Rev*. 2016;57:1596–610. <https://doi.org/10.1016/j.rser.2015.12.202>.
16. Zheng Y, Tao L, Yang X, Huang Y, Liu C, Zheng Z. Study of the thermal behavior, kinetics, and product characterization of biomass and low-density polyethylene co-pyrolysis by thermogravimetric analysis and pyrolysis-GC/MS. *J Anal Appl Pyrolysis*. 2018;133:185–97. <https://doi.org/10.1016/j.jaat.2018.04.001>.
17. Lin X, Kong L, Cai H, Zhang Q, Bi D, Yi W. Effects of alkali and alkaline earth metals on the co-pyrolysis of cellulose and high density polyethylene using TGA and Py-GC/MS. *Fuel Process Technol*. 2019;191:71–8. <https://doi.org/10.1016/j.fuproc.2019.03.015>.
18. Jahirul M, Rasul M, Chowdhury A, Ashwath N. Biofuels production through biomass pyrolysis —a technological review. *Energies*. 2012;5:4952–5001. <https://doi.org/10.3390/en5124952>.
19. Brown R, Holmgren J (2009) Fast Pyrolysis and bio-oil upgrading . https://www.driveonwood.com/static/media/uploads/pdf/fast_pyrolysispdf Data accessed May 2021.
20. Puy N, Murillo R, Navarro MV, López JM, Rieradevall J, Fowler G, Aranguren I, García T, Bartrolí J, Mastral AM. Valorisation of forestry waste by pyrolysis in an auger reactor. *Waste Manag*. 2011;31:1339–49. <https://doi.org/10.1016/j.wasman.2011.01.020>.
21. Veses A, Aznar M, Callén MS, Murillo R, García T. An integrated process for the production of lignocellulosic biomass pyrolysis oils using calcined limestone as a heat carrier with catalytic properties. *Fuel*. 2016;181:430–7. <https://doi.org/10.1016/j.fuel.2016.05.006>.
22. Veses A, Aznar M, López JM, Callén MS, Murillo R, García T. Production of upgraded bio-oils by biomass catalytic pyrolysis in an auger reactor using low cost materials. *Fuel*. 2015;141:17–22. <https://doi.org/10.1016/j.fuel.2014.10.044>.
23. Chen X, Che Q, Li S, Liu Z, Yang H, Chen Y, Wang X, Shao J, Chen H. Recent developments in lignocellulosic biomass catalytic fast pyrolysis: strategies for the optimization of bio-oil quality and yield. *Fuel Process Technol*. 2019;196:106180. <https://doi.org/10.1016/j.fuproc.2019.106180>.
24. Demirbas A. Determination of calorific values of biochars and pyro-oils from pyrolysis of beech trunkbarks. *J Anal Appl Pyrolysis*. 2004;72:215–9. <https://doi.org/10.1016/j.jaat.2004.06.005>.
25. Ahmad M, Rajapaksha AU, Lim JE, Zhang M, Bolan N, Mohan D, Vithanage M, Lee SS, Ok YS. Biochar as a sorbent for contaminant management in soil and water: a review. *Chemosphere*. 2014;99:19–33. <https://doi.org/10.1016/j.chemosphere.2013.10.071>.
26. Mašek O, Brownsort P, Cross A, Sohi S. Influence of production conditions on the yield and environmental stability of biochar. *Fuel*. 2013;103:151–5. <https://doi.org/10.1016/j.fuel.2011.08.044>.
27. Laird DA. The charcoal vision: a win-win-win scenario for simultaneously producing bioenergy, permanently sequestering carbon, while improving soil and water quality. *Agron J*. 2008;100:178–81. <https://doi.org/10.2134/agronj2007.0161>.
28. Kim KH, Kim J-Y, Cho T-S, Choi J. Influence of pyrolysis temperature on physicochemical properties of biochar obtained from the fast pyrolysis of pitch pine (*Pinus rigida*). *Bioresour Technol*. 2012;118:158–62. <https://doi.org/10.1016/j.biortech.2012.04.094>.
29. Czernik S, Bridgwater AV. Overview of applications of biomass fast pyrolysis oil. *Energy Fuels*. 2004;18:590–8. <https://doi.org/10.1021/ef034067u>.
30. Oasmaa A, Peacocke C. A guide to physical property characterisation of biomass-derived fast pyrolysis liquids. VTT Publications; 2001. 87 pp
31. Stedile T, Ender L, Meier HF, Simionatto EL, Wiggers VR. Comparison between physical properties and chemical composition of bio-oils derived from lignocellulose and triglyceride sources. *Renew Sust Energ Rev*. 2015;50:92–108. <https://doi.org/10.1016/j.rser.2015.04.080>.

32. Badger PC, Fransham P. Use of mobile fast pyrolysis plants to densify biomass and reduce biomass handling costs: a preliminary assessment. *Biomass Bioenergy*. 2006;30:321–5. <https://doi.org/10.1016/j.biombioe.2005.07.011>.
33. Oasmaa A, Lehto J, Solantausta Y, Kallio S. Historical review on VTT fast pyrolysis bio-oil production and upgrading. *Energy Fuel*. 2021;13(35):5683–95. <https://doi.org/10.1021/acs.energyfuels.1c00177>.
34. Baloch HA, Nizamuddin S, Siddiqui MTH, Riaz S, Jatoi AS, Dumbre DK, Mubarak NM, Srinivasan MP, Griffin GJ. Recent advances in production and upgrading of bio-oil from biomass: a critical overview. *J Environ Chem Eng*. 2018;6:5101–18. <https://doi.org/10.1016/j.jece.2018.07.050>.
35. Tan S, Zhang Z, Sun J, Wang Q. Recent progress of catalytic pyrolysis of biomass by HZSM-5. *Cuihua Xuebao/Chinese J Catal*. 2013;34:641–50. [https://doi.org/10.1016/S1872-2067\(12\)60531-2](https://doi.org/10.1016/S1872-2067(12)60531-2).
36. Shan Ahamed T, Anto S, Mathimani T, Brindhadevi K, Pugazhendhi A. Upgrading of bio-oil from thermochemical conversion of various biomass – mechanism, challenges and opportunities. *Fuel*. 2020;287:119329. <https://doi.org/10.1016/j.fuel.2020.119329>.
37. Hernando H, Moreno I, Fermoso J, Ochoa-Hernández C, Pizarro P, Coronado JM, Čejka J, Serrano DP. Biomass catalytic fast pyrolysis over hierarchical ZSM-5 and Beta zeolites modified with Mg and Zn oxides. *Biomass Conv Bioref*. 2017;7:289–304. <https://doi.org/10.1007/s13399-017-0266-6>.
38. Sanahuja-Parejo O, Veses A, López JM, Callén MS, Solsona B, Richards N, Taylor SH, García T. Insights into the production of upgraded biofuels using Mg-loaded mesoporous ZSM-5 zeolites. *ChemCatChem*. 2020;12:5236–49. <https://doi.org/10.1002/cctc.202000787>.
39. Abnisa F, Wan Daud WMA, Arami-Niya A, Ali BS, Sahu JN. Recovery of liquid fuel from the aqueous phase of pyrolysis oil using catalytic conversion. *Energy Fuel*. 2014;28:3074–85. <https://doi.org/10.1021/ef5003952>.
40. Moraes MSA, Georges F, Almeida SR, Damasceno FC, da Silva Maciel GP, Zini CA, Jacques RA, Caramão EB. Analysis of products from pyrolysis of Brazilian sugar cane straw. *Fuel Process Technol*. 2012;101:35–43. <https://doi.org/10.1016/j.fuproc.2012.03.004>.
41. Madsen AT, Søndergaard H, Fehrman R, Riisager A. Challenges and perspectives for catalysis in production of diesel from biomass. *Biofuels*. 2011;2:465–83. <https://doi.org/10.4155/bfs.11.115>.
42. Mohanty P, Pant KK, Mittal R. Hydrogen generation from biomass materials: challenges and opportunities. *Wiley Interdiscip Rev: Energy Environ*. 2015;4:139–55. <https://doi.org/10.1002/wene.111>.
43. Gupta S, Mondal P, Borugadda VB, Dalai AK. Advances in upgradation of pyrolysis bio-oil and biochar towards improvement in bio-refinery economics: a comprehensive review. *Environ Technol Innovation*. 2021;21:101276. <https://doi.org/10.1016/j.eti.2020.101276>.
44. Michel R, Rapagnà S, Di Marcello M, Burg P, Matt M, Courson C, Gruber R. Catalytic steam gasification of *Miscanthus X giganteus* in fluidised bed reactor on olivine based catalysts. *Fuel Process Technol*. 2011;92:1169–77. <https://doi.org/10.1016/j.fuproc.2010.12.005>.
45. Vogt ETC, Weckhuysen BM. Fluid catalytic cracking: recent developments on the grand old lady of zeolite catalysis. *Chem Soc Rev*. 2015;44:7342–70. <https://doi.org/10.1039/CSCS00376H>.
46. Stefanidis SD, Karakoulia SA, Kalogiannis KG, Iliopoulos EF, Delimitis A, Yiannoulakis H, Zampetakis T, Lappas AA, Triantafyllidis KS. Natural magnesium oxide (MgO) catalysts: a cost-effective sustainable alternative to acid zeolites for the in situ upgrading of biomass fast pyrolysis oil. *Appl Catal B*. 2016;196:155–73. <https://doi.org/10.1016/j.apcatb.2016.05.031>.
47. Lee SL, Wong YC, Tan YP, Yew SY. Transesterification of palm oil to biodiesel by using waste obtuse horn shell-derived CaO catalyst. *Energy Convers Manag*. 2015;93:282–8. <https://doi.org/10.1016/j.enconman.2014.12.067>.

48. Lin Y, Zhang C, Zhang M, Zhang J. Deoxygenation of bio-oil during pyrolysis of biomass in the presence of CaO in a fluidized-bed reactor. *Energy Fuel*. 2010;24(10):5686–95. <https://doi.org/10.1021/ef1009605>.
49. Bulushev DA, Ross JRH. Catalysis for conversion of biomass to fuels via pyrolysis and gasification: a review. *Catal Today*. 2011;171(1):1–13. <https://doi.org/10.1016/j.cattod.2011.02.005>.
50. Zhang H, Zheng J, Xiao R. Catalytic pyrolysis of willow wood with Me/ZSM-5 (Me = Mg, K, Fe, Ga, Ni) to produce aromatics and olefins. *Bioresources*. 2013;8:5612–21. <https://doi.org/10.15376/biores.8.4.5612-5621>.
51. Carretier V, Delcroix J, Pucci MF, Rublon P, Lopez-Cuesta J-M. Influence of sepiolite and lignin as potential synergists on flame retardant systems in polylactide (PLA) and polyurethane elastomer (PUE). *Materials*. 2020;13(11):2450. <https://doi.org/10.3390/ma13112450>.
52. Han T, Ding S, Yang W, Jönsson P. Catalytic pyrolysis of lignin using low-cost materials with different acidities and textural properties as catalysts. *Chem Eng J*. 2019;373:846–56. <https://doi.org/10.1016/j.cej.2019.05.125>.
53. Wu Z, Wang F, Xu J, Zhang J, Zhao X, Hu L, Jiang Y. Improved lignin pyrolysis over attapulgite-supported solid acid catalysts. *Biomass Convers Biorefin*. 2020;3. <https://doi.org/10.1007/s13399-020-00667-4>.
54. Plastics Europe (association of plastics manufacturers), EPRO (European Association of Plastics Recycling and Recovery Organisations). Plastics – the Facts (2020): An analysis of European plastics production, demand and waste data [Internet]. Date accessed May 2021. https://www.plasticeurope.org/application/files/3416/2270/7211/Plastics_the_facts-WEB-2020_versionJun21_final.pdf.
55. Plastics Europe Deutschland e.V., and Messe Düsseldorf, Plastics Europe (association of plastics manufacturers), EPRO (European Association of Plastics Recycling and Recovery Organisations). Plastics – the Facts 2019: An analysis of European plastics production, demand and waste data [Internet]. Date accessed May 2021. https://www.plasticeurope.org/application/files/9715/7129/9584/FINAL_web_version_Plastics_the_facts2019_14102019.pdf.
56. Sugumaran V, Prakash S, Arora AK, Kapur GS, Narula AK. Thermal cracking of potato-peel powder-polypropylene biocomposite and characterization of products—pyrolysed oils and bio-char. *J Anal Appl Pyrolysis*. 2017;126:405–14. <https://doi.org/10.1016/j.jaat.2017.04.014>.
57. Wasielewski R, Siudyga T. Energy recovery from waste plastics. *Odzysk energetyczny odpadów tworzyw sztucznych*. *Chemik*. 2013;67(5):435–45.
58. Wong SL, Ngadi N, Abdullah TAT, Inuwa IM. Current state and future prospects of plastic waste as source of fuel: a review. *Renew Sust Energ Rev*. 2015;50:1167–80. <https://doi.org/10.1016/j.rser.2015.04.063>.
59. Miranda M, Pinto F, Gulyurtlu I. Polymer wastes pyrolysis for liquid fuel production. In: Domenica C, editor. Liquid fuels: types, properties and production; 2011. p. 147–68. ISBN: 978-1-61470-513-0.
60. Miandad R, Barakat MA, Aburiazaiza AS, Rehan M, Nizami AS. Catalytic pyrolysis of plastic waste: a review. *Process Saf Environ Prot*. 2016;102:822–38. <https://doi.org/10.1016/j.psep.2016.06.022>.
61. Abnisa F, Daud WMAW, Sahu JN. Recovery of liquid fuel from the aqueous phase of pyrolysis oil using catalytic conversion. *Environ Prog Sustain Energy*. 2014;33:1026–33. <https://doi.org/10.1002/ep.11850>.
62. Shadangi KP, Mohanty K. Co-pyrolysis of Karanja and Niger seeds with waste polystyrene to produce liquid fuel. *Fuel*. 2015;153:492–8. <https://doi.org/10.1016/j.fuel.2015.03.017>.
63. Abnisa F, Wan Daud WMA. Optimization of fuel recovery through the stepwise co-pyrolysis of palm shell and scrap tire. *Energy Convers Manag*. 2015;99:334–45. <https://doi.org/10.1016/j.enconman.2015.04.030>.

64. Brebu M, Ucar S, Vasile C, Yanik J. Co-pyrolysis of pine cone with synthetic polymers. *Fuel*. 2010;89:1911–8. <https://doi.org/10.1016/j.fuel.2010.01.029>.
65. Suriapparao DV, Boruah B, Raja D, Vinu R. Microwave assisted co-pyrolysis of biomasses with polypropylene and polystyrene for high quality bio-oil production. *Fuel Process Technol*. 2018;175:64–75. <https://doi.org/10.1016/j.fuproc.2018.02.019>.
66. Akancha KN, Singh RK. Co-pyrolysis of waste polypropylene and rice bran wax—production of biofuel and its characterization. *J Energy Inst*. 2019;92:933–46. <https://doi.org/10.1016/j.joei.2018.07.011>.
67. Martínez JD, Veses A, Mastral AM, Murillo R, Navarro MV, Puy N, Artigues A, Bartrolí J, García T. Co-pyrolysis of biomass with waste tyres: Upgrading of liquid bio-fuel. *Fuel Process Technol*. 2014;119:263–71. <https://doi.org/10.1016/j.fuproc.2013.11.015>.
68. Stančin H, Šafář M, Růžičková J, Mikulčíč H, Raclavská H, Wang X, Duić N. Co-pyrolysis and synergistic effect analysis of biomass sawdust and polystyrene mixtures for production of high-quality bio-oils. *Process Saf Environ Prot*. 2021;145:1–11. <https://doi.org/10.1016/j.psep.2020.07.023>.
69. Sarker M, Rashid MM. Polyvinyl Chloride (PVC) waste plastic treatment using zinc oxide (ZnO) with activated carbon and produced hydrocarbon fuel for petroleum refinery. *Int J Eng Sci*. 2012;1(8):29–41. <https://doi.org/10.2514/1.46753>.
70. Abnisa F, Daud WMAW, Sahu JN. Pyrolysis of mixtures of palm shell and polystyrene: an optional method to produce a high-grade of pyrolysis oil. *Environ Prog Sustain Energy*. 2014;33:1026–33. <https://doi.org/10.1002/ep.11850>.
71. Conrow EH. Estimating technology readiness level coefficients. *J Spacecraft Rockets*. 2011;48:146–52. <https://doi.org/10.2514/1.46753>.
72. Rybicka J, Tiwari A, Leek GA. Technology readiness level assessment of composites recycling technologies. *J Clean Prod*. 2016;112:1001–12. <https://doi.org/10.1016/j.jclepro.2015.08.104>.
73. Sauser B, Ramirez-Marquez J, Verma D, Gove R (2006) From TRL to SRL: the concept of systems readiness levels. In: Paper read at Conference on Systems Engineering Research. Paper #126.
74. Oyedun AO, Tee CZ, Hanson S, Hui CW. Thermogravimetric analysis of the pyrolysis characteristics and kinetics of plastics and biomass blends. *Fuel Process Technol*. 2014;128:471–81. <https://doi.org/10.1016/j.fuproc.2014.08.010>.
75. Zhang X, Lei H, Zhu L, Zhu X, Qian M, Yadavalli G, Wu J, Chen S. Thermal behavior and kinetic study for catalytic co-pyrolysis of biomass with plastics. *Bioresour Technol*. 2016;220:233–8. <https://doi.org/10.1016/j.biortech.2016.08.068>.
76. Liu G, Song H, Wu J. Thermogravimetric study and kinetic analysis of dried industrial sludge pyrolysis. *Waste Manag*. 2015;41:128–33. <https://doi.org/10.1016/j.wasman.2015.03.042>.
77. Gerassimidou S, Velis CA, Williams PT, Komilis D. Characterisation and composition identification of waste-derived fuels obtained from municipal solid waste using thermogravimetry: a review. *Waste Manage Res*. 2020;38:942–65. <https://doi.org/10.1177/0734242X20941085>.
78. Wang Q, Ji C, Sun J, Zhu Q, Liu J. Structure and properties of polylactic acid biocomposite films reinforced with cellulose nanofibrils. *Molecules*. 2020;25:3306. <https://doi.org/10.3390/molecules25143306>.
79. Park K-B, Jeong Y-S, Guzelciftci B, Kim J-S. Two-stage pyrolysis of polystyrene_ Pyrolysis oil as a source of fuels or benzene, toluene, ethylbenzene, and xylenes. *Appl Energy*. 2020;259:114240. <https://doi.org/10.1016/j.apenergy.2019.114240>.
80. Arabiourrutia M, Lopez G, Artetxe M, Alvarez J, Bilbao J, Olazar M. Waste tyre valorization by catalytic pyrolysis: a review. *Renew Sustain Energy Rev*. 2020;129:109932. <https://doi.org/10.1016/j.rser.2020.109932>.
81. Navarro MV, López JM, Veses A, Callén MS, García T. Kinetic study for the co-pyrolysis of lignocellulosic biomass and plastics using the distributed activation energy model. *Energy*. 2018;165:731–42. <https://doi.org/10.1016/j.energy.2018.09.133>.

82. Hameed Z, Naqvi SR, Naqvi M, Ali I, Taqvi SAA, Gao N, Hussain SA, Hussain S. A comprehensive review on thermal coconversion of biomass, sludge, coal, and their blends using thermogravimetric analysis. *J Chem.* 2020;23:5024369. <https://doi.org/10.1155/2020/5024369>.
83. Alam M, Bhavanam A, Jana A, Viroja J kumar S, Peela NR (2020) Co-pyrolysis of bamboo sawdust and plastic: synergistic effects and kinetics. *Renew Energy* 149:1133–1145. doi: <https://doi.org/10.1016/j.renene.2019.10.103>.
84. Önal E, Uzun BB, Pütün AE. Bio-oil production via co-pyrolysis of almond shell as biomass and high density polyethylene. *Energy Convers Manag.* 2014;78:704–10. <https://doi.org/10.1016/j.enconman.2013.11.022>.
85. Wang S, Ru B, Lin H, Dai G, Wang Y, Luo Z. Kinetic study on pyrolysis of biomass components: a critical review. *Curr Org Chem.* 2016;20:2489–513. <https://doi.org/10.2174/1385272820666160525115832>.
86. Cai J, Wu W, Liu R. An overview of distributed activation energy model and its application in the pyrolysis of lignocellulosic biomass. *Renew Sust Energ Rev.* 2014;36:236–46. <https://doi.org/10.1016/j.rser.2014.04.052>.
87. Mahmood H, Moniruzzaman M, Yusup S, Khan MI, Khan MJ. Kinetic modeling and optimization of biomass pyrolysis for bio-oil production. *Energy Sources, Part A: Recov Util Environ Effects.* 2016;38:2065–71. <https://doi.org/10.1080/15567036.2015.1007404>.
88. Wu Z, Li Y, Zhao J, Zhang B, Xu D, Yang B. Fast pyrolysis behavior of lignocellulosic biomass model compound: releasing properties, kinetic analysis of the primary gaseous products and char structure evolution from cellulose. *Energy Procedia.* 2019;158:79–84. <https://doi.org/10.1016/j.egypro.2019.01.049>.
89. Wang S, Lin H, Ru B, Dai G, Wang X, Xiao G, Luo Z. Kinetic modeling of biomass components pyrolysis using a sequential and coupling method. *Fuel.* 2016;185:763–71. <https://doi.org/10.1016/j.fuel.2016.08.037>.
90. Ding Y, Huang B, Wu C, He Q, Lu K. Kinetic model and parameters study of lignocellulosic biomass oxidative pyrolysis. *Energy.* 2019;181:11–7. <https://doi.org/10.1016/j.energy.2019.05.148>.
91. Ding Y, Zhang J, He Q, Huang B, Mao S. The application and validity of various reaction kinetic models on woody biomass pyrolysis. *Energy.* 2019;179:784–91. <https://doi.org/10.1016/j.energy.2019.05.021>.
92. Hameed S, Sharma A, Pareek V, Wu H, Yu Y. A review on biomass pyrolysis models: kinetic, network and mechanistic models. *Biomass Bioenergy.* 2019;123:104–22. <https://doi.org/10.1016/j.biombioe.2019.02.008>.
93. Lei X, Bi Y, Zhou W, Chen H, Hu J. Catalytic fast pyrolysis of cellulose by integrating dispersed nickel catalyst with HZSM-5 zeolite. *IOP Conf Ser Earth Environ Sci.* 2018;108 (2):022017. <https://doi.org/10.1088/1755-1315/108/2/022017>.
94. Jeong J, Lee HW, Jang SH, Ryu S, Kim Y-M, Park R-S, Jung S-C, Jeon J-K, Park Y-K (2019) In-situ catalytic fast pyrolysis of pinecone over HY catalysts. *Catal* 9: art. 1034. doi: <https://doi.org/10.3390/catal9121034>.
95. Nishu LR, Rahman MM, Li C, Chai M, Sarker M, Wang Y, Cai J. Catalytic pyrolysis of microcrystalline cellulose extracted from rice straw for high yield of hydrocarbon over alkali modified ZSM-5. *Fuel.* 2021;285:119038. <https://doi.org/10.1016/j.fuel.2020.119038>.
96. Durmuş A, Koç SN, Pozan GS, Kaşgöz A. *Appl Catal. B.* 2005;61:316–22. <https://doi.org/10.1016/j.apcatb.2005.06.009>.
97. Marcilla A, Gómez-Siurana A, Quesada JCG, Berenguer D. Characterization of high-impact polystyrene by catalytic pyrolysis over Al-MCM-41: study of the influence of the contact between polymer and catalyst. *Polym Degrad Stab.* 2007;92:1867–72. <https://doi.org/10.1016/j.polymdegradstab.2007.06.016>.
98. Kim Y-M, Jae J, Kim B-S, Hong Y, Jung S-C, Park Y-K. Catalytic co-pyrolysis of torrefied yellow poplar and high-density polyethylene using microporous HZSM-5 and mesoporous

- Al-MCM-41 catalysts. *Energy Convers Manag.* 2017;149:966–73. <https://doi.org/10.1016/j.enconman.2017.04.033>.
99. Wang Z, Burra KG, Lei T, Gupta AK. Co-pyrolysis of waste plastic and solid biomass for synergistic production of biofuels and chemicals: a review. *Prog Energy Combust Sci.* 2021;84:100899. <https://doi.org/10.1016/j.pecs.2020.100899>.
100. Rahman MM, Chai M, Sarker M, Nishu LR. Catalytic pyrolysis of pinewood over ZSM-5 and CaO for aromatic hydrocarbon: analytical Py-GC/MS study. *J Energy Inst.* 2019;93 (1):425–35. <https://doi.org/10.1016/j.joei.2019.01.014>.
101. Kavimonica V, Parasuraman S, Ravikrishnan V. Kinetic studies of catalytic upgradation of biomass model compounds using analytical Py-gc/ms. *Chem Eng Trans.* 2020;80:1–6. <https://doi.org/10.3303/CET2080001>.
102. Xing S, Yuan H, Huhetaoli QY, Lv P, Yuan Z, Chen Y. Characterization of the decomposition behaviors of catalytic pyrolysis of wood using copper and potassium over thermogravimetric and Py-GC/MS analysis. *Energy.* 2016;114:634–46. <https://doi.org/10.1016/j.energy.2016.07.154>.
103. Zheng X, Chen C, Ying Z, Wang B, Chi Y. Py-GC/MS study on Tar formation characteristics of MSW key component pyrolysis. *Waste Biomass Valor.* 2017;8:313–9. <https://doi.org/10.1007/s12649-016-9596-z>.
104. Sarker M, Liu R, Rahman MM, Li C, Chai M, Nishu HY. Impact of acid-modified ZSM-5 on hydrocarbon yield of catalytic co-pyrolysis of poplar wood sawdust and high-density polyethylene by Py-GC/MS analysis. *J Energy Inst.* 2020;93:2435–43. <https://doi.org/10.1016/j.joei.2020.08.001>.
105. Xue J, Zhuo J, Liu M, Chi Y, Zhang D, Yao Q. Synergetic effect of co-pyrolysis of cellulose and polypropylene over an all-silica mesoporous catalyst MCM-41 using thermogravimetry–fourier transform infrared spectroscopy and pyrolysis–gas chromatography–mass spectrometry. *Energy Fuel.* 2017;31:9576–84. <https://doi.org/10.1021/acs.energyfuels.7b01651>.
106. Van Daele T, Fernandes del Pozo D, Van Hauwermeiren D, Gernaey K, Wohlgemuth R, Nopens I. A generic model-based methodology for quantification of mass transfer limitations in microreactors. *Chem Eng J.* 2016;300:193–208. <https://doi.org/10.1016/j.cej.2016.04.117>.
107. Butler E, Devlin G, McDonnell K. Waste polyolefins to liquid fuels via pyrolysis: review of commercial state-of-the-art and recent laboratory research. *Waste Biomass Valor.* 2011;2:227–55. <https://doi.org/10.1007/s12649-011-9067-5>.
108. Dai L, Wang Y, Liu Y, He C, Ruan R, Yu Z, Jiang L, Zeng Z, Wu Q. A review on selective production of value-added chemicals via catalytic pyrolysis of lignocellulosic biomass. *Sci Total Environ.* 2020;749:142386. <https://doi.org/10.1016/j.scitotenv.2020.142386>.
109. Kan T, Strezov V, Evans T, He J, Kumar R, Lu Q (2020) Catalytic pyrolysis of lignocellulosic biomass: a review of variations in process factors and system structure. *Renewable Sustainable Energy Rev* 134:art. 110305. doi: <https://doi.org/10.1016/j.rser.2020.110305>.
110. Ryu S, Lee HW, Kim Y-M, Jae J, Jung S-C, Ha J-M, Park Y-K. Catalytic fast co-pyrolysis of organosolv lignin and polypropylene over in-situ red mud and ex-situ HZSM-5 in two-step catalytic micro reactor. *Appl Surf Sci.* 2020;511:145521. <https://doi.org/10.1016/j.apsusc.2020.145521>.
111. Zhao Y, Yang X, Fu Z, Li R, Wu Y. Synergistic effect of catalytic co-pyrolysis of cellulose and polyethylene over HZSM-5. *J Therm Anal Calorim.* 2020;140:363–71. <https://doi.org/10.1007/s10973-019-08633-7>.
112. Fan L, Ruan R, Li J, Ma L, Wang C, Zhou W. Aromatics production from fast co-pyrolysis of lignin and waste cooking oil catalyzed by HZSM-5 zeolite. *Appl Energy.* 2020;263:114629. <https://doi.org/10.1016/j.apenergy.2020.114629>.
113. Kim Y-M, Lee HW, Jae J, Jung KB, Jung S-C, Watanabe A, Park Y-K. Catalytic co-pyrolysis of biomass carbohydrates with LLDPE over Al-SBA-15 and mesoporous ZSM-5. *Catal Today.* 2017;298:46–52. <https://doi.org/10.1016/j.cattod.2017.06.006>.

114. Lee HW, Choi SJ, Park SH, Jeon J-K, Jung S-C, Kim SC, Park Y-K. Pyrolysis and co-pyrolysis of *Laminaria japonica* and polypropylene over mesoporous Al-SBA-15 catalyst. *Nanoscale Res Lett*. 2014;9:1–8. <https://doi.org/10.1186/1556-276X-9-376>.
115. Shafaghat H, Lee HW, Yang L, Oh D, Jung S-C, Rhee GH, Jae J, Park Y-K. Catalytic co-conversion of Kraft lignin and linear low-density polyethylene over mesoZSM-5 and Al-SBA-15 catalysts. *Catal Today*. 2020;355:246–51. <https://doi.org/10.1016/j.cattod.2019.04.052>.
116. Wu Q, Wang Y, Jiang L, Yang Q, Ke L, Peng Y, Yang S, Dai L, Liu Y, Ruan R. Microwave-assisted catalytic upgrading of co-pyrolysis vapor using HZSM-5 and MCM-41 for bio-oil production: Co-feeding of soapstock and straw in a downdraft reactor. *Bioresour Technol*. 2020;299:122611. <https://doi.org/10.1016/j.biortech.2019.122611>.
117. Hu Y, Wang H, Lakshmikandan M, Wang S, Wang Q, He Z, Abomohra AE-F. Catalytic co-pyrolysis of seaweeds and cellulose using mixed ZSM-5 and MCM-41 for enhanced crude bio-oil production. *J Therm Anal Calorim*. 2020;143:827–42. <https://doi.org/10.1007/s10973-020-09291-w>.
118. Chi Y, Xue J, Zhuo J, Zhang D, Liu M, Yao Q. Catalytic co-pyrolysis of cellulose and polypropylene over all-silica mesoporous catalyst MCM-41 and Al-MCM-41. *Sci Total Environ*. 2018;633:1105–13. <https://doi.org/10.1016/j.scitotenv.2018.03.239>.
119. Li Y, Xing X, Ma P, Zhang X, Wu Y, Huang L. Effect of alkali and alkaline earth metals on co-pyrolysis characteristics of municipal solid waste and biomass briquettes. *J Therm Anal Calorim*. 2020;139:489–98. <https://doi.org/10.1007/s10973-019-08278-6>.
120. Kay Lup AN, Abnisa F, Daud WMAW, Aroua MK. A review on reaction mechanisms of metal-catalyzed deoxygenation process in bio-oil model compounds. *Appl Catal A Gen*. 2017;541:87–106. <https://doi.org/10.1016/j.apcata.2017.05.002>.
121. Zheng Y, Wang J, Liu C, Lu Y, Lin X, Li W, Zheng Z. Catalytic copyrolysis of metal impregnated biomass and plastic with Ni-based HZSM-5 catalyst: synergistic effects, kinetics and product distribution. *Int J Energy Res*. 2020;44:5917–35. <https://doi.org/10.1002/er.5370>.
122. Iliopoulou EF, Stefanidis SD, Kalogiannis KG, Delimitis A, Lappas AA, Triantafyllidis KS. Catalytic upgrading of biomass pyrolysis vapors using transition metal-modified ZSM-5 zeolite. *Appl Catal B Environ*. 2012;127:281–90. <https://doi.org/10.1016/j.apcatb.2012.08.030>.
123. Ghorbannezhad P, Park S, Onwudili JA. Co-pyrolysis of biomass and plastic waste over zeolite- and sodium-based catalysts for enhanced yields of hydrocarbon products. *Waste Manag*. 2020;102:909–18. <https://doi.org/10.1016/j.wasman.2019.12.006>.
124. Zheng Y, Tao L, Yang X, Huang Y, Liu C, Zheng Z. Insights into pyrolysis and catalytic co-pyrolysis upgrading of biomass and waste rubber seed oil to promote the formation of aromatics hydrocarbon. *Int J Hydrog Energy*. 2018;43:16479–96. <https://doi.org/10.1016/j.ijhydene.2018.07.079>.
125. Lin X, Kong L, Ren X, Zhang D, Cai H, Lei H. Catalytic co-pyrolysis of torrefied poplar wood and high-density polyethylene over hierarchical HZSM-5 for mono-aromatics production. *Renew Energy*. 2021;164:87–95. <https://doi.org/10.1016/j.renene.2020.09.071>.
126. Lin X, Zhang D, Ren X, Zhang Q, Cai H, Yi W, Lei H. Catalytic co-pyrolysis of waste corn stover and high-density polyethylene for hydrocarbon production: The coupling effect of potassium and HZSM-5 zeolite. *J Anal Appl Pyrolysis* 150:art. 104895. 2020; <https://doi.org/10.1016/j.jaap.2020.104895>.
127. Cao Q, Jin L, Bao W, Lv Y. Investigations into the characteristics of oils produced from co-pyrolysis of biomass and tire. *Fuel Process Technol*. 2009;90:337–42. <https://doi.org/10.1016/j.fuproc.2008.10.005>.
128. Ryu HW, Tsang YF, Lee HW, Jae J, Jung S-C, Lam SS, Park ED, Park Y-K. Catalytic co-pyrolysis of cellulose and linear low-density polyethylene over MgO-impregnated catalysts with different acid-base properties. *Chem Eng J*. 2019;373:375–81. <https://doi.org/10.1016/j.cej.2019.05.049>.

129. Ahmed MHM, Batalha N, Qiu T, Hasan MM, Atanda L, Amiralian N, Wang L, Peng H, Konarova M. Red-mud based porous nanocatalysts for valorisation of municipal solid waste. *J Hazard Mater* 396:art. 122711. 2020; <https://doi.org/10.1016/j.jhazmat.2020.122711>.
130. Sanahuja-Parejo O, Veses A, Navarro MV, López JM, Murillo R, Callén MS, García T. Catalytic co-pyrolysis of grape seeds and waste tyres for the production of drop-in biofuels. *Energy Convers Manag.* 2018;171:1202–12. <https://doi.org/10.1016/j.enconman.2018.06.053>.
131. Veses A, Sanahuja-Parejo O, Navarro MV, López JM, Murillo R, Callén MS, García T. From laboratory scale to pilot plant: Evaluation of the catalytic co-pyrolysis of grape seeds and polystyrene wastes with CaO. *Catal Today*, in press. 2020; <https://doi.org/10.1016/j.cattod.2020.04.054>.
132. Sanahuja-Parejo O, Veses A, Navarro MV, López JM, Murillo R, Callén MS, García T. Drop-in biofuels from the co-pyrolysis of grape seeds and polystyrene. *Chem Eng J.* 2019;377:120246. <https://doi.org/10.1016/j.cej.2018.10.183>.
133. Anellotech Inc. Sustainable technology company, New York [Internet]. Date accessed 2021. <https://anellotech.com/>
134. Marker TL, Felix LG, Linck MB, Roberts MJ. Integrated hydropyrolysis and hydroconversion (IH 2) for the direct production of gasoline and diesel fuels or blending components from biomass. Part 1: Proof of principle testing. *Environ Prog Sustain Energy.* 2012;31:191–9. <https://doi.org/10.1002/ep.10629>.
135. Marker TL, Felix LG, Linck MB, Roberts MJ, Ortiz-Toral P, Wangerow J. Integrated hydropyrolysis and hydroconversion (IH2®) for the direct production of gasoline and diesel fuels or blending components from biomass. Part 2: Continuous testing. *Environ Prog Sustain Energy.* 2014;33:762–8. <https://doi.org/10.1002/ep.11906>.
136. Park JY, Kim J-K, Oh C-H, Park J-W, Kwon EE. Production of bio-oil from fast pyrolysis of biomass using a pilot-scale circulating fluidized bed reactor and its characterization. *J Environ Manage.* 2019;234:138–44. <https://doi.org/10.1016/j.jenvman.2018.12.104>.
137. Miranda NT, Dianin LM, Fernandes DS, Filho RM, Maciel MRW. Experimental study on sugarcane bagasse pyrolysis in a thermochemical processes pilot plant. *Chem Eng Trans.* 2020;80:37–42. <https://doi.org/10.3303/CET2080007>.
138. Treedet W, Suntivarakorn R. Design and operation of a low cost bio-oil fast pyrolysis from sugarcane bagasse on circulating fluidized bed reactor in a pilot plant. *Fuel Process Technol.* 2018;179:17–31. <https://doi.org/10.1016/j.fuproc.2018.06.006>.
139. Pfitzer C, Dahmen N, Tröger N, Weirich F, Sauer J, Günther A, Müller-Hagedorn M. Fast pyrolysis of wheat straw in the bioliq pilot plant. *Energy Fuel.* 2016;30:8047–54. <https://doi.org/10.1021/acs.energyfuels.6b01412>.
140. Dayton DC, Carpenter JR, Kataria A, Peters JE, Barbee D, Mante OD, Gupta R. Design and operation of a pilot-scale catalytic biomass pyrolysis unit. *Green Chem.* 2015;17:4680–9. <https://doi.org/10.1039/C5GC01023C>.
141. Veses A, Aznar M, Martínez I, Martínez JD, López JM, Navarro MV, Callén MS, Murillo R, García T. Catalytic pyrolysis of wood biomass in an auger reactor using calcium-based catalysts. *Bioresour Technol.* 2014;162:250–8. <https://doi.org/10.1016/j.biortech.2014.03.146>.

Chapter 3

Roadmap to Low-Cost Catalytic Pyrolysis of Plastic Wastes for Production of Liquid Fuels



Oraléou Sangué Djandja, Dabo Chen, Lin-Xin Yin, Zhi-Cong Wang,
and Pei-Gao Duan

Abstract Catalytic pyrolysis is an emerging process that can help eliminate the harmful effects of plastic wastes by turning them into liquid fuels. This chapter presents an overview of low-cost catalytic processing of plastic wastes with a focus on biomass-derived activated carbons (BACs) as low-cost catalysts. BACs are cost-effective, environmentally friendly and exhibit high porosity, flexibility of surface modification, and heteroatom surface functional groups, making them versatile as catalysts. Types of biomass, chemical reagents used for activation, reagent to biomass ratio and activation temperature influence the catalytic properties of BACs. Excessive reagent to biomass ratio leads to a high number of acid sites on the BAC that enhance cracking reactions and decrease liquid yield. Extreme activation temperature promotes degradation and volatilization of acid functional groups and thus, reduces catalytic activity. Overall, enhanced aromatization, hydrogen transfer and cracking reactions have been observed over biomass-derived BACs that exhibit strong acidity, large surface area, and large total pore volume. Coprocessing of plastic wastes with lignocellulosic biomass is a good option for reducing the activation energy of plastic waste decomposition and improving the composition of liquid fuels.

Keywords Plastic wastes · Catalytic pyrolysis · Activated carbon · Co-pyrolysis · Liquid fuel

O. S. Djandja · L.-X. Yin · Z.-C. Wang · P.-G. Duan (✉)

Shaanxi Key Laboratory of Energy Chemical Process Intensification, School of Chemical Engineering and Technology, Xi'an Jiaotong University, Xi'an, Shaanxi, People's Republic of China

e-mail: pgduan@xjtu.edu.cn

D. Chen

New More Graphene Application Technology Co., Ltd., Jinhua, Zhejiang, People's Republic of China

3.1 Introduction

According to the World Bank, 2.01 billion tons of solid wastes including 242 million tons of plastic wastes were generated in 2016, of which more 33% were not properly managed, are responsible for 1.6 billion tons of CO₂-equivalent greenhouse gas emissions, which is about 5 percent of global emissions [1]. Table 3.1 presents statistics about wastes generated around the world. It can be seen that large amounts of wastes are released in the world, and significant growth in generation is expected given the increasing population and industrial development. Statistics of each type of waste vary according to region due to different kinds of activities and regulation policies. In all regions presented, the wastes are disposed of mainly by open dumping and landfill, which could explain the higher greenhouse gas emissions associated with these wastes. In most regions, plastic wastes account for about 12% of all solid wastes—nevertheless, plastics contributing enormously to our daily activities. Durability, flexibility, strength, lightness, ability to be molded into different shapes, and endurance (thermal, electrical and chemical) are some physicochemical characteristics that make plastics attractive [2]. In 2015, polyolefins accounted for about 55% of global plastics materials demand, namely, 23% for Polypropylene

Table 3.1 Global solid waste management in 2016 with projections to 2050 [1]

Regions	Amount of waste generated by region (millions of tons per year)			Waste collection coverage (%)	Share of plastic (mass fraction, %) 2016	Share of most represented waste treatment method		Share (%) of recycling in the treatment method
	2016	2030	2050			Method	(%)	
Middle East and North Africa	129	177	255	82	12	Open dumping	52.7	9
Sub-Saharan Africa	174	269	516	44	8.6	Open dumping	69	6.6
Latin America and the Caribbean	231	290	369	84	12	Landfill	68.5	4.5
North America	289	342	396	99.7	12	Sanitary landfill	54.3	33.3
South Asia	334	466	661	51	8	Open dumping	75	5
Europe and Central Asia	392	440	490	90	11.5	Landfill	25.9	20
East Asia and Pacific	468	602	714	71	12	Landfill	46	9
Global	2010	2590	3040		12	Landfill	36.7	13.5

(PP), 15% for high-density polyethylene (HDPE) and 17% for low-density polyethylene (LDPE) and linear low-density polyethylene (LLDPE), followed by 16% for polyvinyl chloride (PVC), 6% for polyurethane (PUR), 7% for polyethylene terephthalate (PET) and 7% for polystyrene (PS) and expanded polystyrene (EPS) [3]. The share of a total loss to the environment per year for PE, PP, PVC, PET, PS, PUR are estimated to be 20%, 14%, 3%, 6%, 4%, and 1%, respectively [4], which shows that the most abundant plastic materials in demand are among the most abundant fractions of plastic wastes ending up in the environment. In India, plastic wastes (daily generation of approximately 26,000 tons) accounts for 8% of the total solid waste annually generated, with more than 50% of these plastic wastes not recycled, and thus escaping into the environment [5]. In 2017, more than 70 million tons of plastic wastes were reported for China [6]. Hence, these plastic wastes required proper management.

Synthetic organic polymers in most plastic wastes are generally non-biodegradable. The large proportion of monomers used to produce plastics, such as ethylene and propylene, are made from fossil hydrocarbons. Thus, disposal of plastic wastes in landfills not only creates significant environmental issues, such as soil leaching and contamination of groundwater but also constitutes a major waste of fossil fuel resources. Although incineration can help to reduce the amount of plastic waste, costly treatment of large amounts of flue gases is required [7]. Although direct recycling processes are being developed, they are limited, in contrast to single component plastic waste. Real-world plastic waste is a mixture of many components, including PVC, PET, PE, PP, PS, and other types of waste that can be difficult to separate. Most of these components are not compatible with each other for processing together during direct recycling. They vary in polymer type, intermolecular bonding, and added inorganic fillers, stabilizers, and pigments that affect their mechanical properties [8]. Another reason is that they are made of different resin compounds and have different degrees of transparency and colors [9]. Subsequently, a significant fraction of plastic wastes collected for recycling cannot be processed, which is estimated to be 40% for post-consumer plastic wastes collected in the European Union in 2012 [10]. Given these limitations, new technologies that can turn plastic wastes into valuable resources in an optimized way are needed. These technologies would eliminate not only the harmful effects of plastic wastes but also create an opportunity to recover resources such as fuels and chemicals. Catalytic pyrolysis is one of these emerging technologies that can turn plastic wastes into high-quality liquid fuels in an environmentally friendly way, and that can help to alleviate energy shortages that the world is facing. However, widely used catalysts are expensive, and their deactivation readily occurs with waste plastics. Therefore, recent works are exploring new ways of low-cost catalysts design, including biomass-derived activated carbon (BAC).

This chapter aims to highlight the positive impact that can provide low-cost catalysts such as BAC and some industrial byproducts in the pyrolysis processing of plastic wastes for liquid fuels production and to provide areas of future research for further development. The advantages of the co-pyrolysis of plastic wastes with

lignocellulosic biomass and sewage sludge are briefly introduced to illustrate challenges in the pyrolysis of real-world plastic wastes.

3.2 Pyrolysis Processing of Plastic Wastes: Why and How?

3.2.1 Motivation Behind Pyrolysis Processing of Waste Plastics

Results of elemental and proximate analysis and higher heating value (HHV) of different types of plastic wastes are presented in Table 3.2. In fact, plastic wastes contain high-value chemicals and high energy density [11], with an HHV of (15–49) MJ/kg (Table 3.2). Ash is composed of inorganic matter that comes from materials employed for plastics manufacturing. Halogens in plastics include Cl, Br, and F, while the most important metals include Pb, Al, Sb, Ti, Sn, Zn, Fe, Ni, Cu, Cd, Cr, and Co. Sulfur and alkaline earth metal compounds such as Ca, Ba, Mg, are also present. Typical concentration ranges of these elements in each type of plastic are summarized in Ref. [12]. PE, PP, and PS have the highest volatile matter content and HHV, with almost no ash and fixed carbon, while PET has high carbon content but low hydrogen content [13]. Given the properties of plastic wastes and that large proportions of monomers for plastics manufacturing are made from fossil hydrocarbons, pyrolysis is a suitable method to recover fossil hydrocarbons from plastic wastes. A comparison of typical recycling and pyrolysis of plastic wastes is presented in Fig. 3.1. Pyrolysis processes can significantly increase the recycling rate as it can use a wider range of plastic wastes than traditional recycling [14]. Although pyrolysis is a mature technology for char generation from solid material [15, 16], it has been recently used extensively to produce liquid fuels (Fig. 3.2). As depicted in Fig. 3.2, the liquid oil obtained can be used as transportation fuels, burned to generate heat/electricity or used to synthesize value-added chemicals that can be used as fertilizers, resins, and light aromatics such as benzene, xylene, toluene and dl-limonene. These chemicals can also be obtained directly from the pyrolysis process, depending on chosen conditions, the catalyst employed, and feedstock type. By-products, including gaseous and solid char products, can be used in many fields, as showed in Fig. 3.2. During pyrolysis, the ash is melted, and inorganic compounds such as glass and heavy metals are mainly fixed in the solid product. They can be recovered as carbon black and reused for several applications such as additives or fillers for other plastics.

Table 3.2 Elemental and proximate analysis and HHV of subgroups of waste plastics

Waste plastic	Proximate analysis (mass fraction)					Ultimate analysis (mass fraction)					HHV (MJ/kg)	HHV (MJ/kg)	Refs.
	Moisture	Ash (%)	Volatile (%)	Fixed-carbon (%)	C (%)	H (%)	O (%)	N (%)	S (%)	Cl (%)			
PP	0.33	10.65	81.27	7.75	70.19	11.27	17.75	0.00	0.79	—	—	—	[17]
PE	—	0.06–0.60	98.96–99.94	0.00–0.48	84.97–86.66	13.26–14.57	0.00–0.32	< 0.70	< 0.70	0.30	37.60–46.48	—	[13]
PP	—	0.02–1.10	98.90–99.97	0.00–0.13	83.75–86.72	12.51–15.23	0.00–2.27	< 0.23	< 0.23	0.03	45.77–46.24	—	[17]
PS	—	0.01–0.51	99.39–99.57	0.00–0.60	89.06–92.14	7.68–10.02	0.00–1.80	0.00	< 0.00	0.37	38.93–40.12	—	[17]
PVC	—	< 14.99	65.06–95.16	4.80–20.47	37.81–41.79	4.25–5.83	0.00–0.21	0.01–0.23	< 0.23	1.25	52.46–57.66	15.88–22.57	—
PET	—	0.09–0.31	90.44–94.09	5.60–9.47	62.00–62.93	4.06–5.20	32.64–33.69	0.00–0.32	< 0.32	0.13	23.09	—	[1]
HDPE	—	—	—	—	85.70	14.30	0	—	—	—	43.00	—	[1]
PP	—	—	—	—	85.70	14.30	0	—	—	—	44	—	[1]
PET	—	—	—	—	62.50	4.20	33.30	—	—	—	24	—	[1]
PS	—	—	—	—	92.30	7.70	0	—	—	—	40	—	[1]
Mixture	—	—	—	—	84.40	12.90	2.70	—	—	—	42	—	[1]
PET	0.22	6.83	86.75	6.20	63.94	4.52	31.49	0.01	0.04	0	—	—	[9]
HDPE	0.01	0.22	99.77	0	86.99	12.12	0.56	0.27	0.07	0	—	—	[1]
PVC	0	9.11	85.77	5.12	37.24	4.99	0	0.08	0.08	57.61	—	—	[2]
LDPE	0.03	0.12	99.85	0	85.60	13.40	0.74	0.26	0	0	—	—	[2]
PP	0	0.36	99.64	0	86.88	12.50	0.32	0.28	0.03	0	—	—	[2]
PS	0	0.22	99.78	0	91.57	7.80	0.45	0.15	0.04	0	—	—	[2]
LDPE	—	19.25	79.99	0.76	—	—	—	—	—	—	44.25	—	[2]
HDPE	—	0.59	99.32	0.09	—	—	—	—	—	—	45.38	—	[2]
PP	—	0.05	99.68	0.27	—	—	—	—	—	—	46.05	—	[2]

(continued)

Table 3.2 (continued)

Waste plastic	Proximate analysis (mass fraction)					Ultimate analysis (mass fraction)					HHV (MJ/kg)	HHV (MJ/kg)	Refs.
	Moisture	Ash (%)	Volatile (%)	Fixed-carbon (%)	C (%)	H (%)	O (%)	N (%)	S (%)	Cl (%)			
HDPE	0.25	4.98	94.77	—	78.18	12.84	3.61	0.06	0.08	—	—	—	[18]
PP	0.40	1.06	98.54	—	83.74	13.71	0.98	0.02	0.08	—	—	—	
PS	0.20	0.50	99.30	—	90.40	8.56	0.18	0.07	0.08	—	—	—	[19]
PET	0.23	—	—	—	61.4 ± 2.4	4.32 ± 3.1	32.7 ± 0.4	0.052 ± 47	0.17	—	22.87	—	
HDPE	0.21	—	—	—	82.4 ± 3.6	15.2 ± 6.2	0.3 ± 8.6	0.063 ± 49	—	—	49.20	—	
PVC	0.46	—	—	—	35.6 ± 5.2	4.83 ± 3.6	4.1 ± 9.2	0.23 ± 136	—	—	19.05	—	
LDPE	0.54	—	—	—	87.3 ± 4.6	15.2 ± 7.1	0.2 ± 12.4	0.060 ± 46	—	—	46.95	—	
PP	0.30	—	—	—	79.1 ± 3.7	14.4 ± 11	1.7 ± 15	0.42 ± 60	0.15	—	49.42	—	
PS	0.57	—	—	—	93.5 ± 4.5	8.49 ± 7.0	0.2 ± 32	0.060 ± 46	—	—	42.13	—	
Other plastics	0.80	—	—	—	85.0 ± 4.4	15.0 ± 8.3	1.2 ± 4.7	0.064 ± 44	—	—	45.85	—	
HDPE	—	—	—	—	80.58	13.98	5.19	0.60	0.08	—	45.78	—	[20]
Real world plastic waste	1	28.20	—	—	58.70	8.70	—	0.50	< 0.1	1	30.60	—	[21]
Simulated mixture plastic waste	0.10	0	—	—	84.70	12.50	—	< 0.10	0.00	1.10	43.90	—	“not reported

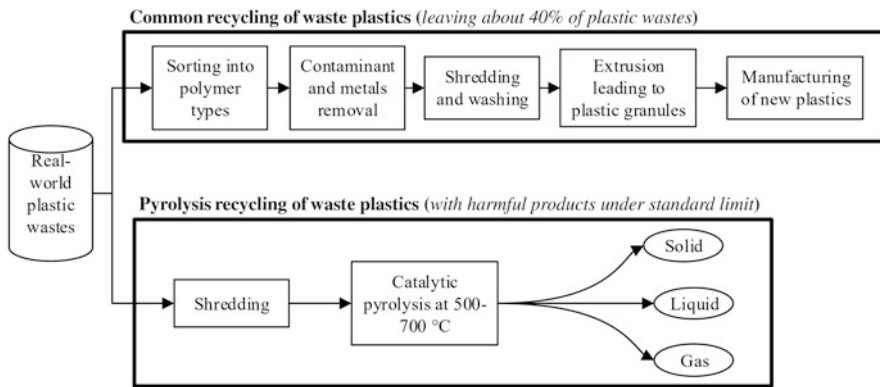


Fig. 3.1 Comparison of direct recycling and pyrolysis conversion of plastic wastes.

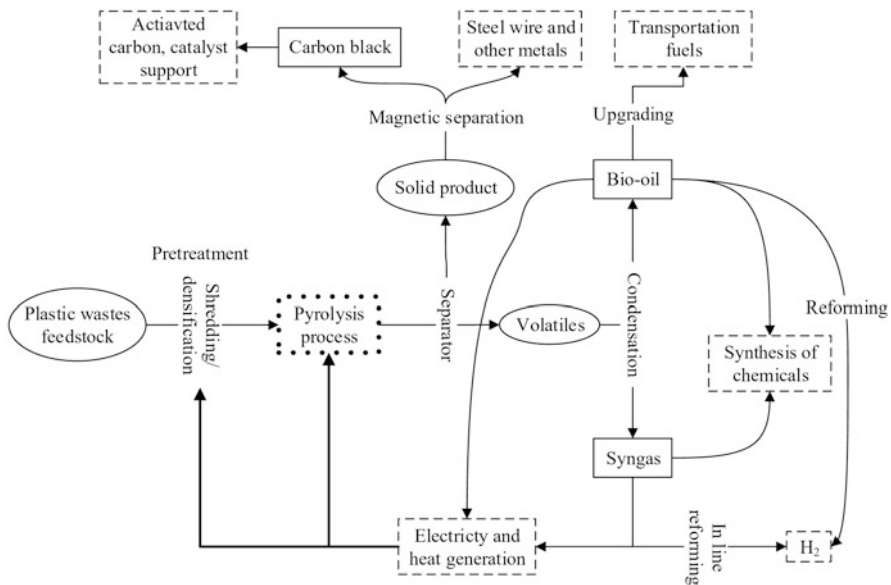


Fig. 3.2 Plastic wastes valorization through pyrolysis

3.2.2 Overview of Pyrolysis Processing of Plastic Wastes

The pyrolysis process refers to organic matter decomposition in an oxygen-free environment. The main factors impacting the distribution and properties of the resulting liquid product include reactor type, process temperature, residence time, heating rate, pressure, turbulence, and feedstock characteristics. Ranges of values and combined factors that are commonly reported are presented in Table 3.3. Although many works have reported on the influence of these factors on the

Table 3.3 Reaction conditions and expected products from pyrolysis processes [30–33]

Heating mode	Residence time	Heating rate (°C/s)	Temperature (°C)	Typical reactors	Expected products
Slow	>10 min	10	290–400	Cylindrical fixed-bed, batch, rotary kiln, and packed bed	30% of liquid, 35% of char, and 35% of gas
Intermediate	5–10 min	1–1000	400–500	Auger screw, vacuum, rotary ovens, microwave	50% of liquid, 25% of char, and 25% gas
Fast	0.5–5 s	10–200	425–650	Rotary kiln, bubbling fluidized bed, spouted fluidized bed, rotating cone, vortex, ablative, entrained microwave, and radiative/conductive reactors	Maximization of the bio-oil (60–75% of liquids, 12–25% of char, and 10–20% of gas)
Flash-liquid	< 1 s	>1000	> 650		Maximization of bio-oil with low water content
Flash-gas	< 1 s	>1000	> 650		Production of chemicals and gas
Ultra	< 0.5	Very high	1000	–	Production of chemicals, gas
Vacuum	2–30s	Medium	400	vacuum	Reduction of the nitrogen flow rate requirements, Maximization of the bio-oil (minimization of secondary reactions and the enhancement of the devolatilization process), the resulted char has more “open” structure and should be suitable for activated carbon production.
Hydro-pyro.	< 10s	High	< 500	–	Maximization of the bio-oil with an increased yield of hydrocarbons,
Methano-pyro.	< 10s	High	> 700	–	Production of chemicals

products, less information is available on the effect of turbulent flow conditions. Lower temperatures ($T < 700^{\circ}\text{C}$) yield solids and waxes/oil, while higher temperatures favor light molecular weight hydrocarbons and non-condensable gases. The effect of pressure is dominant at lower temperatures and reduces with increasing temperature. Char formation is predominant at a lower heating rate, while a higher heating rate enhances the bond cleavage. Computational models reveal that high turbulence promotes heat and mass transfer in the core flow, leading to a uniform distribution reaction [22]. Therefore, medium turbulence would promote liquid oil yield, while higher turbulence would result in extensive destruction of the tar [23]. Further investigations are needed to confirm reported observations. The low thermal conductivity and melting temperatures of plastics make the design of reactors very important, mainly from the viewpoint of heat and mass transfer [24]. TGA, TG-MS, TG-FTIR, and Py-GCMS studies can help to confirm the degradation ranges of plastics and the product trends and further set the pyrolytic conditions for macro-scale operations [25, 26]. Although batch reactors can provide information in terms of yields and quality on a lab scale, they are limited on an industrial scale given the relatively high operation cost associated with feedstock loading, product discharge and heat loss between different batches [24]. Reactors that can be adapted to continuous operation mode are more promising than batch mode reactors. Reactors commonly reported for plastics pyrolysis include bubbling fluidized bed, conical spouted bed, vacuum, stirred tank and screw/rotary kiln reactors [24, 27–29]. These reactors can provide high heat and mass transfer and sufficient solid mixing regimes. Although microwave pyrolysis is an attractive way for providing efficient heat transfer via core volumetric internal heating, this method has some disadvantages such as poor mixing, uncertain scale-up factors and requirements for mixing plastics with heat adsorbent materials such as graphitic carbon or inorganic oxides [25, 29]. However, a continuous microwave-assisted pyrolysis system has been proposed that combines microwave heating with a mixed SiC ball-bed as a promising system for energy recovery from plastic waste pyrolysis on an industrial scale [24]. For PVC, cascade reactors with two steps (a low-temperature step for dechlorination and a higher temperature step for degradation) are convenient [27].

Besides the above studies, many research works focus on the use of catalysts that can improve the composition and yield of the liquid oil. Over a high acidic catalyst and well-selected reaction conditions, long-chain polymers of plastic wastes can be easily degraded into smaller chain molecules via random chain scission, thereby improving oil quality. The mixing of plastic waste with other feedstocks is also another option that is being examined to promote liquid oil yield and to control the oil liquid composition.

3.3 Progress in Catalytic Pyrolysis of Plastic Wastes

3.3.1 Catalytic Pyrolysis Mechanism

Most plastic waste pyrolysis plants use high temperatures (700 °C) to moderate temperatures (500 °C) in the presence of a catalyst [2]. The use of catalysts can alter reaction kinetics during pyrolysis, helping to improve the properties of the pyrolysis oil. Many types of catalysts have been examined for plastic wastes pyrolysis. Metals impregnated fluid-cracking catalysts and acid silica-alumina and zeolites catalysts exhibit enhanced selectivity for aromatics and alkenes, while others such as MCM-41 and Al-MCM-41 promote yield and content of aliphatic compounds in the oil [34–37]. Further improved performance has been achieved in staged catalysis combining MCM-41 and ZSM-5 [34]. These catalysts promote carbocationic cracking of volatiles, and subsequent isomerization, cyclisation, oligomerization, aromatization and hydrogen transfer reactions [34, 35] to help achieve high quality and high yield oil at relatively low temperatures compared with non-catalytic pyrolysis. Acid strength, high specific surface area, and porosity of a catalyst are decisive factors for achieving high catalytic performance [35]. The high acidity and microporous structure of zeolites catalysts are responsible for forming lighter hydrocarbons [17, 38]. In fact, the microporous structure limits the range of higher molecular weight hydrocarbons that can enter the pores of the catalyst for the reaction [34]. Some recent papers have extensively discussed these catalysts [39, 40].

3.3.2 In-Situ and Ex-Situ Catalytic Pyrolysis

As shown in Fig. 3.3, catalytic pyrolysis of plastic wastes can be implemented as an in-situ or ex-situ process. For the in-situ process, the catalyst is mixed into the feedstock, and the mixture is pyrolyzed. The ex-situ process includes two main steps. In the first step, the plastic waste is separately pyrolyzed, which causes thermal degradation to produce relatively short chains radicals that undergo H shift and rearrangement reactions during cooling down to room temperature to form stable short polymers [35]. In the second step, products from thermal degradation are conveyed to a catalytic bed for upgrading into fuel compounds. Although the in-situ process is simple and does not require mechanical modification to existing reactors as well as offering low degradation temperatures, it is difficult to recover the catalyst from its mixture with the biochar. Also, high ash or metal elements contents in the plastic waste feedstock can promote catalyst deactivation [41]. The ex-situ catalytic pyrolysis requires an external catalytic bed and moderately high temperatures. However, ex-situ catalytic pyrolysis is a good option when processing high ash content plastic wastes as it favors the cracking reactions of pyrolytic volatiles and facilitates subsequent separation between catalyst and pyrolysis solid residues [35].

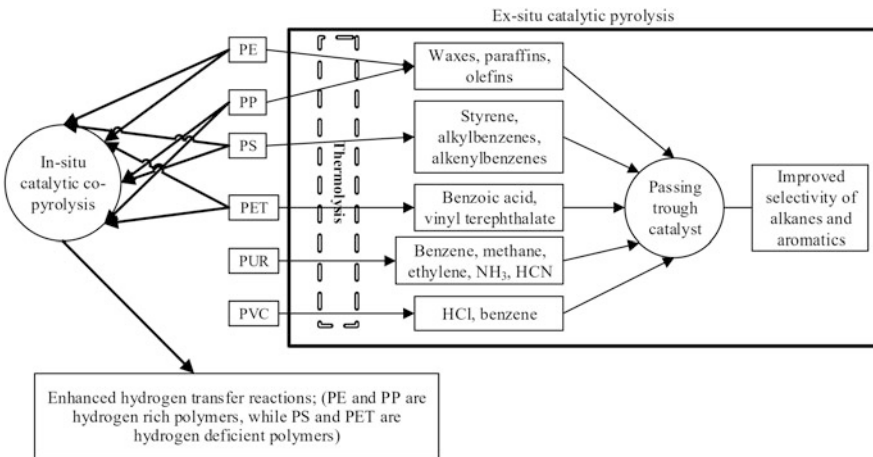


Fig. 3.3 Possible pathways during catalytic pyrolysis of plastic wastes [14, 35, 36, 41].

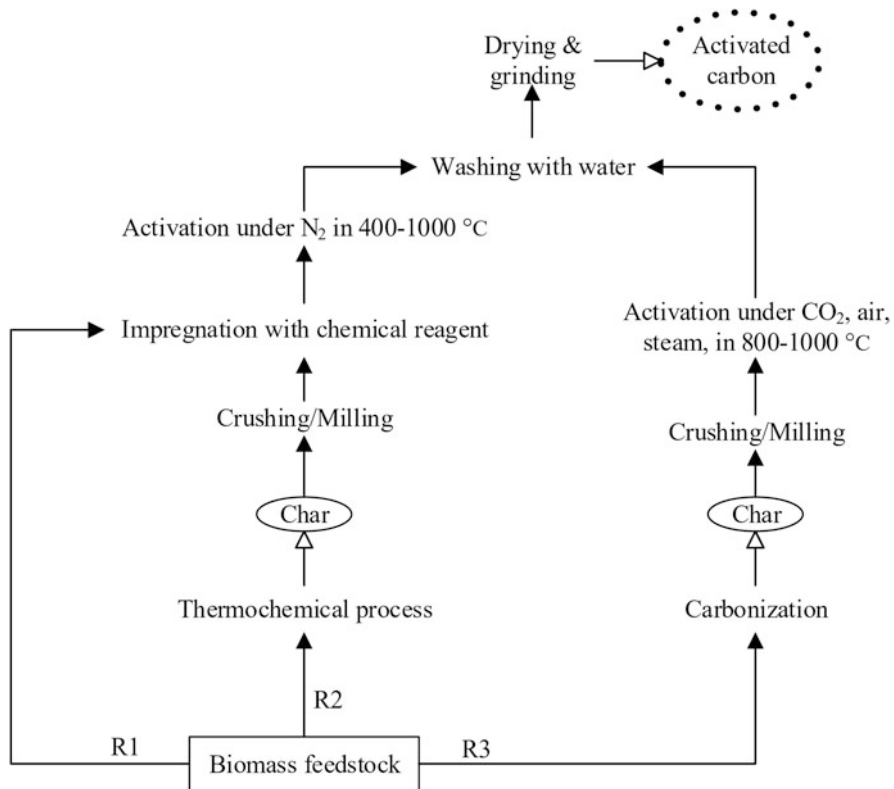
3.3.3 *Limits of Widely Used Catalysts and New Concepts About Catalyst Design for Waste Plastics Pyrolysis*

Despite the appreciable results with catalysts shown in Sect. 3.3.1, most of those approaches are expensive. Quick deactivation induced by coke formation and limited adaptability to feedstocks severely retard performance of many catalysts [36, 38]. Therefore, it still a challenge to develop cost-efficient catalysts. In recent years, activated carbons have received increased interest as catalysts [36, 42], due to their relatively low production cost, high porosity structure, and surface modification flexibility [36]. Enhanced aromatization, hydrogen transfer and cracking reactions can be observed over an activated carbon that exhibits at the same time strong acidity, large Brunauer-Emmett-Teller (BET) surface area, large total pore volume, and low percentage of micropores [35].

3.3.4 *Biomass-Derived activated Carbons as Catalysts for Plastic Waste Pyrolysis*

3.3.4.1 Preparation of Biomass-Derived Activated Carbons

As a material with a well-developed amorphous and porous texture, activated carbon is commonly used as an adsorbent in industries [43, 44]. These porous carbon materials constitute a large part of the support materials that are used to prepare heterogeneous catalysts [45]. Their inert nature, especially under strongly acidic and basic conditions, is an advantage as they do not decompose or only decompose very slowly, and given that the interaction between carrier and active phase such as noble



R1: Chemical activation; R2: Mixture; R3: Physical activation;

Fig. 3.4 Typical preparation steps for biomass activated carbon (BAC)

metals is small and that their pore size distribution and the chemical properties of their surface can be adjusted (polarity and hydrophobicity) according to the intended application, the possibility to recover the metal particles by simply burning the carbon support, are some of the motivations behind their application as catalyst supports. However, commercial activated carbons, having a small surface area and poor adsorption properties, cannot provide good performance in the aforementioned applications [46]. Thus, authors have explored many kinds of biomass feedstocks, including coal, wood, and agriculture wastes, to produce BACs for catalyst or catalyst support applications [45]. Besides being cost-effective and environmentally friendly, BACs are characterized by high porosity and heteroatom surface functional groups, making them suitable as catalysts or as catalyst supports [47].

As depicted in Fig. 3.4, activation of biomass for BAC preparation is commonly performed by physical or chemical activation or a combination of the two methods [48]. In physical activation, biomass is subjected to carbonization, and the obtained char is activated at high temperatures in the second stage with steam, air or CO_2 . In chemical activation, carbonization and activation processes occur in a single step and

at relatively lower temperatures making the process faster [48, 49]. In the third method that can be used for activation, the biomass feedstock is subjected to carbonization, and the resulting biochar is impregnated with a chemical reagent for activation. This can be qualified as a mixture of physical and chemical activation processes and is usually applied to biochar obtained from thermochemical treatment of biomass where other products are expected besides the biochar.

The BAC produced via chemical activation usually has a high specific surface area, good pore development, and the method gives a high carbon yield compared with that of physical activation [48, 49]. In fact, in chemical activation methods, suitable modifications are made by the addition of chemical dehydrating reagents to the biomass and the entire feedstock is then decomposed in an inert atmosphere [49, 50]. To date, the chemical method is widely employed for BAC preparation for plastic waste pyrolysis. To achieve good quality BAC (textural and surface properties), careful attention is required to a selection of the type of biomass and to the activation conditions.

Biomass used for BAC should contain high carbon and low inorganic (ash) content [43, 50–52], and it should be cheap, abundant, and able to be easily activated. A wide variety of BAC with different characteristics can be obtained from low-cost biomass, including cherry stones [51], nutshells and fruit stones [50], bamboo, wheat straw, corn cobs, almond shells, sewage sludge, sugar cane bagasse, grape processing industry waste, date stones, and coconut shells [49]. Differences in cellulose, lignin and holocellulose content in the biomass impact the pore structure and pore size distribution of the resulting BAC [43]. Biomass with a low-density and a high volatile matter content can promote pore volume but decrease bulk density [50]. Biomass with high bulk density, such as coconut shells or fruit stones, provides a non-graphitizable activated carbon in granular form with a large pore volume and can be used in many applications such as catalysts or catalyst support or materials for supercapacitor electrodes. As shown in Table 3.4, at appropriate activation conditions, corn cob, chestnut shell and wood chips provide BACs that exhibit good catalytic properties on liquid oil obtained from pyrolysis of plastic wastes.

Activation with H_3PO_4 is commonly used for lignocellulosic material and at lower temperatures [55]. Other reagents, such as zinc chloride ($ZnCl_2$), potassium hydroxide (KOH) and iron chloride ($FeCl_3$) have been examined with promising results [44]. For each type of biomass, there is an optimal value of activation agent (H_3PO_4) to biomass ratio to keep for activation. At a very low ratio, biomass is hardly destroyed, and pores are barely formed. Increasing the H_3PO_4 to biomass ratio below the optimal value enhances BET surface area, micropore volume and acidity of the resulting BAC. In contrast, at a ratio higher than the optimal value, micropores react with excessive H_3PO_4 to convert into mesopores and macropores [56], or some compounds such as phosphorus pentoxide are formed and block the pore structure, decreasing the area and volume of micropores [54]. Especially for liquid oil production, a very high number of acid sites on the BAC promotes C-C random scission and cracking and rearrangement reactions, which would decrease the liquid yield.

Table 3.4 Impact of activated carbon (AC) activation conditions and subsequent plastic waste pyrolysis on liquid oil properties

Activation conditions			Properties of AC			catalytic pyrolysis conditions			liquid oil properties		
Activation reagent	Reagent to feedstock ratio	T (°C)	BET surface (m ² /g)	Total pore volume (cm ³ /g)	d (nm)	Feed	T (°C)	Ex-situ	Weight ratio of catalyst to plastic waste	Yield (%)	Selectivity (area %)
Biomass	H ₃ PO ₄	0.6	500	721.87	0.424	2.35	LDPE	500	1	60	51.9% of ARH (<C17); 41.47% of C8-C16 alkanes; 4.05% of C17-C23 alkanes
Corn cob		0.8	550.17 (with acidity of 0.4422 mmol/g)	0.426	3.1				0.6	77.3	32% of ARH (<C17); 56.63% of C8-C16 alkanes; 7.99% of C17-C23 alkanes
		0.8							0.8	75.6	48.93% of ARH (<C17); 35.98% of C8-C16 alkanes; 12.7% of C17-C23 alkanes
		0.8							1	75.3	54.2% of ARH (<C17); 39.11% of C8-C16 alkanes; 3.7% of C17-C23 alkanes
		0.8							1.5	42	72.8% of ARH (<C17); 22.25% of C8-C16 alkanes; 0% of C17-C23 alkanes
		1.6	950.41 (with acidity of 0.3733 mmol/g)	1.145	4.82				1	63.3	43.81% of ARH (<C17); 41.62% of C8-C16 alkanes; 12.19% of C17-C23 alkanes

		0.8	400	1454.73	0.978	2.69			1	60	44.25% of ARH (<C17); 48.21% of C8-C16 alkanes; 4.63% of C17-C23 alkanes
		0.8	600	775.91	0.376	1.94			1	49	59.21% of ARH (<C17); 30.21% of C8-C16 alkanes; 9.07% of C17-C23 alkanes
Chestnut shell	H ₃ PO ₄	0.4	850	752.52	0.511	2.715	LDPE	Ex-situ 550	1	55.5	31.63% of mono-ARH (<C17); 41.33% of total ARH (<C17); 58.16% of ALH (<C17)
		0.6	850	1147.37	0.677	2.362			1	53	50% of mono-ARH (<C17); 68.87% of total ARH (<C17); 31.12% of ALH (<C17)
		0.8	750	1137.88	0.601	2.111			1	53.5	41.21% of mono-ARH (<C17); 60.48% of total ARH (<C17); 39.52% of ALH (<C17)
		0.8	850	1413.02	0.738	2.09			0.5	53.5	38.39% of mono-ARH (<C17); 58.93% of total ARH (<C17); 41.07% of ALH (<C17)
		0.8							1	44	63.53% of mono-ARH (<C17); 95.88% of total ARH (<C17); 4.12% of ALH (<C17)

(continued)

Table 3.4 (continued)

Activation conditions			Properties of AC			catalytic pyrolysis conditions			liquid oil properties				
Biomass	Activation reagent	Reagent to feedstock ratio	T (°C)	BET surface (m ² /g)	Total pore volume (cm ³ /g)	d (nm)	Feed	T (°C)	Weight ratio of catalyst to plastic waste	Yield (%)	Selectivity (area %)	Refs.	
0.8	0.8	0.8	950	1460.24	0.749	2.05	1	35	52.86% of mono-ARH (<C17); 75.00% of total ARH (<C17); 26.74% of ALH (<C17)	38	45.41% of mono-ARH (<C17); 63.77% of total ARH (<C17); 36.73% of ALH (<C17)	[36]	
1	ZnCl ₂	1	850	1489.99	0.924	2.481				61.6	40.9% of alkenes; 23.4% of alkanes; 35.1% of ARH		
										0.25	51.8	23.8% of alkenes; 27% of alkanes; 47.5% of ARH	

ARH aromatic hydrocarbon; ALH aliphatic hydrocarbon

Activation temperature is responsible for the carbonization of the biomass and is an important factor in the production of BAC. Carbonization leads to a decrease in volatile matter content of the biomass and increases elemental carbon content and the formation of pores [49]. Compared with conventional heating, microwave heating offers advantages such as uniform heating [46], rapid heating, negligible energy loss and an easily controllable heating process [52]. Increasing temperature enhances the devolatilization process, destroying BAC's surface to a different extent with more pores that can enlarge BET surface area resulting in more active sites. Above the optimal temperature (e.g., 850 °C for chestnut shell [54]; 500 °C for corncob [56]), increasing temperature enhances the reaction rate of C-H₃PO₄ and breaks up some acid functional groups that are volatilized.

3.3.4.2 Pyrolysis of Plastic Wastes Over Biomass-Derived Activated Carbon Catalysts

The use of BACs as catalysts is attracting attention in the processing of plastic wastes. Good results have been pointed out by authors, making this way of catalyst design a promising way for enhanced recycling of plastics wastes. The significant catalytic effect of these alternatives low-cost catalysts is mainly attributed to the conditions of activation and carbonization. From Table 3.4, one can see that at some given conditions, BAC exhibits good quality and can promote yield and improved properties of the liquid oil. Wan et al. [53] examined LDPE pyrolysis in a fixed bed reactor at 500 °C over corncob BACs (activation with H₃PO₄). Without a catalyst, the liquid produced by pyrolysis of LDPE (86.7% yield) turned into solid white wax at room temperature. BACs prepared through different temperatures (400 °C to 700 °C) and H₃PO₄ to corncob ratios (0.2–1.6) had different pore size distributions and acidities, corresponding to changes in their product distributions. At a catalyst to LDPE ratio of 1, the BAC prepared at 500 °C and H₃PO₄ to corncob ratio of 0.8 provided the highest liquid yield with 93.13 area % of jet fuel-range hydrocarbons. In comparison, BACs obtained at 400 °C and 600 °C with H₃PO₄ to corncob ratio of 0.8 produced a liquid yield of 60% (highest alkane content, 48.2 area %) and 49% (highest aromatic content, 59.2 area %), respectively. Overall, BACs prepared at 500 °C and ratio of 0.8 were found suitable, which can be attributed to the relative stronger acidity (0.4422 mmol/g) of the material. By varying the catalyst to LDPE ratio from 0.3 to 1.5, liquid yield gradually decreased from 82% to 42%. The content of C₈-C₂₃ alkanes in the liquid also decreased (C₁₇-C₂₃ completely absent at a ratio of 1.5). In contrast, the aromatic content gradually increased to reach a maximum of 72.8 area % at a ratio of 1.5. These results imply that a higher catalyst to LDPE ratio increased the number of acid sites, which enhances aromatic cyclization, and scission reactions converting long-chain hydrocarbons into lighter ones. An excessive amount of acid sites decreases liquid yield at the expense of increasing the amount of gaseous product. Duan et al. [54] pyrolyzed LDPE at 550 °C over chestnut shell BAC (H₃PO₄/ chestnut shell ratio of 0.8) at a catalyst to LPDE ratio of 1. The authors observed that when using BACs activated at 550 °C and 650 °C,

the obtained liquid oils remained in the solid phase at room temperature. For BACs at high activation temperatures (750 °C to 950 °C), the BET surface area and total volume of the BAC were enhanced, promoting the catalytic reaction of volatiles and liquid yields decreased from 55.5 (thermal process) to 38%, while quality was improved. The best results were found for BACs activated at 850 °C, which led to 44% of the liquid with 63.5 and 32.5 area % of mono-aromatics and polyaromatics, respectively. It was also found that the liquid yield decreased for BACs obtained with increasing H₃PO₄/ chestnut shell ratio from 0.4 to 1 (catalytic pyrolysis at 550 °C and catalyst to LPDE ratio of 1). The mono-aromatics and polyaromatics content in the liquid increased gradually for ratios from 0.4 to 0.8 and decreased thereafter. Zhang et al. [35] investigated the catalytic effect of corn stover BAC (H₃PO₄ to corn stover ratio of 0.85) for pyrolysis of LDPE in a fixed bed at 500 °C. At a catalyst to LDPE ratio of 2.5, the prepared BACs produced more content of aromatic hydrocarbons (<C₁₆) and C₁₇-C₂₃ alkanes, and lower contents of C₈-C₁₆ alkanes, in comparison to five commercial activated carbons, except one that was also activated with H₃PO₄ and produced high aromatic hydrocarbon content (36.4 area %). The selectivity of alkanes and aromatic hydrocarbons in the liquid obtained when the prepared BACs were used accounted for 48.0 and 28.7 area %, respectively.

These results show that biomass-derived AC rich in P-containing functional groups are favorable for aromatization reactions, and moreover, P-containing functional groups can also provide effective catalytic acid sites (such as -C=O and -PO) that could promote the C-C and C-H bond cracking of LDPE, resulting in the production of relatively light alkanes. For each type of AC, there is an optimal catalyst to plastic wastes ratio. Ratios lower than this optimal value promote catalytic activity that favors liquid product quality, while at ratios higher than this optimal value, a very high number of acid sites are offered, which accelerates C-C random scission and cracking and rearrangement reactions [54], which increases the content of aliphatics while decreasing aromatics.

The desire to achieve a more eco-efficient process has lead researchers to investigate the mixing of alternative BAC catalysts with other low-cost catalysts. In this regard, Huo et al. [42] explored ex-situ catalytic pyrolysis of LDPE over a mixture of corncob BAC (activation with H₃PO₄ at 600 °C) and MgO. The placement of the catalysts and catalyst to LDPE ratio (0.1, 1, 2, and 3) were examined at 500 °C. Although homogeneous mixing of these catalysts provided a high liquid yield (81%), the liquid was, unfortunately, mainly composed of waxes. The base catalyst MgO blocks the pore structure of the acidic BAC, inhibiting its catalytic effect for the pyrolysis process. When pyrolytic volatiles first flowed through MgO and then BAC, the liquid yield was 72%, and almost 100% of the liquid belonged to fuel hydrocarbons with the selectivity of aromatic hydrocarbons (<C₁₆), and C₈-C₁₆ and C₁₇-C₂₃ alkanes accounting for (33.4, 65.3, and 1.3) area %, respectively. The large average pore size of MgO favors long-chain hydrocarbons, which further undergoes cracking and aromatization over-acidic sites of BAC to produce C₈-C₁₆ alkanes along with aromatic hydrocarbons(<C₁₆). In contrast, when pyrolytic volatiles first flowed through AC and then MgO, the selectivity of aromatic

hydrocarbons ($<\text{C}_{16}$), and $\text{C}_8\text{-}\text{C}_{16}$ and $\text{C}_{17}\text{-}\text{C}_{23}$ alkanes were (18.1, 58.9 and 20.8) area %, respectively, which suggests that the remaining long-chain hydrocarbons from the reaction over AC flowed through the large pore of MgO to form diesel range alkanes. The authors also noticed that at low catalyst to LDPE ratios (0, 0.5, and 1) for AC to MgO ratio=1, waxes were the main product. With increasing catalyst to LDPE ratio from 2 to 3, no waxes were formed, but the liquid yields decreased. The content of alkanes decreased from 66.6 to 61.2 area %, while the content of aromatic hydrocarbons ($<\text{C}_{16}$) increased from 33.4 to 38.8 area %. The selectivity of mono-ring aromatic hydrocarbons increased to reach a maximum of 29.3 area % at a ratio of 3, which can be attributed to an increase in acidic sites according to the amount of catalyst that promotes cleavage of C-C bonds.

BAC activated with ZnCl_2 has also been tested for pyrolysis of plastic wastes. Sun et al. [36] conducted catalytic pyrolysis of mixed plastic wastes over wood chip BAC (activated with ZnCl_2 at 600 °C, ZnCl_2 / wood chip ratio of 1). The non-catalytic process yielded 61.6% of the liquid with the high alkenes (40.9 area %), while alkanes and aromatics accounted for 23.4 and 35.1 area %, respectively. The use of BAC reduced the liquid yield to 51.8% and its alkenes, while the selectivity of alkanes and aromatics were improved to 27 and 47.5 area %, respectively. The selectivity of two-ring aromatics was enhanced to 90.7 area % of aromatics, with 1,3-diphenylpropane occupying the highest area (40.9%). Zn species introduced on the BAC during activation promotes the formation of Lewis acid sites, which enhances the transformation of alkenes into aromatic and alkanes through dehydrogenation, hydrogen transfer, alkylation and Diels–Alder reactions.

3.3.5 Pyrolysis of Waste Plastics with Other Low-Cost Material Catalysts

Another means to increase the efficiency and the rate of waste recycling is to make all kinds of waste profitable. In this regard, some industrial and municipal wastes are being employed as catalyst or co-feedstock in the pyrolysis processing of waste plastics. López et al. [57] used red mud, which is an inexpensive by-product of the alumina industry, as a catalyst to pyrolyze a mixture of plastic wastes with mass fractions of 40% PE, 35% PP, 18% PS, 4% PET and 3% PET. The red mud was mostly composed of metal oxides (Fe_2O_3 (36.5%), Al_2O_3 (23.8%), TiO_2 (13.5%), SiO_2 (8.5%), CaO (5.3%), Na_2O (1.8%)). The catalytic effect of red mud was significant at 500 °C, while no positive contribution was observed at 440 °C. At 500 °C, red mud catalyst provided more liquid yield (57%) than ZSM-5 (39.8 wt.%), while the non-catalytic process provided 65.2%. The selectivity of aromatic compounds in the liquid obtained at 500 °C with red mud was 89.6 area %, higher than that obtained from the non-catalytic run (73.9 area %) and lower than that from ZSM-5 (98.4 area %). The range of the liquid carbons from the red mud catalytic run was the same as the zeolite ($\text{C}_7\text{-}\text{C}_{16}$), while the non-catalytic run liquid reached C_{19} .

compounds. The Fe_2O_3 and TiO_2 present in red mud promoted hydrogenation of styrene to produce ethyl-benzene, while the acid nature of Al_2O_3 and SiO_2 promoted cracking reactions of styrene to form toluene. Na_2O may hinder the catalytic activity of red mud. Overall, the cracking ability of red mud is lower than that of the zeolite. Fekhar et al. [27] also mentioned a significant reduction of the concentration of chlorinated compounds and the acid number at higher ratios of red mud: $\text{Ca}(\text{OH})_2\text{-Ni}/\text{ZSM-5}$ (0.5:0.25:0.25 and 0.25: 05:0.25) mixed catalyst, after having pyrolyzed a mixture of HDPE, LDPE, and PVC at 550 °C. These ratios promoted light oil and HHV while decreasing heavy oil content. A slight improvement in the liquid oil properties was reported by Luo et al. [17], who pyrolyzed a reworked PP at 600 °C over HCl-modified low-cost kaolin as a catalyst. Compared to the non-catalytic process and the use of non-modified kaolin, the HCl-modified kaolin improved the cracking of heavy components into diesel range components (alkanes and alkenes). HCl modification enhances the catalytic effect via the increase of the number of Al-O and Si-O bonds on the kaolin, which not only promotes the decomposition of PP through b-scission reaction and carbonium ion mechanisms. But also enhances secondary cracking of diesel components and aromatization and Diels-Alder reaction of alkanes and alkenes. The liquid oil yields for this case decreased, while aromaticity increased with high naphthalene content. A significant increase was observed for a fraction of $\text{C}_6\text{-C}_{11}$ compounds, with reduced content of straight alkenes and cycloparaffins being obtained.

3.4 Co-pyrolysis Processing of Plastic Waste with Lignocellulosic Biomass and Sewage Sludge

Many works report on the co-pyrolysis of plastic wastes and biomass as a promising way to improve the properties of the oil from biomass pyrolysis, with synergistic effects being discussed in several reviews [26, 39, 40, 58]. In fact, hydrocarbons from the hydrogen-rich plastics provide hydrogen for biomass-derived oxygenates, which may decrease coke formation from dehydration and other deoxygenation reactions of hydrogen deficient oxygenates [59]. Notable findings have been reported for improving plastic wastes conversion. Through thermogravimetric analysis (TGA), Salvilla et al. [60] observed a significantly reduced activation energy of decomposition of waste PP, LDPE and HDPE when pyrolyzed with wood and corn stover in the temperature range of (30 to 850) °C. Similarly, after examination of the co-pyrolysis of bamboo sawdust (BSD) and LLDPE using TGA at (30 to 900) °C, Alam et al. [61] reported average apparent activation energies (isoconversional method) of pure BSD, LLDPE and their mixtures at LLDPE:BSD ratios of 3 to be 294 kJ/mol, 204 kJ/mol, and 188 kJ/mol, respectively. It is believed that hydroxyl groups resulting from the degradation of cellulose from lignocellulosic biomass react with vinyl groups from polyolefin bond cleavage to produce alcohols, while furan and its derivatives combine with unsaturated hydrocarbons to produce aromatic

hydrocarbons through dehydration and Diels-Alder reactions [58]. During co-pyrolysis of PVC with biomass, the degradation of PVC will generate HCl as an intermediate that can act as an acid catalyst to accelerate cleavage of intra-ring in glycosidic units promoting dehydration, remove -COOH from carbohydrates, promote depolymerization, and thereby providing high liquid yields with reduced oxygenated compounds [62]. The presence of solid-solid and solid-gas interactions affects synergism, as the biochar formed during the co-pyrolysis process is able to act as a catalyst [63].

The co-pyrolysis of sewage sludge and waste LDPE through TGA was investigated [63], where the authors observed significant synergistic effects for co-pyrolysis and found mixture ratios of 1:1 to be optimal, as observed by lower activation energy and lower char formation. The activation energies for sewage sludge, LDPE and mixture, were 30.01 kJ/mol, 187.40 kJ/mol and 37.2 kJ/mol, respectively. In this work, the active pyrolysis zone of sewage sludge and LDPE were in the same temperature range of (200 to 600) °C, while in the case of lignocellulosic biomass in the work of Salvilla et al. [60], biomass degradation occurred at (200 to 400) °C and plastic degradation at (400 to 500) °C.

Although the above-mentioned works present co-pyrolysis as a possible alternative for enhancing the overall efficiency and economic feasibility of plastic wastes and biomass pyrolysis, several issues have yet to be addressed. The chlorine content in waste plastics, the increased viscosity of the produced oil can be listed among the obstacles that need to be overcome [64]. Higher concentrations of intermediate HCl can decrease aromatic yields at the expense of gaseous products, causing poor oil quality, and can also promote the production of highly toxic chemicals such as dioxins and furans [62]. Therefore, it is necessary to select an effective catalyst and convenient reaction conditions that can address these limitations. As eco-effectiveness of the co-pyrolysis process is expected for mixed wastes that already contain both plastics and biomass or other wastes that are difficult to be separated [64], such as real-world plastic wastes, further research is needed on the processing of plastic wastes using inexpensive BAC catalysts.

3.5 Conclusions and Perspectives

Low cost and easily manufacturable BACs with high porosity and heteroatoms surface functional groups are gaining more attention in pyrolysis processing of plastic waste for liquid fuels production. However, catalytic properties of a BAC depend on type of biomass, type of reagent, reagent to biomass ratio and activation temperature, all of which can impact the BET surface area, total pore volume, and acidity of the resulting BAC. Biomass having high carbon content and low ash content is preferable among the many forms of biomass. H_3PO_4 is a common reagent that can be used advantageously for activation of lignocellulosic biomass. When activating with H_3PO_4 , increasing carbonization temperature and H_3PO_4 to biomass ratio promote the catalytic activity of the BAC by enhancing its BET surface area,

volume of micropores and acidity. However, excessive values of each of these parameters can be counterproductive because of enhanced devolatilization of acid functional groups and reduction of micropores. When an excessive H₃PO₄ to biomass ratio is used, a high number of acid sites on the BAC enhances scission, cracking, and rearrangement reactions, thus decreasing liquid oil yield. Overall, BAC rich in P-containing functional groups is favorable for aromatization and C-C and C-H bond cracking reactions, resulting in the production of aromatics and light alkanes. Red mud as a low-cost additive, has the ability to improve hydrogenation and cracking reactions, and dechlorination of the liquid oil. During co-pyrolysis of plastic waste and lignocellulosic biomass, Diels-Alder reactions are promoted between furan or its derivatives from cellulose and unsaturated hydrocarbons from plastic waste, promoting aromatic hydrocarbons in the liquid oil.

The reported works that use BACs and the above mentioned low-cost wastes as additives for catalytic pyrolysis of plastic wastes mainly examine single plastic wastes or simulated mixtures of a given number of plastic wastes. More works are expected to examine the co-pyrolysis process over BACs, as the real-world plastic wastes contain both plastics and other types of waste that are difficult to separate. New studies in this area would enhance the effectiveness of technology for plastic wastes valorization. BACs prepared from high-carbon biomass activated with different reagents, including KOH, ZnCl₂ and FeCl₃, should also be examined for catalytic pyrolysis of plastic wastes. BACs with high selectivity of high value-added compounds such as naphtha can be expected one of the focal points in future research.

References

1. Kaza S, Yao L, Bhada-Tata P, Woerden FV (2018) What a Waste 2.0: A global snapshot of solid waste management to 2050. In: Urban Development series. Washington, DC: World Bank. <https://openknowledge.worldbank.org/handle/10986/30317>
2. Das P, Tiwari P. The effect of slow pyrolysis on the conversion of packaging waste plastics (PE and PP) into fuel. *Waste Manag.* 2018;79:615–24. <https://doi.org/10.1016/j.wasman.2018.08.021>.
3. PlasticsEurope World plastics materials demand 2015 by types. <https://committee.iso.org/files/live/sites/tc61/files/The%20Plastic%20Industry%20Berlin%20Aug%202016%20-%20Copy.pdf>
4. Ryberg MW, Laurent A, Hauschild M. Mapping of global plastics value chain and plastics losses to the environment (with a particular focus on marine environment). Nairobi, Kenya: United Nations Environment Programme; 2018. <https://sites.miiis.edu/bluepioneers/files/2019/06/Mapping-of-global-plastics-value-chain-and-hotspots.pdf>
5. DCC- Zero waste recycler. Plastic Waste Management. <https://www.zerowasterecycler.com/plastic-waste-management/> (accessed on May 28th, 2021).
6. Cai N, Yang H, Zhang X, Xia S, Yao D, Bartocci P, Fantozzi F, Chen Y, Chen H, Williams PT. Bimetallic carbon nanotube encapsulated Fe-Ni catalysts from fast pyrolysis of waste plastics and their oxygen reduction properties. *Waste Manag.* 2020;109:119–26. <https://doi.org/10.1016/j.wasman.2020.05.003>.

7. Parku GK, Collard FX, Görgens JF. Pyrolysis of waste polypropylene plastics for energy recovery: Influence of heating rate and vacuum conditions on composition of fuel product. *Fuel Process Technol.* 2020;209:36–8. <https://doi.org/10.1016/j.fuproc.2020.106522>.
8. Götze R (2016) Composition of waste materials and recyclables. Ph.D. thesis, department of environmental engineering, technical university of Denmark. <https://orbit.dtu.dk/en/publications/composition-of-waste-materials-and-recyclables>
9. Anuar Sharuddin SD, Abnisa F, Wan Daud WMA, Aroua MK. Energy recovery from pyrolysis of plastic waste: Study on non-recycled plastics (NRP) data as the real measure of plastic waste. *Energy Convers Manag.* 2017;148:925–34. <https://doi.org/10.1016/j.enconman.2017.06.046>.
10. Shen L, Worrell E. Plastic recycling. In: Worrell E, Reuter MA, editors. *Handbook of recycling: state-of-the-art for practitioners, analysts, and scientists*. Elsevier Inc.; 2014. p. 179–90. <https://doi.org/10.1016/B978-0-12-396459-5.00013-1>.
11. Uzoejinwa BB, He X, Wang S, El-Fatah Abomohra A, Hu Y, Wang Q. Co-pyrolysis of biomass and waste plastics as a thermochemical conversion technology for high-grade biofuel production: Recent progress and future directions elsewhere worldwide. *Energy Convers Manag.* 2018;163:468–92. <https://doi.org/10.1016/j.enconman.2018.02.004>.
12. Ranta-Korpi M, Vainikka P, Konttinen J, Saarimaa A, Rodriguez M. Ash forming elements in plastics and rubbers. In: VTT Technology series; 2014. <http://www.vtt.fi/inf/pdf/technology/2014/T186.pdf>
13. Zhou H, Meng A, Long Y, Li Q, Zhang Y. Classification and comparison of municipal solid waste based on thermochemical characteristics. *J Air Waste Manag Assoc.* 2014;64:597–616. <https://doi.org/10.1080/10962247.2013.873094>.
14. Qureshi MS, Oasmaa A, Pihkola H, Deviatkin I, Tenhunen A, Mannila J, Minkkinen H, Pohjakallio M, Laine-ylijoki J. Pyrolysis of plastic waste : Opportunities and challenges. *J Anal Appl Pyrolysis.* 2020;152:104804. <https://doi.org/10.1016/j.jaap.2020.104804>.
15. Abdel-Shafy HI, Mansour MSM. Solid waste issue: Sources, composition, disposal, recycling, and valorization. *Egypt J Pet.* 2018;27:1275–90. <https://doi.org/10.1016/j.ejpe.2018.07.003>.
16. Chanashetty VB, Patil BM. Fuel from plastic wastes. *Int J Emerg Technol.* 2015;6(2):121–8. <https://www.researchtrend.net/ijet/ijet61/24%20NCRIET.pdf>
17. Luo W, Hu Q, Fan Z, Wan J, He Q, Huang S, Zhou N, Song M, Zhang J, Zhou Z. The effect of different particle sizes and HCl-modified kaolin on catalytic pyrolysis characteristics of reworked polypropylene plastics. *Energy.* 2020;213:119080. <https://doi.org/10.1016/j.energy.2020.119080>.
18. Yao D, Yang H, Chen H, Williams PT. Co-precipitation, impregnation and so-gel preparation of Ni catalysts for pyrolysis-catalytic steam reforming of waste plastics. *Appl Catal B Environ.* 2018;239:565–77. <https://doi.org/10.1016/j.apcatb.2018.07.075>.
19. Komilis D, Evangelou A, Giannakis G, Lympertis C. Revisiting the elemental composition and the calorific value of the organic fraction of municipal solid wastes. *Waste Manag.* 2012;32: 372–81. <https://doi.org/10.1016/j.wasman.2011.10.034>.
20. Kumar S, Singh RK. Pyrolysis kinetics of waste high-density polyethylene using thermogravimetric analysis. *Int J ChemTech Res.* 2014;6:131–7. [https://sphinxsai.com/2014/ChemTech/JM14CT1_50/CT=16\(131-137\)JM14.pdf](https://sphinxsai.com/2014/ChemTech/JM14CT1_50/CT=16(131-137)JM14.pdf)
21. Adrados A, de Marco I, Caballero BM, López A, Laresgoiti MF, Torres A. Pyrolysis of plastic packaging waste: a comparison of plastic residuals from material recovery facilities with simulated plastic waste. *Waste Manag.* 2012;32:826–32. <https://doi.org/10.1016/j.wasman.2011.06.016>.
22. Feng Y, Liu S, Qin J, Cao Y, Jiang Y, Zhang S. Numerical study on the influence of turbulence on the pyrolysis of hydrocarbon fuel in mini-channel. *Int J Heat Mass Transf.* 2018;119:768–76. <https://doi.org/10.1016/j.ijheatmasstransfer.2017.12.002>.
23. Mellin P, Yu X, Yang W, Blasiak W. Influence of reaction atmosphere (H_2O , N_2 , H_2 , CO_2 , CO) on fluidized-bed fast pyrolysis of biomass using detailed tar vapor chemistry in computational fluid dynamics. *Ind Eng Chem Res.* 2015;54:8344–55. <https://doi.org/10.1021/acs.iecr.5b02164>.

24. Zhou N, Dai L, Lyu Y, Li H, Deng W, Guo F, Chen P, Lei H, Ruan R. Catalytic pyrolysis of plastic wastes in a continuous microwave assisted pyrolysis system for fuel production. *Chem Eng J.* 2021;418:129412. <https://doi.org/10.1016/j.cej.2021.129412>.
25. Das P, Gabriel JCP, Tay CY, Lee JM. Value-added products from thermochemical treatments of contaminated e-waste plastics. *Chemosphere.* 2021;269:129409. <https://doi.org/10.1016/j.chemosphere.2020.129409>.
26. Wang Z, Burra KG, Lei T, Gupta AK. Co-pyrolysis of waste plastic and solid biomass for synergistic production of biofuels and chemicals: a review. *Prog Energy Combust Sci.* 2021;84: 100899. <https://doi.org/10.1016/j.pecs.2020.100899>.
27. Fekhar B, Zsinka V, Miskolczi N. Value added hydrocarbons obtained by pyrolysis of contaminated waste plastics in horizontal tubular reactor: In situ upgrading of the products by chlorine capture. *J Clean Prod.* 2019;241:118166. <https://doi.org/10.1016/j.jclepro.2019.118166>.
28. Butler E, Devlin G, McDonnell K. Waste polyolefins to liquid fuels via pyrolysis: Review of commercial state-of-the-art and recent laboratory research. *Waste Biomass Valorization.* 2011;2:227–55. <https://doi.org/10.1007/s12649-011-9067-5>.
29. Qureshi MS, Oasmaa A, Lindfords C (2019) Thermolysis of plastic waste: reactor comparison. In: Pyroliq 2019: Pyrolysis and liquefaction of biomass and wastes, Engineering Conferences International Digital Archives. Cork, Ireland, https://dc.engconfintl.org/cgi/viewcontent.cgi?article=1015&context=pyroliq_2019
30. Djandja OS, Wang Z, Wang F, Xu Y-P, Duan P-G. Pyrolysis of municipal sewage sludge for biofuel production: a review. *Ind Eng Chem Res.* 2020;59:16939–56. <https://doi.org/10.1021/acs.iecr.0c01546>.
31. Li L, Rowbotham JS, Christopher Greenwell H, Dyer PW. An introduction to pyrolysis and catalytic pyrolysis: Versatile techniques for biomass conversion. In: Suib SL, editor. New and future developments in catalysis: catalytic biomass conversion. Elsevier B.V.; 2013. p. 173–208. <https://doi.org/10.1016/B978-0-444-53878-9.00009-6>.
32. Collard FX, Carrier M, Görgens JF. Fractionation of lignocellulosic material with pyrolysis processing. In: Mussatto SI, editor. Biomass fractionation technologies for a lignocellulosic feedstock based biorefinery. Elsevier Inc.; 2016. p. 81–101. <https://doi.org/10.1016/B978-0-12-802323-5.00004-9>.
33. Arabiourrutia M, Lopez G, Artetxe M, Alvarez J, Bilbao J, Olazar M. Waste tyre valorization by catalytic pyrolysis – a review. *Renew Sust Energ Rev.* 2020;129:109932. <https://doi.org/10.1016/j.rser.2020.109932>.
34. Ratnasari DK, Nahil MA, Williams PT. Catalytic pyrolysis of waste plastics using staged catalysis for production of gasoline range hydrocarbon oils. *J Anal Appl Pyrolysis.* 2017;124: 631–7. <https://doi.org/10.1016/j.jaat.2016.12.027>.
35. Zhang Y, Duan D, Lei H, Villota E, Ruan R. Jet fuel production from waste plastics via catalytic pyrolysis with activated carbons. *Appl Energy.* 2019;251:113337. <https://doi.org/10.1016/j.apenergy.2019.113337>.
36. Sun K, Huang Q, Chi Y, Yan J. Effect of $ZnCl_2$ -activated biochar on catalytic pyrolysis of mixed waste plastics for producing aromatic-enriched oil. *Waste Manag.* 2018;81:128–37. <https://doi.org/10.1016/j.wasman.2018.09.054>.
37. Li K, Lee S, Yuan G, Lei J, Lin S, Weerachanchai P, Yang Y, Wang J-Y. Investigation into the catalytic activity of microporous and mesoporous catalysts in the pyrolysis of waste polyethylene and polypropylene mixture. *Energies.* 2016;9:431. <https://doi.org/10.3390/en9060431>.
38. Khalil U, Vongsvivut J, Shahabuddin M, Samudrala SP, Srivatsa SC, Bhattacharya S. A study on the performance of coke resistive cerium modified zeolite Y catalyst for the pyrolysis of scrap tyres in a two-stage fixed bed reactor. *Waste Manag.* 2020;102:139–48. <https://doi.org/10.1016/j.wasman.2019.10.029>.
39. Ryu HW, Kim DH, Jae J, Lam SS, Park ED, Park YK. Recent advances in catalytic co-pyrolysis of biomass and plastic waste for the production of petroleum-like hydrocarbons. *Bioresour Technol.* 2020;310:123473. <https://doi.org/10.1016/j.biortech.2020.123473>.

40. Ahmed MHM, Batalha N, Mahmudul HMD, Perkins G, Konarova M. A review on advanced catalytic co-pyrolysis of biomass and hydrogen-rich feedstock: insights into synergistic effect, catalyst development and reaction mechanism. *Bioresour Technol.* 2020;310:123457. <https://doi.org/10.1016/j.biortech.2020.123457>.
41. Xue Y, Johnston P, Bai X. Effect of catalyst contact mode and gas atmosphere during catalytic pyrolysis of waste plastics. *Energy Convers Manag.* 2017;142:441–51. <https://doi.org/10.1016/j.enconman.2017.03.071>.
42. Huo E, Lei H, Liu C, Zhang Y, Xin L, Zhao Y, Qian M, Zhang Q, Lin X, Wang C, Mateo W, Villota EM, Ruan R. Jet fuel and hydrogen produced from waste plastics catalytic pyrolysis with activated carbon and MgO. *Sci Total Environ.* 2020;727:138411. <https://doi.org/10.1016/j.scitotenv.2020.138411>.
43. Arami-Niya A, Daud WMAW, Mjalli FS. Using granular activated carbon prepared from oil palm shell by ZnCl₂ and physical activation for methane adsorption. *J Anal Appl Pyrolysis.* 2010;89:197–203. <https://doi.org/10.1016/j.jaat.2010.08.006>.
44. Bedia J, Peñas-Garzón M, Gómez-Avilés A, Rodriguez JJ, Belver C. Review on activated carbons by chemical activation with FeCl₃. *C - J Carbon Res.* 2020;6:21. <https://doi.org/10.3390/c6020021>.
45. Iwanow M, Gärtner T, Sieber V, König B. Activated carbon as catalyst support: precursors, preparation, modification and characterization. *Beilstein J Org Chem.* 2020;16:1188–202. <https://doi.org/10.3762/bjoc.16.104>.
46. Ji Y, Li T, Zhu L, Wang X, Lin Q. Preparation of activated carbons by microwave heating KOH activation. *Appl Surf Sci.* 2007;254:506–12. <https://doi.org/10.1016/j.apsusc.2007.06.034>.
47. Veerakumar P, Panneer Muthuselvam I, Hung C Te, Lin KC, Chou FC, Liu S Bin (2016) Biomass-derived activated carbon supported Fe₃O₄ nanoparticles as recyclable catalysts for reduction of nitroarenes. *ACS Sustain Chem Eng* 4:6772–6782. doi: <https://doi.org/10.1021/acssuschemeng.6b01727>
48. Hui TS, Zaini MAA. Potassium hydroxide activation of activated carbon: a commentary. *Carbon Lett.* 2015;16:275–80. <https://doi.org/10.5714/CL.2015.16.4.275>.
49. Ateş F, Özcan Ö. Preparation and characterization of activated carbon from poplar sawdust by chemical activation: comparison of different activating agents and carbonization temperature. *Eur J Eng Res Sci.* 2018;3:6–11. <https://doi.org/10.24018/ejers.2018.3.11.939>.
50. Rodríguez-Reinoso F, Sepúlveda-Escribano A. Porous carbons in adsorption and catalysis. In: Nalwa HS, editor. *Handbook of surfaces and interfaces of materials*, vol. 5. Elsevier Inc.; 2001. p. 309–55. <https://doi.org/10.1016/b978-012513910-6/50066-9>.
51. Olivares-Marín M, Fernández-González C, Macías-García A, Gómez-Serrano V. Preparation of activated carbon from cherry stones by chemical activation with ZnCl₂. *Appl Surf Sci.* 2006;252:5967–71. <https://doi.org/10.1016/j.apsusc.2005.11.008>.
52. Gerçel Ö, Gerçel HF. Preparation and characterization of activated carbon from vegetable waste by microwave-assisted and conventional heating methods. *Arab J Sci Eng.* 2016;41:2385–92. <https://doi.org/10.1007/s13369-015-1859-7>.
53. Wan K, Chen H, Zheng F, Pan Y, Zhang Y, Long D. Tunable production of jet-fuel range alkanes and aromatics by catalytic pyrolysis of LDPE over biomass-derived activated carbons. *Ind Eng Chem Res.* 2020;59:17451–61. <https://doi.org/10.1021/acs.iecr.0c02482>.
54. Duan D, Feng Z, Dong X, Chen X, Zhang Y, Wan K, Wang Y, Wang Q, Xiao G, Liu H, Ruan R. Improving bio-oil quality from low-density polyethylene pyrolysis: effects of varying activation and pyrolysis parameters. *Energy.* 2021;232:121090. <https://doi.org/10.1016/j.energy.2021.121090>.
55. Heidarinejad Z, Dehghani MH, Heidari M, Javedan G, Ali I, Sillanpää M. Methods for preparation and activation of activated carbon: a review. *Environ Chem Lett.* 2020;18:393–415. <https://doi.org/10.1007/s10311-019-00955-0>.
56. Idumah CI, Nwuzor IC. Novel trends in plastic waste management. *SN Appl Sci.* 2019;1:1402. <https://doi.org/10.1007/s42452-019-1468-2>.

57. López A, de Marco I, Caballero BM, Laresgoiti MF, Adrados A, Aranzabal A. Catalytic pyrolysis of plastic wastes with two different types of catalysts: ZSM-5 zeolite and Red Mud. *Appl Catal B Environ.* 2011;104:211–9. <https://doi.org/10.1016/j.apcatb.2011.03.030>.
58. Gin AW, Hassan H, Ahmad MA, Hameed BH, Mohd Din AT. Recent progress on catalytic co-pyrolysis of plastic waste and lignocellulosic biomass to liquid fuel: the influence of technical and reaction kinetic parameters. *Arab J Chem.* 2021;14:103035. <https://doi.org/10.1016/j.arabjc.2021.103035>.
59. Li X, Zhang H, Li J, Su L, Zuo J, Komarneni S, Wang Y. Improving the aromatic production in catalytic fast pyrolysis of cellulose by co-feeding low-density polyethylene. *Appl Catal A Gen.* 2013;455:114–21. <https://doi.org/10.1016/j.apcata.2013.01.038>.
60. Salvilla JNV, Ofraido BIG, Rollon AP, Manegdeg FG, Abarca RRM, de Luna MDG. Synergistic co-pyrolysis of polyolefin plastics with wood and agricultural wastes for biofuel production. *Appl Energy.* 2020;279:115668. <https://doi.org/10.1016/j.apenergy.2020.115668>.
61. Alam M, Bhavanam A, Jana A, Viroja S, Rao N. Co-pyrolysis of bamboo sawdust and plastic: synergistic effects and kinetics. *Renew Energy.* 2020;149:1133–45. <https://doi.org/10.1016/j.renene.2019.10.103>.
62. Lee DJ, Lu JS, Chang JS. Pyrolysis synergy of municipal solid waste (MSW): a review. *Bioresour Technol.* 2020;318:123912. <https://doi.org/10.1016/j.biortech.2020.123912>.
63. Zaker A, Chen Z, Zaheeruddin M, Guo J. Co-pyrolysis of sewage sludge and low-density polyethylene – a thermogravimetric study of thermo-kinetics and thermodynamic parameters. *J Environ Chem Eng.* 2020;9:104554. <https://doi.org/10.1016/j.jece.2020.104554>.
64. Johansson AC, Sandström L, Öhrman OGW, Jilvero H. Co-pyrolysis of woody biomass and plastic waste in both analytical and pilot scale. *J Anal Appl Pyrolysis.* 2018;134:102–13. <https://doi.org/10.1016/j.jaap.2018.05.015>.

Chapter 4

Production of Valuable Compounds from Leaves by Supercritical CO₂ Extraction



Takafumi Sato

Abstract Although leaves contain many useful compounds, they are typically considered as a waste. Extraction of leaves with carbon dioxide (CO₂) in its supercritical state (sc-CO₂) allows effective recovery of valuable compounds due to the unique properties of CO₂. Recovered components such as terpenes, phenolics and phytosterols can be isolated and depend on the types of leaves and conditions of the extraction. The extraction kinetics consisted of three steps, that is, extraction of accessible solute from the cells, slower extraction of the solute protected by the cell walls and transition state of these situations. Antioxidants, phenolics and flavonoids can be recovered by sc-CO₂ extraction and antioxidant capacity (AOC), total phenolic content (TPC) and total flavonoid content (TFC) in the extract are shown in this chapter overview. The addition of co-solvent such as ethanol generally increases AOC, TPC and TFC. The temperature and pressure influences AOC, TPC and TFC depends on the contribution of solvent density and vapor pressure of solute. Extraction of plant leaves with sc-CO₂ can provides valuable new chemicals from biomass and can create new sources of biochemicals.

Keywords Leaf · Supercritical carbon dioxide · Extraction · Antioxidant · Phenolics · Flavonoid

4.1 Leaf Extraction with Supercritical CO₂

4.1.1 *Background of Supercritical CO₂ Extraction of Leaf*

Leaves of many plants are typically treated as biomass waste. On the other hand, the extracted liquid of some tea leaves is popular as a drink that contains desirable compounds such as catechins. The process for recovery of these compounds from

T. Sato (✉)

Department of Fundamental Engineering, Utsunomiya University, Utsunomiya, Tochigi, Japan
e-mail: takafumi@cc.utsunomiya-u.ac.jp

plant leaves by extraction can be used to produce supplements, food additives, fertilizers and so on or to develop a product with added value and a system for efficient use of biomass waste. The appropriate use of leaves contributes to the establishment of a sustainable society.

The solvent for a separation process should be friendly to the human body and environment. CO_2 is an environmentally friendly solvent and safe for humans and different from typical organic solvents, because it can be brought to its supercritical state at temperatures just above room temperature. In particular, it is not necessary to worry about residual solvent in extract where the extract is used for food additives. The solvent properties of supercritical CO_2 (sc- CO_2) will be discussed in this chapter that shows an effective extraction system for obtaining useful components from plant materials including leaf [1].

Extracts from plant leaves contains bioactive compounds such as antioxidants including phenolics and flavonoids. Antioxidants are important component because they prevent neurodegenerative diseases such as cancer and Alzheimer's disease and have protective activity against a multitude of non-communicable human conditions [2, 3].

In this chapter, the specific features of sc- CO_2 for extraction solvent are firstly introduced. After that, extraction of several kinds of leaves is explained from the view point of extraction kinetics, extracted compounds, amount of antioxidants, and compounds such as phenolics and flavonoids in the extract.

4.1.2 *Properties of Leaf*

The body of vascular plants consists of roots, stems and leaves. The leaf is typically attached to the stem and has a flat shape. The most important function of leaves is photosynthesis. Leaf exchanges water, carbon dioxide, oxygen and water outside of itself and produces organic compounds.

Figure 4.1 shows the cross-section of the tissue of leaf. Each component represents a cell surrounded by cell walls. The major tissue in leaf is the epidermal system, vascular system, and fundamental tissue system other than the former two systems. The epidermal system is the outer layer of the leaf, which is impermeable to water and covered with a cuticle that is the boundary separating the inner cell from the outside. The roles of it are to protect the plant from water loss, regulation of gas exchange and secretion of metabolic compounds. The vascular system consists of veins located in the fundamental tissue system and transport water and nutrition. The fundamental tissue system includes palisade tissue and spongy tissue. The palisade tissue typically exists on the front side of the leaf and consists of one or two vertically elongated cells. The sponge tissue typically exists on the backside of the leaf. The cells in this area are not so tightly packed in an irregular arrangement and there are large intercellular spaces and this is connected outside through the stoma to transport gas to the photosynthetic system.

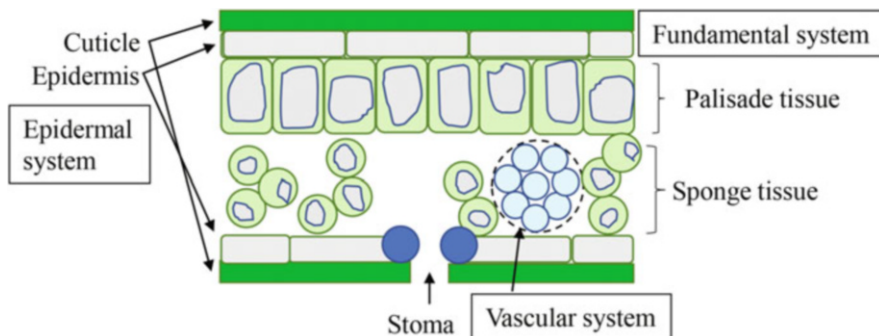


Fig. 4.1 Cross-sectional schematic of leaf tissue

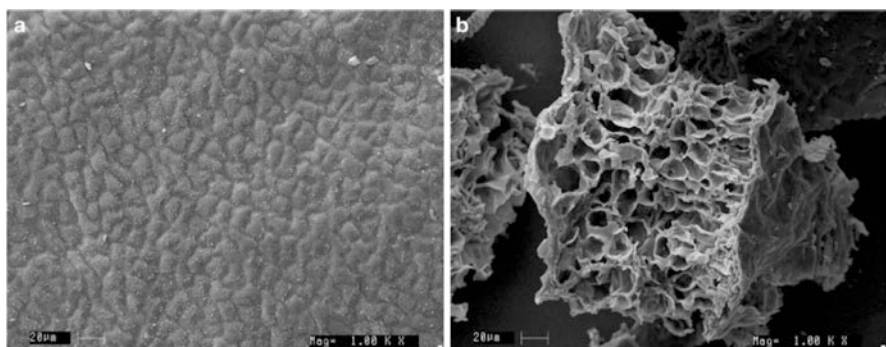


Fig. 4.2 Scanning electron micrographs of the unprocessed tea leaves and sc-CO₂ processed tea leaves. a: Untreated leaves; b: sc-CO₂ processed leaves at 35 MPa, reprinted with permission from [4] Copyright © 2015 Springer Nature

Leaf contains some useful components such as phenolics [2] that have antioxidant properties. Some phenolic compounds exhibit therapeutic benefits including cardio- and neuroprotective effect and health benefits such as preventing many chronic diseases and the integrity of DNA. The antioxidant property and total phenolic content are important to understand the usefulness of extraction of the leaf.

4.1.3 Morphology of Leaf

The solvent power of sc-CO₂ influences the morphology of leaves during extraction. Figure 4.2 shows SEM images of unprocessed tea leaf and tea leaf after extraction of sc-CO₂ at 35 MPa [4]. In the case of the unprocessed leaf, there is an epidermal system on the surface of the leaf. After the extraction with sc-CO₂, the structure of the leaf is cracked and pores in leaf tissue are opened. Sc-CO₂ strongly influences the

structure of leaves such as tissue and cell wall to enhance mass transfer of solvent into the inner side of the leaf, which helps release compounds from the matrix of the leaf.

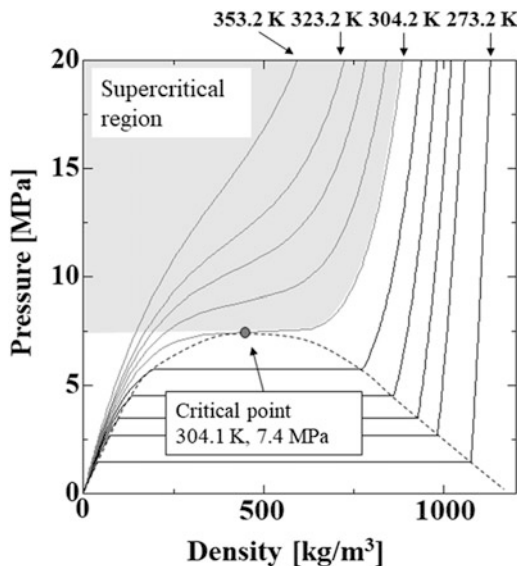
4.2 Properties of Supercritical CO₂ as an Extraction Solvent

4.2.1 Specific Properties of CO₂

The critical point of CO₂ is 304.1 K and 7.38 MPa as depicted in the P-ρ-T diagram (Fig. 4.3) of CO₂ [5]. Above the critical temperature and critical pressure, CO₂ is in a supercritical state and is thus called supercritical CO₂ (sc-CO₂) fluid. In the supercritical state, the density of CO₂ is continuously varied with temperature and pressure without phase change. In particular, the magnitude of change in density with temperature and pressure is large near the critical point. The high pressure and low-temperature region produces high fluid densities, and the low pressure and high-temperature region gives a low fluid density. Physical properties of CO₂ such as viscosity and diffusivity also greatly change according to the change in the density of CO₂.

The density of sc-CO₂ is between those of a gas phase and a liquid phase. The viscosity and diffusivity of sc-CO₂ are also between those of the gas and liquid phase. The higher density of sc-CO₂ than that of gaseous CO₂ enables sc-CO₂ to dissolve larger amounts of solute than that of the gaseous state. Further, the viscosity

Fig. 4.3 Pressure-density-temperature diagram of CO₂ based on data from Ref. [5]



of sc-CO₂ is lower and the diffusivity of sc-CO₂ is larger than those respective properties for liquid CO₂, which leads to an improvement in the permeation of CO₂ into leaf tissue. In sc-CO₂ extraction of plant materials, bioactive compounds such as phenolic compounds, flavonoids, phytosterol, tocopherols, carotenoids can be separated [1].

In addition, sc-CO₂ becomes gas by regulating pressure and the extract dissolved in sc-CO₂ is easily precipitated due to the decrease in solvent power by low density in the low-pressure region. The separation of extract from solvent to obtain the desired compounds is simple when sc-CO₂ is used as solvent, because no CO₂ remains in the substrate at atmospheric pressure in contrast to the case in which an organic liquid solvent is used.

4.2.2 *Properties of Mixture of CO₂ and Co-solvent*

The polarity of CO₂ is low, which means that the solubility of compounds having high polarity is low in CO₂. The addition of high polarity solvent as co-solvent into sc-CO₂ improves the solubility of high polarity compounds in the solvent. The co-solvents generally used are ethanol, methanol or water, because they are popular substances and especially water and ethanol are relatively safe for the human body. The dielectric constants of ethanol, methanol and water at ambient conditions are 25.3, 33.0 and 80.4, respectively [6] and the polarity of co-solvent is in this order. The fraction of co-solvent is usually 5–20 wt%.

The phase behavior of the mixture of CO₂ and co-solvent is important for the extraction process. sc-CO₂ + ethanol mixture is homogeneous above about 12 MPa and below 333 K [7, 8]. sc-CO₂ + methanol mixture is homogeneous above about 8 MPa below 323 K [8]. So the extraction with sc-CO₂ + methanol and sc-CO₂ + ethanol is usually operated under homogeneous conditions. On the other hand, sc-CO₂ + water mixtures are generally in the two-phase region. The vapor-liquid equilibrium for sc-CO₂ + water system from 308 K to 333 K can be estimated with the Peng-Robinson type equation of state [9]. There are CO₂-rich phase and water-rich phase at least less than 30 MPa below 333 K. For example, the mole fraction of CO₂ in CO₂-rich phase and in water-rich phase are 0.96 and 0.03, respectively, at 308 K and 20 MPa. At this condition, the volumetric ratio of the CO₂-rich phase is above 90% in the case of the molar ratio of water/CO₂ being less than 0.3. CO₂ rich phase containing a few % of water would be a major situation of the solvent in the sc-CO₂ + water system.

A mixture of CO₂ and polar co-solvent provides good solvent power for both nonpolar and polar components by the contribution of sc-CO₂ and co-solvent.

4.2.3 Principles of Supercritical CO₂ Extraction System

Figure 4.4 shows the typical CO₂ extraction system in a laboratory scale. In the literature, almost all of the extraction systems are semi-batch system. The principle of a supercritical CO₂ extraction system is as follows.

At first, the leaf is introduced into the extractor. The leaf is generally crushed and sometimes dried before introducing the extractor. CO₂ is supplied with a CO₂ supply pump that can supply CO₂ by cooling the pump head to maintain CO₂ in a liquid phase. The co-solvent that is a liquid is supplied with a high-pressure pump. The feed rate of CO₂ and co-solvent are controlled with the flow rate of each pump. The CO₂ and co-solvent are mixed in line and the mixture is supplied to the preheater as a solvent. The preheater and extractor are in the thermostat that is a water bath or an oven in the case of laboratory scale. In the case of large-scale extraction, preheater and extractor are directly heated with a heater. The solvent is heated in the preheater to the extraction temperature and then flows into the extractor. In the typical extraction, the solvent contact with the leaf ground or whole leaf in the extractor and then penetrates each tissue of a leaf to extract the components in the leaf. Then the extract is moved into the solvent. After that, the solvent flows to the outlet of the extractor.

The solvent dissolving extract is exhausted through a back-pressure regulator. In some cases, a filter is set between the extractor and back-pressure regulator to protect the regulator from dust. The extraction pressure, that is, the system pressure is controlled with a back-pressure regulator. The solvent through the back-pressure regulator is released to the trap to ambient pressure. If the solvent is homogeneous in high pressure, a metering valve can be used instead of back-pressure regulator to control the pressure and flow rate.

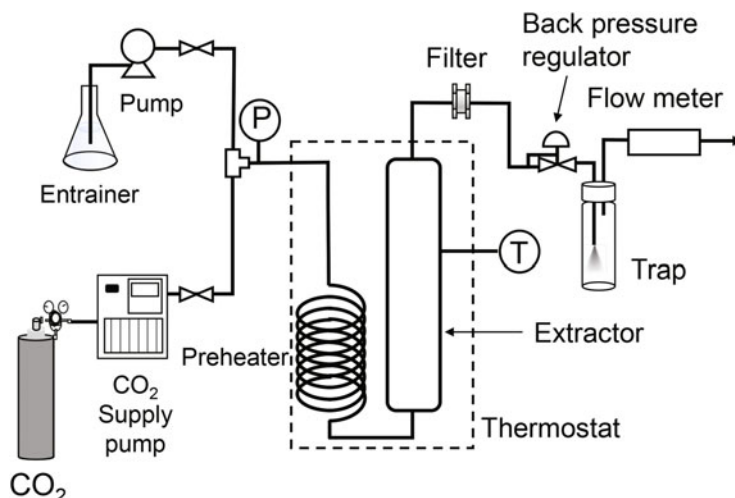


Fig. 4.4 Typical CO₂ extraction system

In the trap, the solvent dissolving extract is separated into CO₂ gas and the precipitated solid or liquid containing extract and co-solvent. The gas is released into the atmosphere after measuring its flow rate. The precipitate in the trap is recovered as the extract. In some cases, the liquid co-solvent is volatilized to obtain the solid extract.

4.3 Extract Obtained by Supercritical CO₂ Extraction of Leaves

4.3.1 Compounds Extracted by Supercritical Extraction of Various Leaves

The extraction of various leaves with sc-CO₂ has been reported (Table 4.1). There are over fifty kinds of leaves extracted with sc-CO₂ and many compounds were recovered. The structures of the main compounds are shown in Fig. 4.5. It was found that the leaves are widely distributed and not limited. The typical co-solvent for leave extraction process in sc-CO₂ is ethanol, methanol and water.

In the extraction of Green Tea (*Camellia sinesis*) leaves with sc-CO₂, triacontanol ((a) in Fig. 4.5) is an important compound that is straight-chain alcohol and improves plant growth by its effect on photosynthesis and plant metabolism [10]. Caffeine ((b) in Fig. 4.5) is also one of the major compounds in tea leaves and should be removed due to its significant effects on the cardiovascular system and gastric acid secretion [11]. Sc-CO₂, sc-CO₂ + water and sc-CO₂ + ethanol solvent extracted caffeine [11–13] from tea leaves. The (–)-epigallocatechin-3-gallate ((c) in Fig. 4.5) was extracted with sc-CO₂ + ethanol from Green Tea (*Camellia assamica L.*) leaves and it has strong antioxidant and health benefitted potential [4].

In the case of the extraction from Spearmint (*Mentha spicata L.*) leaves, flavonoids such as catechin, epicatechin, rutin, luteolin, myricetin, apigenin and naringenin [14] were extracted with sc-CO₂ + ethanol. Carvone ((d) in Fig. 4.5), Limonene ((f) in Fig. 4.5) and 1,8-cineole ((e) in Fig. 4.5) were extracted with sc-CO₂ [15, 16]. In the extraction of Peppermint with sc-CO₂ + ethanol, *l*-menthol ((g) in Fig. 4.5) and menthone ((h) in Fig. 4.5) were major extracted compounds [17].

Eugenol ((i) in Fig. 4.5) [18, 19] and 1,8-cineole ((e) in Fig. 4.5) [18] were extracted from Tulsi (*Ocimum sanctum*) leaves with sc-CO₂ and these compounds have strong antioxidant potency.

Hempedu bumi (*Andrographis paniculata*) grows widely in the tropical area of southeast Asia and is used for traditional medicine. Andrographolide ((j) in Fig. 4.5) that is one of the main components of its leaves were extracted with sc-CO₂ [20, 21].

Pharmacologically active anthraquinones such as aloë-emodin ((k) in Fig. 4.5) and barbaloin ((l) in Fig. 4.5) were extracted with sc-CO₂ from Aloe (*Aloe vera L.*) leaves [22, 23].

Table 4.1 Main components extracted from leaves with supercritical CO₂

Name	Primary active compounds that are extracted ^a	Co-sol. ^b	Ref.
Aloe (<i>Aloe vera L.</i>)	Aloesin, Aloe-emodin (k), Barbaloins (l)		[22]
	Aloe-emodin (k), Barbaloins (l)		[23]
Annual wormwood (<i>Artemisia annua L.</i>)	Artemisinin	E	[64]
Asteraceae (<i>Tithonia diversifolia</i>)	Tagitinine C (t)		[33, 34]
Bamboo (<i>Sasa palmata</i>)	β-Amyrene, α-Amyrin acetate, Gluconic acid	E, W	[52]
Balu (<i>Rhododendron anthopogon</i>)	γ-Terpinene, Limonene (f), β-Caryophyllene		[65]
Bright eyes (<i>Catharanthus roseus</i>)	Vindoline, Catharanthine		[66]
Bushy matgrass (<i>Lippia alba</i> (Mill.) N. E. Brown)	Carvone (d), β-Guaiene, Thymol		[67]
Cajuput (<i>Melaleuca cajuputi</i>)	β-Caryophyllene, Humulene, Eugenin		[68]
Common juniper (<i>Juniperus communis L.</i>)	Limonene (f), β-Selinene, α-Terpinyll acetate		[26]
	Limonene (f), α-thoujone		[27]
Congo Bololo (<i>Vernonia amygdalina</i> Delile)	Hexadecanoic acid, 9,12-Octadecadienonic acid, α-Linolenic acid		[37]
Cupressaceae (<i>Juniperus oxycedrus</i> ssp. <i>oxycedrus</i>)	Germacrene D (n), Manoyl oxide (o), 1- <i>epi</i> -Cubenol (p)		[28]
Date palm (<i>Phoenix dactylifera</i>)	Tetratriacontanol, Tetratriacontanoic acid, Hexadecanoic acid		[69]
Dandelion (<i>Teraxacum officinale</i> Ewber et Wiggers)	β-Amyrin, β-Sitosterol		[35]
Five leaved chaste tree (<i>Vitex negundo L.</i>)	Benzoic acid, Caryophyllene, Caryophyllene oxide		[70]
Ginkgo (<i>Ginkgo biloba L.</i>)	Bilobalide, Ginkgolides	M, E, W	[71]
Grecian foxglove (<i>Digitalis lanata Ehrh.</i>)	Digoxin, Acetyldigoxin	M	[72]
Green Tea (<i>Camellia assamica L.</i>)	(–)-Epiagallocatechin-3-gallate (c)	E	[4]
Green Tea (<i>Camellia sinensis</i>)	Triacontanol (a)		[9]
Green Tea	Caffeine (b)	W	[10]
Hempedu bumi (<i>Andrographis paniculata</i>)	Andrographolide (j)		[20, 21]
Herb (<i>Orthosiphon stamineus</i>)	Sinensetin, Isosinensetin, Rosmarinic acid	E	[73]
Indian borage (<i>Coleus aromaticus</i>)	Carvacrol (q)		[74]
Jambú (<i>Spilanthes acmella ver oleracea</i>)	Spilanthalol	E, W	[53]
Lamiaceae (<i>Origanum vulgare L.</i>)	Carvacrol (q)		[29]
	Carvacrol (q), <i>trans</i> -Sabinene hydrate (r)		[30]

(continued)

Table 4.1 (continued)

Name	Primary active compounds that are extracted ^a	Co-sol. ^b	Ref.
Lantana (<i>Lantana camera</i>)	Ar-curcumene, α -humulene, α -Zingiberene		[75]
Laurel (<i>L. nobilis L.</i> Lauraceae)	1,8-Cineole (e), Linalool, α -Terpinyl acetate		[38]
Lemon balm (<i>Melissa officinalis L.</i>)	α -Citral, β -Citral		[76]
Lemon-scented gum (<i>Corymbia citriodora</i>)	Citronellal		[77]
Limau purut (<i>Citrus hystrix</i>)	Cinnamic acid, <i>m</i> -Coumaric acid, Vanillic acid	E	[61]
Lupine (<i>Lupinus albuscens</i>)	Stigmasterol, Ergosterol		[39]
Maté tea	Caffeine (b)	E	[11]
	Caffeine (b), Theophylline, Theobromine		[12]
Moringa (<i>Moringa oleifera</i>)	α -Linoleic acid	E	[40]
Palo Negro (<i>Leptocarpha rivularis</i>)	α -Thujone, β -Caryophyllene, Resveratrol	E	[54]
	α -Thujone, β -Caryophyllene, Caryophyllene oxide		[41]
Pandan (<i>Pandanus amaryllifolius Roxb.</i>)	2-Acetyl-1-pyrroline (s)		[31, 32]
Pecah Kaca (<i>Strobilanthes crispus</i>)	Rutin, Luteolin, Kaempferol	E	[62]
Peppermint	<i>l</i> -Menthol (g), Menthone (h)	E	[17]
Pimento (<i>Pimenta dioica Merrill.</i>)	Eugenol (i)		[78]
Piper Betle	2,3-Dimethyl-benzoic acid, 9-Octadecenoic acid (Z)-, methyl ester		[79]
<i>Piper klotzschianum</i>	Germacrene D (n), Piper callosidine, 14-oxy- α -Muuroleno	M, E, P	[42]
Physic nut (<i>Jatropha curcas Linn.</i>)	Gallic acid	M	[80]
River red gum (<i>Eucalyptus camaldulensis Dehn.</i>)	1,8-Cineole (e), Allo-aromadendrene, Globulol		[81]
Rock Samphire (<i>Crithmum maritimum L.</i>)	Dillapiole, γ -terpinene, thymol methyl ether		[82]
Rose cactus (<i>Pereskia bleo</i>)	Cholest-5-en-3-ol (3beta)-, Erythritol, 9-Octadecenoic acid		[58]
Rosemary (<i>Rosmarinus officinalis L.</i>)	Carnosic acid (m), 1,8-Cineole (e), Camphor		[24]
	Carnosic acid (m), Wogonin		[25]
Rose-scented geranium (<i>Pelargonium graveolens</i>)	Citronellol, Geraniol, 6,9-Guaiadiene		[83]
Sage (<i>Salvia officinalis L.</i>)	Carnosol, Fatty acids (C18), Allobetulonlactone-1-en-2-ol		[25]
<i>Seseli bocconi</i> Guss. Subsp. <i>praecox</i> Gamisans (Apiaceae)	β -Phellandrene, α -Humulene		[84]

(continued)

Table 4.1 (continued)

Name	Primary active compounds that are extracted ^a	Co-sol. ^b	Ref.
Southern magnolia (<i>Magnolia grandiflora</i>)	Parthenolide, Costunolide, Cyclocolorenone		[85]
Spearmint (<i>Mentha spicata L.</i>)	Luteolin, Apigenin, Naringenin	E	[14]
	Carvone (d), Pulegone, Limonene (f)		[15]
	Carvone (d), 1,8-Cineole (e), Limonene (f)		[16]
Swamp mallet (<i>Eucalyptus spathulata</i>), Coolabah (<i>Eucalyptus microtheca</i>)	1,8-Cineole (e), α -Pirene	M	[43]
Sweet cherry (<i>Prunus avium L.</i>)	D _L -Malic acid, α,α -Trehalose, D-(-)-Mannitol		[86]
Tasmanian bluegum (<i>Eucalyptus globulus L.</i>)	Eudesmol, 1,2-Benzenedicarboxylic acid		[87]
Tulsi (<i>Ocimum sanctum</i>)	Eugenol (i), 1,8-Cineole (e)		[18]
	Eugenol (i)		[19]
Yerba mate folium (<i>Ilex paraguariensis A. St.-Hil., Aquifoliaceae</i>)	Theobromine, Caffeine (b)		[44]

^aCharacter in parenthesis is chemical structure in Fig. 4.5

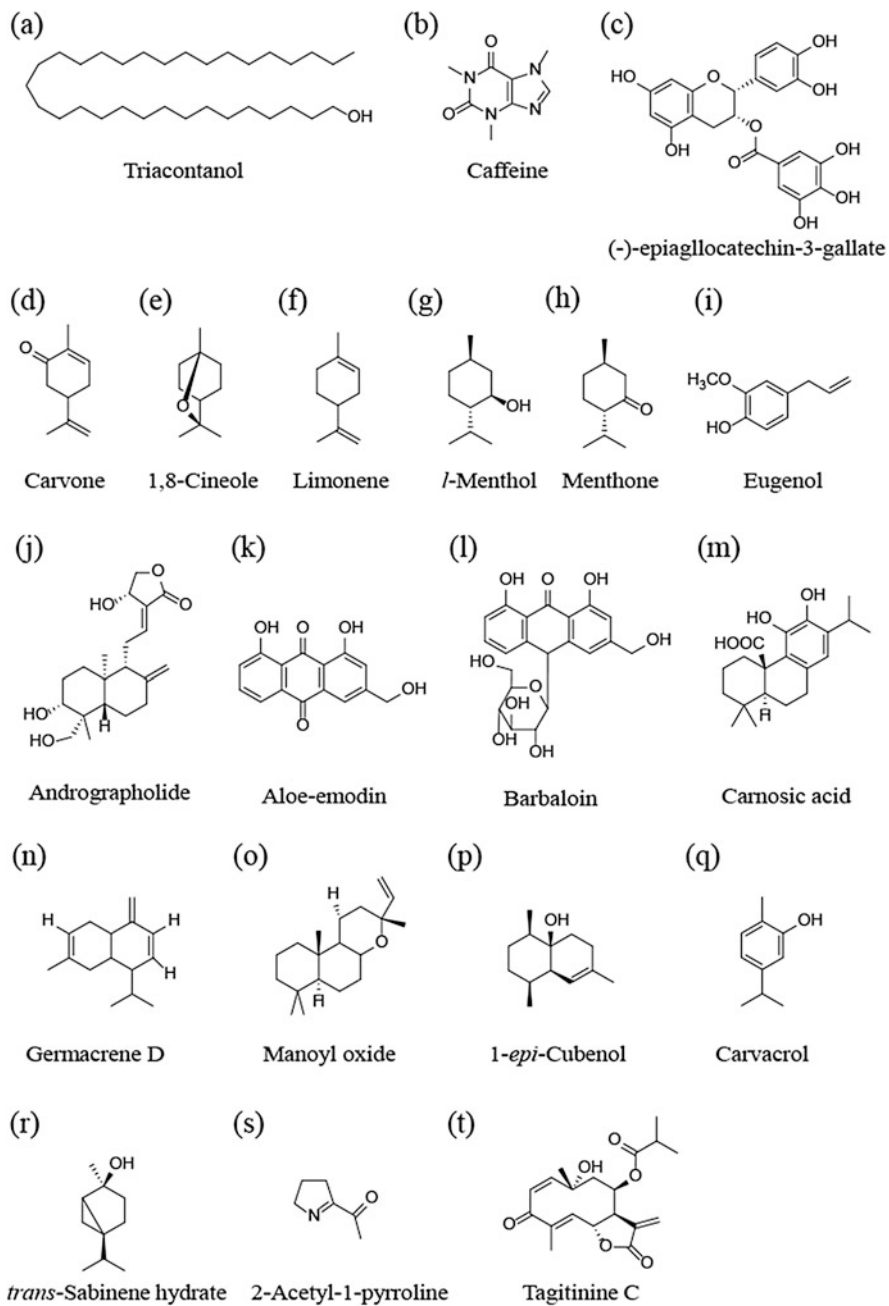
^bCo-solvent, W: water, M: methanol, E: ethanol

Rosemary (*Rosmarinus officinalis L.*) has been recognized as the plant with a high antioxidant capacity. The extraction of rosemary leaves with sc-CO₂ gives carnosic acid ((m) in Fig. 4.5) as the main product [24], and abietane-type diterpenoids including carnosic acid ((m) in Fig. 4.5) and flavonoids including wogonin were also detected in the extract [25].

The extraction of Common juniper (*Juniperus communis L.*) leaves with sc-CO₂ was studied and the main product was limonene ((f) in Fig. 4.5) [26, 27]. Cupressaceae (*Juniperus oxycedrus* ssp. *oxycedrus*) that is a big tree being native to the Mediterranean region, the extraction of the leaves of it with sc-CO₂ provided germacrene D, manoyl oxide and 1-*epi*-cubenol (n, o and p in Fig. 4.5, respectively) [28].

The extraction of Lamiaceae (*Origanum vulgare L.*) leaves with sc-CO₂ was conducted. Lamiaceae is a kind of oregano that is widely used in the flavoring of food products as well as perfume compositions. The components in the extract were slightly different depending on the region harvested [29], and the main components for all samples were carvacrol ((q) in Fig. 4.5) [29, 30] and *trans*-sabinene hydrate ((r) in Fig. 4.5) [30].

Pandan (*Pandanus amaryllifolius* Roxb.) is a tropical plant and a source of natural flavoring. The main component obtained in the extraction of Pandan leaves with sc-CO₂ was 2-acetyl-1-pyrroline ((s) in Fig. 4.5) [31, 32].

**Fig. 4.5** Structure of primary compounds found in leaves obtained with supercritical CO₂

Asteraceae (*Tithonia diversifolia*) is a shrub and its general extract has been used for the treatment of diarrhea, fever and malaria. The extraction of its leaves with sc-CO₂ gave tagitinine C ((t) in Fig. 4.5) as main product that has significant antiproliferative activity [33, 34].

β -Sitosterol was extracted from Dandelion (*Teraxacum officinale* Ewber et Wiggers) leaves [35]. β -Sitosterol is one of phytosterols that are useful components because that provide health benefit to lower cholesterol.

There are many other compounds extracted as shown in Table 4.1. As a whole, terpenes, phenolics and phytosterols were mainly detected as compounds extracted from various leaves with sc-CO₂.

4.4 Kinetics of Supercritical CO₂ Extraction of Leaves

4.4.1 Extraction Model

Extraction of natural products such as leaf includes the extraction of components in the cell and absorbed on the solid in the cell and bound to the cell, which leads to complicated extraction kinetics. The extraction step consists of (1) penetration of solvent into the cellular tissue, (2) dissolution of solute to the solvent, (3) transportation of solute from the cell to the surface of the solid matrix, (4) transportation of solute from the surface of solid to bulk solvent in the laminar film of fluid. The transportation step of (3) is often a rate-limiting step. A typical extraction curve is the properties of extract such as extract yield against the total amount of solvent supplied. The example of the extraction curve is shown in Fig. 4.6 afterward. In the early extraction stage, the solubility of the solute controls the extraction rate because there is a lot of solute in the extraction atmosphere and the extraction proceeds towards saturated concentration. After that, the effect of transportation inner the sample becomes major and the extraction rate decreases.

Several models for the extraction curve have been established. Eqs. (4.1)–(4.6) is one of the basic models [36]. This model is based on the fixed-bed extractor that solvent flows axially with superficial velocity through a bed of milled plant material in a cylindrical extractor.

$$e = qy_r[1 - \exp(-Z)] \quad (4.1)$$

$$e = y_r[q - q_m \exp(z_m - Z)] \quad (4.2)$$

$$e = x_0 - \frac{y_r}{W} \ln \left\{ 1 + \left[\exp \left(\frac{Wx_0}{y_r} \right) - 1 \right] \exp[W(q_m - q)]x_k/x_0 \right\} \quad (4.3)$$

$$\frac{z_W}{Z} = \frac{y_r}{Wx_0} \ln \frac{x_0 \exp[W(q - q_m)] - x_k}{x_0 - x_k} \quad (4.4)$$

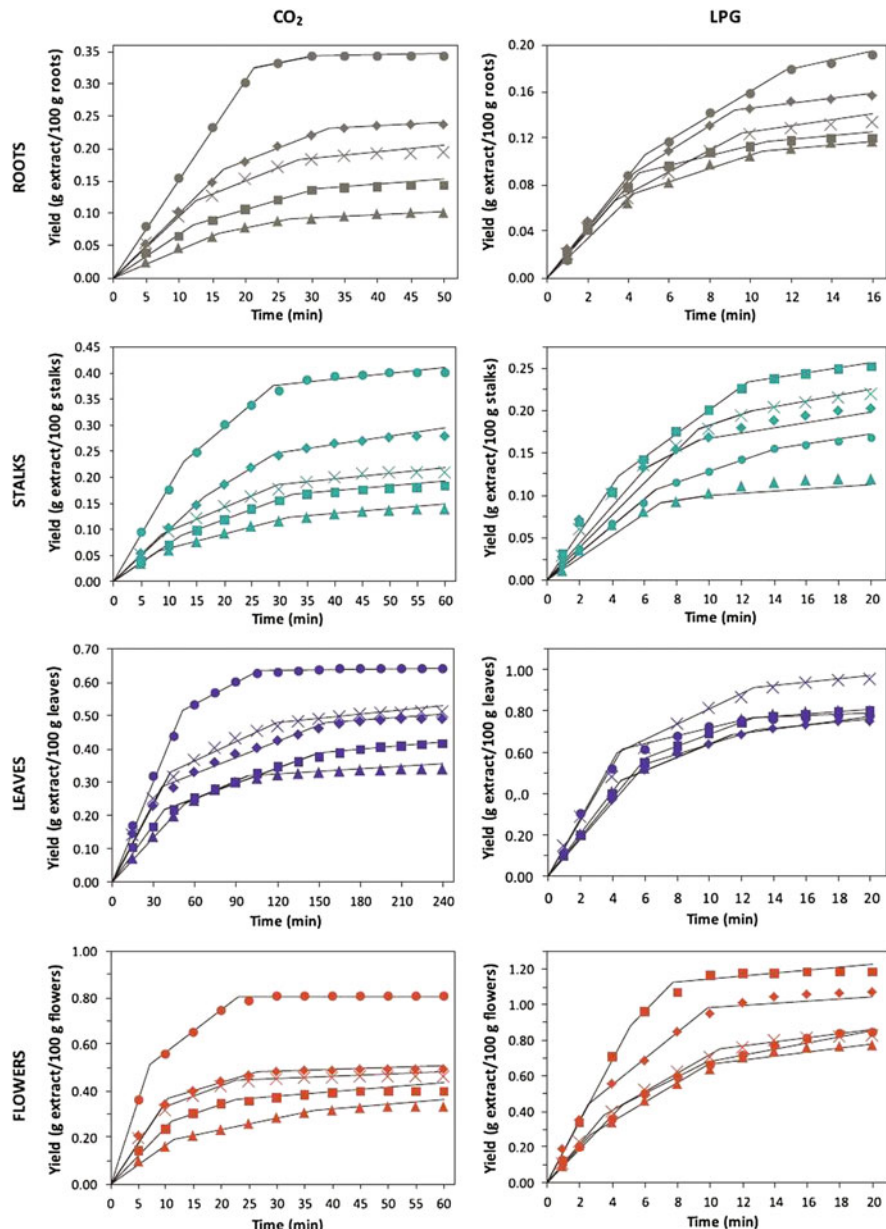


Fig. 4.6 Kinetic yields of extracts obtained from Lupine (*Lupinus albenscens*) by sc-CO₂ and LPG (For sc-CO₂, ■: 313 K, 15 MPa, ♦: 313 K, 25 MPa, ▲: 333 K, 15 MPa, ●: 333 K, 25 MPa, ×: 323 K, 25 MPa; For LPG, ■: 298 K, 1.5 MPa, ♦: 298 K, 3.5 MPa, ▲: 318 K, 1.5 MPa, ●: 318 K, 3.5 MPa, ×: 323 K, 25 MPa; sold line: calculated results, reprinted with permission from [39] Copyright © 2017 Elsevier)

$$Z = \frac{k_f a_0 \rho}{[\dot{q}(1 - \varepsilon)]\rho_s} \quad (4.5)$$

$$W = \frac{k_s a_0}{[\dot{q}(1 - \varepsilon)]} \quad (4.6)$$

where a_0 : specific interfacial area [m^{-1}], e ($=E/N$): extract yield [−], E : weight of extract [kg], k_f : solvent-phase mass transfer coefficient [m s^{-1}], k_s : solid-phase mass transfer coefficient [$\text{m} \cdot \text{s}^{-1}$], N : weight of initial sample [kg], Q : mass of solvent [kg], q ($=Q/N$): specific amount of solvent [−], \dot{q} : mass flow rate of solvent related to $N [\text{s}^{-1}]$, x_0 : initial concentration of solute related to solute-free solvent [−], x_k : initial concentration of solute in easily accessible area related to solute-free solvent, y_r : solubility [g-solute/g-solvent], ε : void fraction [−], ρ : density of solvent [kg/m^3], ρ_s : density of sample [kg/m^3].

Equations (4.1)–(4.3) indicate the extraction curve considering firstly extraction of accessible solute from the cell (Eq. 4.1), then slower extraction of the solute protected by the cell walls (Eq. 4.3) that is controlled by diffusion in the solid phase and there is a transition state between these two situations (Eq. 4.2).

The extraction kinetics of leaves with sc-CO₂ is analyzed for various leaves. The profiles of the properties of extract such as extract yield against the amount of solvent supplied or time are useful to analyze the kinetics [11–13, 15–17, 19–21, 23, 25, 29, 31, 33, 34, 37–51].

In the case of extraction of leaves, the complicated structure of leaf including the existence of plant cell provides various barriers against dissolution and transfer of solute, which leads to influences on extraction kinetics. The typical extraction curve is shown in Fig. 4.6 that is the extraction curve for Lupine (*Lupinus albuscens*) [39]. Although there are extraction curves of sc-CO₂ and liquid propane in this figure, the extraction curves of sc-CO₂ were only concerned in this chapter. The figures in the left row are sc-CO₂ extraction. The parameter related to the extract, that is, extract yield in this case, generally increases with increasing extraction time. The extraction is classified into three steps [37, 39, 45]. The first step is the constant extraction rate step (CER) corresponding to the firstly extraction of accessible solute from the cell. The second step is the falling extraction rate step (FER) corresponding to the transition state between the first step and third step. The third step is diffusion-controlled (DC) step corresponding to slower extraction of the solute protected by the cell walls that being controlled by diffusion in the solid phase.

Some researchers conducted a detailed analysis for extraction. The theoretically mathematical model is proposed [11, 17, 20]. The mathematical model contains two differential solute mass balances in fluid and solid phase, and local equilibrium adsorption representing the relationship between the fluid and solid.

The mass balance of solute on the fluid phase is.

$$\alpha \frac{\partial C}{\partial t} + U_s \frac{\partial C}{\partial z} = -k_f a_p (1 - \alpha) (C - C_{ps}) \quad (4.7)$$

where C : solute concentration in the fluid phase, t : time, z : bed height, C_{ps} : solute concentration in pore at the surface of the particle, α : void fraction, a_p : specific surface area, U_s : superficial velocity, k_f : external mass transfer coefficient.

The mass balance for the solute on the solid phase is.

$$\beta \frac{\partial C_p}{\partial t} = D_e \frac{\partial^2 C_p}{\partial r^2} - (1 - \beta) \frac{\partial C_s}{\partial t} \quad (4.8)$$

where C_p : solute concentration in pores within the particle, β : particle porosity, D_e : effective interparticle diffusion coefficient, r : particle radius, C_s : solute concentration in solid phase.

Consequently, the cumulative fractional yield of solute extracted is.

$$F(\theta) = \left[\frac{A}{1 - \alpha} \right] \times \left\{ \left[\frac{\exp(a_1 \theta) - 1}{a_1} \right] - \left[\frac{\exp(a_2 \theta) - 1}{a_2} \right] \right\} \quad (4.9)$$

$$a_1 = \frac{-b + (b^2 - 4c)^{1/2}}{2} \quad (4.10)$$

$$a_2 = \frac{-b - (b^2 - 4c)^{1/2}}{2} \quad (4.11)$$

$$b = \frac{\phi}{\beta + (1 - \beta)K} + \frac{1}{\alpha} + \frac{\phi(1 - \alpha)}{\alpha} \quad (4.12)$$

$$c = \frac{\phi}{\beta + (1 - \beta)K\alpha} \quad (4.13)$$

$$A = \frac{(1 - \alpha)\phi}{[\beta + (1 - \beta)K]\alpha(a_1 - a_2)} \quad (4.14)$$

where $\theta = t/\tau$, $\phi = K_p a_p \tau$, K : equilibrium adsorption constant.

The most common regression calculation with the above equation and experimental data is performed by mass transfer coefficient k_f and the equilibrium constant K as a fitting parameter.

The simple models are proposed by considering three steps in the extraction [37, 39]. Confortin et al. [39] conducted the extraction of several parts of Lupine (*Lupinus albuscens*) at (313–333) K and (15–25) MPa with sc-CO₂ and LPG. The extraction curve of this system is shown as Fig. 4.6. The proposed sprine model is as follows:

$$Yield(t) = b_1 t \quad (t \leq t_{CER}) \quad (4.15)$$

$$Yield(t) = (b_1 + b_2) t - b_2 t_{CER} \quad (t_{CER} < t \leq t_{FER}) \quad (4.16)$$

$$Yield(t) = (b_1 + b_2 + b_3) t - b_2 t_{CER} - b_3 t_{FER} \quad (t_{FER} \leq t) \quad (4.17)$$

where b_i : adjustable parameters of spline model, t : extraction time variable, t_{CER} : time-span period of CER region, t_{FER} : time-span period of FER region.

Costa et al. [37] analyzed the extraction kinetics about Congo Bololo (*Vernonia amygdalina* Delile) leaves for extract yield. They also proposed a similar simple extraction model (Spline model) considering three extraction steps and claimed that the Spline model presented the best fit to experimental data among other models and was able to characterize constant and decreasing extraction rate periods. When three steps are presented in the extraction curve, the spline model is one of the appropriate models.

Further, a very simple model is shown in Eq. (4.18) and applied for Palo Negro (*Leptocarpha rivularis*) [41].

$$\frac{q}{q_0} = \frac{k_1 t}{1 + k_2 t} \quad (4.18)$$

where k_1 : the parameter related to extraction rate at the very beginning of the process [min^{-1}], k_2 : the parameter related to maximum extraction yield [min^{-1}], q : amount of extract [$\text{g}\cdot\text{kg}^{-1}$ d. s.], q_0 : maximum amount of extracted [$\text{g}\cdot\text{kg}^{-1}$ d. s.], t : time [min].

Other very simple model is proposed in the case of Sage (*Salvia officinalis L.*) leaves [46].

$$\text{Extract yield [\%]} = 100 (1 - \exp(a t + b)) \quad (4.19)$$

where t : extraction time, a, b : constant.

By using this model, the experimental data are correlated by using two parameters.

4.5 Antioxidant Capacity, Total Phenolic Content and Total Flavonoid Content in the Extract Obtained with Supercritical CO₂ Extraction of Leaves

4.5.1 Typical Experimental Conditions

Table 4.2 shows the experimental condition of sc-CO₂ extraction of leaves for evaluation of antioxidant capacity and total phenolic content in the extract. The extraction conditions of these studies are almost at (313–333) K and (10–30) MPa.

Table 4.2 Conditions used to obtain antioxidants and phenolics from leaves with supercritical CO₂

Name	Temp. Press.	Co-sol. ^a	AOC ^b	TPC ^b	Ref.
Aloe (<i>Aloe vera</i>)	305–323 K, 35–45 MPa	M	+		[59]
Bamboo (<i>Sasa palmata</i>)	323–483 K, 10–25 MPa	E, W	+	+	[52]
Congo Bololo (<i>Vernonia amygdalina</i> Delile)	313–333 K, 20–25 MPa		+		[37]
Firespike (<i>Odontonema strictum</i>)	328–338 K, 20–25 MPa	E	+		[63]
Green Tea (<i>Camellia sinensis L.</i>)	313–333 K, 10–20 MPa	E	+		[55]
Hempedu bumi (<i>Andrographis Paniculata</i>)	333 K, 30 MPa	M	+	+	[56]
Jambú (<i>Spilanthes acmella ver oleracea</i>)	323 K, 25 MPa	E, W	+	+	[53]
Lemon balm (<i>Melissa officinalis L.</i>), Rosemary (<i>Rosmarinus officinalis L.</i>), Spanish lavender (<i>Lavandula stoechas</i> ssp.), Thyme (<i>Thymus serpyllum</i>)	313–333 K, 20–30 MPa		+		[76]
Lemon-scented gum (<i>Corymbia citriodora</i>)	309–343 K, 5.18–10 MPa		+		[77]
Limau purut (<i>Citrus hystrix</i>)	313–333 K, 10–36.3 MPa	E	+	+	[61]
Moringa (<i>Moringa oleifera</i>)	313–333 K, 10–20 MPa	E		+	[40]
Palo Negro (<i>Leptocarpha rivularis</i>)	313–333 K 10–20 MPa	E	+		[54]
	313–333 K, 9–15 MPa		+	+	[41]
Rose cactus (<i>Pereskia bleo</i>)	313–333 K, 25–45 MPa	E	+		[58]
Rosemary (<i>Rosmarinus officinalis L.</i>)	313 K, 15–30 MPa		+		[24]
Rosemary (<i>Rosmarinus officinalis L.</i>), Sage (<i>Salvia officinalis L.</i>)	313–373 K, 30 MPa		+		[25]
Spearmint (<i>Mentha spicata</i>)	313–333 K, 10–30 MPa		+		[60]
Strawberry (<i>Fragaria ananassa</i>)	308–333 K, 10–30 MPa	E, W, Ac	+	+	[50, 57]
Tasmanian bluegum (<i>Eucalyptus globulus L.</i>)	313–353 K, 10–35 MPa		+	+	[87]

^aCo-solvent, W: water, M: methanol, E: ethanol, Ac: acetone^bAntioxidant capacity (AOC) and total phenolic content (TPC) +: Evaluated

This is because of easy operation under relatively milder conditions in supercritical states and considering the thermal stability of natural compounds. The extraction temperature in a few studies is over 333 K and it is a rare case. The range for optimization of temperature and pressure is conducted only 20 K and 20 MPa. Further, co-solvent such as methanol, ethanol and water are sometimes used.

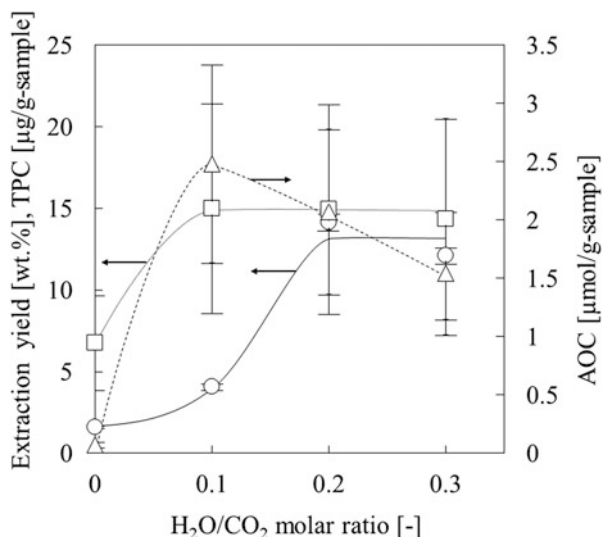
4.5.2 Antioxidant Capacity

Leaves contain antioxidants and the extraction of antioxidants with sc-CO₂ have been widely studied. Table 4.2 summarizes the studies of antioxidant and total phenolic content in the extract obtained with sc-CO₂ extraction of the leaf. One of the major methods for antioxidant capacity is DPPH radical-scavenging assay relative to 2,6-di-*tert*-butyl-*p*-cresol (Butylated hydroxytoluene). “Antioxidant capacity (AOC)” in this chapter means the radical eliminating activity defined in each literature and is not standardized value. It is difficult to organize the condition of extraction and the magnitude of AOC in the extract obtained with sc-CO₂ at this time. In this section, the introduction of some examples of trends are introduced.

The effect of co-solvent for antioxidant capacity were studied [50, 52–57]. In the extraction of Strawberry (*Fragaria ananassa*) leaf with sc-CO₂ + co-solvent at 308 K, 20 MPa and 0.1 of co-solvent/CO₂ molar ratio, the magnitude of AOC was in the order of ethanol > acetone > water > without co-solvent [50]. The solvent probably enhances the extraction of antioxidant compounds in the deep tissue of the leaf. Both nonpolar and polar components were probably present in the extract as an antioxidant because amphiphilic solvents such as ethanol and acetone were effective. In the extraction of Green Tea (*Camellia sinensis L.*) [55], AOC increased with increasing the flow rate of ethanol as co-solvent under constant temperature, pressure and CO₂ flow rate. The addition of polar solvents enhanced the change in the structure of the cellular matrix via intra-crystalline and osmotic swelling and break analyte-matrix bindings. The extraction of Rose cactus (*Pereskia bleo*) with sc-CO₂ + ethanol, AOC increased with increasing the ratio of ethanol to water [58]. The increase in the amount of co-solvent significantly increased AOC. On the other hand, in the case of extraction of Aloe (*Aloe vera*) with sc-CO₂, the effect of co-solvent on AOC was small [59].

In some cases, there is the optimal concentration of co-solvent. The extraction of Bamboo (*Sasa palmata*) leaves with a ternary system of sc-CO₂, ethanol and water were conducted and 25:75 (mol:mol) ethanol-water composition gave the highest AOC at 323 K and 25 MPa [52]. The phenolics contained in Bamboo leaves probably consisted of both ethanol-soluble and water-soluble compounds. Similar results were obtained in the extraction of Jambú (*Spilanthes acmella ver oleracea*) leaves [53]. In the extraction of Strawberry (*Fragaria ananassa*) leaves with sc-CO₂ + water, AOC once increased increasing in water/CO₂ molar ratio and then decreased as shown in Fig. 4.7 [57]. The maximal AOC was 2.48 μmol-BHT/g-sample. The existence of water that is a polar solvent enhanced the dissolution of

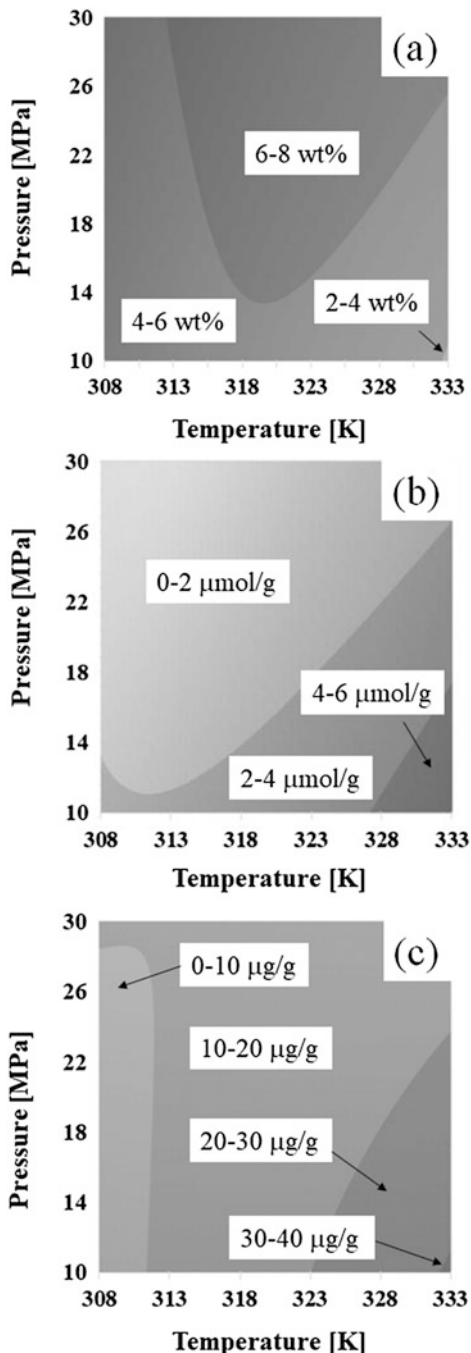
Fig. 4.7 Extraction yield, AOC and TPC at 308 K, 20 MPa and 7.58×10^{-4} mol/s of CO₂ flow rate for 120 min (○: extraction yield, Δ: AOC, □: TPC) of the extract in the extraction of Strawberry (*Fagaria ananassa*) leaves, reprinted with permission from [57] Copyright © 2021 The Society of Chemical Engineers, Japan



antioxidants in the solvent. On the other hand, the phase behavior of sc-CO₂ + water is two-phase regions and the ratio of the volume of CO₂ rich phase decreased with increasing water/CO₂ ratio, which leads to the suppression of the contact between leaves and solvent in CO₂ rich phase as main fluid. The optimal water/CO₂ ratio was probably determined by the balance of positive and negative effects.

The effect of temperature and pressure on AOC was evaluated. The extraction of Strawberry (*Fagaria ananassa*) leaves with sc-CO₂ + water at (308–333) K and (10–30) MPa and 0.1 molar ratio of water/CO₂ was examined [57]. The results were correlated with temperature and pressure, and the response surface against temperature and pressure were constructed as shown in Fig. 4.8. The typical method of response surface analysis is as follows. At first, the experimental conditions such as temperature, pressure and amount of co-solvent are converted to the simple parameter. The parameter is typically between -1 to 1 in the experimental range. After that, the experimental results are correlated with a quadratic polynomial by the determination of the parameters in the equation. AOC was high in higher temperature and lower pressure region. The maximal AOC was 5.65 μmol-BHT/g-sample at 333 K and 10 MPa. The density of solvent decreased with increasing temperature in each pressure. For example, the density of CO₂ decreases from 866 kg/m³ to 724 kg/m³ at 20 MPa when temperature increases from 308 to 333 K [5]. This decrease in density is a factor that decreases the amount of solute dissolving in a solvent. On the other hand, the solubility of compounds generally increases with increasing temperature due to an increase in the vapor pressure of compounds. The effect of change in solubility with temperature was probably the main factor in the extraction of antioxidants from strawberry leaves. The extraction of Aloe (*Aloe vera*) with sc-CO₂ + methanol was examined and AOC was the highest at 305 K, 45 MPa and 24% methanol [59]. The relatively lower temperature and higher pressure region

Fig. 4.8 Response surface analysis of (a) extraction yield, (b) AOC and (c) TPC of the extract in the extraction of Strawberry (*Fragaria ananassa*) leaves at 0.1 of H₂O/CO₂ molar ratio and 7.58 × 10⁻⁴ mol/s of CO₂ flow rate for 120 min



was preferred to obtain high AOC. The author of this paper claimed that higher pressure contributed to the diffusion of polar components and a heat-sensitive property of polar antioxidants suppressed AOC at high-temperature regions. In the case of the extraction of *leptocarpha rivularis* leaves with sc-CO₂, AOC was high in higher pressure and lower temperature region [41]. The high density of solvent probably promoted the extraction of antioxidants.

In some cases, AOC took a maximal value against temperature or pressure. Maran et al. [55] conducted the extraction of Green Tea (*Camellia sinensis L.*) leaves with sc-CO₂ + ethanol at (313–333) K and (10–20) MPa. AOC once increased and then decreased with increasing temperature and increased with increasing pressure. The high solvent density at high pressure decreased the distance between the molecules and thereby strengthening interactions between the fluid and matrix, which leads to the acceleration of mass transfer rate and diffusion of the solvent into the system to improve the extraction of solute. The increase in temperature increased the solute vapor pressure and contributed to damage the particle cell walls increasing mass transfer of solute whereas decomposition of antioxidants during the extraction would occur. A similar trend is reported in the case of extraction of Spearmint (*Mentha spicata*) with sc-CO₂ [60]. AOC tended to higher in high-pressure region and once increased and then decreased with increasing temperature. In the case of extraction of Strawberry (*Fragaria ananassa*) leaf with sc-CO₂ + ethanol, AOC had a maximal value at 20 MPa and was independent of pressure at 308 K [50]. The balance of vapor pressure and solvent density with temperature and pressure determined the extraction of antioxidants. The extraction of Rose cactus (*Pereskia bleo*) was conducted with sc-CO₂ + ethanol [58] and AOC was relatively high in high-pressure region and the low and high-temperature region. In the extraction of Bamboo (*Sasa palmata*) leaves with sc-CO₂ + ethanol or water, the effect of temperature and pressure on AOC depended on the kind of co-solvent [52]. In sc-CO₂ + ethanol, AOC decreased with increasing temperature at 20 MPa, and once increased and then decreased at 323 K. In sc-CO₂ + water, AOC increased with increasing temperature at 20 MPa and increased and became almost constant with increasing pressure at 323 K. Extraction of Limau purut (*Citrus hystrix*) leaves with sc-CO₂ + ethanol was examined [61] and the optimal condition was 323 K and 31.4 MPa estimated by response surface analysis.

4.5.3 Total Phenolic Content

Total phenolic content (TPC) in the extract was evaluated in several studies. TPC is typically measured by the Folin-Ciocalteu method and the content of phenolics is evaluated relative to gallic acid as the standard. The referral of “TPC” in this chapter means that the TPC values were determined according to procedures in each literature reference.

The addition of a polar co-solvent increases TPC by enhancing the extraction of phenolics. In the extraction of Strawberry (*Fragaria ananassa*) leaves with sc-CO₂ at

308 K and 20 MPa, TPC with sc-CO₂ + ethanol, acetone and water were higher than that with sc-CO₂ [50, 57]. These results indicate that the polar solvent was effective for the extraction of phenolic compounds. In the extraction of Bamboo (*Sasa palmata*) leaves with sc-CO₂+ co-solvent, a mixture of 25:75 (mol) ethanol-water co-solvent gave the highest TPC in the whole composition of water-ethanol mixtures [52]. The phenolic compounds consisted of both ethanol and water-soluble compounds.

The trend of the effect of temperature and pressure on TPC resembled that on AOC. In the case of TPC in the extraction of Strawberry (*Fragaria ananassa*) leaves with sc-CO₂ + water at (308–333) K and (10–30) MPa, TPC tended to increase with increasing temperature and decreasing pressure as shown in Fig. 4.8, and the maximal TPC was 31.0 µg-gallic acid/g-sample at 333 K and 10 MPa [57]. In the extraction of Bamboo (*Sasa palmata*) leaves, TPC increased with decreasing temperature and increasing pressure in sc-CO₂ + ethanol while TPC increased with increasing temperature and pressure in sc-CO₂ + water [52].

In some cases, there were optimal conditions. The extraction of Green Tea (*Camellia sinensis L.*) leaves was conducted with sc-CO₂ + ethanol at (313–333) K and (10–20) MPa, and TPC had an optimal value against temperature and increased with increasing pressure [55]. In the extraction of Strawberry (*Fragaria ananassa*) with sc-CO₂ + ethanol at (308–333) K and (10–30) MPa, TPC had maximal value for the temperature at 20 MPa and pressure at 308 K [50].

4.5.4 Total Flavonoid Content

Flavonoids are contained in plants, belong to a class of plant secondary metabolites and contain polyphenolic structure [3]. The flavonoid in the extract from leaves are analyzed. The total flavonoid content (TFC) is measured typically aluminum chloride method and also evaluated as the sum of individual compounds in some cases. In the extraction of leaves with sc-CO₂, the contents of flavonoids in the extract were reported [14, 25, 51, 54, 56, 62, 63].

TFC was measured for Green Tea (*Camellia sinensis L.*) leaves [55], Hempedu bumi (*Andrographis paniculata*) leaves [56] and Palo Negro (*Leptocarpha rivularis*) leaves [54]. In the extraction of Green Tea (*Camellia sinensis L.*) leaves with sc-CO₂ + ethanol at (313–333) K and (10–20) MPa, the estimated maximal of TFC by response surface analysis was 194.60 mg of quercetin equivalents per 100 ml of extract at 323 K and 18.8 MPa [55]. In the extraction of Hempedu bumi (*Andrographis paniculata*) leaves with sc-CO₂, TFC was 179.81 mg per g of extract at 333 K and 30 MPa [56].

The compounds classified as a flavonoid was detected in the extract. The structures of some flavonoids detected are shown in Fig. 4.9. In the extract of Pecah Kaca (*Strobilanthes crispus*) leaves with sc-CO₂ + ethanol at 333 K and 20 MPa, rutin (a), luteolin (b), epicatechin (mixture of c, d), catechin (mixture of e, f), kampferol (g), myricetin (h), naringenin (i) and apigenin (j) were contained [62]. In the extraction of

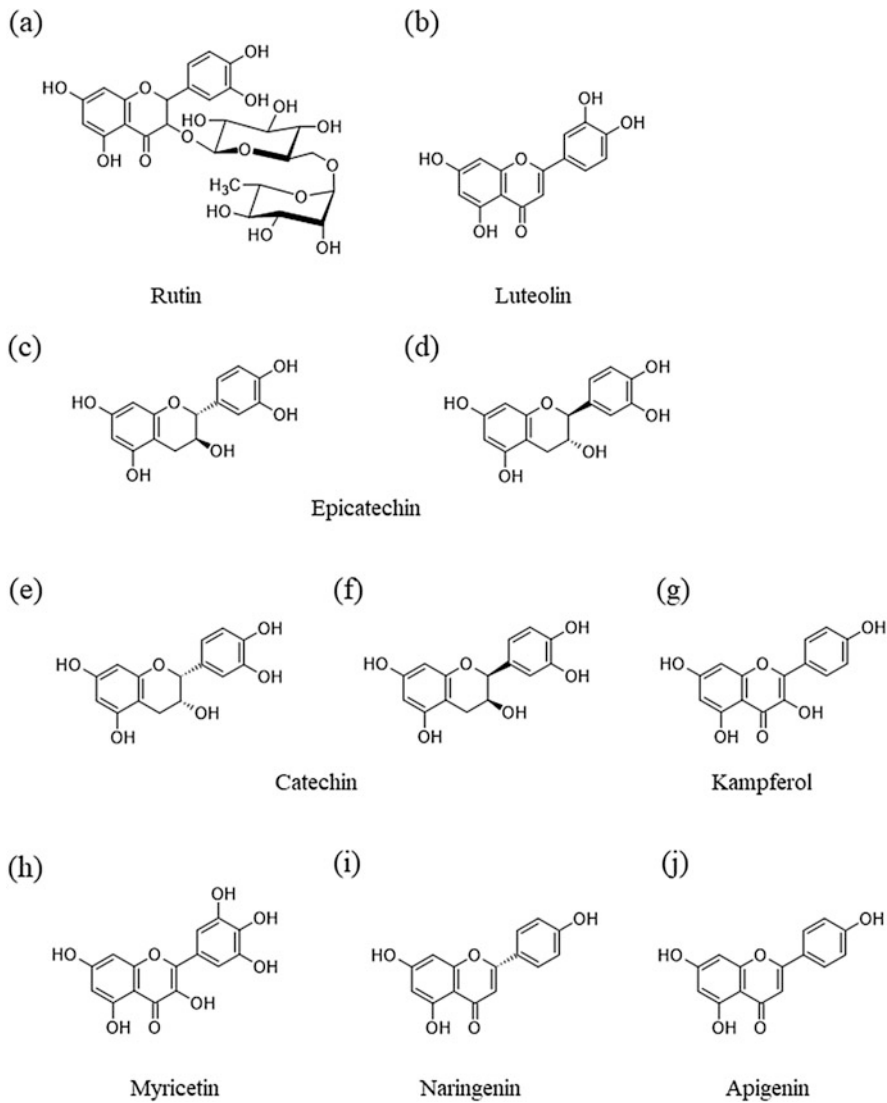


Fig. 4.9 Structure of flavonoids extracted with supercritical CO₂ extraction of leaves from Pecah Kaca (*Strobilanthes crispus*) [62] and Spearmint (*Andrographis paniculata*) [14]

Spearmint (*Andrographis paniculata*) leaves with sc-CO₂ + ethanol at 333 K and 30 MPa, the amount of luteolin (b), apigenin (j), naringenin (i), myricetin (h), epicatechin (c,d), rutin (a), catechin (e,f) was large in this order [14]. The extract from the extraction of Rosemary (*Rosmarinus officinalis L.*) leaves with sc-CO₂ at 373 K and 30 MPa, wogonin, genkwanin, oroxylin A, biochanin A, acacitin and 5,7-dihydroxy-6-methoxyflavone were detected in the extract [25].

4.5.5 Effect of Temperature and Pressure on Kinetics of Supercritical CO₂ Extraction

The effect of temperature and pressure on sc-CO₂ extraction was discussed throughout this chapter. Here, the contribution of temperature and pressure are summarized. Fig. 4.10 shows the effect of vapor pressure of solute and solvent density with temperature and pressure on sc-CO₂ extraction of compounds from leaves.

In low temperature and high-pressure regions, the density of CO₂ is high and the solubility of compounds becomes high. In this case, there are a lot of solvent molecules around the leaf tissue, which probably enhances the transportation of solute from the leaf tissue to solvent by a high saturated concentration of solute in the solvent. On the other hand, low-temperature conditions make the vapor pressure of the solute low and so vaporization of solute from the leaf is suppressed.

In high temperature and low-pressure region, high temperature leads to the high vapor pressure of solute and the solute easily vaporizes into the solvent. The solvent density in high temperature and low-pressure region is low, which leads to the decrease of the number of solvent molecules, which makes the solubility of the solute low. The amount of solute such as antioxidants, phenolics and flavonoids at each condition is determined by considering above factors [50] and the contribution of these factors depends on the kind of leaves. So it is important to evaluate the effect of solvent properties manipulated with temperature and pressure on the extraction kinetics.

4.5.6 Comparison of Supercritical CO₂ Extraction and Conventional Extraction

The comparison of AOC and TPC obtained by sc-CO₂ extraction and that by conventional extraction such as Soxhlet and hydrodistillation were sometimes

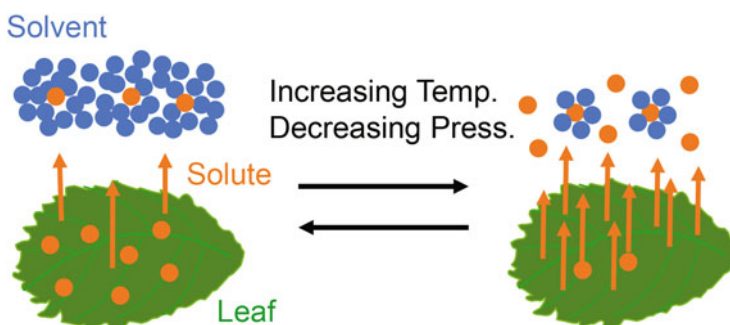


Fig. 4.10 Effect of vapor pressure of solute and solvent density with temperature and pressure on sc-CO₂ extraction of compounds from leaves

examined. In the extraction of Delile (*Vernonia amygdalina*) leaves, AOC and TPC were larger in the order of ethanol > dichloromethane > sc-CO₂ > hexane, which indicates that high polarity of solvent was advantageous of the extraction of antioxidants [37]. In the extraction of Palo Negro (*Leptocar pharivularis*), AOC obtained with hydrodistillation was lower than that with sc-CO₂ extraction because high temperature distillation probably enhanced decomposition of antioxidants. AOC and TPC obtained from the distillation of ethanol-water mixture was larger than sc-CO₂ [41]. In the extraction of Bamboo (*Sasa palmata*) leaves, the ethanol -water solvent (molar ratio 25:75) gave higher AOC than that obtained with sc-CO₂ + ethanol -water solvent (molar ratio 25:75), and TPC for those condition was similar [52]. In the extraction of Jambú (*Spilanthes acmella ver oleracea*), TPC was in the order of hydrodistillation > Soxhlet ethanolic distillation (ethanol-water mixture) > sc-CO₂ extraction [53].

These results indicate that the quantitative comparison was difficult because the extraction system between conventional solvent and sc-CO₂ were different, high polarity of solvent is effective for extraction of antioxidants and phenolics as well as sc-CO₂. In the view of comparison of sc-CO₂ extraction system with conventional extraction one, the advantage of sc-CO₂ system is reducing the amount of polar solvent required for conventional extraction and easier separation of extract from solvent, and disadvantage would be the system being complicated and difficult to make it larger.

4.6 Conclusions and Future Outlook

Extraction of useful components such as antioxidants from leaves with supercritical carbon dioxide (sc-CO₂) is a promising technology for effective usage of biomass. The properties of CO₂ in its supercritical state give it high permeability and provide high solubility of solutes compared with CO₂ in the gas or liquid state. The addition of a polar co-solvent improves extraction of compounds by promoting molecular interactions that are attractive for polar compounds in leaves. Extraction of leaves is typically conducted with a semi-batch system.

Considering the extraction studies of over fifty different types of leaves with sc-CO₂, recovered components such as terpenes, phenolics and phytosterols depend vary widely with the type of leaves. There are three steps in the kinetics of extraction with sc-CO₂ due to the rigid structure of the cell in the leaf. The first step is the constant extraction rate step corresponding to the firstly extraction of accessible solute from the cell. The second step is the falling extraction rate step corresponding to the transition state between the first step and third step. The third step is the diffusion-controlled step corresponding to slower extraction of the solute protected by the cell walls that are controlled by diffusion in the solid phase. Several extraction models were proposed for the extraction curve and some models expressed the extraction curve including the above three steps well.

The total antioxidants (AOC), total phenolics (TPC), total flavonoid content (TFC) in the extract were evaluated. The addition of polar co-solvent such as ethanol and water increased AOC and TPC due to the improvement of solubility of polar compounds in most cases. The effect of temperature and pressure differed according to the kind of leaves. The contribution of both solvent density that becomes large in low temperature and high-pressure region and vapor pressure of solute that becomes large in high-temperature region probably governed the dependence of AOC, TPC and TFC on temperature and pressure.

In the future, generalization of the extract process will be important by extending the extraction conditions, especially to milder conditions. In this case, extraction kinetics in liquid CO₂ just below the critical temperature and critical pressure becomes interesting due to the mingling of different phases. Co-solvents are necessary for the extraction of polar components to compensate for low solubility of CO₂ at low pressures. Water is an inexpensive and environmentally friendly solvent and will become major co-solvent for application in extraction systems. Analysis of extraction kinetics of multiphase systems for sc-CO₂ + water will be necessary.

The extension of the present extraction system to different kinds of leaves is also expected. The recovery of useful components from leave mixtures as a biomass waste is one of the directions of development of this technology. The key factor is finding high added value and highly biological activity compounds from the extraction. It is expected that there will be great progress by making detailed evaluations of compounds obtained from sc-CO₂ extraction of leaves.

References

1. Essien SO, Young B, Baroutian S. Recent advances in subcritical water and supercritical carbon dioxide extraction of bioactive compounds from plant materials. Trends Food Sci Technol. 2020;97:156–69. <https://doi.org/10.1016/j.tifs.2020.01.014>.
2. řtefătesanescu BE, Szabo K, Mocan AS, Crișan G. Phenolic compounds from five ericaceae species leaves and their related bioavailability and health benefits. Molecules. 2019;24:2046. <https://doi.org/10.3390/molecules24112046>.
3. Panche AN, Diwan AD, Chandra SR. Flavonoids: an overview. J Nutr Sci. 2016;5:1–15. <https://doi.org/10.1017/jns.2016.41>.
4. Gadkari PV, Balarman M, Kadimi US. Polyphenols from fresh frozen tea leaves (*Camellia assamica* L.) by supercritical carbon dioxide extraction with ethanol entrainer – application of response surface methodology. J Food Sci Technol. 2015;52:720–30. <https://doi.org/10.1007/s13197-013-1085-9>.
5. NIST, NIST Chemistry Webbook, NIST Standard Reference Database Number 69 (<https://webbook.nist.gov/chemistry/>).
6. Dean JA. Lange's handbook of chemistry. 15th ed. New York: McGraw-Hill; 1972.
7. Secuiianu C, Froiu V, Geană D. Phase behavior for carbon dioxide + ethanol system: experimental measurements and modeling with a cubic equation of state. J Supercrit Fluids. 2008;47: 109–16. <https://doi.org/10.1016/j.supflu.2008.08.004>.
8. Chang CJ, Day C-Y, Ko C-M, Chiu K-L. Densities and P-x-y diagrams for carbon dioxide dissolution in methanol, ethanol and acetone mixtures. Fluid Phase Equilib. 1997;131:243–58. [https://doi.org/10.1016/S0378-3812\(96\)03208-6](https://doi.org/10.1016/S0378-3812(96)03208-6).

9. Peppa GD, Perakis C, Tsimpanogiannis IN, Voutsas EC. Thermodynamic modeling of the vapor-liquid equilibrium of the CO₂/H₂O mixture. *Fluid Phase Equil.* 2009;284:56–63. <https://doi.org/10.1016/j.fluid.2009.06.011>.
10. Sontakke S, Nagavekar N, Dubey KK, Singhal R. Supercritical carbon dioxide extraction of triacontanol from green tea leaves and its evaluation as an unconventional plant growth regulator for spinach tissue culture. *Biocatal Agric Biotechnol.* 2018;16:476–82. <https://doi.org/10.1016/j.bcab.2018.09.018>.
11. Kim W-J, Kim J-D, Oh S-G. Supercritical carbon dioxide extraction of caffeine from Korean green tea. *Sep Sci Tech.* 2007;42:3229–42. <https://doi.org/10.1080/01496390701513008>.
12. Saldaña MDA, Zetzl C, Mohamed RS, Brunner G. Extraction of methylxanthines from Guarana seeds, Maté leaves, and Cocoa beans using supercritical carbon dioxide and ethanol. *J Agric Food Chem.* 2002;50:4820–6. <https://doi.org/10.1021/jf020128v>.
13. Saldaña MDA, Mohamed RS, Mazzafera P. Supercritical carbon dioxide extraction of methylxanthines from Maté tea leaves. *Braz J Chem Eng.* 2000;17:251–9. <https://doi.org/10.1590/S0104-66322000000300001>.
14. Bimakr M, Rahman RA, Ganjloo A, Taip FS, Salleh LM, Sarker MZI. Optimization of supercritical carbon dioxide extraction of bioactive flavonoid compounds from spearmint (*Mentha spicata* L.) leaves by using response surface methodology. *Food Bioprocess Technol.* 2012;5:912–20. <https://doi.org/10.1007/s11947-010-0504-4>.
15. Shahsavarpour M, Lashkarloooki M, Eftekhari MJ, Esmaeilzadeh F. Extraction of essential oils from *Mentha spicata* L. (*Labiateae*) via optimized supercritical carbon dioxide process. *J Supercrit Fluids.* 2017;130:253–60. <https://doi.org/10.1016/j.supflu.2017.02.004>.
16. Özer EÖ, Platin S, Akman U, Hortaçsu Ö. Supercritical carbon dioxide extraction of spearmint oil from mint-plant leaves. *Can J Chem Eng.* 1996;74:920–8. <https://doi.org/10.1002/cjce.5450740615>.
17. Goto M, Sato M, Hirose T. Extraction of peppermint by supercritical carbon dioxide. *J Chem Eng J.* 1993;26:401–7. <https://doi.org/10.1252/jcej.26.401>.
18. Ghosh S, Dutta S, Ghosh PK, Bhattacharjee P, Das S. Design of a polyherbal mix by supercritical carbon dioxide extraction and its encapsulation by spray drying: phytochemical properties and shelf-life study of the encapsulate. *J Food Process Eng.* 2016;40:e12505. <https://doi.org/10.1111/jfpe.12505>.
19. Chatterjee D, Ghosh PK, Ghosh S, Bhattacharjee P. Supercritical carbon dioxide extraction of eugenol from tulsi leaves: process optimization and packed bed characterization. *Chem Eng Res Des.* 2017;118:94–102. <https://doi.org/10.1016/j.cherd.2016.11.025>.
20. Kumoro AC, Hasan M. Modeling of supercritical carbon dioxide extraction of andrographolide from *Andrographis paniculata* leaves. *Chem Eng Comm.* 2008;195:72–80. <https://doi.org/10.1080/00986440701555233>.
21. Kumoro AC, Hasan M. Supercritical carbon dioxide extraction of andrographolide from *Andrographis paniculata*: effect of the solvent flow rate, pressure, and temperature. *Chin J Chem Eng.* 2007;15:877–83. [https://doi.org/10.1016/S1004-9541\(08\)60018-X](https://doi.org/10.1016/S1004-9541(08)60018-X).
22. El-Shemy HA, Aboul-Soud MAM, Nassr-Allah AA, Aboul-Enein KM, Kabash A, Yagi A. Antitumor properties and modulation of antioxidant enzymes' activity by Aloe vera leaf active principles isolated via supercritical carbon dioxide extraction. *Curr Med Chem.* 2010;17:129–38. <https://doi.org/10.2174/092986710790112620>.
23. Kabbash A, Se'oud KAE, Zalat E, Shoeib N, Yagi A. Supercritical carbon dioxide extraction of aloe emodin and barbaloin from aloe vera L. leaves and their in-vitro cytotoxic activity. *Saudi Pharm J.* 2008;16:75–81.
24. Vicente G, Martín D, García-Risco MM, Fornari T, Regiero G. Supercritical carbon dioxide extraction of antioxidants from rosemary (*Rosmarinus officinalis*) leaves for use in edible vegetable oils. *J Oleo Sci.* 2012;61:689–97. <https://doi.org/10.5650/jos.61.689>.
25. Ivanović J, Dilas S, Jadranin M, Vajs V, Babović N, Petrović S, Žižović I. Supercritical carbon dioxide extraction of antioxidants from rosemary (*Rosmarinus officinalis* L.) and sage (*Salvia officinalis* L.). *J Serb Chem Soc.* 2009;74:717–32. <https://doi.org/10.2298/JSC0907717I>.

26. Marongiu B, Porcedda S, Piras A, Sanna G, Murreddu M, Loddo R. Extraction of *Juniperus communis* L. ssp. *nana* Willd essential oil by supercritical carbon dioxide. Flavour Fragr J. 2006;21:148–54. <https://doi.org/10.1002/ffj.1549>.
27. Pourmortazavi SM, Baghaee P, Mirhosseini A. Extraction of volatile compounds from *Juniperus communis* L. leaves with supercritical fluid carbon dioxide: comparison with hydrodistillation. Flavour Fragr J. 2004;19:417–20. <https://doi.org/10.1002/ffj.1327>.
28. Marongiu B, Porcedda S, Caredfda A, Gioannis BD, Vargiu L, Colla PL. Extraction of *Juniperus oxycedrus* ssp. *oxycedrus* essential oil by supercritical carbon dioxide: influence of some process parameters and biological activity. Flavour Fragr J. 2003;18:390–7. <https://doi.org/10.1002/ffj.1224>.
29. Simándi B, Oszagyán M, Lemberkovics É, Kéry Á, Kaszács J, Thyrión F, Mátyás. Supercritical carbon dioxide extraction and fractionation of oregano oleoresin. Food Res Int. 1998;31:723–8. [https://doi.org/10.1016/S0963-9969\(99\)00051-4](https://doi.org/10.1016/S0963-9969(99)00051-4).
30. Santoyo S, Cavero S, Jaime L, Ibañez E, Señoráns FJ, Reglero G. Supercritical carbon dioxide extraction of compounds with antimicrobial activity from *Origanum vulgare* L.: determination of optimal extraction parameters. J Food Prot. 2006;69:369–75. <https://doi.org/10.4315/0362-028x-69.2.369>.
31. Yahya F, Lu T, Santos RCD, Fryer PJ, Bakalis S. Supercritical carbon dioxide and solvent extraction of 2-acetyl-1-pyrroline from Pandan leaf: The effect of pre-treatment. J Supercrit Fluids. 2010;55:20–207. <https://doi.org/10.1016/j.supflu.2010.05.027>.
32. Bhattacharjee P, Kshirsagar A, Singhal RS. Supercritical carbon dioxide extraction of 2-acetyl-l-pyrroline from *Pandanus amaryllifolius* Roxb. Food Chem. 2005;91:255–9. <https://doi.org/10.1016/j.foodchem.2004.01.062>.
33. Ziemons E, Barillaro V, Rozet E, Mbakop NW, Lejeune R, Angenot L, Thunus L, Hubert P. Direct determination of tagitinine C in *Tithonia diversifolia* leaves by on-line coupling of supercritical carbon dioxide extraction to FT-IR spectroscopy by means of optical fibres. Talanta. 2007;71:911–7. <https://doi.org/10.1016/j.talanta.2006.05.076>.
34. Ziemons E, Goffin E, Lejeune R, Cunha AP, Angenot L, Thunus L. Supercritical carbon dioxide extraction of tagitinine C from *Tithonia diversifolia*. J Supercrit Fluids. 2005;33:53–9. <https://doi.org/10.1016/j.supflu.2004.04.001>.
35. Simándi B, Kristo Sz T, Kéry Á, Selmezi LK, Kmecz I, Kemény S. Supercritical fluid extraction of dandelion leaves. J Supercrit Fluids. 2002;23:135–42. [https://doi.org/10.1016/S0896-8446\(02\)00012-8](https://doi.org/10.1016/S0896-8446(02)00012-8).
36. Sonová H. Rate of the vegetable oil extraction with supercritical CO₂ I. Modeling of the extraction curves. Chem Eng Sci. 1993;49:409–14. [https://doi.org/10.1016/0009-2509\(94\)87012-8](https://doi.org/10.1016/0009-2509(94)87012-8).
37. Costa FM, Lemos COT, Arvelos S, Traczynski MR, Silva EA, Cardozo-Filho L, Hori CE, Watanabe EO. Evaluation of supercritical carbon dioxide extraction to obtain bioactive compounds from *Vernonia amygdalina* delile leaves. Chem Ind Chem Eng Q. 2020;26:113–24. <https://doi.org/10.2298/CICEQ190226030C>.
38. Careda A, Marongiu B, Porcedda S, Soro C. Supercritical carbon dioxide extraction and characterization of *Laurus nobilis* essential oil. J Agric Food Chem. 2002;50:1492–6. <https://doi.org/10.1021/jf0108563>.
39. Confortin TC, Todero I, Soares JF, Brun T, Luft L, Ugalde GA, Prá VD, Mazutti MA, Tres MV. Extraction and composition of extracts obtained from *Lupinus albuscens* using supercritical carbon dioxide and compressed liquified petroleum gas. J Supercrit Fluids. 2017;128:395–403. <https://doi.org/10.1016/j.supflu.2017.06.006>.
40. Rodríguez-Pérez C, Mendiola JA, Quirantes-Piné R, Ibáñez E, Segura-Carretero A. Green downstream processing using supercritical carbon dioxide, CO₂-expanded ethanol and pressurized hot water extractions for recovering bioactive compounds from *Moringa oleifera* leaves. J Supercrit Fluids. 2016;116:90–100. <https://doi.org/10.1016/j.supflu.2016.05.009>.

41. Uquiche E, Garcés F. Recovery and antioxidant activity of extracts from *leptocarpha rivularis* by supercritical carbon dioxide extraction. *J Supercrit Fluids*. 2016;110:257–64. <https://doi.org/10.1016/j.supflu.2015.12.003>.
42. Lima RN, Ribeiro AS, Cardozo-Filho L, Vedoy D, Alves PB. Extraction from leaves of *Piper klotzschianum* using supercritical carbon dioxide and co-solvents. *J Supercrit Fluids*. 2019;147:205–12. <https://doi.org/10.1016/j.supflu.2018.11.006>.
43. Ashtiani F, Sefidkon F, Yamin Y, Khajeh K. Supercritical carbon dioxide extraction of volatile components from two *Eucalyptus* species (*E. spathulata* and *E. microtheca*). *J Essent Oil Bear Plants*. 2007;10:198–208. <https://doi.org/10.1080/0972060X.2007.10643543>.
44. Teoflović B, Grujić-Letić N, Kovačević S, Podunavac-Kuzmanović S, Gadžurić S. Analysis of operating variables for yerba mate leaves supercritical carbon dioxide extraction. *Chem Ind Chem Eng Q*. 2018;24:231–8. <https://doi.org/10.2298/CICEQ170217035T>.
45. Quispe-Condori S, Sánchez D, Foglio MA, Rosa PTV, Zetzl C, Brunner G, Meireles MAA. Global yield isotherms and kinetic of artemisinin extraction from *Artemisia annua* L leaves using supercritical carbon dioxide. *J Supercrit Fluids*. 2005;36:40–8. <https://doi.org/10.1016/j.supflu.2005.03.003>.
46. Mićić V, Yusup S, Damjanović V, Chan YH. Kinetic modelling of supercritical carbon dioxide extraction of sage (*Salvia officinalis* L.) leaves and jatropha (*Jatropha curcas* L.) seeds. *J Supercrit Fluids*. 2015;100:142–5. <https://doi.org/10.1016/j.supflu.2015.01.018>.
47. Žižović I, Stamenić M, Orlonić A, Skala D. Energy saving in the supercritical carbon dioxide extraction of essential oils from species of the lamiaceae family. *CI & CEQ*. 2006;12:164–7. <https://doi.org/10.2298/CICEQ0603164Z>.
48. Zizovic I, Stamenić M, Orlonić A, Skala D. Supercritical carbon dioxide essential oil extraction of Lamiaceae family species: mathematical modelling on the micro-scale and process optimization. *Chem Eng Sci*. 2005;60:6747–56. <https://doi.org/10.1016/j.ces.2005.03.068>.
49. Hamdan S, Daood HG. Changes in the chlorophyll and carotenoid content and composition of ground thyme leaves as a function of supercritical carbon dioxide and subcritical propane extraction. *Acta Alim*. 2011;40:8–18. <https://doi.org/10.1556/aalim.2010.0015>.
50. Sato T, Ikeya Y, Adachi S, Yagasaki K, Nihei K, Itoh N. Extraction of strawberry leaves with supercritical carbon dioxide and entrainers: antioxidant capacity, total phenolic content, and inhibitory effect on uric acid production of the extract. *Food Bioprod Process*. 2019;117:160–9. <https://doi.org/10.1016/j.fbp.2019.07.003>.
51. Casas L, Mantell C, Rodríguez M, Torrs A, Macías FA, Ossa EJM. Supercritical fluid extraction of bioactive compounds from sunflower leaves with carbon dioxide and water on a pilot plant scale. *J Supercrit Fluids*. 2008;45:37–42. <https://doi.org/10.1016/j.supflu.2007.12.002>.
52. Zulkafli ZD, Wnag H, Miyashita F, Utsumi N, Tamura K. Cosolvent-modified supercritical carbon dioxide extraction of phenolic compounds from bamboo leaves (*Sasa palmata*). *J Supercrit Fluids*. 2014;94:123–9. <https://doi.org/10.1016/j.supflu.2014.07.008>.
53. Dias AMA, Santos P, Seabra IJ, Júnior RNC, Braga MEM, Sousa HC. Spilanthol from *Spilanthes acmella* flowers, leaves and stems obtained by selective supercritical carbon dioxide extraction. *J Supercrit Fluids*. 2012;61:62–70. <https://doi.org/10.1016/j.supflu.2011.09.020>.
54. Uquiche EL, Toro MT, Quevedo RA. Supercritical extraction with carbon dioxide and co-solvent from *Leptocarpha rivularis*. *J Appl Res Med Aromat Plants*. 2019;14:100210. <https://doi.org/10.1016/j.jarmap.2019.100210>.
55. Maran JP, Manikandan S, Priya B, Gurumoorthi. Box-Behnken design based multi-response analysis and optimization of supercritical carbon dioxide extraction of bioactive flavonoid compounds from tea (*Camellia sinensis* L.) leaves. *J Food Sci Technol*. 2015;52:92–104. <https://doi.org/10.1007/s13197-013-0985-z>.
56. Rithwan F, Zhari S, Yunus MAC, Hadzri HM. Efficacy of biological activity of *Andrographis Paniculata* extracted by using supercritical carbon dioxide (Sc-CO₂) extraction. *J Teknol*. 2014;69:61–4. <https://doi.org/10.11113/jt.v69.3175>.

57. Ikeya Y, Aramaki S, Sato T, Itoh N. Extraction of antioxidants from Strawberry leaves with supercritical carbon dioxide and water mixtures. *Kagaku Kogaku Ronbunshu*. 2021;47:1–6. <https://doi.org/10.1252/kakoronbunshu.47.1>.
58. Sharif KM, Rahman MM, Azmir J, Shamsudin SH, Uddin MS, Fahim TK, Zaidul ISM. Ethanol modified supercritical carbon dioxide extraction of antioxidant rich extract from *Pereskia bleo*. *J Ind Eng Chem*. 2015;21:1314–22. <https://doi.org/10.1016/j.jiec.2014.05.047>.
59. Hu Q, Hu Y, Xu J. Free radical-scavenging activity of *Aloe vera* (*Aloe barbadensis* Miller) extracts by supercritical carbon dioxide extraction. *Food Chem*. 2005;91:85–90. <https://doi.org/10.1016/j.foodchem.2004.05.052>.
60. Mandana B, Russly AR, Ali G, Farah ST. Antioxidant activity of spearmint (*Mentha spicata* L.) leaves extracts by supercritical carbon dioxide (SC-CO₂) extraction. *Int Food Res J*. 2011;18: 543–7.
61. Jamilah B, Abdulkadir Gedi M, Suhaila M, Md Zaidul IS. Phenolics in *Citrus hystrix* leaves using supercritical carbon dioxide extraction. *Int Food Res J*. 2011;18:941–8.
62. Liza MS, Rahman RA, Mandana B, Jinap S, Rahmat A, Zaidul ISM, Hamid A. Supercritical carbon dioxide extraction of bioactive flavonoid from *strobilanthes crispus* (Pecah Kaca). *J Supercrit Fluids*. 2010;88:319–26. <https://doi.org/10.1016/j.jfbp.2009.02.001>.
63. Ouédraogo JCW, Dicjo C, Kini FB, Bonzi-Coulibaly YL. Enhanced extraction of flavonoids from *Odontonema strictum* leaves with antioxidant activity using supercritical carbon dioxide fluid combined with ethanol. *J Supercrit Fluids*. 2018;131:66–71. <https://doi.org/10.1016/j.supflu.2017.08.017>.
64. Ciftci ON, Cahyadi J, Guigard SE, Saldaña MDA. Optimization of artemisinin extraction from *Artemisia annua* L. with supercritical carbon dioxide + ethanol using response surface methodology. *Electrophoresis*. 2018;39:1926–33. <https://doi.org/10.1002/elps.201800084>.
65. Guleria S, Jaitak V, Saini R, Kaul VK, Lal B, Babu GDK, Singh B, Singh RD. Comparative studies of volatile oil composition of Rhododendron anthopogon by hydrodistillation, supercritical carbon dioxide extraction and head space analysis. *Nat Prod Res*. 2011;25:1271–7. <https://doi.org/10.1080/14786419.2011.576395>.
66. Lee H, Hong W, Yoon J, Song K, Kwak S, Liu J. Extraction of indole alkaloids from *Catharanthus roseus* by using supercritical carbon dioxide. *Biotechnol Tech*. 1992;6:127–30. <https://doi.org/10.1007/BF02438817>.
67. Pino JA, Garcia J, Martinez MA. Solvent extraction and supercritical carbon dioxide extraction of *Lippia alba* (Mill.) N. E. Brown leaf. *J Essent Oil Res*. 1997;9:341–3. <https://doi.org/10.1080/10412905.1997.10554256>.
68. Kueh BWB, Yusup S, Osman N. Supercritical carbon dioxide extraction of *Melaleuca cajuputi* leaves for herbicides allelopathy: Optimization and kinetics modeling. *J CO₂ Util*. 2018;24: 220–7. <https://doi.org/10.1016/j.jcou.2018.01.005>.
69. Bulushi KA, Attard TM, North M, Hunt AJ. Optimisation and economic evaluation of the supercritical carbon dioxide extraction of waxes from waste date palm (*Phoenix dactylifera*) leaves. *J Clean Prod*. 2018;186:988–96. <https://doi.org/10.1016/j.jclepro.2018.03.117>.
70. Mohd TAT, Alias N, Ghazali NA, Azizi A, Idris SA, Arina S. Potential of five-leaved chaste tree (*Vitex negundo* L.) leaves as source of natural dye from supercritical carbon dioxide (sc-CO₂) extraction. *Key Eng Mater*. 2014;594-595:207–13. <https://doi.org/10.4028/www.scientific.net/KEM.594-595.207>.
71. Choi YH, Kim J, Yoo K. Supercritical-fluid extraction of bilobalide and ginkgolides from *Ginkgo biloba* leaves by use of a mixture of carbon dioxide, methanol, and water. *Chromatographia*. 2002;56:753–7. <https://doi.org/10.1007/BF02492479>.
72. Moore WN, Taylor LT. Extraction and quantitation of digoxin and acetyldigoxin from the *Digitalis lanata* leaf via near-supercritical methanol-modified carbon dioxide. *J Nat Prod*. 1996;59:690–3. <https://doi.org/10.1021/np960432g>.
73. Aziz AHA, Putra NR, Kong H, Yunus MAC. Supercritical carbon dioxide extraction of sinensetin, isosinensetin, and rosmarinic acid from *Orthosiphon stamineus* leaves: optimization and modeling. *Arab J Sci Eng*. 2020;45:7467–76. <https://doi.org/10.1007/s13369-020-04584-6>.

74. Pino JA, Garcia J, Martinez MA. Comparative chemical composition of the volatiles of *Coleus aromaticus* produced by steam distillation, solvent extraction and supercritical carbon dioxide extraction. *J Essent Oil Res.* 1996;8:373–5. <https://doi.org/10.1080/10412905.1996.9700643>.
75. Marongiu B, Maxia A, Piras A, Porcedda S, Tuveri E, Deriu A, Zanetti S. Extraction of *Lantana camera* essential oil by supercritical carbon dioxide: influence of the grinding and biological activity. *Nat Prod Res.* 2007;21:33–6. <https://doi.org/10.1080/14786410601036108>.
76. Topal U, Sasaki M, Goto M, Otles S. Chemical compositions and antioxidant properties of essential oils from nine species of Turkish plants obtained by supercritical carbon dioxide extraction and steam distillation. *Int J Food Sci Nutr.* 2008;59:619–35. <https://doi.org/10.1080/09637480701553816>.
77. Dogenski M, Ferreira NJ, Oliveira AL. Extraction of *Corymbia citriodora* essential oil and resin using near and supercritical carbon dioxide. *J Supercrit Fluids.* 2016;115:54–64. <https://doi.org/10.1016/j.supflu.2016.04.015>.
78. Pino JA, Garcia J, Martinez MA. Solvent extraction and supercritical carbon dioxide extraction of *Pimenta dioica* Merrill. leaf. *J Essent Oil Res.* 1997;9:689–91. <https://doi.org/10.1080/10412905.1997.9700812>.
79. Foo LW, Salleh E, Hana SN. Green extraction of antimicrobial bioactive compound from *Piper betle* leaves: Probe type ultrasound-assisted extraction vs supercritical carbon dioxide extraction. *Chem Eng Trans.* 2017;56:109–14. <https://doi.org/10.3303/CET1756019>.
80. Manpong P, Douglas S, Douglas PL, Pongamphai S, Teppaitoon W. Preliminary investigation of gallic acid extraction from *Jatropha curcas* Linn leaves using supercritical carbon dioxide with methanol co-solvent. *J Food Process Eng.* 2009;34:1408–18. <https://doi.org/10.1111/j.1745-4530.2009.00506.x>.
81. Francisco J C, Järvenpää E P, Huopalahti R, Sivik B (2001) Comparison of *Eucalyptus camaldulensis* Dehn oils from Mozambique as obtained by hydrodistillation and supercritical carbon dioxide extraction. *J Agric Food Chem* 49:2339–2342, doi: <https://doi.org/10.1021/jf0013611>.
82. Marongiu B, Maxia A, Piras A, Porcedda S, Tuveri E, Gonçalves MJ, Cavaleiro C, Salgueiro L. Isolation of *Cirthmum maritimum* L. volatile oil by supercritical carbon dioxide extraction and biological assays. *Nat Prod Res.* 2007;21:1145–50. <https://doi.org/10.1080/14786410600911616>.
83. Machalova Z, Sajfrtova M, Pavela R, Topiar M. Extraction of botanical pesticides from *Pelargonium graveolens* using supercritical carbon dioxide. *Ind Crop Prod.* 2015;67:310–7. <https://doi.org/10.1016/j.indcrop.2015.01.070>.
84. Marongiu B, Piras A, Porcedda S, Tuveri E, Maxia A. Isolation of *Seseli bocconi* Guss., subsp. *praeox* Gamisans (Apiaceae) volatile oil by supercritical carbon dioxide extraction. *Nat Prod Res.* 2006;20:820–6. <https://doi.org/10.1080/14786410500364684>.
85. Casrañeda-Acosta J, Cain AW, Fischer NH, Knopf FC. Extraction of bioactive sesquiterpene lactones from *Magnolia grandiflora* using supercritical carbon dioxide and near-critical propane. *J Agric Food Chem.* 1995;43:63–8. <https://doi.org/10.1021/jf00049a013>.
86. Zhang H, Li Q, Qiao G, Qiu Z, Wen Z, Wen X. Optimizing the supercritical carbon dioxide extraction of sweet cherry (*Prunus avium* L.) leaves and UPLC-MS/MS analysis. *Anal Methods.* 2020;12:3004–13. <https://doi.org/10.1039/D0AY00718H>.
87. Singh A, Ahmad A, Bushra R. Supercritical carbon dioxide extraction of essential oils from leaves of *Eucalyptus globulus* L., their analysis and application. *Anal Methods.* 2016;8:1339–50. <https://doi.org/10.1039/C5AY02009C>.

Part III

Production of Biofuels and Chemicals by

Biodegradation

Chapter 5

Recovery of Biohydrogen and Biomethane by Anaerobic Fermentation of Organic Solid Waste



Yu Qin, Aijun Zhu, and Yu-You Li

Abstract Organic solid waste, which mainly consists of biowaste, around the world is increasing at an alarming rate. Much of the carbon in this biowaste originates from photosynthesis of atmospheric CO₂. Long before human existence, microorganisms have been returning biomass carbon to the atmosphere to close the carbon cycle loop. Nowadays, anaerobic biotechnology has been developed to intentionally strengthen those microbial abilities to reduce waste and recover biofuels at the same time. CH₄ is one of the major components in the final product of anaerobic digestion, and H₂ is the gaseous intermediate product during the CH₄ fermentation. After years of intensive researches on hydrogen and methane fermentation, co-production of H₂ and CH₄ via the R-TPAD (recirculated two-phase anaerobic digestion) process has been found to be both feasible and desirable. In this chapter, the fundamentals of H₂ and CH₄ fermentation are summarized. As the most outstanding features of the R-TPAD process, its characteristics of hydraulic separation are calculated and discussed. Then, the potential of R-TPAD is highlighted by recent applications in treating different types of organic solid waste for co-production of H₂ and CH₄.

Keywords Hydrogen · Methane · Hythane · Anaerobic digestion · Fermentation · Food waste · Two-phase · Recirculation

5.1 Introduction

Biomass plays a complex role in the carbon cycle on the earth. Whether plant- or animal- sources, the origin of biomass is photosynthesis, with the conversion of atmospheric CO₂ in the presence of solar energy. As it flows through the food chains,

Y. Qin · A. Zhu · Y.-Y. Li (✉)

Laboratory of Environmental Protection Engineering, Department of Civil and Environmental Engineering, Graduate School of Engineering, Tohoku University, Sendai, Japan
e-mail: gyokuyu.ri.a5@tohoku.ac.jp

the biochemical energy in the biomass is released and utilized by ecological producers, consumers, and decomposers. The decomposers, which in most cases are microorganisms, clean up biomass at the ends of the food chains. This is one of the great contributors to the self-cleaning capacity of the nature. As society has developed over time, the amount of biowaste has increased along with human activities and the efforts to find techniques to diminish this waste have been intensified along with it.

Anaerobic digestion/fermentation can contribute to achieving sustainable development goals. By applying anaerobic techniques, the direction of waste management turns from a passive way of reducing biowaste into a proactive way of generating valuable products, like gaseous biofuels. It provides sustainable alternatives for the industrial ecology. Anaerobic digestion/fermentation is the natural degradability enhanced by engineering methodologies. The final products of anaerobic fermentation are CH_4 and CO_2 , with H_2 being the gaseous intermediate product during anaerobic fermentation process. Some liquid biofuels (e.g. bioethanol) or value-added products (e.g. middle-chain fatty acids, lactic acid, or from glutamate to antibiotics) can also be produced by fermentation [1]. Since all products and by-products are converted from biomass, anaerobic fermentation is carbon neutral [2]. From these considerations, anaerobic fermentation has a promising future.

Anaerobic fermentation involves a number of biochemical reactions conducted by anaerobic or facultative microorganisms, where the organics or CO_2 act as electron acceptors rather than O_2 . The electron donors during the fermentation can be other (functional groups of) organics or H_2 . The substrates considered for H_2 and CH_4 fermentation are the types of biowaste that are generated in massive quantities. Biowaste like sewage sludge, food waste, and paper waste can be collected from the municipal system and other types of biowaste, like animal manure or corn stalk, can be collected from agricultural fields. In recent times, certain agricultural industries also produce such organic solid waste as algae, molasses and bagasse. All of these types of biowaste have one point in common: their relatively high moisture content makes them unsuitable for combustion.

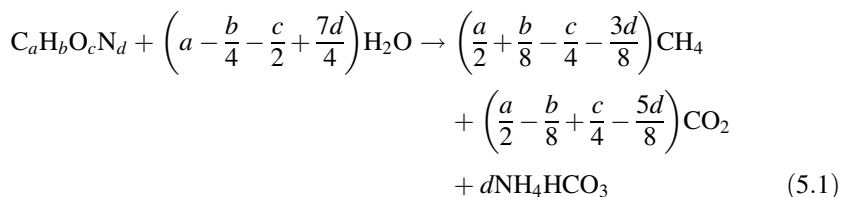
Advantages of recovering H_2 and CH_4 from organic solid waste are many [3]: (1) Fermentation can be conducted under standard pressure and mild temperature conditions; (2) the gaseous biofuels, can be spontaneously separated from the liquid phase; and (3) low cost of energy consumption, for extraction or evaporation. There are, however, shortcomings of anaerobic fermentation, which are associated with the key players in the process: the fermentative microorganisms. Since the biochemical conversions are conducted under mild conditions, the reaction rates are much slower than other methods, e.g. hydrothermal reactions or pyrolysis. Anaerobic microorganisms have to be cultured under appropriate and stable conditions and extra time is needed for domestication when encountering atypical organics. They can be inhibited by some common molecules, e.g. NH_3 , H_2S or long-chain fatty acids (LCFA). Some other compounds, like lignin or synthetic polymers, are absent from the menu of the anaerobic microorganisms. Therefore, while the successful operation of anaerobic fermentation has many benefits, the system must be carefully controlled to maintain stable performance.

This chapter summarizes the basic principles and application of H₂ and CH₄ fermentation. The term “anaerobic digestion” is seen equivalent to “CH₄ fermentation” when organic solid waste is treated. As an efficient combination of H₂ and CH₄ fermentation, R-TPAD (recirculated two-phase anaerobic digestion) process, is introduced. To explain the effect of hydraulic separation within this process, hydraulic characteristics are calculated. Applications of the R-TPAD process for treating different types of organic solid waste are summarized.

5.2 Basic Principles in Methane and Hydrogen Fermentation

5.2.1 Stoichiometry

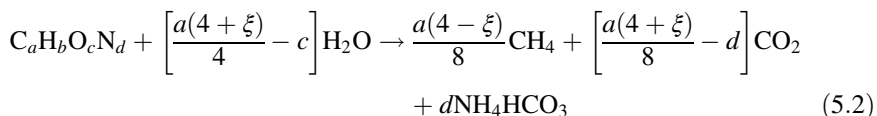
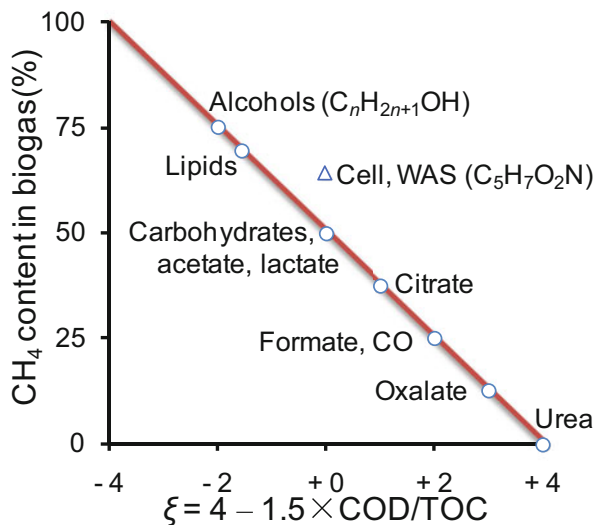
The potential of methane production from biomass is determined by its elemental components. Supposing that organic compounds are completely degraded and converted to methane, the reaction equation of methane fermentation is



where *a*, *b*, *c*, and *d* are the coefficients of C, H, O, and N in the (estimated) formula of the organic compound, respectively. While the coefficients *a*, *b*, *c*, and *d* of the same compound may differ according to the base elements, their ratios must be the same. In other words, C₅H₇O₂N must not be confused, for example, with CH_{1.4}O_{0.4}N_{0.2}. The nitrogen in the final products is ammonia nitrogen. While nitrogen sometimes exists in the substrate in the form of nitrate and nitrite, the majority of nitrogen should be derived from the amino group in the particulate proteins. Ammonia is the source of alkalinity in anaerobic conditions, and its alkalinity is transferred to the bicarbonate ion, which will be discussed in detail in Sect. 5.2.3.2. Before anaerobic fermentation is started, the chemical oxygen demand (COD) of the compound is analyzed with the unit of g-O₂/kg-biowaste. Although the results may not be accurate due to incomplete oxidation of some aromatic compounds, the COD determination with potassium dichromate is broadly used because its oxidability is high enough while the nitrogen is still in the form of ammonia. In elemental analysis with combustion, sulfur content can also be provided in addition to C, H, N, and O. In practical cases, however, S is seldom quantified since it has such wide viability with actual conditions.

More concisely, Eq. (5.1) can be rewritten as

Fig. 5.1 Relation between CH₄ content in produced biogas and ξ (average oxidation state of carbon) in substrate



where ξ is the average oxidation state of C in the formula of the organics, $a\xi = -b + 2c + 3d$. The relation between ξ and COD is

$$\xi = 4 - \frac{\text{COD}}{8} / \frac{\text{TOC}}{12} = 4 - 1.5 \times \frac{\text{COD}}{\text{TOC}} \quad (5.3)$$

where TOC is the total organic carbon with the unit of g-C/kg-biomass. The relation between ξ and the CH₄ content is shown in Fig. 5.1.

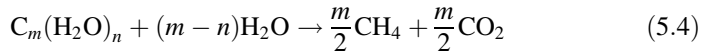
The stoichiometric coefficients in methane fermentation of common compounds are listed in Table 5.1. Carbohydrates, proteins, and lipids are the three major components in biomass, whose compositions determine the average ξ of the biomass. The carbohydrates category includes monosaccharides (glucose, fructose, xylose, arabinose, etc.), disaccharides (maltose, sucrose, lactose, cellobiose, etc.), and polysaccharides (starch, cellulose, hemicellulose, etc.). In the case of monosaccharides, members within the group of hexoses (C₆H₁₂O₆) or pentoses (C₅H₁₀O₅) share the same equation as that for methane fermentation. Of the three major components, only proteins provide nitrogen, and lipids own the highest potential biomethane yield in theory.

The reaction equation for CH₄ fermentation of carbohydrates can be written as:

Table 5.1 Stoichiometric coefficients of methane fermentation for common compounds

Substrates	Reactants	Products				Water demand	Biogas production		Ammonia or alkalinity production		
	Molecular formula	H ₂ O	CH ₄	CO ₂	NH ₄ ⁺	HCO ₃ ⁻	NL-biogas/kg-VS ^a	NL-CH ₄ /kg-VS	CH ₄ % in biogas	g-NH ₃ -N/kg-VS	g-CaCO ₃ /kg-VS
Formic acid	CH ₂ O ₂	-0.5	0.25	0.75	-	-1.96	487	122	25.00	0	0
Acetic acid	C ₂ H ₄ O ₂	0	1	1	-	0	746	373	50.00	0	0
Propionic acid	C ₃ H ₆ O ₂	0.5	1.75	1.25	-	-121	907	529	58.33	0	0
Butyric acid	C ₄ H ₈ O ₂	1	2.5	1.5	-	-204	1017	636	62.50	0	0
SFA ^b	C _n H _{2n} O ₂	$\frac{n-2}{2}$	$\frac{3n-2}{4}$	$\frac{n+2}{4}$	-	-	$\frac{n-2}{4(7n+16)}$	$\frac{22.4n}{[14n+32]}$	$\frac{25(3n-2)}{8(n+16)}$	0	0
Lactic acid	C ₃ H ₆ O ₃	0	1.5	1.5	-	-0	746	373	50.00	0	0
Ethanol	C ₂ H ₅ OH	0	1.5	0.5	-	-0	972	729	75.00	0	0
Cells (WAS ^c)	C ₅ H ₁₀ O ₂ N	4	2.5	1.5	1	1	637	792	495	62.50	124
Glucose	C ₆ H ₁₂ O ₆	0	3	3	-	-0	746	373	50.00	0	0
Cellulose/starch	(C ₆ H ₁₀ O ₅) _n	<i>n</i>	3 <i>n</i>	3 <i>n</i>	-	-111	829	414	50.00	0	0
Protein[4]	C ₁₆ H ₂₄ O ₅ N ₄	14.5	8.25	3.75	4	4	741	763	524	68.75	159
Lipid[4]	C ₅₀ H ₉₀ O ₆	24.5	34.75	15.25	-	-	560	1423	989	69.50	0
Primary sludge[5]	C ₂₂₂ H ₃₉ O ₁₀ N	9	13	8	1	1	339	985	610	61.90	29
Sewage sludge[5]	C ₁₀ H ₁₉ O ₃ N	5.5	6.25	2.75	1	1	492	1002	696	69.44	70
Night soil[5]	C ₇ H ₁₂ O ₄ N	3.8	3.625	2.375	1	1	388	772	466	60.42	80
Cow manure[6]	C ₂₂ H ₃₁ O ₁₁ N	10.5	11.75	9.25	1	1	389	969	542	55.95	29
Kitchen waste[7]	C ₁₇ H ₂₉ O ₁₀ N	6.5	9.25	6.75	1	1	287	880	509	57.81	34
Food waste[8]	C ₄₆ H ₇₃ O ₃₁ N	14	24	21	1	1	222	887	473	53.33	12
Paper waste[5]	C ₂₆₆ H ₄₃₄ O ₂₁₀ N	54.3	134.4	130.6	1	1	139	847	430	50.71	2
											7

^aVS: volatile solids^bSFA: saturated fatty acids
^cWAS: waste activated sludge



where m and n are the coefficients of C and (H_2O) in the formula of the carbohydrate, respectively.

According to their chemical formula, the average oxidation state of C is 0. When Eq. (5.4) is used to describe the anaerobic degradation of carbohydrates (neglecting the cell growth), the ratios of CH_4 to CO_2 are fixed at 1:1.

Protein is an important component of biomass for methane fermentation because it brings nitrogen and alkalinity to the liquid phase of the anaerobic system. Proteins are synthesized after being dehydrated from diverse α -amino acids. Apart from $-\text{NH}_2$ and $-\text{COOH}$, the carbon chain of the amino acids consists of either methyl ($-\text{CH}_3$) or methylene ($=\text{CH}_2$). For this reason, the ratios of CH_4 to CO_2 in the biogas are always greater than 1. Because some portion of CO_2 will react with NH_3 to increase the solubility in the liquid phase, CH_4 in the gas phase will be higher than without proteins.

Lipids are important substances for all life forms since they are essential parts of cell membranes. In organic solid waste, lipids are the fats, i.e. triacyl glycerol, which is dehydrated from glycerol and LCFA. Because most carbons in the carbon chains are saturated, the ratio of CH_4 to CO_2 in the degradation products of lipids is also greater than 1. According to Table 5.1, lipids can potentially reach high CH_4 yield, but they are not the typical substrate of CH_4 fermentation because of the strong inhibition by LCFA. The major problems of lipid substrates are as follows: (a) their hydrophobic nature limits mass transfer with the liquid (water) phase, and (b) they have an inhibitory effect on anaerobes, especially methanogens. For oily biowaste, extraction is required to recover bioenergy in the form of biodiesel.

According to Eqs. (5.1) and (5.2), the theoretical mass balance can be calculated. The results are also listed in Table 5.1.

$$\begin{aligned} \text{Water demand [g-H}_2\text{O/g-VS]} &= \frac{4a - b - 2c + 7d}{4M} \times 18 \\ &= \frac{18}{M} \left(a + \frac{a\xi}{4} - c + d \right) \end{aligned} \quad (5.5)$$

$$\text{Biogas production [NL/g-VS]} = \frac{a - d}{M} \times 22.4 \quad (5.6)$$

$$\text{CH}_4 \text{ production [NL-CH}_4/\text{g-VS]} = \frac{(4 - \xi)a}{8M} \times 22.4 = \frac{a}{M} \cdot \frac{\text{COD}}{\text{TOC}} \times 4.2 \quad (5.7)$$

$$\begin{aligned}\text{CH}_4 \text{ content in biogas [\%]} &= \frac{4a + b - 2c - 3d}{8(a - d)} \times 100 \\ &= \frac{(4 - \xi)a}{8(a - d)} \times 100 \\ &= \frac{3a}{16(a - d)} \cdot \frac{\text{COD}}{\text{TOC}} \times 100\end{aligned}\quad (5.8)$$

$$\text{Ammonia production [g-NH}_3\text{-N/g-VS]} = \frac{d}{M} \times 14 \quad (5.9)$$

$$\text{Alkalinity production [g-CaCO}_3\text{/g-VS]} = \frac{d}{M} \times 50 \quad (5.10)$$

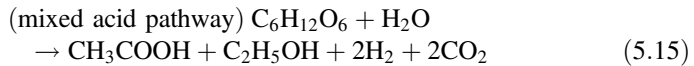
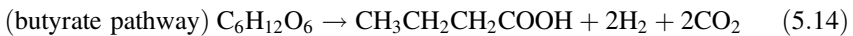
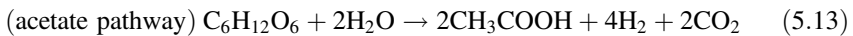
where M is the relative molecular mass of $\text{C}_a\text{H}_b\text{O}_c\text{N}_d$, $M = 12a + b + 16c + 14d$.

Ammonia or alkalinity production can be estimated using the biogas volume and C/N ratio.

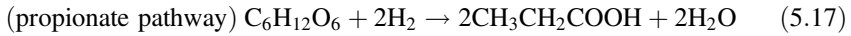
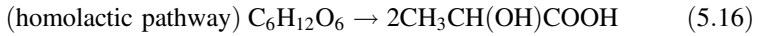
$$\begin{aligned}\text{Ammonia production [g-NH}_3\text{-N/NL-biogas]} &= \frac{d}{a - d} \times \frac{14}{22.4} \\ &= \frac{1}{\text{C/N} - 1} \times \frac{5}{8}\end{aligned}\quad (5.11)$$

$$\text{Alkalinity production [g-CaCO}_3\text{/NL-biogas]} = \frac{1}{C/N - 1} \times \frac{1}{0.448} \quad (5.12)$$

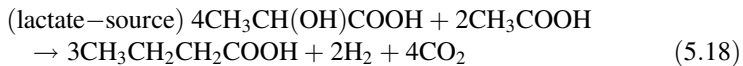
Unlike the wide range of choices for CH_4 fermentation, substrates for H_2 fermentation are carbohydrates in most cases. From hexose (glucose), hydrogen fermentation proceeds along the following pathways.



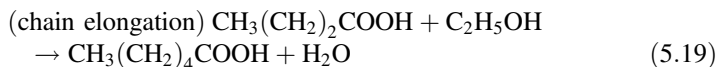
In some cases, some pathways compete or inhibit H_2 fermentation.



Hydrogen can also be generated from lactate.



A portion of butyrate may be converted to caproate. Chain elongation converts volatile fatty acids (VFA, i.e. short-chain fatty acids, SCFA) into middle-chain fatty acids (MCFA), which are also high-value products, for conditions of H₂ fermentation.



These reactions suggest that acetate, butyrate and ethanol are the common by-products of H₂ fermentation. Theoretically, the acetate pathway exhibits the highest yield as 4 mol-H₂/mol-hexose. The existence of caproate does not affect the hydrogen yield. Details will be discussed in Sect. 5.2.2.2.

5.2.2 Four Steps and Two Phases

The major reactions of anaerobic digestion are shown in Fig. 5.2. A complete map of methane fermentation consists of many reactions that basically can be divided into four steps: hydrolysis, acidogenesis, acetogenesis, and methanogenesis [9]. Another way to describe the reactions is to classify them into two phases: the acidogenic phase, which includes hydrolysis and acidogenesis, and the methanogenic phase, which includes acetogenesis and methanogenesis.

5.2.2.1 Hydrolysis

Hydrolysis makes organic solids soluble and ready for a series of reactions. The three major components of the organic solid waste undergo the following reactions: polysaccharides are hydrolyzed into monosaccharides, proteins are hydrolyzed into polypeptide and finally α -amino acids, and lipids, generally fats, are hydrolyzed into glycerol and long-chain fatty acids.

Cellulose is the typical components in biowaste. The common cellulolytic bacteria, are *Acetivibrio* sp., *Bacteroides* sp., *Cellulonomas* sp., *Clostridium* sp., *Ruminococcus* sp., *Spirochaeta* sp., *Fibrobacter* sp. etc. Fungi are also considered to be contributors to the anaerobic cellulolysis. The general proteolytic bacteria are *Bacteroides* sp., *Clostridium* sp., *Peptococcus* sp., *Bacterium* sp., *Bacillus* sp., and *Thermobacteroides* sp. Hydrolysis is generally performed by extracellular enzymes, which proceed as first-order reactions. While the phenomenon of hydrolysis is solubilizing the polymers into the liquid, it does not necessarily mean that they become soluble only when the organics are fully hydrolyzed. During hydrolysis, the

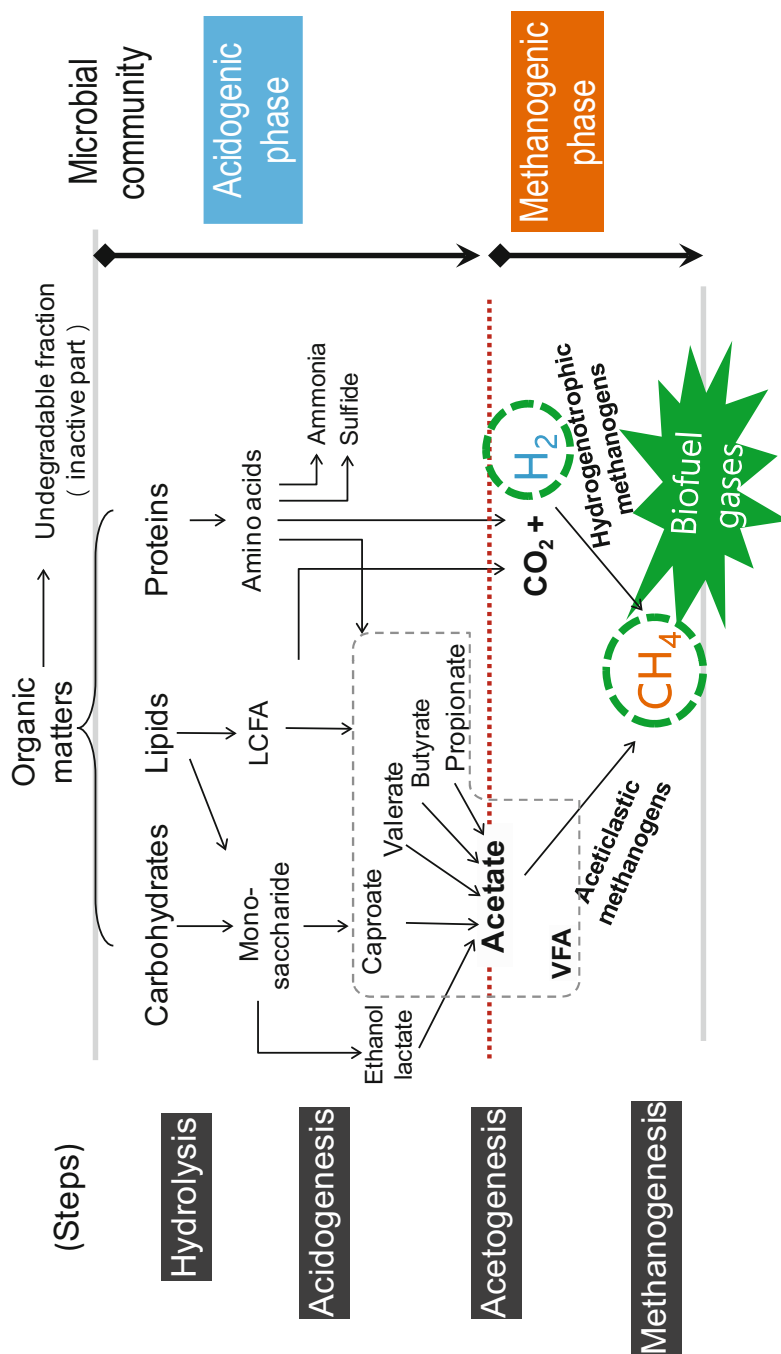


Fig. 5.2 General reactions in methane fermentation

COD remains constant, whereas the TS (total solids) or VS (volatile solids) will increase as a result of the free water added back onto the bonds where condensation reactions occurred during synthesis.

5.2.2.2 Acidogenesis

Acidogenesis refers to reactions that generate VFA for the methanogenic phase. When the operation involves a high-loading rate, the pH drops during this step. This drop in pH is the basis of the term, “the acidogenic phase”. In the continuous operation of CH₄ fermentation, no pH drop is not always observed because the produced organic acids are neutralized by the bicarbonate alkalinity.

Typically, acidogenesis occurs soon after hydrolysis. Acidogens could be obligate anaerobic bacteria, e.g. *Bacteroides* sp., *Butyrivibrio* sp., *Clostridium* sp., *Eubacterium* sp., *Fibrobacter* sp., *Fusobacterium* sp., *Peptococcus* sp., *Ruminococcus* sp., and *Selenomonas* sp., etc., or facultative anaerobic bacteria, e.g. *Bacillus* sp., *Lactobacillus* sp., *Micrococcus* sp., *Staphylococcus* sp., and *Streptococcus* sp.

Hydrogen fermentation is the special case of acidogenesis of carbohydrates. It can also be called dark fermentation, which sets it in contrast to H₂ production via photo-fermentation. Figure 5.3 shows the common pathways of dark fermentation [10], and the reactions are listed above in Eqs. (5.13)–(5.15).

In those conversions, the electrons from dehydrogenation are transferred to NADH and FdH₂. When the FdH₂ accumulates, the electrons and the protons escape as molecular H₂. Fd plays an important role in H₂ fermentation by serving as the active site of hydrogenase, which generally has a structure of iron-sulphur cluster. Figure 5.4 shows the typical iron-sulphur cluster in a hydrogenase. Compared to the [FeFe] hydrogenase, other types, e.g. [NiFe] hydrogenase and [NiFeSe] hydrogenase, have also been found [11]. Their existence indicates that the elements, S, Fe, Ni, and Se, are important for the hydrogen and methane fermentation.

5.2.2.3 Acetogenesis

Acetogenesis includes the reactions that convert the products of acidogenesis into acetates so that the methanogens can directly utilize them. Acetogenesis generally oxidizes the VFA into acetate and molecular hydrogen, where the acetate is the oxidized product.



Molecular H₂ can also be produced from the oxidation of VFA (acetogenesis). However, the H₂ from acetogenesis is different from that from acidogenesis (H₂

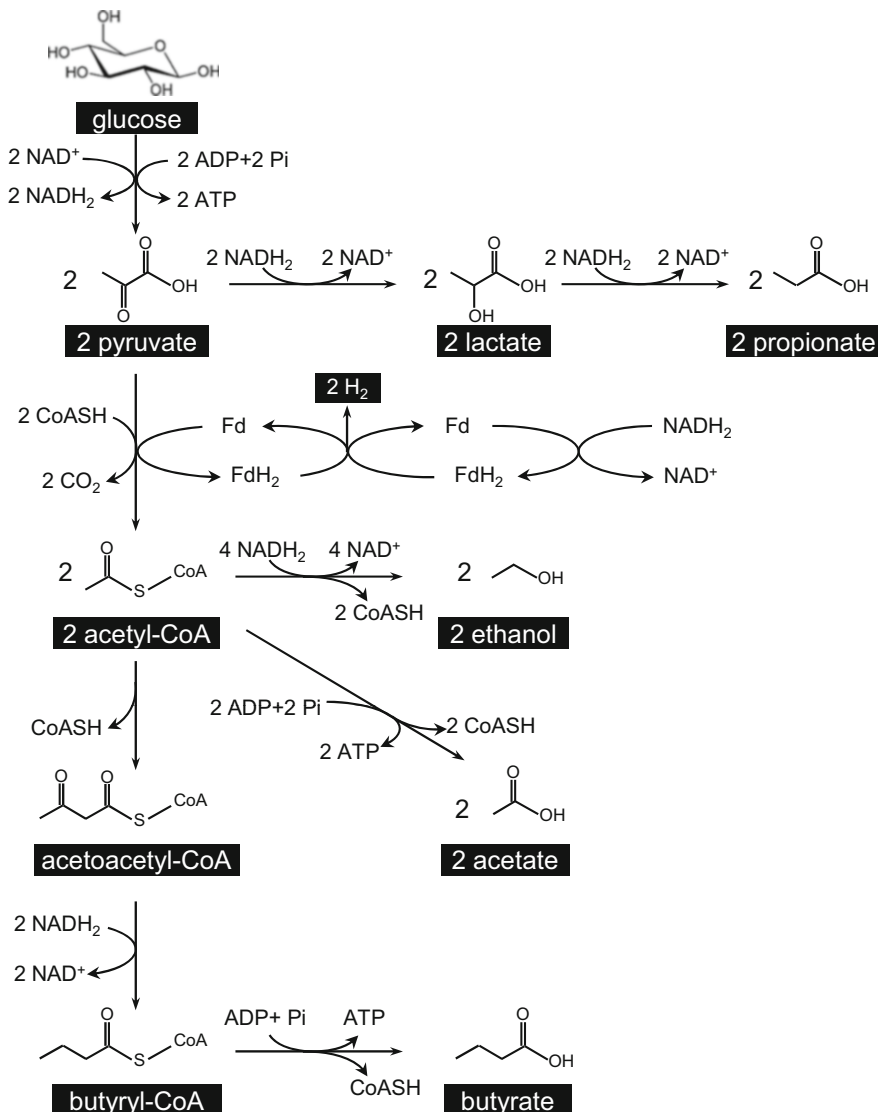


Fig. 5.3 Common pathways of dark fermentation. Fd/FdH₂ is the oxidized/reduced state of ferredoxin. CoA-SH is coenzyme A with its thiol group. NAD⁺/NADH₂ is oxidized/reduced state of nicotinamide adenine dinucleotide. Pi, ADP and ATP are free phosphate, adenosine diphosphate and adenosine triphosphate, respectively

fermentation) because the former is thermodynamically unfavorable under standard conditions. The VFA-oxidizing bacteria, i.e. acetogens, have to work syntrophically with hydrogenotrophic methanogens, which reduce the partial pressure of the produced H₂.

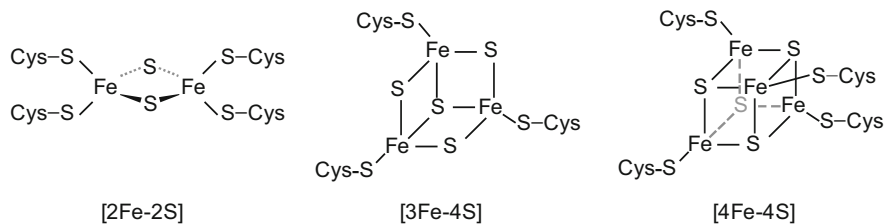
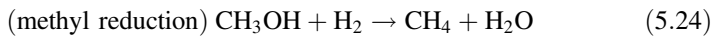
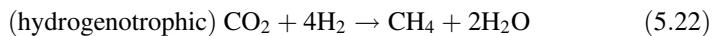
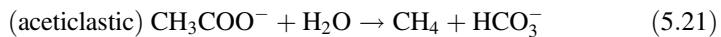


Fig. 5.4 Three common structures of ion-sulphur cluster in ferredoxin. Cys is short for cysteine

5.2.2.4 Methanogenesis

Methanogenesis is the final step of CH_4 fermentation. The electrons from the organic compounds are transferred into CH_4 to escape from the liquid. Four methanogenic pathways are discovered as the elemental reactions for methanogens, as shown in Eqs. (5.21)–(5.24) and Fig. 5.5 [12, 13]. For the CH_4 fermentation from organic solid waste, aceticlastic and hydrogenotrophic pathways are the major paths to produce methane. From Eqs. (5.21) and (5.22), both the generated bicarbonate and the consumed CO_2 lead to a significant pH increase in the liquid phase.



The factor F_{430} in coenzyme M is a nickel-containing compound. The methyl group in $\text{CH}_3\text{-H}_4\text{MPT}$ is firstly transferred to cobolamin then to coenzyme M [14]. Cobolamin, i.e. vitamin B_{12} , is a cobalt-containing compound. Again, these factors highlight the importance of the trace elements Ni and Co in CH_4 fermentation.

Recent studies have revealed that the direct interspecies electron transfer (DIET) is a kinetically efficient pathway for syntrophic methanogenesis [15]. The electrons from the oxidation of molecules were transferred through the (semi-)conductors, which is much faster than the electron carriers through the mass transfer of liquid. The DIET can occur by outer-surface *c*-type cytochromes, by the conductive pili or endogenous nanowires (in *Geobacter* sp.) or by exogenous conductive materials (activated carbon, nanoparticles or graphene) [16–18]. More mechanisms are being discovered to accelerate the methanogenesis in different microflora.

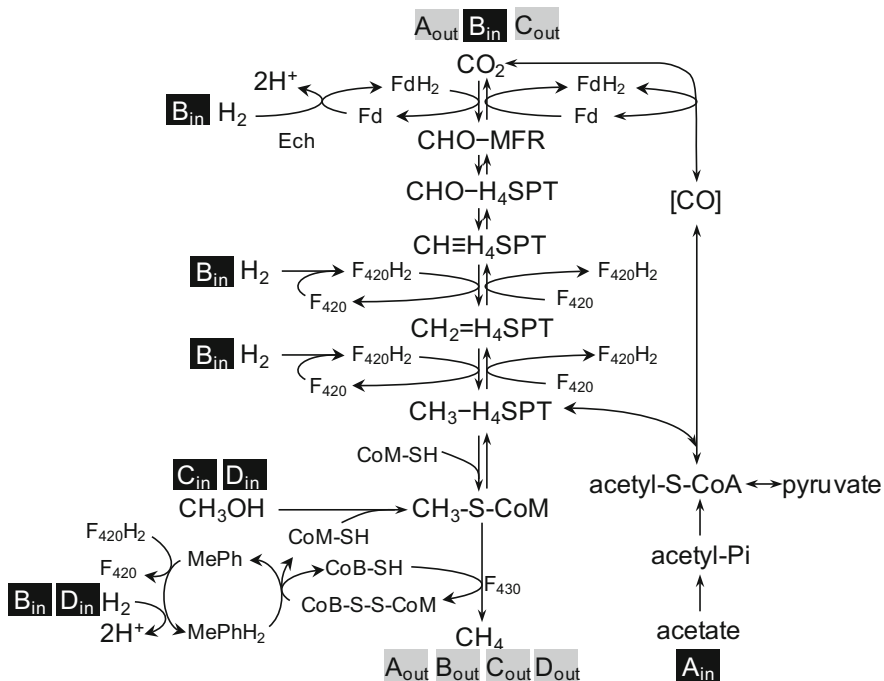


Fig. 5.5 Pathway A, B, C, and D are aceticlastic methanogenesis, hydrogenotrophic methanogenesis, methylotrophic methanogenesis, and methyl reduction methanogenesis, respectively. CHO-MFR is formyl-methanofuran. CHO- H_4 MPT, $CH\equiv H_4$ MPT, $CH_2=H_4$ MPT, and CH_3H_4 MPT are formyl-, methenyl-, methylene-, and methyl-tetrahydromonopterin. CoB-SH and CoM-SH are the thiol groups from coenzyme B and coenzyme M, respectively. $F_{420}/F_{420}H_2$ are the oxidized and reduced states of coenzyme F_{420} . MePh/MePhH₂ are the oxidized and reduced states of methanophenazine. F_{430} is coenzyme F_{430} . The substrates and the products of each pathway are labeled by the subscript “in” and “out”, respectively

5.2.3 Operational Parameters

5.2.3.1 Temperature

Both H_2 and CH_4 fermentation are conducted by microorganisms. The stable production of those products requires the process to run stably at the appropriate ranges of temperatures, especially in the case of CH_4 fermentation, which needs different microbes in order to cooperate with one another through all of the pathways. Generally, the temperature ranges can be divided into these domains: psychrophilic (0 – 20 °C), mesophilic (30 – 38 °C), thermophilic (50 – 60 °C) and hyperthermophilic (65 – 90 °C).

For CH_4 fermentation, mesophilic temperatures are most applied because the energy input for heating is low. Because mesophilic conditions allow a large microbial community to be retained, the system is more stable to the shock of

loading rates or inhibitors. VFA accumulation tends to occur less frequently under mesophilic conditions with better effluent quality. As the second most commonly applied conditions, thermophilic conditions are associated with higher reaction rates than those under mesophilic conditions, especially for cellulose. Under thermophilic conditions, the performance of pathogen deactivation is better, as well [19]. Since thermophilic conditions are associated with an increase in the leftover VFA, a low diversity in the microbial community and an increased risk of instability, these conditions are more suitable to pretreatment [20]. As for other ranges, psychrophilic condition will greatly slower the reaction rates of microbes and hyper-thermophilic condition will deactivate the aceticlastic methanogens.

In the case of H₂ fermentation, temperature is less restricted because it is mostly conducted by bacteria rather than methanogenic archaea. The thermophilic condition is broadly used for its high conversion rates. Still, a relatively stable temperature is necessary to avoid the malfunction of microbial communities.

5.2.3.2 pH and Alkalinity

The pH is the prime parameter for microorganisms to grow and function. Acidogenic bacteria have a wide optimal range of 4.0–9.0 while the general pH range for methanogenic archaea is 7.0–8.0. When discussing the inhibition caused by NH₃ or H₂S, their forms of free molecules are considered to be the direct cause of inhibition because the neutral forms can permeate through the cell membrane by free diffusion.

As shown in Fig. 5.6(a), the pH in the bulk liquid influences the distributions of acid/base pairs. For certain acid/base pairs, e.g. NH₃/NH₄⁺ or H₃PO₄/H₂PO₄⁻/HPO₄²⁻/PO₄³⁻, a given pH fixes the distribution coefficients in those different forms under a certain temperature. The distribution coefficients are also determined by the dissociation coefficient pK_a of the acid/base pairs. Because different acid/base pairs have different dissociation coefficients, the pH-buffering capacity, which could be determined by Eq. (5.25), varies over different pH range. Still, the buffering capacity is a monotonic function of pH. The pH that the solution presents is the “compromised” result of all the acid/base pairs.

$$\beta = \frac{1}{Vc} \cdot \frac{dn}{dpH} \quad (5.25)$$

where β is the buffering capacity; V is the volume of the solution (regardless of the added strong acid or base); c is the total concentration of the acid/base pairs; and n is the amount of proton or hydroxyl ions added to the system with a strong acid or base.

To obtain the integrated buffering capacity of a solution from one pH to another, alkalinity is measured by titration. As shown in Fig. 5.7, the relation between alkalinity and pH is given by

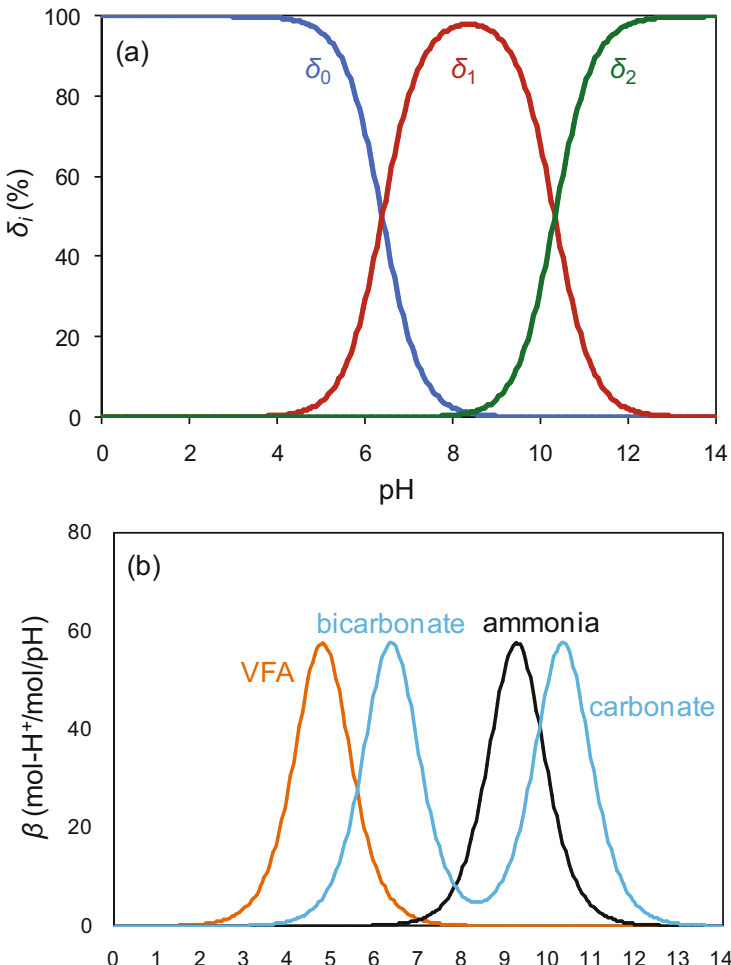


Fig. 5.6 (a) Distribution coefficients of H_2CO_3 (δ_0), HCO_3^- (δ_1), and CO_3^{2-} (δ_2) over pH with $\text{p}K_{\text{a}1} = 6.38$ and $\text{p}K_{\text{a}2} = 10.30$; (b) the buffering capacity of carbonate, ammonia, and VFA systems over pH, which were calculated by the grid of $\Delta\text{pH} = 0.05$

$$\text{Alkalinity}_{a-b} = \sum_i \left(c_i \int_a^b \beta_i \text{d}\text{pH} \right) \quad (5.26)$$

where β_i is the buffering coefficient of the acid/base pair i ; c_i is the total concentration of the acid/base pairs i ; a and b are the initial and the terminal pH of titration, respectively.

The word alkalinity can refer to the property of a matter to neutralize acids and the measure of its capacity of neutralizing acids. When referring to the property,

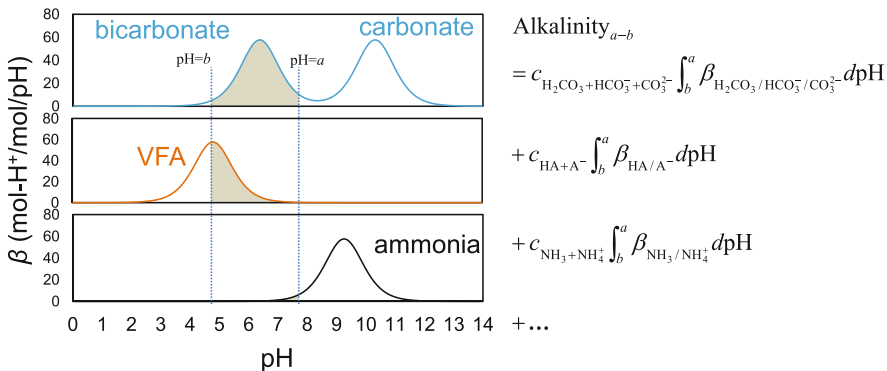


Fig. 5.7 Relations between alkalinity and buffering capacities.

alkalinity could be ranked by strength depending on how high the pK_a is. When referring to the capacity, it has the dimension of concentration and presents as the equivalent content as that of CaCO_3 . It is difficult to calculate the alkalinity even if all the concentrations of acid/base pairs are exhaustively known unless a numeric approximation is considered reasonable. On the other hand, it is reasonably easy to determine alkalinity via experimental titration.

As shown in Fig. 5.6(b), the acid anions of VFA also have buffering capacity in the range of 4.0–5.0, which explains the stability of pH in the acidogenic phase even after a considerable quantity of organic acids are produced. However, in the pH range of methanogenesis, which is 7.0–8.0, bicarbonate is the most alkalinity contributor.

Ammonia is considered the source of alkalinity in anaerobic digestion. The amino groups in proteins are primarily degraded into free ammonia, which has the property of alkalinity. Then, when the free ammonia reacts with carbonic acid as soon as it was formed, its alkalinity is also “transferred” to the bicarbonate anion. Therefore, the free ammonium and the produced bicarbonate have equivalent molar concentrations. With regard to the properties, free ammonia has stronger alkalinity than bicarbonate anions.

5.2.3.3 Retention Time

A high rate of treatment requires a short retention time, whereas the retention time cannot be too short because the microorganisms take time to grow. In cases when cell loss is at a faster rate than the cell growth, the process cannot run continuously. The hydraulic retention time (HRT) is defined to assess the treatment capability of the process and the sludge retention time (SRT) is defined to ensure the growth of the microorganisms. In the fields of waste and wastewater treatment, many processes are able to retain biosolids (microorganisms) within the process so that the SRT is longer than the HRT, allowing enrichment with slow-growing microbes (especially

anaerobes) and the degradation of pollutants with high-loading rates. Typical processes with this feature are the UASB (up-flow anaerobic sludge bed) and the MBR (membrane biological reactor). The sludge in the UASB granulates itself with a good settleability to precipitate before the outlets. The MBR retains sludge with membrane rejection. In both of these processes, a high-solid content will result in failure by either pushing out the granular sludge or blocking the pores on the membrane. For those reasons, the CSTR (completely stirred tank reactor) is widely used for high-solid biowaste. The HRT in the CSTR is equivalent to the SRT since, rather than being separated, the sludge flows out of the process with the liquids.

5.2.3.4 Common Challenges in Methane Fermentation

The rate-limiting steps in CH_4 fermentation can be either hydrolysis or methanogenesis depending on a range of different phenomena. In most cases, hydrolysis is the rate-limiting step due to the microbial limits by mild temperature and the contact surface. Hydrolysis can be promoted by enhancing pretreatment or solubilization, e.g. by heat treatment, steam explosion, acid/alkaline adjustment, or adding external enzymes. The phenomena of low removal efficiency in combination with the low accumulation of intermediate products (VFA) could imply the limitation of hydrolysis.

The limitation of methanogenesis is more indirectly mentioned but it is more frequently described as acidification or failure. Generally, the methanogenic archaea have lower abundances and slower growth rates than the acidogenic bacteria. Slow methanogenesis essentially loses the dynamic equilibrium with acidogenesis, resulting in the accumulation of intermediate products (VFA, e.g. acetate, propionate, etc.), and reducing the pH of the liquid until it is irreversible. The limitation of methanogenesis can be caused by many factors, e.g. overly high-loading rates, an overly short SRT, a lack of trace elements, the inhibition of NH_3 (3–5 g/L), H_2S (0.1–0.8 g/L), and LCFA (0.74–2.56 g/L), etc [19, 21, 22]. Those factors share similar consequences of acidification and VFA accumulation but some of them were attributed to the characteristics of the biowaste. The limitation of methanogenesis can be considered a limitation of the feeding materials unless the cause can be removed.

5.2.3.5 Common Challenges in Hydrogen Fermentation

The key to carrying out H_2 fermentation is to eliminate the hydrogenotrophic methanogens while keeping the acidogenic bacteria. Since general natural inocula contain both acidogenic and methanogenic microorganisms, the key option to generate H_2 is to inhibit the hydrogenotrophic methanogenesis. At present, H_2 fermentation can be achieved by heat treatment, washing out and inhibiting hydrogenotrophic methanogens. Heat treatment involves heating the inoculum, to at 90 °C for 30 min, to deactivate the methanogens while the H_2 producers,

e.g. *Clostridium sp.*, can preserve themselves as spores. It is also possible for methanogenic inhibitors to deactivate the methanogens, but continuous addition is required after being washed out. In the continuous operation, controlling the SRT (=HRT in CSTR) is the effective method to eliminate methanogens. The time course of the microorganisms (sludge or volatile suspended solids, VSS) is described as

$$X(t) = e^{(\mu - \frac{1}{\tau})t} X_0 + \frac{1}{1 - \mu\tau} \left[1 - e^{(\mu - \frac{1}{\tau})t} \right] \cdot X_{in} \quad (5.27)$$

where X is the microbial concentration; X_0 and X_{in} are the microbial concentration in CSTR and in the feeding stream, respectively; τ is the HRT of the process, $\tau = V/Q$; and μ is the (average) relative microbial growth rate, in a batch mode $\mu = d(\ln X)/dt$.

Supposing the microbe content in the influent is negligible and the relative microbial growth rate remains constant, the ultimate concentration of the microbes depends on whether the term $(\mu - 1/\tau)$ is positive or negative. Even if the methanogens are growing, when their growth rates are not high enough ($0 < \mu < 1/\tau$), they will still be washed out from the CSTR.

Continuous H_2 fermentation requires specific environmental conditions than CH_4 fermentation. The pH values in the dark fermentation for H_2 are kept low by the accumulated VFA. One risk is that the pH may become uncontrollable by lactic acid from the influent, and another is that typical bacteria may not grow under low pH. As mentioned before, the digested effluent has a higher pH and alkalinity concentration. An important design for the continuous process is introducing the effluent of CH_4 fermentation to supply bacteria and alkalinity for the H_2 fermentation [23]. After years of trials, researchers have found that a configuration of R-TPAD process is suitable and flexible for stabilizing and optimizing the H_2 and CH_4 fermentation.

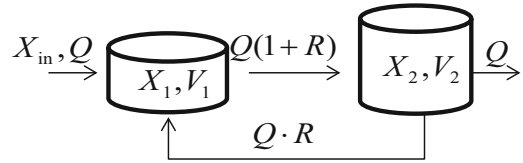
5.3 Characteristics of recirculated R-TPAD process

5.3.1 Model of Two-Stage CSTR with Recirculation

Before introducing applications of R-TPAD processes, the characteristics of R-TPAD need to be presented. In this section, the hydraulic characteristics of recirculated two-stage CSTR process are explained.

A schematic diagram of a two-stage CSTR process is illustrated in Fig. 5.8. The mixing in each reactor is presumably sufficient because they are CSTRs. The flow rates in the influent and effluent are Q . The volume of the first and second reactors are V_1 and V_2 ($V_1 \neq V_2$), respectively. The concentration of the tracer in the feeding stream, first, and second stages are c_{in} , c_1 , and c_2 , respectively. R is the ratio of the recirculated stream to the feeding stream. The hydraulic retention time (HRT) of each stage is not defined at this point, because it alternates due to R . Still, the time constants are defined as the ratio of the working volume over the flow rate, i.e. $\tau_1 =$

Fig. 5.8 Recirculated two-stage CSTR process and process parameters



$V_1/Q, \tau_2 = V_2/Q$. All of the parameters above are constant in an operating condition except c_1 and c_2 , which are variant by time to discuss the transient properties. Thus, the time course of $c_1(t)$ and $c_2(t)$ is described by the following equation set. All the time course functions are defined on $[0, +\infty)$ by default and turn out 0 for the rest of the real numbers, i.e. the step function is invisibly multiplied.

$$\begin{cases} V_1 \frac{dc_1}{dt} = Qc_{\text{in}} - (1+R)Qc_1 + RQc_2 \\ V_2 \frac{dc_2}{dt} = (1+R)Qc_1 - (1+R)Qc_2 \end{cases} \quad (5.28)$$

To efficiently solve the ordinary differential equation set, the Laplace transform is applied,

$$\begin{cases} sC_1 - c_{1,0} = \frac{1}{\tau_1} [c_{\text{in}}/s - (1+R)C_1 + RC_2] \\ sC_2 - c_{2,0} = \frac{1}{\tau_2} [(1+R)C_1 - (1+R)C_2] \end{cases} \quad (5.29)$$

where $C_1 = C_1(s) = \mathcal{L}\{c_1(t)\}$, $C_2 = C_2(s) = \mathcal{L}\{c_2(t)\}$; $c_{1,0}$ and $c_{2,0}$ are the constants denoting the initial concentrations of the tracer spiked into the first and second stages, respectively.

The solutions of the set of equations, Eq. (5.30) are

$$\begin{cases} C_1 = \frac{1+R+\tau_2 s}{sA(s)} c_{\text{in}} + \frac{1+R+\tau_2 s}{A(s)} \tau_1 c_{1,0} + \frac{R}{A(s)} \tau_2 c_{2,0} \\ C_2 = \frac{1+R}{sA(s)} c_{\text{in}} + \frac{1+R}{A(s)} \tau_1 c_{1,0} + \frac{1+R+\tau_1 s}{A(s)} \tau_2 c_{2,0} \end{cases} \quad (5.30)$$

where $A(s) = (1+R+\tau_1 s)(1+R+\tau_2 s) - R(1+R)$.

The roots of the quadratic equation $A(s) = 0$ are $\omega_1 = \frac{-2}{\tau_1 + \tau_2 - \tau_\Delta}$ and $\omega_2 = \frac{-2}{\tau_1 + \tau_2 + \tau_\Delta}$, respectively, where the intermediate parameter $\tau_\Delta := \sqrt{\tau_1^2 + \tau_2^2 - 2\tau_1\tau_2 \frac{1-R}{1+R}}$, which can be regarded as the third side of a triangle when two sides (τ_1, τ_2) and the included angle (θ , such that $\cos \theta = \frac{1-R}{1+R}$) are given.

Therefore, the time course concentrations are obtained after the inverse Laplace transform of Eq. (5.30).

$$c_1(t) = \left[\frac{1}{\tau_\Delta} \left(\frac{1}{\omega_2} e^{\omega_2 t} - \frac{1}{\omega_1} e^{\omega_1 t} \right) + 1 + \frac{e^{\omega_2 t} - e^{\omega_1 t}}{(1+R)\tau_\Delta} \tau_2 \right] c_{in}$$

$$+ \left[\frac{e^{\omega_2 t} - e^{\omega_1 t}}{\tau_\Delta} + \frac{\omega_2 e^{\omega_2 t} - \omega_1 e^{\omega_1 t}}{(1+R)\tau_\Delta} \tau_2 \right] \tau_1 c_{1,0} + \frac{e^{\omega_2 t} - e^{\omega_1 t}}{(1+R)\tau_\Delta} R \tau_2 c_{2,0} \quad (5.31)$$

$$c_2(t) = \frac{1}{\tau_\Delta} \left(\frac{1}{\omega_2} e^{\omega_2 t} - \frac{1}{\omega_1} e^{\omega_1 t} \right) c_{in} + \frac{e^{\omega_2 t} - e^{\omega_1 t}}{\tau_\Delta} \tau_1 c_{1,0}$$

$$+ \left[\left(\frac{e^{\omega_2 t} - e^{\omega_1 t}}{\tau_\Delta} \right) + \frac{\omega_2 e^{\omega_2 t} - \omega_1 e^{\omega_1 t}}{(1+R)\tau_\Delta} \tau_1 \right] \tau_2 c_{2,0} \quad (5.32)$$

The solutions above were sorted according to the sources of the tracers. The coefficients of c_{in} in the reactor are the integration of the corresponding coefficient of $\tau_1 c_{1,0}$. Equations (5.31) and (5.32) can also be sorted as

$$c_1(t) = \left[\frac{-1}{\tau_\Delta \omega_1} c_{in} + \frac{-\tau_2}{(1+R)\tau_\Delta} c_{in} + \frac{-\tau_1}{\tau_\Delta} c_{1,0} + \frac{-\omega_1 \tau_1 \tau_2}{(1+R)\tau_\Delta} c_{1,0} + \frac{-R\tau_2}{(1+R)\tau_\Delta} c_{2,0} \right] e^{\omega_1 t}$$

$$+ \left[\frac{1}{\tau_\Delta \omega_2} c_{in} + \frac{\tau_2}{(1+R)\tau_\Delta} c_{in} + \frac{\tau_1}{\tau_\Delta} c_{1,0} + \frac{\omega_2 \tau_1 \tau_2}{(1+R)\tau_\Delta} c_{1,0} + \frac{R\tau_2}{(1+R)\tau_\Delta} c_{2,0} \right] e^{\omega_2 t}$$

$$+ c_{in} \quad (5.33)$$

$$c_2(t) = \left[\frac{-1}{\omega_1 \tau_\Delta} c_{in} + \frac{-\tau_1}{\tau_\Delta} c_{1,0} + \frac{-\tau_2}{\tau_\Delta} c_{2,0} + \frac{-\omega_1 \tau_1 \tau_2}{(1+R)\tau_\Delta} c_{2,0} \right] e^{\omega_1 t}$$

$$+ \left[\frac{1}{\omega_2 \tau_\Delta} c_{in} + \frac{\tau_1}{\tau_\Delta} c_{1,0} + \frac{\tau_2}{\tau_\Delta} c_{2,0} + \frac{\omega_2 \tau_1 \tau_2}{(1+R)\tau_\Delta} c_{2,0} \right] e^{\omega_2 t} + c_{in} \quad (5.34)$$

Both concentrations have the time-variant (transient-state) components and the constant (steady-state) component. The time-variant components approach 0 since they are controlled by the decaying items, $e^{\omega_1 t}$ and $e^{\omega_2 t}$ ($\omega_1, \omega_2 < 0$). The constant components in both stages are the influent concentration c_{in} , which is also the final concentration of $c_{1,0}$ and $c_{2,0}$.

For a process with $V_1 = V_2$, the above results are still functionable if $R \neq 0$, whereas, if $V_1 = V_2 = V$ and $R = 0$, there will be $\tau_\Delta = 0$ in the denominator of the time-variant components. Since $\omega_1 = \omega_2$ at the same time, the solutions can be achieved by $\tau_1 \rightarrow \tau_2 = \tau$. In this case, where the cascaded CSTRs have been intensively discussed, Eqs. (5.31)–(5.34) will be

$$\begin{cases} c_1(t) = \left(1 - e^{-\frac{t}{\tau}}\right)c_{\text{in}} + e^{-\frac{t}{\tau}} \cdot c_{1,0} \\ c_2(t) = \left[1 - \left(1 + \frac{t}{\tau}\right)e^{-\frac{t}{\tau}}\right]c_{\text{in}} + \frac{t}{\tau}e^{-\frac{t}{\tau}} \cdot c_{1,0} + e^{-\frac{t}{\tau}} \cdot c_{2,0} \end{cases} \quad (5.35)$$

$$\begin{cases} c_1(t) = (c_{1,0} - c_{\text{in}})e^{-\frac{t}{\tau}} + c_{\text{in}} \\ c_2(t) = (c_{1,0} - c_{\text{in}}) \cdot \frac{t}{\tau}e^{-\frac{t}{\tau}} + (c_{2,0} - c_{\text{in}})e^{-\frac{t}{\tau}} + c_{\text{in}} \end{cases} \quad (5.36)$$

Whether $V_1 = V_2$ and $R = 0$ or not determines the forms of the equations of the time course. The hydraulic characteristics of the process are still continuous with respect to the other parameters since the limits of $V_1 \rightarrow V_2$ on both sides are equal to the case when $V_1 = V_2$.

5.3.2 Spatial Distribution

The hydraulic characteristics of the recirculated two-stage process can be explained as follows. Firstly, to obtain the total amount of the tracer from each source, the equivalence between the initial amount and the final amount is utilized. The initial concentrations in the first and second stage are from a pulse in the influent. When $t = 0$, the function of the initial concentration can be described as $c_{1,\text{ini}}(t) = k_1\delta(t)$ and $c_{2,\text{ini}}(t) = k_2\delta(t)$.

$$\begin{aligned} \int_{-\infty}^{+\infty} Qc_{1,\text{ini}}(t)dt &= \text{input} = \text{output} = \int_{-\infty}^{+\infty} Q \frac{\partial c_2}{\partial c_{1,0}} c_{1,0} dt \\ &= Qc_{1,0} \frac{\partial C_2(s)}{\partial c_{1,0}} \Big|_{s=0} = Qc_{1,0}\tau_1 \end{aligned} \quad (5.37)$$

where $\delta(t)$ is the unit pulse function; $\int_{-\infty}^{+\infty} c_2(t)dt = \left[\int_{-\infty}^{+\infty} c_2(t)e^{-st}dt\right]_{s=0} = \mathcal{L}[c_2(t)]|_{s=0} = C_2(s)|_{s=0}$; $\frac{\partial c_2}{\partial c_{1,0}}$ indicates the coefficient of $c_{1,0}$ as its contribution to the effluent concentration c_2 . Therefore, $k_1 = c_{1,0}\tau_1$ and $c_{1,\text{ini}}(t) = c_{1,0}\tau_1\delta(t)$. Similarly, $c_{2,\text{ini}}(t) = c_{2,0}\tau_2\delta(t)$.

The HRT of the tracers from the initial condition $c_{i,0}$ till the outlet of the reactor j is defined ($i, j = 1, 2$) by

$$\text{HRT}_{i@j} = \frac{\int_{-\infty}^{+\infty} t \cdot Q \frac{\partial c_j(t)}{\partial c_{i,0}} c_{i,0} dt}{\int_{-\infty}^{+\infty} Qc_{i,\text{ini}}(t)dt} = \frac{1}{\tau_i} \cdot \left(-\frac{d}{ds} \frac{\partial C_j(s)}{\partial c_{i,0}} \Big|_{s=0} \right) = \mu_{1,i@j} \quad (5.38)$$

Also, the hydraulic variance (2nd moment about the mean value) is calculated by the 2nd moment about the origin point.

$$\mu_{2,i@j} := \frac{\int_{-\infty}^{+\infty} t^2 \cdot Q \frac{\partial c_j(t)}{\partial c_{i,0}} c_{i,0} dt}{\int_{-\infty}^{+\infty} Q c_{i,\text{ini}}(t) dt} = \frac{1}{\tau_i} \cdot (-1)^2 \frac{d^2}{ds^2} \frac{\partial C_j(s)}{\partial c_{i,0}} \Big|_{s=0} \quad (5.39)$$

$$\sigma_{i@j}^2 := \mu_{2,i@j} - \mu_{1,i@j}^2 \quad (5.40)$$

The results of the HRT and the hydraulic variance are expressed in matrices.

$$\mathbf{M}_1 := \begin{bmatrix} \text{HRT}_{1@1} & \text{HRT}_{2@1} \\ \text{HRT}_{1@2} & \text{HRT}_{2@2} \end{bmatrix} = \begin{bmatrix} \tau_1 + \frac{R}{1+R} \tau_2 & \frac{R}{1+R} (\tau_1 + \tau_2) \\ \tau_1 + \tau_2 & \frac{R}{1+R} \tau_1 + \tau_2 \end{bmatrix} \quad (5.41)$$

$$\mathbf{M}_2 := \begin{bmatrix} \sigma_{1@1}^2 & \sigma_{2@1}^2 \\ \sigma_{1@2}^2 & \sigma_{2@2}^2 \end{bmatrix} = \left(\tau_1^2 + \tau_2^2 + \frac{2R\tau_1\tau_2}{1+R} \right) \begin{bmatrix} 1 & 1 \\ 1 & 1 \end{bmatrix} - \frac{1}{(1+R)^2} \begin{bmatrix} \tau_2^2 & \tau_1^2 + \tau_2^2 \\ 0 & \tau_1^2 \end{bmatrix} \quad (5.42)$$

The results indicate that the R will increase the HRT and the hydraulic variance of the tracers within the process. For the tracers that initially departed from the second stage, recirculation makes it possible to retain those tracer in the first stage. The number of theoretical plates N in the R-TPAD is defined as

$$N := \frac{\mu_{1@2}^2}{\sigma_{1@2}^2} = \frac{(\tau_1 + \tau_2)^2}{(\tau_1 + \tau_2)^2 - 2\tau_1\tau_2/(1+R)} = \frac{1}{1 - \frac{2\tau_1\tau_2}{(\tau_1 + \tau_2)^2}/(1+R)} \quad (5.43)$$

The CSTR and plug flow reactor (PFR) are the two extremes of the typical reactors. In the case of the CSTR, $\text{HRT} = \tau$, $\sigma^2 = \tau^2$. For PFR, $\text{HRT} = \tau$, $\sigma^2 = 0$. It is clear that while HRT is always the quotient of V to Q regardless of the flow types inside the reactor, the hydraulic variance is related to the flow type. The maximal variance of the reactor is achieved in CSTR as τ^2 and the minimum is in PFR as 0.

For the R-TPAD process, when $R = 0$, $\mathbf{M}_1 = \begin{bmatrix} \tau_1 & 0 \\ \tau_1 + \tau_2 & \tau_2 \end{bmatrix}$, $\mathbf{M} = \begin{bmatrix} \tau_1^2 & 0 \\ \tau_1^2 + \tau_2^2 & \tau_2^2 \end{bmatrix}$, $N = \frac{(\tau_1 + \tau_2)^2}{\tau_1^2 + \tau_2^2} \in (1, 2]$. Without recirculation, the tracers departed from the initial 1st or 2nd stage act as a 1-stage CSTR. There will not be a tracer from the initial 2nd stage flowing back into the 1st stage. The tracer from the initial 1st stage has to take averagely $\tau_1 + \tau_2$ to pass through the 2nd stage, which represents the HRT of the whole process. Compared to the 1-stage CSTR, the variance of the two-stage CSTRs is reduced from the square of the HRT of the whole process $(\tau_1 + \tau_2)^2$ to the sum of the square of the total HRT of each stage, i.e. $\tau_1^2 + \tau_2^2$. It can be induced that the hydraulic variance of n -stage CSTR is $\sigma_n^2 = \sum_{i=1}^n \tau_i^2$. When n goes to infinity, σ_n^2 goes

to 0, which is the reason why PFR can be regarded as the infinite stages of cascaded CSTRs.

$$\text{When } R \text{ goes to infinity, } \mathbf{M}_1 \rightarrow \begin{bmatrix} \tau_1 + \tau_2 & \tau_1 + \tau_2 \\ \tau_1 + \tau_2 & \tau_1 + \tau_2 \end{bmatrix}, \mathbf{M}_2 \rightarrow \begin{bmatrix} (\tau_1 + \tau_2)^2 & (\tau_1 + \tau_2)^2 \\ (\tau_1 + \tau_2)^2 & (\tau_1 + \tau_2)^2 \end{bmatrix},$$

$N \rightarrow 1$. Now the HRT of all the tracer in both stages increases to the same value as $\tau_1 + \tau_2$, which is the HRT of the whole process, and all the hydraulic variances are the same as well as the square of the HRT. Those characteristics suggest that the two-stage CSTR becomes one-stage if the R is sufficiently large.

$$\text{When } R = 1, \mathbf{M}_1 = \begin{bmatrix} \tau_1 + \frac{\tau_2}{2} & \frac{\tau_1 + \tau_2}{2} \\ \tau_1 + \tau_2 & \frac{\tau_1}{2} + \tau_2 \end{bmatrix}, \mathbf{M}_2 = \begin{bmatrix} \tau_1^2 + \frac{3}{4}\tau_2^2 + \tau_1\tau_2 & \frac{3}{4}\tau_1^2 + \frac{3}{4}\tau_2^2 + \tau_1\tau_2 \\ \tau_1^2 + \tau_2^2 + \tau_1\tau_2 & \frac{3}{4}\tau_1^2 + \tau_2^2 + \tau_1\tau_2 \end{bmatrix},$$

$N = \frac{1}{1 - \tau_1\tau_2 / (\tau_1 + \tau_2)^2} \in (1, \frac{4}{3}]$. The HRT of all tracers from each stage is just the midpoint between $\mathbf{M}_1(R = 0)$ and $\mathbf{M}_1(R = \infty)$, which means the condition of $R = 1$ places the R-TPAD process right in the middle between the one-stage and two-stage CSTRs.

As for the number of theoretical plates N , when $R = 0$, the N in R-TPAD reaches a maximum of 2 when $\tau_1 = \tau_2$. The other limits is 1 when R goes to infinity and whatever the τ_1 and τ_2 are. When $R = 1$, $\tau_1 = \tau_2$ also leads to the maximum of N but the maximum is 4/3. The HRTs, τ_1 and τ_2 , are fixed once the process was designed, but R can be adjusted to finely control the hydraulic properties of N .

5.4 Applications of the R-TPAD Processes

5.4.1 Separation of Acidogenic Phase and Methanogenic Phase

The co-production of H_2 and CH_4 from organic solid waste dates back to the two-phase UASB process used to treat organic wastewater in 1971 [24, 25]. A conventional methane fermentation reactor contains both an acidogenic phase and a methanogenic phase within 1 stage. When the process is comprised of two stages and the HRT in the first stage is shorter than 3–5 days, the first stage cannot retain methanogens and the intermediate products, i.e. VFA and H_2 , accumulate, which is referred to as “phase separation”. After decades of development, the process for organic wastewater treatment has been adapted to treat organic solid waste. For wastewater treatment, the feeding concentration is relatively low as 1–2% (on TS) or 10–20 g-COD/L, where UASB is applicable and the biosolids (wastewater/micro-organisms) can be easily separated from the liquid within the reactor. However, in the case of organic solid waste, the feeding concentration can reach 5–20% (on TS) or 50–200 g-COD/L. High concentrations of solid waste require both higher concentrations of microorganisms and a longer time for hydrolysis. Hence, the CSTR is used more widely in the treatment of organic solid waste.

5.4.2 Coupling Recirculation

Besides phase separation, more requirements are needed for H₂ production including appropriate pH, functional microorganisms, and limited H₂-consumers. The desired pH range, about 4.5–6.0, can be achieved via pH adjustment by external alkaline and acid. Typical H₂ producers are rumen bacteria, many of which hardly grow in the pH range of H₂ fermentation. Low growth rates under a low pH range can result in the H₂-producers being washed out of the reactor. As shown in Fig. 5.9, coupling the effluent recirculation to the two-phase process can solve the problems of adjusting pH and losing H₂-producers, with a third advantage of diluting the feeding materials.

The recirculated effluent also introduces a new problem: it introduces H₂-consumers in the form of hydrogenotrophic methanogens. Some researchers have turned to conventional methods to deactivate or separate the methanogens, like heat treatment, sedimentation, and aeration. Recently, researchers have been focusing on the fine control of R , and have succeeded in running the reactor while avoiding hydrogenotrophic methanogenesis. In Eq. (5.41), the HRT_{2@1} of the tracers describes the hydraulic behavior of the methanogens in the first stage, which increases from 0 to $\tau_1 + \tau_2$ with R from 0 to infinity. The equation suggests that small R values are preferable so that HRT_{2@1} is short enough to wash out those methanogens. The R also increases the HRT_{1@1} by $\tau_2 \cdot R / (1+R)$, allowing more slow-growing microbes to grow within the first stage and also to avoid the washout. Since different cases may require different values or ranges of R to produce hydrogen, a strategy was proposed to find out the appropriate R by narrowing the probable range (Fig. 5.10). [26] Another strategy is to apply a dynamic R according to performance. [27]

In the R-TPAD process, the acidogenic phase, as the first stage, can pre-convert the feeding organic solid waste into soluble compounds and produce H₂. It can also

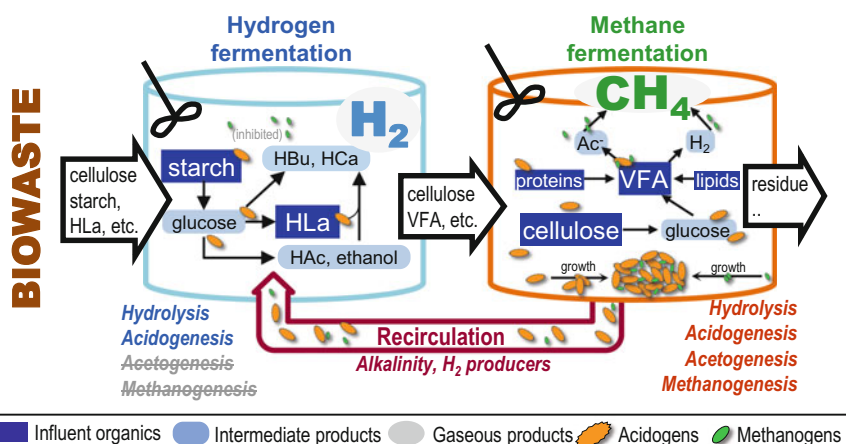
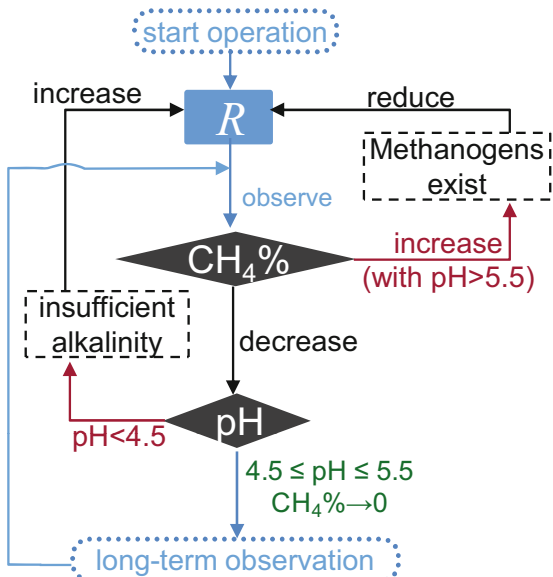


Fig. 5.9 Mechanisms of H₂ and CH₄ fermentation in recirculated two-phase anaerobic digestion

Fig. 5.10 Strategy of adjusting recirculation ratio R to produce H_2 in R-TPAD



hydrolyze the biosolids in the recirculated sludge so that the total organic removal is higher than that without recirculation. [28] The methanogenic phase, as the second stage, degrades the leftover intermediate products after H_2 fermentation, produces CH_4 and provides the alkalinity and H_2 -producers for the first stage. By coupling recirculation in the two-phase process, fermentation of H_2 and CH_4 becomes mutually beneficial with R-TPAD.

5.4.3 Co-production of Hydrogen and Methane

5.4.3.1 Food Waste

Food waste (FW) is commonly used as the substrate for the co-production of H_2 and CH_4 . The largest or the second-largest fraction of municipal solid waste (MSW) is FW [86]. Typical FW consists of starch, cellulose, proteins, and lipids with varying compositions. During its storage before treatment, lactic acid fermentation occurs even at a low temperature of 4 °C, resulting in high concentrations of lactic acid and low pH in the feedstock. A low pH, at around 4.0, helps to reduce the pH in the acidogenic phase. [87] On the other hand, after anaerobic degradation, the proteins in FW can generate sufficient alkalinity to sustain the appropriate pH for CH_4 fermentation. The low pH makes FW the most suitable biomass for the co-production of H_2 and CH_4 with the R-TPAD. Similar types of biowaste, e.g. household solid waste, fruit waste or vegetable waste are also suitable.

Results of studies on H₂ and CH₄ fermentation of FW are listed in Table 5.2. Initially, some cases could produce H₂ and CH₄ without pH adjustment and recirculation. In most cases, however, pH adjustment and recirculation were required, and in some cases the recirculated sludge required treatment, implying that running the two-phase process by itself might not be sufficient to produce H₂ due to different compositions of the source biowaste. Liquid/solid separation, aeration, pH and heat treatment were used in the early studies. Many researchers equipped online systems for automatic pH adjustment, where their target pH for hydrogen fermentation is 5.5. Since methanogenesis converts the anions of organic acids into bicarbonate, the increasing pH in the methanogenic effluent confirmed that alkaline was consumed to adjust the pH in H₂ fermentation. [55] A number of different processes have met with success at promoting the stable operation of the system by recirculating raw effluent with small *R* values of less than 1.0.

5.4.3.2 Agro-Industrial Waste

Crop processing industries produce carbohydrates in the form of starch, sugar, and ethanol. The relevant wastes are root bagasse, sugarcane bagasse, and stillage, which are lignocellulosic plant tissues. In traditional small-scale agriculture, such leftover biomass was used as feed for livestock. There are, however, cases where the biowaste does not meet the standards for husbandry feedstock. In large-scale industry of modern agriculture, those residues tend to be converted into high-value products. Fermentation for H₂ and CH₄ has great potential in the treatment of agricultural biowaste. Results of studies on H₂ and CH₄ fermentation from agro-industrial waste are listed in Table 5.3. Compared with FW, which is the mixture of different sources of materials, whose nitrogen content is sufficient for buffering the pH for CH₄ fermentation, the deficiency of nitrogen and trace elements occurs in most cases of agro-industrial waste, which is attributed to their being collected from single sources [88]. For some types of waste, e.g. straw or algae, their compact structures of lignocellulose were remained during the treatment of fermentation. The compact structure is formed by the lignin wrapping around the cellulose (or hemicellulose) fibers but the lignin is undegradable for anaerobic microorganisms. Pretreatment is needed to destroy such structure and expose the cellulose or hemicellulose, thus optimizing their pretreatment is a research topic for not only two-phase processes, but also for any other types of fermentation.

5.4.3.3 Co-Digestion

Nitrogen-rich biowaste from municipal and agricultural sources, e.g. sewage sludge, including primary sludge and waste activated sludge, or animal manure, can maintain the pH at levels higher than 7.0 during anaerobic degradation (CH₄ fermentation). Sewage sludge and animal manure are typical materials for CH₄ fermentation since early times, but their acidification for H₂ fermentation is almost impossible.

Table 5.2 Hydrogen and methane fermentation from food waste

Source biowaste (default units)	Process configuration					Feeding conc.	COD g/kg	VS %	pH	H ₂ yield L/kg VS _{fed}	First stage		Second stage		R	Ref.
	Type (CSTR)	Temp. °C	HRT ₁ days	HRT ₂ days	TS %						pH	H ₂ yield L/kg VS _{fed}	CH ₄ yield L/kg VS _{fed}			
Household solid waste	+/+	37/37	2	15	10.2	7.58	—	4.8-5.2	43	7.5	500	—	—	—	—	[29]
Organic waste	+/PBR	55/55	0.6-1.2	4.3-6.8	6.83	6.66	140	5.8-6.0*	11-46	7.8-8.0	1,35-296	—	—	—	—	[30]
FW	+/ABR	55/35	1.3	5.0	11.7	10.8	142	5.5*	205	7.5	464	2 precipitated	—	—	—	[31]
FW	+/+	40	4-10	16-40	20.5	17.6	212	5-6	49-71	7.0-7.5	480-551	—	—	—	—	[32]
FW	+/+	55/55	1.9	15.4	10.0	9.5	150	5.5	114	7.7	451	1 aerated	—	—	—	[33]
Biowaste	+/+	55/55	3.3-6.6	12.6	24.1-26.7	20.3-21.3	206-249	3.5-5.4	2.6-51.2	7.6-8.3	580-630	1.0 ^g liquid	—	—	—	[34, 35]
FW	+/+	37/37	2	7	4.25	2.89	91.7	5-6	180-332	6.9-7.2	344-510	—	—	—	—	[36]
FW	+/+	55/55	3.3	12.6	26.6	21.9	257	5.7	66.7	8.4	490	~1.0	—	—	—	[37]
FW	+/ABR	55/55	2.87	14.4	9.09-10.69	84.8-114.1	5.5-5.6*	5.9-147.3	—	383-470	2.9 ^g heated	—	—	—	—	[38]
FW	+/+	52/52	7.8-15.8	31.2-63.2	24.8	23.6	248	4.6-5.8	0-117	5.72-7.80	77-484	1.6-4.3	—	—	—	[39]
FW	+/+	55/55	3.3	12.6	26.0	21.6	248	5.2	48.3	8.1	400	0-0.5	—	—	—	[27]
Vegetable waste	+/+	37/37	4.2-6	8.9.8	5.5	4.8	88	5.4-6.9	(0-344)	—	200-442	0-1.6	—	—	—	[40]
Vegetable waste hydrolysate	+/+	60/37	—	—	—	—	—	5.5-6.0	(42.4-62.3)	—	234-259	—	—	—	—	[41]
FW	+/+	55/35	6	24	7.62	7.21	101	3.6	0	7.3	450	0	—	—	—	[28]
FW	+/PBR	55/37	3.7	1.5	22.2	—	397	—	115	—	—	—	—	—	—	[42]
FW	+/+	55/35	5	8-30	10.5	9.1	152	5.5*	105	6.9-8.0	456-526	—	—	—	—	[43, 44]
FW	+/+	55/55	3.3	12.6	28.1	26.0	312	5.2-5.4	68	8.1-8.3	515	—	—	—	—	[45]
FW + brown water	+/+	37/37	0.33-2	20	5.67	4.78	127	5.0-5.5*	68.5-99.8	7.0-7.5*	676-728	—	—	—	—	[46]
FW	+/+	37/37	4	25	26.0	24.1	362	—	—	7-8	401-503	0-0.3	—	—	—	[47]
FW	+/+	35/35	4	20-33.3	10.3	9.70	133.3	3.4	—	7.3-7.5	390-511	—	—	—	—	[48]
FW	+/+	35/35	4	20	26.2	24.6	—	5.3*	47.7	7.1*	335	0-1.0	—	—	—	[49]
FW	Leach bed / UASB	-/37	—	—	15	—	—	—	7.2-31.7	—	177.3	0-0.75	—	—	—	[50]
FW	Hybrid UASB	M	0.1-0.6	1.9-9.4	4.93	3.73	40.9	—	0-11.5	7.0*	27.5-67.4	—	—	—	—	[51]
FW+biochar	+/+	Ambient	3	7	6.12	5.95	—	>4	46	—	301	—	—	—	—	[52]
FW	+/+	55/35	5	9	10.5	9.1	152	5.1-5.4*	43.8-135	7.3-7.8	234-526	0-1.0	—	—	—	[53]
FW	+/+	37/37	2-8	20	23.7	23.3	—	—	—	7.7	467-500	0-0.6	—	—	—	[54]
FW	+/+	—	4-16	22-42	13.0-18.0	12.4-17.1	132.2	3.6-6.0*	0-31.1	7.2-8.2	392-482	—	—	—	—	[55]

Note: 1. Reactor types: “+” means CSTR, ABR: anaerobic baffled reactor, 2. “*” after pH value denotes online pH adjustment, 3. Values with round brackets in H₂ yields mean they are CH₄ yields in first stage. 4. Superscripts in values of R denote treatment conducted to recirculated sludge.

Table 5.3 Hydrogen and methane fermentation of agro-industrial waste

Source biowaste (default units)	Process configuration				Feeding conc.				First stage		Second stage		Ref.
	Type	Temp. (CSTR)	HRT ₁	HRT ₂	TS	VS	COD	pH	H ₂ yield L/kg-VS _{fed}	CH ₄ yield L/kg-VS _{fed}	pH		
Cassava stillage	+/+	60/55	1	4	4.74–6.22	4.0–5.3	48–65	5.78	56.6	–	249	–	[56]
Cassava residue	+/+	55/35	6	24	10.0	9.19	136	5.0	58–83	7.1	375–525	1.0	[57, 58]
Potato waste	+/+	35/35	0.25	1.25	1.08	1.03	12.6	5.5*	31.5	7.0	192	–	[59]
Potato waste	+/+	55/36	3–11.2	6–44.8	17.4	16.5	181	5.0–5.5	65.5	7.6	249–332	1.0	[60, 61]
Grass	+/+	35/35	0.75	11.3–19.3	5.47	4.80	66.7	5.5*	6.7	7.0	305–349	–	[62]
Hydrothermal hydrolysate of wheat straw	UASB/UASB	70/55	1.0	1.0–5.5	–	9.9	4.65	5.1	89	7.0–7.1	211–307	–	[63]
Hydrothermal liquefied cornstalk	UASB/UASB/PBR/PBR	37/37	–	–	–	76	–	0–146	–	158–302	–	[64]	
Macro-µ-algae	+/+	37/37	4	12–24	2.38–4.53	1.53–2.95	–	–	19.0–55.3	–	237–245	–	[65]
POME	SBR/UASB	55/28–34	2	14	6.2	5.50	85.5	5.5	40	7.3–7.5	486	–	[66]
POME	SBR/UASB	55/55	2	10	4.05	3.03	75.6	6.6	73	7.5	342	–	[67]
POME	UASB/+	55/37	2	5	3.2	2.6	56.5	5.5*	215 ^{COD}	7.3–7.5	320 ^{COD}	–	[68, 69]
Dairy processing waste	IBR/IBR	60/40	3	15	6.11	5.53	98.7	4.8–5.5	2.36 [L/L/d]	7.2	0.48 [L/L/d]	–	[70]

Cheese whey	+/+	35/35	1	20	8.7 TSS	8.1 VSS	60.5	5.2*	2.9 1.9	-	6.7 [L/L- feeds]	-	[71]
Cheese whey	+/ABR	35/35	1	4.4	6.77 TSS	6.27 VSS	61.0	5.2*	7.53 [L/d]	8.01	75.6 [L/d]	-	[72]
Skim latex serum	UASB/ UASB	55/55	1–2.5	9	4.13	3.8	35.8	5.4– 5.5	41.4– 59.2	7.4– 7.9	168.6	-	[73]
Maize silage	+/+	38/38	16.9	16.9	9.8	9.5	118	5.0– 5.5*	53.8	7.1	133.9	-	[74]

Note: 1. POME: palm oil mill effluent. 2 Reactor types: “+” means CSTR, SBR: sequencing batch reactor. ABR: induced bed reactor. IBR: anaerobic baffled reactor. PBR: packed bed reactor. 3. “*”: after pH adjustment. 4. Values with round brackets in H₂ yields mean they are CH₄ yields in first stage. Values with square brackets in H₂ or CH₄ yields denote units used by literature rather than heading units. Items in superscripts, e.g. TSS (total suspended solids), VSS (volatile suspended solids), COD (chemical oxygen demand) are terms used in original literature references rather than heading units

Even at hyper-thermophilic temperatures, the pH was reported to be 6.5, at a stage with an abundance of hydrogenotrophic methanogens and methane being produced [89, 90]. As listed in Table 5.4, biowastes that were not considered suitable for H₂ fermentation have been co-digested with other wastes, e.g. FW or FW-containing MSW. The nitrogen-rich biowaste can provide nitrogen and alkalinity for the H₂ fermentation of mixed waste. However, in the R-TPAD process, the nitrogen and alkalinity from the influent become less necessary but the recirculated sludge from CH₄ fermentation can also provide the living H₂-producers. Although co-digestion is a hot topic in treating biowaste, increasing the nitrogen content of the feeding mixture for R-TPAD is not as significant as other types of processes. Moreover, alkaline fermentation is another way to generate H₂ from nitrogen-rich waste. [85]

5.5 Conclusions and Future Outlook

In this chapter, the fundamentals of anaerobic fermentation for H₂ and CH₄ are introduced. Methane fermentation is the natural reaction of anaerobic degradation, but anaerobic H₂ production requires a more controlled set of conditions since H₂ is an intermediate product of CH₄ fermentation. Methane can be generated from a diverse source of organic solid waste, while hydrogen can only be generated from starch or soluble carbohydrates. The recirculated two-phase anaerobic digestion (R-TPAD) process, which converts biowaste into H₂ and CH₄ simultaneously, can be finely adjusted by the recirculation ratio to hydraulically separate the biological phases. With regard to the sources of biowaste, food waste is the major source and agro-industrial waste is the second most plentifully available source. The major challenges of H₂ and CH₄ fermentation are that lignin cannot be degraded by anaerobic microorganisms and that the conversion rates are slow compared to other methods with high temperatures or high pressure, or other physical and chemical treatments. Enhancing saccharification within the acidogenic phase can increase the H₂ yield from the source biomass.

Still, most of the studies on these systems have been conducted at the lab-scale or in pilot-scale reactors, where some problems might be hidden in the continuous operation of H₂ and CH₄ fermentation. This does not detract from the enormous potential of anaerobic H₂ and CH₄ fermentation to fully realize the biogasification of the organic solid waste. The combination of R-TPAD with recently attracting topics, e.g. direct interspecies electron transfer, membrane bioreactor, etc., is considered to be the remarkable studies in the recent future. Applying the automatic control and artificial intelligence will also solve the problem of continuous stability. With deepened understanding towards the process, configuration of R-TPAD can be applied for other purposes or in other fields. For the whole R-TPAD process, which can be seen as a multiple-input multiple-output system, more studies are required to investigate the relations between the operation parameters to the variables of yields and stability. Further optimization of the R-TPAD should be conducted both in theory and practice.

Table 5.4 Hydrogen and methane fermentation by co-digestion

Source biowaste	Process configuration				Feeding conc.			First stage		Second stage		Ref.
	Type	Temp.	HRT ₁	HRT ₂	TS	VS	COD	pH	H ₂ yield	CH ₄ yield	R	
(default units)	(CSTR)	°C	days	days	%	%	g/kg	-	L/kg-VS _{fed}	-	-	-
Garbage, waste paper, canteen waste, shredded paper	+/+	55/55	2.1–5.7	1.5–24	5.43–9.76	5.19–9.19	75.5–128	4.0–5.8*	10–60	7.4	490–570	0–2.0
Fruit waste, Vegetable waste, cow manure, straw	+/+	35/35	–	–	12.7–16.3	11.9–15.0	–	–	7–40	–	157–290	–
FW, paper waste	+/+	55/37.5	6	24	10.4–10.9	9.5–10.2	130–159	4.6–5.3	50–79	7.3–7.8	329–426	0.4
FW, sewage sludge	+/+	55/55	3.3	15	24.9	22.6	243	5.1	40	8.2	320	–
MSW, WAS	+/+	55/55	3	16	7.0	5.6	63.7	4.8	29	7.97	287	–
FW, sewage sludge	+/+	37/37	5	10	3.13	2.97	–	5.5*	44	6.5*	327	–
Urban organic wastes, WAS	+/+	55/55	3	17	15.5	13.0	146	5.3	24	8.2	570	–
Cattle manure, vegetable, WAS, MSW	+/SBR	–	5.3–10	8–15	5.57	4.21	89.8	5.2–6.9	21.0–79.4	–	130–530	–
Swine manure, market waste	+/+	55/55	3	22	3.95	3.77	85.9	5.5	140	7.61	351	–
Stillage, cake, glycerol	+/+	55/55	1–3	12–14	4.75–6.85	4.5–6.82	61.9–97.3	5.2–5.3	40–69	–	320–348	–
WAS	+/+	55/37	5	10	1.06	0.96	9.8	10*	6.7–74.5	–	123–150	–
		37/37										[85]

Note: 1. WAS: waste activated sludge (secondary sludge). MSW: municipal solid waste. 2. Reactor types: “+” means CSTR. SBR: sequencing batch reactor.

3. “*” after pH value denotes online pH adjustment

Acknowledgement This work is supported by the Grant-in-Aid for Research Activity Start-up (19K23528) from Japan Society for the Promotion of Science (JSPS).

References

1. Stephanopoulos G. Challenges in engineering microbes for biofuels production. *Science*. 2007;315:801–4. <https://doi.org/10.1126/science.1139612>.
2. Sun X, Atiyeh HK, Huhnke RL, Tanner RS. Syngas fermentation process development for production of biofuels and chemicals: a review. *Bioresource Technol Rep*. 2019;7:100279. <https://doi.org/10.1016/j.biteb.2019.100279>.
3. Li Y, Chen Y, Wu J. Enhancement of methane production in anaerobic digestion process: a review. *Appl Energy*. 2019;240:120–37. <https://doi.org/10.1016/j.apenergy.2019.01.243>.
4. Kaoru M, Toru F, Sang-Yul K, Kazuei I (2012) Experimental study of methane fermentation characteristics of waste biomass with different mixture ratio of carbohydrate, lipid, and protein. Proceedings of Annual Meeting of Environmental Systems Research 95–100 (Japanese), Japan Society of Civil Engineers, Tokyo. <https://iss.ndl.go.jp/books/R100000002-I00000162535-00?ar=4e1f&locale=en>
5. Yu-You LI (2004) Recent development of biomethanation technology [in Japanese]. *Journal of Japan Society on Water Environment* 27:622–626, Japan Society on Water Environment, Tokyo. <https://ci.nii.ac.jp/naid/10013650442/en/?range=0&sortorder=0&start=0&count=0>
6. Sakurai K, Li Y-Y, Noike T. Characteristics of mesophilic methane fermentation of high-solid content cow manure. *J Japan Soc Waste Manag Exp*. 2005;16:65–73. <https://doi.org/10.3985/jswme.16.65>.
7. Okuno Y, Li Y-Y, Sasaki H, Seki K, Kamigochi I. Influence of sludge ratio and temperature on the integrated methane fermentation of organic fraction of municipal solid waste and biosludge. *Doboku Gakkai Ronbunshu*. 2003;2003:75–84. https://doi.org/10.2208/jscej.2003.734_75.
8. Fang HHP. Environmental anaerobic technology: applications and new developments. London: World Scientific, Imperial College Press; 2010. <https://doi.org/10.1142/p706>.
9. Batstone DJ, Keller J, Angelidaki I, Kalyuzhnyi SV, Pavlostathis SG, Rozzi A, Sanders WTM, Siegrist H, Vavilin VA. The IWA Anaerobic Digestion Model No 1 (ADM1). *Water Sci Technol*. 2002;45:65–73. <https://doi.org/10.2166/wst.2002.0292>.
10. Wong YM, Wu TY, Juan JC. A review of sustainable hydrogen production using seed sludge via dark fermentation. *Renew Sustain Energy Rev*. 2014;34:471–82. <https://doi.org/10.1016/j.rser.2014.03.008>.
11. Shafaat HS, Rüdiger O, Ogata H, Lubitz W. [NiFe] hydrogenases: A common active site for hydrogen metabolism under diverse conditions. *Biochim Biophys Acta (BBA): Bioenergetics*. 2013;1827:986–1002. <https://doi.org/10.1016/j.bbabiobio.2013.01.015>.
12. Guss AM, Mukhopadhyay B, Zhang JK, Metcalf WW. Genetic analysis of mch mutants in two Methanosaerica species demonstrates multiple roles for the methanopterin-dependent C-1 oxidation/reduction pathway and differences in H(2) metabolism between closely related species. *Mol Microbiol*. 2005;55:1671–80. <https://doi.org/10.1111/j.1365-2958.2005.04514.x>.
13. Meuer J, Kuettner HC, Zhang JK, Hedderich R, Metcalf WW. Genetic analysis of the archaeon Methanosaerica barkeri Fusaro reveals a central role for Ech hydrogenase and ferredoxin in methanogenesis and carbon fixation. *Proc Natl Acad Sci U S A*. 2002;99:5632–7. <https://doi.org/10.1073/pnas.072615499>.
14. DiMarco AA, Bobik TA, Wolfe RS. Unusual coenzymes of methanogenesis. *Annu Rev Biochem*. 1990;59:355–94. <https://doi.org/10.1146/annurev.bi.59.070190.002035>.
15. Cheng Q, Call DF. Hardwiring microbes via direct interspecies electron transfer: mechanisms and applications. *Environ Sci: Processes Impacts*. 2016;18:968–80. <https://doi.org/10.1039/C6EM00219F>.

16. Barua S, Dhar BR. Advances towards understanding and engineering direct interspecies electron transfer in anaerobic digestion. *Bioresour Technol.* 2017;244:698–707. <https://doi.org/10.1016/j.biortech.2017.08.023>.
17. Lovley DR. Syntrophy goes electric: direct interspecies electron transfer. *Annu Rev Microbiol.* 2017;71:643–64. <https://doi.org/10.1146/annurev-micro-030117-020420>.
18. Lin R, Cheng J, Zhang J, Zhou J, Cen K, Murphy JD. Boosting biomethane yield and production rate with graphene: The potential of direct interspecies electron transfer in anaerobic digestion. *Bioresour Technol.* 2017;239:345–52. <https://doi.org/10.1016/j.biortech.2017.05.017>.
19. Niu Q, Hojo T, Qiao W, Qiang H, Li Y-Y. Characterization of methanogenesis, acidogenesis and hydrolysis in thermophilic methane fermentation of chicken manure. *Chem Eng J.* 2014;244:587–96. <https://doi.org/10.1016/j.cej.2013.11.074>.
20. Riau V, De la Rubia MÁ, Pérez M. Temperature-phased anaerobic digestion (TPAD) to obtain class A biosolids: a semi-continuous study. *Bioresour Technol.* 2010;101:2706–12. <https://doi.org/10.1016/j.biortech.2009.11.101>.
21. Yuan H, Zhu N. Progress in inhibition mechanisms and process control of intermediates and by-products in sewage sludge anaerobic digestion. *Renew Sustain Energy Rev.* 2016;58:429–38. <https://doi.org/10.1016/j.rser.2015.12.261>.
22. Astals S, Batstone DJ, Mata-Alvarez J, Jensen PD. Identification of synergistic impacts during anaerobic co-digestion of organic wastes. *Bioresour Technol.* 2014;169:421–7. <https://doi.org/10.1016/j.biortech.2014.07.024>.
23. Srisowmeya G, Chakravarthy M, Nandhini Devi G. Critical considerations in two-stage anaerobic digestion of food waste: a review. *Renew Sustain Energy Rev.* 2020;119:109587. <https://doi.org/10.1016/j.rser.2019.109587>.
24. Ghosh S, Ombregt JP, Pipyn P. Methane production from industrial wastes by two-phase anaerobic digestion. *Water Res.* 1985;19:1083–8. [https://doi.org/10.1016/0043-1354\(85\)90343-4](https://doi.org/10.1016/0043-1354(85)90343-4).
25. Ghosh S, Buoy K, Dressel L, Miller T, Wilcox G, Loos D. Pilot- and full-scale two-phase anaerobic digestion of municipal sludge. *Water Environ Res.* 1995;67:206–14. <https://doi.org/10.2175/106143095X131367>.
26. Qin Y, Wu J, Xiao B, Cong M, Hojo T, Cheng J, Li Y-Y. Strategy of adjusting recirculation ratio for biohythane production via recirculated temperature-phased anaerobic digestion of food waste. *Energy.* 2019;179:1235–45. <https://doi.org/10.1016/j.energy.2019.04.182>.
27. Micolucci F, Gottardo M, Bolzonella D, Pavan P. Automatic process control for stable bio-hythane production in two-phase thermophilic anaerobic digestion of food waste. *Int J Hydrogen Energy.* 2014;39:17563–72. <https://doi.org/10.1016/j.ijhydene.2014.08.136>.
28. Wu L-J, Kobayashi T, Li Y-Y, Xu K-Q. Comparison of single-stage and temperature-phased two-stage anaerobic digestion of oily food waste. *Energ Convers Manage.* 2015;106:1174–82. <https://doi.org/10.1016/j.enconman.2015.10.059>.
29. Liu D, Liu D, Zeng RJ, Angelidaki I. Hydrogen and methane production from household solid waste in the two-stage fermentation process. *Water Res.* 2006;40:2230–6. <https://doi.org/10.1016/j.watres.2006.03.029>.
30. Ueno Y, Fukui H, Goto M. Operation of a two-stage fermentation process producing hydrogen and methane from organic waste. *Environ Sci Technol.* 2007;41:1413–9. <https://doi.org/10.1021/es062127f>.
31. Chu C-F, Li Y-Y, Xu K-Q, Ebie Y, Inamori Y, Kong H-N. A pH- and temperature-phased two-stage process for hydrogen and methane production from food waste. *Int J Hydrogen Energy.* 2008;33:4739–46. <https://doi.org/10.1016/j.ijhydene.2008.06.060>.
32. Wang X, Zhao Y. A bench scale study of fermentative hydrogen and methane production from food waste in integrated two-stage process. *Int J Hydrogen Energy.* 2009;34:245–54. <https://doi.org/10.1016/j.ijhydene.2008.09.100>.
33. Lee D-Y, Ebie Y, Xu K-Q, Li Y-Y, Inamori Y. Continuous H₂ and CH₄ production from high-solid food waste in the two-stage thermophilic fermentation process with the recirculation of

- digester sludge. *Bioresour Technol.* 2010;101:S42–7. <https://doi.org/10.1016/j.biortech.2009.03.037>.
34. Cavinato C, Bolzonella D, Fatone F, Cecchi F, Pavan P. Optimization of two-phase thermophilic anaerobic digestion of biowaste for hydrogen and methane production through reject water recirculation. *Bioresour Technol.* 2011;102:8605–11. <https://doi.org/10.1016/j.biortech.2011.03.084>.
35. Cavinato C, Bolzonella D, Fatone F, Giuliano A, Pavan P. Two-phase thermophilic anaerobic digestion process for biohythane production treating biowaste: preliminary results. *Water Sci Technol.* 2011;64:715–21. <https://doi.org/10.2166/wst.2011.698>.
36. Elbeshbishi E, Nakhla G. Comparative study of the effect of ultrasonication on the anaerobic biodegradability of food waste in single and two-stage systems. *Bioresour Technol.* 2011;102: 6449–57. <https://doi.org/10.1016/j.biortech.2011.03.082>.
37. Cavinato C, Giuliano A, Bolzonella D, Pavan P, Cecchi F. Bio-hythane production from food waste by dark fermentation coupled with anaerobic digestion process: a long-term pilot scale experience. *Int J Hydrogen Energy.* 2012;37:11549–55. <https://doi.org/10.1016/j.ijhydene.2012.03.065>.
38. Kobayashi T, Xu K-Q, Li Y-Y, Inamori Y. Effect of sludge recirculation on characteristics of hydrogen production in a two-stage hydrogen–methane fermentation process treating food wastes. *Int J Hydrogen Energy.* 2012;37:5602–11. <https://doi.org/10.1016/j.ijhydene.2011.12.123>.
39. Chinellato G, Cavinato C, Bolzonella D, Heaven S, Banks CJ. Biohydrogen production from food waste in batch and semi-continuous conditions: Evaluation of a two-phase approach with digestate recirculation for pH control. *Int J Hydrogen Energy.* 2013;38:4351–60. <https://doi.org/10.1016/j.ijhydene.2013.01.078>.
40. Zuo Z, Wu S, Qi X, Dong R. Performance enhancement of leaf vegetable waste in two-stage anaerobic systems under high organic loading rate: Role of recirculation and hydraulic retention time. *Appl Energy.* 2015;147:279–86. <https://doi.org/10.1016/j.apenergy.2015.03.001>.
41. Ravi PP, Lindner J, Oechsner H, Lemmer A. Effects of target pH-value on organic acids and methane production in two-stage anaerobic digestion of vegetable waste. *Bioresour Technol.* 2018;247:96–102. <https://doi.org/10.1016/j.biortech.2017.09.068>.
42. Yeshanew MM, Frunzo L, Pirozzi F, Lens PNL, Esposito G. Production of biohythane from food waste via an integrated system of continuously stirred tank and anaerobic fixed bed reactors. *Bioresour Technol.* 2016;220:312–22. <https://doi.org/10.1016/j.biortech.2016.08.078>.
43. Algapani DE, Qiao W, di Pumbo F, Bianchi D, Wandera SM, Adani F, Dong R. Long-term bio-H₂ and bio-CH₄ production from food waste in a continuous two-stage system: Energy efficiency and conversion pathways. *Bioresour Technol.* 2017; <https://doi.org/10.1016/j.biortech.2017.05.164>.
44. Algapani DE, Qiao W, Su M, di Pumbo F, Wandera SM, Adani F, Dong R. Bio-hydrolysis and bio-hydrogen production from food waste by thermophilic and hyperthermophilic anaerobic process. *Bioresour Technol.* 2016;216:768–77. <https://doi.org/10.1016/j.biortech.2016.06.016>.
45. Gottardo M, Micolucci F, Bolzonella D, Uellendahl H, Pavan P. Pilot scale fermentation coupled with anaerobic digestion of food waste: effect of dynamic digestate recirculation. *Renew Energy.* 2017;114:455–63. <https://doi.org/10.1016/j.renene.2017.07.047>.
46. Paudel S, Kang Y, Yoo Y-S, Seo GT. Effect of volumetric organic loading rate (OLR) on H₂ and CH₄ production by two-stage anaerobic co-digestion of food waste and brown water. *Waste Manag.* 2017;61:484–93. <https://doi.org/10.1016/j.wasman.2016.12.013>.
47. Wu C, Huang Q, Yu M, Ren Y, Wang Q, Sakai K. Effects of digestate recirculation on a two-stage anaerobic digestion system, particularly focusing on metabolite correlation analysis. *Bioresour Technol.* 2018;251:40–8. <https://doi.org/10.1016/j.biortech.2017.12.020>.
48. Jo Y, Kim J, Hwang K, Lee C. A comparative study of single- and two-phase anaerobic digestion of food waste under uncontrolled pH conditions. *Waste Manag.* 2018;78:509–20. <https://doi.org/10.1016/j.wasman.2018.06.017>.

49. Mustafa AM, Chen X, Lin H, Sheng K. Effect of ammonia concentration on hythane (H_2 and CH_4) production in two-phase anaerobic digestion. *Int J Hydrogen Energy*. 2019;44:27297–310. <https://doi.org/10.1016/j.ijhydene.2019.08.229>.
50. Luo L, Wong JWC. Enhanced food waste degradation in integrated two-phase anaerobic digestion: Effect of leachate recirculation ratio. *Bioresour Technol*. 2019;291:121813. <https://doi.org/10.1016/j.biortech.2019.121813>.
51. Vo T-P, Lay C-H, Lin C-Y. Effects of hydraulic retention time on biohythane production via single-stage anaerobic fermentation in a two-compartment bioreactor. *Bioresour Technol*. 2019;121869 <https://doi.org/10.1016/j.biortech.2019.121869>.
52. Sunyoto NMS, Sugiarto Y, Zhu M, Zhang D. Transient performance during start-up of a two-phase anaerobic digestion process demonstration unit treating carbohydrate-rich waste with biochar addition. *Int J Hydrogen Energy*. 2019;44:14341–50. <https://doi.org/10.1016/j.ijhydene.2019.04.037>.
53. Algapani DE, Qiao W, Ricci M, Bianchi DM, Wandera S, Adani F, Dong R. Bio-hydrogen and bio-methane production from food waste in a two-stage anaerobic digestion process with digestate recirculation. *Renew Energy*. 2019;130:1108–15. <https://doi.org/10.1016/j.renene.2018.08.079>.
54. Ma X, Yu M, Yang M, Zhang S, Gao M, Wu C, Wang Q. Effect of liquid digestate recirculation on the ethanol-type two-phase semi-continuous anaerobic digestion system of food waste. *Bioresour Technol*. 2020;313:123534. <https://doi.org/10.1016/j.biortech.2020.123534>.
55. Feng K, Wang Q, Li H, Zhang Y, Deng Z, Liu J, Du X. Effect of fermentation type regulation using alkaline addition on two-phase anaerobic digestion of food waste at different organic load rates. *Renew Energy*. 2020;154:385–93. <https://doi.org/10.1016/j.renene.2020.03.051>.
56. Luo G, Xie L, Zou Z, Wang W, Zhou Q, Shim H. Anaerobic treatment of cassava sludge for hydrogen and methane production in continuously stirred tank reactor (CSTR) under high organic loading rate (OLR). *Int J Hydrogen Energy*. 2010;35:11733–7. <https://doi.org/10.1016/j.ijhydene.2010.08.033>.
57. Jiang H, Qin Y, Gadow SI, Ohnishi A, Fujimoto N, Li Y-Y. Bio-hythane production from cassava residue by two-stage fermentative process with recirculation. *Bioresour Technol*. 2017; <https://doi.org/10.1016/j.biortech.2017.09.102>.
58. Jiang H, Qin Y, Fujimoto N, Ohnishi A, Y-Y LI. Optimization of two-stage recirculated biohythane fermentation from high-solids cassava residue (in Japanese). *J Environ Eng Res*. 2017;73:III_483–93.
59. Zhu H, Stadnyk A, Béland M, Seto P. Co-production of hydrogen and methane from potato waste using a two-stage anaerobic digestion process. *Bioresour Technol*. 2008;99:5078–84. <https://doi.org/10.1016/j.biortech.2007.08.083>.
60. Ohba M, Li Y-Y, Noike T. Analysis of microbial community in two-phase circulating process for hydrogen and methane fermentation (in Japanese). *J Japan Soc Water Environ*. 2006;29: 399–406. <https://doi.org/10.2965/jswe.29.399>.
61. Ohba M, Li Y-Y, Noike T. Characteristics of hydrogen and methane fermentation of potato processing waste by two-phase circulating process without dilution water. *J Japan Society Water Environ*. 2005;28:629–36. <https://doi.org/10.2965/jswe.28.629>.
62. Massanet-Nicolau J, Dinsdale R, Guwy A, Shipley G. Utilising biohydrogen to increase methane production, energy yields and process efficiency via two stage anaerobic digestion of grass. *Bioresour Technol*. 2015;189:379–83. <https://doi.org/10.1016/j.biortech.2015.03.116>.
63. Kongjan P, O-Thong S, Angelidaki I. Performance and microbial community analysis of two-stage process with extreme thermophilic hydrogen and thermophilic methane production from hydrolysate in UASB reactors. *Bioresour Technol*. 2011;102:4028–35. <https://doi.org/10.1016/j.biortech.2010.12.009>.
64. Si B-C, Li J-M, Zhu Z-B, Zhang Y-H, Lu J-W, Shen R-X, Zhang C, Xing X-H, Liu Z. Continuous production of biohythane from hydrothermal liquefied cornstalk biomass via two-stage high-rate anaerobic reactors. *Biotechnol Biofuels*. 2016;9:254. <https://doi.org/10.1186/s13068-016-0666-z>.

65. Ding L, Chan Gutierrez E, Cheng J, Xia A, O'Shea R, Guneratnam AJ, Murphy JD. Assessment of continuous fermentative hydrogen and methane co-production using macro- and micro-algae with increasing organic loading rate. *Energy*. 2018;151:760–70. <https://doi.org/10.1016/j.energy.2018.03.103>.
66. Mamimin C, Singkhala A, Kongjan P, Suraraksa B, Prasertsan P, Imai T, O-Thong S. Two-stage thermophilic fermentation and mesophilic methanogen process for biohythane production from palm oil mill effluent. *Int J Hydrogen Energy*. 2015;40:6319–28. <https://doi.org/10.1016/j.ijhydene.2015.03.068>.
67. Seengenyoung J, Mamimin C, Prasertsan P, O-Thong S. Pilot-scale of biohythane production from palm oil mill effluent by two-stage thermophilic anaerobic fermentation. *Int J Hydrogen Energy*. 2018; <https://doi.org/10.1016/j.ijhydene.2018.08.021>.
68. Krishnan S, Singh L, Sakinah M, Thakur S, Nasrul M, Otieno A, Wahid ZA. An investigation of two-stage thermophilic and mesophilic fermentation process for the production of hydrogen and methane from palm oil mill effluent. *Environmental Progress & Sustain Energy*. 2017;36: 895–902. <https://doi.org/10.1002/ep.12537>.
69. Krishnan S, Singh L, Sakinah M, Thakur S, Wahid ZA, Alkasrawi M. Process enhancement of hydrogen and methane production from palm oil mill effluent using two-stage thermophilic and mesophilic fermentation. *Int J Hydrogen Energy*. 2016;41:12888–98. <https://doi.org/10.1016/j.ijhydene.2016.05.037>.
70. Zhong J, Stevens DK, Hansen CL. Optimization of anaerobic hydrogen and methane production from dairy processing waste using a two-stage digestion in induced bed reactors (IBR). *Int J Hydrogen Energy*. 2015;40:15470–6. <https://doi.org/10.1016/j.ijhydene.2015.09.085>.
71. Venetsaneas N, Antonopoulou G, Stamatelatou K, Kornaros M, Lyberatos G. Using cheese whey for hydrogen and methane generation in a two-stage continuous process with alternative pH controlling approaches. *Bioresour Technol*. 2009;100:3713–7. <https://doi.org/10.1016/j.biortech.2009.01.025>.
72. Antonopoulou G, Stamatelatou K, Venetsaneas N, Kornaros M, Lyberatos G. Biohydrogen and methane production from cheese whey in a two-stage anaerobic process. *Ind Eng Chem Res*. 2008;47:5227–33. <https://doi.org/10.1021/ie071622x>.
73. Kongjan P, Jariyaboon R, O-Thong S. Anaerobic digestion of skim latex serum (SLS) for hydrogen and methane production using a two-stage process in a series of up-flow anaerobic sludge blanket (UASB) reactor. *Int J Hydrogen Energy*. 2014;39:19343–8. <https://doi.org/10.1016/j.ijhydene.2014.06.057>.
74. Benito Martin PC, Schlienz M, Greger M. Production of bio-hydrogen and methane during semi-continuous digestion of maize silage in a two-stage system. *Int J Hydrogen Energy*. 2017;42:5768–79. <https://doi.org/10.1016/j.ijhydene.2017.01.020>.
75. Kataoka N, Ayame S, Miya A, Yoneyama Y, Watanabe A, Suzuki T. Biogasification of garbage and waste-paper by hydrogen-methane two-stage fermentation system (in Japanese). *Environ Eng Res*. 2006;43:15–22. <https://doi.org/10.11532/proes1992.43.15>.
76. Ganesh R, Torrijos M, Sousbie P, Lugardon A, Steyer JP, Delgenes JP. Effect of increasing proportions of lignocellulosic cosubstrate on the single-phase and two-phase digestion of readily biodegradable substrate. *Biomass Bioenergy*. 2015;80:243–51. <https://doi.org/10.1016/j.biombioe.2015.05.019>.
77. Qin Y, Li L, Wu J, Xiao B, Hojo T, Kubota K, Cheng J, Li Y-Y. Co-production of biohydrogen and biomethane from food waste and paper waste via recirculated two-phase anaerobic digestion process: bioenergy yields and metabolic distribution. *Bioresour Technol*. 2019;276:325–34. <https://doi.org/10.1016/j.biortech.2019.01.004>.
78. Gottardo M, Micolucci F, Mattioli A, Faggian S, Cavinato C, Pavan P. Hydrogen and methane production from biowaste and sewage sludge by two phases anaerobic codigestion. *Chem Eng Trans*. 2015;43:379–84. <https://doi.org/10.3303/CET1543064>.
79. Zahedi S, Solera R, Micolucci F, Cavinato C, Bolzonella D. Changes in microbial community during hydrogen and methane production in two-stage thermophilic anaerobic co-digestion process from biowaste. *Waste Manag*. 2016;49:40–6. <https://doi.org/10.1016/j.wasman.2016.01.016>.

80. Siddiqui Z, Horan NJ, Salter M. Energy optimisation from co-digested waste using a two-phase process to generate hydrogen and methane. *Int J Hydrogen Energy*. 2011;36:4792–9. <https://doi.org/10.1016/j.ijhydene.2010.12.118>.
81. Bolzonella D, Micolucci F, Battista F, Cavinato C, Gottardo M, Provesan S, Pavan P. Producing biohythane from Urban Organic Wastes. *Waste Biomass Valor*. 2019; <https://doi.org/10.1007/s12649-018-00569-7>.
82. Farhat A, Miladi B, Hamdi M, Bouallgui H. Fermentative hydrogen and methane co-production from anaerobic co-digestion of organic wastes at high-loading rate coupling continuously and sequencing batch digesters. *Environ Sci Pollut Res Int*. 2018; <https://doi.org/10.1007/s11356-018-2796-2>.
83. Schievano A, Tenca A, Scaglia B, Merlini G, Rizzi A, Daffonchio D, Oberti R, Adani F. Two-stage vs single-stage thermophilic anaerobic digestion: comparison of energy production and biodegradation efficiencies. *Environ Sci Technol*. 2012;46:8502–10. <https://doi.org/10.1021/es301376n>.
84. Luo G, Xie L, Zhou Q, Angelidaki I. Enhancement of bioenergy production from organic wastes by two-stage anaerobic hydrogen and methane production process. *Bioresour Technol*. 2011;102:8700–6. <https://doi.org/10.1016/j.biortech.2011.02.012>.
85. Wan J, Jing Y, Rao Y, Zhang S, Luo G. Thermophilic alkaline fermentation followed by mesophilic anaerobic digestion for efficient hydrogen and methane production from waste-activated sludge: dynamics of bacterial pathogens as revealed by the combination of metagenomic and quantitative PCR analyses. *Appl Environ Microbiol*. 2018;84. <https://doi.org/10.1128/AEM.02632-17>.
86. Zamri MFMA, Hasmady S, Akhiar A, Ideris F, Shamsuddin AH, Mofijur M, Fattah IMR, Mahlia TMI. A comprehensive review on anaerobic digestion of organic fraction of municipal solid waste. *Renew Sustain Rev*. 2021;137:110637. <https://doi.org/10.1016/j.rser.2020.110637>.
87. Qin Y, Wu J, Xiao B, Hojo T, Li Y-Y. Biogas recovery from two-phase anaerobic digestion of food waste and paper waste: Optimization of paper waste addition. *Sci Total Environ*. 2018;634:1222–30. <https://doi.org/10.1016/j.scitotenv.2018.03.341>.
88. García-Depraect O, Muñoz R, van Lier JB, Rene ER, Diaz-Cruces VF, León-Becerril E. Three-stage process for tequila vinasse valorization through sequential lactate, biohydrogen and methane production. *Bioresour Technol*. 2020;307:123160. <https://doi.org/10.1016/j.biortech.2020.123160>.
89. Wu L-J, Higashimori A, Qin Y, Hojo T, Kubota K, Li Y-Y. Comparison of hyper-thermophilic-mesophilic two-stage with single-stage mesophilic anaerobic digestion of waste activated sludge: Process performance and microbial community analysis. *Chem Eng J*. 2016;290:290–301. <https://doi.org/10.1016/j.cej.2016.01.067>.
90. Qin Y, Higashimori A, Wu L-J, Hojo T, Kubota K, Li Y-Y. Phase separation and microbial distribution in the hyperthermophilic-mesophilic-type temperature-phased anaerobic digestion (TPAD) of waste activated sludge (WAS). *Bioresour Technol*. 2017;245:401–10. <https://doi.org/10.1016/j.biortech.2017.08.124>.

Chapter 6

Recycling of Multiple Organic Solid Wastes into Biogas via Anaerobic Digestion



Nima Hajinajaf, Manali Das, Pradipta Patra, Amit Ghosh,
and Arul M. Varman

Abstract The accumulation of solid organic wastes (SOW) has reached critical levels globally and therefore, sustainable management of wastes is the key to minimize the risks to human health, avoid depletion of natural resources, reduce environmental burden and maintain the ecological balance. SOWs mainly include food waste, animal manure, waste activated sludge, yard waste, and agricultural waste. Anaerobic digestion (AD) is one of the most viable and popular technologies for recycling the organic fraction of solid wastes for the production of renewable energy in the form of biogas that can be crucial in meeting the world's ever-increasing energy demands. Employing sophisticated treatment techniques for the diverse organic fractions present in solid wastes enable proper waste management as well as add value to the economy. Detailed knowledge about the physical properties of these SOWs to determine suitable operating conditions as well as research on the genetic engineering of microbes involved in the AD process are needed to produce biogas efficiently. This chapter summarizes the science underlying the anaerobic digestion process, different feedstock types, the diverse array of microorganisms involved, process variables crucial for AD efficiency, industrial scope of the

N. Hajinajaf · A. M. Varman (✉)

Chemical Engineering, School for Engineering of Matter, Transport, and Energy, Arizona State University, Tempe, AZ, USA

e-mail: Arul.M.Varman@asu.edu

M. Das

School of Bioscience, Indian Institute of Technology Kharagpur, Kharagpur, West Bengal, India

P. Patra

School of Energy Science and Engineering, Indian Institute of Technology Kharagpur, Kharagpur, West Bengal, India

A. Ghosh

School of Energy Science and Engineering, Indian Institute of Technology Kharagpur, Kharagpur, West Bengal, India

P.K. Sinha Centre for Bioenergy and Renewables, Indian Institute of Technology Kharagpur, Kharagpur, West Bengal, India

different reactor modes, and the optimization and pretreatment methods to improve process efficiency.

Keywords Renewable energy · Solid organic wastes · Anaerobic digestion models · Resource recovery · Pretreatment

6.1 Introduction

The energy crisis in the twenty-first century caused by global population swelling and the development of industries has reached an unprecedented level. Currently, fossil fuels are the main source of world energy which are non-renewable and cause environmental pollution that has triggered scientists' motivation to look for renewable, clean sources [1]. Besides, the world is currently witnessing a tremendous increase in the production of solid wastes. A major quantity of the generated solid wastes is organic by nature, and they originate from the municipal, industrial and agricultural sectors. Municipal solid wastes (MSW) are one of the most common organic solid wastes and it is projected that by 2025, the annual MSW production could reach 2.2 billion tonnes [2]. Agricultural wastes are another class of biodegradable wastes that are generated during livestock and food production which can be utilized for biogas production, thereby contributing to the economics of agriculture. However, in many countries, a major percentage of the organic wastes end up in landfills or are disposed off in water bodies, resulting in serious soil and water pollution, which can affect human health and hygiene. Hence, using appropriate processing methods to convert biodegradable organic wastes into biofuel such as biogas is of utmost importance to allow energy recovery and prevent adverse environmental effects. Anaerobic digestion (AD) is a simple yet powerful process that can be used to overcome the challenge posed by organic wastes to the environment. AD is primarily used to convert organic wastes into gaseous biofuel, biogas (biogas is a mixture of methane, carbon dioxide, and other trace gases). Biogas produced in rural areas is mainly used for cooking and heating homes. Additionally, the biogas produced in large scale plants can be used for steam generation in boilers or combined heat and power (CHP) generation in power station or heat engines. Through anaerobic digestion as the organic wastes which is usually released to the environment or landfills is diverted for biogas production it helps in the fight against greenhouse gas emissions by reducing methane and nitrous oxide emissions from landfills. Furthermore, AD process can be used to promote soil fertility by using digestates as a nutrient rich material for the production of compost and organic fertilizer [3].

Although organic wastes appear in solid form, they contain up to 90% moisture. This restricts the application of thermo-chemical treatment such as incineration for energy recovery as the process would end up requiring excessive heat to overcome the high-water percentage, making it energy intensive. AD overcomes this limitation by allowing the controlled release of energy from the chemical bonds present in the

organic compounds that makeup the wastes. Therefore, AD has become a prevailing choice for the sustainable treatment of organic wastes having high moisture content. It involves the microbial degradation of organic feedstocks through a series of anaerobic stages to produce methane-rich biogas for renewable energy production and use.

Based on the total solid content of the waste and the percentage of moisture present, the AD can be classified as either liquid-state AD (solid content <15%) or solid-state AD (solid content >15%) [4]. Liquid state AD, also called as wet AD, is primarily used to treat substrates with high moisture content, such as waste activated sludge and animal manures. However, the large water content in this process significantly lowers the volumetric methane productivity as well as creating the problem of generating a large amount of digestate as waste product [5]. On the other hand, solid-state AD (dry AD) involves digestion of feedstocks with high organic loading and minimal water content. Solid-state AD is generally preferred for digestion of the organic fraction derived from municipal solid waste and agricultural wastes, and often results in a high volumetric methane productivity. Moreover, the heating-energy requirement and wastewater generation are also reduced in the solid-state AD. However, due to inadequate mass transfer, solid-state AD has disadvantages such as longer retention time, high cost, and a tendency to accumulate inhibitors [6]. Thus, the major focus of this chapter is on the different methods of AD of organic wastes and how matching the treatment process to the selected type of waste can help in the maximization of the biogas production for renewable energy generation. This chapter also deals with the different microbial conditions and species required for facilitating the different stages of AD, synthetic biology approaches for engineering strains towards AD as well as models available to better understand the molecular processes. Also, the primary conditions such as organic loading rate (OLR, a definition for OLR is provided in Sect. 6.4.5), biogas production rates, and the influencing environmental conditions like temperature, pH, alkalinity, etc., have been discussed that contribute significantly towards the successful design and operations of the treatment process. In addition, this chapter also highlights emerging technologies like solid-state AD and the different processes available for large-scale AD.

6.2 Feedstocks for AD

Solid wastes are broadly grouped into three categories of municipal, industrial, and agricultural-based on their source. Considering that, municipal solid waste generation will reach 6.1 million metric tonnes/day in 2025 [7], consolidated solid waste management approaches such as AD are required to create a pollution-free environment. However, a more rigorous classification of AD feedstocks is necessary to better manage the wastes and to optimize the operating conditions of AD. More specifically, solid organic wastes are also classified into agricultural wastes (AW), animal manure (AM), waste activated sludge (WAS), yard waste (YW), and food

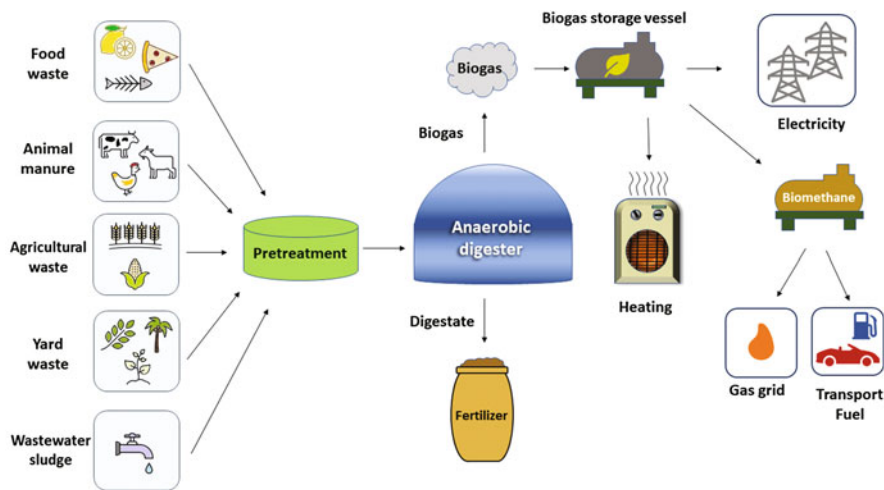


Fig. 6.1 Schematic depicting the different types of organic solid wastes fed into anaerobic digester and the common applications of the products generated via AD

waste (FW). Figure 6.1 shows the classification of solid wastes fed into AD and the applications of the products generated via AD.

6.2.1 Agricultural Waste

As the name indicates, residues of agriculture such as corn stover, rice straw, etc., can be used as the feedstock for the AD [8]. It has been estimated that around 90.7 million dry tonnes of primary crop residues are projected to be collected in the US out of which 75% is corn stover [9]. These wastes are composed of cellulose, hemicellulose, and lignin, which are hard to be broken down by natural enzymes and consumed by bacteria, and therefore, AD of these materials without pretreatment would not be effective. For instance, the corn stover silage is composed of 35% cellulose, 25.2% hemicellulose, and 4.3% lignin in which using a biological pretreatment (fungal) can increase methane yield by 23% [10]. Another strategy to improve the anaerobic digestion of agricultural wastes is to reduce their particle size. For example, Menardo et al. [11], adopted physical pretreatment to reduce the barley straw's size from 5.0 cm to 0.5 cm and this improved the methane yield by 54.2%. In the same work, thermal pretreatment at 120 °C on barley and wheat straw increased methane production by 40.8% and 64.3%, respectively. Table 6.1 provides the composition of various lignocellulosic feedstocks found in agricultural wastes.

Table 6.1 Composition of various lignocellulosic materials found in agricultural and yard wastes

No.	Biomass	Cellulose (%)	Hemicellulose (%)	Lignin (%)	Ref.
1	Rice Straw	34.63	29.74	15.34	[24]
2	Wheat Straw	35.19	22.15	22.09	[25]
3	Sugarcane bagasse	46.21	20.86	22.67	[25]
4	Pinewood	44.50	28.00	26.80	[26]
5	Elmwood	46.40	26.30	26.20	[26]
6	Corn stover	42.62	22.99	12.75	[27]
7	Sunflower Stalks	34.00	20.80	29.70	[28]
8	Banana Waste	13.20	14.80	14.00	[29]

6.2.2 Animal Manure

Animal manure is a good source of organic matter that can act as a feedstock for biogas production. As the quality of different animal manure is subtly different from each other, the conditions at which the AD operates are different as well [12]. A study in 2011 showed that out of the total animal manure feedstock used for AD, about 13.62% is recovered as energy in the form of biogas, while the remaining 73.14% is present as digestate [13]. The digestate also has the value of being used as fertilizer [14]. Animal manure is considered as a complex waste which contains a high amount of nitrogen that might cause reactor failure due to ammonia (NH_3) inhibition [15]. In this regard, when the concentration of NH_3 in an AD process exceeds a threshold, process failure might happen. Both free NH_3 and ammonium ion (NH_4^+) can inhibit the process if their concentration surpass $\sim 1800 \text{ mg.L}^{-1}$ in high-rate digesters [16, 17]. Various techniques for recovery from ammonia inhibition have been discussed by Yenigün and Demirel, such as periodic removal of supernatants, reduction of protein content in wastewater feedstock, adjustment of pH and C:N ratio, etc. [15].

6.2.3 Waste Activated Sludge

Sludge generated during the treatment of municipal wastewater is considered as waste activated sludge. Its disposal can account for up to 50% of the wastewater plant's operating costs and one of the most preferred methods for sludge disposal and recycling is AD [18]. The disposed sludge of wastewater treatment plant can also be used as the feedstock which has a low carbon-to-nitrogen (C/N) ratio due to the high amount of nitrogen present in this type of waste [19]. However, the optimal C/N ratio of anaerobic digestion is around 20–30 [20]. To counterbalance the nutrients and ammonia inhibition the sludge can be used in co-digestion along with other wastes such as agricultural wastes that have a high C/N ratio.

6.2.4 Yard Waste

Yard waste or garden waste mostly includes leaves falling from trees and bushes, grasses and other various parts of plants that are mostly aggregated in the green cities and areas which can be used as the raw material of AD [21]. Table 6.1 provides the composition of various lignocellulosic feedstocks found in yard wastes as well. Garden wastes also have the same problem and difficulties to be used for AD as agricultural wastes as they are also composed of lignin, cellulose and hemicellulose which need to use pretreatments. For instance, Dussadee et al. [22] conducted AD of Napier grass (*Pennisetum purpureum*) for biogas production with and without pretreatment. After AD, they obtained 164 L biogas per kilogram volatile solids (L/kg VS) without pretreatment, whereas by integrating AD with chemical pretreatment they obtained 179 L/kg VS. In another study by Panigrahi et al. [23], four different pretreatments of hot air oven, hot water bath, autoclave and microwave applied on yard wastes and they obtained approximately 10% increase in biochemical methane potential from 328.9 ± 15 mL/g VS (untreated after 45 days) to 364.5 ± 11 mL/g VS (after 26 days) using microwave pretreatment.

6.2.5 Food Waste

Food waste is another important organic solid waste that can be used to produce biogas via AD, which mostly contains uneaten or discarded food from houses, restaurants or even industrial sectors. A study conducted by European Union reported that 88 million tonnes of edible and non-edible food wastes were generated in 2012 [30], which is shocking as it is equal to 20% of the total food produced. These food wastes can be used to produce biogas and further in electricity which studies have shown that 9900 ton of corn silage can be replaced by 6600 ton of food waste to reduce the carbon footprint by 42% [31]. Food wastes also are used as co-digestion feedstock to balance the nutrients in an anaerobic digester and improve the biogas production of various feedstocks. Yong et al. [32], investigated the biogas production from food wastes as well as using it as a co-digestion with straw. They obtained $0.16 \text{ m}^3 \text{ CH}_4 / \text{kgvs}$ from AD of food waste individually, while using it as co-digestion improved the methane production yield of straw by 149.7% confirming using food waste as a desirable feedstock for nutrient balancing in AD.

As mentioned earlier, characterizing the properties of these solid organic wastes can provide researchers the necessary knowledge to design optimal conditions for AD. Table 6.2 shows a literature review on the AD of various substrates for biogas production and their operational conditions.

Table 6.2 A literature review on the AD of various feedstocks and their biogas/methane production

No.	Feedstock	System	OLR	Pre-treatment	pH	Biogas composition	Biogas/methane production	Ref.
1	Napier grass (<i>Pennisetum purpureum</i>)	Batch		Alkali	7.9	Methane 63.5% CO ₂ 30.1%	179.38 L biogas kg ⁻¹ VS	[22]
2	Municipal solid waste	Semi-continuous	6 kg VS m ⁻³ day ⁻¹	Mechanical(combination of a shear shredder, rotary cutter and wet macerator)	7.3	Methane 59%	0.54 STP m ³ biogas kg ⁻¹ VS _{added}	[33]
3	Municipal solid waste	Semi-continuous	6 kg VS m ⁻³ day ⁻¹	Mechanical(a combination of a shear shredder, rotary cutter and wet macerator)	8.4	Methane 59%	0.48 STP m ³ biogas kg ⁻¹ VS _{added}	[33]
4	Landfill leachate	Batch		Pulsed electric field	8.25–8.54		155.61–220.06 mL biogas g ⁻¹ VS	[34]
5	Fruit/Vegetable	Batch		Pulsed electric field	3.81–3.92		804.51–368.80 mL biogas g ⁻¹ VS	[34]
6	Organic fraction of municipal solid waste (OFMSW)	Batch		Sonication time 30 min Specific energy 7200 kJ/kg TS Power density 0.6 W/mL			455 mL biogas g ⁻¹ VS	[35]
7	Municipal solid waste			High-pressure extruding with 40 MPa pressure	6.96–7.64		674 mL CH ₄ g ⁻¹ VS	[36]
8	Rice straw	Batch		Citric acid	7		197.86 mL biogas g ⁻¹ VS _{total}	[24]
9	Corn stover silage			Fungal (<i>Phanerochaete chrysosporium</i>)	4.3		265.1 mL CH ₄ g ⁻¹	[10]
10	Drinking sludge	Batch			7.3		160 mL ^a CH ₄ g ⁻¹ DM	[37]
11	Sludge	Batch	—		7–7.5		64.8 mL biogas g ⁻¹ VS	[38]

(continued)

Table 6.2 (continued)

No.	Feedstock	System	OLR	Pre-treatment	pH	Biogas composition	Biogas/methane production	Ref.
12	<i>Scenedesmus</i> spp. (microalgae)	Continuous	0.3–0.4 g COD L ⁻¹ d ⁻¹	Rumen microorganisms	6–7		214 mL CH ₄ g ⁻¹ COD In	[39]
13	<i>Chlamydomonas reinhardtii</i> strain CC-1690	2		Thermal pretreatment			464 mL ^a CH ₄ g ⁻¹ VS day ⁻¹	[40]
14	Egeria densa	Semi-continuous		–			231 mL CH ₄ g ⁻¹ VS	[41]
15	Municipal solid waste	Batch		–		70% CH ₄	0.560 m ³ biogas kg ⁻¹ VS	[42]
16	Chicken manure	Batch	5.3 kg VS/m ³ /d	–	7.7–8.4		0.18 m ³ CH ₄ kg ⁻¹ VSFed	[43]
17	Chicken manure	Batch	1.8 kg VS/m ³ /d	–	7.7–8.4		0.35 m ³ CH ₄ kg ⁻¹ VSFed	[43]
18	Activated sludge	Batch		Alkali	9.5		282 mL CH ₄ g ⁻¹ VSS	[44]
19	Corn Straw	Batch		Mechanochemical	7.0		239 mL CH ₄ g ⁻¹ - TS	[45]
20	Paper wastes	Batch		–	7.5		243–316 mL CH ₄ g ⁻¹ -VS	[46]
21	Food wastes	Batch		Microwave 2.45 GHz 1000 W	8.0		783.15 mL CH ₄ g ⁻¹ -VS	[47]
22	Lipid wastes	Batch		Ultrasound 20 kHz 500 W	8.0		927.97 mL CH ₄ g ⁻¹ -VS	[47]

^aN refers to normal or normalized volume of a gas which is the gas volume at 0 ° C and 760 millimeters pressure

6.3 Microbial Communities in AD

6.3.1 Microbial Communities Involved in the Four Stages of AD

The AD process involves a series of biochemical reactions catalyzed by microbial communities and is grouped into four stages: hydrolysis, acidogenesis, acetogenesis, and methanogenesis as shown in Fig. 6.2 [48]. Hydrolysis is the first stage in which the high molecular weight complex organic polymers such as starch, cellulose, lipids, etc. are hydrolyzed into smaller chains/molecules. The breakdown of complex substrate is catalyzed by hydrolases (amylases, proteases, and lipases) produced by hydrolytic bacteria such as *Bifidobacterium* and *Bacteroides* [49]. Following hydrolysis, acidogenesis takes place, wherein anaerobes of the genera *Bacillus*, *Pseudomonas*, *Micrococcus*, *Clostridium*, *Flavobacterium*, and *Proteobacteria* like *Enterobacteriaceae* break down the simpler molecules derived from hydrolysis into short-chain organic acids (formic, acetic, butyric acids, etc.), alcohols (methanol and ethanol), hydrogen and carbon dioxide [50, 51]. In one study, it was reported that *Proteobacteria* make up approximately 53.2% of the total microbial community present in an up-flow anaerobic sludge blanket reactor, making them a crucial phylogenetic group in this process owing to their involvement as glucose, butyrate, propionate, and acetate-consuming microbes [52, 53]. The organic compounds produced during acidogenesis can serve as both electron donors (dehydrogenation) and acceptors (hydrogenation). The accumulation of electrons in the form of organic acids is a bacterial response to the increasing hydrogen concentration in the solution, which may not always be directly used by methanogenic bacteria for biogas production, thus necessitating an intermediate step called acetogenesis. Both hydrolysis and acidogenesis are carried out in acidic pH within the range of 5.2–6.3 [54]. During acetogenesis, bacteria of the genera *Syntrophomonas*, *Syntrophobacter*, *Methanobacterium*, etc. metabolize the organic acids to produce acetic acid along with ammonium, hydrogen gas, carbon dioxide. Acetogenesis determines the efficiency of the AD process because approximately 70% of total methane produced in the AD process is derived from the acetate produced during acetogenesis. In addition, this step accounts for approximately 25% of the total acetate as well as 11% of the hydrogen gas formed during AD [55]. The final stage of AD is methanogenesis and is assisted by the activities of both acetotrophic (*Methanosaeta*) and hydrogenotrophic methanogens (*Methanosarcina*). In methanogenesis, the acetotrophic methanogenic bacteria decompose acetate produced during acetogenesis to methane [56], while the hydrogenotrophic methanogens convert the hydrogen and carbon dioxide gas into methane [57]. Generally, filamentous *Methanosaeta* dominates the microbial population at low concentrations of acetate. But higher concentrations of toxic byproducts of digestions, like volatile fatty acids, hydrogen sulphide, etc. inhibit *Methanosaeta* and allow the growth of hydrogenotrophic methanogens like *Methanosarcina*.

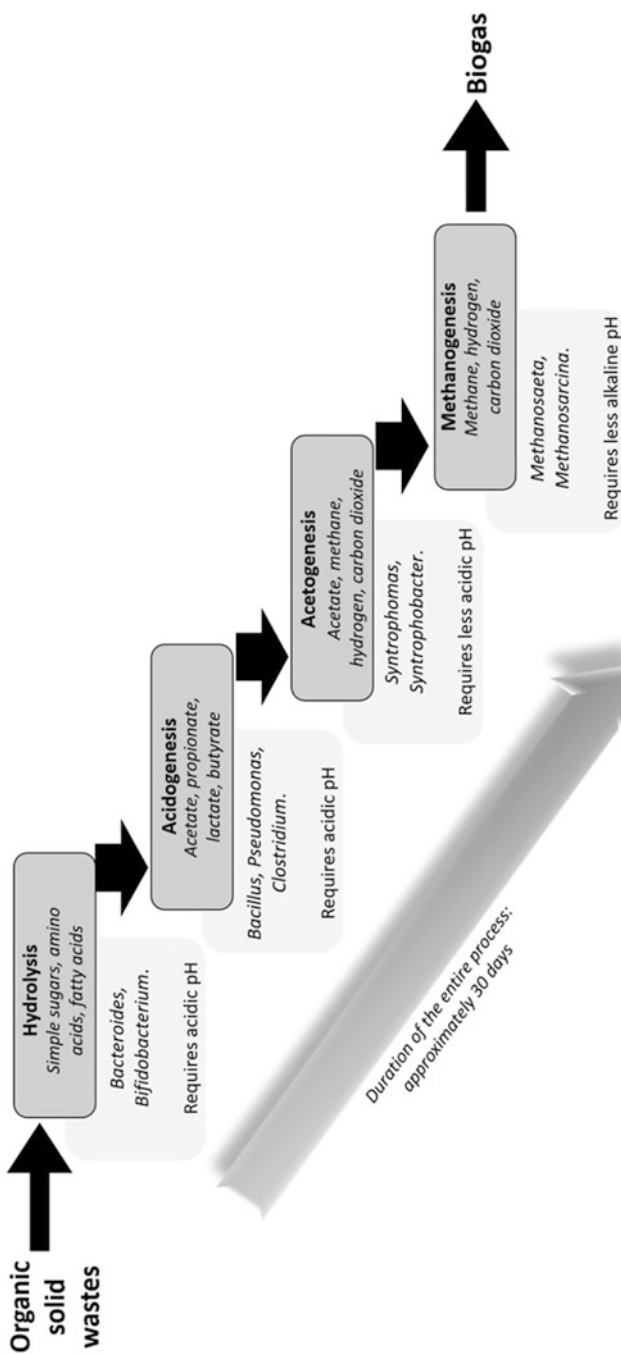


Fig. 6.2 Stages in anaerobic digestion. The organic wastes are digested via microbial action in four stages, i.e., hydrolysis, acidogenesis, acetogenesis, and methanogenesis to produce biogases. The entire process can take up to 30 days to complete.

6.3.2 Synthetic Biology and Genetic Engineering in AD

The efficiency of biogas production, particularly methane, from organic wastes depends on the composition of the microbial consortium used, as well as the behavior or action of the consortium. As the optimal conditions (e.g., temperature, pH, etc.) of each stage are different, engineering the microbial consortium of each stage can help scientists design and optimize the process to improve the biogas production [58]. Till date, wild-type strains of anaerobic microbes are widely used for facilitating the process of AD, however, the advent of genetic and metabolic engineering can assist in improving the performances of these strains. Previously the only option for genetic engineering was to create changes in the DNA sequences, but the development of synthetic biology and metabolic engineering can provide means to radically manipulate bacterial and fungal genes to change their characteristics in order to produce enzymes that can improve the AD of wastes [59]. In recent years, toolsets documenting the different bacterial consortia present in anaerobic digestion cultures, their genomic information, and their physiology have become available, which act as valuable resource for conducting further research. So far, genomic sequences of 21 *Archaeabacteria* and 205 *Eubacteria* have been sequenced, out of which approximately 80% of the *Archaeabacteria* comprises of methanogenic bacteria typically found in sludge or other anaerobic environments [59]. The availability of the genomic and physiological properties can allow the discovery of non-cultivable bacteria in the consortia [60] as well as enable genetic engineering of either the hosts or particular enzyme activities for the enhancement of biogas production from AD [61]. Other tools such as q-PCR, RT-PCR, Sanger sequencing, T-RFLP, next-generation sequencing (NGS) etc., can benefit the researchers to make libraries and identifying markers and genes from microbial consortia involved in AD to assist in targeted redesigning of the entire metabolic pathway using synthetic biology. Additionally, since most methanogenic enzymes function optimally at high K⁺ ion concentrations, genes from other organisms encoding K⁺ transporters and channels can be cloned into the microbes present in AD to increase their electrochemical activity, thereby increasing the efficiency of AD process to produce a higher amount of biogas [62, 63].

Also, for easier analysis of microbial genome and their characteristics, analyzing the 16S rRNA gene in the microbial community of AD has been proposed [58]. In order to assess the microbial community in each stage of AD, the 16S rRNA gene can act as a marker to help scientists specify the identity of organisms in the anaerobic digester [64]. Rivière et al. [65], analyzed the microbial community present in seven anaerobic digesters by creating a total of 9890 16S rRNA clones. The analysis revealed that the Archaea community is represented by the following operational taxonomic units (OTUs): *Methanosaרכinale*, *Methanomicrobiales*, and Arc I. Further phylogenetic affiliation and statistical analysis of the library revealed that the bacterial community present in the anaerobic digesters can be grouped under three categories: (1) a core group of phylotypes, which is common to most digesters; (2) another group of phylotypes shared among a few digesters; and (3) a third group

phylotype specific to each digester [65]. Finally, it is imperative that for improving biogas yield through synthetic biology techniques, key points such as developing efficient genome-editing tools, mapping and cloning of key genes from important phylotypes associated with biogas production, creating metagenomics-based data mining method, as well as further experiments from lab and pilot-scale to full-scale application needs to be conducted for furthering AD research.

6.3.3 Insights into Microbial Community Dynamics in AD

To further understand and investigate the factors and mechanisms governing AD process, studies on the microbial community dynamics are indispensable. They can also be useful in investigating the transformation of compounds during the whole AD process. Analyzing microbial community dynamics can also provide an idea on the interactions and relative abundance of the microbes under different conditions and thereby, help us in creating an appropriate and robust microbial consortium for efficient substrate degradation and biogas production. For example, reactor performance, as well as microbial community dynamics studies on solid-state AD of corn stover conducted at mesophilic and thermophilic conditions revealed that thermophilic AD resulted in faster reduction of cellulose and hemicellulose in the first 12-days, compared to mesophilic conditions. It was found that there was a shift in population of microbes over the 38 days of culture, compared to the initial inoculum. When mesophilic cultures were used as inoculum for thermophilic conditions, it was observed that the populations of thermophilic cellulolytic and xylanolytic microbes were about 10–50 times greater than those in mesophilic ones [6]. The same group investigated the effect of inoculation ratio on microbial community dynamics in solid-state AD and highlighted that non-microbial factor of the inoculum, such as alkalinity, were found to be more decisive on the final methane yield of corn stover. Instead, the microbial population of methanogens affected the kinetics of volatile fatty acids (VFA) consumption and methane production [5, 66]. Determination of microbiome composition and their temporal succession in thermophilic and mesophilic solid-state AD, as well as acidified solid-state AD reactors using Illumina sequencing of 16S rRNA gene amplicons showed that the genus *Methanothermobacter* dominated in the thermophilic solid-state AD reactors, while *Methanoculleus* dominated in the mesophilic reactors [5, 67, 68]. Also, acetate oxidation coupled with hydrogenotrophic methanogenesis was found as an important pathway for biogas production during thermophilic solid-state AD, and the abundance of *Methanomassiliicoccus* was positively correlated to daily biogas yield in the mesophilic solid-state AD process [67]. Additionally, studies were also conducted to study the effect of inhibitors on the microbial community present in solid-state AD. It was found that increasing acetate concentration impacted the population dynamics of dominant hydrogenotrophic methanogenic microbial species including *Methanobacterium*, *Methanosarcina*, and *Methanocorpusculum*.

[69, 70]. It was also discovered that increasing OLR impacted acetotrophic methanogens more than hydrogenotrophic methanogens. This imbalance between the two phylotypes (and the associated metabolic pathways) could lower methane production.

6.3.4 Modeling of AD Systems to Study Molecular Mechanisms

To gain insights into the molecular mechanisms of the reactions involved in the AD process in the reactors, modeling has been used as an effective approach, which can also help in facilitating process design as well as predicting system performance [71]. Theoretical models developed for solid-state AD are diverse and utilize different parameters like reactor designs, reaction kinetics, and mass transfer along with the rate-limiting steps to provide better insights into the complex system mechanisms. However, many of these models cannot be applied for robust simulation of varying process conditions and input substrates as they are structurally and numerically complex [72]. In parallel, liquid-state AD models have also been developed and the most popular among them is the Anaerobic Digestion Model No.1 (ADM1) [73]. In the development of ADM1 researchers have utilized both biochemical reactions and physico-chemical reactions that take place within an AD process. More importantly the reactor design in ADM1 is based on the assumption that the digester is a completely stirred tank reactor with a constant liquid volume and a single input and output stream [73]. Using this most comprehensive liquid-state AD model, the ADM1 as a template, several kinetic models have been further developed that simulate the process of disintegration, acetogenesis and methanogenesis steps of various complex organic substrates. [74–76]. Most of the recent models focused on the effect of total solid content on methane yield and production rate. These models assume that the total solid content is a key parameter that affects the mass transfer of VFAs, H₂, CO₂, etc., between the gas-liquid-solid phases. It was also assumed that the mass transfer effect in turn affected the hydrolysis rate constant, the rate of accumulation of inhibitors [74, 76], maximum microbial growth rate or half-saturation coefficient [74], and the maximum microbial growth rate [77].

Additionally, linear regression models have also been created that calculate how total solid content affects methane production in solid-state AD using artificial neural network [69, 78]. Kinetic models, on the other hand, have also been developed empirically and these models mainly captured the heterogeneous distribution of inoculum in the substrate, which in turn caused heterogeneous accumulation of VFA in the reactor. Kinetic model simulations suggest that vigorous mixing, highly dispersed inoculum, and leachate recirculation can affect methane production during solid-state AD, as these conditions result in the acidification of the inoculated

organic particles by the VFAs [79]. As the experimental designs for the AD process are becoming more advanced, so are the amount of data being generated as well and utilizing these data for the development of mathematical models will play a major role in revealing further details about the molecular mechanisms in AD process.

6.4 Process Variables that Influence AD

AD, like any other process, can operate under various operational conditions and therefore, factors affecting the efficiency of the AD process can be optimized based on the type of waste used. These factors are as follows:

6.4.1 Temperature

Temperature is one of the most important parameters in AD as microbial metabolism and enzyme kinetics vary with temperature. Therefore, the optimal temperature to be employed to obtain higher biogas production is based on the type of organism employed in the AD process. This is due to the fact that psychrophilic ($T < 20$), mesophilic ($35 < T < 40$), and thermophilic ($50 < T < 65$) organisms prefer to grow better at their optimal temperature [59]. Comparing the preferred temperature of various organism types shows that higher energy is required for thermophilic organisms, compared to mesophilic bacteria while using thermophilic bacteria provides a higher volume of biogas generation and guarantees a faster production rate. On the other hand, in processing waste streams that generate ammonium, mesophilic digestion is more stable compared to thermophilic digestion owing to ammonium toxicity [14]. Therefore, for the wastes containing a high amount of nitrogen, using mesophilic digestion would make the process more efficient.

6.4.2 pH

pH is another critical parameter that can regulate the activity of organisms. For example, methanogenic and acidogenic bacteria prefer different pH for their growth. Various researches have reported different optimum pH for the biogas production in the AD process in which generally, the optimal range for pH is reported to be between 6 and 8 [59]. However, different stages of AD require different values of pH as hydrolysis and acidogenesis bacteria prefer the pH of 5.2–6.3, whereas the methanogenic bacteria desire 6.8–7.5 [80]. Therefore, choosing the AD process pH based upon the AD process stage in operation would make the process more efficient.

6.4.3 Hydraulic Retention Time (HRT)

Hydraulic retention time, also hydraulic residence time (HRT) is the average time that liquids remain in the anaerobic digester [81]. It is an important operational parameter in AD as its duration depends on the type of feedstock and can affect the conversion of volatile solids into biogas. Each AD requires a minimum HRT period for completion. A low HRT can result in the accumulation of volatile fatty acids, while a high HRT increases the process operation cost due to longer run-time. Hence, researchers often attempt to lower the HRT to a certain period, where the biogas production is optimum and the volatile fatty acids production is lowered [82, 83]. Another form of retention time is called solid retention time (SRT) which is the average time that microbes are in the digester. SRT and HRT will be the same when the microbial culture and waste are present in the same phase which happens while the waste is in the liquid form; however, when solid wastes are used, HRT and SRT will have a different value. Obviously, the HRT changes with the nature of the feedstock. The average reported HRT is 15–30 days for treating solid organic wastes under mesophilic condition for the biogas production in AD [59]. Recalcitrant wastes containing a high content of fiber or fat require a high HRT, while other easily digestible wastes such as animal manure need a lower HRT. Besides, digestion by mesophilic organisms needs a longer HRT as they are efficient at lower temperatures, whereas thermophilic digestion can be accomplished at a higher rate leading to a shorter HRT. It should also be noted that the size of waste particles can also influence HRT. Due to their high surface area, smaller waste particles lower the HRT and therefore faster digestion will happen.

6.4.4 Organic Loading Rate (OLR)

The amount of SOW necessary to be fed to the anaerobic digester per day per unit working volume is called the organic loading rate [84]. As all the process variables affecting the efficiency of the AD process are interconnected, various OLR have been reported based upon the operating condition. Therefore, the temperature, pH, feedstock characteristics, and hydraulic retention time can influence the organic loading rate. A high OLR means a higher workload on the anaerobic bacteria to convert wastes into biogas, which would result in the availability of a high amount of VFAs in the anaerobic digester that leads to bacteria inhibition, whereas a low OLR may reduce the nutrient availability and therefore, disrupt the performance of the microbial community [85].

6.4.5 C/N ratio

One other factor that affects the AD operation is the C/N ratio. Bacteria need the right supply of carbon and nitrogen for their optimal growth and metabolism and therefore, the C/N ratio of the feedstock is critical. The C/N ratio from 20:1 to 30:1 has been reported as optimal for AD [86]. A high C/N ratio results in a less efficient AD as nitrogen is a vital element for microbial protein synthesis. On the other hand, a low C/N ratio leads to build-up of ammonia and therefore, causes ammonia toxicity [87]. It is noteworthy to mention that the C/N ratio is feedstock specific and it cannot be changed unless wastes with different C/N values are mixed as feed to obtain an optimal C/N ratio. Providing a feed with an optimal C/N ratio for the microbes will maximize biogas production.

6.4.6 Feedstock-to-Inoculum (F/I) Ratio

Feedstock-to-inoculum ratio (F/I) is another important factor to be considered in the AD of solid organic wastes and it can affect the pH as well as inhibitor production. A very high F/I could result in the overproduction of VFAs due to excess organic loads that can significantly lower the pH and inhibit the action of the methanogens [88]. It was found that AD of palm oil mill residues achieved the highest methane production rates at the lowest F/I ratio within the range of 2:1–5:1, while rapid hydrolysis at F/I ratio of 4:1–5:1 resulted in a VFAs accumulation and low methane yield [89].

6.5 Pretreatment Techniques

Various techniques have been suggested to improve the biogas production of solid wastes such as the addition of additives, co-digestion and using pretreatment [59]. Using pretreatment techniques is helpful specifically for the wastes containing a high percentage of lignocellulosic materials to increase the rate of hydrolysis and thereby, achieve high biogas yield through maximum digestion of solid wastes. Pretreatment of agricultural waste is generally divided into chemical, biological, physical, and thermal or their combination. It is noteworthy to mention that a pretreatment technique must not only be economical and environmental-friendly but also should not repress or have a negative effect on the biomass or process [90, 91]. Also, the pretreatment technique required for each waste type might be different and factors such as the availability of lignocellulosic materials, crystallinity, the surface area of the particles, availability of acetyl groups, and the degree of polymerization should be considered [8].

6.5.1 Physical Pretreatment

Organic wastes come in different particle sizes, and knowing the fact that smaller particle size gains a higher surface area, physical pretreatment can be the first solution to enhance the efficiency of any type of organic solid wastes. In physical pretreatment, neither microorganisms nor chemicals are involved. Examples of physical pretreatments are high-pressure homogenizer, electrohydrolysis, microwave, milling, crushing, steam explosion, and ultrasound. Milling not only provides a higher surface area of particles but also decreases the degree of crystallinity and polymerization. Other physical pretreatments such as high-pressure homogenization make an abrupt expansion to rupture the lignocellulosic biomass structure and therefore increase the AD performance. Steam explosion of wheat straw increased the methane yield by 30% [92]. Microwave pretreatment can be applied to the substances that contain water inside their cell in which the sudden increase in water volume, the cell will be destroyed, yielding a higher AD efficiency [93].

In order to reduce the particle size, proper equipment should be used regarding the substrate type and the type of anaerobic digester to be used to not damage the equipment and causing process failure. It should also be noted that the size of the particle has to be within an optimum range as smaller particles might cause media acidification in dry digestion as the result of acid production during fermentation, while they might lead to the formation of foams in the wet digestion [33].

6.5.2 Chemical Pretreatment

Chemical pretreatment includes using acids, alkalis, ionic liquids, oxidants, etc., to enhance the hydrolysis rate. The selection of suitable chemical pretreatment depends on the type of substrate and its characteristics. Generally, the use of chemical pretreatment has received more attention compared to physical pretreatment due to its higher effectiveness on biogas production. It has been suggested not to use acid pretreatments for readily degradable materials as it might cause the accumulation of VFA, along with the degradation of soluble sugars to inhibitory compounds like furfural [94]. However, this type of pretreatment (acid) is mostly used for lignocellulosic substrates as the strong acid disrupts lignin and thereby, releases the cellulose and hemicellulose rendering them more susceptible to enzymatic hydrolysis [95]. On the other hand, dilute acid pretreatment is better to be applied on food wastes, along with thermal pretreatment [96].

As mentioned, the generation of toxic or inhibitory chemicals in the chemical pretreatment is likely to happen, and therefore, actions such as neutralizing the pH of the biomass are recommended. Due to this fact, chemical pretreatment cost is mostly higher than that of physical pretreatments, and therefore economical assessment of chemical pretreatment in the industrial scale should be investigated for the process

design. Currently, alkali hydrolysis is majorly used on solid organic wastes with low lignin content in the industrial scale [97].

6.5.3 Biological Pretreatment

Biological pretreatment is being done by using biological agents such as enzymes that can improve the degradation of biomass by breaking the covalent cross-linkages and non-covalent bonds between hemicellulose and lignin without the generation of any inhibitory chemicals [98], therefore, it can be very useful for AD of agricultural and yard wastes.

Biological pretreatment includes enzymatic, bacterial, and fungal pretreatment. The merits of using biological pretreatment are its low operation cost, less energy requirement for operation, and environmental-friendly. However, the need for a long process time is the main disadvantage of using biological pretreatment, which precludes its application at industrial scale. Also, some bacteria have the ability to degrade cellulose along with hemicellulose, resulting in the reduction of final biogas production [99].

Enzymatic: Laccase and versatile peroxidase are examples of enzymes used for enzymatic pretreatment of lignocellulosic biomass as they can degrade lignin [100]. Schroyen et al. [101], have investigated the effect of various enzymatic pretreatment on corn stover and found 25% and 17% increase in biomethane production after 24 h and 6 h incubation using laccase and peroxidase enzyme, respectively. In another study, enzymatic pretreatment of sugar beet pulp and spent hops yielded 19% and 13% increase in biogas production, respectively, compared to control [102].

Bacterial: Studies on the microbial pretreatment of SOWs have also shown a positive effect on biogas production. In the study of Zhang et al. [103], a microbial consortium pretreatment was applied on cassava residues and 97% increase in methane production from 131.95 mL/g-VS to 259.46 mL/g-VS was observed. Findings of another research study also showed 35% decrease in the digestion time of corn straw AD using a complex microbial agent pretreatment compared to untreated feed [104]. In their study, pretreatment with microbial agents yielded 33% and 76% increase in total biogas and biomethane production, respectively.

Fungal: Shi et al. [105] performed fungal pretreatment of cotton stalks by using *Phanerochaete chrysosporium* and observed 19–36% of lignin being degraded under various pretreatment conditions compared to the control (untreated). Another study by Ge et al. [106] showed 24% lignin degradation using fungal pretreatment on *Albizia* biomass that improved the methane yield by 3.7-fold. A study on biological pretreatment by the fungus *Ceriporiopsis subvermispora* [107] that produces ligninolytic enzymes [108] showed 106% increase in methane production from 21.6 L/kg volatile solid (control) to 44.6 L/kg volatile solid after pretreatment. In general, studies on fungal pretreatments showed that lignin degradation of biomass often improves the methane production.

6.5.4 Thermal Pretreatment

Another type of pretreatment is thermal pretreatment that is applicable to all types of solid organic wastes in a large scale. Thermal pretreatment can improve the solubility of chemical oxygen demand (COD), increase the process efficiency, and reduce the hydraulic retention time. It can also be used for dewatering and improving the digestibility of some type of organic wastes [109]. The two types of thermal pretreatment are (1) thermal, in which only the temperature is controlled, and (2) hydrothermal in which both pressure and temperature are controlled. Hydrothermal pretreatment is a specialized thermal pretreatment process, in which the biomass to be digested is completely submerged in liquid water at both high temperature and pressure. Hence, hydrothermal pretreatment is generally considered suitable for treating wastes already containing high water content.

6.5.5 Combined Pretreatment Techniques

Each pretreatment method described has its own merits and demerits. Although some pretreatment methods have been suggested to be used for some type of substrates, no general suggestion can be made as each substrate type contains a large variety of wastes. Researches have shown that combining two or three pretreatment methods will also further improve biogas/methane production. Table 6.3 presents a literature review on the different pretreatment methods applied to various substrates and their effect on improving biogas production. Figure 6.3 summarizes the various AD process parameters and parameters that need to be monitored during the AD of SOWs, as well as the pretreatment methods that have been employed to improve the product yield.

6.6 Process Operation Types

AD can be carried out in full scale using the following four different types of process operations, depending on the raw material input method as well as number of stages involved: (a) batch, (b) continuous operations, (c) single-stage and (d) multistage operations. Each of the operation types has its pros and cons, and is discussed below in detail.

Table 6.3 Various pretreatment methods used for AD

Pretreatment type	Pretreatment method	Feed	Pretreatment conditions	Methane/biogas yield increase	Ref.
Physical	Microwave	Organic fraction of municipal solid waste (OFMSW)	145 °C and 8 days of digestion	26% methane increase	[93]
	Steam explosion	Corn stover	160 °C for 2 min	22% methane yield increase	[110]
	High-pressure homogenizer	Municipal solid waste	40 MPa pressure	33% methane increase	[36]
	Ultrasound	Organic fraction of municipal solid waste (OFMSW)	Sonication time 30 mins; Specific energy 7200 kJ/kg TS Power density 0.6 W/mL	15% increase in biogas	[35]
	Electroporation	Organic fraction of municipal solid waste (OFMSW)	field strength: 24 kV/cm frequency 12.5 Hz	20%–40% biogas increase	[111]
	Pulsed electric field	Landfill leachate	50 kW h/m ³ Frequency 1.7 Hz Electric field strength 20 (kV/cm)	44% methane increase	[34]
Chemical	Acid	Rice straw	160 °C for 10 min	161% to 533%	[24]
	Alkali	Wheat straw	5 min with 5% w/w H ₂ O ₂ solid:liquid ratio of 1:20	64% methane increase	[25]
	Alkali	Sugarcane bagasse	5 min with 5% w/w H ₂ O ₂ solid:liquid ratio of 1:20	68% methane increase	[25]
	Alkali	Napier grass (<i>Pennisetum purpureum</i>)	1, 2, and 3% sodium hydroxide (NaOH)	9.3% increase in biogas yield	[22]
Biological	Enzymatic	Corn stover	combination of laccase and versatile peroxidase 30 °C for 6 h	50.4% increase in methane production	[100]
	Fungal	Corn Stover Silage	Using <i>Phanerochaete chrysosporium</i> at 28 °C for 30 days	23% in methane production	[10]

(continued)

Table 6.3 (continued)

Pretreatment type	Pretreatment method	Feed	Pretreatment conditions	Methane/biogas yield increase	Ref.
	Microbial	Corn straw	Combination of yeast, cellulolytic bacteria, and the lactic acid bacteria 20–55 °C for 12 h to 20 days	33.07% increase in biogas yield 75.57% increase in methane yield	[104]
Thermal	Thermal autoclaving	Wheat straw	121 °C for 60 min	62% methane increase	[25]
	Thermal autoclaving	Sugarcane bagasse	121 °C for 60 min	58% methane increase	[25]

6.6.1 Batch Operation

Batch operation is one of the most commonly used modes of operation for AD of organic solid wastes. The batch operation is easier to maintain compared to continuous operation as it requires less capital investment and lower operating costs with fewer process control requirements. However, the amount of biogas produced through batch operation would fluctuate with time and a major portion of the biogas would be produced during the peak performance of the AD process. For example, it was reported that in a 55-day batch solid-state AD of corn stover, more than 80% of biogas was produced on day 36, when the AD was at the methanogenic phase [112]. Moreover, the batch operation also requires a large amount of inoculum (i.e., low F/I ratio); a high F/I ratio is known to produce volatile fatty acids in larger amounts compared to biogas [113].

6.6.2 Continuous Operation

Continuous operation is another popular method of operating AD, with a continuous supply of raw materials and resulting in biogas production at a steady state. Continuous operation is primarily affected by OLR, and SRT, and these are the key parameters in designing and evaluating a continuous AD [114]. Contrary to a batch operation, in continuous operations, the solid-to-gas conversion capacity is proportional to OLR. In general, high OLR is preferred as it can achieve a high waste consumption rate in a relatively smaller digester. On the other hand, high OLR can lead to VFA overproduction that can result in an imbalance between acidogens and



Fig. 6.3 Summary of the various process parameters, parameters to be monitored, and pretreatment techniques. In orange are the AD process parameters: Feed/inoculum ratio (F/I); organic loading rate (OLR), carbon/nitrogen ratio (C/N) in the feed, and hydraulic retention time (HRT). In brown are the parameters needed to be monitored during the AD of SOWs (pH, temperature, and inhibitors). In green are the different pretreatment methods used to improve AD yield

methanogens. A maximum OLR level in solid-state AD depends on various parameters such as reactor design, feedstock characteristics, microbial activity, temperature, pH, and toxicity level [115]. SRT is the second critical factor in continuous operation. In a continuous AD operation with food waste as feedstock, increasing SRT from 15 days to 35 days increased methane yield from 360 mL/kg to 454 mL/kg volatile solids [116].

6.6.3 Single-Stage Operation

In addition to depending on the mode of raw-matter feed, another mode of operation focuses on the stages of operation. In a single-stage AD system, all the four stages of digestion are implemented in a single reactor vessel (Fig. 6.4). Thus, the reactor system is easier to design and can be built with less capital costs. However, a major

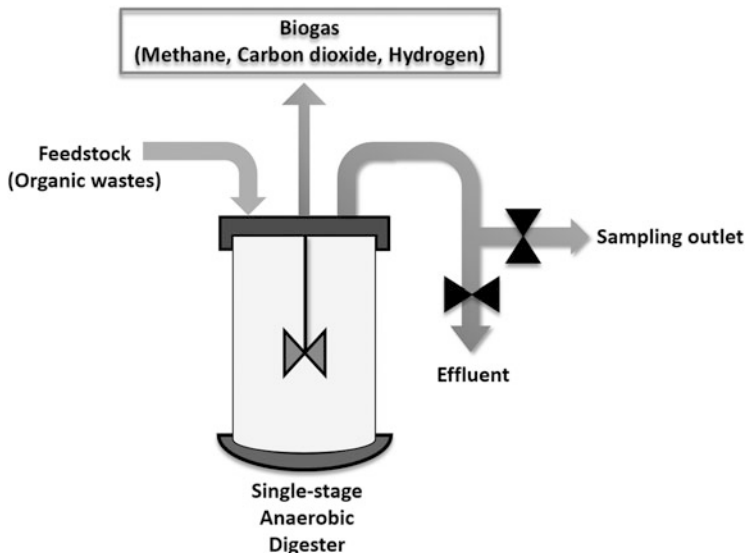


Fig. 6.4 Schematic representation of a single-stage AD operating system. In a single-stage AD all the four stages of decomposition occurs in a single reactor to convert solid wastes into biogas

limitation is the OLR, because excessive OLR can cause rapid pH drop, thus limiting the rate of digestion and overproducing VFAs [4].

6.6.4 Multi-stage Operation

A multiple-stage operation is another type of AD operation method in which the different conversion stages are carried out in multiple reactor vessels. Generally, the first two stages, i.e., hydrolysis and acidogenesis are carried out in one reactor while acetogenesis and methanogenesis are carried out in a separate reactor (Fig. 6.5) [117]. Thus, all the stages can be operated at their optimal process conditions (pH, temperature, OLR, etc.).

It has been suggested that multistage operation perform better than single-stage operations because the former results in a proper fermentation of the loaded wastes with limited generation of inhibitors or by-products [2]. For example, the solid-state AD of brewery spent grain (BSG) in a single-stage reactor was limited by the inhibitors, such as weak acids, furan derivatives, and phenolic substances, generated in the degradation of lignocellulose in BSG [118]. However, it is noteworthy to mention that although multistage AD system has the advantage of improved AD performance, the need for high capital investments and operating costs hampers its implementation at a commercial scale. As a result, single-stage AD is still predominantly used.

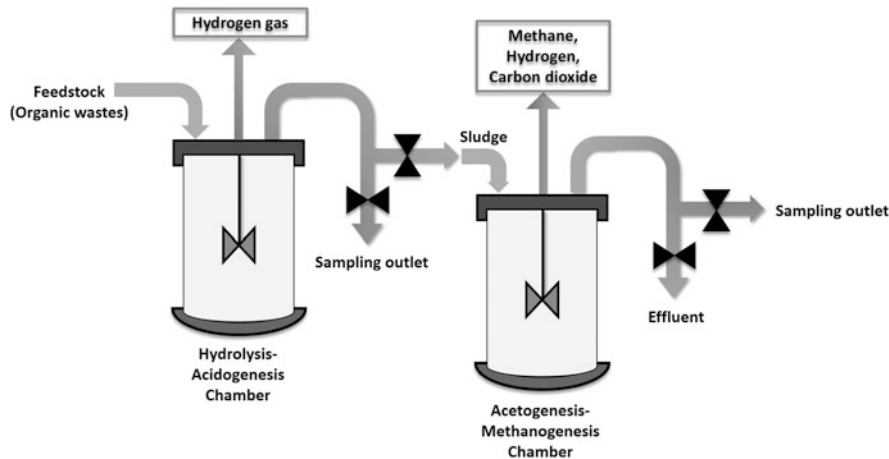


Fig. 6.5 Schematic representation of a multi-stage AD operating system. The reactions occur in separate chambers for conversion of solid wastes to biogas

6.7 Economic Benefits of Biogas Production in AD

As energy production is the main aim for AD operation, a cost-benefit analysis needs to be considered. As stated earlier, apart from biogas production, AD can provide various other benefits such as heat or electricity generation as well as compost and high-quality fertilizer. AD systems can be used in small-scale (approximately 50–500 ft³) for heat production in rural areas or large-scale up to 300,000 ft³ [119, 120].

Most of the total cost of AD systems is spent on capital costs. Items such as digester, piping system, liquid and gas pumps, electrical controllers and wiring, power transmission lines, mixing tanks, the land where the whole system is located, etc. are considered as the main contributor of AD. However, the type of feedstock and its shipping costs are other factors that impact the generation costs. Therefore, the use of centralized systems is prevalent in Europe in which co-digestion of animal manure with other agricultural, yard or food wastes of several farms, provides energy and fertilizer for the farmers.

As biogas is composed of methane and CO₂, its heating value (600 btu/ft³) is less than that of natural gas (1000 btu/ft³) [121]. Hence, upgrading the biogas to biomethane by removing CO₂ should be evaluated economically, based on the aim and location where the system is located. Biomethane has a similar characteristics as natural gas; thus, it can be used as compressed natural gas (CNG) as transportation fuel or to be transferred to other places.

Overall, a feasibility study is required to determine the payback period of investments for AD or investigating based on the feedstock availability and type, project site, community impact and vicinity, shipping, system size and total energy

production estimations, environmental considerations, equipment, and worker costs, etc. based on the location or country where the AD is to be done.

6.8 Conclusions and Future Outlook

Generation of biogas through the AD of organic wastes can not only solve the problems of waste disposal, but also helps energy recovery. The generated biogas can be utilized across different sectors for the production of heat and electricity or be upgraded into biofuels. However, several problems associated with the production of biogas from organic wastes using AD needs to be effectively addressed to implement this method in a large-scale globally. One of the primary gases released during the AD process is methane. Methane is a greenhouse gas and therefore, proper design and operation of the AD are required to avoid the release of methane into the atmosphere. Additionally, the process requires a microbial consortium to operate under a given set of operating conditions, lack of which can result in damaging the stability of the system causing inefficient gas production. Moreover, natural gas is readily available, whereas biogas requires the operation of a long lengthy AD process, making the AD-generated biogas costly in comparison to natural gas. In addition to researching the parameters such as temperature, pH, OLR, etc. engineering the microbial consortia could help in maximizing the methane content, which would help inspire future AD developments.

Acknowledgments Authors are thankful to Scheme for Promotion of Academic and Research Collaboration (SPARC), MHRD, Govt. of India (Grant No. SPARC/2018-2019/P265/SL). MD thanks the support from the Council of Scientific and Industrial Research (CSIR). PP appreciates the support from the Department of Science and Technology (INSPIRE, India) for the award of fellowships, DST). AG acknowledges the support from the Department of Science and Technology (Grant No. CRG/2020/002080), Govt. of India. AMV acknowledges start-up funds from the School for Engineering of Matter, Transport and Energy at Arizona State University.

References

1. Hajinajaf N, Mehrabadi A, Tavakoli O. Practical strategies to improve harvestable biomass energy yield in microalgal culture: a review. *Biomass Bioenergy*. 2021;145:105941. <https://doi.org/10.1016/j.biombioe.2020.105941>.
2. Zhou H, Wen Z. Solid-State anaerobic digestion for waste management and biogas production. In: Steudler S, Werner A, Cheng JJ, editors. *Advances in biochemical engineering/biotechnology*. Cham: Springer International Publishing; 2019. p. 147–68. https://doi.org/10.1007/10_2019_86.
3. Mostafazadeh-Fard S, Samani Z, Bandini P. Production of liquid organic fertilizer through anaerobic digestion of grass clippings. *Waste Biomass Valoriz*. 2019;10:771–81. <https://doi.org/10.1007/s12649-017-0095-7>.

4. Rapport J, Zhang R, Jenkins BM, Williams RB, Schwarzenegger A, Adams LS, Brown MR, Chair B (2008) Current anaerobic digestion technologies used for treatment of municipal organic solid waste.
5. Ge X, Xu F, Li Y. Solid-state anaerobic digestion of lignocellulosic biomass: recent progress and perspectives. *Bioresour Technol.* 2016;205:239–49. <https://doi.org/10.1016/j.biortech.2016.01.050>.
6. Shi J, Wang Z, Stiverson JA, Yu Z, Li Y. Reactor performance and microbial community dynamics during solid-state anaerobic digestion of corn stover at mesophilic and thermophilic conditions. *Bioresour Technol.* 2013;136:574–81. <https://doi.org/10.1016/j.biortech.2013.02.073>.
7. Hoornweg D, Bhada-Tata P (2014) What a waste: a global review of solid waste management cb, Washington, DC.
8. Ravindran R, Jaiswal AK. A comprehensive review on pre-treatment strategy for lignocellulosic food industry waste: challenges and opportunities. *Bioresour Technol.* 2016;199:92–102. <https://doi.org/10.1016/j.biortech.2015.07.106>.
9. Perlick RD, Eaton LM, Turhollow Jr AF, Langholtz MH, Brandt CC, Downing ME, Graham RL, Wright LL, Kavkewitz JM, Shamey AM (2011) US billion-ton update: biomass supply for a bioenergy and bioproducts industry.
10. Liu S, Li X, Wu S, He J, Pang C, Deng Y, Dong R. Fungal pretreatment by Phanerochaete chrysosporium for enhancement of biogas production from corn stover silage. *Appl Biochem Biotechnol.* 2014;174:1907–18. <https://doi.org/10.1007/s12010-014-1185-7>.
11. Menardo S, Airoldi G, Balsari P. The effect of particle size and thermal pre-treatment on the methane yield of four agricultural by-products. *Bioresour Technol.* 2012;104:708–14. <https://doi.org/10.1016/j.biortech.2011.10.061>.
12. Lazarus WF. Economics of anaerobic digesters for processing animal manure. Extension Univ Minnesota; 2015.
13. Banks CJ, Cheshire M, Heaven S, Arnold R. Anaerobic digestion of source-segregated domestic food waste: performance assessment by mass and energy balance. *Bioresour Technol.* 2011;102:612–20. <https://doi.org/10.1016/j.biortech.2010.08.005>.
14. Mortier N, Velghe F, Verstichel S. Organic recycling of agricultural waste today: composting and anaerobic digestion. Amsterdam: Elsevier Inc; 2016.
15. Yenigün O, Demirel B. Ammonia inhibition in anaerobic digestion: a review. *Process Biochem.* 2013;48:901–11. <https://doi.org/10.1016/j.procbio.2013.04.012>.
16. Melbinger NR, Donnellon J, Zablatzky HR. Toxic effects of ammonia nitrogen in high-rate digestion (with Discussion). *J Water Pollut Control Fed.* 1971;1658–70.
17. Albertson OE. Ammonia nitrogen and the anaerobic environment. *J Water Pollut Control Fed.* 1961;978–95.
18. Appels L, Baeyens J, Degrève J, Dewil R. Principles and potential of the anaerobic digestion of waste-activated sludge. *Prog Energy Combust Sci.* 2008;34:755–81. <https://doi.org/10.1016/j.pecs.2008.06.002>.
19. Hallaji SM, Kuroshkarim M, Moussavi SP. Enhancing methane production using anaerobic co-digestion of waste activated sludge with combined fruit waste and cheese whey. *BMC Biotechnol.* 2019;19:1–10. <https://doi.org/10.1186/s12896-019-0513-y>.
20. Chow WL, Chong S, Lim JW, Chan YJ, Chong MF, Tiong TJ, Chin JK, Pan G-T. Anaerobic co-digestion of wastewater sludge: a review of potential co-substrates and operating factors for improved methane yield. *PRO.* 2020;8:39. <https://doi.org/10.3390/pr8010039>.
21. Yao Z, Li W, Kan X, Dai Y, Tong YW, Wang C-H. Anaerobic digestion and gasification hybrid system for potential energy recovery from yard waste and woody biomass. *Energy.* 2017;124:133–45. <https://doi.org/10.1016/j.energy.2017.02.035>.
22. Dussadee N, Ramaraj R, Cheunbam T. Biotechnological application of sustainable biogas production through dry anaerobic digestion of Napier grass. *3 Biotech.* 2017;7 <https://doi.org/10.1007/s13205-017-0646-4>.

23. Panigrahi S, Sharma HB, Dubey BK. Overcoming yard waste recalcitrance through four different liquid hot water pretreatment techniques—structural evolution, biogas production and energy balance. *Biomass Bioenergy*. 2019;127:105268. <https://doi.org/10.1016/j.biombioe.2019.105268>.
24. Amnuaycheewa P, Hengaroonprasan R, Rattanaporn K, Kirdponpattara S, Cheenkachorn K, Sririyanun M. Enhancing enzymatic hydrolysis and biogas production from rice straw by pretreatment with organic acids. *Ind Crop Prod*. 2016;87:247–54. <https://doi.org/10.1016/j.indcrop.2016.04.069>.
25. Bolado-Rodríguez S, Toquero C, Martín-Juárez J, Travaini R, García-Encina PA. Effect of thermal, acid, alkaline and alkaline-peroxide pretreatments on the biochemical methane potential and kinetics of the anaerobic digestion of wheat straw and sugarcane bagasse. *Bioresour Technol*. 2016;201:182–90. <https://doi.org/10.1016/j.biortech.2015.11.047>.
26. Mirmohamadsadeghi S, Karimi K, Zamani A, Amiri H, Horváth IS. Enhanced solid-state biogas production from lignocellulosic biomass by organosolv pretreatment. *Biomed Res Int*. 2014, 2014; <https://doi.org/10.1155/2014/350414>.
27. Zhao X, Wang L, Lu X, Zhang S. Pretreatment of corn stover with diluted acetic acid for enhancement of acidogenic fermentation. *Bioresour Technol*. 2014;158:12–8. <https://doi.org/10.1016/j.biortech.2014.01.122>.
28. Monlau F, Barakat A, Steyer J-P, Carrere H. Comparison of seven types of thermo-chemical pretreatments on the structural features and anaerobic digestion of sunflower stalks. *Bioresour Technol*. 2012;120:241–7. <https://doi.org/10.1016/j.biortech.2012.06.040>.
29. Tumutegyereize P, Muranga FI, Kawongolo J, Nabugoomu F. Optimization of biogas production from banana peels: effect of particle size on methane yield. *Afr J Biotechnol*. 2011;10: 18243–51.
30. Stenmarck Å, Jensen C, Quested T, Moates G (2016) Estimates of European food waste levels (FUSION Reducing food waste through social innovation). Stock Sweden.
31. Bartocci P, Zampilli M, Liberti F, Pistolesi V, Massoli S, Bidini G, Fantozzi F. LCA analysis of food waste co-digestion. *Sci Total Environ*. 2020;709:136187. <https://doi.org/10.1016/j.scitotenv.2019.136187>.
32. Yong Z, Dong Y, Zhang X, Tan T. Anaerobic co-digestion of food waste and straw for biogas production. *Renew Energy*. 2015;78:527–30. <https://doi.org/10.1016/j.renene.2015.01.033>.
33. Zhang Y, Banks CJ. Impact of different particle size distributions on anaerobic digestion of the organic fraction of municipal solid waste. *Waste Manag*. 2013;33:297–307. <https://doi.org/10.1016/j.renene.2015.01.033>.
34. Safavi SM, Unnithorsson R. Methane yield enhancement via electroporation of organic waste. *Waste Manag*. 2017;66:61–9. <https://doi.org/10.1016/j.wasman.2017.02.032>.
35. Raspoor M, Ajabshirchi Y, Adl M, Abdi R, Gharibi A. The effect of ultrasonic pretreatment on biogas generation yield from organic fraction of municipal solid waste under medium solids concentration circumstance. *Energy Convers Manag*. 2016;119:444–52. <https://doi.org/10.1016/j.enconman.2016.04.066>.
36. Xu S, Kong X, Liu J, Zhao K, Zhao G, Bahdolla A. Effects of high-pressure extruding pretreatment on MSW upgrading and hydrolysis enhancement. *Waste Manag*. 2016;58:81–9. <https://doi.org/10.1016/j.wasman.2016.07.012>.
37. Amare DE, Ogun MK, Körner I. Anaerobic treatment of deinking sludge: methane production and organic matter degradation. *Waste Manag*. 2019;85:417–24. <https://doi.org/10.1016/j.wasman.2018.12.046>.
38. Zhang Y, Li H. Energy recovery from wastewater treatment plants through sludge anaerobic digestion: effect of low-organic-content sludge. *Environ Sci Pollut Res*. 2019;26:30544–53. <https://doi.org/10.1007/s11356-017-0184-y>.
39. Giménez JB, Aguado D, Bouzas A, Ferrer J, Seco A. Use of rumen microorganisms to boost the anaerobic biodegradability of microalgae. *Algal Res*. 2017;24:309–16. <https://doi.org/10.1016/j.algal.2017.04.003>.

40. Klassen V, Blifernez-Klassen O, Wibberg D, Winkler A, Kalinowski J, Posten C, Kruse O. Highly efficient methane generation from untreated microalgae biomass. *Biotechnol Biofuels*. 2017;10:186. <https://doi.org/10.1186/s13068-017-0871-4>.
41. Kobayashi T, Wu Y-P, Lu Z-J, Xu K-Q. Characterization of anaerobic degradability and kinetics of harvested submerged aquatic weeds used for nutrient phytoremediation. *Energies*. 2015;8:304–18. <https://doi.org/10.3390/en8010304>.
42. Rao MS, Singh SP. Bioenergy conversion studies of organic fraction of MSW: kinetic studies and gas yield–organic loading relationships for process optimisation. *Bioresour Technol*. 2004;95:173–85. <https://doi.org/10.1016/j.biortech.2004.02.013>.
43. Bi S, Westerholm M, Qiao W, Xiong L, Mahdy A, Yin D, Song Y, Dong R. Metabolic performance of anaerobic digestion of chicken manure under wet, high solid, and dry conditions. *Bioresour Technol*. 2020;296:122342. <https://doi.org/10.1016/j.biortech.2019.122342>.
44. He D, Xiao J, Wang D, Liu X, Fu Q, Li Y, Du M, Yang Q, Liu Y, Wang Q. Digestion liquid based alkaline pretreatment of waste activated sludge promotes methane production from anaerobic digestion. *Water Res*. 2021;199:117198. <https://doi.org/10.1016/j.watres.2021.117198>.
45. Ma S, Wang H, Li L, Gu X, Zhu W. Enhanced biomethane production from corn straw by a novel anaerobic digestion strategy with mechanochemical pretreatment. *Renew Sust Energ Rev*. 2021;146:111099. <https://doi.org/10.1016/j.rser.2021.111099>.
46. Li W, Khalid H, Amin FR, Zhang H, Dai Z, Chen C, Liu G. Biomethane production characteristics, kinetic analysis, and energy potential of different paper wastes in anaerobic digestion. *Renew Energy*. 2020;157:1081–8. <https://doi.org/10.1016/j.renene.2020.04.035>.
47. Yue L, Cheng J, Tang S, An X, Hua J, Dong H, Zhou J. Ultrasound and microwave pre-treatments promote methane production potential and energy conversion during anaerobic digestion of lipid and food wastes. *Energy*. 2021;228:120525. <https://doi.org/10.1016/j.energy.2021.120525>.
48. Zinder S. Microbiology of anaerobic conversion of organic wastes to methane: recent developments. *Am Soc Microbiol News*; (United States). 1984;50(7).
49. Uçkun Kiran E, Stamatelatou K, Antonopoulou G, Lyberatos G. Production of biogas via anaerobic digestion. Cambridge: Elsevier Ltd.; 2016. <https://doi.org/10.1016/B978-0-08-100455-5.00010-2>.
50. Ziemiński K. Methane fermentation process as anaerobic digestion of biomass: transformations, stages and microorganisms. *Afr J Biotechnol*. 2012;11 <https://doi.org/10.5897/ajbx11.054>.
51. Ntaikou I, Antonopoulou G, Lyberatos G. Biohydrogen production from biomass and wastes via dark fermentation: a review. *Waste Biomass Valoriz*. 2010;1:21–39. <https://doi.org/10.1007/s12649-009-9001-2>.
52. Murdoch FK, Murdoch RW, Gürakan GC, Sanin FD. Change of microbial community composition in anaerobic digesters during the degradation of nonylphenol diethoxylate. *Int Biodeterior Biodegrad*. 2018;135:1–8. <https://doi.org/10.1016/j.ibiod.2018.09.002>.
53. Sidhu C, Vikram S, Pinnaka AK. Unraveling the microbial interactions and metabolic potentials in pre-and post-treated sludge from a wastewater treatment plant using metagenomic studies. *Front Microbiol*. 2017;8:1382. <https://doi.org/10.3389/fmicb.2017.01382>.
54. Moo-Young M. Comprehensive biotechnology. Amsterdam: Elsevier; 2019.
55. Schink B. Energetics of syntrophic cooperation in methanogenic degradation. *Microbiol Mol Biol Rev*. 1997;61:262–80. <https://doi.org/10.1128/61.2.262-280.1997>.
56. Karakashev D, Batstone DJ, Angelidaki I. Influence of environmental conditions on methanogenic compositions in anaerobic biogas reactors. *Appl Environ Microbiol*. 2005;71: 331–8. <https://doi.org/10.1128/AEM.71.1.331-338.2005>.
57. Demirel B, Scherer P. The roles of acetotrophic and hydrogenotrophic methanogens during anaerobic conversion of biomass to methane: a review. *Rev Environ Sci Bio/Technol*. 2008;7: 173–90. <https://doi.org/10.1007/s11157-008-9131-1>.

58. Cabezas A, de Araujo JC, Callejas C, Galès A, Hamelin J, Marone A, Sousa DZ, Trably E, Etchebehere C. How to use molecular biology tools for the study of the anaerobic digestion process? *Rev Environ Sci Bio/Technol.* 2015;14:555–93. <https://doi.org/10.1007/s11157-015-9380-8>.
59. Zhang L, Loh KC, Zhang J. Enhanced biogas production from anaerobic digestion of solid organic wastes: current status and prospects. *Bioresour Technol Rep.* 2019;5:280–96. <https://doi.org/10.1016/j.biteb.2018.07.005>.
60. Cho K, Shin SG, Kim W, Lee J, Lee C, Hwang S. Microbial community shifts in a farm-scale anaerobic digester treating swine waste: correlations between bacteria communities associated with hydrogenotrophic methanogens and environmental conditions. *Sci Total Environ.* 2017;601:167–76. <https://doi.org/10.1016/j.scitotenv.2017.05.188>.
61. Lim JW, Ge T, Tong YW. Monitoring of microbial communities in anaerobic digestion sludge for biogas optimisation. *Waste Manag.* 2018;71:334–41. <https://doi.org/10.1016/j.wasman.2017.10.007>.
62. Pham TH, Rabaey K, Aelterman P, Clauwaert P, De Schampheleire L, Boon N, Verstraete W. Microbial fuel cells in relation to conventional anaerobic digestion technology. *Eng Life Sci.* 2006;6:285–92. <https://doi.org/10.1002/elsc.200620121>.
63. Goswami R, Chattopadhyay P, Shome A, Banerjee SN, Chakraborty AK, Mathew AK, Chaudhury S. An overview of physico-chemical mechanisms of biogas production by microbial communities: a step towards sustainable waste management. *3 Biotech.* 2016;6:1–12. <https://doi.org/10.1007/s13205-016-0395-9>.
64. Su C, Lei L, Duan Y, Zhang K-Q, Yang J. Culture-independent methods for studying environmental microorganisms: methods, application, and perspective. *Appl Microbiol Biotechnol.* 2012;93:993–1003. <https://doi.org/10.1007/s00253-011-3800-7>.
65. Riviere D, Desvignes V, Pelletier E, Chaussonnerie S, Guermazi S, Weissenbach J, Li T, Camacho P, Sghir A. Towards the definition of a core of microorganisms involved in anaerobic digestion of sludge. *ISME J.* 2009;3:700–14. <https://doi.org/10.1038/ismej.2009.2>.
66. Shi J, Xu F, Wang Z, Stiverson JA, Yu Z, Li Y. Effects of microbial and non-microbial factors of liquid anaerobic digestion effluent as inoculum on solid-state anaerobic digestion of corn stover. *Bioresour Technol.* 2014;157:188–96. <https://doi.org/10.1016/j.biortech.2014.01.089>.
67. Li YF, Shi J, Nelson MC, Chen PH, Graf J, Li Y, Yu Z. Impact of different ratios of feedstock to liquid anaerobic digestion effluent on the performance and microbiome of solid-state anaerobic digesters digesting corn stover. *Bioresour Technol.* 2016;200:744–52. <https://doi.org/10.1016/j.biortech.2015.10.078>.
68. Li YF, Nelson MC, Chen PH, Graf J, Li Y, Yu Z. Comparison of the microbial communities in solid-state anaerobic digestion (SS-AD) reactors operated at mesophilic and thermophilic temperatures. *Appl Microbiol Biotechnol.* 2015;99:969–80. <https://doi.org/10.1007/s00253-014-6036-5>.
69. Xu F, Wang ZW, Li Y. Predicting the methane yield of lignocellulosic biomass in mesophilic solid-state anaerobic digestion based on feedstock characteristics and process parameters. *Bioresour Technol.* 2014;173:168–76. <https://doi.org/10.1016/j.biortech.2014.09.090>.
70. Nayak BS, Levine AD, Cardoso A, Harwood VJ. Microbial population dynamics in laboratory-scale solid waste bioreactors in the presence or absence of biosolids. *J Appl Microbiol.* 2009;107:1330–9. <https://doi.org/10.1111/j.1365-2672.2009.04319.x>.
71. Fdez-Güelfo LA, Álvarez-Gallego C, Sales D, Romero García LI. Dry-thermophilic anaerobic digestion of organic fraction of municipal solid waste: methane production modeling. *Waste Manag.* 2012;32:382–8. <https://doi.org/10.1016/j.wasman.2011.11.002>.
72. Weinrich S, Nelles M. Critical comparison of different model structures for the applied simulation of the anaerobic digestion of agricultural energy crops. *Bioresour Technol.* 2015;178:306–12. <https://doi.org/10.1016/j.biortech.2014.10.138>.
73. Batstone DJ, Keller J, Angelidaki I, Kaluzhny SV, Pavlostathis SG, Rozzi A, Sanders WTM, Siegrist HA, Vavilin VA. The IWA anaerobic digestion model no 1 (ADM1). *Water Sci Technol.* 2002;45:65–73. <https://doi.org/10.2166/wst.2002.0292>.

74. Liotta F, Chatellier P, Esposito G, Fabbricino M, Frunzo L, Van Hullebusch ED, Lens PNL, Pirozzi F. Modified Anaerobic Digestion Model No.1 for dry and semi-dry anaerobic digestion of solid organic waste. *Environ Technol (United Kingdom)*. 2015;36:870–80. <https://doi.org/10.1080/09593330.2014.965226>.
75. Bollon J, Le-hyartic R, Benbelkacem H, Buffiere P. Development of a kinetic model for anaerobic dry digestion processes: focus on acetate degradation and moisture content. *Biochem Eng J*. 2011;56:212–8. <https://doi.org/10.1016/j.bej.2011.06.011>.
76. Abbassi-Guendouz A, Brockmann D, Trably E, Dumas C, Delgenès JP, Steyer JP, Escudié R. Total solids content drives high solid anaerobic digestion via mass transfer limitation. *Bioresour Technol*. 2012;111:55–61. <https://doi.org/10.1016/j.biortech.2012.01.174>.
77. Xu F, Wang ZW, Tang L, Li Y. A mass diffusion-based interpretation of the effect of total solids content on solid-state anaerobic digestion of cellulosic biomass. *Bioresour Technol*. 2014;167:178–85. <https://doi.org/10.1016/j.biortech.2014.05.114>.
78. Motte JC, Escudié R, Bernet N, Delgenes JP, Steyer JP, Dumas C. Dynamic effect of total solid content, low substrate/inoculum ratio and particle size on solid-state anaerobic digestion. *Bioresour Technol*. 2013;144:141–8. <https://doi.org/10.1016/j.biortech.2013.06.057>.
79. Vavilin VA, Lokshina LY, Jokela JPY, Rintala JA. Modeling solid waste decomposition. *Bioresour Technol*. 2004;94:69–81. <https://doi.org/10.1016/j.biortech.2003.10.034>.
80. Zhang C, Su H, Tan T. Batch and semi-continuous anaerobic digestion of food waste in a dual solid-liquid system. *Bioresour Technol*. 2013;145:10–6. <https://doi.org/10.1016/j.biortech.2013.03.030>.
81. Mao C, Feng Y, Wang X, Ren G. Review on research achievements of biogas from anaerobic digestion. *Renew Sust Energ Rev*. 2015;45:540–55. <https://doi.org/10.1016/j.rser.2015.02.032>.
82. Bi S, Hong X, Yang H, Yu X, Fang S, Bai Y, Liu J, Gao Y, Yan L, Wang W. Effect of hydraulic retention time on anaerobic co-digestion of cattle manure and food waste. *Renew Energy*. 2020;150:213–20. <https://doi.org/10.1016/j.renene.2019.12.091>.
83. Gaby JC, Zamanzadeh M, Horn SJ. The effect of temperature and retention time on methane production and microbial community composition in staged anaerobic digesters fed with food waste. *Biotechnol Biofuels*. 2017;10:1–13. <https://doi.org/10.1186/s13068-017-0989-4>.
84. Mattocks R (1984) Understanding biogas generation (Technical paper No. 4. volunteers in technical Assistance, p. 13). Virginia Volunt Tech Assist, Arlington.
85. Zhang L, Loh K, Zhang J. Enhanced biogas production from anaerobic digestion of solid organic wastes: current status and prospects. Department of Chemical and Biomolecular Engineering , National University of Singapore , Singapore NUS Environment; 1936. p. 1–6. <https://doi.org/10.1016/j.biteb.2018.07.005>.
86. Wang X, Zhang L, Xi B, Sun W, Xia X, Zhu C, He X, Li M, Yang T, Wang P. Biogas production improvement and C/N control by natural clinoptilolite addition into anaerobic co-digestion of Phragmites australis, feces and kitchen waste. *Bioresour Technol*. 2015;180: 192–9. <https://doi.org/10.1016/j.biortech.2014.12.023>.
87. Fricke K, Santen H, Wallmann R, Hüttner A, Dichtl N. Operating problems in anaerobic digestion plants resulting from nitrogen in MSW. *Waste Manag*. 2007;27:30–43. <https://doi.org/10.1016/j.wasman.2006.03.003>.
88. Zhou Y, Li C, Nges IA, Liu J. The effects of pre-aeration and inoculation on solid-state anaerobic digestion of rice straw. *Bioresour Technol*. 2017;224:78–86. <https://doi.org/10.1016/j.biortech.2016.11.104>.
89. Suksong W, Jehlee A, Singkhala A, Kongjan P, Prasertsan P, Imai T, O-Thong S. Thermophilic solid-state anaerobic digestion of solid waste residues from palm oil mill industry for biogas production. *Ind Crop Prod*. 2017;95:502–11. <https://doi.org/10.1016/j.indcrop.2016.11.002>.
90. Choi JH, Jang SK, Kim JH, Park SY, Kim JC, Jeong H, Kim HY, Choi IG. Simultaneous production of glucose, furfural, and ethanol organosolv lignin for total utilization of high

- recalcitrant biomass by organosolv pretreatment. *Renew Energy*. 2019;130:952–60. <https://doi.org/10.1016/j.renene.2018.05.052>.
91. Derman E, Abdulla R, Marbawi H, Sabullah MK. Oil palm empty fruit bunches as a promising feedstock for bioethanol production in Malaysia. *Renew Energy*. 2018;129:285–98. <https://doi.org/10.1016/j.renene.2018.06.003>.
92. Bauer A, Leonhartsberger C, Bösch P, Amon B, Friedl A, Amon T. Analysis of methane yields from energy crops and agricultural by-products and estimation of energy potential from sustainable crop rotation systems in EU-27. *Clean Techn Environ Policy*. 2010;12:153–61. <https://doi.org/10.1007/s10098-009-0236-1>.
93. Shahriari H. Enhancement of anaerobic digestion of organic fraction of municipal solid waste by microwave pretreatment. University of Ottawa. (Ph.D. Dissertation); 2011. <https://doi.org/10.20381/ruor-4874>.
94. Vavouraki AI, Angelis EM, Kornaros M. Optimization of thermo-chemical hydrolysis of kitchen wastes. *Waste Manag*. 2013;33:740–5. <https://doi.org/10.1016/j.wasman.2012.07.012>.
95. Sarto S, Hidayati R, Syaichurrozi I. Effect of chemical pretreatment using sulfuric acid on biogas production from water hyacinth and kinetics. *Renew Energy*. 2019;132:335–50. <https://doi.org/10.1016/j.renene.2018.07.121>.
96. Ariunbaatar J, Panico A, Frunzo L, Esposito G, Lens PNL, Pirozzi F. Enhanced anaerobic digestion of food waste by thermal and ozonation pretreatment methods. *J Environ Manag*. 2014;146:142–9. <https://doi.org/10.1016/j.jenvman.2014.07.042>.
97. Shah FA, Mahmood Q, Rashid N, Pervez A, Raja IA, Shah MM. Co-digestion, pretreatment and digester design for enhanced methanogenesis. *Renew Sust Energ Rev*. 2015;42:627–42. <https://doi.org/10.1016/j.rser.2014.10.053>.
98. Panigrahi S, Dubey BK. A critical review on operating parameters and strategies to improve the biogas yield from anaerobic digestion of organic fraction of municipal solid waste. *Renew Energy*. 2019;143:779–97. <https://doi.org/10.1016/j.renene.2019.05.040>.
99. Kiran EU, Stamatelatou K, Antonopoulou G, Lyberatos G. Production of biogas via anaerobic digestion. In: *Handbook of biofuels production*. Elsevier; 2016. p. 259–301. <https://doi.org/10.1016/B978-0-08-100455-5.00010-2>.
100. Schroyen M, Vervaeren H, Vandepitte H, Van Hulle SWH, Raes K. Effect of enzymatic pretreatment of various lignocellulosic substrates on production of phenolic compounds and biomethane potential. *Bioresour Technol*. 2015;192:696–702. <https://doi.org/10.1016/j.biortech.2015.06.051>.
101. Schroyen M, Vervaeren H, Van Hulle SWH, Raes K. Impact of enzymatic pretreatment on corn stover degradation and biogas production. *Bioresour Technol*. 2014;173:59–66. <https://doi.org/10.1016/j.biortech.2014.09.030>.
102. Zierniński K, Romanowska I, Kowalska M. Enzymatic pretreatment of lignocellulosic wastes to improve biogas production. *Waste Manag*. 2012;32:1131–7. <https://doi.org/10.1016/j.wasman.2012.01.016>.
103. Zhang Q, He J, Tian M, Mao Z, Tang L, Zhang J, Zhang H. Enhancement of methane production from cassava residues by biological pretreatment using a constructed microbial consortium. *Bioresour Technol*. 2011;102:8899–906. <https://doi.org/10.1016/j.biortech.2011.06.061>.
104. Zhong W, Zhang Z, Luo Y, Sun S, Qiao W, Xiao M. Effect of biological pretreatments in enhancing corn straw biogas production. *Bioresour Technol*. 2011;102:11177–82. <https://doi.org/10.1016/j.biortech.2011.09.077>.
105. Shi J, Sharma-Shivappa RR, Chinn M, Howell N. Effect of microbial pretreatment on enzymatic hydrolysis and fermentation of cotton stalks for ethanol production. *Biomass Bioenergy*. 2009;33:88–96. <https://doi.org/10.1016/j.biombioe.2008.04.016>.
106. Ge X, Matsumoto T, Keith L, Li Y. Fungal pretreatment of albizia chips for enhanced biogas production by solid-state anaerobic digestion. *Energy Fuel*. 2015;29:200–4. <https://doi.org/10.1021/ef501922t>.

107. Zhao J, Zheng Y, Li Y. Fungal pretreatment of yard trimmings for enhancement of methane yield from solid-state anaerobic digestion. *Bioresour Technol.* 2014;156:176–81. <https://doi.org/10.1016/j.biortech.2014.01.011>.
108. Martinez AT, Ruiz-Dueñas FJ, Martínez MJ, Del Río JC, Gutierrez A. Enzymatic delignification of plant cell wall: from nature to mill. *Curr Opin Biotechnol.* 2009;20:348–57. <https://doi.org/10.1016/j.copbio.2009.05.002>.
109. Skidas IV, Gavala HN, Lu J, Ahring BK. Thermal pre-treatment of primary and secondary sludge at 70 C prior to anaerobic digestion. *Water Sci Technol.* 2005;52:161–6. <https://doi.org/10.2166/wst.2005.0512>.
110. Lizasoain J, Trulea A, Gittinger J, Kral I, Piringer G, Schedl A, Nilsen PJ, Potthast A, Gronauer A, Bauer A. Corn stover for biogas production: effect of steam explosion pretreatment on the gas yields and on the biodegradation kinetics of the primary structural compounds. *Bioresour Technol.* 2017;244:949–56. <https://doi.org/10.1016/j.biortech.2017.08.042>.
111. Carlsson M, Lagerkvist A, Ecke H. Electroporation for enhanced methane yield from municipal solid waste. *ORBIT 2008 Mov Org Waste Recycl Towar Resour Manag Biobased Econ.* 2008;6:1–8.
112. Liu CM, Wachemo AC, Yuan HR, Zou DX, Liu YP, Zhang L, Pang YZ, Li XJ. Evaluation of methane yield using acidogenic effluent of NaOH pretreated corn stover in anaerobic digestion. *Renew Energy.* 2018;116:224–33. <https://doi.org/10.1016/j.renene.2017.07.001>.
113. Capson-Tojo G, Trably E, Rouez M, Crest M, Steyer JP, Delgenès JP, Escudié R. Dry anaerobic digestion of food waste and cardboard at different substrate loads, solid contents and co-digestion proportions. *Bioresour Technol.* 2017;233:166–75. <https://doi.org/10.1016/j.biortech.2017.02.126>.
114. Fagbohungbe MO, Dodd IC, Herbert BMJ, Li H, Ricketts L, Semple KT. High solid anaerobic digestion: Operational challenges and possibilities. *Environ Technol Innov.* 2015;4:268–84. <https://doi.org/10.1016/j.eti.2015.09.003>.
115. Amani T, Nosrati M, Sreekrishnan TR. Anaerobic digestion from the viewpoint of microbiological, chemical, and operational aspects: a review. *Environ Rev.* 2010;18:255–78. <https://doi.org/10.1139/A10-011>.
116. Wu D, Lü F, Shao L, He P. Effect of cycle digestion time and solid-liquid separation on digestate recirculated one-stage dry anaerobic digestion: use of intact polar lipid analysis for microbes monitoring to enhance process evaluation. *Renew Energy.* 2017;103:38–48. <https://doi.org/10.1016/j.renene.2016.11.016>.
117. Fox P, Pohland FG. Anaerobic treatment applications and fundamentals: substrate specificity during phase separation. *Water Environ Res.* 1994;66:716–24. <https://doi.org/10.2175/wer.66.5.8>.
118. Panjičko M, Zupančič GD, Zelić B. Anaerobic biodegradation of raw and pre-treated brewery spent grain utilizing solid state anaerobic digestion. *Acta Chim Slov.* 2015;62:818–27. <https://doi.org/10.17344/acsi.2015.1534>.
119. Nielsen HB, Angelidaki I. Codigestion of manure and industrial organic waste at centralized biogas plants: process imbalances and limitations. *Water Sci Technol.* 2008;58:1521–8. <https://doi.org/10.2166/wst.2008.507>.
120. Surendra KC, Takara D, Hashimoto AG, Khanal SK. Biogas as a sustainable energy source for developing countries: opportunities and challenges. *Renew Sust Energ Rev.* 2014;31:846–59. <https://doi.org/10.1016/j.rser.2013.12.015>.
121. Korres N, O'Kiely P, Benzie JAH, West JS. Bioenergy production by anaerobic digestion: using agricultural biomass and organic wastes. New York: Routledge; 2013.

Chapter 7

Recycling of Multiple Organic Solid Wastes into Chemicals via Biodegradation



Trevor J. Shoaf and Abigail S. Engelberth

Abstract Much of the solid waste produced annually is high in organic content, and while the definition of what exactly is considered to be organic waste differs based on locale, the sheer volume of organic waste produced is shocking. Organic waste contributes to greenhouse gas (GHG) emissions and often carries costly disposal fees. Redirecting the organics from the waste into a higher value use can (1) mitigate emissions, (2) potentially reduce cost, (3) save time and effort on producing primary resources, (4) produce valuable goods and commodity chemicals. The organic fraction of municipal solid waste (OFMSW) can be recycled via biodegradation into readily used methane gas or into chemical building blocks such as acids or alcohols. Biodegradation may include anaerobic digestion, fungal transformation, and composting. This chapter will explore selected types of biodegradation, factors affecting each type, how the composition of the organic fraction affects the outcome of the biodegradation products, and the mitigation potential for recycling OFMSW via biodegradation. Upcycling, recycling, or repurposing carbon-rich wastes will enhance the carbon circular economy and reduce the burden on primary production. This chapter aims to demonstrate the utility of biodegradation to produce market-ready products from otherwise wasted resources.

T. J. Shoaf

Department of Agricultural & Biological Engineering, Purdue University, West Lafayette, IN, USA

Laboratory of Renewable Resources Engineering, Purdue University, West Lafayette, IN, USA

A. S. Engelberth (✉)

Department of Agricultural & Biological Engineering, Purdue University, West Lafayette, IN, USA

Laboratory of Renewable Resources Engineering, Purdue University, West Lafayette, IN, USA

Environmental & Ecological Engineering, Purdue University, West Lafayette, IN, USA

Center for the Environment, Purdue University, West Lafayette, IN, USA

e-mail: aengelbe@purdue.edu

Keywords Agricultural residues · Biodegradation · Anaerobic digestion · Lactic acid · Food waste · Organic fraction municipal solid waste

7.1 Introduction

Global waste generation and disposal has become a salient issue after the turn of the century. In an effort to shift from a linear to a more circular economy, reuse and conversion of wastes away from the landfill and into more suitable and higher value products is necessary. A potential solution is to use the carbon present in the organic fraction of municipal solid waste (OFMSW) – in the form carbohydrates (*i.e.* sugars) – as a resource for biochemical degradation and conversion. OFMSW is rich in both simple and complex sugars: food waste has been shown to have concentrations of up to 71.5% total sugars on a dry basis [1], and cotton waste fibers are around 95.4 wt % cellulose [2].

Sugar-rich waste is an ideal candidate for biodegradation to mitigate the ever growing stream of organic waste by diverting it from a landfill and into a process by which microorganisms consume the sugars to produce higher-value products. The aim of this chapter is to highlight recent findings and to demonstrate the current understanding of how OFMSW and other organic wastes can act as a feedstock for biodegradation.

Biodegradation of OFMSW into valuable products – specifically commodity chemicals or petro-chemical replacements – reduces demand on virgin resources and assists in the goal for national energy independence. In 2007, the United States passed the “Energy Independence and Security Act” with a goal to reduce reliance on foreign entities for their energy sources [3]. While energy independence is a significant driving force, reduction in volume of organic solid wastes annually landfilled is another. Of the 268 million tons of municipal solid waste (MSW) produced in the USA in 2017, the majority (53%) was landfilled [4]. Due to the organic nature of the OFMSW, degradation continues regardless of final resting place. When landfilled, OFMSW degrades resulting in both leachate and greenhouse gas emissions [5]. The leachate, which is the liquid excreted from landfills to the environment, levels increase with OFMSW decomposition and can reduce landfill gas collection operation [6]. Landfilling as a waste management solution for organic wastes also increases the negative impacts on human health (*e.g.*, cardiovascular, pulmonary) by the waste treatment chemicals used [7, 8].

Background and current status of research into OFMSW and other waste organics as they pertain to biodegradation to produce either liquid or gaseous products that have a demonstrated market demand will be elucidated [3]. First, liquid-based products produced through the acetone-butanol-ethanol (ABE) fermentation schema will be discussed followed by the sequential production of lactic acid and methane gas.

The major organic wastes that will be discussed are categorized as either agricultural residues or organic fraction of municipal solid wastes. All wastes discussed

are organic in composition and have either been previously studied as potential candidates for a biodegradation or have a high potential for conversion to higher value products.

7.1.1 Agricultural Residues

Agricultural residues are considered to be wastes derived from agricultural processing. The term ‘agricultural processing’ refers to anything from tapioca production, resulting in cassava bagasse, to rice harvesting, resulting in rice straw generation. The defining characteristic of agricultural residues, as applied to this chapter, is that these parts of the crop are generally deemed inedible and are conventionally discarded as refuse [9]. The term bagasse is used to describe the more fibrous waste of a crop [10]. The agricultural residues highlighted in this chapter are cassava bagasse, three different straws (rice, barley, and wheat), sugar beet pulp, and corn stover.

Cassava is predominately found in diets of the people living in Asian, African, and Latin American locales, making cassava the sixth most important global food crop. The major solid wastes from cassava processing are bagasse and peels, which are inedible due to their deadly concentration of cyanide [11]. For every 250–300 tons of edible tubers of cassava processed, about 280 tons of bagasse and 1.6 tons of peels are produced [9]. Cassava bagasse contains water, residual starches, and cellulose fibers, where the residual starches and cellulose fibers can be used in microbial biodegradation [3, 12]. The global production of cassava in 2019 was 304 million tons, up from 287 million tons in 2017 [13].

Rice straw is the residue remaining in the field after harvest [14, 15]. The volume is dependent upon the techniques employed for grain removal, including the cutting height, as well as the choices by the growers regarding the treatment of the straw not harvested with the grains. When these factors are considered, the global rice straw production in 2019 was between 370 and 520 million tons [13]. Of the rice straw production in 2017 the United States produced only 4.3 million dry tons and the United States Department of Energy (DOE) forecasts there to be 10.8 million dry tons by 2030 [3]. The DOE used an estimate of the moisture content of the grain to be 13.5% and a ratio of 1 dry gram of rice to 1 dry gram rice straw [16]. While grown to a lesser extent globally than rice, barely straw is also a significant agricultural residue to consider. The worldwide production of barley straw in 2019 was 159 million tons and it is estimated that between 0.33 to 0.53 kg of straw is produced per kg of barley [17].

Sugar beets are mainly grown for use as a source of crystalline sugars with 270 million tons produced annually with a dry basis of five million tons of sugar beet pulp annually, 20% of which is produced within the USA [18, 19]. The process to transform sugar beets into crystalline sugar also results in three major byproducts: tops, pulp, and molasses [20]. While sugar beet molasses has been used in

fermentation to produce alcohol and methane, sugar beet pulp is the residue of focus for this chapter due to its high-solids composition [20, 21].

Corn stover is the solid agricultural waste byproduct created when growing corn; generally, corn stover is most every part of the grass that is not the ear. [22]. Barley straw and rice straw account for less than a 1:1 ratio for their product by weight, corn stover accounts for 1 kg stover per kg grain [3]. This fact, along with the fact that corn takes up over 12 times more land in the USA for growing than barley and rice combined, makes corn stover an attractive potential waste residue for biodegradation [3].

7.1.2 Municipal Solid Wastes (MSW)

The specific organic content of OFMSW is highly dependent on source, season, and region [17, 23, 24], though it is usually abundant in food wastes (FW), whether they be from residences, markets, or restaurants [24]. In 2015 the DOE reported that 15.1% of OFMSW was food wastes, 6.2% was wood, 13.3% from yard trimmings, and 25.9% was non-recycled paper products [25]. OFMSW tends to have higher moisture content than MSW and varied concentrations of rejected materials. Materials that may inhibit a biodegradation process and are present to varying degrees within OFMSW include plastics, cardboard, paper, metal, glass, bones, and fruit kernels [16]. Glass (4.4% of MSW), metals (9.1% of MSW), plastics (13.1% of MSW), as well as “other inorganic species found in MSW” (3.6% of MSW) are not usable as feedstock for anaerobic digestion [16, 26]. It is estimated that between 1.6 and 2.0 billion tons of MSW are produced globally per year. Of that, around 70% is landfilled, and only around 19% is recycled [27]. The production of MSW is around three times that of the combined production of agricultural residues of rice straw (520 Mt), barley straw (84 Mt), and cassava bagasse (76 Mt).

Food wastes are not the only organic-rich feedstock in MSW; textiles are another fraction of MSW and have a cellulosic makeup between 30 and 40% on average [28, 29]. In the United States, over the past two decades, the production of textile MSW by weight has increased 80%, from 9.48 million tons in 2000 to 17.03 million tons in 2018 [30]. Of the textile waste produced in these two decades, on average, 66% was landfilled, which is equivalent to 11.3 million tons in 2018 [30].

In 2019, the fraction of textile waste in MSW found in Lahore, Pakistan was 9.21%. This percentage was determined through a case study and does not define the percent of textiles found in MSW worldwide. In 2015 the fraction of MSW that can be attributed to rubber, leather, and textiles was 9.3% [26]. In the textile market globally, cotton is attributed to 30% of the market share and cellulose from cotton requires significantly more time to degrade naturally as compared to amorphous cellulose [2].

7.1.3 Biodegradation Processes Overview

The biodegradation processes discussed in this chapter focus on the production of either a liquid or gaseous product. The focus will be on two general schema, acetone-butanol-ethanol (ABE) and anaerobic digestion for the production of lactic acid and methane. Each will be discussed in detail in the Sects. 7.3 and 7.4. Table 7.1 is included here to highlight and summarize microorganism type and use on the substrates of interest. Table 7.1 displays strain, along with key operating parameters, sorted by process and also highlights the feedstocks pertinent to the present work.

Table 7.1 Key operating parameters for highlighted microorganisms

Process	Microorganism	pH range	Temperature range (°C)	Relevant feedstocks	References	
ABE	<i>Clostridium acetobutylicum</i>	5.0–7.0	30–42	Barley Straw	[31–33]	
				Rice Straw		
				Cotton Fibers		
				OFMSW		
	<i>Clostridium beijerinckii</i>	5.0–6.8	34–40	Barley Straw Switchgrass and Corn Stover Packing Peanuts	[34–36]	
Lactic Acid	<i>Clostridium tyrobutyricum</i>	5.0–6.0	20–37	Cassava Bagasse	[37–39]	
	<i>Clostridium thermocellum</i> and <i>Clostridium saccharoperbutylacetonicum</i>		5.0–6.0	30	Rice Straw	[40–42]
	<i>Bacillus coagulans</i>	6.0–6.4	50–52	OFMSW	[43, 44]	
	<i>Lactobacillus casei</i>	6.5	30–45	Cassava Bagasse	[45]	
	<i>Lactobacillus delbrueckii</i> sp. <i>Bulgarcus</i>	–	–	Corn Stover	[46]	
	<i>Lactobacillus plantarum</i>	6.25	35	Food Waste	[1]	
	<i>Streptococcus</i> sp.	6	35	Food Waste	[24]	

ABE—acetone-butanol-ethanol

OFMSW—organic fraction of municipal solid waste

7.2 Pretreatment to Overcome Substrate Challenges

To maximize yield of a desired product from organic solid waste, pretreatment may be required [36, 47–52]. Pretreatment methods that have been employed for organic wastes and agricultural residues can be categorized by one of the following groups: mechanical, physical, chemical, physicochemical, or biological. The prevalence and availability of these methods depends upon the scale of the study, the composition of the waste, and the availability of the resource. Section 7.2 aims to provide sufficient background to more acutely explain the differences in parameters and reasons for increased yield in each of the products discussed. Table 7.2 illustrates how different combinations of the pretreatment methods are related to each of the main feedstocks and how the pretreatment methods relate to the final products of interest. Note that while other pretreatment methods exist and are common for lignocellulosic materials that are not considered waste, such as switchgrass grown for energy production, they will only be discussed if they have demonstrated use in the pretreatment of organic solid wastes as well.

7.2.1 Physical and Mechanical Pretreatments

Physical and mechanical pretreatments employ either a physical or mechanical action or change to the substrate to increase yields of target components (e.g., cellulose, hemicellulose) [51]; examples include ultrasonication [67, 68], grinding [69, 70], rotary drum reactor [59, 63], and microwave treatment [65, 71, 72].

Grinding is a basic pretreatment that uses mechanical blades or impellers to reduce the size of the substrate [69, 70]. A hammer mill was used to grind wheat straw, barley straw, and corn stover with the goal of determining the physical properties at three particle sizes (0.8 mm, 1.6 mm, and 3.2 mm screen sizes) [70]. The bulk density achieved for the wheat straw, barely straw, and corn stover was highest for the smallest hammer mill screen sizes tested [70]. A household garbage disposal, which imparted the same type of action as a hammer mill, was compared to a bead mill to reduce FW particle and increase VFA production and methane yield [69]. A household garbage disposal was tested as a pretreatment option due to the distributed nature and volume of food waste production. It was reported that reducing FW particle size below a lower limit threshold of 0.6 mm particles resulted in VFA accumulation and decreased methane yield, as well as a reduction in FW particle solubility in the anaerobic chamber. The optimal particle size for methane production from FW was 0.62 mm [69]. Note that standard garbage disposal was only able to reduce the FW particles to 0.88 mm, whereas the bead mill achieved the optimal size of 0.62 mm and could further reduce the FW particles to 0.4 mm [69].

Ultrasonication uses targeted sound waves to sunder substrates prior to fermentation [67, 68]. Ultrasonic waves between 10 kHz and 20 MHz are emitted and

Table 7.2 Pretreatment combinations for solid waste feedstocks used in biodegradation

	Substrate	Pretreatment by type			Physicochemical (s)	Product (s)	References
		Mechanical and physical	Chemical	Biological			
Agricultural residues	Barley Straw	Ground, milled	Sulfuric acid	Cellulase, β -glucosidase, xylanase	—	ABE	[53]
	Cassava Bagasse	Milled	—	Glucamylase, cellulase, endoglucanase, β -glucosidase	—	ABE	[38]
	—	—	—	α -amylase, glucamylase	—	Lactic acid	[31]
Corn Stover	Ground, milled	Sulfuric acid	Cellulase, β -glucosidase, xylanase	—	ABE	[54]	
	Crushed, dried	Hydrochloric Acid	Cellulase	—	Lactic Acid	[46]	
	—	Sulfuric acid	—	Steam explosion	ABE	[55]	
<i>Eucalyptus grandis</i> wood	Milled, dried	—	Cellulase	—	—	—	
Rice Straw	Dried, milled	Alkaline (NaOH), Phosphoric Acid	Cellulase, β -glucosidase	—	ABE	[52]	
	Milled	Organosolv (EtOH)	Cellulase, β -glucosidase	—	ABE	[56]	
Sugar Beet Pulp	Sonicated, magnetic field, ground	—	Pectinase	—	Methane	[57]	
—	—	—	—	Hydrothermal	Methane	[58]	
Sugar Cane Bagasse	Rotary Drum Reactor	Alkaline (NaOH)	Accelerase™ 1000 enzyme complex from Genencor International Inc.	—	Ethanol	[59]	
Sonicated	—	—	Enzymatic Hydrolysis	Supercritical CO ₂	—	[60]	
Wheat Straw	Ground, milled	Sulfuric acid	Cellulase, β -glucosidase, xylanase	—	ABE	[61]	
OFMSW	Cotton Waste	—	Phosphoric Acid – Acetone	Cellic® CTec2 (Novazymes)	—	ABE	[2]

(continued)

Table 7.2 (continued)

Substrate	Pretreatment by type				Product(s)	References
	Mechanical and physical	Chemical	Biological	Physiochemical		
Food Waste	—	—	Enzopeptidase	Hydrothermal	Methane	[62]
MSW	Ground	—	—	—	VFA, Methane	[24]
	Rotary Drum Reactor	—	—	—	Methane	[63]
	Shredded	—	—	Hydrothermal	Methane	[50]
	Dried, milled, homogenized	Organosolv (EtOH)	Cellulase, hemicellulase	—	ABE	[64]
OFMSW	Ground, microwave	—	—	—	Biogas	[65]
Polyester- Cotton	Cut, milled	Alkaline (NaOH)	β -glucosidase, cellulase	—	Ethanol	[66]

ABE—acetone-butanol-ethanol

VFA—volatile fatty acids

weaken cell walls and break down lignin to improve accessibility of sugars to microorganisms [73]. The ultrasonic waves cause the formation of cavitation bubbles that, when disrupted, create a high pressure burst to lyse cells [73]. Ultrasonication was used on sugar beet pulp pellets that had been ground to 2 mm pieces to increase methane production 26% and methane concentration 79% when ultrasonication was paired with enzyme pretreatment, a magnetic field pretreatment, and grinding [74].

The rotary drum reactor has the same technological basis to traditional composting techniques, in that air is added to drums from the unloading side to assist in aerobic biodegradation and mechanical force degradation [59, 63]. A rotary drum reactor was able to separate biodegradable materials from MSW which resulted in a feedstock that was consistent in biogas yield to the quantity produced from FW alone [63]. A rotary drum reactor was successfully scaled-up to a 100-L capacity for use in the pretreatment of sugar cane bagasse to produce ethanol using SSF operating conditions [59].

Microwave pretreatment irradiates substrates with electromagnetic waves, between 0.3 and 300 GHz frequency, and can be used concurrently with chemical pretreatments to enhance cellulose concentrations from organic solid wastes by disrupting cells through polar and dielectric molecular interactions [65, 71, 72]. Microwave pretreatment has shown to increase glucose concentrations while reducing the concentration of fermentative inhibitors (e.g., 5-hydroxymethylfurfural and furfural) [71]. When microwave pretreatment was applied to a stand-in version of OFMSW, formulated based on previous characterization of Canadian kitchen waste, after size reduction pretreatment, resulted in an increased biogas production between 4 and 7%, suggesting synergy from combining pretreatments [65].

7.2.2 *Chemical Pretreatments*

Chemical pretreatments employ solvents – often acids – to reduce the long chain carbohydrates into shorter chain sugars that are more readily consumed during biodegradation. Organosolv is conventionally used for delignification of lignocellulosic biomass and it relies on an organic solvent (e.g., MgSO_4 , HCl , $(\text{NH}_4)_3\text{PO}_4$) to degrade the lignin barrier of biomass [75]. For rice straw, an ethanol organosolv pretreatment (with a solid-to-liquid ratio of 1:8 and 75% (v/v) aqueous ethanol containing 1% (w/w) sulfuric acid catalyst) was shown to improve butanol production from 43.6 g/kg rice straw to 80.3 g/kg rice straw [56].

Alkaline pretreatment was considered as an alternative to organosolv to improve the yield of ABE from rice straw [52]. Alkaline pretreatment is often viewed as a promising path for pretreatment of agricultural residues due to its ability to simultaneously increase the internal surface area, decrease in cellulose crystallinity, and disrupt the lignin [52].

Phosphoric acid-acetone is a combination of two organic acids for enhanced organosolv pretreatment that has been shown to effectively pretreat cotton-based

textile wastes to recover cellulose [2, 76]. The two-step method follows: (1) phosphoric acid (H_3PO_4) is used to treat solid textile cotton waste (2) acetone ($(CH_3)_2CO$) is used to recover cellulose. Step 1 dissolved 94% solids using 19 g H_3PO_4/g cotton compared to the initial solid mass. Step 2 recovered 97% cellulose using 41 g $(CH_3)_2CO/g$ solid. Recovered cellulose here is defined by: grams cellulose precipitated per gram of dissolved cellulose [2]. Phosphoric acid-acetone pretreatment was shown to increase the glucose yield compared to untreated rice straw from 101.8 g glucose/kg rice straw [52].

7.2.3 Physiochemical Pretreatments

Physiochemical pretreatments take advantage of the discord between physical and chemical properties to synergistically create a force that breaks the barrier between complex substrates and fermentation. Examples of physiochemical pretreatments are hydrothermal pretreatment [50, 58], steam explosion [55, 77], and the use of supercritical CO_2 (SC- CO_2) [60, 78, 79].

Hydrothermal pretreatment (HTP) uses a high temperature water bath, between 160 °C and 180 °C for 30–60 min, to surround a vessel containing the substrate of interest in an effort to increase the hydrolysis rate [58]. HTP structurally changes organic solid wastes to allow more straightforward degradation and increases the soluble chemical oxygen demand by degrading insoluble organic carbohydrates and proteins [50]. The production of inhibitory compounds (i.e., melanoidins) is an inherent pitfall of HTP due to interactions between carbohydrates and amino acids during HTP, but it is possible to design the reaction vessel to counteract this by addition of acid consuming bacteria (i.e., *Lactobacillus plantarum SF5.6*) [50]. A two-phase anaerobic digestion of MSW was coupled with HTP and it was determined that biogas production in the two-phase anaerobic digestion was 31.5% higher if HTP was employed first as compared to the control; two-phase anaerobic digestion could reach a net energy output 97.4% higher than the one phase anaerobic digestion with HTP [50].

Steam explosion is an attractive pretreatment method for lignocellulosic biomass since it requires no chemical bar water and generates small amounts of waste [55]. Steam explosion and hydrothermal pretreatments both take advantage of high temperature water, but steam explosion uses saturated steam, whereas hydrothermal pretreatment uses the liquid phase of water [77]. The scientific basis behind steam explosion is that the high temperatures and high pressure is applied to the biomass, followed by a rapid drop in pressure, causing an explosive decompressive state that breaks down the hemicellulose [77].

Supercritical CO_2 (SC- CO_2) is another temperature dependent physiochemical pretreatment technique, but it uses CO_2 to break down complex organic wastes [79]. When SC- CO_2 was used to pretreat sugarcane bagasse resulting in an increase in fermentable sugar by 280%, compared to untreated sugarcane bagasse [60]. This

pretreatment is favorable when used on biomass or organic solid waste because it does not result in the formation of harmful solvent byproducts [78].

7.2.4 Biological Pretreatments

Biological pretreatments use microorganisms, enzymes, or a combination thereof to reduce substrates, with similar complexity as to what is found in organic solid waste, and to maximize the fermentative production potential improving the carbon accessibility in the substrates [73, 80, 81].

Enzymatic hydrolysis may be necessary to access the organic solid waste as a carbon source in the fermentation media [73]. Selection of enzymatic hydrolysis over other pretreatment methods is based on both substrate composition and the downstream degradation process. The main goal of the enzymes used for pretreatment of organic solid wastes is to reduce carbon chain length [73, 82]. Enzymatic hydrolysis often targets hydrogen bonding within a carbon chain at designated bonding sites to reduce chain length [82]. Microorganisms can more readily consume a shortened carbon chain and thus increase the yield of a given product of interest. Cellulase, amylase, and β -glucosidase are commonly used enzymes for cellulose hydrolysis [81]. Microbial selections involving some *Clostridia* species, render enzymatic hydrolysis unnecessary, due to the innate enzymatic production of these microbes [83–85]. Section 7.3.1 will explore these features of *Clostridium* bacteria in more depth.

One of the microorganism-based approaches uses fungus to synthesize enzymes, with the goal of reducing operational cost increases seen from the use of industrially produced enzymes [28]. One example of such a fungus is *Aspergillus niger* which produces several hydrolysis enzymes such as α -amylase, β -glucosidase, xylanase, and cellulase [28].

7.3 Acetone-Butanol-Ethanol (ABE) Process

ABE fermentation is an anaerobic process reliant upon bacteria to produce acetone, butanol, and ethanol [86]. While early reports of butanol production using the ABE process revolved around the *Clostridia* genus, more recent industrial processes have used genetically modified *Clostridium* or *Saccharomyces cerevisiae* [87]. Fermentations with these specific species have controlled the genetics greatly, but use of mixed cultures has also been explored; combining *Clostridium cellulovorans* and *Clostridium beijerinckii* [88]. Mixed culture fermentation (MCF) is often employed in the fermentation of organic solids, but does not always lead to increased yields [57, 85, 89–91]. ABE fermentation uses a bi-phasic schema of acidogenesis, which produces butyrate, hydrogen, and CO₂, followed by solventogenesis

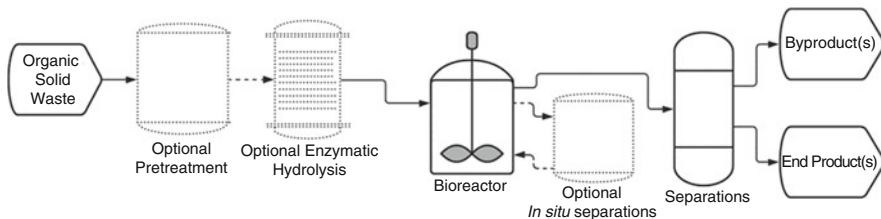


Fig. 7.1 Generic process flow diagram for Acetone-butanol-ethanol (ABE) fermentation. Dotted lines represent operations that are not required but may be implemented based on the feedstock or desired yield

[86]. Microorganisms consume the products of the acidogenic phase and produce acetone-butanol-ethanol during a second phase called the solventogenesis phase [92].

ABE fermentation emerged in response to a growing acetone market during World War I, but production began to wane in the 1980s, as the petrochemical industry expanded its reach and portfolio [87, 93]. However, due to the rise of interest in alternative liquid fuels and renewable chemicals – namely in the form of biobutanol – research on ABE fermentation has reemerged [87, 93]. Butanol is commonly considered a drop-in ready liquid fuel and is an intermediate for the production in three disparate industries: artificial flavoring, solvents, and cosmetics [94].

Figure 7.1 depicts a generic process flow for an ABE fermentation. The unit operations shown in Fig. 7.1 include: pretreatment and enzymatic hydrolysis, fermentation, in situ separations, and a final separation to purify the product of interest from the mixture. The pretreatment and enzymatic hydrolysis steps are optional and depend on the substrate used; the fermentation contains an optional in situ separation process to assist in increasing yield as butanol is toxic to the microbes present.

The ABE production process – outlined in Fig. 7.1 – is a biphasic process where microorganisms (historically *Clostridia*) consume feedstock to produce acetic acid and butyric acid in the acidogenic phase (phase 1), and acetone, butanol, and ethanol in the solventogenic phase (phase 2) generally in a ratio of 3:6:1 respectively [87]. Variables that have been explored in the optimization of ABE production in terms of butanol production will be discussed. Butanol is produced in the second phase of the ABE fermentation, when microorganisms convert the organic acids produced in the solventogenic phase into acetone, butanol, and ethanol. The microorganisms that produce butanol through ABE fermentation at the industrial and lab scales are reviewed and then the organic solid substrates are presented and ranked by yield of butanol, and finally the impact of in situ separation of inhibitory compounds produced during the biodegradation mechanisms is discussed.

7.3.1 Microorganisms

Aerobic conditions, pH, and temperature used within a given ABE fermentation depend on microorganism selection. The genus Clostridia is often selected for this fermentation due to Clostridia's ability to produce butanol [95]. Issues regarding use of Clostridia will be discussed and have led to increases in research into genetically modifying *Escherichia coli* and *Saccharomyces cerevisiae* [94, 96]. Of the Clostridia species, biobutanol is most prevalently produced from *Clostridium acetobutylicum* and *Clostridium beijerinckii*, however the exploration of other species with similar characteristics have been explored, but to a lesser extent [61, 97].

7.3.1.1 Clostridia

The Clostridia species most prevalent in the production of butanol are *Clostridium acetobutylicum*, *Clostridium beijerinckii*, *Clostridium saccharoperbutylacetonicum*, and *Clostridium saccharobutylicum* [95]. Clostridia bacteria digest sugar, starch, cellulose, and lignin – a trait that is especially advantageous when using an alternative feedstocks like agricultural residues and OFMSW [87]. These species produce butanol under the following optimal conditions: 30–40 °C, pH between 6.0 and 7.5, and anaerobic conditions [87]. The effect of pH on butanol production using a non-waste feedstock was reported; the initial pH of 6.2 yielded the highest concentration of butanol (6.28 g/L) of the pH values tested (5.0, 5.5, 6.0, 6.2, 6.5, 7.0) on the *C. acetobutylicum* YM1 strain [33]. Table 7.3 displays the range of pH values that have been used for ABE production along with the organic solid substrates used and their butanol yields.

Optimal temperatures used in ABE fermentation using Clostridia species are reported in Table 7.3 as well, however there has been interest in increasing the optimal temperature for this process by genetically modifying *Clostridium* strains to improve cellulase activity and hence butanol production. A shift towards temperatures around 42 °C yields 0.18 g/g-substrate compared to between (0.08 and 0.12) g/g-substrate in usual simultaneous saccharification and fermentation (SSF) processes using temperatures of 36 °C [32].

SSF processes allow for the reduction of unit operations due to the removal of pretreatment steps that take place in the same SSF reactor [32]. One of the major challenges of SSF was the temperature optimization conundrum due to the fact that enzymatic hydrolysis operates mostly between 45 °C and 50 °C, whereas *Clostridium* fermentation for ABE operates between 30 °C and 40 °C [32, 76]. Non-isothermal simultaneous saccharification and fermentation (NSSF) is a process designed to circumnavigate the temperature-based challenges of SSF, namely the differences in the optimal temperatures of enzymatic hydrolysis and fermentation, where the operation is set to the optimal enzymatic temperatures until

Table 7.3 Comparative review of various acetone-butanol-ethanol (ABE) substrates and butanol production

	Substrate	pH ¹ (C/UC) ²	Residence Time (h)	T (°C) Mixing RPM	Microorganism	Butanol Production (g/L)	Yield (g/kg)	Reference
Agricultural residue	Barley Straw and grain	6.5 (UC)	120	37 (0)	<i>C. acetobutylicum</i>	7.8	235.6	[53]
	Barley Straw Hydrolysate	6.5 (UC)	68	35 (0)	<i>C. beijerinckii</i>	18.01	285 ³	[61]
	Cassava bagasse	6.0 (C)	85	37 (0)	<i>C. tyrobutyricum</i>	15.0	300	[38]
	Rice Straw	6.5 (UC)	72	37 (0)	<i>C. acetobutylicum</i>	2.0	112.7	[56]
	— (UC)	14 days		30 (0)	<i>C. thermocellum</i> and <i>C. saccharoperbutylacetonicum</i>	5.5	—	[42]
	Switchgrass and corn stover	6.5 (UC)	85	35 (0)	<i>C. beijerinckii</i>	14.5	241.3 ³	[97]
OFMSW	Cotton Fibers	6.8 (UC)	72	37 (160)	<i>C. acetobutylicum</i>	3.28	109.3	[2]
	OFMSW	6.8 (UC)	96	37 (0)	<i>C. acetobutylicum</i>	8.57	102.43	[64]
	OFMSW	6.8 (UC)	72	37 (0)	<i>C. acetobutylicum</i>	—	83.9	[108]
	Packing Peanuts	6.8 (UC)	96	36 (0)	<i>C. beijerinckii</i>	15	155.6 ³	[109]

1: pH adjustment prior to fermentation

2: C – controlled pH throughout fermentation; UC—uncontrolled pH throughout fermentation

3: Yield reported in a gram product/kg sugars basis

the enzymatic hydrolysis has achieved the desired hydrolysis before shifting the temperature within the reactor to a more desirable fermentative temperature [81, 98].

One development to counteract downsides of SSF and NSSF is consolidated bioprocessing (CBP). The main aspect to CBP that sets it apart from SSF and NSSF is the use of a single organism to produce enzymes and carry out the fermentation [81]. This strategy takes advantage of the advances of recombinant DNA technology that have allowed extensive modification of microbial species to carry out these tasks [81]. A few reports on these genetic modifications on *Clostridium* have shown enhanced yields of up to 0.39 g/g of butanol and ethanol using CBP [81, 99].

7.3.1.2 *Escherichia coli* and *Saccharomyces cerevisiae*

Escherichia coli and *Saccharomyces cerevisiae* are model organisms due to the abundance of information and genomics surrounding their use and functionality [100]. A strong baseline knowledge of both *E. coli* and *S. cerevisiae* allow for reasonable modifications to optimize ABE fermentation processes and to improve butanol yield.

A butanol production pathway was added into the native bacterial chassis of *E. coli* which resulted in 33 native gene deletions and five heterologous gene introductions [101]. The strain was enhanced to produce a 34% yield with 20 g/L of butanol from a synthetic medium; a marked increase over engineered *Clostridia* strains which can produce 18.9 g/L with yield of 29% [101].

S. cerevisiae is another model organism that has been modified to include a butanol production pathway [102–106]. One goal behind implementing *S. cerevisiae*, co-cultured with *C. acetobutylicum*, was to raise the butanol toxicity threshold [107]. From this exploration, the butanol concentration was able to reach 16.3 g/L, over double the threshold of 8 g/L discussed in Sect. 7.3.3 [107].

7.3.2 Substrate Selection

OFMSW has been either homogenized or left as a heterogeneous mixture for use as the carbon source in ABE fermentation. Table 7.3 compares the output of butanol, as it pertains to various organic solid substrates, and is sorted by highest to lowest butanol yield, while maintaining categorical separation between OFMSW and agricultural residues.

The fermentations shown in Table 7.3 were conducted with the Clostridia genus, with the majority (60%) of those being of *C. acetobutylicum*, followed by 30% from *C. beijerinckii*, while only one used *C. tyrobutyricum*. Microorganism selection is consistent with research trends in the past few years. It should be noted that each fermentation was performed at 36 ± 1 °C with 70% of the fermentations conducted at 37 °C. Only two studies used agitated vessels, with the final yield not among the highest yields achieved indicating that agitation may not be required. The highest yield of butanol per kg of agricultural residue was achieved from cassava bagasse at

300 g/kg [38], whereas the lowest yield from an agricultural residue was from rice straw at 112.7 g/kg [56]. Of the municipal solid waste substrates, the OFMSW from Isfahan, Iran and was pretreated with a combination of ethanol extraction, dilute acid pretreatment, and enzymatic hydrolysis, demonstrated the lowest yield of 83.9 g butanol/kg substrate [108]. The decreased yield in butanol for OFMSW as compared to agricultural residues may indicate that the sugars may not be accessible for the microorganisms and that additional pretreatment may be required to increase yield.

7.3.3 Separation

In situ separation processes are advantageous due to the inhibitory effect of butanol at concentrations greater than 8 g/L with regards to ABE production from *Clostridium* bacteria [39]. Pervaporation [110–113] and gas stripping [112, 114, 115] are conventional separation processes employed for product recovery during fermentation. Gas stripping removes the solvents produced from the media throughout the fermentation process by bubbling hydrogen or carbon dioxide through the fermentation broth, effectively stripping away ABE products as they are produced [115]. Pervaporation relies on membrane permeabilities to allow selected vapors to pass through the membrane pores with assistance of a vacuum [111]. This procedure partially vaporizes the fermentation broth by increasing the temperature of the feed broth to the heat of vaporization, then the vaporized broth passes by the membrane at which point the ABE products are pulled through the membrane via vacuum and condensed back into a liquid on the other side [111].

Gas stripping has been shown to maintain butanol concentrations below the critical inhibitory concentration of 8 g/L [112, 114]. When using a gas recycle flowrate between 0.3 and 0.6 vvm (gas volume per liquid volume per minute), 18.6 g/L of butanol was produced from industrial juices, such as sugar cane juice and sweet sorghum juice, when gas-stripping was used, compared to 10.5 g/L butanol from industrial juices without gas stripping [115]. When gas-stripping was applied to cassava bagasse hydrolysate, the butanol yield shifted from 0.22 g/g to 0.25 g/g, but the fermentation was able to produce 59.81 g/L with gas-stripping, and only 9.71 g/L without gas stripping [31], demonstrating that the more significant impact of in situ gas stripping lies in production over time, and not the yield.

Pervaporation relies on a liquid-to-vapor phase change, along with membrane technology, to separate butanol, along with other ABE products, from the fermentation media [110]. A model of a pervaporation membrane was constructed to determine efficacy in ABE production and was determined that an in situ process showed 250% higher butanol concentrations compared to control with no in situ separation [111]. A techno-economic analysis on the feasibility of pervaporation, along with gas-stripping, determined that biobutanol from MSW an economically viable process only if these two separations were incorporated. Pervaporation remains a relatively new yet technologically advanced separation technique [111, 112]; the most appropriate membranes for this separation are likely still under development.

7.4 Lactic Acid and Methane Process

Lactic acid and methane are generally concurrently produced – especially during anaerobic digestion. First, current approaches for optimizing production of lactic acid from organic solid wastes will be discussed followed by variables that can be modified to optimize lactic acid production and consequently achieve higher methane yields in the second phase. Lactic acid (LA) can be used in the production of various marketable products (e.g., anti-aging moisturizers, chemical cleaning agents, food preservatives, and dialysis solutions) [24]. The market size of lactic acid is estimated to increase by 254%, from \$2.64 billion to \$9.0 billion, between 2018 and 2025 [116]. Lactic acid produced by biodegradation is viewed as a more cost-effective and environmentally beneficial alternative to chemical synthesis because of the ability to utilize in-expensive waste streams as substrates and because chemical synthesis to produce lactic acid requires elevated temperatures and higher energy input [117].

Figure 7.2 illustrates a generic process flow for LA production via biodegradation, followed by optional methanogenesis of the volatile fatty acids (VFA). The unit operations shown in Fig. 7.2 include: pretreatment and enzymatic hydrolysis, acidogenic fermentation, optional *in situ* separation, separation of LA as a purified product, optional methanogenesis of remaining VFAs and media, *in situ* separation, and a final separation to purify the methane.

Figure 7.2 shows both the acidogenesis step and the methanogenesis step of organic solid waste fermentation. Methanogens transform organic acids into methane [118, 119]. The dotted line flowing from “Other Organic Acids” to

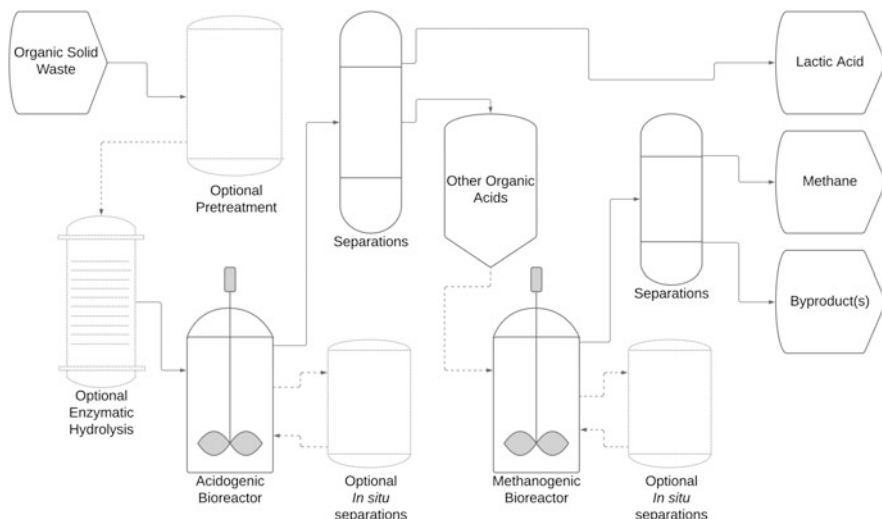


Fig. 7.2 Generic flow diagram for lactic acid and methane production from organic solid wastes. The dotted lines indicate an optional process or connection between processes

“Methanogenic Bioreactor” represent an optional step to harvest the lactic acid and utilize the remaining broth, including other VFAs, produced during acidogenesis to produce methane. This flow is one potential route to maximize the profitability of methane production [120, 121].

The sequential production of lactic acid and methane is advantageous in anaerobic digestion because it overcomes an economic hurdle of methanogenesis [24]. In the European Union (EU), LA fermentation production costs can range between 0.72 and 1.13 €/kg lactic acid with the market value at 1.36 €/kg lactic acid [24].

The microorganisms that are involved in acidogenesis include: lactic acid bacteria (LAB) [122] and *Saccharomyces cerevisiae* [121], whereas methanogenesis is carried out by: *Methanomicrobium mobile* [123] and *Methanosarcina* [21]. Similar to ABE production, lactic acid production has been carried out with mixed cultures, such as the combination of LAB monocultures with various fermentative abilities that were used to produce lactic acid from sugar beet pulp [49].

7.4.1 Lactic Acid

Anaerobic digestion is performed as either a single or two-stage process with the transformation occurring in four phases beginning with hydrolysis, followed by acidogenesis, then acetogenesis, and finally ending with the methanogenesis [50, 124–126]. While anaerobic digestion can be conducted using a single reactor, or in sequential reactors; the choice between one or two reactors for the production of lactic acid and/or methane influences both microorganism selection and operating conditions [24].

7.4.1.1 Microorganisms

Microorganisms for lactic acid production from municipal solid wastes often include a mix of various lactic acid bacteria (LAB) [122, 127], and *S. cerevisiae* [120, 121]. Refer to Table 7.1 for a summary and Table 7.4 for more specifics.

7.4.1.1.1 Lactic Acid Bacteria (LAB)

LAB is a classification that encompasses a wide variety of bacterium that efficaciously produce lactic acid; the two genera encompassed by LAB are Enterococci and Lactobacilli [128, 129].

The Enterococci genus includes species that operate at higher temperatures than any currently known Lactobacilli strain [128, 129]. *Enterococcus faecium* has been studied in a scale-up operation from 3 L to 100 L. It was concluded that *E. faecium* was a feasible option for industrial uses with a pilot scale production rate of 3.91 g/L-h. The lab scale production rate was 4.96 g/L-h, but the slower rate in the pilot scale

Table 7.4 Lactic acid yields from various substrates

	Substrate	pH ¹ (C/ UC) ²	Residence time [h]	T [°C] (Mixing RPM)	Microorganism	Lactic Acid Production [g/L]	Yield [g/g – TS]	Ref.
Agricultural residues	Cassava Bagasse	6.5 (C)	60	37	<i>Lactobacillus casei</i>	83.8	96.3%	[132]
	Corn Stover	–	48	–	<i>Lactobacillus delbreuckii</i> <i>sp. bulgaricus</i>	18.0	–	[46]
OFMSW	Sugar Beet Pulp	5 (C)	48	37 (0)	<i>Lactobacillus delbreuckii</i> and <i>Lacto-</i> <i>bacillus plantarum</i>	–	–	[57]
	FW	6.25 (UC)	4 days	35 (200)	<i>Lactobacillus plantarum</i>	98.51	88.75%	[1]
OFMSW	6 (UC)	24	35 (0)	<i>Streptococcus</i> sp.	66.5	0.33	[24]	
	4.4 (UC)	7 days	37 (120)	Mixed culture	52	0.18	[50]	
	5 (C)	72	37 (0)	Methanogenic Sludge	20.7	0.36	[133]	
	5 (C)	168	37 (0)	Anaerobic Sludge	22.6	0.41		
	5 (C)	84	37 (0)	Non-sterilized FW	28.4	0.46		
	5 (C)	72	37 (150)	<i>Lactobacillus delbreuckii</i> dominated Mixed culture	29.9	–	[50]	
	6 (C)	19	52 (400)	<i>Bacillus coagulans</i>	60.7	0.91	[23]	

1: pH adjustment prior to fermentation

2: C—controlled pH throughout fermentation; UC—uncontrolled pH throughout fermentation

3: Yield reported in a gram product/kg sugars basis

was deemed a significant hurdle as the yield was not significantly different between the 3 L and 100 L scales [129].

Lactobacilli is the other main genus represented within LABs, spanning over 200 species of microorganisms [118]. With the abundance of species represented in LABs a versatility is present allowing operation anywhere from 2 °C to 53 °C as well as an ability to operate under many oxygenated states for growth [118].

7.4.1.1.2 *Saccharomyces cerevisiae*

S. cerevisiae can be engineered to produce D-lactic acid at a purity of 99.9% [46, 121]. The two enantiomeric forms of lactic acid that can be produced by fermentation are D and L forms of lactic acid. When used in the production of biologically derived plastics, L-lactic acid is more susceptible to thermal modifications at temperatures as low as 58 °C, lower than D-lactic acid [46, 128]. Furthermore, mixtures of D and L enantiomers of lactic acid can form an enhanced racemic crystal stereo-complex capable of increasing the melting temperature of the bioplastic by around 50 °C [130].

S. cerevisiae, combined with indigenous microorganism consortium within food waste, rich in *Enterococcus* spp., was used to determine the effectiveness of breaking down FW by measuring metabolite yield. The results showed that the use of both the indigenous consortium of bacteria and yeast together achieved metabolite yields of 81%, and the conclusion stated that this is a feasible combination of microorganisms to produce lactic acid through a more targeted fermentation than the one tested in this study [131].

7.4.1.2 Substrate Selection

Substrate selection for the production of lactic acid through anaerobic digestion is shown in Table 7.4. As can be seen in Table 7.4, mixed cultures are a popular choice for lactic acid production in the organic solid waste sector, with 55% of studies listed utilizing this approach. Interestingly, each of the reported pH values for this acidogenic fermentation are skewed acidic. It should also be noted that the results from the studies using specific organisms, and not mixed cultures, mostly achieved higher yields than any of the mixed culture studies reported here with the average lactic acid yield for single culture studies being 79.3 g/L and the average lactic acid yield for mixed cultures being 30.7 g/L.

7.4.1.3 Separations

Commonly used separation techniques for lactic acid include precipitation, solvent extraction, adsorption, distillation, electrodialysis, and nanofiltration [134–

136]. Section 7.4.1.3 will explore solvent extraction, electrodialysis, and nanofiltration as they have been applied to lactic acid produced from the substrates of interest.

Electrodialysis (ED) is a membrane separation technology that operates based on differences in electric potential of the solutes [134]. ED poses issues with scaling on the membrane, resulting in shorter membrane life or requires costly descaling techniques. To improve upon ED challenges, the coupling of nanofiltration membranes with electrodialysis or the use of anion-exchange membranes along with electrodialysis was explored and it was determined that both combinations resulted in greater deacidification, and demineralization, but these approaches are generally more energy intensive than more traditional electrodialysis configurations [134].

Solvent extraction is a liquid-liquid extraction technique used to isolate lactic acid post fermentation. Solvent extraction takes advantage of the solubility differences between extraction solvent and lactic acid. However, this extraction method is not often employed industrially due to the weaknesses that economically feasible solvents have demonstrated when separating lactic acid. Environmental impact can be addressed when choosing solvents for this liquid-liquid extraction; the lower miscibility is proportional to reductions in environmental impacts [136].

Nanofiltration has its merits individually in the separations of lactic acid, but it operates even better coupled with the other previously discussed extraction techniques. Nanofiltration is generally less energy intensive as it uses crossflow filtration which does not require as much energy input when compared to other separation techniques [134–136].

7.4.1.4 pH Control

Lactic acid was produced using three inocula under different pH values and procedures and it was determined that for the methanogenic sludge, the highest yield of lactic acid (20.7 g/L) was at pH 5 after 72 h compared to the same sludge producing 9.7 g/L of lactic acid after 144 h with uncontrolled pH [45]. The same methods were tested on anaerobic sludge and showed similar trends. The uncontrolled pH trial with anaerobic sludge produced 11.5 g/L of lactic acid after 120 h, versus the pH 5 trial with anaerobic sludge, producing 22.6 g/L after 84 h. The pH-controlled experiments were completed in a shortened time frame as compared to the uncontrolled experiments due to the noticeably faster rate of carbohydrate degradation [133].

7.4.2 Methane

Lactic acid production can be coupled with methane production (see Fig. 7.2) as the acidogenesis phase is a precursor in methane production. Section 7.4.2 will explore biodegradation of organic solid feedstocks used for the production of methane gas as part of the anaerobic digestion process.

7.4.2.1 Microorganisms

Methanogens are a class of archaea microorganisms known for the production of methane from organic acids [119, 137]. These archaea are a part of the phylum *Euryarchaeota*, consisting of seven orders: *Methanococcales*, *Methanobacteriales*, *Methanosarcinales*, *Methanomicrobiales*, *Methanopyrales*, *Methanocellales*, and *Methanomassiliicoccales* [119, 137].

The environments that methanogens can withstand are vast and diverse, but always anoxic [119, 137]. There have been reports of methanogens in extreme locations: hydrothermal vents and saline lakes; simple environments: rice fields and marshes; the feces of animals: cattle and horses; the human body: human feces and human dental plaques; man-made environments: landfills and biogas plants [137, 138].

Two of the more important parameters for biogas production are pH and temperature [119]. The temperature ranges that methanogens operate under are range from 4 °C to 65 °C. Values for pH in which the production of methane from methanogens is optimized is similarly large (between 5.1 and 9.5, with most methanogens exhibiting optimal production near neutral pH) [119].

7.4.2.2 Substrate Selection

Table 7.5 shows selected studies to produce methane from agricultural residues and OFMSW. Five aspects of the studies have been reported here: substrate used, the number of bioreactor stages used, hydraulic retention time (HRT), temperature, and yield. Note that Table 7.5 does not list microorganism information; this omission is intentional as methanogenic processes most often use mixed cultures and not specific organisms [21, 24, 50, 58, 139].

Table 7.5 Substrate yields for methane gas production

	Substrate	Stages	HRT (days)	Temperature (°C)	Yield (Nm ³ /kgvs)	Reference
Agricultural residues	Sugar Beet Molasses	2	–	–	7.43 L/working volume/day	[21]
	Sugar Beet Pulp	1	28	37	502.50 L /kg VS accumulated	[58]
OFMSW	FW	2	20	37	0.398	[24]
	OFMSW	1	–	33	73.2 m ³ /metric ton feedstock	[50]
	Wool Textile Waste	1	46	55	0.43	[139]

VS—volatile solids

HRT—hydraulic retention time

7.5 Technoeconomic Comparisons for Biodegradation Processes

Technoeconomic assessment (TEA) is often employed as a tool to compare nascent or inchoate processes to probe into potential trade-offs – both in terms of cost and energy use. TEA provides insight in early stages of process design and allows for early directional shifts if it is clear that a particular unit operation will be cost prohibitive for a conversion. While TEA is a useful prediction tool, it is not as widely reported as expected. Table 7.6 is included to demonstrate the dearth of TEA reports for organic wastes as feedstocks within biodegradation transformations. Of the multitude of studies published, only two were identified which included any economic information on the process. This lack of information indicates that further research is needed to demonstrate the potential utility – or lack thereof – for these types of feedstocks. A general assumption may be that since the feedstocks of interest are considered to be wastes, then the process will be profitable since material costs will be low. However, this is not necessarily the case and cursory TEA may indicate that a particular process may never be fruitful since yield or some other such variable might be too low to overcome. Food waste upgrading is best performed in a facility focused on producing a variety of products with more than one feedstock entering the facility [5].

7.6 Conclusions and Future Outlook

Use of organic wastes and agricultural residues as substrates to produce valuable chemical products is possible. While many substrates have specific challenges, these can be overcome through additional unit operations; ABE fermentation of cassava bagasse has been shown to produce upwards of 76 g/L of butanol when in situ separation techniques were applied as compared to 9.71 g/L without [31]. Not only are modifications to process configurations a possibility to for increasing production, genetic manipulations of the microorganisms themselves may prove most beneficial.

Increasing the tolerance to butanol within certain *Clostridium* bacteria for ABE fermentation or reducing required fermentation time are two of the most promising directions regarding microbial manipulations [150]. A significant focus on metabolic engineering has been to increase the butanol titers from ABE fermentation by modifications to *Clostridium cellulovorans* [99, 151], *Clostridium cellulolyticum* [150, 152], as well as genetic modifications of other *Clostridium* species. Metabolic engineering of *Clostridium cellulovorans* has focused on improving butanol titers for cellulosic biomass through consolidated bioprocessing (CBP) [99, 151]. Modifications to *Clostridium cellulovorans* can increase butanol production at least 138 times, from 0.025 g/L to 3.47 g/L after only 84 h, when using cellulose,

Table 7.6 Techno-economic analysis of biodegradation processes. Lack of economic results indicates need for analysis for moving research forward.

End Product	Fermentation Pathway	Microorganism Selection	Feedstock	Pretreatment	Yield	Initial Rate of Return	ROI	Payback Time	References
ABE	Standard ABE pathway	<i>Clostridium acetobutylicum</i>	Cotton Fibers	Phosphoric-acid-acetone, enzymatic hydrolysis	0.107	–	–	–	[2]
			MSW	Hammer mill, magnet separator, drum sieve, organosolv, enzymatic hydrolysis	0.102	–	–	–	[64]
			OFMSW	Hammer mill, magnet separator, drum sieve, organosolv, enzymatic hydrolysis	0.084	–	–	–	[108]
			Rice Straw	Enzymatic hydrolysis, alkaline pretreatment, phosphoric-acid-acetone	0.113	–	–	–	[52]
				Organosolv, enzymatic hydrolysis	0.080	–	–	–	[56]
				Phosphoric-acid-acetone, alkaline, enzymatic hydrolysis	0.113	–	–	–	[52]

		Waste Starch Medium	-	0.346	-	-	[340]
Standard ABE with <i>in situ</i> gas stripping	Cassava Bagasse	Enzymatic hydrolysis	0.250	-	-	-	[31]
	Industrial Juices of 75% Sugar Cane and 25% Sweet Sorghum	-	0.160	-	-	-	[115]
CBP	Corn Fiber Arabinoxylan	Integrated hydro- lysis, fermenta- tion, recovery process	0.440	-	-	-	[141]
SSF	Clostridium acetobutylicum with <i>S. cerevisiae</i>	Corn Stover Corn Flour	Pre-hydrolysis Enzymatic hydrolysis	0.180 0.347 ^a	-	-	[32]
	2-stage with <i>S. cerevisiae</i> added during solventogenesis		Enzymatic hydrolysis	0.240	-	-	[142]
CBP	<i>C. acetobutylicum</i> with <i>Thermoanaerobacterium</i> <i>thermosaccharolyticum</i>	Corn cob	-	0.260	-	-	[143]
Standard ABE Pathway	<i>Clostridium beijerinckii</i>	Barley Straw	Hammer mill, H_2SO_4 , NaOH, Enzymatic Hydrolysis	0.430 ^a	-	-	[61]
		Corn Stover	Hydrolysis	-	-	-	[144]
		Corn Stover and Switchgrass	Hydrolysis	0.260	-	-	[97]

(continued)

Table 7.6 (continued)

End Product	Fermentation Pathway	Microorganism Selection	Feedstock	Pretreatment	Yield	Initial Rate of Return	Payback Time	ROI	Payback Time	References
			Corncobs and Corn Steep Liquor	Grinding, Hydrolysis	0.300	–	–	–	–	[145]
		<i>Eucalyptus grandis</i> wood	<i>Eucalyptus grandis</i> wood	Steam Explosion	0.220	–	–	–	–	[55]
		P2 Medium	P2 Medium	–	0.240	–	–	–	–	[144]
		P2 Medium	P2 Medium	–	0.230	–	–	–	–	[146]
		Packing peanuts, apple droppings, cracked corn	Packing peanuts, apple droppings, cracked corn	Blended	9.8 g/L butanol	–	–	–	–	[109]
		Glucose	Glucose	–	0.470	–	–	–	–	[147]
		Pinewood, Timothy Grass, Wheat Straw	Pinewood, Timothy Grass, Wheat Straw	Air dried, pulverized, sieved, acid treatment, enzymatic hydrolysis	0.120	–	–	–	–	[107]
Standard ABE with <i>in situ</i> gas stripping										
Standard ABE with fibrous-bed bioreactor		<i>Clostridium tyrobutyricum</i>	Cassava Bagasse	Milled, hydrolysis	0.300	–	16.78%	6 years	–	[38]
Standard ABE Pathway		<i>Clostridium thermocellum</i> and <i>Clostridium saccharoperbutylacetonicum</i>	Rice Straw	Alkaline (NaOH)	0.140	–	–	–	–	[42]
	Fed Batch		Food Waste	Crushed	29.9 g/L	–	–	–	–	[148]

Lactic acid	<i>Lactobacillus delbrueckii</i> dominated mixed culture						
	<i>Lactobacillus casei</i>	Cassava Bagasse	—	81.9 g/L	—	—	[132]
	<i>Lactobacillus delbrueckii</i> sp. <i>bulgaricus</i>	Corn Stover	Sulfuric acid, hydrochloric acid, sieved, crushed, enzymatic hydrolysis	18 g/L	—	—	[46]
	<i>Lactobacillus plantarum</i>	Food Waste	Homogenized	98.51 g/L	—	—	[1]
	<i>Lactobacillus delbrueckii</i> and <i>Lactobacillus plantarum</i>	Sugar Beet Pulp	Enzymatic Hydrolysis	58.39 g/L	—	—	[57]
Two-phase AD	Mixed Culture	OFMSW	Hydrothermal	—	—	—	[50]
	<i>Streptococcus</i> sp.	Food Waste	Blended	0.290	—	—	[24]
Not Specified	Anaerobic Sludge	Food Waste	—	0.410	—	—	[133]
	<i>Lactobacillus casei</i> Shirota	Pulverized, microbial pretreatment by <i>Aspergillus</i>	0.920	31.1%	22.9%	5.1 years	[149]
Methane	Methanogenic Sludge		—	0.360	—	—	[133]
	Non-sterilized FW		—	0.460	—	—	[133]
	<i>Bacillus coagulans</i>	OFMSW	Enzymatic Hydrolysis	60.7 g/L	—	—	[133]
Methane	<i>Rhizopus oryzae</i>	Potato Starch	Shredded	0.300	—	—	[117]
	—	Food Waste	—	0.90 Nm ³ / kg _{VS}	—	—	[24]
	Mixed Culture	OFMSW	Hydrothermal	0.59 L biogas/g _{VS}	—	—	[50]
Methane	Activated Sludge	Sugar Beet Molasses	—	743 L-CH ₄ /	—	—	[21]

(continued)

Table 7.6 (continued)

End Product	Fermentation Pathway	Microorganism Selection	Feedstock	Pretreatment	Yield	Initial Rate of Return	Payback Time	References
					working volume/day			
					502.50 L-CH ₄ /kg _{vfs}	–	–	[58]
					0.43 N m ³ /kg _{vfs}	–	–	[139]

ABE—acetone-butanol-ethanol

AD—anaerobic digestion

CBP—consolidated bioprocessing

MSW—municipal solid waste

OFMSW—organic fraction of municipal solid waste

SSF—simultaneous saccharification and fermentation

^aABE yield

indicating that genetic manipulations of this organism show enough potential for additional investigation with a lower-cost feedstock [99].

The use of *Clostridium cellulolyticum* could be advantageous for the lignocellulosic agricultural residues, such as rice straw, due to its ability to digest the lignin [152]. However, proof-of-concept studies for *Clostridium cellulolyticum* show limited potential; sometimes only achieving a titer of 0.04 g/L up to 0.12 g/L of butanol [150, 152].

The combination of *Thermoanaerobacterium thermosaccharolyticum* and *Clostridium acetobutylicum* was studied to determine their ability to produce butanol from hemicellulose and with 13.28 g/L of butanol produced, the concept was promising enough to explore with food waste, namely corncob [153]. With untreated corncob, CBP produced 7.61 g/L of butanol, signifying an advance in the field of butanol production through fermentation sans pretreatment [153, 154]. However, there remains many routes for expanding the use of biodegradation of agricultural residues or OFMSW.

An engineered strain of *Clostridium beijerinckii* was used on corn stover hydrolysate to increase the production in the solventogenic phase of ABE fermentation showing comparable results, of 20.7 g/L total solvents, to the solventogenic production when using corn alone as feedstock [154]. The histidine kinases in *C. beijerinckii* were altered to increase butanol titer and production rate, concluding that deletion of *cbeT2073*, a histidine kinase coding region, increased production rate by 40% and increased the butanol biosynthesis by 40.8%, from 9.8 g/L to 13.8 g/L of butanol [144]. This provides evidence of the role in histidine kinase in butanol production and provides insight into specific strategies moving forward in metabolic engineering of *Clostridium* strains for enhanced butanol production.

When anaerobic digestion is used, the production of lactic acid and methane generally rely on the use of a consortia of microorganisms rather than a specific strain like that of ABE fermentations. For this reason, only minimal effort has been spared with respect to strain development. Though there is significant attention paid to research in mixed microbial communities [57, 88, 155]. In the coming years, significant attention on the economic feasibility of biodegradation processes of organic wastes should be given. Economic potential and profitability are seminal for commercialization of these potentially valuable feedstocks.

References

1. Ye Z-L, Lu M, Zheng Y, Li Y-H, Cai W-M. Lactic acid production from dining-hall food waste by *Lactobacillus plantarum* using response surface methodology. *J Chem Technol Biotechnol*. 2008;83:1541–50. <https://doi.org/10.1002/jctb.1968>.
2. Seifollahi M, Amiri H. Phosphoric acid-acetone process for cleaner production of acetone, butanol, and ethanol from waste cotton fibers. *J Clean Prod*. 2018;193:459–70. <https://doi.org/10.1016/j.jclepro.2018.05.093>.
3. Oak Ridge National Laboratory. 2016 billion-ton report. U.S. Department of Energy; 2016. <https://doi.org/10.1089/ind.2016.29051.doe>.

4. American Society of Civil Engineers. ASCE's 2021 infrastructure report card: solid waste, 2021.
5. Engelberth AS. Evaluating economic potential of food waste valorization: Onward to a diverse feedstock biorefinery. *Green Sustain Chem.* 2020;1–6:100385. <https://doi.org/10.1016/j.cogsc.2020.100385>.
6. Xu Q, Qin J, Ko JH. Municipal solid waste landfill performance with different biogas collection practices: Biogas and leachate generations. *J Clean Prod.* 2019;222:446–54. <https://doi.org/10.1016/j.jclepro.2019.03.083>.
7. Laurent A, Bakas I, Clavreul J, Bernstad A, Niero M, Gentil E, Hauschild MZ, Christensen TH. Review of LCA studies of solid waste management systems—Part I: Lessons learned and perspectives. *Waste Manag.* 2014;34(3):573–88. <https://doi.org/10.1016/j.wasman.2013.10.045>.
8. Giusti L. A review of waste management practices and their impact on human health. *Waste Manag.* 2009;29(8):2227–39. <https://doi.org/10.1016/j.wasman.2009.03.028>.
9. John RP. Chapter 11: Biotechnological potentials of Cassava Bagasse. In: Pandey A, Nigam PS-N, editors. *Biotechnology for agro-industrial residues utilisation.* Dordrecht: Springer; 2009. p. 225–37. <https://doi.org/10.1007/978-1-4020-9942-7>.
10. Food and Agriculture Organization of the United Nations. Cassava Production Globally, 2019, from <http://www.fao.org/faostat/en/#data/QC>, accessed 3-5-2021.
11. Parmar A, Sturm B, Hensel O. Crops that feed the world: Production and improvement of cassava for food, feed, and industrial uses. *Food Security.* 2017;9(5):907–27. <https://doi.org/10.1007/s12571-017-0717-8>.
12. Teixeira EDM, Pasquini D, Curvelo AAS, Corradini E, Belgacem MN, Dufresne A. Cassava bagasse cellulose nanofibrils reinforced thermoplastic cassava starch. *Carbohydr Polym.* 2009;78(3):422–31. <https://doi.org/10.1016/j.carbpol.2009.04.034>.
13. van Hung N, Maguyon-Detras MC, Migo MV, Quilloy R, Balingbing C, Chivenge P, Gummert M. Rice straw overview: availability, properties, and management practices. In: Gummert M, van Hung N, Chivenge P, Douthwaite B, editors. *Sustainable rice straw management.* Cham: Springer International Publishing; 2020. p. 1–13. https://doi.org/10.1007/978-3-030-32373-8_1.
14. González-García S, Morales PC, Gullón B. Estimating the environmental impacts of a brewery waste-based biorefinery: Bio-ethanol and xylooligosaccharides joint production case study. *Ind Crop Prod.* 2018;123:331–40. <https://doi.org/10.1016/j.indcrop.2018.07.003>.
15. Garcia-Garcia G, Rahimifard S. Life-cycle environmental impacts of barley straw valorisation. *Resources Conserv Recycl.* 2019;149:1–11. <https://doi.org/10.1016/j.resconrec.2019.05.026>.
16. Office of Energy Efficiency & Renewable Energy. (2019). Waste-to-energy from municipal solids wastes, U. S. Department of Energy.
17. Alibardi L, Cossu R. Composition variability of the organic fraction of municipal solid waste and effects on hydrogen and methane production potentials. *Waste Manag.* 2015;36:147–55. <https://doi.org/10.1016/j.wasman.2014.11.019>.
18. Maitah M, Řezbová H, Smutka L, Tomšík K. European sugar production and its control in the world market. *Sugar Tech.* 2016;18(3):236–41. <https://doi.org/10.1007/s12355-016-0439-9>.
19. Alexandri M, Schneider R, Papapostolou H, Ladakis D, Koutinas A, Venus J. Restructuring the conventional sugar beet industry into a novel biorefinery: fractionation and bioconversion of sugar beet pulp into succinic acid and value-added coproducts. *ACS Sustain Chem Eng.* 2019;7(7):6569–79. <https://doi.org/10.1021/acssuschemeng.8b04874>.
20. Cheesman OD. Use and impacts of by-products. In: Environmental impacts of sugar production: the cultivation and processing of sugarcane and sugar beet. Wallingford, UK: CABI Publishing; 2004. p. 151–72. <https://doi.org/10.1079/9780851999814.0151>.
21. Chojnacka A, Szczęsny P, Błaszczyk MK, Zielenkiewicz U, Detman A, Salamon A, Sikora A. Noteworthy facts about a methane-producing microbial community processing acidic effluent from sugar beet molasses fermentation. *PLoS One.* 2015;10(5):1–23. <https://doi.org/10.1371/journal.pone.0128008>.

22. Kim S, Dale BE, Jenkins R. Life cycle assessment of corn grain and corn stover in the United States. *Int J Life Cycle Assess.* 2009;14(2):160–74. <https://doi.org/10.1007/s11367-008-0054-4>.
23. López-Gómez JP, Latorre-Sánchez M, Unger P, Schneider R, Coll Lozano C, Venus J. Assessing the organic fraction of municipal solid wastes for the production of lactic acid. *Biochem Eng J.* 2019;150:107251. <https://doi.org/10.1016/j.bej.2019.107251>.
24. Demichelis F, Pleissner D, Fiore S, Mariano S, Navarro Gutiérrez IM, Schneider R, Venus J. Investigation of food waste valorization through sequential lactic acid fermentative production and anaerobic digestion of fermentation residues. *Bioresour Technol.* 2017;241:508–16. <https://doi.org/10.1016/j.biortech.2017.05.174>.
25. Gutberlet J. Cooperative urban mining in Brazil: collective practices in selective household waste collection and recycling. *Waste Manag.* 2015;45:22–31. <https://doi.org/10.1016/j.wasman.2015.06.023>.
26. Office of Energy Efficiency & Renewable Energy. Agricultural residues and energy crops. U.S. Department of Energy; 2016.
27. Azam M, Jahromy SS, Raza W, Raza N, Lee SS, Kim KH, Winter F. Status, characterization, and potential utilization of municipal solid waste as renewable energy source: Lahore case study in Pakistan. *Environ Int.* 2019;134:105291. <https://doi.org/10.1016/j.envint.2019.105291>.
28. Hu Y, Du C, Pensupa N, Lin CSK. Optimisation of fungal cellulase production from textile waste using experimental design. *Process Saf Environ Prot.* 2018;118:133–42. <https://doi.org/10.1016/j.psep.2018.06.009>.
29. Hu Y, Du C, Leu SY, Jing H, Li X, Lin CSK. Valorisation of textile waste by fungal solid state fermentation: an example of circular waste-based biorefinery. *Resources Conserv Recycl.* 2018;129:27–35. <https://doi.org/10.1016/j.resconrec.2017.09.024>.
30. EPA. (n.d.). 1960–2018 Data on Textiles in MSW by Weight (in thousands of U.S. tons), from <https://www.epa.gov/facts-and-figures-about-materials-waste-and-recycling/textiles-material-specific-data>. Accessed 1-5-2020.
31. Lu C, Zhao J, Yang ST, Wei D. Fed-batch fermentation for n-butanol production from cassava bagasse hydrolysate in a fibrous bed bioreactor with continuous gas stripping. *Bioresour Technol.* 2012;104:380–7. <https://doi.org/10.1016/j.biortech.2011.10.089>.
32. Wu Y, Wang Z, Ma X, Xue C. High temperature simultaneous saccharification and fermentation of corn stover for efficient butanol production by a thermotolerant *Clostridium acetobutylicum*. *Process Biochem.* 2021;100:20–5. <https://doi.org/10.1016/j.procbio.2020.09.026>.
33. Al-Shorgani NKN, Kalil MS, Yusoff WMW, Hamid AA. Impact of pH and butyric acid on butanol production during batch fermentation using a new local isolate of *Clostridium acetobutylicum* YM1. *Saudi J Biol Sci.* 2018;25(2):339–48. <https://doi.org/10.1016/j.sjbs.2017.03.020>.
34. Jin Q, Qureshi N, Wang H, Huang H. Acetone-butanol-ethanol (ABE) fermentation of soluble and hydrolyzed sugars in apple pomace by *Clostridium beijerinckii* P260. *Fuel.* 2019;244: 536–44. <https://doi.org/10.1016/J.FUEL.2019.01.177>.
35. Mutschlechner O, Swoboda H, Gapes JR. Continuous two-stage ABE-fermentation using *Clostridium beijerinckii* HRRL B592 operating with a growth rate in the first stage vessel close to its maximal value. *J Mol Microbiol Biotechnol.* 2000;2(1):101–5.
36. Lépez-Aguilar L, Rodríguez-Rodríguez CE, Arias ML, Lutz G, Ulate W. Butanol production by *Clostridium beijerinckii* BA101 using cassava flour as fermentation substrate: enzymatic versus chemical pretreatments. *World J Microbiol Biotechnol.* 2011;27(8):1933–9. <https://doi.org/10.1007/s11274-010-0630-1>.
37. Li L, Ai H, Zhang S, Li S, Liang Z, Wu ZQ, Yang ST, Wang JF. Enhanced butanol production by coculture of *Clostridium beijerinckii* and *Clostridium tyrobutyricum*. *Bioresour Technol.* 2013;143:397–404. <https://doi.org/10.1016/J.BIORTECH.2013.06.023>.
38. Huang J, Du Y, Bao T, Lin M, Wang J, Yang ST. Production of n-butanol from cassava bagasse hydrolysate by engineered *Clostridium tyrobutyricum* overexpressing adhE2: kinetics

- and cost analysis. *Bioresour Technol.* 2019;292:121969. <https://doi.org/10.1016/j.biortech.2019.121969>.
39. Zhang J, Zong W, Hong W, Zhang ZT, Wang Y. Exploiting endogenous CRISPR-Cas system for multiplex genome editing in *Clostridium tyrobutyricum* and engineer the strain for high-level butanol production. *Metab Eng.* 2018;47:49–59. <https://doi.org/10.1016/J.YMBEN.2018.03.007>.
40. Nakayama S, Kiyoshi K, Kadokura T, Nakazato A. Butanol production from crystalline cellulose by Cocultured *Clostridium thermocellum* and *Clostridium saccharoperbutylacetonicum* N1-4. *Appl Environ Microbiol.* 2011;77(18):6470–5. <https://doi.org/10.1128/AEM.00706-11>.
41. Thang VH, Kanda K, Kobayashi G. Production of Acetone-Butanol-Ethanol (ABE) in direct fermentation of cassava by *Clostridium saccharoperbutylacetonicum* N1-4. *Appl Biochem Biotechnol.* 2010;161(1–8):157–70. <https://doi.org/10.1007/s12010-009-8770-1>.
42. Kiyoshi K, Furukawa M, Seyama T, Kadokura T, Nakazato A, Nakayama S. Butanol production from alkali-pretreated rice straw by co-culture of *Clostridium thermocellum* and *Clostridium saccharoperbutylacetonicum*. *Bioresour Technol.* 2015;186:325–8. <https://doi.org/10.1016/j.biortech.2015.03.061>.
43. Payot T, Chemaly Z, Fick M. Lactic acid production by *Bacillus coagulans*—kinetic studies and optimization of culture medium for batch and continuous fermentations. *Enzyme Microb Technol.* 1999;24(3–4):191–9. [https://doi.org/10.1016/S0141-0229\(98\)00098-2](https://doi.org/10.1016/S0141-0229(98)00098-2).
44. Cubas-Cano E, Venus J, González-Fernández C, Tomás-Pejó E. Assessment of different *Bacillus coagulans* strains for l-lactic acid production from defined media and gardening hydrolysates: Effect of lignocellulosic inhibitors. *J Biotechnol.* 2020;323:9–16. <https://doi.org/10.1016/J.JBIOTEC.2020.07.017>.
45. Hujanen M, Linko YY. Effect of temperature and various nitrogen sources on L (+)-lactic acid production by *Lactobacillus casei*. *Appl Microbiol Biotechnol.* 1996;45(3):307–13. <https://doi.org/10.1007/s002530050688>.
46. Wang X, Wang G, Yu X, Chen H, Sun Y, Chen G. Pretreatment of corn stover by solid acid for D-lactic acid fermentation. *Bioresour Technol.* 2017;239:490–5. <https://doi.org/10.1016/j.biortech.2017.04.089>.
47. Mussatto SI, Dragone GM. Biomass pretreatment, biorefineries, and potential products for a bioeconomy development. In: Biomass fractionation technologies for a lignocellulosic feedstock based biorefinery. Elsevier Inc.; 2016. p. 1–22. <https://doi.org/10.1016/B978-0-12-802323-5.00001-3>.
48. Yang B, Wyman CE. Pretreatment: the key to unlocking low-cost cellulosic ethanol. *Biofuels Bioprod Biorefining.* 2007;6(3):246–56. <https://doi.org/10.1002/bbb.49>.
49. Ziemiński K, Kowalska-Wentel M. Effect of different sugar beet pulp pretreatments on biogas production efficiency. *Appl Biochem Biotechnol.* 2017;181(3):1211–27. <https://doi.org/10.1007/s12010-016-2279-1>.
50. Li W, Guo J, Cheng H, Wang W, Dong R. Two-phase anaerobic digestion of municipal solid wastes enhanced by hydrothermal pretreatment: viability, performance and microbial community evaluation. *Appl Energy.* 2017;189:613–22. <https://doi.org/10.1016/j.apenergy.2016.12.101>.
51. Lomovsky O, Bychkov A, Lomovsky I. Mechanical pretreatment. In: Mussatto SI, editor. Biomass fractionation technologies for a lignocellulosic feedstock based biorefinery. Amsterdam: Elsevier; 2016. p. 23–55. <https://doi.org/10.1016/B978-0-12-802323-5.00002-5>.
52. Moradi F, Amiri H, Soleimanian-Zad S, Ehsani MR, Karimi K. Improvement of acetone, butanol and ethanol production from rice straw by acid and alkaline pretreatments. *Fuel.* 2013;112:8–13. <https://doi.org/10.1016/j.fuel.2013.05.011>.
53. Yang M, Kuittinen S, Zhang J, Vepsäläinen J, Keinänen M, Pappinen A. Co-fermentation of hemicellulose and starch from barley straw and grain for efficient pentoses utilization in acetone-butanol-ethanol production. *Bioresour Technol.* 2015;179:128–35. <https://doi.org/10.1016/j.biortech.2014.12.005>.

54. Luo H, Zeng Q, Han S, Wang Z, Dong Q, Bi Y, Zhao Y. High-efficient n-butanol production by co-culturing *Clostridium acetobutylicum* and *Saccharomyces cerevisiae* integrated with butyrate fermentative supernatant addition. *World J Microbiol Biotechnol.* 2017;33(4) <https://doi.org/10.1007/s11274-017-2246-1>.
55. Cebrieros F, Rizzo F, Cagno M, Cabrera MN, Rochón E, Jauregui G, Boix E, Böthig S, Ferrari MD, Lareo C. Enhanced production of butanol and xylosaccharides from *Eucalyptus grandis* wood using steam explosion in a semi-continuous pre-pilot reactor. *Fuel.* 2020;290 <https://doi.org/10.1016/j.fuel.2020.119818>.
56. Amiri H, Karimi K, Zilouei H. Organosolv pretreatment of rice straw for efficient acetone, butanol, and ethanol production. *Bioresour Technol.* 2014;152:450–6. <https://doi.org/10.1016/j.biortech.2013.11.038>.
57. Berlowska J, Cieciura W, Borowski S, Dudkiewicz M, Binczarski M, Witonska I, Otlewska A, Kregiel D. Simultaneous saccharification and fermentation of sugar beet pulp with mixed bacterial cultures for lactic acid and propylene glycol production. *Molecules.* 2016;21(10) <https://doi.org/10.3390/molecules21101380>.
58. Ziemiński K, Romanowska I, Kowalska-Wentel M, Cyran M. Effects of hydrothermal pretreatment of sugar beet pulp for methane production. *Bioresour Technol.* 2014;166:187–93. <https://doi.org/10.1016/j.biortech.2014.05.021>.
59. Lin YS, Lee WC, Duan KJ, Lin YH. Ethanol production by simultaneous saccharification and fermentation in rotary drum reactor using thermotolerant *Kluveromyces marxianus*. *Appl Energy.* 2013;105:389–94. <https://doi.org/10.1016/j.apenergy.2012.12.020>.
60. Benazzi T, Calgaroto S, Astolfi V, Dalla Rosa C, Oliveira JV, Mazutti MA. Pretreatment of sugarcane bagasse using supercritical carbon dioxide combined with ultrasound to improve the enzymatic hydrolysis. *Enzyme Microb Technol.* 2013;52(4–5):247–50. <https://doi.org/10.1016/j.enzmictec.2013.02.001>.
61. Qureshi N, Saha BC, Dien B, Hector RE, Cotta MA. Production of butanol (a biofuel) from agricultural residues: Part I—Use of barley straw hydrolysate. *Biomass Bioenergy.* 2010;34(4):559–65. <https://doi.org/10.1016/j.biombioe.2009.12.024>.
62. Chu CY, Wu SY, Tsai CY, Lin CY. Kinetics of cotton cellulose hydrolysis using concentrated acid and fermentative hydrogen production from hydrolysate. *Int J Hydrogen Energy.* 2011;36, Pergamon:8743–50. <https://doi.org/10.1016/j.ijhydene.2010.07.072>.
63. Gikas P, Zhu B, Batistatos NI, Zhang R. Evaluation of the rotary drum reactor process as pretreatment technology of municipal solid waste for thermophilic anaerobic digestion and biogas production. *J Environ Manage.* 2018;216:96–104. <https://doi.org/10.1016/j.jenvman.2017.07.050>.
64. Farmanbordar S, Amiri H, Karimi K. Simultaneous organosolv pretreatment and detoxification of municipal solid waste for efficient biobutanol production. *Bioresour Technol.* 2018;270:236–44. <https://doi.org/10.1016/j.biortech.2018.09.017>.
65. Shahriari H, Warith M, Hamoda M, Kennedy KJ. Anaerobic digestion of organic fraction of municipal solid waste combining two pretreatment modalities, high temperature microwave and hydrogen peroxide. *Waste Manag.* 2012;32(1):41–52. <https://doi.org/10.1016/j.wasman.2011.08.012>.
66. Gholamzad E, Karimi K, Masoomi M. Effective conversion of waste polyester-cotton textile to ethanol and recovery of polyester by alkaline pretreatment. *Chem Eng J.* 2014;253:40–5. <https://doi.org/10.1016/j.cej.2014.04.109>.
67. Lee KM, Hong JY, Tey WY. Combination of ultrasonication and deep eutectic solvent in pretreatment of lignocellulosic biomass for enhanced enzymatic saccharification. *Cellulose.* 2021;28(3):1513–26. <https://doi.org/10.1007/s10570-020-03598-5>.
68. Elbeshbishy E, Nakhla G. Comparative study of the effect of ultrasonication on the anaerobic biodegradability of food waste in single and two-stage systems. *Bioresour Technol.* 2011;102(11):6449–57. <https://doi.org/10.1016/j.biortech.2011.03.082>.
69. Izumi K, Okishio YK, Nagao N, Niwa C, Yamamoto S, Toda T. Effects of particle size on anaerobic digestion of food waste. *Int Biodeter Biodegr.* 2010;64(7):601–8. <https://doi.org/10.1016/j.ibiod.2010.06.013>.

70. Mani S, Tabil LG, Sokhansanj S. Grinding performance and physical properties of wheat and barley straws, corn stover and switchgrass. *Biomass Bioenergy*. 2004;27(4):339–52. <https://doi.org/10.1016/j.biombioe.2004.03.007>.
71. Mikulski D, Kłosowski G, Menka A, Koim-Puchowska B. Microwave-assisted pretreatment of maize distillery stillage with the use of dilute sulfuric acid in the production of cellulosic ethanol. *Bioresour Technol*. 2019;278:318–28. <https://doi.org/10.1016/j.biortech.2019.01.068>.
72. Mishra P, ab Wahid Z, Singh L, Zaid RM, Tabassum S, Sakinah M, Jiang X. Synergistic effect of ultrasonic and microwave pretreatment on improved biohydrogen generation from palm oil mill effluent. *Biomass Convers Biorefinery*. 2021; <https://doi.org/10.1007/s13399-021-01285-4>.
73. Rudakiya DM. Strategies to improve solid-state fermentation technology. In: New and future developments in microbial biotechnology and bioengineering: from cellulose to cellulase: strategies to improve biofuel production; 2019. p. 155–80. <https://doi.org/10.1016/B978-0-444-64223-3.00010-2>.
74. Pessoa M, Sobrinho MAM, Kraume M. The use of biomagnetism for biogas production from sugar beet pulp. *Biochem Eng J*. 2020;164:107770. <https://doi.org/10.1016/j.bej.2020.107770>.
75. Brodeur G, Yau E, Badal K, Collier J, Ramachandran KB, Ramakrishnan S. Chemical and physicochemical pretreatment of lignocellulosic biomass: a review. *Enzyme Res*. 2011; <https://doi.org/10.4061/2011/787532>.
76. Li H, Kim NJ, Jiang M, Kang JW, Chang HN. Simultaneous saccharification and fermentation of lignocellulosic residues pretreated with phosphoric acid-acetone for bioethanol production. *Bioresour Technol*. 2009;100(13):3245–51. <https://doi.org/10.1016/j.biortech.2009.01.021>.
77. Carrere H, Antonopoulou G, Affes R, Passos F, Battimelli A, Lyberatos G, Ferrer I. Review of feedstock pretreatment strategies for improved anaerobic digestion: from lab-scale research to full-scale application. *Bioresour Technol*, Elsevier Ltd., 2016:386–97. <https://doi.org/10.1016/j.biortech.2015.09.007>.
78. Schacht C, Zetzl C, Brunner G. From plant materials to ethanol by means of supercritical fluid technology. *J Supercrit Fluids*, Elsevier. 2008;299–321. <https://doi.org/10.1016/j.supflu.2008.01.018>.
79. Gu T, Held MA, Faik A. Supercritical CO₂ and ionic liquids for the pretreatment of lignocellulosic biomass in bioethanol production. *Environ Technol (United Kingdom)*. 2013;34(13–14):1735–49. <https://doi.org/10.1080/09593330.2013.809777>.
80. Ng CH, He J, Yang KL. Purification and characterization of a GH11 Xylanase from biobutanol-producing *Clostridium beijerinckii* G117. *Appl Biochem Biotechnol*. 2015;175(6):2832–44. <https://doi.org/10.1007/s12010-014-1470-5>.
81. Jouzani GS, Taherzadeh MJ. Advances in consolidated bioprocessing systems for bioethanol and butanol production from biomass: a comprehensive review. *Biofuel Res J*. 2015;2(1):152–95. <https://doi.org/10.18331/BRJ2015.2.1.4>.
82. Singh-Nee Nigam, P.; Pandey, A.; Gupta, N. (2009). Chapter 2: Pre-treatment of agro-industrial residues. In: P. Singh-Nee Nigam, A. Pandey (Eds.), *Biotechnology for agro-industrial residues utilisation* utilisation of agro-residues, Dordrecht, pp. 13–33.
83. Paquet V, Croux C, Goma G, Soucaille P. Purification and characterization of the extracellular α-amylase from *Clostridium acetobutylicum* ATCC 824. *Appl Environ Microbiol*. 1991;57(1):212–8. <https://doi.org/10.1128/aem.57.1.212-218.1991>.
84. Szymanowska-Połańska D, Orczyk D, Leja K. Biotechnological potential of *Clostridium butyricum* bacteria. *Braz J Microbiol*. 2014;45(3):892–901. <https://doi.org/10.1590/S1517-83822014000300019>.
85. Cai J, Wang R, Wu Q, Wang G, Deng C. Characterization of a hydrogen-producing bacterium *Clostridium* sp. 5A-1. *Int J Green Energy*. 2021; <https://doi.org/10.1080/15435075.2021.1875469>.
86. Ahmad A, Banat F, Taher H. A review on the lactic acid fermentation from low-cost renewable materials: recent developments and challenges. *Environ Technol Innov*. 2020;20:101138. <https://doi.org/10.1016/j.eti.2020.101138>.

87. Veza I, Muhamad Said MF, Latiff ZA. Recent advances in butanol production by acetone-butanol-ethanol (ABE) fermentation. *Biomass Bioenergy*. 2021;144:105919. <https://doi.org/10.1016/j.biombioe.2020.105919>.
88. Valdez-Vazquez I, Sanchez A. Proposal for biorefineries based on mixed cultures for lignocellulosic biofuel production: a techno-economic analysis, *Biofuels*. *Bioprod Biorefining*. 2018;12(1):56–67. <https://doi.org/10.1002/bbb.1828>.
89. Xue C, Zhao J, Chen L, Yang ST, Bai F. Recent advances and state-of-the-art strategies in strain and process engineering for biobutanol production by *Clostridium acetobutylicum*. *Biotechnol Adv.* 2017;35(2):310–22. <https://doi.org/10.1016/j.biotechadv.2017.01.007>.
90. Uçkun Kiran E, Trzciński AP, Liu Y. Platform chemical production from food wastes using a biorefinery concept. *J Chem Technol Biotechnol*. 2015;90(8):1364–79. <https://doi.org/10.1002/jctb.4551>.
91. Detman A, Chojnacka A, Mielecki D, Błaszczyk MK, Sikora A. Inhibition of hydrogen-yielding dark fermentation by ascomycetous yeasts. *Int J Hydrogen Energy*. 2018;43(24):10967–79. <https://doi.org/10.1016/j.ijhydene.2018.05.004>.
92. Zakaria ZA, Boopathy R, Dib JR, editors. *Valorisation of agro-industrial residues – Volume I: Biological approaches*. 1st ed; 2020.
93. Bharathiraja B, Jayamuthunagai J, Sudharsanaa T, Bharghavi A, Praveenkumar R, Chakravarthy M, Devarajan Y. Biobutanol – an impending biofuel for future: a review on upstream and downstream processing techniques. *Renew Sustain Energy Rev.* 2017;68:788–807. <https://doi.org/10.1016/j.rser.2016.10.017>.
94. Swidah R, Ogundabi O, Grant CM, Ashe MP. n-Butanol production in *S. cerevisiae*: co-ordinate use of endogenous and exogenous pathways. *Appl Microbiol Biotechnol*. 2018;102(22):9857–66. <https://doi.org/10.1007/s00253-018-9305-x>.
95. Moon HG, Jang YS, Cho C, Lee J, Binkley R, Lee SY. One hundred years of clostridial butanol fermentation. *FEMS Microbiol Lett*. 2016;363(3) <https://doi.org/10.1093/femsle/fnw001>.
96. Swidah R, Wang H, Reid PJ, Ahmed HZ, Pisanelli AM, Persaud KC, Grant CM, Ashe MP. Butanol production in *S. cerevisiae* via a synthetic ABE pathway is enhanced by specific metabolic engineering and butanol resistance. *Biotechnol Biofuels*. 2015;8(1):1–9. <https://doi.org/10.1186/s13068-015-0281-4>.
97. Qureshi N, Saha BC, Hector RE, Dien B, Hughes S, Liu S, Iten L, Bowman MJ, Sarah G, Cotta MA. Production of butanol (a biofuel) from agricultural residues: Part II—Use of corn stover and switchgrass hydrolysates. *Biomass Bioenergy*. 2010;34(4):566–71. <https://doi.org/10.1016/j.biombioe.2009.12.023>.
98. Ibrahim MF, Ramli N, Kamal Bahrin E, Abd-Aziz S. Cellulosic biobutanol by Clostridia: challenges and improvements. *Renew Sustain Energy Rev.*, Elsevier Ltd. 2017;1241–54. <https://doi.org/10.1016/j.rser.2017.05.184>.
99. Yang X, Xu M, Yang ST. Metabolic and process engineering of *Clostridium cellulovorans* for biofuel production from cellulose. *Metab Eng.* 2015;32:39–48. <https://doi.org/10.1016/j.ymben.2015.09.001>.
100. Müller B, Grossniklaus U. Model organisms: a historical perspective. *J Proteomics*. Elsevier. 2010;2054–63. <https://doi.org/10.1016/j.jprot.2010.08.002>.
101. Dong H, Zhao C, Zhang T, Zhu H, Lin Z, Tao W, Zhang Y, Li Y. A systematically chromosomally engineered *Escherichia coli* efficiently produces butanol. *Metab Eng.* 2017;44:284–92. <https://doi.org/10.1016/j.ymben.2017.10.014>.
102. Galazzo JL, Bailey JE. Fermentation pathway kinetics and immobilized *Saccharomyces cerevisiae*. *Enzyme Microbial Technol*. 1990;12(3):162–72.
103. Lin Y, Zhang W, Li C, Sakakibara K, Tanaka S, Kong H. Factors affecting ethanol fermentation using *Saccharomyces cerevisiae* BY4742. *Biomass Bioenergy*. 2014;47:395–401. <https://doi.org/10.1016/j.biombioe.2012.09.019>.
104. Patnaik PR. Oscillatory metabolism of *Saccharomyces cerevisiae*: an overview of mechanisms and models. *Biotechnol Adv.* Elsevier Inc., 2003;183–92. [https://doi.org/10.1016/S0734-9750\(03\)00022-3](https://doi.org/10.1016/S0734-9750(03)00022-3).

105. Lau MW, Dale BE. Cellulosic ethanol production from AFEX-treated corn stover using *Saccharomyces cerevisiae* 424A(LNH-ST). Proc Natl Acad Sci U S A. 2009;106(5):1368–73. <https://doi.org/10.1073/pnas.0812364106>.
106. Jin H, Liu R, He Y. Kinetics of batch fermentations for ethanol production with immobilized *Saccharomyces cerevisiae* growing on Sweet Sorghum Stalk Juice. Procedia Environ Sci. 2012;12:137–45. <https://doi.org/10.1016/j.proenv.2012.01.258>.
107. Nanda S, Dalai AK, Kozinski JA. Butanol and ethanol production from lignocellulosic feedstock: biomass pretreatment and bioconversion. Energy Sci Eng. 2014;2(3):138–48. <https://doi.org/10.1002/ese3.41>.
108. Farmanbordar S, Karimi K, Amiri H. Municipal solid waste as a suitable substrate for butanol production as an advanced biofuel. Energy Convers Manage. 2017;157:396–408. <https://doi.org/10.1016/j.enconman.2017.12.020>.
109. Jesse TW, Ezeji TC, Qureshi N, Blaschek HP. Production of butanol from starch-based waste packing peanuts and agricultural waste. J Ind Microbiol Biotechnol. 2002;29(3):117–23. <https://doi.org/10.1038/sj.jim.7000285>.
110. Shao P, Huang RYM. Polymeric membrane pervaporation. J Membr Sci. 2007;287(2):162–79. <https://doi.org/10.1016/j.memsci.2006.10.043>.
111. Azimi H, Tezel H, Thibault J. Optimization of the in situ recovery of butanol from ABE fermentation broth via membrane pervaporation. Chem Eng Res Des. 2019;150:49–64. <https://doi.org/10.1016/j.cherd.2019.07.012>.
112. Cai D, Chen H, Chen C, Hu S, Wang Y, Chang Z, Miao Q, Qin P, Wang Z, Wang J, Tan T. Gas stripping-pervaporation hybrid process for energy-saving product recovery from acetone-butanol-ethanol (ABE) fermentation broth. Chem Eng J. 2016;287:1–10. <https://doi.org/10.1016/j.cej.2015.11.024>.
113. Qureshi N, Blaschek HP. Production of acetone butanol ethanol (ABE) by a hyper-producing mutant strain of *Clostridium beijerinckii* BA101 and recovery by pervaporation. Biotechnol Prog. 1999;15(4):594–602. <https://doi.org/10.1021/bp990080e>.
114. Lin Z, Liu H, Yan X, Zhou Y, Cheng K, Zhang J. High-efficiency acetone-butanol-ethanol production and recovery in non-strict anaerobic gas-stripping fed-batch fermentation. Appl Microbiol Biotechnol. 2017;101(21):8029–39. <https://doi.org/10.1007/s00253-017-8520-1>.
115. Rochón E, Ferrari MD, Lareo C. Integrated ABE fermentation-gas stripping process for enhanced butanol production from sugarcane-sweet sorghum juices. Biomass Bioenergy. 2017;98:153–60. <https://doi.org/10.1016/j.biombioe.2017.01.011>.
116. López-Gómez JP, Pérez-Rivero C, Venus J. Valorisation of solid biowastes: the lactic acid alternative. Process Biochem. 2020;99:222–35. <https://doi.org/10.1016/J.PROCBIO.2020.08.029>.
117. Kim MS, Na JG, Lee MK, Ryu H, Chang YK, Triolo JM, Yun YM, Kim DH. More value from food waste: lactic acid and biogas recovery. Water Res. 2016;96:208–16. <https://doi.org/10.1016/j.watres.2016.03.064>.
118. Duar RM, Lin XB, Zheng J, Martino ME, Grenier T, Pérez-Muñoz ME, Leulier F, Gänzle M, Walter J. Lifestyles in transition: evolution and natural history of the genus *Lactobacillus*. FEMS Microbiol Rev. 2017;41(1):S27–48. <https://doi.org/10.1093/femsre/fux030>.
119. Enzmann F, Mayer F, Rother M, Holtmann D. Methanogens: biochemical background and biotechnological applications. AMB Express. 2018;8(1):1–22. <https://doi.org/10.1186/s13568-017-0531-x>.
120. Baek SH, Kwon EY, Bae SJ, Cho BR, Kim SY, Hahn JS. Improvement of d-lactic acid production in *Saccharomyces cerevisiae* under acidic conditions by evolutionary and rational metabolic engineering. Biotechnol J. 2017;12(10):1–7. <https://doi.org/10.1002/biot.201700015>.
121. Ishida N, Suzuki T, Tokuhiro K, Nagamori E, Onishi T, Saitoh S, Kitamoto K, Takahashi H. d-Lactic acid production by metabolically engineered *Saccharomyces cerevisiae*. J Biosci Bioeng. 2006;101(2):172–7. <https://doi.org/10.1263/jbb.101.172>.

122. Hayek SA, Ibrahim SA. Current limitations and challenges with lactic acid bacteria: a review. *Food Nutr Sci.* 2013;4:73–87.
123. Dworkin M, Falkow S, Rosenberg E, Karl-Heinz Schleifer ES. Bacteria: firmicutes cyanobacteria. *Prokaryotes.* 2006;4
124. Paudel SR, Banjara SP, Choi OK, Park KY, Kim YM, Lee JW. Pretreatment of agricultural biomass for anaerobic digestion: current state and challenges. *Bioresour Technol.* Elsevier Ltd. 2017;1194–205. <https://doi.org/10.1016/j.biortech.2017.08.182>.
125. Zhang Q, Wang M, Ma X, Gao Q, Wang T, Shi X, Zhou J, Zuo J, Yang Y. High variations of methanogenic microorganisms drive full-scale anaerobic digestion process. *Environ Int.* 2019;126:543–51. <https://doi.org/10.1016/j.envint.2019.03.005>.
126. Yabu H, Sakai C, Fujiwara T, Nishio N, Nakashimada Y. Thermophilic two-stage dry anaerobic digestion of model garbage with ammonia stripping. *J Biosci Bioeng.* 2011;111(3):312–9. <https://doi.org/10.1016/j.jbiosc.2010.10.011>.
127. Doyle N, Mbandlwa P, Kelly WJ, Attwood G, Li Y, Ross RP, Stanton C, Leahy S. Use of lactic acid bacteria to reduce methane production in ruminants, a critical review. *Front Microbiol.* 2019;10 <https://doi.org/10.3389/fmicb.2019.02207>.
128. Zhang Y, Yoshida M, Vadlani P v. Biosynthesis of d-lactic acid from lignocellulosic biomass. *Biotechnol Lett.* 2018;40(8):1167–79. <https://doi.org/10.1007/s10529-018-2588-2>.
129. Nolasco-Hipolito C, Carvajal-Zarrabal O, Kelvin E, Tan YH, Kohei M, Nyoel SA, Shoji E, Dieng H, Bujang K. Scaling up of lactic acid fermentation using *Enterococcus faecalis*. IOP Conference Series: Mater Sci Eng. 2019;495(1) <https://doi.org/10.1088/1757-899X/495/1/012049>.
130. Sarasua, J. R.; Arraiza, O.; Balerdi, P.; Fundací, I. M. (n.d.). Crystallization and thermal behaviour of optically pure polylactides and their blends.
131. Peinemann JC, Rhee C, Shin SG, Pleissner D. Non-sterile fermentation of food waste with indigenous consortium and yeast – effects on microbial community and product spectrum. *Bioresour Technol.* 2020;306:123175. <https://doi.org/10.1016/j.biortech.2020.123175>.
132. John, R. P.; Nampoothiri, M.; Pandey, A. (2006). Simultaneous saccharification and fermentation of Cassava Bagasse for L-(+)-lactic acid production using lactobacilli.
133. Tang J, Wang XC, Hu Y, Zhang Y, Li Y. Effect of pH on lactic acid production from acidogenic fermentation of food waste with different types of inocula. *Bioresour Technol.* 2017;224:544–52. <https://doi.org/10.1016/j.biortech.2016.11.111>.
134. Beaulieu M, Perreault V, Mikhaylin S, Bazinet L. How overlimiting current condition influences lactic acid recovery and demineralization by electrodialysis with nanofiltration membrane: comparison with conventional electrodialysis. *Membranes.* 2020;10(6):1–19. <https://doi.org/10.3390/membranes10060113>.
135. Laube H, Schneider R, Venus J. Investigation of spiral-wound membrane modules for the cross-flow nanofiltration of fermentation broth obtained from a pilot plant fermentation reactor for the continuous production of lactic acid. *Bioresour Bioprocess.* 2017;4(1) <https://doi.org/10.1186/s40643-016-0133-5>.
136. Komesu A, Maciel MRW, Filho RM. Separation and purification technologies for lactic acid: a brief review. *BioResources.* 2017;12(3):6885–901. <https://doi.org/10.15376/biores.12.3.6885-6901>.
137. Thauer RK, Kaster AK, Seedorf H, Buckel W, Hedderich R. Methanogenic archaea: ecologically relevant differences in energy conservation. *Nat Rev Microbiol.* 2008;6(8):579–91. <https://doi.org/10.1038/nrmicro1931>.
138. Conrad R. Importance of hydrogenotrophic, aceticlastic and methylotrophic methanogenesis for methane production in terrestrial, aquatic and other anoxic environments: a mini review. *Pedosphere Soil Sci Soc China.* 2020;25:39 [https://doi.org/10.1016/S1002-0160\(18\)60052-9](https://doi.org/10.1016/S1002-0160(18)60052-9).
139. Kabir MM, Forgács G, Sárvári Horváth I. Enhanced methane production from wool textile residues by thermal and enzymatic pretreatment. *Process Biochem.* 2013;48(4):575–80. <https://doi.org/10.1016/j.procbio.2013.02.029>.
140. Kheyrandish M, Asadollahi MA, Jeihanpour A, Doostmohammadi M, Rismani-Yazdi H, Karimi K. Direct production of acetone-butanol-ethanol from waste starch by free and

- immobilized *Clostridium acetobutylicum*. Fuel. 2014;142:129–33. <https://doi.org/10.1016/j.fuel.2014.11.017>.
141. Qureshi N, Li XL, Hughes S, Saha BC, Cotta MA. Butanol production from corn fiber xylan using *Clostridium acetobutylicum*. Biotechnol Prog. 2006;22(3):673–80. <https://doi.org/10.1021/bp050360w>.
142. Luo H, Ge L, Zhang J, Ding J, Chen R, Shi Z. Enhancing acetone biosynthesis and acetone-butanol-ethanol fermentation performance by co-culturing *Clostridium acetobutylicum/Saccharomyces cerevisiae* integrated with exogenous acetate addition. Bioresour Technol. 2016;200:111–20. <https://doi.org/10.1016/j.biortech.2015.09.116>.
143. Wen Z, Li Q, Liu J, Jin M, Yang S. Consolidated bioprocessing for butanol production of cellulolytic Clostridia: development and optimization. J Microbial Biotechnol. 2020;13(2): 410–22. <https://doi.org/10.1111/1751-7915.13478>.
144. Xin X, Cheng C, Du G, Chen L, Xue C. Metabolic engineering of histidine kinases in *Clostridium beijerinckii* for enhanced butanol production. Front Bioeng Biotechnol. 2020;8: 1–8. <https://doi.org/10.3389/fbioe.2020.00214>.
145. Zhang J, Jia B. Enhanced butanol production using *Clostridium beijerinckii* SE-2 from the waste of corn processing. Biomass Bioenergy. 2018;115:260–6. <https://doi.org/10.1016/j.biombioe.2018.05.012>.
146. Xu M, Zhao J, Yu L, Tang IC, Xue C, Yang ST. Engineering *Clostridium acetobutylicum* with a histidine kinase knockout for enhanced n-butanol tolerance and production. Appl Microbiol Biotechnol. 2015;99(2):1011–22. <https://doi.org/10.1007/s00253-014-6249-7>.
147. Ezeji TC, Qureshi N, Blaschek HP. Acetone butanol ethanol (ABE) production from concentrated substrate: reduction in substrate inhibition by fed-batch technique and product inhibition by gas stripping. Appl Microbiol Biotechnol. 2004;63(6):653–8. <https://doi.org/10.1007/s00253-003-1400-x>.
148. Probst M, Walde J, Pümpel T, Wagner AO, Schneider I, Insam H. Lactic acid fermentation within a cascading approach for biowaste treatment. Appl Microbiol Biotechnol. 2015;99(7): 3029–40. <https://doi.org/10.1007/s00253-015-6414-7>.
149. Kwan TH, Hu Y, Lin CSK. Techno-economic analysis of a food waste valorisation process for lactic acid, lactide and poly(lactic acid) production. J Clean Prod. 2018;181:72–87. <https://doi.org/10.1016/j.jclepro.2018.01.179>.
150. Gaida SM, Liedtke A, Jentges AHW, Engels B, Jennewein S. Metabolic engineering of *Clostridium cellulolyticum* for the production of n-butanol from crystalline cellulose. Microb Cell Fact. 2016;15(1):1–11. <https://doi.org/10.1186/s12934-015-0406-2>.
151. Wen Z, Ledesma-amaro R, Lin J, Jiang Y. Improved n-butanol production from clostridium cellulovorans by integrated metabolic and evolutionary engineering. Appl Environ Microbiol. 2019;85(7):1–17. <https://doi.org/10.1128/aem.02560-18>.
152. Fedorova I, Arseniev A, Selkova P, Pobegalov G, Goryanin I, Vasileva A, Musharova O, Abramova M, Kazalov M, Zyubko T, Artamonova T, Artamonova D, Shmakov S, Khodorkovskii M, Severinov K. DNA targeting by *Clostridium cellulolyticum* CRISPR-Cas9 Type II-C system. Nucleic Acids Res. 2020;48(4):2026–34. <https://doi.org/10.1093/nar/gkz1225>.
153. Jiang Y, Lv Y, Wu R, Lu J, Dong W, Zhou J, Zhang W, Xin F, Jiang M. Consolidated bioprocessing performance of a two-species microbial consortium for butanol production from lignocellulosic biomass. Biotechnol Bioeng. 2020;117(10):2985–95. <https://doi.org/10.1002/bit.27464>.
154. Liu J, Jiang Y, Chen J, Yang J, Jiang W, Zhuang W, Ying H, Yang S. Metabolic engineering and adaptive evolution of *Clostridium beijerinckii* to increase solvent production from corn stover hydrolysate. J Agric Food Chem. 2020;68(30):7916–25. <https://doi.org/10.1021/acs.jafc.0c03048>.
155. Yousuf A, Bastidas-Oyanedel JR, Schmidt JE. Effect of total solid content and pretreatment on the production of lactic acid from mixed culture dark fermentation of food waste. Waste Manag. 2018;77:516–21. <https://doi.org/10.1016/j.wasman.2018.04.035>.

Part IV

**Production of Liquid Biofuels with New
Technologies**

Chapter 8

Producing Value-Added Products from Organic Bioresources via Photo-BioCatalytic Processes



Silvia Magri and David Cannella

Abstract The interplay between light and bioprocesses represents an opportunity to develop high-value products from organic waste. In the past decade, the field of green chemistry was overturned by applications of photobiocatalysis, despite being investigated since the early 1900s. New developments allow fine-tuning control and accelerated kinetics of enzymatic redox reactions by light. Indeed, solar irradiation can be deployed either to directly activate or to ensure the in-situ regeneration of reducing equivalent promoting redox enzymes activity. Till now, organic wastes are only partially utilized as biomass growth support in biorefinery processes and its fully exploitation is far to be achieved. Photobiocatalysis exemplifies a strategic way to design new biotransformation processes. In this context, the production of high-value molecules is achieved by using organic waste as primary chemical precursors that provides electrons upon oxidation, also widely defined as sacrificial molecules. In this chapter, the organic wastes recovery through photobiocatalytic processes, including enzymatic systems, electron reservoirs and final acceptors, are discussed. In addition, a special focus will be given toward the light-driven valorisation of organic by-products involving whole-cell biotransformation approaches. These technologies are considered as the new frontiers in the biorefinery field.

Keywords Photobiocatalysis · Redox enzymes · Biomass · Light · Pigments · Biorefinery

S. Magri · D. Cannella (✉)

PhotoBioCatalysis Unit, Crop Nutrition and Biostimulation Lab (CPBL) and Biomass Transformation Lab (BTL), Université libre de Bruxelles (ULB), Bruxelles, Belgium
e-mail: david.cannella@ulb.be

8.1 Introduction

At its onset, life on Earth started with sparkles of energy ultimately caused by electromagnetic radiations originating from the Sun. Sunlight driven reactions were probably the very first happening on primordial Earth and could have contributed on generating the reservoir of prebiotic molecules, necessary for the incumbent evolution of life [1]. Since then, light had become the basic energy input for the Earth ecosystems, and its energy conversion through photosynthesis produce today 100–200 Gton/year of reduced carbon compounds, which represents a vast resource to look at if we want to harness the very first source of renewable energy available, with the goal of guiding the transition of our society out of the fossil-based era.

For long, scientific challenges reproducing *in vitro* the biological photosynthesis able at splitting water for production of viable electrons, had been endured in what is known today as artificial photosynthesis. Thought with limited success, in terms of quantum efficiency, this had laid the fundaments of new domain of studies among which the Photobiocatalysis (PBC) is emerging.

The PBC concept sees the use of light-excitable photosensitizers coupled with biocatalysts, i.e., redox enzymes, fueled directly or via electron's conveyor pigments, ultimately sacrificing an inexpensive source of electrons. PBC provides us with a basic tool to initiate and expand research on the biggest challenges within chemistry, physics and biology: a completely renewable/green technology capable of converting light energy into chemical energy. In a PBC system the light energy is used to promote the electron transfer among the catalytic components and to allow thermodynamic challenging reactions.

The substrate-to-product conversion in a classic PBC setup is usually achieved by the concerted action of four main elements: (i) photosensitizer (PS), (ii) electron mediator (EM), (iii) biocatalyst (i.e., enzymes) and (iv) electron donor (or sacrificial molecule). Photosensitizers are single molecules or complexes able to absorb light and generate photoexcited electrons, and their exposure to their specific wavelength is considered the starting event in PBC. Then, the excited photosensitizer (PS^*) can either reduce the biocatalyst (usually a single redox enzyme) with a direct electron transfer or alternatively activate it by an indirect electron transfer through the reduction of an electron mediator (usually a prosthetic group of enzymes). In both cases, the presence of a sacrificial external electron donor is needed for the regeneration of the photosensitizer (or to fill the electron void) and thus assuring the photocatalytic turnover (Fig. 8.1). Depending on the specific system, the electron mediator can be either a small artificial redox molecule or the natural cofactor of the enzyme catalyzing the reaction. Inspired by this basic architecture, various PBC systems have been developed to cope with specific reaction conditions, component incompatibilities or electron transfer optimization. For example, an additional mediator can be added to improve the indirect electron transfer from the photosensitizer to the biocatalyst. The use of a whole-cell approach, in which the biocatalyst is the entire recombinant cells expressing the enzyme of interest, can bypass the addition of expensive cofactors or improve the overall system stability.

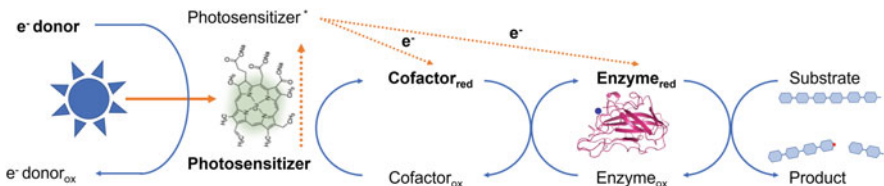


Fig. 8.1 Schematic diagram of photobiocatalysis process via direct or indirect photoelectron transfer from photosensitizer to enzymatic active site

This chapter will provide the reader with the insights on the basic working principles of photobiocatalysis and on the features of the main bioresources that can be valorised through it. Some examples of the latest advancements in the still young PBC field are reported, mainly as proof-of-concept studies at small scales, yet representing valid greener alternatives to actual harsh chemical or fossil-based processes (summarized in Table 8.1). We will start by introducing the first elements for PBC as choice of light sources and photosensitizers aiming at practical application of the technology at lab scale and discuss possible up-scaling. Then we will report the most important examples based on light-driven enzymes couple to common biowaste sources of their substrates (summarized in Table 8.2), indeed a unique point of view not yet covered in the literature.

8.2 Light Sources and Pigments

Exposure to appropriate light energy induces changes in the electronic structure of a photosensitizer thus promoting its transition from the *ground state* (more stable) to an energy-rich state namely *excited state*. At the excited state, a charge separation occurs resulting from the formation of electron-hole pair in the conduction and valence band of the photosensitizer, respectively. In a photocatalytic process, the light-driven charge separation is used as driving force for thermodynamically challenging redox reactions. As only the absorbed light is effective and photosensitizer compounds display intrinsic absorbing properties at specific wavelength, the choice of the appropriate light source is of primary relevance for the accomplishment of the photoinduced reaction. The light spectrum currently exploited in PBC systems spans from 280–700 nm, being composed by UV light (mainly UVB and UVA) and visible light, strictly depending on the aimed photosensitizer, electrochemical features and the process applications. Beside the type of light source, another parameter influencing photoconversion is the light energy supply in terms of quantity (light intensity) and duration/period (continuous or intermittent). The formation of electron-hole pairs linearly increases with the light intensity until a certain low threshold, but at high photon intensity, the rate of electron-holes recombination outcompetes the rate of redox reactions between the photosensitizer and the catalyst. Therefore, a tunable light dosage is not only necessary for the economy of the process but also for its

Table 8.1 Summary of PBC systems reviewed in this chapter. Photoactivation mode (direct/indirect), enzyme, cofactor, photosensitizer and substrate class are listed

Direct/ indirect electron transfer	Enzyme	Cofactor	Photosensitizer	Generic substrate	Ref.
Direct	<i>TtAA9E</i> , <i>TtAA9H</i> , <i>TaAA9A</i>	—	Chlorophyllin, thylakoid, Water-soluble chlorophyll-binding protein	Polysaccharide	[12, 13, 56]
	<i>BsAA10</i> , CPB21	—	V-TiO ₂ , chlorophyllin	Polysaccharide	[14]
	LAC3	—	V-TiO ₂ , chlorophyllin	Cyclic alkene	[15, 60]
	Commercial Laccase	—	Laccase/carbon dots decorated with phosphate groups complex	Low-molecular weight mediator	[61]
	<i>AaeUPO</i>	—	Carbon nitride (CN-OAm)	Cyclic alkene	[6]
	<i>AaeUPO</i>	—	Sodium AnthraquinoneSulfonate (SAS)	Cyclic alkene	[70]
	<i>AaeUPO</i>	—	Nitrogen-doped Carbon Nanodots (N-CNDs)	Cyclic alkene	[71]
Indirect	CHMO	NADPH	Intact cyanobacterial photosystem (whole-cell)	Cyclic alkene	[21]
	CHMO	NADPH	Au-TiO ₂ , g-C ₃ N ₄	Cyclic alkene	[8]
	CHMO, HAPMO	NADPH	Sodium AnthraquinoneSulfonate (SAS)	Ketoalkene	[76]
	CvFAP	FAD	FAD	Fatty acids	[78, 79]
	YqjM	NADPH	Intact Cyanobacterial photosystem (whole-cell)	Alkenes	[81]
	<i>YersER</i>	FMNH	Iridium complex [Ir-(dmppy) ₂ (dtbbpy)]PF ₆	Alkenes	[82]

intrinsic electrochemistry. Moreover, the use of intermittent light has been seen to reduce the electron-holes recombination phenomenon and prevent the overproduction of highly reactive ROS species thus improving the quantum yield and stability of the photobiocatalysis conversion [2]. Here we provide the reader with an overview of the most common light sources investigated up to date.

Table 8.2 A summary of main bioresources suitable for PBC conversion and valorization. PBC set up and obtained products are listed

Substrate	BioResource	Enzyme	Light/PS	Products	Ref.
Cellulose	Lignocellulose, pulping paper	LPMO - <i>TiAA9E-H, TaAA9A</i>	Chlorophyllin - Sunlight, LED, Bulb, 150-200 μ E, continuous and intermittent	Cellooligosaccharides various DP, Cello-aldonic acids, keto-cellooligosaccharides	[12, 13, 15, 58]
Hemicellulose	Agricultural waste, food waste, lignocellulose	LPMO - <i>TiAA9E</i>	Chlorophyllin - Sunlight, LED, Bulb, 150-200 μ E, continuous	Xyloglucans oligosaccharides, xyloglucan aldonic acid	[12]
Chitin	Fishery industry, food waste, restauration sector	LPMO - <i>BsAA10, CPB21</i>	Chlorophyllin, V-TiO ₂ - visible light - 42 W cm ⁻² , continuous	Chitoooligosaccharides and their aldonic acids	[14]
Lignin	Pretreated lignocellulose	LPMO - <i>MiAA91-A, TiAA9E w/ Laccase</i>	Chlorophyllin - Sunlight, LED, Bulb, 150-200 μ E, continuous	Water soluble lignols, carboxylate lignols, lignin oligomers, lignin nanoparticles	[12, 64, 98]
Lipids	Fatty acids and PUFAs, algal production, agricultural oil, WCO	CvFAP	LED - 68 μ mol m ⁻² m ⁻¹ - continuous	Decarboxylated fatty acids, biodiesel	[78, 79]
Terpenoids	Lignocellulose, microbial communities	CtVCPO	Sodium Anthraquinone Sulfonate (SAS) - white light bulb - continuous	Halogenated terpenoids and cyclized halogenated terpenoids	[70]
Aromatic hydrocarbons	Lignocellulose, microbial communities	<i>AaeUPO</i>	Sodium Anthraquinone Sulfonate (SAS) - white light bulb, – continuous	Alcohol and ketone form of aromatic hydrocarbon	[70]

8.2.1 *Sunlight*

Natural sunlight is an ideal starter for highly sustainable PBC processes being renewable, economical and offering a complete array of suitable electromagnetic radiation. However, its supply is discontinuous due to changes between day and night, seasonal turnover and latitudinal variations that are important constraints for developing robust industrial processes. The sun electromagnetic spectra radiation reaching the Earth's surface is also influenced by the weather conditions, whereas on a cloudy day, direct sunlight is less intense and short wavelengths are strongly reduced [3]. Sunlight-fueled approaches are well developed for biomass and high-valued compounds production using photoautotroph microorganisms as in the case of microalgae cultivation in open-ponds and outdoor photobioreactors. The effect of discontinuous sunlight supply on outdoor plants productivity can be modelled and mathematical predictions are a powerful tool for adaptation to other tunable parameters e.g. for preventing cell self-shading or photoinhibition mechanisms [4]. Photosynthetic organisms are naturally provided with adaptative mechanisms enabling them to cope with fluctuating illumination, while artificial PBC systems are more sensible to environmental light variations. It is thus necessary to intensify investigation on the electrochemical properties of photosensitizers to further develop more stable and efficient molecules for assuring constant photoconversion yields under variable conditions. Xanthene-based organic dyes are reported to successfully mediate in vitro light catalyzed production of molecular hydrogen (H_2) through a cyanobacterial hydrogenase under ambient daylight irradiation [5]. The bio-inspired simplified system activated by visible light and stable H_2 productivity has been reported [5] despite daily light intensity variations, proving the possibility of its application outside standardized laboratory conditions.

8.2.2 *Gas Discharge Lamps*

Gas discharge lamps are widely used light sources composed of tiny glass ampules containing two electrodes and a mixture of noble gases at low pressure. The composition of the gas mixture determines the emission spectrum of the lamp. Neon bulbs are characterized by emission wavelengths in the red-orange (above 600 nm) range while argon lamps are shifted towards blue-violet (below 500 nm). Fluorescent lamps are typically mercury-based and a phosphor coating is used to produce visible light that appear white to the human eye. Despite fluorescent light is perceived as a homogenous beam, its spectrum is quite discontinuous, displaying discrete high intensity emission peaks related to the noble gas employed. Generally, gas discharge lamps present a substantial time delay in the full intensity emission since the current supply, this can hamper their application in PBC reaction with an intermittent illumination setup.

8.2.3 *Light Emitting Diode—LED*

Light emitting diodes (LEDs) are a relative recent light source having huge interest in industrial applications as their price is continuously decreasing and the technology improving leading to remarkable decrease in electricity consumption for amount of light produced. The light emission spectrum of a LED is narrow enough to be depicted by a single wavelength. The actual range of semiconductor materials suitable for this technology allow a wide diversification of LED colors and, a broader overall emission spectrum can be achieved by LEDs combinations (like RGB LED array) or by recent white LED. Having a spectral width in the range of 20–50 nm, LED devices allow a fine control of photocatalytic conversions where combination and alternation of irradiation with different wavelengths is required to drive specific reactions [6]. LED are nowadays replacing conventional lighting systems, such as incandescent bulbs and fluorescent tubes, because of the lack of infrared emissions ascribed to heating of the radiated surfaces thus reducing the need of cooling systems for the reactor volumes. When intermittent illumination is needed, LED technology represents a reliable light source being able to assure on/off cycles within a time range in the order of milliseconds. Notably, the use of LED in pulsed mode results in an extended lifespan and diminished power dissipation and heating generation. Lastly, the main challenge for LEDs implementation in photobiocatalytic processes at industrial scale, is the low in-depth penetration power of the emitted beam. This limitation must be taken in account especially for applications where UV-LEDs are used to drive biocatalytic conversions in high turbidity streams.

8.2.4 *Pigments Photo-Oxidation/Reduction*

Nowadays several photosensitizers have been identified for PBC processes that are either biologically derived and thus renewable, or chemically synthesized. Generally, after absorbing light, the photosensitizer is promoted to its excited state (PS^*), and interacts with other molecules via electron transfer, energy transfer or atom transfer pathways. In PS^* , an electron in the highest occupied molecular orbitals (HOMO, or valence band) is promoted to the lower unoccupied molecular orbital (LUMO, or conduction band) leading to charge separation. PS^* is thus a strong redox agent and tend to undergo electron transfer by donating it to an appropriate electron acceptor (reductive quenching) or by receiving it from an electron donor (oxidative quenching). The photosensitizer is then regenerated via a second electron transfer that restore the ground state. The electron transfer direction and thermodynamic feasibility depends on the redox potentials of the involved species and competes with other relaxation mechanisms such as the radiative deactivation by emission of less energetic photon and the nonradiative deactivation by heat dissipation [7]. Thus, to achieve efficient photoconversion, the photobiocatalytic system must be careful designed by coupling the redox partners favoring the electron transfer over other

concurrent deactivation mechanisms. After light excitation, intersystem crossing can promote the PS to its triplet excited state (${}^3\text{PS}^*$) allowing the direct energy transfer to ground state substrate causing the formation of triplet excited substrate (${}^3\text{SUB}^*$). This event is commonly occurring after light exposition of chlorophyll in aerobic condition. The excited pigment interacts with molecular oxygen leading to the formation of highly reactive oxygen species which then disproportionate forming H_2O_2 . Light-driven in-situ production of hydrogen peroxide is a mechanism extensively used to activate peroxygenases in photobiocatalytic conversions [8, 9]. Each photosensitizer possesses only one ground state but multiple excited states with specific energetic levels, physiochemical features, and lifetimes. Excited triplet states are usually preferred than singlet states due to their longer lifetime (in microseconds and nanoseconds order, respectively) making the electron transfer more efficient. Lastly, a PS^* can interact with other molecules by atom abstraction from a suitable substrate usually displaying an accessible hydrogen atom. A common chemical structure feature of photosensitive molecules is the presence of large and stable π -aromatic configuration which assure electron delocalization making them excellent electron donors/acceptors [10]. In current PBC reactions, the successful use of a wide range of photosensitizers is reported, including natural and natural-derived pigments or complexes, organic dyes, transitions metal complexes and carbon-base nanomaterials (Fig. 8.2).

8.2.4.1 Natural Chlorophyll and Derivatives

Taking inspiration from photosynthesis, which is the most powerful natural process for storing light energy into chemical energy, a wide number of PBC setups have implemented porphyrin-based molecules as the light harvesting component. Photoactive porphyrins display a large and rigid tetrapyrrolic conformation coordinating a transition metal (e.g. Mg, Fe), in which the extended conjugated system determine a strong absorption in visible electromagnetic spectrum (Fig. 8.2a). Modifications in the peripheral decoration or in the transition metal allow a fine tuning of their physiochemical properties such as the modulation of the ground- and excited-state optical and electronic features, excited state stability and absorption shift [11]. The abundance in natural feedstock and the plasticity of these chromophores attracted the interest of researchers working on sustainable PBC processes. Water-soluble chlorophyl complexes and chlorophyl copper substituted derivative, (chlorophyllin), were used to photoactivate oxidative enzymes active on polysaccharides [12–14], while a zinc-based porphyrin was shown to perform multielectron transfer to laccase enzyme via long stable triplet excited state [15].

8.2.4.2 Complexes Phycobilisomes, Thylakoids, Cell Lysates

In higher photosynthetic organisms (plants) the light energy absorption take place in well organized and compartmentalized environment (the chloroplast) in which series

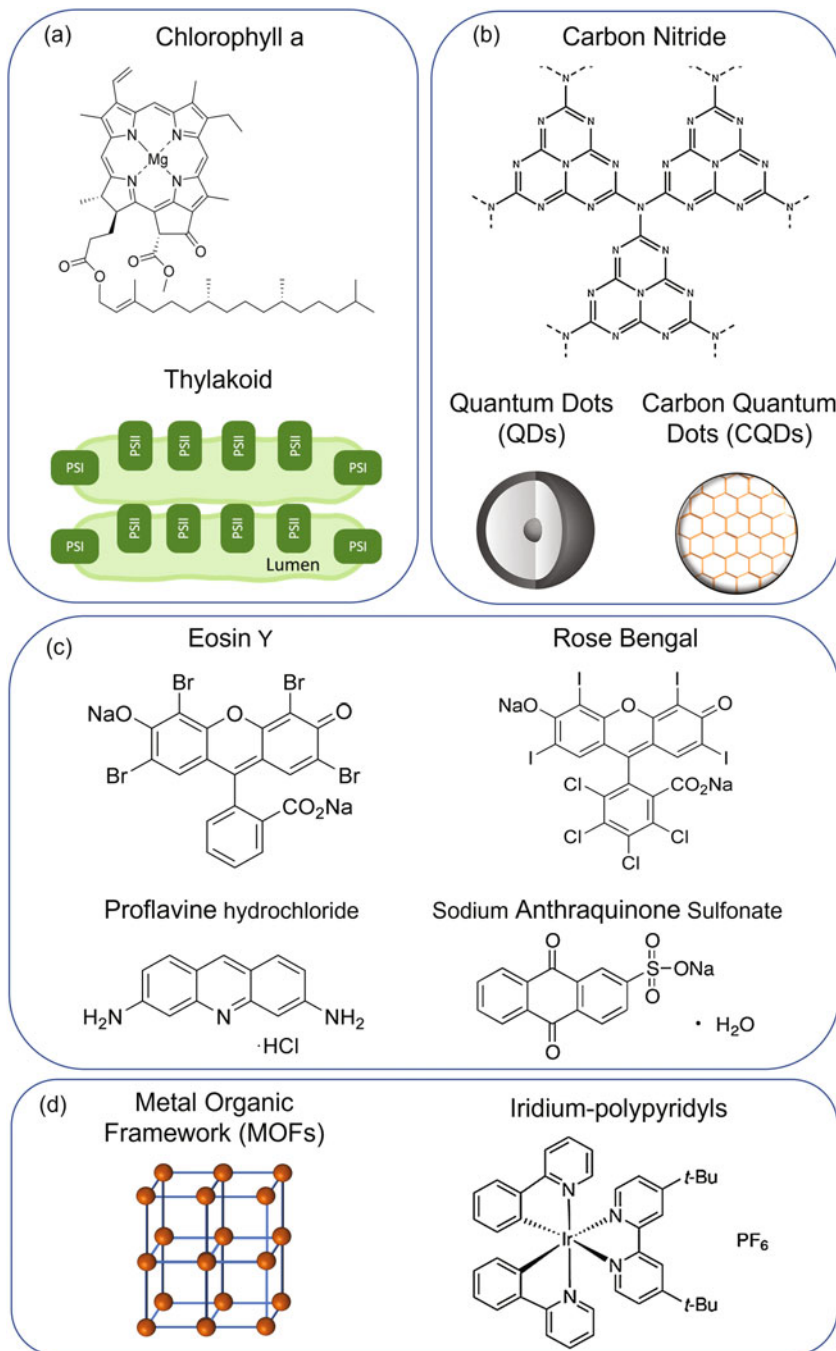


Fig. 8.2 Structures of commonly used photosensitizers grouped by class: (a) natural chlorophyll; (b) Quantum dots and functionalized materials; (c) microbial derived xanthenes; (d) metal complexes

of light harvesting complexes (photosystems) concentrate the incident photons and the electron transport chain maximize the charges separation across the membrane of the thylakoids (Fig. 8.2a). Exploiting this kind of structure can be beneficial for some reactions in which the orientation of the electron flux and the presence of a compatible interface between the photocatalyst and the biocatalyst are needed [16]. Isolated photosystems have been used to create *in vitro* chromophore-enzymatic complexes for efficient H₂ at the only expense of water oxidation [17, 18]. Many attempts are reported to artificially reproduce photosynthetic processes and mimic chloroplast organized and stable environments. A bio-based artificial photosynthetic system was produced by Park and co-workers using lignocellulosic derivatives to encapsulate hydrophobic porphyrins and regenerate enzymatic redox cofactors [19]. Other whole-cell biocatalytic approaches demonstrated the possibility to exploit natural photosynthesis to drive the production of target compounds via metabolic engineering of cyanobacteria. Photosynthetic direct electron transfer or reducing agent production (in form of NAD(P)H) can be employed for enzymatic production of bioactive-compounds, organic molecules and their oxy-functionalization [20–22].

8.2.4.3 Microbial Derived Xanthenes

Alongside photosynthetic pigments, other biobased compounds present ideal features for green photobiocatalytic applications. Xanthenes and xanthenes derivatives are organic dyes with heterocyclic structure able to absorb light in the central region of visible spectrum (500–600 nm) and, when photoexcited, are able to undergo reductive and oxidative quenching. Eosin Y and E, Rose Bengal and flavin-based compounds are the most widely used in light driven reactions being able to direct activate the catalytic site of redox enzymes [23, 24] to sustain the photoregeneration of several redox cofactors or to photoactivate substrate for further enzymatic conversion [25]. Photophysical and electrochemical properties of xanthene can be tailored by specific structure modifications and peripheral functionalization with, for example, halide groups (Fig. 8.2c). Aromatic heterocycles with broad absorption properties are abundant secondary metabolites naturally produced by plants and microorganisms during symbiotic and pathogenic interactions [26]. New natural structures are constantly discovered and characterized, thus representing an unlimited source of green photosensitizer building blocks.

8.2.4.4 Metal Complexes

Photocatalysts containing precious metals like iridium, platinum and ruthenium (Fig. 8.2d) are broadly used to drive challenging redox reactions due to their high chemical stability and long-lived excited states. However, the actual need for more environment friendly and affordable conversion strategies resulted in the development of new metal complexes with on Earth more abundant first-row transition metals such as copper, zinc and nickel and titanium. UV absorbing titanium oxides

are the most exploited photosensitizers especially for in situ generation of hydrogen peroxide, electron donor transfer [9, 14, 27] and reducing agent regeneration [28] for oxidoreductase activation. TiO₂ nanoparticles can also be doped with other metal oxides (like Cu₂O) to improve their stability and modulate the absorbance range [29] or be incorporated in bioderived carrier, such as cellulose, for application in photocatalytic-biodegradation coupled processes [30]. A subsequent evolution of metal complex is the design of metal-organic frameworks (MOFs) in which metal clusters are coordinated with organic ligands allowing multidimensional structures (Fig. 8.2d). Structure and properties depend on the nature of the ligand (valence and functional groups) and of the coordination preference of the metal. MOFs can thus be designed to host stable pores which improve the contact surface area with the reactants, target goal especially for application in H₂ storage and CO₂ capturing and fixation. Ligand electron delocalization and introduction of antenna groups (–OH; –NH₂) can broaden and shift from UV range the absorption spectrum and favor charge transfer kinetics of MOFs rendering them suitable photosensitizers [31].

8.2.4.5 Quantum Dots and Functionalized Materials

Developments in nanomaterial science led to the design of practical semiconducting nanoparticles called quantum dots (QDs, Fig. 8.2b). QDs find application in a broad range of technologies like microelectronic, biomedical, bioimaging and solar cell, just to mention few. Due to their unique photophysical characteristics, QDs are successfully used as photosensitizer in PBC. QDs absorption spectra, emission quantum yield and excited state lifetime are all features depending on the particle size and atom composition allowing high degree of freedom in their design and adaptability. Common sizes span from 2 to 10 nm in diameter, with smaller crystals absorbing high light intensity (UV – blue spectrum region) and bigger size being excited at longer wavelengths. Contrary to organic dyes and pure pigments, QDs are more prone to photobleaching, thus showing a higher stability over repeated cycles of excitation. Moreover, nanocrystals optical and photo-physic characteristics can be further shaped by varying their composition using different transition metals for their fabrication [32]. Besides, metal based QDs, more sustainable and less toxic semiconducting nanoparticles are now made upon carbon structure (Fig. 8.2b). Carbon quantum dots (BQDs) can be synthesized either with a top-down approach by fragmentation of graphite and carbon nanotubes structures or by bottom-up processes where small precursors (e.g., sugars and citrate) are assembled via hydrothermal or solvothermal treatments. This latter production approach allows their straightforward synthesis from simple carbohydrate-rich natural biomass such pear juice, peach blossom and agricultural waste hydrolysates [33–35]. CQDs are suitable photosensitizers for PBC thanks to their high solubility in aqueous solution, biocompatibility, light harvesting and electron transfer properties. All these characteristics can be tuned by surface groups modifications and modulated by the environmental pH conditions [36].

8.3 Biocatalysts- Enzymes and Whole Cell Applications

The term biocatalyst usually refers to the specific isolated enzyme that catalyzes the aimed substrate-to-product conversion. Commonly, PBC conversions are based on the use of enzymes belonging to the oxidoreductase class (EC 1) which catalyze the electron exchange between a donor and an acceptor molecule. To perform the reaction, these enzymes often require the presence of reduced nicotinamide (NAD (P)H) cofactors or prosthetic groups such as metal-ions, flavins and heme groups. Oxidases and oxygenases use O₂ as an electron acceptor, the latter directly incorporate at least one oxygen atom into the substrate. H₂O₂ is the co-substrate of peroxygenases, while dehydrogenases use molecules other than oxygen as electron acceptors [37]. Many approaches have been proposed for the regeneration (reduction) of monooxygenases or for their cofactor, spanning from chemical, electrochemical to enzymatic approaches but all at the expenses of a valuable donating electron molecule [38]. When considering applying these enzymes in biotechnological processes, electron donation can pose a limitation due to the high costs of these reducing agents. A renewable and inexpensive source of electrons that can regenerate these molecules, or that can bypass it and directly donate the electrons to the enzymes, will finally enable to exploit all the potentials of these enzymes. In a broader definition a biocatalyst can be used to depict the whole organism able to express (produce) the enzyme and ideally sustain its activity over time by continuously providing suitable cofactors, as a part its endogenous metabolism [39].

8.3.1 *Pigment Mediated Photo Excitable Enzymes Without Cofactor*

8.3.1.1 Lytic Polysaccharide MonoOxygenases - LPMOs

Lytic Polysaccharide MonoOxygenases (LPMOs, EC 1.14.99.-) discovered in 2010 [40], are redox enzymes able at cleaving by oxidation the β-1,4-glycosidic bond in numerous polysaccharides. This had abruptly changed all our understanding of polysaccharide degradation. The new scenarios see LPMOs creating rupture in the fibers tension via oxidative cleavage of polysaccharide chains leaving new entry sites for the further depolymerization actuated by cellobiohydrolase enzymes, that were thought to operate in synergy only with endoglucanases [41]. LPMOs were firstly identified in bacteria (*Serratia marcescens*, SmAA10A) but shortly after, numerous LPMOs-coding sequences were found in many different organisms including archaea, eukaryotes and viruses. Up-to-date, according to the CAZy classification [42] LPMOs are grouped into 7 families of Auxiliary Activity enzymes (AA9-11, AA13-15 and AA16). The AA9s, AA11s, AA13s, AA14s and AA16s are widespread in eukaryotes, while the AA15s are also found in insect and viruses and the AA10s are mostly common in bacteria [43]. The highly conserved catalytic site

host a single copper atom (type II copper) coordinated with a T-shaped histidine-brace [44, 45]. The enzyme activation requires the electron transfer from an external donor to reduce the catalytic copper which then can oxidatively cleave the glycosidic bond using either O₂ or H₂O₂ as co-substrate [46, 47]. This cleavage leads to the production of oxidized oligosaccharides and their non-oxidized counterpart. Upon enzyme reduction, the catalytic site performs a hydrogen abstraction from carbon in position 1 or 4 in the pyranose ring. The resulting radical intermediate is then hydroxylated causing the subsequent break of the glycosidic bond [48, 49]. The oxidation at C1 or C4 position leads to the formation of aldonic acids or 4-ketoaldehyde gemdiols, respectively. Moreover, some LPMOs are able to release double oxidized products acting on both sides of two different monomers [50].

The first industrial application of LPMOs was their implementation in cellulolytic cocktails for the digestion of pretreated lignocellulosic biomass to obtain molasses of monosaccharides suitable for any bio-productions upon biological fermentations: biofuels, bioplastics and biochemicals [51]. Among other factors, the optimization of LPMOs activity clearly depends on the chemical nature of the electron donor and on its redox potential. Several reducing agents such as small molecules, enzymatic partners, mono- and poly-lignols, and photoexcited pigments have been reported to activate LPMOs [12, 27, 52–55]. In the first study of light-driven cellulose oxidation by LPMOs, the water-soluble form of chlorophyll (chlorophyllin) and isolated thylakoids were used to activate the monocupper enzyme via direct electron transfer (Fig. 8.1). Furthermore, the oxidized pigment was continuously regenerated at the only expense of ascorbic acid. The Photobiocatalytic system dramatically increased the product yield of the fungal *TtAA9E*, and more interestingly revealed a secondary activity on a different substrate (xyloglucan), not detectable under dark conditions [12]. A more recent work highlighted a possible double role played by the light supply in boosting the activity of LPMOs. Along with the electron delivery to the catalytic center, the excited photosensitizer promotes the *in situ* generation of hydrogen peroxide that can be used as a co-substrate by the redox enzyme [14]. The importance and influence of other factors on the efficiency and robustness of this light-driven system are currently under investigations. The balance between all the reaction components (enzyme, photosensitizer and reducing agent) was assessed in a recent study where free or complexed chlorophyll (WCSP-Chl *a*) were used to mediate the light energy conversion. By optimizing the reducing agent concentration and the light intensity it was possible to prevent early enzyme inactivation which may occur in presence of an excess of H₂O₂ [13]. Finally, a beneficial effect on the system stability over time and an energy input gain is assured by the use of illumination on/off cycles [56].

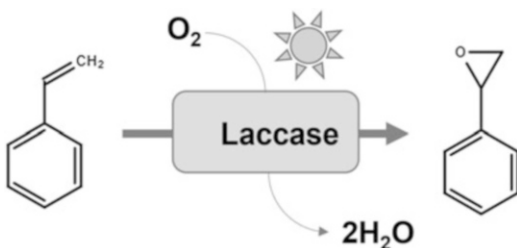
8.3.1.2 Laccases

In nature, the degradation and modification of lignin, which is one of the most abundant and recalcitrant organic polymers, is enabled by the activity of powerful redox enzymes such as class II peroxidases, dye peroxidases and laccases. These

latter are an evolutionary old a family of extracellular copper-containing polyphenol oxidases (EC 1.10.3.2) widespread among the tree of life spanning from fungi, bacteria, plants and in a lesser extent in animals. Expression and secretion of polyphenol oxidases in fungi is also one of the first response lines when harmful conditions are “sensed” such as in the presence of bioactive compounds, xenobiotic toxins and antagonistic microorganisms. Moreover, laccases play a crucial in pathogenic mechanisms by producing melanin and melanin-like pigments recognized as antimicrobial and virulence factors. The abundance of laccases coding genes reflects the wealth of architecture diversity, substrate specificity and kinetic properties displayed by this enzymatic class. Other biological functions of laccases are metal homeostasis/oxidation, morphogenesis, cell pigmentation, plant lignification and wound healing. Laccases molecular masses vary from 40 to 180 kDa having generally slightly acidic pH optima with the exception of bacterial laccases preferring alkaline conditions (e.g., SLAC from *Streptomyces coelicolor* with pH optimum 9.4.). Peculiar feature of laccases is the presence of cupredoxin-like domains hosting the binding site for type I copper (strongly distorted coordination sphere) and of one or two other domains supporting the coordination of one type II copper (planar coordination) and two type III coppers (oxygen bridged Cu-Cu dimer) [57]. The multicopper center allows the oxidation of a variety of phenolic substrates while performing the four electrons reduction of molecular oxygen to water. The substrate is oxidized at the type I copper site which then transfer the electrons to the tri-copper cluster in which the reductive generation of water takes place. The driving force for the substrate oxidation is the redox potential difference between the fully oxidized catalytic cluster and the phenolic compound. Based on their redox potential, laccases are categorized as low-redox-potential enzymes (mainly in bacterial and plants) and high-redox-potential enzymes (mostly found in white rot fungi). An expansion in substrate scope, including non-phenolic lignin subunits, is possible when low molecular weight mediators (such as ABTS; 2,2-azinobis-(3-ethylbenzothiazoline)-6-sulfonic acid) are firstly oxidized by the laccase and then target the substrate performing the final oxidation [58]. Thanks to their substrate versatility, temperature and pH stability, cofactor and hydrogen peroxide independence, laccases are ideal powerful oxidative enzymes for industrial biotechnological application in a wide range of fields like biofuel production, bioremediation, chemical, pharmaceutical and clothing industry, just to mention few.

Classic photoactivation mechanism supports single electron-transfer while the accumulation of multicharges or holes needed to activate metal-cluster enzymes remain challenging. The first complete reduction of a fungal laccase (from *Trametes* sp. strain C30) by light was achieved in 2011 by Tron and co-workers [59]. Excitation with white light of a Ru^{II}-polypyridine-type complex in presence of an exogenous electron donor induced the delivery of four electrons to the multicopper-cluster. The fully reduced laccase was then able to generate water molecules by reducing dioxygen. In a follow up work, the authors overcame the need for the external electron donor and coupled the laccase oxygen reduction with the oxidation of unusual olefin substrates. The model reaction led to the photo-epoxidation of *p*-styrene sulfonate (alkene) mediated by Ruthenium complex using O₂ both as

Fig. 8.3 Epoxidation of styrene to styrene epoxide by photoactivated Laccase in which the molecular oxygen (O_2) has the double role of electron acceptor and O atom donor



electron acceptor as well as O atom donor and laccase as electron sink (Fig. 8.3) [60]. Further investigations on laccase light activation led to the development of a tunable enzymatic-photosensitizer hybrid system showing higher catalytic activity compared to free laccase. Hydrophilic carbon dots decorated with phosphate groups (PCDs) were connected through noncovalent bonds to the type I coppers in the laccase catalytic center, resulting in a hybrid complex with improved oxidative activity and stability. Photoexcited PCDs possess strong electron donating and accepting properties which can favor the electron transfer between the low-molecular weight mediator (ABTS) and the laccase multicopper-cluster. More interestingly, the laccase/PCDs hybrid was sharply regulated by light illumination specifically responding to the provided light intensity and to on/off activation cycles [61]. Lignin removal from lignocellulose biomass is a high energy demanding and fundamental step in carbohydrate derivatization and refinery. The laccase/mediator systems are now exploited for lignin deconstruction in biotechnological processes and more recently the new concept seeing lignin as a precious reservoir of biochemicals is attracting the research interest for their customization. Low-molecular weight lignin (LMWL) pools derived from laccase/ABTS oxidation of steam-exploded sugarcane bagasse and wheat straw have been demonstrated boosting the LPMOs oxidative breakdown of cellulose via long-range electron transfer [62]. Another possible synergism between the two oxidative activities (of laccases and LPMOs) has been recently envisioned when the two enzymes work simultaneously. The phenolic radicals produced by laccases can interact with molecular oxygen forming hydrogen peroxide which in turn promotes LPMOs catalysis [63]. Moreover, lignin valorization via grafting desired compounds in lignin fraction is a further biotechnological route where laccase/mediator systems can be applied. It has been showed that laccase oxidation via ABTS efficiently deconstructs lignin polymers, prevents possible subsequent repolymerization event between phenolic radicals forming relative stable adduct with phenolic lignin dimers [64].

8.3.1.3 Unspecific Peroxygenases – UPOs

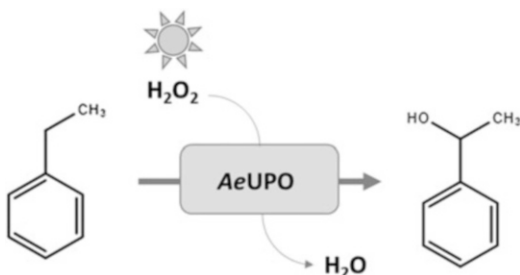
Recently discovered Unspecific Peroxygenases (UPOs, EC 1.11.2.1) are extracellular fungal enzymes grouped under a unique family of peroxygenases due to their broad substrate scope. Few UPOs have been currently isolated and biochemically

characterized, the first one, *Agrocybe aegerita* (*AeUPO*) was found within the Basidiomycota phylum. Current phylogenetic analysis show the presence of diversified putative UPOs sequences in almost 30 classes of Basidiomycota, Ascomycota and fungus-like Oomycota, with some of the hosting species living in extreme pH conditions or saline environments [65]. Like the well-known Cytochrome P-450 and Chloroperoxidases (CPOs), they host in the active site an heme-thiolate prosthetic group with an iron atom coordinating a proximal cysteine residue. UPOs are small monomeric proteins with molecular masses and isoelectric points varying from 32 to 46 kDa and from 3.8 to 6.1, respectively. Because of the high degree of glycosylation, UPOs are appreciated for their water-solubility and stability. Furthermore, the large variety of reactions they can catalyze is attracting the research attention for the design of new biocatalytic routes [66]. At the only expense of hydrogen peroxide (used as electron acceptor) UPOs catalyze the formation of alcohol products starting from short and medium-chain alkanes, and unlike CPOs, also from aromatic compounds and recalcitrant heterocycles [65]. Over 300 possible molecules are reported as a possible substrate for UPOs catalysis, including naphthalene, toluene, pyrene and p-nitrophenol among the aromatic rings and pyridine, dibenzofuran and various others as recalcitrant heterocycles.

Vinyl monomers are industrially important commodity chemicals used to produce polyacrylate, polystyrene, adhesive, protectives coatings, resins, rubbers, and other copolymers. Avasthi et al. [67] reviewed recent catalytic transformation strategies used to produce three important vinyl monomers such as acrylic acid (AA), methacrylic acid (MA) and styrene (ST) which precursors (itaconic acid, glycerol, allyl alcohol, lactic acid and acrolein) can be biomass-derived. Styrene is derived from oxidative dehydrogenation of ethylbenzene. Ethylbenzene can be obtained from selective lignin depolymerization[68]. Ethylbenzene, together with other valuable arenes (benzene, toluene and xylene) are now obtained from lignin [69].

Kroutil and co-workers [6] developed a photocatalytic process for the stereoselective conversion of ethylbenzene to 1-phenylethanol. Highly pure (S)- or (R)-enantiomers were obtained by simply tuning the visible light wavelengths used to activate a carbon nitride (CN-OA-m) photocatalyst. When the carbon nitride is irradiated with green light (528 nm), electron holes with lower oxidation potential are formed and hydrogen peroxide is photocatalitically produced from the water molecules present in the solution. On the contrary, the irradiation of CN-OA-m with more intense photons (440 nm) leads to the formation of a stronger oxidant excited state affording the C-H bonds oxidation to produce acetophenone. In situ generation of H₂O₂ supports the asymmetric hydroxylation of ethylbenzene catalyzed by the unspecific peroxygenase from *A. aegerita* (*AeUPO*), leading to the formation of enantiopure (R)-1-phenylethanol (99% e.e.) (Fig. 8.4). An alcohol dehydrogenase (ADH-A) from *Rhodococcus ruber* is instead employed to enantioselectively convert acetophenone to (S)-1-phenylethanol. The two light-driven reactions are wavelength specific enabling a fine control of the entire photobiocatalytic system by simple governing the emission light stimuli. More interesting, a protective effect against *AeUPO* deactivation was revealed upon green light illumination compared to

Fig. 8.4 *Agrocybe aegerita* (*AaeUPO*) oxidation of ethylbenzene to 1-phenylethanol driven by in situ photocatalytic production of H₂O₂



blue light due to minor production of ROS species. The substrate scope of *AeUPO* was also partially investigated with a series of methyl and halide substituted ethylbenzene. This elegant proof-of-concept pointed out, one more time, the importance of the rational design to assure a full exploitation of the photobiocatalytic system and to maximize its stability. Overoxidation of cyclohexane is a desirable reaction for the production of ε-caprolactame (key precursor of nylon polymers). *AeUPO* can be used for the conversion of cyclohexane into the corresponding ketone via a self-sustainable PBC system exploiting visible light energy. The excited state of the organic dye sodium anthraquinone sulfonate (SAS) was used to both yielding H₂O₂ via oxygen reduction, to drive the substrate hydroxylation catalyzed by *AeUPO*, and to mediate the further oxidation of the alcohol into cyclohexanone [70]. The same PBC system was also able to sustain the halogenation of thymol (a common natural terpenoid) catalyzed by a vanadium-dependent chloroperoxidase from *Curvularia inaequalis* (*CvVCPO*) [70]. In the two above mentioned works, substrate solubilization is required to afford the reaction in an aqueous solution. A study by Selin and colleagues [71] overcame the need for additional solvent supplementation, thus decreasing the number of pre-processing steps. In this case, an engineered *AeUPO* (*AaeUPO PaDa-I*) was immobilized into calcium alginate beads assuring good enzymatic stability in organic media. In situ hydrogen peroxide generation was concomitantly provided by light excitation of nitrogen-doped carbon nanodots and the strategy afforded the production of cyclohexanol in neat cyclohexane solution.

8.3.2 Cofactor Dependent Enzymes

Monooxygenases are a powerful class of enzymes that catalyze the insertion of one oxygen atom (oxidation or hydroxylation) into a wide variety of organic substrates for their functionalization. Monooxygenases can selectively oxidize alkenes, ammonia, methane, cyclohexanones, styrene, dyes and phenols, just to mention few of their substrate [38]. To do that these enzymes have to activate molecular oxygen, and this activation occur only if coupled with donation of electrons to molecular oxygen, and some di-copper monooxygenases share similarity with mono-copper LPMO in the mechanism of activity [72]. Almost all monooxygenases depend upon cofactors

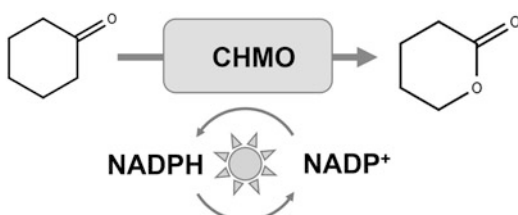
to obtain the electrons (i.e. mostly NADH and NADPH) which implies that this reducing agent equivalent molecule is oxidized then must be regenerated [73].

8.3.2.1 Baeyer-Villiger MonoOxygenases - BVMOs

Baeyer-Villiger monooxygenases (BVMOs) are FAD-containing redox proteins which activate O₂ for the incorporation of one oxygen atom into the substrate and reduce the other forming H₂O (EC 1.14.13.X). BVMOs are largely widespread among the tree of life and currently more than hundred eukaryotic and prokaryotic representatives have been isolated, characterized and crystallized for structure determination. Generally, they catalyze the conversion of ketones and cyclic ketones into esters and lactones, respectively. The binding of a NAD(P)H cofactor and the following two electrons flavine reduction are needed for initiate the catalysis of BVMOs, representing the first reductive half-reaction. During the second half-reaction, dioxygen is activated through the formation of an unprotonated peroxyflavin intermediate that attacks the carbonyl group in the substrate. In the absence of a suitable substrate, the uncoupling reaction leads to the production of hydrogen peroxide, as commonly happens for all monooxygenases. The broad substrate scope and variety of specific reactions catalyzed by BVMOs render this enzyme highly attractive for biotechnological applications but only recent research advances made them suitable for industrial uses [74]. One example is the Cyclohexanone monooxygenase (CHMO) from *Acinetobacter* sp. NCIMB 9871 which shows an impressive substrate scope as well as exquisite chemo-, regio-, and enantioselectivity and is currently employed for the enantioselective sulfoxidation of pyrmetazole to produce esomeprazole [75]. The full exploitation of BVMOs potential at industrial scale lies on some limiting factors such as poor enzyme stability in solution (being intracellular enzymes), sustainable cofactor regeneration and substrate/product inhibition.

A common strategy assuring continuous cofactor regeneration is the use of a whole-cell approach where the biocatalysis is supported by an engineered microorganism overexpressing the aimed enzyme. In 2017, Böhmer and co-workers [21] showed an interesting solution to cope with BVMO cofactor regeneration avoiding the depletion of energy-rich organic molecules, such as glucose in the case of whole-cell approach with heterotroph, or preventing the use of artificial photocatalysts when the reduction of NAD⁺ is mediated by light (Fig. 8.5). By engineering the

Fig. 8.5 Cyclohexanone MonoOxygenase (CHMO) catalyzed oxidation of cyclohexane to ϵ -caprolactone driven by photocatalytic regeneration of NADPH cofactor

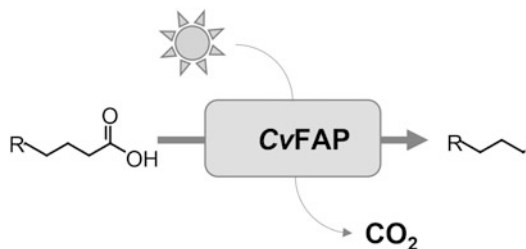


cyanobacteria *Synechococcus elongatus* with the NADPH-dependent Baeyer-Villiger cyclohexanone monooxygenase (CHMO) from *Acinetobacter calcoaceticus*, the authors were able to exploit the natural photosynthetic production of reducing power for the CHMO activity. The cyclohexanone substrate was completely converted into δ -valerolactone within 48 h without affecting the cells viability, thus allowing for further re-cultivation after the biotransformation. Whereas the inhibitory effect of high substrate concentration can be relieved by adopting sequential or simultaneous reaction configurations where the true enzymatic substrate is produced over time by a preliminary (photo)catalysis. The combination of the photocatalysis and enzymatic conversion was developed by Hollmann and colleagues [76] by designing a universal two-phase system for the C-H functionalization of simple alkanes. In this approach the organic phase acts as substrate reservoir while the aqueous phase contains the photocatalyst and the selected enzymes together with the relative cofactor, when needed. The reaction was taking place at the interface between the organic and the aqueous phase preventing the incompatibilities between the photo-organo catalyst and the biocatalyst, such as premature substrate degradation and enzyme inhibition caused by light-driven ROS generation or high substrate concentration. The light energy is directly used to drive small molecules oxidation into aldehydes or ketones by mean of the organophotocatalyst SAS (sodium anthraquinone sulfonate), and specifically in the above-mentioned work, cyclohexanol was oxidized to cyclohexanone. The further substrate functionalization is then catalyzed by CHMO or HAPMO (4-hydroxy-acetophenone) yielding ϵ -caprolactone or phenyl formate, respectively. The compartmentalization into two phases was beneficial for the system productivity compared to what has been achieved by the same system but in a homogeneous environment. Alternatively, a photo-biocatalytic cascade reaction can be designed to build a hybrid system where the catalytic substrate preparation is followed by the enzymatic conversion with a whole-cell approach [8]. The one-pot two-step reaction consists in a first oxidation of the cyclohexane to obtain the relative lactone using in situ photocatalytical generation of H_2O_2 . Secondly, the whole-cell approach is used to support the biocatalytic Baeyer-Villiger oxidation of the cyclohexanone into the desired ϵ -caprolactone employing a cell suspension of *E. coli* expressing the cyclohexane monooxygenase from *Acinetobacter calcoaceticus* (AcCHMO). Here, the photooxidation of cyclohexane mediated by Au-TiO₂ or g-C₃N₄ assured a clean and specific production of the cyclohexanone intermediate and the use of the cell suspension instead of the free extract contributed to the AcCHMO stabilisation.

8.3.2.2 FAP – Fatty Acid Photodecarboxylase

A new natural photo-enzyme named Fatty Acid Photodecarboxilase (CvFAP, EC 4.1.1.106) was discovered in the microalgae *Chlorella variabilis*, by Sorigué and colleagues [77]. This FAD-dependent enzyme belongs to the GMC (glucose-methanol-choline) oxidoreductase family and, contrary to the other members, it is involved in the lipid metabolism by converting fatty acids (FAs) into alkanes in

Fig. 8.6 Light-driven CvFAP (Fatty Acid Photodecarboxylase) decarboxylation of palmitic acid



response of blue light (Fig. 8.6). This discovery pointed out that in nature the light-driven catalysis does not only relay in the photosynthetic processes or in the repair of UV damages in DNA, but it is also exploited in metabolic pathways. The catalytic site of CvFAP is composed by a narrow hydrophobic tunnel harboring the FAD cofactor and allowing the stabilization of the fatty acid substrate. WT CvFAP is able to oxidatively remove the carbonyl group of a wide range of fatty acids but showing higher efficiency for C16–C17 chains. The turnover number measured for palmitic acid decarboxylation is $0.86 + - 0.13 \text{ s}^{-1}$ with a quantum yield higher than 80% [77]. The discovery of FAP is revolutionizing the paradigm of biofuels production. The classical approach is based on the conversion of fatty acids in the corresponding methyl and ethyl esters (FAMEs and FAEEs). The transesterification process carried out in mild condition is an equilibrium reaction in which significant molar surpluses of alcohols are required to arise the conversion yield and subsequent purification steps are needed to remove the formed soap. The possibility to enzymatically decarboxylate FAs offers a sustainable alternative for the conversion of waste bio-oils into biofuels having even a slightly higher specific heat of combustion (ca.9%) compared to classical FAMEs.

Huijbers and co-workers [78] developed a bienzymatic two-step cascade for the conversion of non-edible oils and fats into biofuels. The process allows the enzymatic hydrolysis of triolein to free oleic acids and glycerol using a lipase from *Candida rugose*. The subsequent intermediates are then subjected to photodecarboxylation to obtain the corresponding C1-shortened alkanes. The irreversible reaction of photodecarboxylation is catalyzed by a natural photoenzyme derived from *Chlorella variabilis* (CvFAP) which is activated upon blue light illumination leading to the photoexcitation of the FAD cofactor present in the active site. CvFAP is characterized by a high substrate scope and good tolerance toward organic solvent (up to 50% DMSO). Higher activity and robustness were achieved performing the catalysis in presence of the cell crude extract rather than with the purified enzymatic preparation. In another approach spores of *Bacillus subtilis* were used as cell factories for the recombinant expression on CvFAP and physical support for the enzyme immobilization. The CvFAP was cloned in frame with an abundant endogenous coating protein assuring the localization in the outer layer of the spore coating. Microbial oils and olive oil were used for the hydrocarbon production in a one pot bienzymatic reaction. Commercially available lipase catalyzed the release of

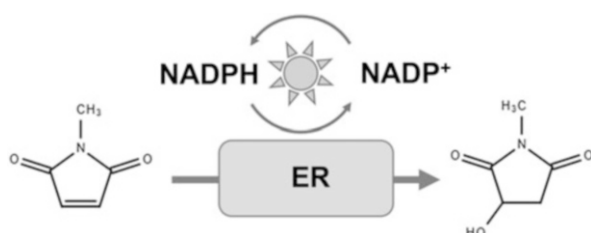
free fatty acids and their decarboxylation was conducted under blue light irradiation by CvFAP [79].

8.3.2.3 Ene-Reductases

Ene-reductases (EC 1.3.1.31), belonging to the Old Yellow Enzyme (OYE) family, are flavin mononucleotide (FMN)-containing redox enzymes catalyzing the reduction of C=C double bonds of a wide range of substrates at the expense of a nicotinamide cofactor. Several biocatalytic processes have been developed to sustain the regeneration of the natural reducing agent (NAD(P)H), to expand the enzymatic scope as well as combine various reactions to diversify the product range. Asymmetric chemical reduction yielding chiral products is an essential reaction for the synthesis of pharmaceutical and valued-chemical compounds. The stereoselective saturation of C–C double bonds in alkenes is currently achieved employing precious metal catalysts and hydrogen gas. Although the chemical conversions boast a perfect atom efficiency, new biocatalytic approaches represent a valid alternative when milder conditions, metal-free reactions and highly enantiopure products are desired [80]. Increasing research efforts are resulting in the enzymatic alkene reduction using ene-reductase as a key biocatalyst.

A first attempt for the sustainable regeneration of reducing power using water and light was proved by König et al. [81] by developing a whole-cell biocatalytic approach based on a recombinant cyanobacteria (*Synechocystis* sp. PCC6803) overexpressing the enoate reductase YqjM from *Bacillus subtilis*. A broad range of cyclic prochiral alkenes were enantioselectively reduced by the viable biocatalyst upon irradiation with visible light and at the only expense of water oxidation (Fig. 8.7). Despite the high enantiopurity of the products (> 99% for 2-methylsuccinimide) and the fine light control of the reaction, further process optimizations are envisioned to achieve industrially relevant product yields. However, the cell tolerance toward high substrate concentration and the repression of side reactions leading to product (or substrate) degradation are still the common main challenges for most of the whole-cell technologies. In a recent work by Wang and colleagues [82] the light energy supply is exploited to both drive the ene-reductase activation and the substrate isomerization from a less to a higher reactive form. Based on the light dual utilization concept, the authors conceived a chemoenzymatic system aimed to convert mixture of alkene isomers into an enantiopure product using

Fig. 8.7 Photocatalytic cofactor regeneration for Ene-reductase (ER) reduction of 2-methyl-*N*-methylmaleimide to (*R*)-2methyl-*N*-methylsuccinimide



blue light irradiation. Mixtures of alkene substrates are often low isomeric homogeneous, and some isomers (*E*) are preferentially targeted by ene-reductases than the (*Z*) counterpart causing a loss of conversion yield. A photosensitized energy transfer process mediated by an iridium catalyst, is used to drive the alkene isomerization from *Z*-alkenes to *E*-alkenes. Those reactive intermediates are then subjected to asymmetric reduction by specific ERs via photoinduced electron transfer for the regeneration of the flavin coenzyme (FMNH_{red}). The chemoenzymatic system has been tested for the conversion of several aryl alkenes with specific reductase enzymes, all of them yielding products with high optical purity (> 95% ee, in average). An improved final yield was observed when the two light-driven reactions worked in a cooperative manner rather than sequentially performed. This is likely due to the benign competition among chemo and enzymatic reactions that prevents the non-specific alkene reduction mediated by the photoexcited free FAD cofactor.

8.3.3 New Proposed System for Conversion of Biomass and CO₂ to Value-Added Bio-alkanes

Very recently Lin and colleagues [83] envisioned a circular cascading system for the production of bio-based fuels combining the latest bioelectrochemical technologies such as electro-fermentation, microbial CO₂ electrosynthesis and photobiocatalysis. Through electro-fermentation, renewable feedstocks can be converted in short chain carboxylic acid (such as acetic and butyric acid) and CO₂ which are then subjected to chain elongation to obtain e.g., caproic acid via microbial CO₂ electro synthesis. Finally, the specific calorific value of medium chain carboxylic acids is enhanced by removing their carbonyl groups yielding relative alkanes through the photoenzymatic catalysis step using CvFAP. The application of an electrical field in fermentation processes allow a fine regulation of the microbial redox metabolism leading to an increased carbon usage efficiency and improved products selectivity compared to traditional fermentation [84]. In this context, the working electrode (acting as electron donor) favors cathodic reactions resulting in the reduction of the substrate and the product enrichment in volatile fatty acids [85]. CO₂ is then used as principal substrate for the sequential carbon chain elongation of short chain carboxylic acids by a microbial electro synthesis driven by reducing power externally supplied from a cathode with higher potential [86]. The entire biorefinery process is envisioned to end up with the photobiocatalytic oxidation to alkanes performed by FAP enzymes under mild conditions. Despite the recent discovery of these photoenzymes, several studies have resulted in an improvement of its catalytic stability and in substrate preference tuning [87].

8.4 Bioresources for Photobiocatalysis and Applications

The PBC processes are particularly attractive for their potential applications to bioresources and biomass transformations, a key strategy to enhance the circularity aspects of our modern biobased society oriented towards the zero-waste goal. The transition from a fossil-based to a greener society is not only linked to consumption of bioderived or renewable goods, but also aims at increasing the sustainability of current production methods still often entirely based on petrol-derived catalysts, toxic metals additives, and non-renewable energy inputs. Therefore, PBC based on natural pigments, sorted directly from the biomass or produced by microorganisms, are particularly attractive in these regards. Imagining a self-sustainable PBC process, an ideal bioresource should then be made of: (i) the substrate for the photoactive enzyme, or contain platform molecules (i.e. glucose) to be converted by a cell-based PBC system; (ii) moreover, should have sacrificial molecules to recharge the PS or to work as electron donors; (iii) and optionally a natural pigment, either sorted directly from the bioresource (i.e. chlorophyll-derived from green grasses), or produced by the cell. Finally, combinations of bioresources and/or waste streams could allow the instauration of the above-mentioned conditions, and if the same bioresource could sustain the endogenous production of the enzymatic catalysts, then it would further increase the entire sustainability of the process towards stand-alone conditions as well. The coupling of photocatalytic and biodegradative process is a relatively recent strategy allowing efficient removal of pollutants contained in waste waters [88] but still differs from PBC as the photoelectron are not directly transferred to the enzymatic active site, and needing of a porous carrier for instauration of a microbial film. The process is known as intimate coupled photocatalysis and biodegradation ICPB, and already found several fields of applications and a patented technology (WO2009023578A1) for general abatement of organics, phenolics removal [89]; and tannery waste waters often containing dyes [90, 91]. Therefore, such waste waters could be blended with lipids rich or lignocellulosic rich slurries for achieving simultaneous removal of toxicants and conversion of the primary organic waste into the desired products.

Several available bioresources or organic wastes could sustain entirely or partially a PBC system and could be divided as naturally occurring bioresources or anthropogenic biowaste. In this paragraph we classified them following the chemical class of the major substrates that are target of enzymatic conversion, specifying the type of PBS that could be sustained by the specific biowaste, their source and sector of application (Fig. 8.8 and Table 8.2).

8.4.1 Lignocellulose

Nonedible lignocellulose bioresources are common in the biorefinery sector for production of bioethanol, lignols and second-generation hydrolysates/molasses.

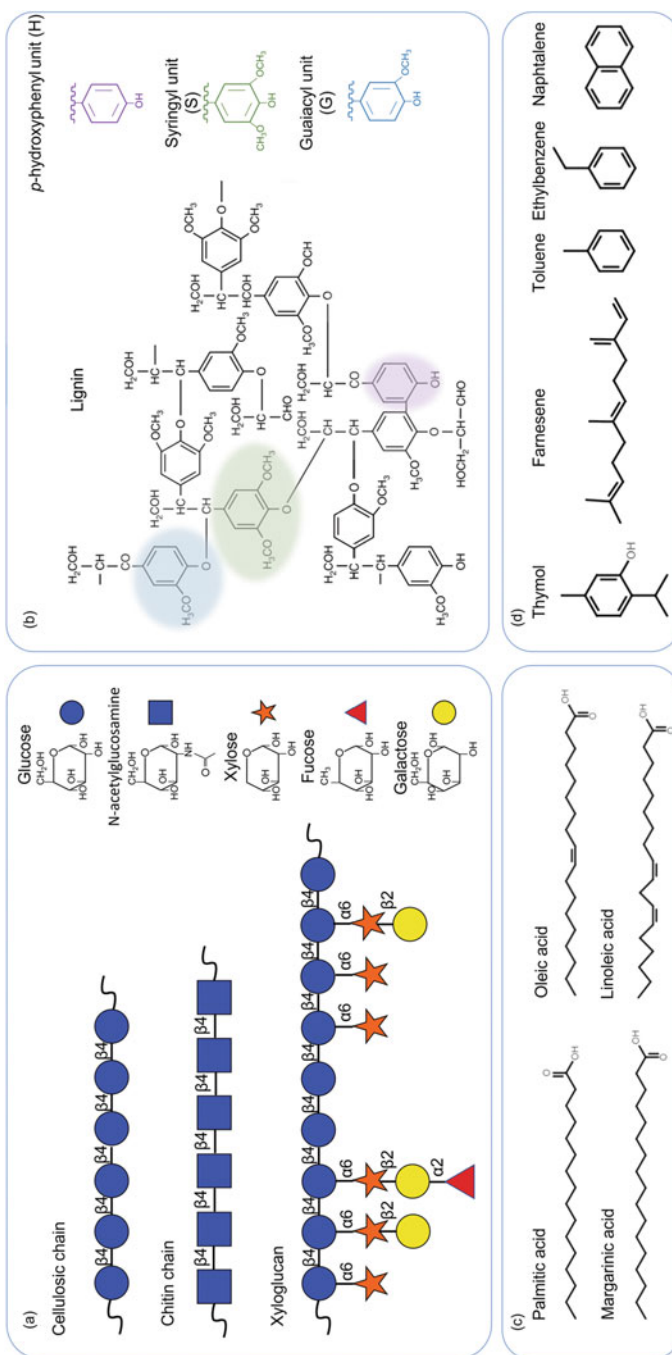


Fig. 8.8 Structure of suitable substrates for photobiocatalysis from bioresources grouped by class: (a) monosaccharide building blocks (right) and polysaccharides (left) from plant biomass; (b) lignin units (right) and a representation of a natural lignin (left); (c) fatty acids; (d) terpenoids. Adapted with permission from [92]. Copyright © 2015, Elsevier

The main source are woody materials, agricultural waste and residues of dedicated crops (i.e., sugarcane bagasse). They originate from plant cell walls that are composed of a limited chemical diversity mainly carbohydrate polymers and phenol-based hetero-molecules: respectively cellulose, hemicellulose and lignin. Polysaccharides are made of relatively few types of monosaccharide building blocks (glucose, xylose, mannose, arabinose and galactose among the others, Fig. 8.8a). Moreover, their composition is further reduced after chemical-physical pretreatment needed for preparing the lignocellulose for subsequent enzymatic hydrolysis steps. Often only glucans- and xylan-based polymers dominate the entire saccharide fractions of pretreated lignocellulose, but still organized in recalcitrant ultrastructure surrounded by phenolic heteropolymer. This highly cross-linked molecule, referred to as lignin does not have a proper polymeric organization as distinct repeating units are not evident, but for easiness of definition is synthesized from three main phenolic units: para-hydroxyphenyl (H), guaiacyl (G) and syringyl (S) (Fig. 8.8b). It is polymerized in a 3D structure enveloping the polysaccharides, filling the voids among them, finally providing inaccessible barrier. The composition of lignin varies among plant species. Softwood (gymnosperms) is rich in G units (G:S:H 94:1:5 in % of total lignin [93]) while angiosperms in general have more G and S lignin (wheat straw, G:S:H 45:46:9 in % of total lignin [94]) and an overall lower amount compared to softwoods.

The role of lignin during enzymatic hydrolysis has been subject of extensive studies often showing negative effects to glycosyl hydrolases inhibition occurring through irreversible non-productive adsorption mainly [95, 96]. However, this paradigm had been recently challenged thanks to seminal discoveries that have seen the lignin derived phenolics being able at activating key redox enzymes, i.e. LPMO [52, 62, 97], that consequently increase the activity of glycosyl hydrolases. In addition, lignin derived molecules could even provide electrons to photo-reduced photosensitizers, also able at donating photo-excited electrons to LPMO, i.e. chlorophyllin [12], therefore making lignin the ultimate donor of electrons in the role of sacrificial molecule for PBC [12]. Because lignin is regarded often as the waste of biorefineries, this confers it the label of the most attractive sacrificial molecule to be used for powering photocatalytic system owing to its wide range of redox potential, availability and low costs [98].

Of note, is that all evidence on the role of lignin as LPMO activator has always dealt with pretreated lignin often using hydrothermal or organosolvent strategies, that tend to preserve the native phenolic structure [12, 99], compared instead to the highly oxidizing technology like alkaline based methods which are found detrimental for preserving the reducing ability of lignin [100]. Potentially photoactive enzymes, such as laccases and peroxydases, have been found that depolymerize lignin [101], laying a major route for future development in the light driven conversion of lignocellulosic biomass. To summarize, the potential uses of lignocellulosic biomass in PBC based on LPMO enzymes are linked to the productions of either cello-oligosaccharides and xylan-oligosaccharides using waste lignin as electron donors and leaving a semi-treated lignocellulose material to ease subsequent enzymatic hydrolysis for molasses productions.

On the side of freshly harvested lignocellulosic resources, it is worth mentioning the green grasses, an emerging source of various components of interest also for PBC. Often green grasses are treated immediately after mowing, leaving the chlorophyll derived pigments still active in donating electrons to redox enzymes although still anchored to the semi-lysates thylakoids membranes from chloroplasts [12]. This is due to the gentle screw-press separation which fractionates the liquid part of green grass (green juice) containing water soluble proteins, thylakoids, sugars and cell lysates, from the fibers, mostly composed of water insoluble polysaccharides and minimal fraction of phenolics. The fiber so obtained could undergoes subsequent physical-chemical pretreatment and later being reunited with the green juice to sustain a PBC process based for example on photoactivable redox enzymes acting on the cellulose fibers for production of oligosaccharides (Table 8.2). Alternatively, other enzymes able at receiving electrons from photoexcited thylakoids could be coupled.

8.4.2 *Chitin*

Chitin is considered the second most abundant polysaccharide in nature after cellulose, with which it shares many chemical and structural similarities, so that often it is referred to as the “animal cellulose”. The backbone of chitin polymers is made of N-acetylglucosamine linked through a β -1,4-glycosidic bond, thus featuring both amorphous and crystalline regions, it can also be isolated in form of nanofibrils. Today, many industrial process and specialty chemical applications are based on chitin rendering this molecule attractive for biotechnological purposes from food additives (edible protective films) to plant elicitors and bio-stimulants. Common into the cell walls of fungi and exoskeleton of insects and mollusks, chitin is often sorted in quantity from different man-made wastes: industrial fishery, fungal cultures, and food-waste. In biocatalysis research, chitin had been a precursor of several discoveries regarding degrading enzymes that later had been also confirmed or applied to cellulose degradation, as for example the discovery of the LPMO class (namely the CPB21 enzyme [40]). Therefore, after proving the photoactivation of LPMO on cellulose substrate, it was also found that similar PBC system could be applied on chitin-active LPMOs AA10 giving an array of native and oxidized chito-oligosaccharides, also confirming an higher turn-over rate when exposed to light and using chlorophyllin as PS [14].

8.4.3 *Lipids*

Lipids and fatty acids represent a wide class of substrates for photoactive enzymes either in PBC mode or whole cells PBC. They are extracted from bioresources or produced as metabolites from growing cultures that often contains also natural

photosensitizers and sacrificial molecules. The major source of renewable lipids for biofuels applications are agricultural dedicated productions (first-generation crops, *i.e.*, palm seeds, soybean, rapeseed), or their direct or processing waste (*i.e.*, not-edible olive oil pomace and their black waste waters, second generation biofuels); then algal productions (advanced biofuels or third generation); and finally, food industry waste (*i.e.*, waste cooking oil - WCO). Those mentioned represent the more common sources of lipids worldwide but obviously there exists many other sources. Particularly at local scale one could find more abundant availability from man-made activities or local biomass productions, and often with already established chains of disposal and collections that could enhance further the feasibility and circularity of their bioprocessing [102].

8.4.3.1 Algal Culture

Algal cultures produce fatty acids for carbon storage purposes (up to 50% in dry weight) or alternatively as secondary metabolites. Starting from CO₂ algae could virtually photo-convert this into any given substrate either naturally or via genetic modifications. For example new cyanobacterial strain, *Synechococcus* sp. PCC 11901, was discovered recently and engineered to produce free fatty acids in yields over 6 mM (1.5 g L⁻¹), an amount produced autotrophically and comparable to that achieved by similarly engineered heterotrophic organisms [103]. The literature is vast on bioresources production form algal cultures [104] (the reader is also redirected to Chap. 12 of this book).

The fatty acids produced by algae are a mixture of saturated and monounsaturated, and different lengths often ranging commonly from 14 to 20 carbons, called polyunsaturated fatty acids (PUFAs). Often their particular ratio or profile is unique for each strain and/or cultivation conditions [105]: among others linoleic, linolenic and arachidonic acids are the most commonly found algal PUFAs [106]. Phycobilisomes are the light harvesting antennae supercomplexes of cyanobacteria and red algae and consist of three types of phycobiliproteins: allophycocyanin, phycoerythrin, phycocyanin [107]. These phycobiliproteins are responsible for absorbing light in the region of 500-650 nm usually not permitted by chlorophyll pigments. Anchored on the surface of thylakoids, they can be used as PS for donating electrons to redox enzymes. Thylakoids of the cyanobacterium *Synechococcus* sp. PCC 7002 were used in combination with LPMO enzymes for successful oxidation of cellulose fibers [12]. Finally, an array of secondary metabolites is usually produced by algal and microbial cultures of which several could serve as sacrificial molecule once the cells are lysate: organic acids (ascorbate, gallate, 3HAA, etc.), phenolics, aromatics.

8.4.3.2 Food Waste

An important source of lipidic substrates is society-made linked to the food waste of various sectors. As for example, we analyze here the waste cooking oil, that in many parts of the world is separated from the general household waste through a dedicated collection system, therefore enabling potentially a series of tailored bioprocesses. The United States generates approximately ten million tons of WCO annually [108], while considering urban scale a particular indicative case is that of Hong Kong. There three million tons of municipal waste is produced every year and based on data reported by Karmee et al., the lipid fraction could sum up to approximately 400 thousand tons, which is attractive for local biodiesel production [102]. The chemical variety of waste cooking oil or lipid fraction of municipal waste can variate greatly among various regions, and in Shanghai in 2010 was reported to be made of linoleic, oleic and palmitic acid (55%, 21% and 8% respectively) (Fig. 8.8c) [109].

8.4.4 *Microbial Production of Relevant Substrates*

Continuous development on genetic engineering technologies, like CRISPR-Cas for example, are easing synthetic biology approaches for isolation of unique cultures for production of chemicals. Virtually no limits could be posed to the variety of molecules achievable with genetically modified strains. Today several de novo enzymes could be introduced in various hosts, for reconstituting entire biosynthetic pathways or creating new enzymatic cascades for producing the desired molecule. In photobiocatalysis these approaches are becoming popular either for producing the substrates to be used for photoactive enzymes or to form entire photocatalytic living cells, where the photosensitizers, enzymes, and substrates are assembled to produce the final product upon light energy and a carbon source (often CO₂). This latter approach is described in paragraph 2 dedicated to enzymes and whole cell applications of PBC, here we limit our discussion in the use of biologically derived substrates for PBC.

8.4.4.1 Terpenoid and other natural hydrocarbons

Terpenoids from plants represent probably the largest class of compounds in terms of chemical diversity. Many terpenoids are the building block for the production of several commodities such as whole are considered platform chemicals. Also, many have optimal reducing ability for donating electrons to exhausted photosensitizer, besides being themselves photoactive or photo-reducing. Olive oil waste waters and solid waste of olive processing often contain several terpenoids [110] and the reducing ability or antioxidant is retained for long time after harvesting or processing [111]. Many interesting compounds are today biorefined enzymatically from this

agricultural waste. Although natural sources are available, many studies are now focusing in producing terpenoids using microbial cells factories using the principle of synthetic biology purposely for increasing yield and ease downstream separation. Often the strategy adopted involves also photoactive enzymes (*i.e.* P450 enzyme) along the biosynthetic pathway reconstructed in microbial hosts [112]. The latter if also naturally containing photosynthetic complexes or modified to express some could indeed represent a self-sustaining cell-based photobiocatalytic process [24].

Farnesene is linear sesquiterpenoid (Fig. 8.8d) of various biological function and substrate of the OYEnzy or ENE reductases which catalyze the double bond rearrangement also in other alkene so allowing production of special stereoisomers of various molecules. Upon improvement by addition of farnesene synthase gene from *Artemesia annua*, *S. cerevisiae* strain could produce farnesene at a yield, when fed with glucose a conversion of 0.12 g/g was achieved [113]. Few other aromatics hydrocarbons are also produced microbiologically. In nature toluene [114] and naphthalene [115] (Fig. 8.8d) have been found in the environment of their relative ecosystems being produced for specific ecological purposes that are still not elucidated yet. However, the existence of the biosynthetic pathways in distinct organisms poses the fundaments for developing future biotechnologies for the enhanced bio-productions of such chemical commodities for direct use as substituent of actual petrol-based production, or as common substrate of photo-catalytically active enzymes for subsequent transformation into other necessary molecules. Styrene is a cyclic alkene (Fig. 8.8d) that can be oxidized to its epoxy form by monooxygenases like laccases [60]. Polystyrene it is probably one the most produced plastic in the world. It has been demonstrated that styrene can also be formed by micro-organisms from renewable substrates such as glucose [116].

8.5 Conclusions and Future Outlook

The idea of converting light-energy directly into chemical-equivalent, biofuels and biomaterial is the Holy Grail for a sustainable fossil-free society. To that end photobiocatalysis applied to the transformation of society-made waste and bioresources represent the closest technological option in our hands. Although the goal is still far as generally accepted, PBC is at its infancy, yet today we can count several scalable enzymatic systems on which could be focused on for future stable application. The scalability of the technology then is influenced upon few basic barriers being the choice of the sacrificial molecule and photosensitizer; the sourcing and composition of organic substrate to be converted; and other engineering aspects like, light supply, volumes/surface, bioreactor design etc.

There exist several classes of molecules that can be used as photosensitizer in PBC, from organic biologically extracted pigments, synthetic molecules based on metal, and semiconducting nanoparticles of which either industrial application already exists (*i.e.*, chlorophyllin) or which its production is facile (carbon and graphene-based nanoparticles). The conversion of the light energy into chemical

energy primarily depends on the ability of a photosensitizer to absorb a photon, be promoted to its excited state, and donate the electron at the conduction band to an external acceptor before return to the ground state. This would leave the organic photosensitizer oxidized or photobleached preventing a new round of photoexcitation almost immediately after light exposure, yet given to its abundance in case of biologically derived (thylakoids etc.) this would be a tolerable cost. Instead, when using metal complexes for photoexcitation, this causes electronic holes that need to be quenched, although more expensive than biologically derived carbon nanoparticles could still undergo several cycles before exhausting.

It is therefore evident that in any photosensitizer option that one could choose, there is a need for refilling the electron photoexcited, and a sacrificial molecule must always be added to PBC. In nature, this is achieved by water molecule splitting, that is considered the most successful photo-biocatalytic example, representing though the final aim of artificial photosynthesis or PBC. Meanwhile, since we have not yet achieved the goal, still an equivalent electron donor has to be sacrificed. Their choice is crucial for the sustainability of the PBC as their chemical and economical value must be lower than the of the final product. Therefore, photobiocatalysis systems based on organic waste, carrying their own pool of sacrificial molecules otherwise not exploitable by any other bioprocesses (*i.e.*, low concentration), are becoming attractive.

Regarding the waste composition as emerged here, several biowastes are found suitable for PBC processes, some bringing all the components needed, substrate, pigments, sacrificial molecule or possibly enzymes. The major problematic issues associated with the use of bioresources in general is then linked to the solid particles, fibers, and membranes that cause light scattering and shading which impair a uniformed transmittance of light. To that end, slurry clarification by dedicated decanter units or membrane-based technology are a valid option as already used at commercial scale for cellulosic ethanol biorefinery. Another beneficial aspect of these strategies is also avoidance of hydrophobic adsorption of PS or enzymes on fibers and lignin.

Although many successful PBC systems have been reported in the literature (Table 8.1), the conversion yields and reaction volumes are still performed on laboratory scales making it difficult to obtain a reliable estimate of their scalability. The lack of studies investigating the robustness and reproducibility of PBC reactions in increasing volumes hamper the transition from “proof-of-concept” set up to the design of platforms at industrial relevant scale, and this is where the next research should be focused. However, the design and development of PBC large-scale reactors may benefit from what it has been already done concerning the optimization of photobioreactors for microalgal cultivation, sourcing then from decades of research for a quick adaptation of the technology to PBC.

Overall, the nascent field of photobiocatalysis holds all the premises for rapid development from lab-scale to commercial scale technology, especially if coupled with transformation of inexpensive substrates today considered waste, into added value chemicals, platform chemicals, and or material. Key to this success will be the adaptation of mature technologies developed for biorefinery and algal cultures.

References

- Rapf RJ, Vaida V. Sunlight as an energetic driver in the synthesis of molecules necessary for life. *Phys Chem Chem Phys.* 2016;18:20067–84. <https://doi.org/10.1039/C6CP00980H>.
- Tokode O, Prabhu R, Lawton LA, Robertson PKJ. Controlled periodic illumination in semiconductor photocatalysis. *J Photochem Photobiol A Chem.* 2016;319–320:96–106. <https://doi.org/10.1016/j.jphotochem.2015.12.002>.
- Bartlett JS, Ciotti ÁM, Davis RF, Cullen JJ. The spectral effects of clouds on solar irradiance. *J Geophys Res Ocean.* 1998;103:31017–31. <https://doi.org/10.1029/1998JC900002>.
- Holdmann C, Schmid-Staiger U, Hirth T. Outdoor microalgae cultivation at different biomass concentrations—assessment of different daily and seasonal light scenarios by modeling. *Algal Res.* 2019;38:101405. <https://doi.org/10.1016/j.algal.2018.101405>.
- Adam D, Bösche L, Castañeda-Losada L, Winkler M, Apfel U-P, Happe T. Sunlight-dependent hydrogen production by photosensitizer/hydrogenase systems. *ChemSusChem.* 2017;10:894–902. <https://doi.org/10.1002/cssc.201601523>.
- Schmermund L, Reischauer S, Bierbäumer S, Winkler CK, Diaz-Rodriguez A, Edwards LJ, Kara S, Mielke T, Cartwright J, Grogan G, Pieber B, Kroutil W. Chromoselective photocatalysis enables stereocomplementary biocatalytic pathways**. *Angew Chemie Int Ed.* 2021;60:6965–9. <https://doi.org/10.1002/anie.202100164>.
- Juris A, Ceroni P, Balzani V. Photochemistry and photophysics: concepts, research, applications, 2014.
- Li P, Ma Y, Li Y, Zhang X, Wang Y. Cascade synthesis from Cyclohexane to ε-caprolactone by visible-light-driven photocatalysis combined with whole-cell biological oxidation. *Chembiochem.* 2020;21:1852–5. <https://doi.org/10.1002/cbic.202000035>.
- Junge NH, Fernandes DLA, Sá J. Phototriggering lignin peroxidase with nanocatalysts to convert veratryl alcohol to high-value chemical veratryl aldehyde. *Mater Today Sustain.* 2018;1–2:28–31. <https://doi.org/10.1016/j.mtsust.2018.11.001>.
- Imahori H, Umeyama T, Ito S. Large π-aromatic molecules as potential sensitizers for highly efficient dye-sensitized solar cells. *Acc Chem Res.* 2009; <https://doi.org/10.1021/ar900034t>.
- Lin VSY, DiMagno SG, Therien MJ. Highly conjugated, acetylenyl bridged porphyrins: new models for light-harvesting antenna systems. *Science* 80. 1994;264:1105–11. <https://doi.org/10.1126/science.8178169>.
- Cannella D, Möllers KB, Frigaard N-U, Jensen PE, Bjerrum MJ, Johansen KS, Felby C. Light-driven oxidation of polysaccharides by photosynthetic pigments and a metalloenzyme. *Nat Commun.* 2016;7:11134. <https://doi.org/10.1038/ncomms11134>.
- Dodge N, Russo DA, Blossom BM, Singh RK, van Oort B, Jensen PE. Water-soluble chlorophyll-binding proteins from *Brassica oleracea* allow for stable photobiocatalytic oxidation of cellulose by a lytic polysaccharide monooxygenase. *Biotechnol Biofuels.* 2020;13(1): 1–12. <https://doi.org/10.21203/rs.3.rs-40886/v1>.
- Bissaro B, Kommedal E, Rørh ÅK, Eijsink VGH. Controlled depolymerization of cellulose by light-driven lytic polysaccharide oxygenases. *Nat Commun.* 2020;11. <https://doi.org/10.1038/s41467-020-14744-9>.
- Lazarides T, Sazanovich IV, Simaan AJ, Kafentzi MC, Delor M, Mekmouche Y, Faure B, Réglier M, Weinstein JA, Coutsolelos AG, Tron T. Visible light-driven O₂ reduction by a porphyrin-laccase system. *J Am Chem Soc.* 2013;135:3095–103. <https://doi.org/10.1021/ja309969s>.
- Zhang S, Shi J, Sun Y, Wu Y, Zhang Y, Cai Z, Chen Y, You C, Han P, Jiang Z. Artificial thylakoid for the coordinated photoenzymatic reduction of carbon dioxide. *ACS Catal.* 2019;9: 3913–25. <https://doi.org/10.1021/acscatal.9b00255>.
- Ihara M, Nishihara H, Yoon K-S, Lenz O, Friedrich B, Nakamoto H, Kojima K, Honma D, Kamachi T, Okura I. Light-driven hydrogen production by a hybrid complex of a [NiFe]-hydrogenase and the cyanobacterial photosystem I. *Photochem Photobiol.* 2006;82:676. <https://doi.org/10.1562/2006-01-16-RA-778>.

18. Lubner CE, Applegate AM, Knörzer P, Ganago A, Bryant DA, Happe T, Golbeck JH. Solar hydrogen-producing bionanodevice outperforms natural photosynthesis. *Proc Natl Acad Sci U S A.* 2011;108:20988–91. <https://doi.org/10.1073/pnas.1114660108>.
19. Lee M, Kim JH, Lee SH, Lee SH, Park CB. Biomimetic artificial photosynthesis by light-harvesting synthetic wood. *ChemSusChem.* 2011;4:581–6. <https://doi.org/10.1002/cssc.201100074>.
20. Włodarczyk A, Gnanasekaran T, Nielsen AZ, Zulu NN, Mellor SB, Luckner M, Thøfner JFB, Olsen CE, Mottawie MS, Burow M, Pribil M, Feussner I, Møller BL, Jensen PE. Metabolic engineering of light-driven cytochrome P450 dependent pathways into *Synechocystis* sp. PCC 6803. *Metab Eng.* 2016;33:1–11. <https://doi.org/10.1016/j.ymben.2015.10.009>.
21. Böhmer S, Königler K, Gómez-Baraibar Á, Bojarra S, Mügge C, Schmidt S, Nowaczyk M, Kourist R. Enzymatic oxyfunctionalization driven by photosynthetic water-splitting in the cyanobacterium *synechocystis* sp. PCC 6803. *Catalysts.* 2017;7:240. <https://doi.org/10.3390/catal7080240>.
22. Lassen LM, Nielsen AZ, Ziersen B, Gnanasekaran T, Møller BL, Jensen PE. Redirecting photosynthetic electron flow into light-driven synthesis of alternative products including high-value bioactive natural compounds. *ACS Synth Biol.* 2014;3:1–12. <https://doi.org/10.1021/sb400136f>.
23. Lee SH, Choi DS, Pesic M, Lee YW, Paul CE, Hollmann F, Park CB. Cofactor-free, direct photoactivation of enoate reductases for the asymmetric reduction of C=C bonds. *Angew Chem Int Ed.* 2017;56:8681–5. <https://doi.org/10.1002/anie.201702461>.
24. Feyza Özgen F, Runda ME, Burek BO, Wied P, Bloh JZ, Kourist R, Schmidt S. Artificial light-harvesting complexes enable rieske oxygenase catalyzed hydroxylations in non-photosynthetic cells. *Angew Chem Int Ed.* 2020;59:3982–7. <https://doi.org/10.1002/anie.201914519>.
25. Biegasiewicz KF, Cooper SJ, Emmanuel MA, Miller DC, Hyster TK. Catalytic promiscuity enabled by photoredox catalysis in nicotinamide-dependent oxidoreductases. *Nat Chem.* 2018;10:770–5. <https://doi.org/10.1038/s41557-018-0059-y>.
26. Richardson SN, Nsiamka TK, Walker AK, McMullin DR, Miller JD. Antimicrobial dihydrobenzofurans and xanthenes from a foliar endophyte of *Pinus strobus*. *Phytochemistry.* 2015;117:436–43. <https://doi.org/10.1016/j.phytochem.2015.07.009>.
27. Bissaro B, Forsberg Z, Ni Y, Hollmann F, Vaaje-Kolstad G, Eijsink VGH. Fueling biomass-degrading oxidative enzymes by light-driven water oxidation. *Green Chem.* 2016;18:5357–66. <https://doi.org/10.1039/c6gc01666a>.
28. Mifsud M, Gargiulo S, Iborra S, Arends IWCE, Hollmann F, Corma A. Photobiocatalytic chemistry of oxidoreductases using water as the electron donor. *Nat Commun.* 2014;5:1–6. <https://doi.org/10.1038/ncomms4145>.
29. Yan L, Yang F, Tao CY, Luo X, Zhang L. Highly efficient and stable Cu₂O–TiO₂ intermediate photocatalytic water splitting. *Ceram Int.* 2020;46:9455–63. <https://doi.org/10.1016/j.ceramint.2019.12.206>.
30. Xiong J, Liang Y, Cheng H, Guo S, Jiao C, Zhu H, Wang S, Liang J, Yang Q, Chen G. Preparation and photocatalytic properties of bagasse-supported nano-TiO₂ photocatalytic-coupled microbial carrier. *Gongneng Cailiao/J Funct Mater.* 2020;51 <https://doi.org/10.3969/j.issn.1001-9731.2020.07.003>.
31. Durgalakshmi D, Ajay Rakkes R, Rajendran S, Naushad M. Green photocatalyst for diverse applications. In: *Green photocatalysts for energy and environmental process*. Cham: Springer; 2020. https://doi.org/10.1007/978-3-030-17638-9_1.
32. Bera D, Qian L, Tseng TK, Holloway PH. Quantum dots and their multimodal applications: a review. *Materials.* 2010;3:2260–345. <https://doi.org/10.3390/ma3042260>.
33. Das GS, Shim JP, Bhatnagar A, Tripathi KM, Kim TY. Biomass-derived carbon quantum dots for visible-light-induced photocatalysis and label-free detection of Fe(III) and ascorbic acid. *Sci Rep.* 2019;9:1–9. <https://doi.org/10.1038/s41598-019-49266-y>.

34. Yao X, Ma C, Huang H, Zhu Z, Dong H, Li C, Zhang W, Yan Y, Liu Y. Solvothermal-assisted synthesis of biomass carbon quantum dots/bismuth oxyiodide microflower for enhanced photocatalytic activity. *Nano.* 2018;13(03):1850031. <https://doi.org/10.1142/S1793292018500315>.
35. Tang X, Yu Y, Ma C, Zhou G, Liu X, Song M, Lu Z, Liu L. The fabrication of a biomass carbon quantum dot-Bi₂WO₆ hybrid photocatalyst with high performance for antibiotic degradation. *New J Chem.* 2019;43:18860–7. <https://doi.org/10.1039/C9nj04764f>.
36. Bhattacharya D, Mishra MK, De G. Carbon dots from a single source exhibiting tunable luminescent colors through the modification of surface functional groups in ORMOSIL films. *J Phys Chem C.* 2017;121:28106–16. <https://doi.org/10.1021/acs.jpcc.7b08039>.
37. Younus H. Oxidoreductases: overview and practical applications. In: Biocatalysis: enzymatic basics and applications. Springer International Publishing; 2019. p. 39–55. https://doi.org/10.1007/978-3-030-25023-2_3.
38. Torres Pazmiño DE, Winkler M, Glieder A, Fraaije MW. Monooxygenases as biocatalysts: classification, mechanistic aspects and biotechnological applications. *J Biotechnol.* 2010;146: 9–24. <https://doi.org/10.1016/j.biote.2010.01.021>.
39. Sakkos JK, Wackett LP, Aksan A. Enhancement of biocatalyst activity and protection against stressors using a microbial exoskeleton. *Sci Rep.* 2019;9:1–12. <https://doi.org/10.1038/s41598-019-40113-8>.
40. Vaaje-kolstad G, Westereng B, Horn SJ, Liu Z, Zhai H, Sørlie M, Eijsink VGH. An oxidative enzyme boosting the enzymatic conversion of recalcitrant polysaccharides. *Science* 80. 2010;330:219–23. <https://doi.org/10.1126/science.1192231>.
41. Lo Leggio L, Simmons TJ, Poulsen JCN, Frandsen KEH, Hemsworth GR, Stringer MA, Von Freiesleben P, Tovborg M, Johansen KS, De Maria L, Harris PV, Soong CL, Dupree P, Tryfona T, Lenfant N, Henrissat B, Davies GJ, Walton PH. Structure and boosting activity of a starch-degrading lytic polysaccharide monooxygenase. *Nat Commun.* 2015;6:1–9. <https://doi.org/10.1038/ncomms6961>.
42. Levasseur A, Drula E, Lombard V, Coutinho PM, Henrissat B. Expansion of the enzymatic repertoire of the CAZy database to integrate auxiliary redox enzymes. *Biotechnol Biofuels.* 2013;6:1–14. <https://doi.org/10.1186/1754-6834-6-41>.
43. Franco Cairo JPL, Cannella D, Oliveira LC, Gonçalves TA, Rubio MV, Terrasan CRF, Tramontina R, Mofatto LS, Carazzolle MF, Garcia W, Felby C, Damasio A, Walton PH, Squina F. On the roles of AA15 lytic polysaccharide monooxygenases derived from the termite *Coptotermes gestroi*. *J Inorg Biochem.* 2021;216:111316. <https://doi.org/10.1016/j.jinorgbio.2020.111316>.
44. Quinlan RJ, Sweeney MD, Lo L, Otten H, Poulsen JN, Tryfona T, Walter CP, Dupree P, Xu F, Davies GJ, Walton PH. Insights into the oxidative degradation of cellulose by a copper metalloenzyme that exploits biomass components. *PNAS.* 2011;108:15079–84. <https://doi.org/10.1073/pnas.1105776108>.
45. Ciano L, Davies GJ, Tolman WB, Walton PH. Bracing copper for the catalytic oxidation of C–H bonds. *Nat Catal.* 2018;1:571–7. <https://doi.org/10.1038/s41929-018-0110-9>.
46. Beeson WT, Phillips CM, Cate JHD, Marletta MA. Oxidative cleavage of cellulose by fungal copper-dependent polysaccharide monooxygenases. *J Am Chem Soc.* 2012;134:890–2. <https://doi.org/10.1021/ja210657t>.
47. Bissaro B, Røhr ÅK, Müller G, Chylenski P, Skaugen M, Forsberg Z, Horn SJ, Vaaje-Kolstad G, Eijsink VGH. Oxidative cleavage of polysaccharides by monocupper enzymes depends on H₂O₂. *Nat Chem Biol.* 2017;13:1123–8. <https://doi.org/10.1038/nchembio.2470>.
48. Kjaergaard CH, Qayyum MF, Wong SD, Xu F, Hemsworth GR, Walton DJ, Young NA, Davies GJ, Walton PH, Johansen KS, Hodgson KO, Hedman B, Solomon EI. Spectroscopic and computational insight into the activation of O₂ by the mononuclear Cu center in polysaccharide monooxygenases. *Proc Natl Acad Sci U S A.* 2014;111:8797–802. <https://doi.org/10.1073/pnas.1408115111>.

49. Kim S, Ståhlberg J, Sandgren M, Paton RS, Beckham GT. Quantum mechanical calculations suggest that lytic polysaccharide monooxygenases use a copper-oxyxl, oxygen-rebound mechanism. *Proc Natl Acad Sci U S A.* 2014;111:149–54. <https://doi.org/10.1073/pnas.1316609111>.
50. Forsberg Z, Mackenzie AK, Sørlie M, Røhr ÅK, Helland R, Arvai AS, Vaaje-Kolstad G, Eijsink VGH. Structural and functional characterization of a conserved pair of bacterial cellulose-oxidizing lytic polysaccharide monooxygenases. *Proc Natl Acad Sci U S A.* 2014;111:8446–51. <https://doi.org/10.1073/pnas.1402771111>.
51. Martínez AT. How to break down crystalline cellulose. *Science* (80). 2016;352:1050–1. <https://doi.org/10.1126/science.aaf8920>.
52. Westereng B, Cannella D, Wittrup Agger J, Jørgensen H, Larsen Andersen M, Eijsink VGH, Felby C. Enzymatic cellulose oxidation is linked to lignin by long-range electron transfer. *Sci Rep.* 2015;5:1–9. <https://doi.org/10.1038/srep18561>.
53. Frommhagen M, Westphal AH, van Berkel WJH, Kabel MA. Distinct substrate specificities and electron-donating systems of fungal lytic polysaccharide monooxygenases. *Front Microbiol.* 2018;9:1–22. <https://doi.org/10.3389/fmicb.2018.01080>.
54. Tan TC, Kracher D, Gandini R, Sygmund C, Kittl R, Haltrich D, Hällberg BM, Ludwig R, Divne C. Structural basis for cellobiose dehydrogenase action during oxidative cellulose degradation. *Nat Commun.* 2015;6:1–11. <https://doi.org/10.1038/ncomms8542>.
55. Kracher D, Scheiblbrandner S, Felice AKG, Breslmayr E, Preims M, Ludwicka K, Haltrich D, Eijsink VGH, Ludwig R. Extracellular electron transfer systems fuel cellulose oxidative degradation. *Science* (80). 2016;352:1098–101. <https://doi.org/10.1126/science.aaf3165>.
56. Blossom BM, Russo DA, Singh RK, van Oort B, Keller MB, Simonsen TI, Perzon A, Gamon LF, Davies MJ, Cannella D, Croce R, Jensen PE, Bjerrum MJ, Felby C. Photobiocatalysis by a lytic polysaccharide monooxygenase using intermittent illumination. *ACS Sustain Chem Eng.* 2020;8:9301–10. <https://doi.org/10.1021/acssuschemeng.0c00702>.
57. Janusz G, Pawlik A, Świderska-Burek U, Polak J, Sulej J, Jarosz-Wilkołazka A, Paszczyński A. Laccase properties, physiological functions, and evolution. *Int J Mol Sci.* 2020;21:966. <https://doi.org/10.3390/ijms21030966>.
58. Munk L, Sitarz AK, Kalyani DC, Mikkelsen JD, Meyer AS. Can laccases catalyze bond cleavage in lignin? *Biotechnol Adv.* 2015;33:13–24. <https://doi.org/10.1016/j.biotechadv.2014.12.008>.
59. Simaan AJ, Mekmouche Y, Herrero C, Moreno P, Aukauloo A, Delaire JA, Réglier M, Tron T. Photoinduced multielectron transfer to a multicopper oxidase resulting in dioxygen reduction into water. *Chem A Eur J.* 2011;17:11743–6. <https://doi.org/10.1002/chem.201101282>.
60. Schneider L, Mekmouche Y, Rousselot-Pailley P, Simaan AJ, Robert V, Réglier M, Aukauloo A, Tron T. Visible-light-driven oxidation of organic substrates with dioxygen mediated by a [Ru(bpy)3]2+/laccase system. *ChemSusChem.* 2015;8:3048–51. <https://doi.org/10.1002/cssc.201500602>.
61. Li H, Guo S, Li C, Huang H, Liu Y, Kang Z. Tuning laccase catalytic activity with phosphate functionalized carbon dots by visible light. *ACS Appl Mater Interfaces.* 2015;7:10004–12. <https://doi.org/10.1021/acsami.5b02386>.
62. Brenelli L, Squina FM, Felby C, Cannella D. Laccase-derived lignin compounds boost cellulose oxidative enzymes AA9. *Biotechnol Biofuels.* 2018;11:1–12. <https://doi.org/10.1186/s13068-017-0985-8>.
63. Perna V, Meyer AS, Holck J, Eltis LD, Eijsink VGH, Wittrup Agger J. Laccase-catalyzed oxidation of lignin induces production of H₂O₂. *ACS Sustain Chem Eng.* 2020;8:831–41. <https://doi.org/10.1021/acssuschemeng.9b04912>.
64. Hilgers R, Vincken JP, Gruppen H, Kabel MA. Laccase/mediator systems: their reactivity toward phenolic lignin structures. *ACS Sustain Chem Eng.* 2018;6:2037–46. <https://doi.org/10.1021/acssuschemeng.7b03451>.

65. Faiza M, Huang S, Lan D, Wang Y. New insights on unspecific peroxygenases: superfamily reclassification and evolution. *BMC Evol Biol.* 2019;19:76. <https://doi.org/10.1186/s12862-019-1394-3>.
66. Hofrichter M, Ullrich R. Oxidations catalyzed by fungal peroxygenases. *Curr Opin Chem Biol.* 2014;19:116–25. <https://doi.org/10.1016/j.cbpa.2014.01.015>.
67. Avasthi K, Bohre A, Grilc M, Likozar B, Saha B. Advances in catalytic production processes of biomass-derived vinyl monomers. *Cat Sci Technol.* 2020;10:5411–37. <https://doi.org/10.1039/docy00598c>.
68. Luo Z, Qin S, Chen S, Hui Y, Zhaoa C. Selective conversion of lignin to ethylbenzene. *Green Chem.* 2020;22(6):1842–50. <https://doi.org/10.1039/x0xx00000x>.
69. Wang A, Song H. Maximizing the production of aromatic hydrocarbons from lignin conversion by coupling methane activation. *Bioresour Technol.* 2018;268:505–13. <https://doi.org/10.1016/j.biortech.2018.08.026>.
70. Yuan B, Mahor D, Fei Q, Wever R, Alcalde M, Zhang W, Hollmann F (2020) Water-soluble anthraquinone photocatalysts enable methanol-driven enzymatic halogenation and hydroxylation reactions. *ACS Catal.* 10(15):8277–8284 doi: <https://doi.org/10.1021/acscatal.0c01958>.
71. Hobisch M, Schie MMCH, Kim J, Røkjær Andersen K, Alcalde M, Kourist R, Park CB, Hollmann F, Kara S. Solvent-free photobiocatalytic hydroxylation of cyclohexane. *ChemCatChem.* 2020;12:4009–13. <https://doi.org/10.1002/cctc.202000512>.
72. Klinman JP. The copper-enzyme family of dopamine β -monooxygenase and peptidylglycine α -hydroxylating monooxygenase: resolving the chemical pathway for substrate hydroxylation. *J Biol Chem.* 2006;281:3013–6. <https://doi.org/10.1074/jbc.R500011200>.
73. Van Den Heuvel RHH, Tahallah N, Kamerbeek NM, Fraaije MW, Van Berkel WJH, Janssen DB, Heck AJR. Coenzyme binding during catalysis is beneficial for the stability of 4-hydroxyacetophenone monooxygenase. *J Biol Chem.* 2005;280:32115–21. <https://doi.org/10.1074/jbc.M503758200>.
74. Fürst MJLJ, Gran-Scheuch A, Aalbers FS, Fraaije MW. Baeyer-Villiger monooxygenases: tunable oxidative biocatalysts. *ACS Catal.* 2019;9:11207–41. <https://doi.org/10.1021/acscatal.9b03396>.
75. Bong YK, Song S, Nazor J, Vogel M, Widegren M, Smith D, Collier SJ, Wilson R, Palanivel SM, Narayanaswamy K, Mijts B, Clay MD, Fong R, Colbeck J, Appaswami A, Muley S, Zhu J, Zhang X, Liang J, Entwistle D. Baeyer-Villiger monooxygenase-mediated synthesis of esomeprazole as an alternative for Kagan sulfoxidation. *J Org Chem.* 2018;83:7453–8. <https://doi.org/10.1021/acs.joc.8b00468>.
76. Zhang W, Fueyo EF, Hollmann F, Martin LL, Pesic M, Wardenga R, Höhne M, Schmidt S. Combining photo-organo redox- and enzyme catalysis facilitates asymmetric C–H bond functionalization. *Eur J Org Chem.* 2019;2019:80–4. <https://doi.org/10.1002/ejoc.201801692>.
77. Sorigué D, Légeret B, Cuiné S, Blangy S, Moulin S, Billon E, Richaud P, Brugiére S, Couté Y, Nurizzo D, Müller P, Brettel K, Pignol D, Arnoux P, Li-Beisson Y, Peltier G, Beisson F. An algal photoenzyme converts fatty acids to hydrocarbons. *Science* (80). 2017;357:903–7. <https://doi.org/10.1126/science.aan6349>.
78. Huijbers MME, Zhang W, Tonin F, Hollmann F. Light-driven enzymatic decarboxylation of fatty acids. *Angew Chem Int Ed.* 2018;57:13648–51. <https://doi.org/10.1002/anie.201807119>.
79. Karava M, Gockel P, Kabisch J. *Bacillus subtilis* spore surface display of photodecarboxylase for the transformation of lipids to hydrocarbons. *Sustain Energy Fuels.* 2021; <https://doi.org/10.1039/d0se01404d>.
80. Toogood HS, Gardiner JM, Scrutton NS. Biocatalytic reductions and chemical versatility of the old yellow enzyme family of flavoprotein oxidoreductases. *ChemCatChem.* 2010;2:892–914. <https://doi.org/10.1002/cctc.201000094>.
81. Königer K, Gómez Baraíbar Á, Mügge C, Paul CE, Hollmann F, Nowacyk MM, Kourist R. Recombinant cyanobacteria for the asymmetric reduction of C=C bonds fueled by the biocatalytic oxidation of water. *Angew Chem Int Ed.* 2016;55:5582–5. <https://doi.org/10.1002/anie.201601200>.

82. Wang Y, Huang X, Hui J, Vo LT, Zhao H. Stereoconvergent reduction of activated alkenes by a nicotinamide free synergistic photobiocatalytic system. *ACS Catal.* 2020;10:9431–7. <https://doi.org/10.1021/acscatal.0c02489>.
83. Lin R, Deng C, Zhang W, Hollmann F, Murphy JD. Production of Bio-alkanes from Biomass and CO₂. *Trends Biotechnol.* 2021; <https://doi.org/10.1016/j.tibtech.2020.12.004>.
84. Schievano A, Pepé Sciarria T, Vanbroekhoven K, De Wever H, Puig S, Andersen SJ, Rabaeij K, Pant D. Electro-fermentation— merging electrochemistry with fermentation in industrial applications. *Trends Biotechnol.* 2016;34:866–78. <https://doi.org/10.1016/j.tibtech.2016.04.007>.
85. Shanthi Sravan J, Butti SK, Sarkar O, Vamshi Krishna K, Venkata Mohan S. Electrofermentation of food waste—regulating acidogenesis towards enhanced volatile fatty acids production. *Chem Eng J.* 2018;334:1709–18. <https://doi.org/10.1016/j.cej.2017.11.005>.
86. Vassilev I, Hernandez PA, Batlle-Vilanova P, Freguia S, Krömer JO, Keller J, Ledezma P, Virdis B. Microbial electrosynthesis of isobutyric, butyric, caproic acids, and corresponding alcohols from carbon dioxide. *ACS Sustain Chem Eng.* 2018;6:8485–93. <https://doi.org/10.1021/acssuschemeng.8b00739>.
87. Zhang W, Ma M, Huijbers MME, Filonenko GA, Pidko EA, Van Schie M, De Boer S, Bastien, Burek O, Blok JZ, WJH VB, Smith WA, Hollmann F. Hydrocarbon synthesis via photoenzymatic decarboxylation of carboxylic acids. *J Am Chem Soc.* 2019; <https://doi.org/10.1021/jacs.8b12282>.
88. Marsolek MD, Torres CI, Hausner M, Rittmann BE. Intimate coupling of photocatalysis and biodegradation in a photocatalytic circulating-bed biofilm reactor. *Biotechnol Bioeng.* 2008;101:83–92. <https://doi.org/10.1002/bit.21889>.
89. Zhou D, Xu Z, Dong S, Huo M, Dong S, Tian X, Cui B, Xiong H, Li T, Ma D. Intimate coupling of photocatalysis and biodegradation for degrading phenol using different light types: visible light vs UV light. *Environ Sci Technol.* 2015;49:7776–83. <https://doi.org/10.1021/acs.est.5b00989>.
90. Kanagasabai S, Kang YL, Manickam M, Ibrahim S, Pichiah S. Intimate coupling of electro and biooxidation of tannery wastewater. *Desalin Water Treat.* 2013;51:6617–23. <https://doi.org/10.1080/19443994.2013.769699>.
91. Xiong J, Guo S, Zhao T, Liang Y, Liang J, Wang S, Zhu H, Zhang L, Zhao JR, Chen G. Degradation of methylene blue by intimate coupling photocatalysis and biodegradation with bagasse cellulose composite carrier. *Cellulose.* 2020;27:3391–404. <https://doi.org/10.1007/s10570-020-02995-0>.
92. Watkins D, Nuruddin M, Hosur M, Tcherbi-Narteh A, Jeelani S. Extraction and characterization of lignin from different biomass resources. *J Mater Res Technol.* 2015;4:26–32. <https://doi.org/10.1016/j.jmrt.2014.10.009>.
93. Erickson M, Larsson S, Miksche GE. Gas-chromatographic analysis of lignin oxidation products. Structure of the spruce lignins. *Acta Chem Scand.* 1973;27 <https://doi.org/10.3891/acta.chem.scand.27-0005>.
94. Kanitskaya LV, Rokhin AV, Kushnarev DF, Kalabin GA. Chemical structure of wheat dioxane lignin studied by ¹H and ¹³C NMR spectroscopy. *Polym Sci Ser A.* 1998;40(5): 459–63.
95. Berlin A, Balakshin M, Gilkes N, Kadla J, Maximenko V, Kubo S, Saddler J. Inhibition of cellulase, xylanase and β-glucosidase activities by softwood lignin preparations. *J Biotechnol.* 2006;125:198–209. <https://doi.org/10.1016/j.jbiotec.2006.02.021>.
96. Kumar L, Arantes V, Chandra R, Saddler J. The lignin present in steam pretreated softwood binds enzymes and limits cellulose accessibility. *Bioresour Technol.* 2012;103:201–8. <https://doi.org/10.1016/j.biotech.2011.09.091>.
97. Frommhagen M, Koetsier MJ, Westphal AH, Visser J, Hinz SWA, Vincken JP, Van Berkel WJH, Kabel MA, Gruppen H. Lytic polysaccharide monooxygenases from Myceliophthora

- thermophila C1 differ in substrate preference and reducing agent specificity. *Biotechnol Biofuels.* 2016;9:1–17. <https://doi.org/10.1186/s13068-016-0594-y>.
98. Karnaouri A, Matsakas L, Krikiglianni E, Rova U, Christakopoulos P. Valorization of waste forest biomass toward the production of cello-oligosaccharides with potential prebiotic activity by utilizing customized enzyme cocktails. *Biotechnol Biofuels.* 2019;12:1–19. <https://doi.org/10.1186/s13068-019-1628-z>.
99. Cannella D, Hsieh CWC, Felby C, Jørgensen H. Production and effect of aldonic acids during enzymatic hydrolysis of lignocellulose at high dry matter content. *Biotechnol Biofuels.* 2012;5:1–10. <https://doi.org/10.1186/1754-6834-5-26>.
100. Rodríguez-Zúñiga UF, Cannella D, Giordano RDC, Giordano RDLC, Jørgensen H, Felby C. Lignocellulose pretreatment technologies affect the level of enzymatic cellulose oxidation by LPMO. *Green Chem.* 2015;17:2896–903. <https://doi.org/10.1039/c4gc02179g>.
101. Lee SH, Choi DS, Kuk SK, Park CB. Photobiocatalysis: activating redox enzymes by direct or indirect transfer of photoinduced electrons. *Angew Chem Int Ed.* 2018;57:7958–85. <https://doi.org/10.1002/anie.201710070>.
102. Karmee SK, Linardi D, Lee J, Lin CSK. Conversion of lipid from food waste to biodiesel. *Waste Manag.* 2015;41:169–73. <https://doi.org/10.1016/j.wasman.2015.03.025>.
103. Włodarczyk A, Selão TT, Norling B, Nixon PJ. Newly discovered *Synechococcus* sp. PCC 11901 is a robust cyanobacterial strain for high biomass production. *Commun Biol.* 2020;3:1–14. <https://doi.org/10.1038/s42003-020-0910-8>.
104. Ferreira GF, Ríos Pinto LF, Maciel Filho R, Fregolente LV. A review on lipid production from microalgae: Association between cultivation using waste streams and fatty acid profiles. *Renew Sust Energ Rev.* 2019;109:448–66. <https://doi.org/10.1016/j.rser.2019.04.052>.
105. Sun H, Ren Y, Mao X, Li X, Zhang H, Lao Y, Chen F. Harnessing C/N balance of *Chromochloris zofingiensis* to overcome the potential conflict in microalgal production. *Commun Biol.* 2020;3:1–13. <https://doi.org/10.1038/s42003-020-0900-x>.
106. López G, Yate C, Ramos FA, Cala MP, Restrepo S, Baena S. Production of polyunsaturated fatty acids and lipids from autotrophic, mixotrophic and heterotrophic cultivation of *Galdieria* sp. strain USBA-GBX-832. *Sci Rep.* 2019;9:1–13. <https://doi.org/10.1038/s41598-019-46645-3>.
107. Wessendorf RL. Introducing an *Arabidopsis thaliana* thylakoid thiol/disulfide-modulating protein into *synechocystis* increases the efficiency of photosystem II photochemistry. *Front Plant Sci.* 2019;10:1284. <https://doi.org/10.3389/fpls.2019.01284>.
108. Gui MM, Lee KT, Bhatia S. Feasibility of edible oil vs. non-edible oil vs. waste edible oil as biodiesel feedstock. *Energy.* 2008;33:1646–53. <https://doi.org/10.1016/j.energy.2008.06.002>.
109. Wen Z, Yu X, Tu S-T, Yan J, Dahlquist E. Biodiesel production from waste cooking oil catalyzed by TiO_2 – MgO mixed oxides. *Bioresour Technol.* 2010;101:9570–6. <https://doi.org/10.1016/j.biortech.2010.07.066>.
110. Mulinacci N, Romani A, Galardi C, Pinelli P, Giaccherini C, Vincieri FF. Polyphenolic content in olive oil waste waters and related olive samples. *J Agric Food Chem.* 2001;49: 3509–14. <https://doi.org/10.1021/jf000972q>.
111. Ahmed PM, Fernández PM, de Figueroa LIC, Pajot HF. Exploitation alternatives of olive mill wastewater: production of value-added compounds useful for industry and agriculture. *Biofuel Res J.* 2019;6:980–94. <https://doi.org/10.18331/BRJ2019.6.2.4>.
112. Zhang C, Hong K. Production of terpenoids by synthetic biology approaches. *Front Bioeng Biotechnol.* 2020;8:347. <https://doi.org/10.3389/fbioe.2020.00347>.
113. Straathof AJJ. Transformation of biomass into commodity chemicals using enzymes or cells. *Chem Rev.* 2014;114:1871–908. <https://doi.org/10.1021/cr400309c>.
114. Fischer-Romero C, Tindall BJ, Jüttner F. *Tolumonas auensis* gen. nov., sp. nov., a toluene-producing bacterium from anoxic sediments of a freshwater lake. *Int J Syst Bacteriol.* 1996;46: 183–8. <https://doi.org/10.1099/00207713-46-1-183>.
115. Chen J, Henderson G, Grimm CC, Lloyd SW, Laine RA. Termites fumigate their nests with naphthalene. *Nature.* 1998;392:558–9. <https://doi.org/10.1038/33305>.

116. McKenna R, Nielsen DR (2011) Styrene biosynthesis from glucose by engineered *E. coli*. In: Food, pharmaceutical and bioengineering division—core programming topic at the 2011 AIChE annual meeting. AIChE, pp 340–350. doi: <https://doi.org/10.1016/j.ymben.2011.06.005>.

Chapter 9

Depolymerisation of Fossil Fuel and Biomass-derived Polyesters



Guido Grause

Abstract Monomer recovery from waste plastic is an essential part of any waste treatment concept. In particular, the depolymerisation of poly(ethylene terephthalate) (PET) by glycolysis and hydrolysis is well established. In addition to the classic products of PET solvolysis, bis(2-hydroxyethyl)terephthalate and terephthalic acid, terephthalic acid amides and rather unconventional terephthalic acid alcohol esters are also obtained. Reactions can take place in ionic liquids or in a microwave oven. Products of depolymerisation can be used as raw materials for virgin polyesters, polyurethanes or bitumen additives. Another group of polyesters that is attracting increasing attention is obtained from biomass. Polymers such as poly(lactic acid), poly(butylene succinate) or polyhydroxyalkanoates are biodegradable. However, the entire effort of production is lost if these materials are returned to the environment untreated. Therefore, recycling of these polymers is an act of resource conservation. Poly(lactic acid) is depolymerised during methanolysis to produce methyl lactate, which can be converted into lactide as a starting material for new polymers. Poly(butylene succinate) and poly(3-hydroxybutyric acid) can be hydrolysed at higher temperatures in the presence of lipases, yielding monomers such as succinic acid, 3-hydroxybutyric acid, and crotonic acid. There are a variety of options for the depolymerisation of polyesters that are examined in this chapter. The increasing number of new polyester monomers requires special solutions for each individual polymer.

Keywords Poly(ethylene terephthalate) · Polylactide/Poly(lactic acid) · Poly(butylene succinate) · Polyhydroxyalkanoates · Glycolysis · Hydrolysis · Microwave · Ionic liquids · Enzymes · Chemical recycling

G. Grause (✉)

Graduate School of Environmental Studies, Tohoku University, Sendai, Japan
e-mail: grause.guido.a2@tohoku.ac.jp; guido.grause@web.de

9.1 Introduction

Polyesters comprise a group of polymers obtained by the reaction of dicarboxylic acids and diols. Sometimes block building units are derived from hydroxycarboxylic acids or lactones. The most commonly used polyester is poly(ethylene terephthalate) (PET), known as the material for soft drink bottles. PET is also used for other food contact applications and for fibres. All aromatic polyesters, including poly(butylene terephthalate) (PBT) and poly(ethylene naphthalate) (PEN), have in common that they are made from fossil fuels, although bio-based routes are available [1]. As society strives to decarbonise, carbon sources may become scarce and the need for resource recovery increases.

Bio-based aliphatic polyesters offer an alternative to these fossil fuel-based polymers, such as poly(lactic acid) or polyhydroxyalkanoates. These materials are biodegradable and can be disposed of in composting facilities. This concept is advantageous when plastic is littered; however, all the effort (harvest, work, energy) required to produce these materials is lost when they are biodegraded [2]. Therefore, recycling is also desirable for these polyesters.

The most beneficial way of recycling is to reuse the material as it is (mechanical recycling). However, the material properties are often modified by dyes and other additives. These can affect the optical properties and the intrinsic viscosity, which makes chemical recycling more attractive [3]. In addition, polyesters are generally sensitive to hydrolysis, and the reaction with other protic compounds offers the possibility of recovering monomers or oligomers.

This process is briefly described by the term depolymerisation, which is defined in this chapter as the recovery of monomers or other valuable chemicals rather than the conversion of polymers into fuel. The aim is to obtain defined compounds with a sufficient high purity through highly selective processes. The product is to be used for the production of polymers or other useful materials after minimal processing.

For the depolymerisation of polyesters, solvolytic processes are the most promising options. Glycolysis and hydrolysis are well established for the depolymerisation of PET, while methanolysis can rather be considered a historical process, as the synthesis of PET from dimethyl terephthalate is obsolete. The strategies successfully used for the depolymerisation of PET are also considered for novel polyesters. However, many researchers favour enzymatic pathways, which in turn can provide alternative routes for the degradation of aromatic polyesters.

9.2 Technologies Used in the Depolymerisation of Polyesters

The depolymerisation of polyesters with sub- or supercritical water has a long tradition [4]. Such methods require high temperatures and pressures, which makes the processes energy intensive and expensive. In addition, sensitive monomers such as ethylene glycol or hydroxyalkanoates could be destroyed in the process [5, 6].

Therefore, strategies have been developed over the years to reduce the heat and pressure requirements. Catalysts have been developed to lower the reaction temperature, as described in the following sections. This trend culminates in the use of lactases and other enzymes [7, 8], pushing reaction temperatures close to ambient temperatures. Although the temperature requirements are drastically reduced, the reaction time can extend to days.

Another strategy is to change the reaction medium. Today, glycolysis is the most studied process for the depolymerisation of PET. One of the main reasons is that the reaction can be carried out below the boiling point of ethylene glycol (196 °C) and therefore pressure reactors are not required. Steam can be used as a reaction medium for the hydrolysis of polyesters [5]. This reduces the pressure requirements but requires temperatures above the melting point of the polymer, which can lead to the destruction of some products.

Most reactions are carried out in autoclaves or in pressureless vessels. With conventional heating, heat is only transferred at the interface between the reactor and reaction medium. From there, the heat is distributed by the thermal conductivity of the medium and by free or forced convection. Reaching thermal equilibrium requires time. Commonly, the reaction time starts when the reaction temperature is reached. By this time, a considerable part of the polymer may already have been degraded [9].

Microwave technology offers an alternative way of heating [10]. Microwave radiation is directly absorbed by various types of materials. Depending on the absorber and the microwave power, rapid heat transfer can be achieved. Water and ethylene glycol are good microwave absorbers because their polar structure is forced by microwave fields into a rotational motion called dipolar polarization. This motion is converted into heat and only material near the absorber is heated. Polymers do not usually act as absorbers. Even if they have a polar structure, they lack the necessary flexibility to follow the electromagnetic field of microwaves. Catalysts with a polar structure can also absorb microwaves and heat up the reaction medium in their vicinity. Ionic catalysts can additionally absorb microwaves by ionic conduction and convert translational energy into heat. Both effects can significantly accelerate the reaction.

9.3 Depolymerisation of Aromatic Polyesters

The most important aromatic polyester is PET. Therefore, most of this section will deal with this polymer. Besides PET, PBT, and PEN are of interest. The best way of reusing these polymers is mechanical recycling, which can be combined with solid state polycondensation (SSP) to obtain a material appropriate for most applications [11]. However, highly contaminated or degraded materials might become inappropriate for this pathway. Then depolymerisation should be considered.

Recent research focuses on glycolysis, hydrolysis, and aminolysis. The products of all these methods can be used for the production of new polymers. Since the production of PET is a two-step process in which terephthalic acid reacts first with ethylene glycol to form bis(2-hydroxyethyl)terephthalate (BHET), which undergoes in a second step further condensation to high molecular weight PET, terephthalic acid from hydrolysis and BHET from glycolysis can directly be reused in this process.

Many works make use of three values for their description of the depolymerisation process [10]. It is important to understand that these values are often used in a different manner than in common chemical technology. The *conversion* is not identical with the number of depolymerisation reactions as one would expect. It describes rather the dissolution of polymer, which is commonly seen as the difference between the weight of the polymer before the depolymerisation process starts and the residual polymer afterwards. As PET is insoluble in any common solvent, residue can be recovered by filtration. The molecular weight might be reduced without changing the solubility significantly. Only short chain oligomers are sufficient soluble in the reaction medium used for the depolymerisation. Therefore, the *selectivity* defines the fraction of desired product in relation to the dissolved fraction of PET. The classical definition assumes that selectivity is reduced when desired product is lost by the formation of undesired by-product. However, low selectivity during the depolymerisation of PET is most likely related to the incomplete reaction of oligomers, which can still be converted into product by changing reaction conditions. That is that the definitions of both conversion and selectivity differ from those commonly used. Only the definition of the *yield* as the ratio of practical and theoretical amount of product is conventionally used.

9.3.1 Glycolysis of Poly(Ethylene Terephthalate)

Most attention in the field of PET depolymerisation in recent years has been given to processes associated with glycolysis. Compared to other solvolytic processes, the high boiling point of ethylene glycol at 197 °C allows operation at considerably lower pressure. Below the boiling point, no additional pressure is required. The compatibility of polarity between PET and ethylene glycol reduces the temperature requirement and depolymerisation can be carried out below the melting point of

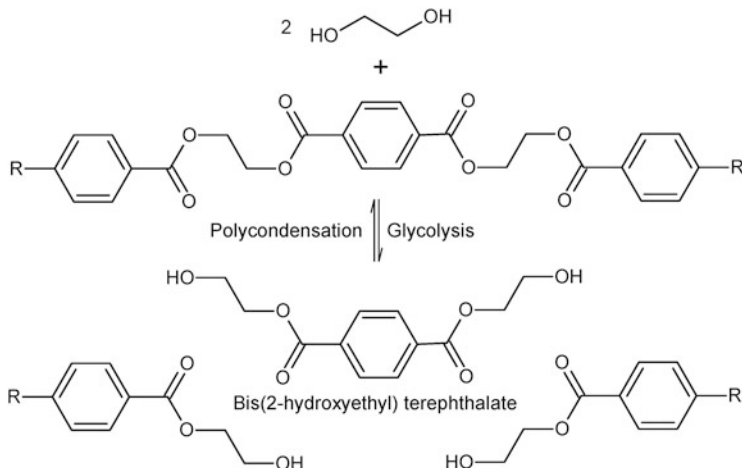


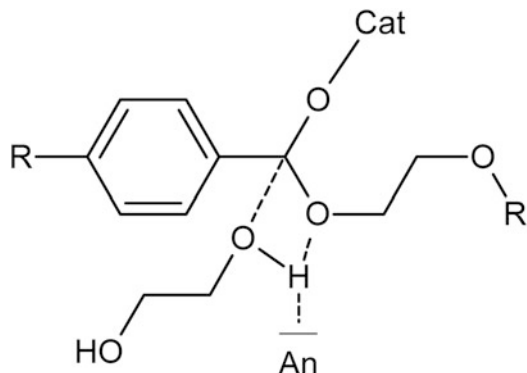
Fig. 9.1 Polycondensation of bis(2-hydroxyethyl) terephthalate (BHET) and glycolysis of poly(ethylene terephthalate) (PET)

PET. However, this comes at the price of long reaction times, which require the presence of suitable catalysts and advanced reaction systems. Therefore, current research focuses on developing new catalysts and performing glycolysis reactions in ionic liquids or microwave ovens.

The glycolysis reaction itself is the reverse second step of the PET polycondensation described earlier and leads to the formation of BHET as the desired main product (Fig. 9.1). The reaction must be catalysed to proceed at a reasonable rate. Efficient catalysts are ionic materials, such as salts [12], ionic liquids [10, 13, 14], protic ionic salts [15], and deep eutectic solvents (DES) [16, 17]. The product BHET can be used directly for the production of PET [3].

Both cation and the anion of the catalyst have a part in the reaction. The cation is coordinated to the ester group and increases its electrophilicity. Liu, et al. [16] reported that the activity of metal ions in deep eutectic solvents decreased in the series $\text{Zn}^{2+} > \text{Mn}^{2+} > \text{Co}^{2+} > \text{Ni}^{2+} > \text{Cu}^{2+} > \text{Fe}^{3+}$ when 1,3-dimethylurea was used, which is consistent with the activity of acetate catalysts providing the series $\text{Zn}^{2+} > \text{Mn}^{2+} > \text{Co}^{2+} > \text{Cu}^{2+} > \text{Na}^+$ [18], with Pb^{2+} being less active than Zn^{2+} and Mn^{2+} [19]. The activity series differed slightly in the presence of urea [17]. The anion should have significant Brønsted basicity, allowing the coordination of the hydroxyl hydrogen of ethylene glycol (Fig. 9.2). The effect can be enhanced by ligands with the ability to form different types of hydrogen bonds with the ethylene glycol. This substantially increases the nucleophilicity of the attacking alcohol. To this end, the catalysts should not have bulky groups that could prevent attack on the polymer chain [10, 13, 16]. Since the reaction is catalysed in both directions, the glycolysis reaction is finished when equilibrium between ethylene glycol, BHET, and oligomers is reached [20].

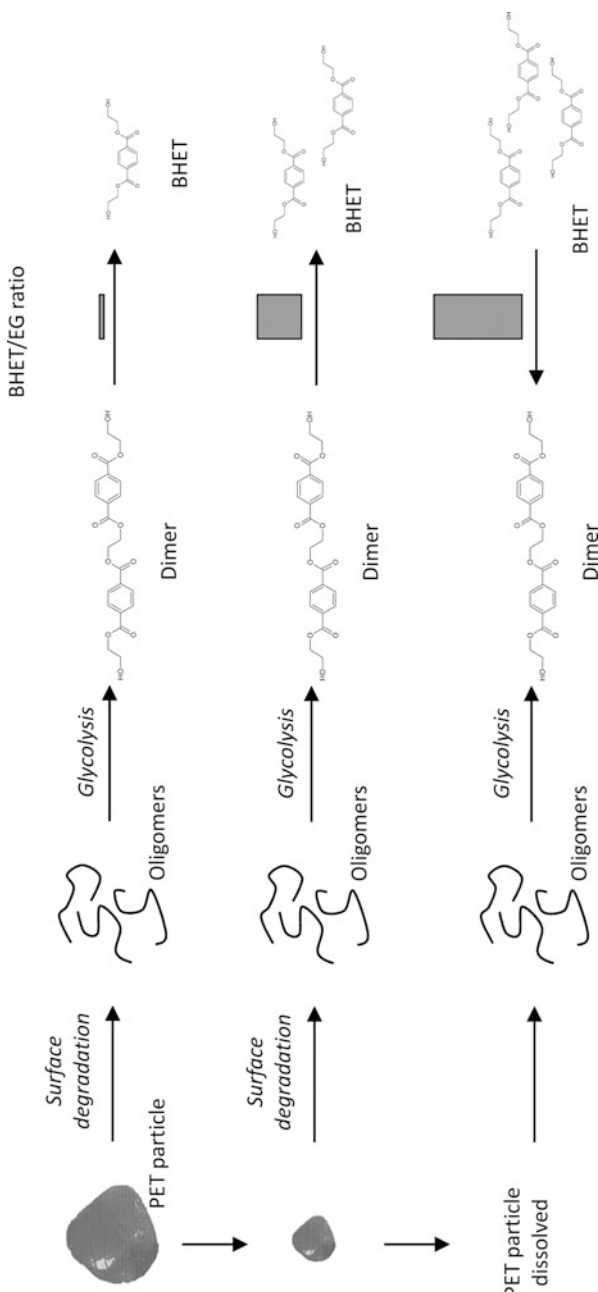
Fig. 9.2 Proposed poly(ethylene terephthalate)-catalyst complex (Cat: cation, An: anion)



Glycolysis at temperatures below the melting point of PET takes place at the interface between PET and solvent [21]. The initial reaction causes chain scission at the surface without the formation of soluble products, which can be observed as an induction time during which no conversion of PET or formation of BHET is observed. As the number of chain ends increases, the probability of BHET formation increases and a loss in weight of the solid phase is observed. Although the particle size decreases with time, the surface area increases due to the formation of cracks as amorphous regions of the semi-crystalline polymer are affected first [22]. Finally, the remaining oligomers are dissolved by the solvent and the reaction proceeds homogeneously [23].

The equilibrium is strongly affected by the molar ratio between PET and ethylene glycol [15]. It is often observed that a molar ethylene glycol/PET repeat unit ratio of more than 15 is required to raise the BHET yield to its maximum of about 80%. Several papers reported a decreasing BHET yield after exceeding the optimal reaction time, which is explained by the formation of dimers from BHET after complete glycolysis of PET. This behaviour requires explanation, as the equilibrium holds over the entire reaction time (Fig. 9.3). However, it can be observed that BHET is formed at the expense of PET long chains, while the amount of dimers remains constant [24]. This leads to high BHET yields at high ethylene glycol concentrations as long as long PET chains are still present in the reactor. Glycolysis of these last chains at the end of the reaction then reduces the ethylene glycol concentration, causing a shift in the equilibrium from BHET to the dimer. The formation of diethylene glycol and triethylene glycol as by-products from PET long chains can also reduce the ethylene glycol concentration [25]. In addition, the reaction of BHET with ethylene glycol di- and trimers, as well as with water formed during the condensation of ethylene glycol, would reduce the BHET yield. This behaviour is poorly understood and the temporal changes in the molecular weight distribution of PET during glycolysis have not yet been studied. The reaction is endothermic with an enthalpy of reaction of 12 kJ mol^{-1} at 196°C [23] and a free energy between -11 and -62 kJ mol^{-1} at temperatures between 300 and 450°C [25]. The equilibrium shifts to higher BHET yields at higher temperatures.

Fig. 9.3 Glycolysis of poly(ethylene terephthalate) (PET): Random chain scission takes place on the surface of the PET particle, steadily reducing its size. Soluble oligomers are formed, which become dimers and bis(2-hydroxyethyl)terephthalate (BHET). Initially, the BHET/EG (ethylene glycol) ratio in the solution is low. As the conversion progresses, the BHET proportion increases and the EG fraction decreases. At the end, an appreciable part of the EG is consumed. Glycolysis of the remaining oligomers consumes even more EG, resulting in the formation of additional dimers from BHET



A kinetic model was developed by Viana, et al. [21] for glycolysis in the presence of zinc acetate, based on a model that considers the reaction of glycol and PET at the interface. The authors found an activation energy of 42 kJ mol^{-1} at temperatures

above 180 °C and 100 kJ mol⁻¹ below this temperature, suggesting that diffusion plays an important role in the reaction at low temperatures. Goje and Mishra [26] found an activation energy of 46 kJ mol⁻¹ and a pre-exponential factor of 1.0×10^5 for a boundary controlled reaction.

The rate of depolymerisation was found to be proportional to the reaction time, while the reaction rate decreased with particle size. The molecular weight of the remaining PET changed only slightly, leading to the assumption that the reaction occurred favourable at the PET-ethylene glycol interface [26]. Reducing of the PET particle size by 40% could reduce the activation energy by 40–50% [18]. Therefore, the shrinking-core model was often adopted for kinetic studies. Choline acetate used as catalyst showed an apparent activation energy of 131 kJ mol⁻¹ and a pre-exponential factor of 1.21×10^{13} , which was still higher than that of metal-based catalysts [13]. The activation energy (149 kJ mol⁻¹) of the deep eutectic solvent system zinc acetate/1,3-dimethylurea was even higher [16]. Other researchers assumed first-order kinetics. The catalyst [bmim][OAc], based on 1-butyl-3-methylimidazole, proceeded with an activation energy of 59 kJ mol⁻¹ [20]. The reaction in the presence of Na₂CO₃ showed first-order kinetics with an activation energy of 185 kJ mol⁻¹ and a pre-exponential factor of 9.4×10^{21} [23].

The parameters that are usually adjusted to optimise BHET yield are temperature, PET/ethylene glycol molar ratio and catalyst concentration. It was found that the most important parameter for the zinc acetate catalysed reaction is the PET/ethylene glycol molar ratio and the other factors have a little influence [12].

Glycolysis without any catalyst requires high temperatures. The reaction gave BHET yields of about 95% after 30–35 min at 450 °C and a pressure of 15.3 MPa under supercritical conditions for different types of PET. Longer reaction times caused a decrease in BHET yield, while the concentrations of the dimer and oligomers rose. The concentrations of diethylene glycol and triethylene glycol increased simultaneously. The reaction under subcritical conditions between 300 and 350 °C required 120 and 70 min, respectively [25].

One of the earliest catalysts used was zinc acetate. A BHET yield of almost 70% was achieved after 1 h at 196 °C [3]. Raising the temperature above the boiling point of ethylene glycol accelerates the reaction. Optimum conditions were found to obtain 85–89% BHET at an ethylene glycol/PET weight ratio of 6:1 after 150 min at 208 °C [12, 27]. A phase transfer reaction in which BHET accumulated in the xylene phase while PET and ethylene glycol formed immiscible droplets, gave 80% BHET and 20% dimer at 220 °C. It was suggested that the separation of BHET from the ethylene glycol phase could shift the equilibrium towards the BHET product [28].

Zinc chloride and didymium chloride (PrNdCl₆) required between 7 and 8 h to reach equilibrium conditions and BHET yields of more than 70% were obtained at 197 °C [29]. In ethylene glycol, soluble Na₂CO₃ gave BHET yields of about 60% after 1 h reaction time at 196 °C [23]. Sodium sulphate, which has a low solubility in ethylene glycol, achieved such BHET yields only after 7 h reaction time [30]. Similar results were obtained for acetic acid, LiOH, and K₂SO₄. These values are lower than those for zinc salts; however, sodium salts are less toxic than heavy metal ions and

therefore provide an environmental viable alternative [3, 30]. For both zinc and sodium salts, it can be assumed that the catalytic activity is limited to the cation.

Heterogeneous catalysts require temperatures above the melting temperature of PET at about 240 °C to support glycolysis, as only the molten PET in such a system can make the required contact with the catalyst. However, the higher temperature should shorten the reaction time and shift the equilibrium towards BHET, thus increasing the yield. The use of silica nanoparticle carrying Mn₃O₄ provided a BHET yield of more than 90% after 80 min at a temperature of 300 °C and a pressure of 1.1 MPa [31]. A BHET yield of 92% was obtained in the presence of the spinel ZnMn₂O₄ at a temperature of 260 °C and a pressure of 0.5 MPa after 60 min. The use of CoMn₂O₄ required 80 min under the same conditions, which was attributed to the smaller surface area and the smaller number of strong acid sites on the surface of this catalyst [24].

The catalytic activity of metal salts acting as Lewis acids can be enhanced by the presence of hydrogen bond acceptors forming deep eutectic solvents. Before the use of deep eutectic solvents was considered, it was already found that the presence of cyclohexyl amine and NaOH in addition to zinc acetate as a catalyst accelerated the reaction rate of glycolysis [26]. The combination of zinc acetate and urea in a ratio of 1–4 gave a BHET yield of 81% after 30 min at 170 °C [17]. It was suggested that the formation of hydrogen bonds between ethylene glycol and amine increased the nucleophilicity of the hydroxyl group and thus facilitated the attack on the PET ester group (Fig. 9.2). A similar result was obtained after 20 min at 190 °C when 1,3-dimethylurea was used instead [16]. The electron-withdrawing effect of the methyl groups in 1,3-dimethylurea increases the basicity of the amine, while more bulky groups sterically prevent any catalytic activity. It was assumed that the ratio of 1–4 was related to the complexation of the metal ion by the amine.

Heterogeneous solid catalysts offer the advantage that they can be easily separated from the reaction solution by filtration or centrifugation. Zinc modified layered double hydroxides gave a maximum BHET yield of 76% after 3 h at a reaction temperature of 196 °C [32].

Sodium titanate nanotubes are comparable to zinc acetate in their catalytic activity. Both catalysts gave comparable results with a BHET yield of about 80% over a time of 2–4 h. Titanate nanotubes gave higher yields for virgin PET, zinc acetate for PET waste. The recovered BHET showed no evidence of the presence of oligomers [33]. The reaction most likely proceeded by coordination of the PET carbonyl oxygen at the titanate Lewis acid site. The adjacent oxygen could act as a Lewis base and increase the nucleophilicity of the ethylene glycol [34].

In recent years, magnetic catalysts have been used that could be recovered after glycolysis. The first, nano-sized γ-Fe₂O₃ (maghemite) provided a BHET yield of 90% after 70 min at 300 °C [35]. The reaction conditions required a pressure of 1.1 MPa. At 255 °C, a yield of more than 80% was still obtained after 80 min. The catalyst acted as a mild acid and had no basic component that could have improved the performance. The nanoscale demobilisation of γ-Fe₂O₃ on nitrogen-doped graphene combines the Lewis acidity of Fe₂O₃ with the Brønstedt basicity of the nitrogen bound to the graphene [36]. In addition, terephthalate units are adsorbed on

the graphene through strong π - π interactions, which provides a reduced distance between catalyst and PET. Magnetite (Fe_3O_4) attached to multi-walled carbon nanotubes (MWCNTs) also acted as an excellent catalyst [37]. Both catalysts yielded 100% BHET at a reaction temperature of 195 °C. The Fe_3O_4 -enhanced MWCNTs required only 2 h, while the maghemite-based catalyst took 3 h to complete the reaction. The reaction in the presence of the ionic liquid coated nanoparticles $\text{Fe}_3\text{O}_4@\text{SiO}_2@(\text{mim})[\text{FeCl}_4]$ resulted in complete conversion after 24 h at 180 °C [38]. These catalysts are recovered after the reaction due to their magnetic properties.

In recent years, research has focussed on ionic liquids, many of which contain zinc or cobalt ions. These can cause concerns about environmental problems arising from the removal of metal ions from the final product [13]. Imidazolium-based ionic liquids also have moderate toxicity. Choline-based ionic liquids are considered less toxic and biodegradable [13].

The Lewis neutral ionic liquids [bmin][Br] and [bmin][Cl] dissolved 1.8 and 2.7 wt% of PET at 180 °C. Solubility increased in the presence of water, which was associated with decreasing pH. Even higher PET solubilities were obtained with [bmin][OAc] and [bmin][AlCl₄] [27]. Although PET was partially soluble in [bmin][Br] and [bmin][Cl], little catalytic activity was observed in the glycolysis of PET [14, 20]. The catalytic activity can be increased by the addition of ZnCl_2 . The resulting catalyst [bmin] ZnCl_3 gave a BHET yield of 83% after 2 h of reaction at 190 °C. Similar results are obtained with high concentrations of [bmin] MnCl_3 as catalyst. However, the Mn-based catalyst was less effective at low concentrations due to the lower Lewis-acidity of the MnCl_3^- -anion [14]. A BHET yield of 58% was obtained after 3 h at 190 °C when [bmin][OAc] was used as the catalyst [20]. A decreasing pH of the reaction medium could indicate the interaction of ethylene glycol with the ionic liquid, leading to the release of acetic acid. Other imidazolium-based catalysts gave yields of about 80% after 24 h reaction time. The catalyst (dimim)[FeCl₄] showed higher catalytic activity than (dimim)₂[Fe₂Cl₆(μ -O)], caused by a higher Brønstedt basicity of the anion and a lower steric hindrance of the cation. Reducing the particle size of the PET dramatically increased the yield by providing a larger surface area for catalyst and ethylene glycol to attack [10]. Choline formate and acetate gave BHET yields of more than 80% in 3 h at 180 °C [13].

The guanidine-based catalyst 1,5,7-triazabicyclo[4.4.0]dec-5-ene (TBD) degraded PET at 190 °C in ethylene glycol in a period of less than 10 min. However, the catalyst was rapidly deactivated by atmospheric CO₂ and other acidic impurities that may be present in PET waste [39]. This drawback was prevented by forming an organic salt with methanesulfonic acid, resulting in BHET yields of about 90%. No inert gas atmosphere is required and glycolysis can be carried out in an air atmosphere [15]. Similar activity to TBD was observed for the reaction with betaine. [40].

The reaction can be accelerated if microwave radiation is used to heat the reaction medium. The reaction time was reduced from 24 h to 2 h for PET waste using the imidazolium-based catalysts (dimim)[FeCl₄] and (dimim)₂[Fe₂Cl₆(μ -O)]. The second catalyst proved to be the more active one, as the polar structure of the iron(III)

complex acted as an additional microwave absorption mechanism besides ionic conduction [10].

Since the glycolysis of PET waste is a recycling process, it is important to avoid the formation of production waste from spent reaction medium and catalyst during processing. Therefore, in addition to economic factors, many researchers also investigated the reusability of the reaction system. A pilot plant with a capacity of 200 tons per year could provide BHET at a price of 4.23 €/kg using zinc acetate as the catalyst. Ethylene glycol consumption was identified as the highest cost factor. Up-scaling to 8000 tons per year and reducing the ethylene glycol/PET ratio could reduce the cost to 1.99 €/kg [12]. The glycolysis process with zinc acetate can also tolerate complex waste fractions containing polyolefins from closures and labels, which are solid balls after the process [12]. However, coloured waste fractions led to discoloration of the BHET and require additional purification steps [3].

Cholin-based catalysts are cheaper than imidazolium-based ionic liquids, with a price of about US\$1100 per tonne [13]. Due to the lower price and lower toxicity, choline acetate is considered the better catalyst, even though formate has the slightly higher activity.

The recyclability of the catalyst must also be considered for the economic evaluation [10]. In many homogeneous catalytic systems, the catalyst remains in the reaction medium, which is reused after BHET separation. As a result, contaminations can accumulate in the reaction medium and reduce the quality of the product. The ionic liquid [bmin][OAc] was recovered by vacuum distillation after filtration of solid BHET and used six times in succession without loss of activity [20]. The deep-eutectic solvent system zinc acetate/1,3-dimethylurea can be recycled at least 5 time. However, in the last cycle only a quarter of the initial catalyst concentration was still present in the reaction medium. Tighter control of the catalyst loss is required [16]. When using the protic salt formed from methanesulfonic acid and triazabicyclo[4.4.0]dec-5-ene, no loss of activity was observed [15].

Heterogeneous catalysts, such as layered double hydroxides [32], can be removed from the reaction medium by filtration or centrifugation. This allows the replacement of the ethylene glycol and the removal of impurities. Catalysts based on Fe_3O_4 [37] or $\gamma\text{-Fe}_2\text{O}_3$ [35, 36], were completely separated from the solvent by their magnetic properties. The recovery of the ionic liquid coated nanoparticles $\text{Fe}_3\text{O}_4@\text{SiO}_2@(\text{mim})[\text{FeCl}_4]$ required 3 min [38]. These catalysts were reused at least 5 times consecutively without loss of activity.

9.3.2 Hydrolysis of Poly(Ethylene Terephthalate)

Besides glycolysis, hydrolysis is the most studied process for the depolymerisation of PET. Hydrolysis occurs when PET reacts with water and as a result terephthalic acid and ethylene glycol are formed, both of which can be reused in the production of new PET. This reaction requires high temperatures and pressures when carried out in aqueous solutions under sub- or supercritical conditions. Therefore, catalysts are

commonly used to reduce these drastic conditions. Most catalytic approaches use acidic [41–43] or basic catalysts [12, 44, 45], but some neutral catalysts are also known [46, 47]. Both acidic and basic catalysts have serious disadvantages. Basic catalysts form terephthalic acid salt solutions that must be neutralized with strong mineral acids to obtain terephthalic acid. Acidic catalysts are commonly strong mineral acids that must be diluted with water to recover terephthalic acid; the mineral acid is disposed of as waste. In addition, like terephthalic acid, these catalysts have the disadvantage of causing corrosion to the equipment. Therefore, attempts have been made to reduce the harsh conditions and instead carry out the reaction in a steam atmosphere [5, 48–50]. More recent approaches try to avoid water as a solvent and use less volatile solvents [46, 51, 52] or use enzymes [53–56] to accelerate the reaction under more ambient conditions.

When hydrolysed in water above the melting point of PET and without a catalyst, an apparent activation energy of 56 kJ mol⁻¹ was observed [4]. The activation energy did not change between 250 and 265 °C when zinc acetate was used as a catalyst. A decreasing activation energy was only observed at a lower temperature, which was explained by a change in the emulsion state [47]. The uncatalysed reaction proceeded in a 75 vol% steam atmosphere with an apparent activation energy of 140 kJ mol⁻¹ and a pre-exponential factor of 1.6×10^9 according to kinetics that most closely follows the models of a contracting cylinder or sphere [49]. Hydrolysis of PET fibres from PVC-coated woven fabrics followed the same models with an activation energy of 56 kJ mol⁻¹ and a pre-exponential factor of 1.3×10^6 [44]. Alkaline hydrolysis of PET with NaOH proceeded with an apparent activation energy of 99 kJ mol⁻¹ [45]. The reaction was diffusion controlled in ethanol/water [57]. In the presence of KOH, an apparent activation energy of 69 kJ mol⁻¹ and a pre-exponential factor of 419 L min⁻¹ cm⁻² were observed. The reaction was assumed to be first-order in terms of both PET surface area and KOH concentration [58]. A much higher apparent activation energy of 173 kJ mol⁻¹ was found for the alkaline hydrolysis carried out in ethylene glycol [52].

A value of 89 kJ mol⁻¹, was achieved by developing a modified shrinking core model for the hydrolysis of PET in sulphuric acid, taking into account the partial dissolution of the PET in the acid [42]. Another modified shrinking core model was applied for the reaction in nitric acid. Taking into account the precipitation of terephthalic acid on the PET surface, a value of 101 kJ mol⁻¹ was obtained [43]. The reaction in supercritical CO₂ was more likely to proceed by a first-order reaction with an apparent activation energy of about 12.5 kJ mol⁻¹ at 160 °C when sulphated TiO₂ was used as a solid acid catalyst [41].

Activation energies ranged from 12.5 to 173 kJ mol⁻¹ depending on the conditions used. Phase boundaries were present in any case; PET was either in the form of solid or molten polymer; the mobile phase was either an aqueous solution, an organic solution, or a gas phase. This implies that in any case mass transfer resistance was present, which had a strong influence on the observed results. It is to be expected that higher activation energies indicate systems with a high degree of chemical control, while lower values indicate an obstruction by phase boundaries.

The hydrolysis of PET in the absence of a catalyst requires high temperatures and pressures. The yield of terephthalic acid was more than 90% at 350 °C after 60 min reaction time [59]. At higher temperatures, the yield decreased because the terephthalic acid was degraded to benzoic acid [60]. The yield of ethylene glycol was lower than that of terephthalic acid. The increasing acid concentration caused the degradation of ethylene glycol. Acetaldehyde, di- and triethylene glycol were found as by-products [59]. Reducing the temperature requires longer reaction times. The reaction was completed after 5 h at 265 °C, with terephthalic acid and ethylene glycol as the main products. A degradation of ethylene glycol was not observed. An equilibrium constant of 0.664 was found, which means that complete hydrolysis of PET cannot be achieved [4].

The addition of zinc or sodium acetate as a catalyst increased the reaction rate by only about 20% compared to the uncatalysed reaction [47]. It was assumed that these catalysts did not directly influence the hydrolysis reaction, but stabilized the emulsion and reduced the droplet size. This was supported by the fact that the apparent activation energy between 250 and 265 °C was equal to the uncatalysed one. When the reaction was catalysed with zinc acetate in xylene, using a minimum amount of water and a detergent to form an emulsion, the average molecular weight of the resulting product at 160 °C was greatly reduced. This process lowered the reaction temperature and pressure and facilitated product recovery, as the recovered ethylene glycol contained little water and PET oligomers were obtained as a fine white powder [46].

The alkaline hydrolysis of PET at 150 °C was completed after 4 h reaction time at a PET/NaOH ratio of 1:2.4. The yield of terephthalic acid was 90% with a purity of more than 95% when PET waste was used [12]. A comparable reaction gave 98% terephthalic acid after 1 h at 200 °C [45]. The reaction temperature was reduced to 80 °C in ethanol/water with a volume ratio of 60–40 with comparable yields [57].

When KOH was used at 160 °C, terephthalic acid with a yield of 91% and ethylene glycol were the only products obtained. The remaining PET hardly changed and retained its high molecular weight even at the end of the reaction, indicating that depolymerisation took place only on the PET surface [58].

Alkaline hydrolysis can also be used to separate PET fibres from poly(vinyl chloride) (PVC) in woven fabrics. The yield of terephthalic acid reached 99% after 2 h at 180 °C in 1 M NaOH solution. Dechlorination of PVC occurred simultaneously and reached 22% at the end of the reaction. Both the hydrolysis of PET and the dechlorination of PVC proceeded independently without the formation of shared by-products [44].

Alkaline hydrolysis in ethylene glycol resulted in complete PET conversion after 1 min at 185 °C. The usual mass transfer resistance caused by the formation of sodium terephthalate at the sample surface was overcome by vigorous stirring. In addition, the molecular weight reduction caused by hydrolytic degradation during processing and aging was also found to shorten the processing time [52]. The reaction with 9 M KOH in Cellusolve ($\text{CH}_3\text{OCH}_2\text{CH}_2\text{OH}$) gave a terephthalic acid yield of 82% after 2.5 h at 120 °C. It was assumed that a higher yield was

prevented by product formation on the PET surface, as potassium terephthalate was not soluble in the reaction medium [45].

Concentrated sulphuric acid (18 M) is able to dissolve PET at room temperature. During the slow hydrolysis of the dissolved polymer, more and more end-groups, carboxylic acids and hydroxyl-groups, are formed. The investigation of precipitated product by XRD showed that amorphous regions are dissolved first before the dissolution process also covers PET crystallites [61]. The solubility of PET decreases with the sulphuric acid concentration, which also leads to a delay in the hydrolysis reaction. Complete hydrolysis at 150 °C was achieved at a concentration of 9 mol L⁻¹ after 2 h, whereas with sulphuric acid at a concentration of 3 mol L⁻¹, only 90% of the PET was degraded after 12 h [42, 62]. The reaction of PET in 13 M HNO₃ resulted in a weight loss of about 80 wt% after 12 h at 100 °C. Removal of terephthalic acid from the surface was able to accelerate the reaction. Ethylene glycol was oxidized to oxalic acid, which was obtained as the second major product [43].

Hydrolysis carried out in the ionic liquid [Bmin][Cl] in the presence of [HSO₃-pmim][HSO₄] (where pmim stands for 1-methyl-3-(3-sulfopropyl)-imidazol) as an acid catalyst gave a yield of 89% of terephthalic acid after 4.5 h at 170 °C. Even without any catalyst, the ionic liquid gave a terephthalic acid yield of 76% [51].

The reaction can be strongly accelerated by the use of microwave radiation. The presence of sodium methoxide as catalyst reduces the reaction time in dimethyl sulphoxide and methanol as solvent to 5 min at 70 °C. The reaction yields a mixture of dimethyl and monomethyl terephthalate and terephthalic acid. The terephthalic acid is recovered from the solution after addition of water. The yield was reported to be about 74% for terephthalic acid [63].

An alternative possibility for hydrolysis is the reaction in supercritical CO₂. The gas acts as a plasticizer under supercritical conditions, promoting swelling and migration within the polymer. However, it also induces crystallization of amorphous PET, which can slow down the hydrolysis process. The reaction in supercritical CO₂ using the solid superacid catalyst SO₄²⁻/TiO₂ was complete after 5 h at 200 °C at any pressure. Hydronium ions were able to migrate together with dissolved water into the polymer matrix. The reaction took place both on the surface and in the bulk material [41].

High pressure can be avoided if hydrolysis is carried out in a steam atmosphere. The reaction in a fluidised bed requires temperatures above 400 °C to ensure volatilization of the terephthalic acid. At 450 °C, a terephthalic acid yield of about 70% was achieved, while ethylene glycol was almost completely degraded when quartz sand was used as bed material. Up to 24% of the terephthalic acid remained bound in oligomers. Decarboxylation also occurred with the formation of benzoic acid and acetylbenzoic acid [5]. Experiments with ¹⁸O-labelled steam showed that at temperatures between 340 and 440 °C, both pyrolysis and hydrolysis occurred in the degradation of PET and other aromatic polyesters. The selectivity of hydrolysis shifted from 46% to 11% in this temperature range when a 75 vol% steam atmosphere was present [49].

Terephthalic acid from the steam hydrolysis of PET can be converted to benzene using CaO as a catalyst. This reaction required 9 h at 450 °C, which could be reduced to 90 min at 550 °C. The benzene yield and purity were between 52 and 65% and between 82 and 89%, respectively. While the benzene yield reached its maximum at 500 °C, the highest purity was obtained at 450 °C. An even higher benzene yield of 74% and a purity of 97% were achieved when a heating rate of 2 K min⁻¹ was applied from 300 to 500 °C [48]. At a heating rate of 5 K min⁻¹, more than 50% of the carbon was converted to benzene. Benzene was obtained as a liquid with a high purity of 99%. Naphthalenes and biphenyls observed during pyrolysis of PET in the presence of CaO are minor impurities and no oxygen-containing compounds were observed [50]. When bottle-PET was hydrolysed at 450 °C and the volatile terephthalic acid was decarboxylated over CaO at 700 °C, benzene was obtained with a yield of 74% and a purity of 96%. The benzene yield from various composites such as X-ray film and magnetic tape decreased to values between 32 and 35%. The main by-product was biphenyl from the secondary reaction of benzene. Oxygenated compounds were negligible [64].

A new way of hydrolytically decomposing PET waste is the use of polyester degrading bacteria and their enzymes [65]. In the past, carboxylic acid hydrolases, lipases, serine esterases and carboxylesterases have been reported to be effective in the hydrolysis of PET [56]. Among these, cutinases, which belong to the group of carboxylic acid hydrolases, are the most efficient. It was found that *Humicola insolens* cutinase (HiC) is more than 20 times faster than other known PET degrading enzymes. One reason for this could be the small size of cutinases compared to other enzymes, which allows better contact with the rigid structure of PET. Terephthalic acid and mono(2-hydroxyethyl)terephthalate (MHET) were the main products of the degradation.

Cutinases are natural polyester hydrolases that have proven to be very efficient in the hydrolysis of PET at a temperature of around 70 °C. Terephthalic acid could then be recovered by filtration and ethylene glycol after distillation. The biodegradation route could be less energy intensive and thus more cost-effective at lower temperature and pressure. However, the biochemical process is more time consuming. Complete hydrolysis of PET film by *Thermobifida fusca* cutinase TfCut2, expressed by *Bacillus subtilis* and isolated from *E. coli*, takes approximately 120 h at 70 °C. With other packaging materials, 50% of the PET was not degraded. The reason for the differences in degradation behaviour was thought to be the inability of the enzyme to attack crystalline and rigid amorphous fractions, neither of which offer sufficient flexibility for an enzymatic reaction [53].

This obstacle is overcome by studying enzymes that are active at temperatures above 70 °C. Degradation of PET by the *Thermobifida cellulosilytica* derived cutinase Thc_Cut1 caused increasing crystallinity, which may also indicate preferential hydrolysis of the amorphous region [66]. When the thermophilic bacterium *Clostridium thermocellum* expresses leaf and branch compost cutinase (LCC) at 60 °C, about 62% of the amorphous PET was converted into terephthalic acid and MHET over a period of 14 days [7]. The stability of LCC against aggregation was improved by glycosylation. The stabilized enzyme showed high activity between

70 and 80 °C. The thickness of an amorphous PET film with a crystallinity of 7% was reduced by $60 \mu\text{m day}^{-1}$ [54]. With improved thermal stability, LCC was able to depolymerise PET by 90% in less than 10 h in a pilot-plant scale set-up. The recovered terephthalic acid was purified and used to make new PET. The bottles made from this material showed similar properties to those made from commercial PET [67].

The hydrolysis of PET in blends with polyethylene or polyamide is accelerated when Thc_Cut1 is used as an enzyme [66]. The enzymatic hydrolysis of highly crystalline PET fibres requires a pretreatment step. Only after hydrolysis of PET fibres at a temperature of 250 °C and a pressure of 39 bar was HiC able to convert the remaining oligomers into terephthalic acid. The presence of zinc cations as hydrolysis catalyst inhibited the action of the enzyme [55]. Furthermore, MHET [56, 68] and BHET [66] showed inhibitory effects on cutinases. Countermeasures are the addition of *Candida Antarctica* lipase B (CALB), which degraded MHET to terephthalic acid [56] or the use of an ultrafiltration membrane reactor to continuously remove MHET [68]. A reduced particle size is favourable for the hydrolysis of PET by enzymes [66].

Terephthalic acid can be produced by alkaline hydrolysis at 150 °C at a cost of 2.71 € kg^{-1} . The main cost factor is the wastewater management in terms of the organic content and the salt load due to the neutralisation of the highly basic solution for the precipitation of the terephthalic acid. The price could be reduced to 1.02 € kg^{-1} , if the wastewater is treated within the production plant [12]. The reaction in ethanol/water at 80 °C could reduce greenhouse gas emissions compared to the energetic conversion of PET waste [57].

The recyclability of production waste from PET hydrolysis is rather poor. Wastewater with an extreme pH is often disposed of. When neutralising the reaction solution from alkaline hydrolysis to recover terephthalic acid, saline solutions are produced from which the salt could be recovered. More promising is the use of ionic liquids as the reaction medium, as the two can be easily separated. Ionic liquid and catalyst were reused eight times in a row without loss of catalytic activity [51].

9.3.3 Aminolysis of Poly(Ethylene Terephthalate)

Poly(ethylene terephthalate) reacts with ammonia (ammonolysis) or organic amines (aminolysis) to form aromatic amides. Strongly basic amines react faster than amines with a low basicity. The reactivity is reduced by steric hindrance [69]. Depending on the amine used, a catalyst may be required. A catalyst is more likely to be needed for the reaction of lipophilic amines than for hydrophilic amines [70]. Since the amine-group is more nucleophilic than the hydroxyl-group, amino alcohols give always terephthalamides [70].

The reaction takes place below the melting temperature of PET at the particle surface. It was observed that methylamine preferentially attacks amorphous areas, while ammonia attacks both amorphous and crystalline areas from the beginning.

This was attributed to the higher nucleophilicity of methylamine [71]. Increasing temperatures cause a softening of the material and facilitate the migration of the amine beyond the surface, which is even more easily penetrated when the temperature exceeds the melting point of PET. The molecular weight of PET has been found to decrease with increasing PET conversion, indicating a random scission process [72].

The apparent activation energy of the aminolysis of PET in ethanolamine was determined to be 153 kJ mol⁻¹ using a modified shrinking core model [72].

Terephthalamides can be obtained from ammonia or various primary or secondary amines. Often, after optimisation the reaction does not require a catalyst [70]. If necessary, catalysts such as zinc acetate [73], sodium sulphate, acetate or bicarbonate [74] are used. Reaction of PET with ammonia under pressure at ambient temperature resulted in complete conversion to terephthalamide after 45 days in the absence of any catalyst and 15 days in the presence of zinc acetate [73]. Reaction with ethanolamine gave bis(hydroxyethyl)terephthalamide (BHETA) after 2 h at 140 °C [70]. Precipitation of the product was observed at high conversion. Reaction of fibres and bottle wastes under reflux in the presence of sodium acetate yielded 91 and 83% of BHETA after 8 h, respectively. The lower rate of degradation of bottle waste was explained by its higher molecular weight and broader molecular weight distribution [75].

The reaction of ethylenediamine with PET required 17 h at 100 °C in the absence of a catalyst. The yield of bis(2-aminoethyl)terephthalamide (BAET) reached 75% at an ethylene diamine/PET ratio of 16. Lower ratios yielded less BAET. The by-products were α,ω -aminoligo(ethylene terephthalamide)s (AOETs), oligomers from the condensation of BAET. The dimer was the most abundant fraction of the AOETs, although trimers and tetramers were also present [76]. The equilibrium shifted towards the AOET with temperature, reaching about 70% at 250 °C [77]. The reaction of triethylenetetramine with PET gave the corresponding terephthalamide after refluxing for 2 h at 130–140 °C [78].

The guanidine derivative 1,5,7-triazabicyclo [4.4.0] dec-5-ene (TBD) accelerated the aminolysis of PET with various aliphatic and aromatic amines. Aminolysis in the presence of ethylenediamine was completed after 1 h at 120 °C. Aminolysis in aniline took 24 h at 180 °C due to its lower basicity. Although piperidine is a strong base, the reaction was slow due to steric limitations [69]. Aminolysis in ethylenediamine in the presence of a TBD derivative (Fig. 9.4) as catalyst gave complete conversion of PET with BAET as the main product after 10 min at 120 °C. The reaction in ethanolamine required only 3 min at 190 °C and gave BHETA [79].

The reaction time can also be shortened by using a microwave reactor. The yield of BAET in the presence of ethylenediamine reached a maximum of 30% after 10 min at 250 °C and a pressure of more than 1 MPa. The main product after the complete conversion of PET was AOET. The reaction rate decreased significantly when the reaction was carried out below the melting point of PET [77]. Aminolysis in the presence of ethanolamine and NaHCO₃ as catalyst required 5 min for PET fibre waste and 7 min for PET bottle waste to obtain BHETA yields of about 90% under reflux [74]. The reaction time could be reduced to 2 min in the absence of a

Fig. 9.4 TBD (1,5,7-triazabicyclo [4.4.0] dec-5-ene) based aminolysis catalyst

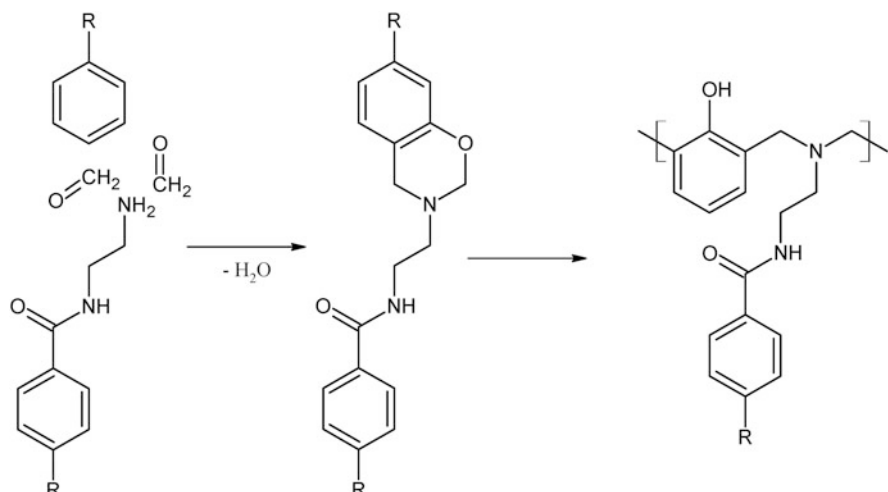
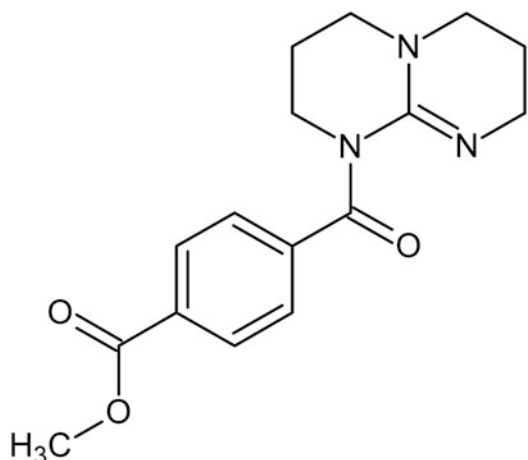


Fig. 9.5 Thermosets from bis(2-aminoethyl)terephthalamide (BAET) and cardanol

catalyst at a microwave power of 150 W when an autoclave was used. The temperature rose above the melting temperature of PET and the pressure exceeded 1 MPa. No reaction was observed below 180 °C [72].

The reaction in the presence of ethanolamine catalysed by dibutyltin oxide gave a complete conversion after 60 days in a sand bath heated by solar radiation in the Egyptian summer [80].

The product of PET depolymerized in ethanolamine, BHETA can be used for the production of polyurethanes [81] and corrosion protection paints [80]. The reaction of BAET with cardanol and paraformaldehyde resulted in bis-benzoxazines derivatives, which were converted to thermosets by ring-opening polymerisation (Fig. 9.5).

Cardanol is obtained from cashew nut shells and provides a route of bio-based resin production [77].

Products from the aminolysis of PET can be used as additives in asphalt [70]. The in-situ polymerisation of BHETA with methylene diphenyl diisocyanate in bitumen at 90–130 °C resulted in a binder suitable for the construction of roads with high traffic loads [82].

9.3.4 Solvolysis Using Other Types of Alcohols

In addition to the reactions described in the sections above, solvolysis can also be carried out in the presence of other alcohols, methanol being the most important. Methanolysis was of some importance in the early days of research, but lost importance when PET production was no longer carried out via the transesterification of dimethyl terephthalate (DMT).

The reaction mechanism is similar to that of the glycolysis process. The same catalytic systems are also applicable. The use of deep eutectic solvents [83] has been reported. A special feature of alcoholysis processes with solvents other than ethylene glycol is that at least two alcohols are present in the system and mixed products can be expected [84, 85]. An ATR-FTIR investigation could show that the Gauche conformation disappeared faster than the Trans conformation during methanolysis. The crystalline fraction also decreased faster than the amorphous fraction [86]. It was found that the transesterification of PET with 2-ethyl-1-hexanol in the presence of choline chloride/zinc acetate as catalyst proceeds by a first-order reaction with an activation energy of 95 kJ mol⁻¹ [83].

The use of methanol requires high pressure due to the low boiling point of methanol (65 °C). The reaction is usually carried out in the supercritical state above the critical point of 239 °C and 8.09 MPa [85]. It is shown that PET cast film was readily penetrated by methanol already at 150 °C, although the low activation energy of 6 kJ mol⁻¹ suggested an impeded mass transfer [86]. However, sufficient solubilisation only occurred under critical conditions. Below the critical pressure, the depolymerisation rate decreased significantly [85]. Below the melting point of PET, degradation occurred mainly at tie molecules reducing the molecular weight to one third. Catalysts can accelerate the formation of oligomers and DMT [87].

Under supercritical conditions, PET is melted and the effect of mass transfer resistance is reduced. It was found that PET dissolution is improved under supercritical conditions [88]. The depolymerisation was completed after 40 min at temperatures between 253 and 273 °C and a pressure of 11 MPa. Most of the by-products are converted into DMT under these conditions and DMT with a purity of 98% could be recovered from waste materials after purification [85]. At a temperature of 300 °C and a pressure of 20 MPa, PET with an average molecular weight of 47 kDa was depolymerised to 3 kDa after 5 min and 1 kDa after 10 min. The main products after 20 min were methyl 2-hydroxyethyl terephthalate, DMT,

and terephthalic acid monomethyl ester (TAMME). The yield of TAMME decreased after reaching its maximum after 15 min. The molecular weight distribution was successfully simulated over the reaction time [89]. The optimal conditions for the uncatalysed reaction were found at 298 °C for 112 min, yielding 99.8% DMT [88]. The addition of toluene promoted swelling and increased the DMT yield in the presence of aluminium isopropoxide as catalyst from 67% in pure methanol to 89% in methanol/toluene (80:20) at a temperature of 200 °C [87]. The temperature and time requirements can be reduced by using microwave reactors. Methanolysis in the presence of zinc acetate gave a DMT yield of 87% after 30 min at 180 °C. After reaching a maximum of 1.6 MPa, the pressure dropped to 1.2 MPa during the reaction, caused by the consumption of methanol [84].

The reaction in supercritical ethanol at a temperature of 255 °C and a pressure of 11.65 MPa gave a diethylterephthalate yield of 80% from multilayer packaging PET coated with aluminium and polyethylene [90].

High boiling alcohols do not require high pressure for their reaction with PET. The reaction with 1,4-butanediol and triethylene glycol can be carried out at 220 °C in the presence of zinc acetate as catalyst. The main product after 10 h of the reaction with 1,4-butanediol was bis(4-hydroxybutenyl)terephthalate with the dimer being the main by-product. When triethylene glycol was used, mainly oligomers with molecular weights between 700 and 800 g mol⁻¹ were obtained [91]. Solvolysis in the presence of 2-ethyl-1-hexanol gave a dioctyl terephthalate yield of 84% after 1 h reaction time and with choline chloride/zinc acetate (molar ratio 1:1) as deep eutectic solvent catalyst. The product could replace phthalate plasticizers and reduce the environmental hazard they pose [83].

9.3.5 Other Aromatic Polyesters

The most common aromatic polyesters besides PET are PBT and PEN. While PBT is used for many applications in the automotive industry and for electrical and electronic equipment, PEN is used as an alternative material to PET for packaging applications due to its better gas barrier properties and higher glass transition temperature. The depolymerisation processes are similar to those for PET.

The hydrolysis of PEN in aqueous ammonia solution at 240 °C was controlled by mass transfer [92]. The activation energy of the hydrolysis of PEN was 95 kJ mol⁻¹ [93], higher than that observed for PET with 56 kJ mol⁻¹ [4]. The activation energies for hydrolysis of PBT and PEN in steam atmosphere were 156 and 161 kJ mol⁻¹, respectively, which were slightly higher than that for PET under the same conditions [49]. For the random scission of PBT in methanol, an activation energy between 84 [9] and 87 kJ mol⁻¹ [94] was determined, which is about 10 kJ mol⁻¹ lower than that for the reaction of PET [9].

Depolymerisation of PEN in hot water is not observed below 227 °C. Yields of 2,6-naphthalene dicarboxylic acid (NDA) and ethylene glycol reached 98 and 86% after 1 h at a temperature of 300 °C [59]. When PEN was heated in water, swelling

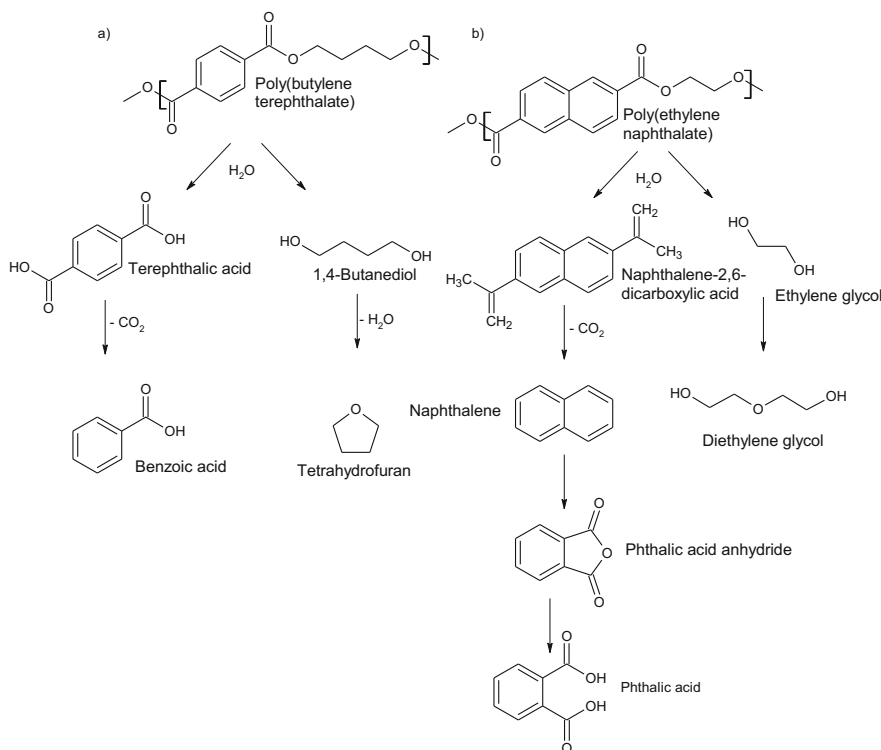


Fig. 9.6 Degradation of a) poly(butylene terephthalate) (PBT), and b) poly(ethylene naphthalate) (PEN) in hot water

was first observed, then above 200 °C the state changed to a liquid. This process ended at 270 °C, after which PEN was dissolved and a homogeneous aqueous phase was formed. The hydrolysis of PEN resulted in 83% of NDA and 80% ethylene glycol after 60 min at 260 °C [93].

The reaction of PBT and PEN catalysed by $\text{Ca}(\text{OH})_2$ in a steam atmosphere led to the formation of benzene and naphthalene, respectively, as was also observed for PET. The highest product yields were observed at 700 °C for PBT and 600 °C for PEN [95]. Pyrolytic processes were also observed during the hydrolytic degradation of PBT and PEN in a steam atmosphere. Pyrolysis increased drastically from 19 to 73% for PBT hydrolysis between 320 and 440 °C, while the contribution of pyrolysis remained constant at about 75% for PEN [49].

The hydrolysis of PBT in hot water can cause the degradation of terephthalic acid and 1,4-butanediol. Benzoic acid and tetrahydrofuran are observed as products instead [60]. During the hydrolysis of PEN, the resulting NDA can be decarboxylated to form naphthalene, which is oxidised to phthalic anhydride and hydrolysed to phthalic acid (Fig. 9.6) [93].

In methanol, PBT was completely depolymerised at 240 °C after 22 min. The highest DMT yield of 95% was observed after 75 min at 290 °C [94]. Shibata, et al. [9] observed complete depolymerisation after 10 min at the same temperature and a pressure of 6 MPa. By the time the reaction temperature was reached, about 50% of the two monomers had already been recovered. Alcoholysis of PBT is faster in methanol than in ethanol or propanol. Complete conversion was achieved in methanol after 20 min at 250 °C, while 25 and 42% of the PBT remained as residue in ethanol and propanol, respectively. The highest yields of dialkyl terephthalates were observed after 75 min at 310 °C with 98.5% of DMT and 76% of diethyl terephthalate [96]. One reason for this behaviour could be the good miscibility of molten PBT with methanol [9].

9.4 Depolymerisation of Aliphatic Polyesters

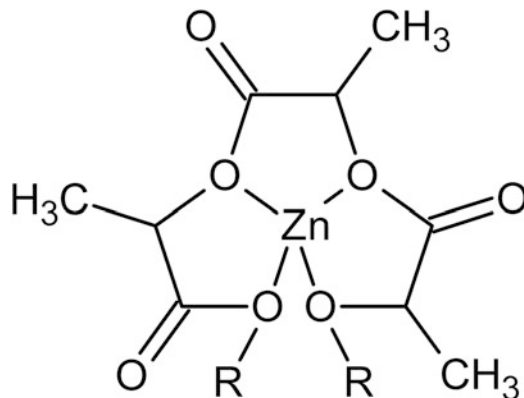
In contrast to aromatic polyesters, aliphatic polyesters are biodegradable. These include poly(lactic acid) (PLA, polylactide), poly(butylene succinate) (PBS), polycaprolactone (PCL), polyhydroxyalkanoates (PHAs) and others. Despite their biodegradability, these polyesters should be recycled to reduce the environmental impact of their production [97]. Most of these polymers can be successfully converted into monomers and other feedstocks for the production of new materials.

9.4.1 Depolymerisation of Poly(Lactic Acid)

The production of PLA begins with the fermentation of sugary biomass by lacto bacteria. The resulting lactic acid is dimerised to lactide in a conventional chemical process and then further converted to PLA by ring-opening polymerisation. Lactic acid occurs in two enantiomers, both produced by different species of *Lactobacillus*. Since usually only one of the enantiomers is used for the production of one type of PLA, the aim of depolymerising used PLA is to recover lactide or other lactic acid derivatives without racemisation [98].

The mechanism of catalysed depolymerisation of PLA is often analogous to that of PET glycolysis (Figs. 9.1 and 9.2) with the cation acting as a Lewis acid and the anion increasing the nucleophilicity of the reactant, water or alcohol [99, 100]. The reaction of PLA in the presence of a zinc catalyst is faster than that of PET. It has been suggested that PLA is able to chelate the zinc ion (Fig. 9.7), while the rigid structure of PET prevents chelation [101]. High solubility of PLA is favourable for the reaction. Ionic liquids with a low ability to dissolve PLA showed limited conversion, while the reaction proceeded easily when PLA was sufficiently dissolved. Small polymer chains were more rapidly dissolved and depolymerised by a random scission process than longer ones, resulting in an extraordinary reduction in polydispersity [100].

Fig. 9.7 Chelation of zinc ions by poly(lactic acid) PLA. The R-groups represent PLA chains



Hydrolysis in water and NaOH solution showed comparable activation energies of 82 kJ mol^{-1} and 72 kJ mol^{-1} , respectively [102]. The activation energy was significantly higher at 134 kJ mol^{-1} when the reaction was catalysed by $[\text{Bmin}][\text{OAc}]$ [100]. Methanolysis using a zinc ring-opening catalyst proceeded by random chain scission with an activation energy of $(39$ and $65)$ kJ mol^{-1} [103]. Using an ethylenediamine-zinc(II) complex, an activation energy of about 40 kJ mol^{-1} was observed [104].

Pyrolysis is the simplest route of PLA depolymerisation, but also the most energy-intensive. In the presence of zinc catalysts at temperatures between 190 and $245 \text{ }^\circ\text{C}$, lactide was obtained as the main product with an enantiomeric excess of more than 99% and a yield of up to 92% [105]. However, racemisation occurs in the presence of some fillers. It was observed that in the presence of MgO less than 3% of the lactide was racemised at temperatures below $270 \text{ }^\circ\text{C}$. The extent of racemisation increased above this temperature. The presence of CaO resulted in $10\text{--}20\%$ racemisation below $250 \text{ }^\circ\text{C}$, while above this temperature racemisation decreased to below 2% . It was suggested that racemisation occurred by a backbiting process, while L,L-lactide was obtained by an unzipping reaction [106, 107].

Hydrolysis of PLA in water and NaOH solution gave lactic acid yields between 92% and 98% at $160 \text{ }^\circ\text{C}$ [102]. Similar results were obtained in the presence of $[\text{Bmin}][\text{OAc}]$ as catalyst, resulting in a PLA conversion of 94% at a temperature of $130 \text{ }^\circ\text{C}$. After precipitation with $\text{Ca}(\text{CO}_3)$, a calcium lactate yield of 76% was obtained [100]. High enantiomeric purity was achieved with *Escherichia coli* strains [102].

Methanolysis in the presence of KF as catalyst gave methyl lactate yields of more than 99% at $180 \text{ }^\circ\text{C}$. The catalyst was able to degrade PLA and poly(bisphenol-A-carbonate) side by side, while PET and nylon-6 interfered with the degradation and reduced the yield of PLA [99]. Reaction in methanol with 4-dimethylaminopyridine (DMAP) as a catalyst resulted in 97% yield of methyl lactate as determined by NMR after heating in a microwave oven at $180 \text{ }^\circ\text{C}$ for 10 min. The catalysts 1,8-diazabicyclo[5.4.0]undec-7-ene (DBU) and 1,5,7-triazabicyclo[4.4.0]dec-5-ene (TBD) even achieved yields close to 100% under the same conditions

[108]. Microwave methanolysis at 160 °C gave reaction yields of more than 99% after 20 min in the presence of tin(II) 2-ethylhexanoate. High turnover frequencies close to $4 \times 10^4 \text{ h}^{-1}$ were observed [109]. The reaction of PLA with methanol, ethanol and butanol was completed after 2 min at room temperature in the presence of TBD. The reaction of sterically hindered alcohols was strongly delayed due to the space requirements of the catalyst. Acidic alcohols deactivated the basic catalyst [110]. Methanolysis in the presence of zinc acetate gave a methyl lactate yield of 70% after 15 h of heating under reflux [101]. The reaction in tetrahydrofuran using a zinc ring-opening catalyst was completed within 60 min and gave 100% methyl lactate although depolymerisation was already observed at 40 °C [103]. Methyl lactate yields of 100% were obtained from PLA waste after 4 h at 110 °C in the presence of an ethylenediamine-Zn(II) complex as catalyst [104].

The reaction of PLA with diamines gave oligomers when carried out under reflux in xylene. The reaction proceeded with 1,6-diaminohexane without catalyst and after 1 h an oligomer with a molecular weight of 5.5 kg mol⁻¹ was obtained containing both lactic acid and diamine units. Oligomers were also obtained in the presence of tin(II) 2-ethylhexanoate as catalyst when 1,3-propanediol was the degradation agent [111]. Ionic liquids could be recovered from PLA hydrolysis and reused 7 times in a row without loss of activity [100].

Lifecycle assessment showed that chemical recycling and polymerisation of virgin PLA from 1 tonne of waste PLA could reduce the global warming potential by 780 kg CO₂-eq. [97]. The energy requirement for the production of lactic acid could be reduced from 55 MJ kg⁻¹ for the production from corn starch to 14 MJ kg⁻¹ for the hydrolysis of PLA [98].

9.4.2 Depolymerisation of Other Aliphatic Polyesters

Other aliphatic polyesters include PBS, PCL, PHAs, and other mostly biomass derived thermoplastics. Although these materials are often biodegradable, depolymerisation for the purpose of recycling has been an emerging issue in recent years. In this section, only a few examples are presented.

It can be seen that many concepts that were successfully applied to the depolymerisation of PET were also adopted for aliphatic polyesters. The reaction mechanisms found for the reaction catalysed by ionic liquids [112, 113] were analogous to those for PET (Figs. 9.1 and 9.2). The hydrolysis of PBS and poly (butylene succinate/adipate) (PBSA) in hot water proceeded with activation energies of 64 and 58 kJ mol⁻¹ [114]. The low activation energy of 27 kJ mol⁻¹ in the methanolysis of PHB catalysed by [Bmin]FeCl₄ [112, 113] indicated mass transport hindrance.

The thermal degradation of PHAs at 190 °C leads to a significant reduction in molecular weight after only 30 min [115]. If PHB was pyrolysed at 310 °C, unsaturated acids are obtained. A yield of about 78% was achieved, including trans-crotonic acid as the main product and 2-pentenoic acid and cis-crotonic acid

as by-products. This method can be used to separate PHB from polypropylene, which is degraded at higher temperatures [116].

The hydrolysis of PBS and poly(butylene succinate/adipate) (PBSA) in hot water provided lower acid yields between 180 and 300 °C than comparable experiments from PET. The highest succinic acid yield of 80% was achieved from PBS after about 30 min at temperatures between 270 and 300 °C. In the same temperature range, the succinic acid and adipic acid yields from PBSA reached 65 and 70%, respectively [114].

The most common strategy for the depolymerisation of aliphatic esters is the use of enzymes. Lipases in particular offer the advantage of wide commercial availability [117]. Such lipases were able to reduce the molecular weight of poly(3-hydroxybutyrate-co-4-hydroxybutyrate) from 300 kg mol⁻¹ to below 5 kg mol⁻¹ after 72 h at 37 °C. The reaction of PCL in toluene required 24 h at 50 °C in the presence of *Candida antarctica* lipase B (CALB) for conversion to di-, tri-, and tetra-oligomers. ε-caprolactone was also observed as a by-product. Depolymerisation proceeded by a random chain scission mechanism. After reaching a minimum after 24 h, the molecular weight increased again significantly [8]. The time required for depolymerisation at moderate temperatures is still too long for technical application. Therefore, higher temperatures are aimed for.

Depolymerisation in the presence of CALB using a twin screw extruder drastically reduced the molecular weight of PBS from 82 kg mol⁻¹ to 2000 g mol⁻¹ after 5 min at a temperature of 120 °C. A maximum succinic acid yield of 44% was achieved, while 1,4-butanediol was not observed among the products. This reaction required catalyst concentrations of up to 10 wt% and the catalyst lost more than 60% of its activity during the process [118]. The depolymerases Est-H and Est-L isolated from the bacterium *Roseateles depolymerans* TB-87 were able to degrade various aliphatic and aliphatic-aromatic polyesters. Succinic acid and 1,4-butanediol were obtained from PBS. In addition, adipic acid was observed in the degradation of poly(butylene succinate-co-adipate) and terephthalic acid and isophthalic acid in the degradation of poly(butylene succinate/terephthalate/isophthalate)-co-(lactate). The depolymerisation of aliphatic-aromatic polyesters proved to be slower than that of purely aliphatic polyesters [119]. The depolymerisation of poly(hexamethylene succinate-co-hexamethylene-hexylthiosuccinate) with CALB reduced the molecular weight from 78 kg mol⁻¹ to 800 g mol⁻¹. All products were cyclic oligomers. Subsequent ring-opening polymerisation with the same catalyst gave a polymer with a molecular weight of 70 kg mol⁻¹, proving the recyclability of this type of polyester [120].

Methanolysis under reflux in the absence of a catalyst at a temperature of 200 °C and a pressure of 18 bar for a period of 6 h converted PHB to methyl crotonate. The product could be used to obtain propylene and methyl acrylate by metathesis [6]. Methanolysis of PHB in the presence of the ionic liquids [Bmin]FeCl₄ and [MIMPS]FeCl₄ (1-(3-sulfonic acid)-propyl-3-methylimidazole ferric chloride) as ferromagnetic catalysts gave methyl (3-hydroxybutyrate) yields of 85 and 87% after a reaction time of 3 h at 140 °C, respectively. The purity of the monomer was over 98%. The catalysts were recovered and used six times in succession

without loss of activity [112, 113]. The reaction carried out under a microwave heating in the presence of methanol or ethanol gave a mixture of 3-hydroxybutyric acid, crotonic acid, and the 3-alkyl butyric acid ethers [121].

9.5 Conclusions and Future Outlook

Climate change will force plastics manufacturers to find new sources of carbon in future, when fossil fuels are no longer considered suitable for technical applications. Fossil carbon could be replaced to some extent by biomass. However, it is questionable whether enough biomass can be made available to meet the increasing demand for plastics. Plastic producers could face carbon scarcity in a future world, which would force them to keep the “harvested” carbon in the cycle.

Established polymers such as PET, PBT, and PEN have been developed from monomers that are readily available from fossil fuels. This paradigm could change if biomass becomes the main feedstock for carbon loss replacement. Biomass as a feedstock provides different types of monomers. New polymers, such as PLA, PBS, and PHAs, are the result and others may follow. The structure of the new polymers may depend strongly on the type of biomass used. This could result in an even wider range of polymers than we see today—and all these polymers have their own process requirements for recycling if monomers are to be the target.

We have seen in this chapter that different types of polyesters require different processes for depolymerisation. However, we have also seen that some processes allow the separation of different types of polymers: PET can be separated from PVC [44]; PLA from PET and nylon-6 [99]; PHB from polyolefins [116]. The increasing number of polymers in the waste stream could make the separation of individual polymers more difficult than it is today. Combining chemical recycling methods for monomer recovery may have some advantages, and therefore there is still much work to be done to develop solutions that offer the possibility of fractional depolymerisation and stepwise monomer recovery. To keep track of the increasing number of possible monomers, more of these solutions will be needed in the future.

References

1. Volanti M, Cespi D, Passarini F, Neri E, Cavani F, Mizsey P, Fozer D. Terephthalic acid from renewable sources: early-stage sustainability analysis of a bio-PET precursor. *Green Chem.* 2019;21:885–96. <https://doi.org/10.1039/C8GC03666G>.
2. Williams ID, Shaw PJ. Reuse in Practice. 4th Symposium on Urban Mining and Circular Economy. Bergamo, Italy; 2018
3. Lopez-Fonseca R, Duque-Ingunza I, de Rivas B, Arnaiz S, Gutierrez-Ortiz JI. Chemical recycling of post-consumer PET wastes by glycolysis in the presence of metal salts. *Polym Degrad Stabil.* 2010;95:1022–8. <https://doi.org/10.1016/j.polymdegradstab.2010.03.007>.

4. Campanelli JR, Kamal MR, Cooper DG. A kinetic-study of the hydrolytic degradation of polyethylene terephthalate at high-temperatures. *J Appl Polym Sci.* 1993;48:443–51. <https://doi.org/10.1002/app.1993.070480309>.
5. Grause G, Kaminsky W, Fahrbach G. Hydrolysis of poly(ethylene terephthalate) in a fluidised bed reactor. *Polym Degrad Stabil.* 2004;85:571–5. <https://doi.org/10.1016/j.polymdegradstab.2003.10.020>.
6. Spekreijse J, Le Notre J, Sanders JPM, Scott EL. Conversion of polyhydroxybutyrate (PHB) to methyl crotonate for the production of biobased monomers. *J Appl Polym Sci.* 2015;132:8. <https://doi.org/10.1002/app.42462>.
7. Yan F, Wei R, Cui Q, Bornscheuer UT, Liu YJ. Thermophilic whole-cell degradation of polyethylene terephthalate using engineered *Clostridium thermocellum*. *Microb Biotechnol.* 2021;14:374–85. <https://doi.org/10.1111/1751-7915.13580>.
8. Aris MH, Annar MSM, Ling TC. Lipase-mediated degradation of poly-epsilon-caprolactone in toluene: Behavior and its action mechanism. *Polym Degrad Stabil.* 2016;133:182–91. <https://doi.org/10.1016/j.polymdegradstab.2016.08.015>.
9. Shibata M, Masuda T, Yosomiya R, Ling-Hui M. Depolymerization of poly(butylene terephthalate) using high-temperature and high-pressure methanol. *J Appl Polym Sci.* 2000;77:3228–33. [https://doi.org/10.1002/1097-4628\(20000929\)77:14<3228::Aid-app260>3.0.Co;2-g](https://doi.org/10.1002/1097-4628(20000929)77:14<3228::Aid-app260>3.0.Co;2-g).
10. Sce F, Cano I, Martin C, Beobide G, Castillo O, de Pedro I. Comparing conventional and microwave-assisted heating in PET degradation mediated by imidazolium-based halometallate complexes. *New J Chem.* 2019;43:3476–85. <https://doi.org/10.1039/c8nj06090h>.
11. Welle F. Twenty years of PET bottle to bottle recycling—An overview. *Resour Conserv Recy.* 2011;55:865–75. <https://doi.org/10.1016/j.resconrec.2011.04.009>.
12. Aguado A, Martinez L, Becerra L, Arieta-araunabena M, Arnaiz S, Asueta A, Robertson I. Chemical depolymerisation of PET complex waste: hydrolysis vs. glycolysis. *J Mater Cycles Waste Manage.* 2014;16:201–10. <https://doi.org/10.1007/s10163-013-0177-y>.
13. Liu YC, Yao XQ, Yao HY, Zhou Q, Xin JY, Lu XM, Zhang SJ. Degradation of poly(ethylene terephthalate) catalyzed by metal-free choline-based ionic liquids. *Green Chem.* 2020;22:3122–31. <https://doi.org/10.1039/d0gc00327a>.
14. Yue QF, Xiao LF, Zhang ML, Bai XF. The glycolysis of poly(ethylene terephthalate) waste: lewis acidic ionic liquids as high efficient catalysts. *Polymers.* 2013;5:1258–71. <https://doi.org/10.3390/polym5041258>.
15. Jehanno C, Flores I, Dove AP, Muller AJ, Ruiperez F, Sardon H. Organocatalysed depolymerisation of PET in a fully sustainable cycle using thermally stable protic ionic salt. *Green Chem.* 2018;20:1205–12. <https://doi.org/10.1039/c7gc03396f>.
16. Liu B, Fu WZ, Lu XM, Zhou Q, Zhang SJ. Lewis acid-base synergistic catalysis for polyethylene terephthalate degradation by 1,3-dimethylurea/Zn(OAc)₂ deep eutectic solvent. *ACS Sustain Chem Eng.* 2019;7:3292–300. <https://doi.org/10.1021/acssuschemeng.8b05324>.
17. Wang Q, Yao XQ, Geng YR, Zhou Q, Lu XM, Zhang SJ. Deep eutectic solvents as highly active catalysts for the fast and mild glycolysis of poly(ethylene terephthalate)(PET). *Green Chem.* 2015;17:2473–9. <https://doi.org/10.1039/c4gc02401j>.
18. Kao CY, Cheng WH, Wan BZ. Investigation of catalytic glycolysis of polyethylene terephthalate by differential scanning calorimetry. *Thermochim Acta.* 1997;292:95–104. [https://doi.org/10.1016/s0040-6031\(97\)00060-9](https://doi.org/10.1016/s0040-6031(97)00060-9).
19. Ghaemy M, Mossadegh K. Depolymerisation of poly(ethylene terephthalate) fibre wastes using ethylene glycol. *Polym Degrad Stabil.* 2005;90:570–6. <https://doi.org/10.1016/j.polymdegradstab.2005.03.011>.
20. Al-Sabagh AM, Yehia FZ, Eissa A, Moustafa ME, Eshaq G, Rabie ARM, ElMetwally AE. Glycolysis of poly(ethylene terephthalate) catalyzed by the lewis base ionic liquid (Bmim)(OAc). *Ind Eng Chem Res.* 2014;53:18443–51. <https://doi.org/10.1021/ie503677w>.

21. Viana ME, Riul A, Carvalho GM, Rubira AF, Muniz EC. Chemical recycling of PET by catalyzed glycolysis: kinetics of the heterogeneous reaction. *Chem Eng J.* 2011;173:210–9. <https://doi.org/10.1016/j.cej.2011.07.031>.
22. Zhou XY, Lu XM, Wang Q, Zhu ML, Li ZX. Effective catalysis of poly(ethylene terephthalate) (PET) degradation by metallic acetate ionic liquids. *Pure Appl Chem.* 2012;84:789–801. <https://doi.org/10.1351/pac-con-11-06-10>.
23. Lopez-Fonseca R, Duque-Ingunza I, de Rivas B, Flores-Giraldo L, Gutierrez-Ortiz JI. Kinetics of catalytic glycolysis of PET wastes with sodium carbonate. *Chem Eng J.* 2011;168:312–20. <https://doi.org/10.1016/j.cej.2011.01.031>.
24. Imran M, Kim DH, Al-Masry WA, Mahmood A, Hassan A, Haider S, Ramay SM. Manganese-, cobalt-, and zinc-based mixed-oxide spinels as novel catalysts for the chemical recycling of poly(ethylene terephthalate) via glycolysis. *Polym Degrad Stabil.* 2013;98:904–15. <https://doi.org/10.1016/j.polymdegradstab.2013.01.007>.
25. Imran M, Kim BK, Han M, Cho BG, Kim DH. Sub- and supercritical glycolysis of polyethylene terephthalate (PET) into the monomer bis(2-hydroxyethyl) terephthalate (BHET). *Polym Degrad Stabil.* 2010;95:1686–93. <https://doi.org/10.1016/j.polymdegradstab.2010.05.026>.
26. Goje AS, Mishra S. Chemical kinetics, simulation, and thermodynamics of glycolytic depolymerization of poly(ethylene terephthalate) waste with catalyst optimization for recycling of value added monomeric products. *Macromol Mater Eng.* 2003;288:326–36. <https://doi.org/10.1002/mame.200390034>.
27. Wang H, Li ZX, Liu YQ, Zhang XP, Zhang SJ. Degradation of poly(ethylene terephthalate) using ionic liquids. *Green Chem.* 2009;11:1568–75. <https://doi.org/10.1039/b906831g>.
28. Guclu G, Kasgoz A, Ozbudak S, Ozgumus S, Orbay M. Glycolysis of poly(ethylene terephthalate) wastes in xylene. *J Appl Polym Sci.* 1998;69:2311–9. [https://doi.org/10.1002/\(SICI\)1097-4628\(19980919\)69:12<2311::AID-APP2%3E3.0.CO;2-B](https://doi.org/10.1002/(SICI)1097-4628(19980919)69:12<2311::AID-APP2%3E3.0.CO;2-B).
29. Pingale ND, Palekar VS, Shukla SR. Glycolysis of postconsumer polyethylene terephthalate waste. *J Appl Polym Sci.* 2010;115:249–54. <https://doi.org/10.1002/app.31092>.
30. Shukla SR, Harad AM. Glycolysis of polyethylene terephthalate waste fibers. *J Appl Polym Sci.* 2005;97:513–7. <https://doi.org/10.1002/app.21769>.
31. Imran M, Lee KG, Imtiaz Q, Kim BK, Han M, Cho BG, Kim DH. Metal-oxide-doped silica nanoparticles for the catalytic glycolysis of polyethylene terephthalate. *J Nanosci Nanotechnol.* 2011;11:824–8. <https://doi.org/10.1166/jnn.2011.3201>.
32. Eshaq G, ElMetwally AE. (Mg-Zn)-Al layered double hydroxide as a regenerable catalyst for the catalytic glycolysis of polyethylene terephthalate. *J Mol Liq.* 2016;214:1–6. <https://doi.org/10.1016/j.molliq.2015.11.049>.
33. Lima GR, Monteiro WF, Ligabue R, Santana RMC. Titanate nanotubes as new nanostructured catalyst for depolymerization of PET by glycolysis reaction. *Mater Res-Ibero-Am J Mater.* 2017;20:588–95. <https://doi.org/10.1590/1980-5373-mr-2017-0645>.
34. Kitano M, Wada E, Nakajima K, Hayashi S, Miyazaki S, Kobayashi H, Hara M. Protonated titanate nanotubes with Lewis and Brønsted acidity: relationship between nanotube structure and catalytic activity. *Chem Mat.* 2013;25:385–93. <https://doi.org/10.1021/cm303324b>.
35. Bartolome L, Imran M, Lee KG, Sangalang A, Ahn JK, Kim DH. Superparamagnetic γ -Fe₂O₃ nanoparticles as an easily recoverable catalyst for the chemical recycling of PET. *Green Chem.* 2014;16:279–86. <https://doi.org/10.1039/c3gc41834k>.
36. Nabid MR, Bide Y, Fereidouni N, Etemadi B. Maghemite/nitrogen-doped graphene hybrid material as a reusable bifunctional catalyst for glycolysis of polyethylene terephthalate. *Polym Degrad Stabil.* 2017;144:434–41. <https://doi.org/10.1016/j.polymdegradstab.2017.08.033>.
37. Al-Sabagh AM, Yehia FZ, Harding DRK, Eshaq G, ElMetwally AE. Fe₃O₄-boosted MWCNT as an efficient sustainable catalyst for PET glycolysis. *Green Chem.* 2016;18:3997–4003. <https://doi.org/10.1039/c6gc00534a>.
38. Cano I, Martin C, Fernandes JA, Lodge RW, Dupont J, Casado-Carmona FA, Lucena R, Cardenas S, Sans V, de Pedro I. Paramagnetic ionic liquid-coated SiO₂@Fe3O4 nanoparticles—The next generation of magnetically recoverable nanocatalysts applied in the

- glycolysis of PET. *Appl Catal B Environ.* 2020;260:118110. <https://doi.org/10.1016/j.apcatb.2019.118110>.
39. Fukushima K, Coulembier O, Lecuyer JM, Almegren HA, Alabdulrahman AM, Alsewailem FD, McNeil MA, Dubois P, Waymouth RM, Horn HW, Rice JE, Hedrick JL. Organocatalytic depolymerization of poly(ethylene terephthalate). *J Polym Sci Pol Chem.* 2011;49:1273–81. <https://doi.org/10.1002/pola.24551>.
40. Kim DH, Han DO, In Shim K, Kim JK, Pelton JG, Ryu MH, Joo JC, Han JW, Kim HT, Kim KH. One-pot chemo-bioprocess of PET depolymerization and recycling enabled by a biocompatible catalyst, betaine. *ACS Catal.* 2021;11:3996–4008. <https://doi.org/10.1021/acscatal.0c04014>.
41. Li XK, Lu H, Guo WZ, Cao GP, Liu HL, Shi YH. Reaction kinetics and mechanism of catalyzed hydrolysis of waste PET using solid acid catalyst in supercritical CO₂. *AICHE J.* 2015;61:200–14. <https://doi.org/10.1002/aic.14632>.
42. Yoshioka T, Motoki T, Okuwaki A. Kinetics of hydrolysis of poly(ethylene terephthalate) powder in sulfuric acid by a modified shrinking-core model. *Ind Eng Chem Res.* 2001;40:75–9. <https://doi.org/10.1021/ie000592u>.
43. Yoshioka T, Okayama N, Okuwaki A. Kinetics of hydrolysis of PET powder in nitric acid by a modified shrinking-core model. *Ind Eng Chem Res.* 1998;37:336–40. <https://doi.org/10.1021/ie970459a>.
44. Kumagai S, Hirahashi S, Grause G, Kameda T, Toyoda H, Yoshioka T. Alkaline hydrolysis of PVC-coated PET fibers for simultaneous recycling of PET and PVC. *J Mater Cycles Waste Manage.* 2018;20:439–49. <https://doi.org/10.1007/s10163-017-0614-4>.
45. Karayannidis GP, Chatziavoustis AP, Achilias DS. Poly(ethylene terephthalate) recycling and recovery of pure terephthalic acid by alkaline hydrolysis. *Adv Polym Technol.* 2002;21:250–9. <https://doi.org/10.1002/adv.10029>.
46. Guclu G, Yalcinyuva T, Ozgumu S, Orbay M. Hydrolysis of waste polyethylene terephthalate and characterization of products by differential scanning calorimetry. *Thermochim Acta.* 2003;404:193–205. [https://doi.org/10.1016/s0040-6031\(03\)00160-6](https://doi.org/10.1016/s0040-6031(03)00160-6).
47. Campanelli JR, Cooper G, Kamal MR. Catalyzed-hydrolysis of polyethylene terephthalate melts. *J Appl Polym Sci.* 1994;53:985–91. <https://doi.org/10.1002/app.1994.070530801>.
48. Grause G, Handa T, Kameda T, Mizoguchi T, Yoshioka T. Effect of temperature management on the hydrolytic degradation of PET in a calcium oxide filled tube reactor. *Chem Eng J.* 2011;166:523–8. <https://doi.org/10.1016/j.cej.2010.11.010>.
49. Kumagai S, Morohoshi Y, Grause G, Kameda T, Yoshioka T. Pyrolysis versus hydrolysis behavior during steam decomposition of polyesters using ¹⁸O-labeled steam. *RSC Adv.* 2015;5:61828–37. <https://doi.org/10.1039/c5ra08577b>.
50. Du SC, Valla JA, Parnas RS, Bollas GM. Conversion of polyethylene terephthalate based waste carpet to benzene-rich oils through thermal, catalytic, and catalytic steam pyrolysis. *ACS Sustain Chem Eng.* 2016;4:2852–60. <https://doi.org/10.1021/acssuschemeng.6b00450>.
51. Liu FS, Cui X, Yu ST, Li Z, Ge XP. Hydrolysis reaction of poly(ethylene terephthalate) using ionic liquids as solvent and catalyst. *J Appl Polym Sci.* 2009;114:3561–5. <https://doi.org/10.1002/app.30981>.
52. Ruvolo A, Curti PS. Chemical kinetic model and thermodynamic compensation effect of alkaline hydrolysis of waste poly(ethylene terephthalate) in nonaqueous ethylene glycol solution. *Ind Eng Chem Res.* 2006;45:7985–96. <https://doi.org/10.1021/ie060528y>.
53. Wei R, Breite D, Song C, Grasing D, Ploss T, Hille P, Schwerdtfeger R, Matysik J, Schulze A, Zimmermann W. Biocatalytic degradation efficiency of postconsumer polyethylene terephthalate packaging determined by their polymer microstructures. *Adv Sci.* 2019;6:10. <https://doi.org/10.1002/advs.201900491>.
54. Shirke AN, White C, Englaender JA, Zwarycz A, Butterfoss GL, Linhardt RJ, Gross RA. Stabilizing leaf and branch compost cutinase (LCC) with glycosylation: mechanism and effect on PET hydrolysis. *Biochemistry.* 2018;57:1190–200. <https://doi.org/10.1021/acs.biochem.7b01189>.

55. Quarintello F, Vajnhandl S, Valh JV, Farmer TJ, Voncina B, Lobnik A, Acero EH, Pellis A, Guebitz GM. Synergistic chemo-enzymatic hydrolysis of poly(ethylene terephthalate) from textile waste. *Microb Biotechnol.* 2017;10:1376–83. <https://doi.org/10.1111/1751-7915.12734>.
56. de Castro AM, Carniel A, Nicomedes J, Gomes AD, Valoni E. Screening of commercial enzymes for poly(ethylene terephthalate) (PET) hydrolysis and synergy studies on different substrate sources. *J Ind Microbiol Biotechnol.* 2017;44:835–44. <https://doi.org/10.1007/s10295-017-1942-z>.
57. Ügdüler S, Van Geem KM, Denolf R, Roosen M, Mys N, Ragaert K, De Meester S. Towards closed-loop recycling of multilayer and coloured PET plastic waste by alkaline hydrolysis. *Green Chem.* 2020;22:5376–94. <https://doi.org/10.1039/D0GC00894J>.
58. Wan BZ, Kao CY, Cheng WH. Kinetics of depolymerization of poly(ethylene terephthalate) in a potassium hydroxide solution. *Ind Eng Chem Res.* 2001;40:509–14. <https://doi.org/10.1021/ie0005304>.
59. Sato O, Arai K, Shirai M. Hydrolysis of poly(ethylene terephthalate) and poly(ethylene 2,6-naphthalene dicarboxylate) using water at high temperature: effect of proton on low ethylene glycol yield. *Catal Today.* 2006;111:297–301. <https://doi.org/10.1016/j.cattod.2005.10.040>.
60. Wang JL, Bei K, Hu ZC, Liu YP, Ma YP, Shen Y, Chou IM, Pan ZY. Depolymerization of waste polybutylene terephthalate in hot compressed water in a fused silica capillary reactor and an autoclave reactor: monomer phase behavior, stability, and mechanism. *Polym Eng Sci.* 2017;57:544–9. <https://doi.org/10.1002/pen.24450>.
61. de Carvalho GM, Muniz EC, Rubira AF. Hydrolysis of post-consume poly(ethylene terephthalate) with sulfuric acid and product characterization by WAXD, ^{13}C -NMR and DSC. *Polym Degrad Stabil.* 2006;91:1326–32. <https://doi.org/10.1016/j.polymdegradstab.2005.08.005>.
62. Yoshioka T, Sato T, Okuwaki A. Hydrolysis of waste PET by sulfuric acid at 150°C for a chemical recycling. *J Appl Polym Sci.* 1994;52:1353–5. <https://doi.org/10.1002/app.1994.070520919>.
63. Mohsin MA, Alnaqbi MA, Busheer RM, Haik Y. Sodium methoxide catalyzed depolymerization of waste polyethylene terephthalate under microwave irradiation. *Catal Ind.* 2018;10:41–8. <https://doi.org/10.1134/s2070050418010087>.
64. Kumagai S, Grause G, Kameda T, Yoshioka T. Simultaneous recovery of benzene-rich oil and metals by steam pyrolysis of metal-poly(ethylene terephthalate) composite waste. *Environ Sci Technol.* 2014;48:3430–7. <https://doi.org/10.1021/es405047j>.
65. Kawai F, Kawabata T, Oda M. Current state and perspectives related to the polyethylene terephthalate hydrolases available for biorecycling. *ACS Sustain Chem Eng.* 2020;8:8894–908. <https://doi.org/10.1021/acssuschemeng.0c01638>.
66. Gamerith C, Zartl B, Pellis A, Guillamot F, Marty A, Acero EH, Guebitz GM. Enzymatic recovery of polyester building blocks from polymer blends. *Process Biochem.* 2017;59:58–64. <https://doi.org/10.1016/j.procbio.2017.01.004>.
67. Tournier V, Topham CM, Gilles A, David B, Folgoas C, Moya-Leclair E, Kamionka E, Desrousseaux ML, Texier H, Gavalda S, Cot M, Guémard E, Dalibey M, Nomme J, Cioci G, Barbe S, Chateau M, André I, Duquesne S, Marty A. An engineered PET depolymerase to break down and recycle plastic bottles. *Nature.* 2020;580:216–9. <https://doi.org/10.1038/s41586-020-2149-4>.
68. Barth M, Wei R, Oeser T, Then J, Schmidt J, Wohlgemuth F, Zimmermann W. Enzymatic hydrolysis of polyethylene terephthalate films in an ultrafiltration membrane reactor. *J Membr Sci.* 2015;494:182–7. <https://doi.org/10.1016/j.memsci.2015.07.030>.
69. Fukushima K, Lecuyer JM, Wei DS, Horn HW, Jones GO, Al-Megren HA, Alabdulrahman AM, Alsewailem FD, McNeil MA, Rice JE, Hedrick JL. Advanced chemical recycling of poly (ethylene terephthalate) through organocatalytic aminolysis. *Polym Chem.* 2013;4:1610–6. <https://doi.org/10.1039/c2py20793a>.

70. Merkel DR, Kuang W, Malhotra D, Petrossian G, Zhong L, Simmons KL, Zhang J, Cosimescu L. Waste PET chemical processing to terephthalic amides and their effect on asphalt performance. *ACS Sustain Chem Eng.* 2020;8:5615–25. <https://doi.org/10.1021/acssuschemeng.0c00036>.
71. Mittal A, Soni RK, Dutt K, Singh S. Scanning electron microscopic study of hazardous waste flakes of polyethylene terephthalate (PET) by aminolysis and ammonolysis. *J Hazard Mater.* 2010;178:390–6. <https://doi.org/10.1016/j.jhazmat.2010.01.092>.
72. Achilias DS, Tsintzou GP, Nikolaidis AK, Bikaris DN, Karayannidis GP. Aminolytic depolymerization of poly(ethylene terephthalate) waste in a microwave reactor. *Polym Int.* 2011;60:500–6. <https://doi.org/10.1002/pi.2976>.
73. Jain A, Soni RK. Spectroscopic investigation of end products obtained by ammonolysis of poly (ethylene terephthalate) waste in the presence of zinc acetate as a catalyst. *J Polym Res.* 2007;14:475–81. <https://doi.org/10.1007/s10965-007-9131-9>.
74. Pingale ND, Shukla SR. Microwave-assisted aminolytic depolymerization of PET waste. *Eur Polym J.* 2009;45:2695–700. <https://doi.org/10.1016/j.eurpolymj.2009.05.028>.
75. Shukla SR, Harad AM. Aminolysis of polyethylene terephthalate waste. *Polym Degrad Stabil.* 2006;91:1850–4. <https://doi.org/10.1016/j.polymdegradstab.2005.11.005>.
76. Hoang CN, Dang YH. Aminolysis of poly(ethylene terephthalate) waste with ethylenediamine and characterization of a,u-diamine products. *Polym Degrad Stabil.* 2013;98:697–708. <https://doi.org/10.1016/j.polymdegradstab.2012.12.026>.
77. Sharma P, Lochab B, Kumar D, Roy PK. Sustainable Bis-benzoxazines from cardanol and PET-derived terephthalamides. *ACS Sustain Chem Eng.* 2016;4:1085–93. <https://doi.org/10.1021/acssuschemeng.5b01153>.
78. Leng Z, Sreeram A, Padhan RK, Tan Z. Value-added application of waste PET based additives in bituminous mixtures containing high percentage of reclaimed asphalt pavement (RAP). *J Clean Prod.* 2018;196:615–25. <https://doi.org/10.1016/j.jclepro.2018.06.119>.
79. Nica S, Duldner M, Hangau A, Iancu S, Cursaru B, Sarbu A, Filip P, Bartha E. Functionalized 1,5,7-triazabicyclo [4.4.0] dec-5-ene (TBD) as novel organocatalyst for efficient depolymerization of polyethylene terephthalate (PET) wastes. *Rev Chim.* 2018;69:2613–6. <https://doi.org/10.37358/rc.18.10.6591>.
80. Tawfik ME, Ahmed NM, Eskander SB. Aminolysis of poly(ethylene terephthalate) wastes based on sunlight and utilization of the end product [bis(2-hydroxyethylene) terephthalamide] as an ingredient in the anticorrosive paints for the protection of steel structures. *J Appl Polym Sci.* 2011;120:2842–55. <https://doi.org/10.1002/app.33350>.
81. Shamsi R, Abdouss M, Sadeghi GMM, Taromi FA. Synthesis and characterization of novel polyurethanes based on aminolysis of poly(ethylene terephthalate) wastes, and evaluation of their thermal and mechanical properties. *Polym Int.* 2009;58:22–30. <https://doi.org/10.1002/pip.2488>.
82. Padhan RK, Gupta AA. Preparation and evaluation of waste PET derived polyurethane polymer modified bitumen through in situ polymerization reaction. *Constr Build Mater.* 2018;158:337–45. <https://doi.org/10.1016/j.conbuildmat.2017.09.147>.
83. Zhou L, Lu XM, Ju ZY, Liu B, Yao HY, Xu JL, Zhou Q, Hu YF, Zhang SJ. Alcoholysis of polyethylene terephthalate to produce diethyl terephthalate using choline chloride-based deep eutectic solvents as efficient catalysts. *Green Chem.* 2019;21:897–906. <https://doi.org/10.1039/c8gc03791d>.
84. Siddiqui MN, Redhwani HH, Achilias DS. Recycling of poly(ethylene terephthalate) waste through methanolic pyrolysis in a microwave reactor. *J Anal Appl Pyrolysis.* 2012;98:214–20. <https://doi.org/10.1016/j.jaap.2012.09.007>.
85. Yang Y, Lu YJ, Xiang HW, Xu YY, Li YW. Study on methanolytic depolymerization of PET with supercritical methanol for chemical recycling. *Polym Degrad Stabil.* 2002;75:185–91. [https://doi.org/10.1016/s0141-3910\(01\)00217-8](https://doi.org/10.1016/s0141-3910(01)00217-8).

86. Andanson JM, Kazarian SG. In situ ATR-FTIR spectroscopy of poly(ethylene terephthalate) subjected to high-temperature methanol. *Macromol Symp.* 2008;265:195–204. <https://doi.org/10.1002/masy.200850521>.
87. Kurokawa H, Ohshima M, Sugiyama K, Miura H. Methanolysis of polyethylene terephthalate (PET) in the presence of aluminium triisopropoxide catalyst to form dimethyl terephthalate and ethylene glycol. *Polym Degrad Stabil.* 2003;79:529–33. [https://doi.org/10.1016/s0141-3910\(02\)00370-1](https://doi.org/10.1016/s0141-3910(02)00370-1).
88. Liu QL, Li RS, Fang T. Investigating and modeling PET methanolysis under supercritical conditions by response surface methodology approach. *Chem Eng J.* 2015;270:535–41. <https://doi.org/10.1016/j.cej.2015.02.039>.
89. Goto M, Koyamoto H, Kodama A, Hirose T. Degradation kinetics of polyethylene terephthalate in supercritical methanol. *AICHE J.* 2002;48:136–44. <https://doi.org/10.1002/aic.690480114>.
90. Favaro SL, Freitas AR, Ganzerli TA, Pereira AGB, Cardozo AL, Baron O, Muniz EC, Girotto EM, Radovanovic E. PET and aluminum recycling from multilayer food packaging using supercritical ethanol. *J Supercrit Fluids.* 2013;75:138–43. <https://doi.org/10.1016/j.supflu.2012.12.015>.
91. Mansour SH, Ikladious NE. Depolymerization of poly(ethylene terephthalate) wastes using 1,4-butanediol and triethylene glycol. *Polym Test.* 2002;21:497–505. [https://doi.org/10.1016/s0142-9418\(01\)00115-5](https://doi.org/10.1016/s0142-9418(01)00115-5).
92. Arai R, Zenda K, Hatakeyama K, Yui K, Funazukuri T. Reaction kinetics of hydrothermal depolymerization of poly(ethylene naphthalate), poly(ethylene terephthalate), and polycarbonate with aqueous ammonia solution. *Chem Eng Sci.* 2010;65:36–41. <https://doi.org/10.1016/j.ces.2009.03.023>.
93. Bei K, Ma PX, Wang JL, Li K, Lyu JH, Hu ZC, Chou IM, Pan ZY. Depolymerization of poly(ethylene naphthalate) in fused silica capillary reactor and autoclave reactor from 240 to 280°C in subcritical water. *Polym Eng Sci.* 2017;57:1382–8. <https://doi.org/10.1002/pen.24523>.
94. Huang J, Yang JH, Chyu MK, Wang QM, Zhu ZB. Continuous-distribution kinetics for degradation of polybutylene terephthalate (PBT) in supercritical methanol. *Polym Degrad Stabil.* 2009;94:2142–8. <https://doi.org/10.1016/j.polymdegradstab.2009.09.011>.
95. Yoshioka T, Grause G, Otani S, Okuwaki A. Selective production of benzene and naphthalene from poly(butylene terephthalate) and poly(ethylene naphthalene-2,6-dicarboxylate) by pyrolysis in the presence of calcium hydroxide. *Polym Degrad Stabil.* 2006;91:1002–9. <https://doi.org/10.1016/j.polymdegradstab.2005.08.010>.
96. Yang JH, Huang J, Chyu MK, Wang QM, Xiong DL, Zhu ZB. Degradation of poly(butylene terephthalate) in different supercritical alcohol solvents. *J Appl Polym Sci.* 2010;116:2269–74. <https://doi.org/10.1002/app.31649>.
97. Maga D, Hiebel M, Thonemann N. Life cycle assessment of recycling options for polylactic acid. *Resour Conserv Recycl.* 2019;149:86–96. <https://doi.org/10.1016/j.resconrec.2019.05.018>.
98. Piemonte V, Sabatini S, Gironi F. Chemical recycling of PLA: a great opportunity towards the sustainable development? *J Polym Environ.* 2013;21:640–7. <https://doi.org/10.1007/s10924-013-0608-9>.
99. Alberti C, Damps N, Meissner RRR, Hofmann M, Rijono D, Enthaler S. Selective degradation of end-of-life poly(lactide) via alkali-metal-halide catalysis. *Adv Sustain Syst.* 2020;4:9. <https://doi.org/10.1002/adsu.201900081>.
100. Song XY, Wang H, Yang XQ, Liu FS, Yu ST, Liu SW. Hydrolysis of poly(lactic acid) into calcium lactate using ionic liquid [Bmin][OAc] for chemical recycling. *Polym Degrad Stabil.* 2014;110:65–70. <https://doi.org/10.1016/j.polymdegradstab.2014.08.020>.
101. Sanchez AC, Collinson SR. The selective recycling of mixed plastic waste of polylactic acid and polyethylene terephthalate by control of process conditions. *Eur Polym J.* 2011;47:1970–6. <https://doi.org/10.1016/j.eurpolymj.2011.07.013>.

102. Chauliac D, Pullammanappallil PC, Ingram LO, Shanmugam KT. A combined thermochemical and microbial process for recycling polylactic acid polymer to optically pure L-lactic acid for reuse. *J Polym Environ.* 2020;28:1503–12. <https://doi.org/10.1007/s10924-020-01710-1>.
103. Roman-Ramirez LA, McKeown P, Jones MD, Wood J. Poly(lactic acid) degradation into methyl lactate catalyzed by a well-defined Zn(II) complex. *ACS Catal.* 2019;9:409–16. <https://doi.org/10.1021/acscatal.8b04863>.
104. Román-Ramírez LA, McKeown P, Shah C, Abraham J, Jones MD, Wood J. Chemical degradation of end-of-life poly(lactic acid) into methyl lactate by a Zn(II) complex. *Ind Eng Chem Res.* 2020;59:11149–56. <https://doi.org/10.1021/acs.iecr.0c01122>.
105. Noda M, Okuyama H. Thermal catalytic depolymerization of poly(L-lactic acid) oligomer into LL-lactide : effects of Al, Ti, Zn and Zr compounds as catalysts. *Chem Pharm Bull.* 1999;47:467–71. <https://doi.org/10.1248/cpb.47.467>.
106. Fan YJ, Nishida H, Mori T, Shirai Y, Endo T. Thermal degradation of poly(L-lactide): effect of alkali earth metal oxides for selective L,L-lactide formation. *Polymer.* 2004;45:1197–205. <https://doi.org/10.1016/j.polymer.2003.12.058>.
107. Fan YJ, Nishida H, Shirai Y, Endo T. Control of racemization for feedstock recycling of PLLA. *Green Chem.* 2003;5:575–9. <https://doi.org/10.1039/b304792j>.
108. Alberti C, Damps N, Meissner RRR, Enthaler S. Depolymerization of end-of-life poly(lactide) via 4-dimethylaminopyridine-catalyzed methanolysis. *ChemistrySelect.* 2019;4:6845–8. <https://doi.org/10.1002/slct.201901316>.
109. Hofmann M, Alberti C, Scheliga F, Meißner RRR, Enthaler S. Tin(ii) 2-ethylhexanoate catalysed methanolysis of end-of-life poly(lactide). *Polym Chem.* 2020;11:2625–9. <https://doi.org/10.1039/DOPY00292E>.
110. Leibfarth FA, Moreno N, Hawker AP, Shand JD. Transforming polylactide into value-added materials. *J Polym Sci Polym Chem Ed.* 2012;50:4814–22. <https://doi.org/10.1002/pola.26303>.
111. Plichta A, Lisowska P, Kundys A, Zychewicz A, Debowski M, Florjanczyk Z. Chemical recycling of poly(lactic acid) via controlled degradation with protic (macro)molecules. *Polym Degrad Stabil.* 2014;108:288–96. <https://doi.org/10.1016/j.polymdegradstab.2014.03.006>.
112. Song XY, Wang H, Wang C, Liu FS, Yu ST, Liu SW, Song ZY. Chemical recycling of bio-based poly(3-hydroxybutyrate) wastes under methanolysis condition catalyzed by Fe-containing magnetic ionic liquid. *J Polym Environ.* 2019;27:862–70. <https://doi.org/10.1007/s10924-018-1347-8>.
113. Song XY, Liu FS, Wang H, Wang C, Yu ST, Liu SW. Methanolysis of microbial polyester poly(3-hydroxybutyrate) catalyzed by Bronsted-Lewis acidic ionic liquids as a new method towards sustainable development. *Polym Degrad Stabil.* 2018;147:215–21. <https://doi.org/10.1016/j.polymdegradstab.2017.12.009>.
114. Tsuji H, Yamamura Y, Ono T, Saeki T, Daimon H, Fujie K. Hydrolytic degradation and monomer recovery of poly(butylene succinate) and poly(butylene succinate adipate) in the melt. *Macromol React Eng.* 2008;2:522–8. <https://doi.org/10.1002/mren.200800027>.
115. Sin MC, Tan IKP, Annuar MSM, Gan SN. Characterization of oligomeric hydroxyalkanoic acids from thermal decomposition of palm kernel oil-based biopolyester. *Int J Polym Anal Charact.* 2011;16:337–47. <https://doi.org/10.1080/1023666x.2011.588306>.
116. Norrrahim MNF, Ariffin H, Hassan MA, Ibrahim NA, Nishida H. Performance evaluation and chemical recyclability of a polyethylene/poly(3-hydroxybutyrate-co-3-hydroxyvalerate) blend for sustainable packaging. *RSC Adv.* 2013;3:24378–88. <https://doi.org/10.1039/c3ra43632b>.
117. Rodriguez-Contreras A, Calafell-Monfort M, Marques-Calvo MS. Enzymatic degradation of poly(3-hydroxybutyrate-co-4-hydroxybutyrate) by commercial lipases. *Polym Degrad Stabil.* 2012;97:597–604. <https://doi.org/10.1016/j.polymdegradstab.2012.01.007>.

118. Jbilou F, Dole P, Degraeve P, Ladaviere C, Joly C. A green method for polybutylene succinate recycling: depolymerization catalyzed by lipase B from *Candida antarctica* during reactive extrusion. *Eur Polym J.* 2015;68:207–15. <https://doi.org/10.1016/j.eurpolymj.2015.04.039>.
119. Shah AA, Eguchi T, Mayumi D, Kato S, Shintani N, Kamini NR, Nakajima-Kambe T. Degradation of aliphatic and aliphatic-aromatic co-polyesters by depolymerases from Roseateles depolymerans strain TB-87 and analysis of degradation products by LC-MS. *Polym Degrad Stabil.* 2013;98:2722–9. <https://doi.org/10.1016/j.polymdegradstab.2013.10.003>.
120. Yagihara T, Matsumura S. Enzymatic synthesis and chemical recycling of novel polyester-type thermoplastic elastomers. *Polymers.* 2012;4:1259–77. <https://doi.org/10.3390/polym4021259>.
121. Yang X, Odelius K, Hakkainen M. Microwave-assisted reaction in green solvents recycles PHB to functional chemicals. *ACS Sustain Chem Eng.* 2014;2:2198–203. <https://doi.org/10.1021/sc500397h>.

Chapter 10

Producing Value-added Products from Organic Solid Wastes with Mechanochemical Processes



Haixin Guo, Xiao Zhang, and Feng Shen

Abstract Mechanochemical process is a versatile technique that is induced by mechanical forces such as shearing, friction, compression, stretching, and grinding. Recycling organic solid wastes (e.g. biomass) to value-added products from organic solid wastes *via* mechanochemical processes has received increasing interest due to its high efficiency, low cost and eco-friendly nature (solvent-less or solvent-free). In this chapter, a brief overview of the historical development of mechanochemistry, kinds of mechanochemistry equipment, the relationship between mechanochemistry and organic solid wastes (e.g. waste biomass) conversion into value-added products (chemicals, fuels, and carbon materials) will be introduced for the general reader. Emphasis is placed on typical mechanochemical processes for conversion of waste biomass to chemicals (glucose, xylose, furfural, 5-HMF, sorbitol, phenol, etc.) and functional carbon materials (adsorbents, catalysts, electrodes, etc.). The role and mechanism of mechanochemical technology on the waste biomass transformation into value-added products were also presented. Limitations and opportunities associated with the mechanochemical synthesis of valuable products from organic solid wastes (biomass) are highlighted.

Keywords Ball milling · Waste management · Biochar · Lignocellulose · Biorefinery

H. Guo

Graduate School of Environmental Studies, Tohoku University, Sendai, Japan

X. Zhang

School of Energy and Environmental Engineering, Hebei University of Technology, Tianjin, China

F. Shen (✉)

Agro-Environmental Protection Institute, Ministry of Agricultural and Rural Affairs, Tianjin, China

e-mail: shenfeng@caas.cn

10.1 Introduction

Mechanochemistry process technology refers to chemical reactions induced by the application of mechanical energy. Shear and compressive forces are developed through grinding and impacts [1]. The mechanochemical reaction process provides a new way to reduce or avoid the use of solvents. In solvent-free or solvent-less conditions, new synthetic is realized, improving the product selectivity, yield or reaction rate. Mechanochemistry, especially when implemented in a continuous process, has been identified by the International Union of Pure and Applied Chemistry (IUPAC) [2] as one of the ten world-changing technologies.

In 2000, Boldyrev, V. V and co-workers reported one of the earliest applications of mechanochemistry in the book “On Stones” in 315 B.C, which discussed the grinding of cinnabar and acetic acid with a mortar and pestle could produce elemental mercury (Hg) [3]. Since then, mechanochemical reactions were almost ignored by twentieth century scientists until the last few decades. In 1820, Faraday et al. [4] discovered that silver chloride could be reduced to its elemental form by a solvent-free grinding method. Then, M. Carey Lea (1823–1897) performed systematic investigations on the mechanochemical reaction and thus he is known as “the father of mechanochemistry.” During the past two decades, mechanochemistry has been rapidly established as a green and environmentally friendly synthetic method.

Investigations using a mortar and pestle were the first to implement mechanochemical reactions since they are cheap and convenient tools [5]. However, manual grinding is susceptible to variable factors that are difficult to control, such as operator variability and laboratory environments. These factors frequently render results obtained by mortar and pestle unrepeatable. Today, machine-driven ball milling has become one of the most important tools for mechanochemical reactions. As shown in Fig. 10.1, laboratories typically implement two different kinds of ball milling equipment that represent different applications of mechanical force. These are the shaker (or mixer) mill and planetary mill. In shaker mills, the reaction jars are rapidly oscillated from side to side, or in complex paths which results in the enclosed ball bearings applying shear and compressive force to realize grinding [6]. While in the planetary mills (Fig. 10.1), the reaction vessels are spun at high speed,

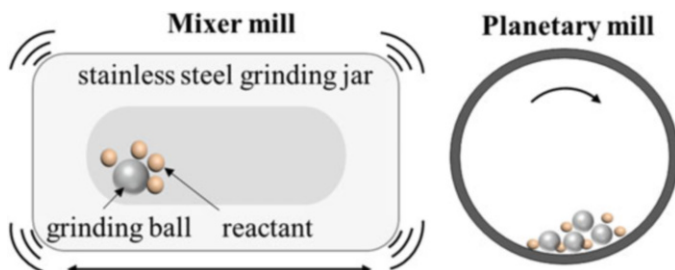


Fig. 10.1 Typical automatic ball milling equipment used for mechanochemical reactions

counter-rotatory to the main spinning “sun wheel” (thus, the term planetary) results in the balls grinding the solids within the jars.

Recently, mechanochemical reaction technology has been applied in various fields such as materials synthesis, industrial chemistry, extractive metallurgy, minerals engineering, and bioengineering [7]. Mechanochemical processing offers a lot of advantages such as ecological safety and process simplicity when compared to solution-based wet processing. Practically, the mechanochemical treatment processes not only avoid the complex post-treatment steps (e.g. reuse of solvent and separation of product) but also the use of large amounts of solvents. Importantly, most mechanochemical reaction systems are completed within minutes to hours. Another advantage of mechanochemistry is enabling applications under mild conditions (e.g. at ambient temperature). These factors make mechanochemical approaches an attractive solution for biomass waste management. Considering environmental and economic factors, mechanochemistry offers a time-saving, eco-friendly and labor-saving process for the conversion of waste biomass into sustainable platform chemicals, fuels, and functional carbon materials.

10.2 Chemicals from Waste Biomass

10.2.1 Reducing Sugars

The efficient hydrolysis of carbohydrates (e.g. cellulose and hemicellulose) of the biomass into reducing sugars (RS) is essential for the organic solid wastes transformation process. It is due to the RS (C5 sugars and C6 sugars) can be further transformed into value-added products (e.g. biofuels and chemicals) [8, 9]. However, the hydrolysis of biomass offers great challenges because raw biomass has a recalcitrant structure that protects its carbohydrate from degradation/attack by the enzymes [10]. Therefore, pretreatment is an essential step for waste biomass hydrolysis into reducing sugars, which can reduce the crystallinity of the cellulose and particle size of the biomass thus increasing the cellulose accessibility.

Pretreatment methods (e.g. chemical pretreatments including acid, alkaline and organic solvents, steam explosion, biological, and hydrothermal methods) have been used to promote the biomass hydrolysis into reducing sugars, however, these methods are usually limited by their corrosivity, recyclability of solvents, and waste generated. Most pretreatment methods of biomass limits the production of undesirable dehydration products (such as levoglucosan, levoglucosenone and 5-hydroxymethylfurfural) and improves susceptibility towards further hydrolysis through enzymatic processes [11]. Practically, chemical pretreatment methods limit further enzymatic hydrolysis [12]. So, it is necessary to develop environmentally friendly pretreatments methods that avoid strong acid and alkalis. Various equipment has been developed to implement mechanochemical processes such as automated mortar grinders, shaker mills, screw extruders and drum mixers [13].

Table 10.1 Effect of mechanical pretreatment on total reducing sugar (TRS) yields by biomass hydrolysis

Substrate	Milling time	TRS yields (%)	Ref.
	h	Without pretreatment	With pretreatment
Bagasse	2	<150 mg/g	531.6 mg/g [25]
Jatropha hulls	24	29.5	35.4 [26]
Plukenetia hulls	24	34.0	40.8 [26]
Rice straw	1	23.4	89.4 [19]
Cellulose	6	20.9	84.5 [27]
Oil palm	2	11.4	71.9 [28]

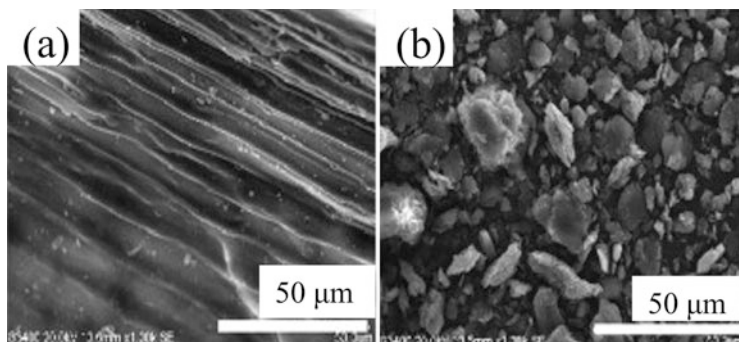


Fig. 10.2 Scanning electron micrographs of pretreated rice straws. (a) rice straw cutter milled to less than 2 mm and (b) rice straw ball milled for 60 min. (Reprinted with permission from [19]. Copyright © 2009, Elsevier)

Mechanical pretreatment processes enabled by the ball milling of raw biomass have appeared as an environmentally friendly, efficient, and economically feasible alternative the traditional pretreatment process. This approach was pioneered by Blair (dry) [14] and Schüth (wet) [15] for the realization of C5 and C6 sugars from cellulose and biomass. Larger scale experiments showed improved energy consumption [16–18]. Table 10.1 given the effect of mechanical pretreatment on the yields of total reducing sugar by hydrolysis of various raw biomass. Compared with direct hydrolysis of biomass, the TRS yields increasing 1.1–14.8% after ball pretreatment of biomass (Table 10.1). Gu et al. [12] reported that after pre-milled Douglas-fir forest residuals, the crystallinity of cellulose was reduced from 40% to 11%. The particle size of samples on D 90% decreased from 416 μm to 41 μm and on D 10% decreased from 20 μm to 3 μm after ball milled. Scanning electron microscopy (SEM) images result show that the particle size of rice straw after 60 min dry ball-milling pretreatment decreases from 500 μm to 2 mm to less than 30 μm (Fig. 10.2), and the surface changed from smooth to rough which lead to an increase in the overall surface area [19]. Wide-Angle X-ray Diffraction (WAXD) and ATR-FTIR analysis showed that both the mean size of the crystalline domains and crystallinity

index were decreased after 2–60 min of treatment with ball milling [20]. The average length of the fibers decreased to 12 µm from 200 µm after 60 min of ball milling. Proton NMR and ^{13}C NMR spectra were used to investigate the functional structure of the biomass during the ball milling process [21, 22]. It was shown that ball milling broke chains in cellulose (or hemicellulose), resulting in a disruption of the biomass structure and conversion into oligosaccharides or monosaccharides [22, 23]. Moreover, Zhang et al. [17] reported that the rolling mode (shear > compressive) promotes cellulose conversion into glucose, while the shaking mode (compressive > shear) promotes the levoglucosan formation. Wu et al. [24] reported that glucose yield from enzymatic hydrolysis of biomass greatly increased from 38.7% to 66.5% after the introduction of intermittent ball milling by enhancing the adsorption of enzymes into cellulose.

In conclusion, mechanical pretreatment (milling/grinding) is an efficient way to promote biomass hydrolysis into total RS. Mechanical pretreatment offers advantages through changes in the structure of biomass including the amorphization of biomass crystalline structures, breaking hydrogen bonding, decreasing the degree of polymerization (DP) of biomass and increasing the accessible surface area. Due to avoid strong acid and alkalis, the mechanical pretreatment (e.g. ball milling) as an environmentally friendly is also beneficial for enzymatic hydrolysis of biomass to reducing sugars.

10.2.2 Furfural and 5-HMF

Furfural and 5-hydroxymethylfurfural (5-HMF), which are obtained from the acid dehydration of C5/C6 sugars, are regarded as important biomass-derived platform compounds of the biorefinery [29–31], moreover furfural and 5-HMF offers a rich source of derivatives that are potential biofuel components such as ethyl levulinate (EL) [32], methyl tetrahydrofuran (MTHF) [29], 5-ethoxymethylfurfural (5-EMF) [32], 2,5-dimethylfuran (DMF) [33]. Extensive research has been carried out on direct preparation of furfural and 5-HMF from fructose and xylose with a homogeneous and heterogeneous acid catalyst such as modified biochar, zeolite, and AlCl_3 [30, 34, 35]. However, it is still a challenge to efficiently producing furfural and 5-HMF direct from raw biomass (e.g. long reaction times and harsh reaction conditions) so that the large-scale production of platform chemicals (furfural and 5-HMF) is still not feasible at reasonable prices. As shown in the above section, mechanical pretreatment (e.g. ball milling treatment) is beneficial for the hydrolysis of biomass into total RS (glucose, fructose and xylose), in this section the catalyst-assisted mechanochemical (or mechanocatalytic) process for the preparation of platform chemicals (furfural and 5-HMF) from raw-biomass (e.g. Cellulose, Bamboo powder) is discussed.

As shown in Table 10.2, compared with synthesis platform chemicals (5-HMF and furfural) single catalyst reaction, the objective product (5-HMF and furfural) yields increased via catalyst-assisted mechanochemistry reaction. As Fig. 10.3

Table 10.2 Conversion of C5/C6 sugars into furfural and 5-hydroxymethylfurfural *via* catalyst-assisted mechanochemical method (BM: ball-milling)

Substrate	Catalyst	Product	Without BM (%)	With BM (%)	Ref.
Cellulose	$\text{Al}_2(\text{SO}_4)_3$	5-HMF	39.8	44.6	[36]
α -cellulose	AlCl_3	5-HMF	—	79	[37]
<i>C. japonica</i>	[Py]Cl	5-HMF	<3 wt. %	6.9 wt.%	[39]
Pine sawdust	AlCl_3	Furfural	<82	85	[40]
Bamboo powder	Zeolite	Furfural	55	~65	[41]

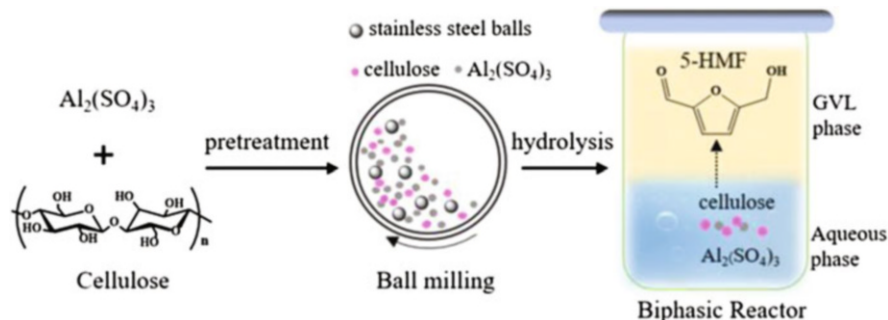


Fig. 10.3 $\text{Al}_2(\text{SO}_4)_3$ -assisted mechanochemical synthesis of 5-HMF from cellulose (Reprinted with permission from [36]. Copyright ©2020, Springer)

shows, Shen et al. [36] using ball-milling with $\text{Al}_2(\text{SO}_4)_3$ -assisted pretreatment in preparation of 5-HMF from cellulose, in which $\text{Al}_2(\text{SO}_4)_3$ not only acts as a catalyst but also promotes cellulose comminution during the milling pretreatment step. Mechanochemical pretreatment also reduces reaction time, with ball milling, a 79% yield of 5-HMF and 80% yield of furfural were obtained after 9 min at 170 °C from glucan and xylan, respectively [37, 38]. This is due to soluble molecules obtained in the catalyst-assisted mechanochemical biomass pretreatment step. It is demonstrated that the catalyst-assisted mechanochemical method is an efficient technology in biomass transformation into furfural and 5-HMF, in which the objective product yield increase and short reaction time are possible compared to the traditional solution-based catalytic method.

10.2.3 Sorbitol

Sorbitol is notable among biomass-related materials, as it can be used for the production of pharmaceutical intermediates, monomers of polymers or fuels [42]. Sorbitol can be synthesized from cellulose *via* acidic hydrolysis into sugars and their further hydrogenation in the presence of hydrogen donor sources [43, 44]. Although some processes have succeeded in the conversion of cellulose

Table 10.3 Catalytic results for single ball-milling of biomass and mixed ball-milling

Catalyst	Conv. (%)	Sorbitol (%)	Ref.
Ru/AC	86	17	[50]
(Ru/AC) _{mix}	100	46	[50]
Ru/AC	88	42	[48]
(Ru/AC) _{mix}	89	69	[51]
Ru-Ni/AC	54.1	31.7	[51]
(Ru-Ni/AC) _{mix}	86.1	74.3	[51]
Ru-Ni/CNT	74.5	41.4	[51]
(Ru-Ni/CNT) _{mix}	99.3	70.8	[51]

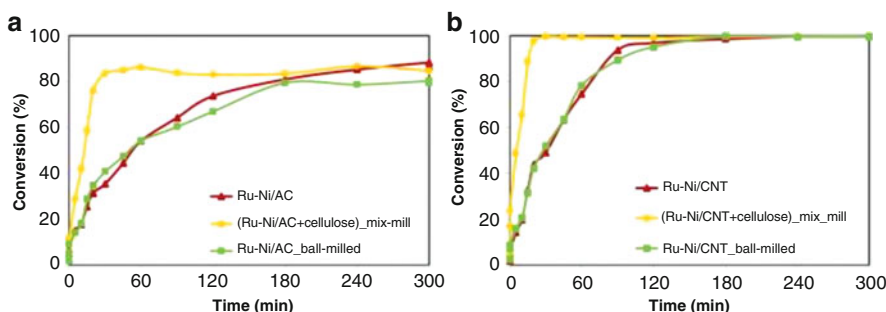


Fig. 10.4 Conversion of cellulose via a mixed feedstock/catalyst milling process. (a) Ru-Ni/AC ball-milled together with cellulose and (b) Ru-Ni/CNT ball-milled together with cellulose. (Reaction conditions: cellulose 0.75 g, catalyst 0.3 g, water 300 mL, at 205 °C under 5 MPa H₂ (Reprinted with permission from [51]. Copyright © 2017, Springer)

into sorbitol with various metal catalysts such as Ru-containing composites [45, 46], there are still many challenges, such as the limit sorbitol selectivity and harsh reaction conditions.

In the previous section, mechanical pretreatment of biomass and acid catalyst-assisted mechanochemical ball milling pretreatment of biomass promoted biomass hydrolysis and dehydration. Results show that the selectivity of sorbitol and cellulose conversion can be increased after pretreatment by single ball milling [47] or catalyst ball-milling together with biomass (Table 10.3) [48–50]. Geboers et al. [47] reported a 27% yield of sorbitol with a 65% yield of sugar alcohol from ball milled cellulose. Ribeiro et al. [48, 51] reported that after milling cellulose with catalyst, the activity of catalyst and selectivity of sorbitol can be greatly increased. A 69% yield of sorbitol was realized by shaker milling a Ru/AC catalyst with cellulose without any acidic catalyst [51]. With cellulose ball-milled together with Ru-Ni/CNT catalyst, a yield of sorbitol of 70.8% was achieved from cellulose after just 1 h reaction time (Table 10.3). Based above section, the selectivity to sorbitol can be related to the improved physical contact between the catalyst and the solid substrate after ball-milling treatment. For both Ru-Ni/AC and Ru-Ni/CNT, the conversions of cellulose achieved with mixed-ball-milling were higher than that without ball-milling pretreatment or single ball milling pretreatment (Fig. 10.4). The concurrent milling of catalyst and

cellulose gives a significant increase in the initial reaction rate (Fig. 10.4) that is due to mix-milling that can facilitate good solid-solid contact between substrate and active sites that become accessible to cellulose and promote the cellulose hydrolysis [50, 52]. In summary, the selectively and yield of sorbitol from hydrogenation of biomass can be increased if the reaction substrate is ball-milled together with catalyst.

10.2.4 Phenol

Phenol is a key feedstock in the chemical industry. It is mainly used for synthetic pharmaceuticals, herbicides, polymer precursors, resins, and plasticizers such as bisphenol-A [53–55]. Traditionally phenol is synthesized from petrochemical sources. However, there growing concerns about the environmental impact of petrochemical technologies and the declining reserves of such sources. Lignin has attracted much attention for supplanting petrochemicals for chemical precursors, due to it being a rich source of aromatics [56, 57]. Lignin (15–20%) along with cellulose (40–50%) and hemicellulose (25–35%) are the main basic structural components of lignocellulosic materials [58]. The procedure for the synthesis of lignin into phenol involves the separation of lignin from lignocellulosic materials and catalytic lignin depolymerization, dehydrogenation/oxidation into phenol [53, 59].

In the conversion of lignin into phenol, the most important step is mechanical milling (e.g. ball-milling and ultrafine grinding) of raw biomass (e.g. wood, corn stover, wheat straw) to disrupt the lignocellulosic cell wall polymers and promote the separation of lignin with cellulose/hemicellulose (Fig. 10.5) [22, 60–62]. The lignin in biomass is likely a branched polymer and cross-linked (Fig. 10.5) [63]. Some works have reported a schematic for heterogeneity of ball-milled treatment in lignin separation [64, 65]. In general, ball-milled pretreatment can reduce native cell wall

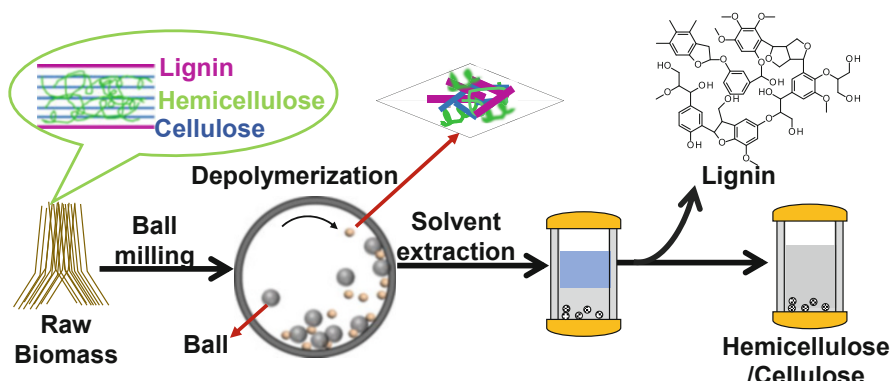


Fig. 10.5 Separation of lignin with cellulose and hemicellulose with ball-milling pretreatment

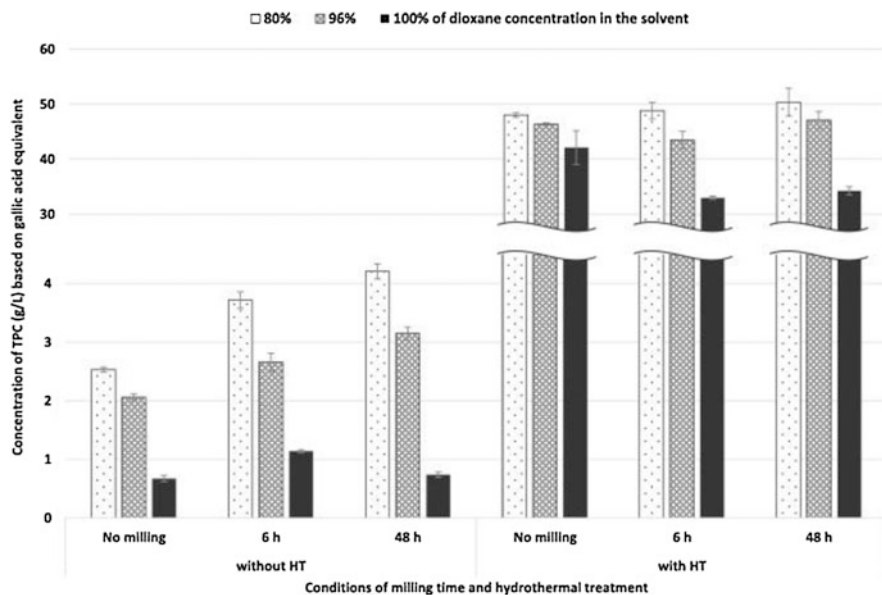


Fig. 10.6 Concentration of total phenolic compounds (TPC) (g/L) of hydrothermal conversion of lignin after ball-milling pretreatment (Reprinted with permission from [62]. Copyright © 2020, Springer)

recalcitrance, modify the supramolecular structure of the lignin-cellulose-hemicellulose matrix and depolymerization the cell wall of waste biomass (Fig. 10.5), which results in increasing the lignin separation.

The limited phenol yield from lignin is also due to the complex structure, heterogeneity and variety of lignin [66]. Mechanochemical processes (e.g. ball-milling) were also used in the second step to promote lignin depolymerization into lower molecular weight liquid products and further catalytic cracking into phenols [62, 67–70]. Chemical catalysis with mechanochemical treatment of biomass (e.g. ball milling treatment methods) has become a promising technology for lignin conversion into phenol. Bolm et al. [69] develop mechanochemical base-catalyzed degradation of lignin to the phenol derivatives under mild conditions. This was followed by Dabral *et al.* [71] who obtained excellent yields of phenol derivatives from lignin through mechanochemical-oxidation of lignin with HO-TEMPO/KBr in presence of ozone. Jang et al. [62] showed that that in the extraction of lignin, the total extracted phenolic compounds (TPC) concentration after ball milling pretreatment increased (Fig. 10.6). Moreover, Nair et al. [67] developed a combined mechanochemical and photocatalytic (titania consisting of anatase and rutile) oxidation process that transformed lignin into phenol. High yields of phenolic compounds from ball-milled lignin were obtained after 3–4 h of UV exposure and phenolic compounds formed even when milled without light. Compared to photocatalysis-assisted dry milling, catalysis of wet-milled mixtures with water or organic solvents (hexane) resulted in high yields of phenolics. Powder X-ray

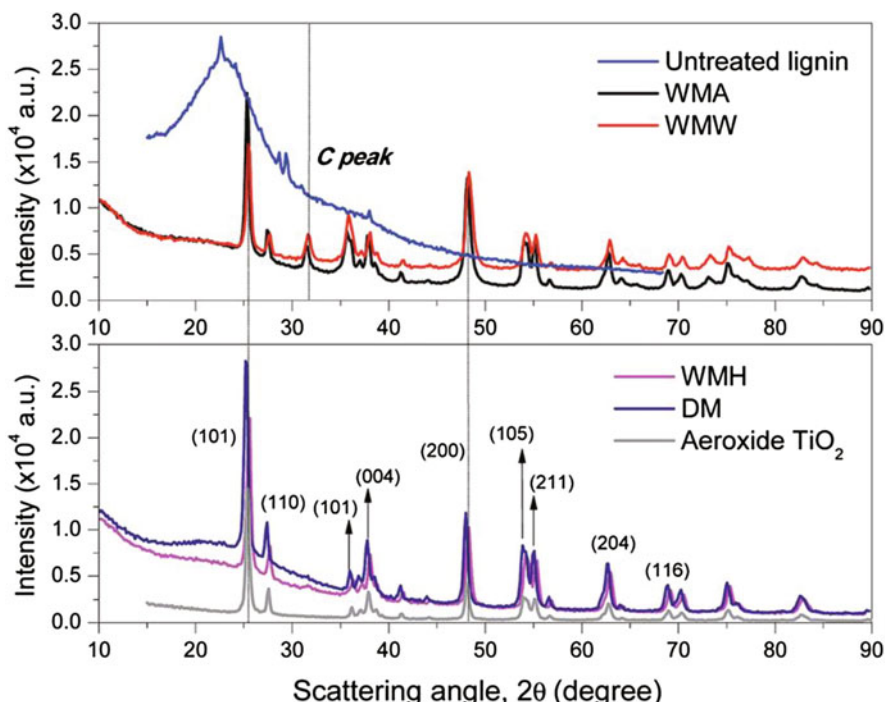


Fig. 10.7 Diffractograms of titania, lignin, and other milled samples under wet condition (Reprinted with permission from [67]. Copyright © 2016, Royal Society of Chemistry)

diffraction of pristine lignin milled with titania produced a new diffraction peak at 31.7° which was only realized after wet milling of lignin with acetone and water. This was attributed to the interaction between lignin and catalyst (Fig. 10.7).

Mechanochemical processes are highly effective that can be used in various waste biomass transformation steps, such as hydrolysis to reducing sugars, dehydration of reducing sugars to 5-HMF and furfural, hydrogenation for the realization of sorbitol, and lignin depolymerization, dehydrogenation-oxidation into phenol. Application of mechanochemical pretreatments (e.g. ball milling) can efficiently disrupt the crystalline structure of biomass, reduce particle sizes (communition), break complex molecular and macromolecular networks. Many works have developed catalysis-assisted mixed mechanochemical processes to reduce the reaction time and improve product yields. This is due to the mechanochemical pretreatment not only produces comminution but also facilitates catalytic processes during the pretreatment step.

10.3 Functional Materials from Waste Biomass

Using waste biomass as a carbon source has emerged as an efficient way to synthesis high-value functional carbon materials. Mechanical ball milling technology has been widely used for the valorization of waste biomass to carbon-based materials such as adsorbents, catalysts, electrodes, flame retardants, and soil remediation agents.

10.3.1 Adsorbents

Carbon materials synthesized from waste biomass are potential substitutes for binder/filter media in adsorption areas. Generally, the adsorption capacity was observed to increase with higher surface areas, rich electrostatic interactions, and abundant functional groups. Mechanical treatment is an efficient way to improve the total surface area of functional carbon materials [72]. The physical- and chemical-properties of carbon material induced by ball milling are controlled by preparation temperatures of pristine biochar, pretreatment times, substrate-ball mass ratios (BPR), and milling media. After a ball milling pretreatment, the specific surface area can be greatly increased to $\sim 350\text{ m}^2/\text{g}$ from 2 to $10\text{ m}^2/\text{g}$ [72]. With treatment by ball milling, high surface area carbon materials were obtained through particle size reduction of porous biochar [73]. Additionally, the ball mill pretreatment of biochar influences the oxygen-containing functional groups resulting in improved diffusion properties, the introduction of ionic defects, and the formation of graphitic structures [74].

Biochar or biochar-based composites materials synthesized *via* ball milling are efficient for the removal of inorganic and heavy metal pollutants (Ni, Hg, Cr, As and Cd) from wastewater [75]. For instance, the adsorption capacities of ball-milled bone biochar for Cd(II), Cu(II) and Pb(II) were 165.8 mg/g, 287.6 mg/g and 558.9 mg/g, respectively (25°C , pH 5.0), which was much higher than that the un-milled biochar (75.2 mg/g, 163.8 mg/g and 389.5 mg/g, respectively) [76]. The mechanism investigated showed that the enhancement of the adsorption capacity of the biochar is due to the increased total surface area and oxygen-containing groups on the carbon frame after ball-milling treatment.

Carbon materials from waste biomass *via* ball-milling were reported to be effective in the adsorption and removal of antibiotics [77, 78]. For instance, negligible sulfonamide antibiotics were removed by biochars synthesized directly from raw bamboo, bagasse, and hickory chips. However, ball milling biochars prepared from the above waste biomass all showed high removal efficiencies of sulfamethoxazole from 33.4% to 83.3% and sulfapyridine from 39.8% to 89.6% [79]. The introduction of oxygen and nitrogen-containing groups into the biochar *via* ball milling resulted in improved adsorption capacities for antibiotics [80] which can be attributed to the interaction of the biochar functional groups with the adsorbate

through the formation of hydrophobic interaction, π - π interaction, and electrostatic interaction.

Ball milled carbon materials also show good adsorption performance for gaseous molecules due to internal pore structures developed during processing. The surface area of hickory wood biochar increasing to 285 m²/g from ~10 m²/g after ball milling. The adsorbent had a high capacity for different VOCs (toluene, cyclohexane, chloroform, ethanol, and acetone) [81]. In addition to an improvement in the total surface area, the increased polarity of carbon materials induced by ball milling pretreatment also benefits adsorption of VOCs.

Hierarchical porous carbon adsorbents, with application in Hg⁰ removal, can be fabricated mechanochemically using waste biomass rice straw. Large numbers of oxygen-containing functional groups were generated simultaneously after removal of a hard CaCO₃ template. The ball milled carbon adsorbent showed higher removal efficiency for Hg⁰ from flue gas than that of conventional biochar (65% vs. 40) due to its hierarchical porous structures and oxygen-containing functional groups [82].

Ball milling is also a feasible method for the modification of biochar. Lyu et al. [83] obtained thiol-modified biochar from poplar wood biochar with 3-mercaptopropyltrimethoxysilane *via* the ball-milling treatment process. The thiol-modified biochar that has -SH groups, larger surface area and more negatively charged surface. It was demonstrated to be efficient for removal of CH₃Hg⁺ and Hg²⁺ (CH₃Hg⁺:104.9 mg/g and Hg²⁺: 320.1 mg/g), which is much higher than the pristine biochar (CH₃Hg⁺:8.21 mg/g and Hg²⁺: 105.7 mg/g).[83].

10.3.2 Catalysts

Waste biomass-derived biochars/biochar-metal composites with catalytically-active groups introduced *via* mechanochemical processing have been used for photocatalysis [77], thermocatalysis [84], and electrocatalysis [85].

In a photocatalytic reaction system, the electrons of carbon defects in waste biomass derived-biochars were excited and shifted to oxygen-containing groups thus leading to the formation of ·O₂⁻ and H⁺. It was demonstrated that the milling process generally produced in more oxygen-containing functional groups as well as more reactive oxygen species on the carbon materials. Xiao et al. [86] reported that the concentrations of oxygen-containing groups including carboxyl, lactic, and phenolic hydroxyls of unmilled biochar were 0.1–0.3, 0–1.1, and 0.1–0.7 mmol/g, respectively. The concentrations of the above oxygen-containing groups increased to 0.2–0.5, 0.4–1.2, and 0.2–1.1 mmol/g, respectively after ball milling. The O/C ratio of biochar from poplar at 300 °C increased from 28.4% to 35.0% after ball milling. Photocatalysis experiments showed that the ball milled biochar exhibited a much higher enrofloxacin degradation rate (80.2%) compared with unmilled biochar (13.9%). Additionally, the mineralization ability improved from 0% to 66.4% after ball milling [86].

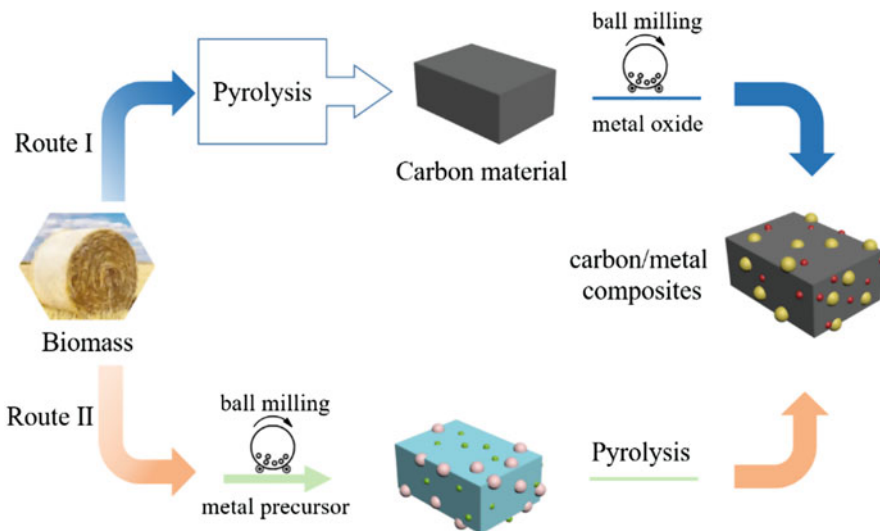


Fig. 10.8 Metal/biochar composites can be realized through the milling of catalysts with biochar or milling of precursors followed by pyrolysis (Reprinted with permission from [5]. Copyright © 2020, Springer)

When being used as thermal catalysis, waste biomass could be mechanochemically converted into biochar with more surface defects and rich catalytic sites such as heteroatoms (B, O, S). Due to the high stability of carbon materials under reaction conditions, catalytically active waste biomass-derived biochars could be employed as heterogeneous catalysts for different catalytic reactions. For example, surface-oxidized coke powder could be used as catalyst in the hydrolysis of cellulose [52, 87]. In conventional approaches, oxidation of biochar involves large amounts of liquid waste and requires high temperatures. Fukuoka et al. [88] reported a solvent-free ball milling strategy to fabricate -COOH rich biochars, in which the oxidant of persulfate salts (e.g. KHSO_5 and $(\text{NH}_4)_2\text{S}_2\text{O}_8$) was mixed with biochars by ball milling. By this way, highly carboxylated porous carbon materials were produced without the use of solvent. In this strategy, ball milling enhanced the contact between the biochar support and the persulfate salts and the mechanical processing gradually introduced surface defects in the carbons. The modified biochar obtained possessed a high-density of -COOH groups and showed good activity for the acid hydrolysis of cellulose into glucose with yields of 85% [68].

Metal/biochar composite catalysts can be directly synthesized *via* a physical solvent-free ball milling process. There are two ways to prepare metal/biochar composite as shown in Fig. 10.8. The first way is to prepare biochar and then ball mill the biochar with metal oxide. In another way, the waste biomass can be mixed with metal precursors by first milling a mixture of metal catalyst with waste biomass followed by pyrolysis to realize carbon/metal oxide composites.

In this way, the milling process can ensure complete dispersal of metal/metal oxides into waste biomass-derived biochars and facilitate carbon precursor particle refinement. He et al. [89] prepared an iron sulfide and biochar (FeS@BC) composite through ball milling and applied it to the oxidative degradation of tetracycline. The FeS@BC showed excellent performance which could be attributed to the fact that the milling process reduced the agglomeration of FeS, and increased the total surface area of the biochar.

Mechanochemically synthesized carbonaceous materials from waste biomass have also shown great potential in the electrocatalytic reactions. Lyu et al. [85] used ball-milled biochar as glassy carbon electrodes. These electrodes showed high electrocatalytic activity towards reduction of $\text{Fe}(\text{CN})_6^{3-}$. The electrochemical properties including electrical conductivity, peak-to-peak separation, series resistance, and charge transfer resistance were all improved after the milling pretreatment. Such properties play an important role in promoting electron transfer kinetics and reducing the interface resistance of carbon support materials [86].

10.3.3 *Electrodes*

Porous conductive carbons from waste biomass with a high surface area are desired materials for electrodes especially for electrical double-layer (EDL). The electrochemical performance is greatly affected by surface area since micropores provide abundant adsorbing sites for the electrolyte ions and mesopores promote diffusion of electrolyte ions [90]. Ball milling can greatly increase the surface area, pore-volume, oxygen-containing functional groups, hydrophilicity, crystallinity, and graphitization of waste biomass-derived carbons [74, 85]. This special structure facilitates electron transfer and reduces interface resistance of carbon materials as electrodes. To further improve the electrochemical performance of carbon electrodes, it is essential to increase the total microporous surface area of carbon materials. Mechanical ball milling could provide a powerful force for mixing waste biomass with other solid reagents. It can then be integrated into the chemical activation process to produce porous carbon materials from waste biomass and applied as electrodes for energy storage and electrochemical applications.

Traditional methods to prepare porous carbon materials are chemical activation *via* impregnation of waste biomass with KOH or KHCO_3 solutions and then pyrolysis at high temperatures [91, 92]. Mechanical ball milling provides an alternative solvent-free way to fabricate porous carbon materials. Zhai et al. [93] mixed the waste biomass of vinasse with the activating agent KOH *via* ball milling under solvent-free conditions. The ball milling process enhances homogenous contact between carbon precursor and KOH and improves pore production. Additionally, the ball milling process improves surface wettability of carbon materials since more surface defects are formed. In this way, porous carbons with surface area up to 3047 m^2/g have been obtained and have excellent characteristics for supercapacitor electrodes.

To further improve the electrochemical performance of carbon-based electrodes, heteroatom (N, S, B) doped porous carbon could be obtained from waste biomass *via* a one-pot ball milling method [94]. In this facile approach, waste biomass is employed as a carbon precursor, urea or melamine are used as heteroatom precursor, and K_2CO_3 (or $KHCO_3$) is used as the activator [95]. After ball milling and high temperature pyrolysis, high-surface porous carbons (up to $3000\text{ m}^2/\text{g}$) with a high concentration of covalently modified heteroatoms are formed. In this way, the specific capacitances of the carbon materials can reach 302.7 F/g at a current density of 0.5 A/g in 6 M KOH .

10.3.4 Flame Retardants

Flame-retardants are a class of compounds that are added to combustible materials to prevent fires or slow the ignition of fire. Phosphorylation is one of the most important ways to fabricate flame-retardant carbon materials. Traditionally, phosphorylated carbons are obtained *via* the direct treatment of waste biomass with concentrated liquid phosphoric acid which is corrosive and difficult to recycle [96]. Fiss et al. [97] describe a facile, green, solvent-free and previously unreported way for direct phosphorylation of cellulose and lignin *via* ball milling method with solid phosphorus pentoxide (P_2O_5). Based on ^{31}P MAS NMR and TGA analysis, it was shown that phosphorus groups could be grafted onto the carbon support *via* mechanochemical treatment, and the obtained cellulose nanocrystals have high thermally stability.

10.3.5 Soil Remediation Agent

Because of the high content of carbon, large specific surface area and unique surface properties (i.e., more functional groups), carbon materials prepared from waste biomass *via* the mechanical milling process have been applied in the soil remediation. The biochar-soil composites prepared by sing-step dry ball milling wheat straw could be used for the retention of organic pollutants. Yan et al. [98] reported that the complexation of biochar with soil minerals was enhanced after ball milling of biochar due to its rich oxygen-containing functional groups. In this way, the sorption capacity and uptake rate of biochar-soil composites for phthalate esters in soil was greatly improved.

10.4 Conclusions and Future Outlook

Waste biomass as renewable and sustainable sources have a strong potential for supplanting traditional fossil sources in the production of platform chemicals, fuels and high-value carbon materials. However, it is still a challenging task due to the complex characteristics and robust structure of the waste biomass. This chapter has provided an overview of mechanochemical technology that can be developed into a green and efficient process for transformation of waste solid biomass. The mechanochemical treatment (*e.g.* ball milling) is an important step in conversion of waste biomass into chemicals and functional carbon materials, since it can disrupt the recalcitrant structure of biomass, break hydrogen bonding in biomass, decreasing the polymerization degree of biomass and facilitate the good solid-solid contact between catalyst and biomass substrate.

Generally, high yields of chemicals (*e.g.* reducing sugars, 5-HMF, furfural, sorbitol, phenol) can be obtained from waste biomass *via* mechanochemical pretreatment (*e.g.* ball milling) and selective hydrolysis, dehydration, hydrogenation or oxidation reactions. It is found that mechanochemical assisted conditions such as the type of ball milling method (single ball milling or mixed ball milling method), milling mode, milling time, ball material, ball size and other parameters, can greatly affect the yield of products. Practically, homogeneous catalyst ball-milled together with biomass prior to use in biomass transformation reactions, where the mechanical process promotes good physical contact between the catalyst and biomass, increases solid-solid mass transfer and increases chemical productivity.

Mechanochemistry provides a new way to design and fabricate functional carbon materials from waste biomass. Compared with conventional wet processing, the mechanochemical approach is solvent-lite or solvent-free, requires short reaction times, and can be performed at ambient temperatures. Highly porous carbon materials with surface area up to 3047 m²/g have been obtained by mechanochemically-assisted (ball-milling treatment) from waste biomass. The mechanochemical processing can promote the introduction of active sites such as oxygen-rich groups, metal oxides and heteroatoms into the carbon materials. The obtained functional carbon materials have a range of applications such as adsorbents, catalysts, electrodes and soil amendments.

Despite the outstanding contribution of mechanochemistry in waste biomass valorization, high consumption of energy limits its large-scale industrialization. Combining mechanical ball milling with other methods such as enzyme and cryoprocessing is a potential way to reduce energy input. Energy savings are also realized when processes are scaled beyond the laboratory. Unfortunately, such large-scale studies may be resource prohibitive. In addition, the impact of the mechanochemical process on the conversion of solid waste biomass at the molecular level is not yet fully understood and further investigations are needed to quantify and model frictional effects on reactive materials. As research in this field expands, many of these hurdles will be overcome and mechanochemical processing will become a mainstay in chemical plant design for sustainable society.

References

1. Bertran J. Mechanochemistry: an overview. *Pure Appl Chem.* 1999;71:581–6. <https://doi.org/10.1351/pac199971040581>.
2. Gomollón-Bel F. Ten chemical innovations that will change our world: IUPAC identifies emerging technologies in chemistry with potential to make our planet more sustainable. *Chem Int.* 2019;41:12–7. <https://doi.org/10.1515/ci-2019-0203>.
3. Boldyrev VV, Tkáčová K. Mechanochemistry of solids: past, present, and prospects. *J Mater Synth Process.* 2000;8:121–32. <https://doi.org/10.1023/A:1011347706721>.
4. Takacs L. The mechanochemical reduction of AgCl with metals. *J Therm Anal Calorim.* 2007;90:81–4. <https://doi.org/10.1007/s10973-007-8479-8>.
5. Shen F, Xiong X, Fu JY, Yang JR, Qiu M, Qi XH, Tsang DCW. Recent advances in mechanochemical production of chemicals and carbon materials from sustainable biomass resources. *Renew Sust Energ Rev.* 2020;130:109944. <https://doi.org/10.1016/j.rser.2020.109944>.
6. Tan D, García F. Main group mechanochemistry: from curiosity to established protocols. *Chem Soc Rev.* 2019;48:2274–92. <https://doi.org/10.1039/C7CS00813A>.
7. Howard JL, Cao Q, Browne DL. Mechanochemistry as an emerging tool for molecular synthesis: what can it offer? *Chem Sci.* 2018;9:3080–94. <https://doi.org/10.1039/C7SC05371A>.
8. Guo H, Lian Y, Yan L, Qi X, Smith RL. Cellulose-derived superparamagnetic carbonaceous solid acid catalyst for cellulose hydrolysis in an ionic liquid or aqueous reaction system. *Green Chem.* 2013;15:2167–74. <https://doi.org/10.1039/C3GC40433A>.
9. Rinaldi R, Schüth F. Acid hydrolysis of cellulose as the entry point into biorefinery schemes. *ChemSusChem.* 2009;2:1096–107. <https://doi.org/10.1002/cssc.200900188>.
10. Vyver SV, Peng L, Geboers J, Schepers H, Clippel F, Gommes CJ, Goderis B, Jacobs PA, Sels BF. Sulfonated silica/carbon nanocomposites as novel catalysts for hydrolysis of cellulose to glucose. *Green Chem.* 2010;12:1560–3. <https://doi.org/10.1039/C0GC00235F>.
11. Lee JW, Jeffries TW. Efficiencies of acid catalysts in the hydrolysis of lignocellulosic biomass over a range of combined severity factors. *Bioresour Technol.* 2011;102:5884–90. <https://doi.org/10.1016/j.biortech.2011.02.048>.
12. Gu BJ, Wang J, Wolcott MP, Ganjyal GM. Increased sugar yield from pre-milled Douglas-fir forest residuals with lower energy consumption by using planetary ball milling. *Bioresour Technol.* 2018;251:93–8. <https://doi.org/10.1016/j.biortech.2017.11.103>.
13. Szczesniak B, Borysiuk S, Choma J, Jaroniec M. Mechanochemical synthesis of highly porous materials. *Mate Horiz.* 2020;7:1457–73. <https://doi.org/10.1039/DOMH00081G>.
14. Hick SM, Griebel C, Restrepo DT, Truitt JH, Baker EJ, Bylda C, Blair RG. Mechanocatalysis for biomass-derived chemicals and fuels. *Green Chem.* 2010;12:468–74. <https://doi.org/10.1039/B923079C>.
15. Meine N, Rinaldi R, Schüth F. Solvent-free catalytic depolymerization of cellulose to water-soluble oligosaccharides. *ChemSusChem.* 2012;5:1322–9. <https://doi.org/10.1002/cssc.201100770>.
16. Kaufman RMD, Käldström M, Richter U, Schüth F, Rinaldi R. Mechanocatalytic depolymerization of lignocellulose performed on hectogram and kilogram scales. *Ind Eng Chem Res.* 2015;54:4581–92. <https://doi.org/10.1021/acs.iecr.5b00224>.
17. Zhang Q, Jérôme F. Mechanocatalytic deconstruction of cellulose: an emerging entry into biorefinery. *ChemSusChem.* 2013;6:2042–4. <https://doi.org/10.1002/cssc.201300765>.
18. Blair RG, Chagoya K, Biltek S, Jackson S, Sinclair A, Tarabocchi A, Restrepo DT. The scalability in the mechanochemical syntheses of edge functionalized graphene materials and biomass-derived chemicals. *Faraday Discuss.* 2014;170:223–33. <https://doi.org/10.1039/C4FD00007B>.
19. Hideno A, Inoue H, Tsukahara K, Fujimoto S, Minowa T, Inoue S, Endo T, Sawayama S. Wet disk milling pretreatment without sulfuric acid for enzymatic hydrolysis of rice straw. *Bioresour Technol.* 2009;100:2706–11. <https://doi.org/10.1016/j.biortech.2008.12.057>.

20. Avolio R, Bonadies I, Capitani D, Errico ME, Gentile G, Avella M. A multitechnique approach to assess the effect of ball milling on cellulose. *Carbohydr Polym*. 2012;87:265–73. <https://doi.org/10.1016/j.carbpol.2011.07.047>.
21. Dornath P, Cho HJ, Paulsen A, Dauenhauer P, Fan W. Efficient mechano-catalytic depolymerization of crystalline cellulose by formation of branched glucan chains. *Green Chem*. 2015;17:769–75. <https://doi.org/10.1039/C4GC02187H>.
22. Liu H, Chen X, Ji G, Yu H, Gao C, Han L, Xiao W. Mechanochemical deconstruction of lignocellulosic cell wall polymers with ball-milling. *Bioresour Technol*. 2019;286:121364. <https://doi.org/10.1016/j.biortech.2019.121364>.
23. Ji G, Gao C, Xiao W, Han L. Mechanical fragmentation of corncob at different plant scales: impact and mechanism on microstructure features and enzymatic hydrolysis. *Bioresour Technol*. 2016;205:159–65. <https://doi.org/10.1016/j.biortech.2016.01.029>.
24. Wu Y, Ge S, Xia C, Mei C, Kim KH, Cai L, Smith LM, Lee J, Shi SQ. Application of intermittent ball milling to enzymatic hydrolysis for efficient conversion of lignocellulosic biomass into glucose. *Renew Sust Energ Rev*. 2021;136:110442. <https://doi.org/10.1016/j.rser.2020.110442>.
25. Da SAS, Inoue H, Endo T, Yano S, Bon EPS. Milling pretreatment of sugarcane bagasse and straw for enzymatic hydrolysis and ethanol fermentation. *Bioresour Technol*. 2010;101:7402–9. <https://doi.org/10.1016/j.biortech.2010.05.008>.
26. Su TC, Fang Z, Zhang F, Luo J, Li XK. Hydrolysis of selected tropical plant wastes catalyzed by a magnetic carbonaceous acid with microwave. *Sci Rep*. 2015;5:17538. <https://doi.org/10.1038/srep17538>.
27. Jiang LQ, Zheng AQ, Meng JG, Wang XB, Zhao ZL, Li HB. A comparative investigation of fast pyrolysis with enzymatic hydrolysis for fermentable sugars production from cellulose. *Bioresour Technol*. 2019;274:281–6. <https://doi.org/10.1016/j.biortech.2018.11.098>.
28. Zakaria MR, Fujimoto S, Hirata S, Hassan MA. Ball milling pretreatment of oil palm biomass for enhancing enzymatic hydrolysis. *Appl Biochem Biotechnol*. 2014;173:1778–89. <https://doi.org/10.1007/s12010-014-0964-5>.
29. Lange JP, Van DHE, Van BJ, Price R. Furfural-a promising platform for lignocellulosic biofuels. *ChemSusChem*. 2012;5:150–66. <https://doi.org/10.1002/cssc.201100648>.
30. Ramli NAS, Amin NAS. Kinetic study of glucose conversion to levulinic acid over Fe/HY zeolite catalyst. *Chem Eng J*. 2016;283:150–9. <https://doi.org/10.1016/j.cej.2015.07.044>.
31. Van PRJ, Van DWJC, De JE, Rasrendra CB, Heeres HJ, De VJG. Hydroxymethylfurfural, a versatile platform chemical made from renewable resources. *Chem Rev*. 2013;113:1499–597. <https://doi.org/10.1021/cr300182k>.
32. Guo H, Hirosaki Y, Qi X, Smith RL. Synthesis of ethyl levulinate over amino-sulfonated functional carbon materials. *Renew Energy*. 2020;157:951–8. <https://doi.org/10.1016/j.renene.2020.05.103>.
33. Qian Y, Zhu L, Wang Y, Lu X. Recent progress in the development of biofuel 2,5-dimethylfuran. *Renew Sust Energ Rev*. 2015;41:633–46. <https://doi.org/10.1016/j.rser.2014.08.085>.
34. Qi X, Guo H, Li L, Smith RL. Acid-catalyzed dehydration of fructose into 5-hydroxymethylfurfural by cellulose-derived amorphous carbon. *ChemSusChem*. 2012;5:2215–20. <https://doi.org/10.1002/cssc.201200363>.
35. Zhang L, Yu H, Wang P, Dong H, Peng X. Conversion of xylan, D-xylose and lignocellulosic biomass into furfural using AlCl₃ as catalyst in ionic liquid. *Bioresour Technol*. 2013;130:110–6. <https://doi.org/10.1016/j.biortech.2012.12.018>.
36. Shen F, Sun S, Zhang X, Yang JR, Qiu M, Qi XH. Mechanochemical-assisted production of 5-hydroxymethylfurfural from high concentration of cellulose. *Cellulose*. 2020;27:3013–23. <https://doi.org/10.1007/s10570-020-03008-w>.
37. Carrasquillo-Flores R, Kaldstrom M, Schuth F, Dumesic JA, Rinaldi R. Mechanocatalytic depolymerization of dry (ligno) cellulose as an entry process for high-yield production of furfurals. *ACS Catal*. 2013;3:993–7. <https://doi.org/10.1021/cs400133z>.

38. Schüth F, Rinaldi R, Meine N, Käldström M, Hilgert J, Rechulski MDK. Mechanocatalytic depolymerization of cellulose and raw biomass and downstream processing of the products. *Catal Today.* 2014;234:24–30. <https://doi.org/10.1016/j.cattod.2014.02.019>.
39. Yoshioka K, Yamada T, Ohno H, Miyafuji H. Production of furan compounds from Cryptomeria japonica using pyridinium chloride under various conditions. *BioResources.* 2018;13:208–19. <https://doi.org/10.15376/biores.13.1.208-219>.
40. Lappalainen K, Dong Y. Simultaneous production of furfural and levulinic acid from pine sawdust via acid-catalysed mechanical depolymerization and microwave irradiation. *Biomass Bioenergy.* 2019;123:159–65. <https://doi.org/10.1016/j.biombioe.2019.02.017>.
41. Yoshida K, Nanao H, Kiyozumi Y, Sato K, Sato O, Yamaguchi A, Shirai M. Furfural production from xylose and bamboo powder over chabazite-type zeolite prepared by interzeolite conversion method. *J Taiwan Inst Chem Eng.* 2017;79:55–9. <https://doi.org/10.1016/j.jtice.2017.05.035>.
42. Chen J, Wang S, Huang J, Chen L, Ma L, Huang X. Conversion of cellulose and cellobiose into sorbitol catalyzed by ruthenium supported on a polyoxometalate/metal-organic framework hybrid. *ChemSusChem.* 2013;6:1545–55. <https://doi.org/10.1002/cssc.201200914>.
43. Zhang X, Durnell LJ, Isaacs MA, Parlett CMA, Lee AF, Wilson K. Platinum-catalyzed aqueous-phase hydrogenation of D-glucose to D-sorbitol. *ACS Catal.* 2016;6:7409–17. <https://doi.org/10.1021/acscatal.6b02369>.
44. Rey-Raap N, Ribeiro LS, Órfão JJDM, Figueiredo JL, Pereira MFR. Catalytic conversion of cellulose to sorbitol over Ru supported on biomass-derived carbon-based materials. *Appl Catal B Environ.* 2019;256:117826. <https://doi.org/10.1016/j.apcatb.2019.117826>.
45. Gromov NV, Medvedeva TB, Rodikova YA, Timofeeva MN, Parmon VN. One-pot synthesis of sorbitol via hydrolysis-hydrogenation of cellulose in the presence of Ru-containing composites. *Bioresour Technol.* 2020;319:124122. <https://doi.org/10.1016/j.biortech.2020.124122>.
46. Mao F, Chen S, Zhang Q, Yang L, Fu Z. Ru/p-containing porous biochar-efficiently catalyzed cascade conversion of cellulose to sorbitol in water under medium-pressure H₂ atmosphere. *Bull Chem Soc Jpn.* 2020;93:1026–35. <https://doi.org/10.1246/bcsj.20200095>.
47. Geboers J, Van DVS, Carpentier K, De BK, Jacobs P, Sels B. Efficient catalytic conversion of concentrated cellulose feeds to hexitols with heteropoly acids and Ru on carbon. *Chem Commun.* 2010;46:3577–9. <https://doi.org/10.1039/C001096K>.
48. Ribeiro LS, Órfão JJM, Pereira MFR. Enhanced direct production of sorbitol by cellulose ball-milling. *Green Chem.* 2015;17:2973–80. <https://doi.org/10.1039/C5GC00039D>.
49. Ribeiro LS, Delgado JJ, Órfão JJM, Pereira MFR. Direct conversion of cellulose to sorbitol over ruthenium catalysts: influence of the support. *Catal Today.* 2017;279:244–51. <https://doi.org/10.1016/j.cattod.2016.05.028>.
50. Almohalla M, Rodríguez-Ramos I, Ribeiro LS, Órfão JJM, Pereira MFR, Guerrero-Ruiz A. Cooperative action of heteropolyacids and carbon supported Ru catalysts for the conversion of cellulose. *Catal Today.* 2018;301:65–71. <https://doi.org/10.1016/j.cattod.2017.05.023>.
51. Ribeiro LS, Delgado JJ, Órfão JJM, Pereira MFR. Carbon supported Ru-Ni bimetallic catalysts for the enhanced one-pot conversion of cellulose to sorbitol. *Appl Catal B Environ.* 2017;217:265–74. <https://doi.org/10.1016/j.apcatb.2017.04.078>.
52. Kobayashi H, Yabushita M, Komanoya T, Hara K, Fujita I, Fukuoka A. High-yielding one-pot synthesis of glucose from cellulose using simple activated carbons and trace hydrochloric acid. *ACS Catal.* 2013;3:581–7. <https://doi.org/10.1021/cs300845f>.
53. Wang M, Liu M, Li H, Zhao Z, Zhang X, Wang F. Dealkylation of lignin to phenol via oxidation-hydrogenation strategy. *ACS Catal.* 2018;8:6837–43. <https://doi.org/10.1021/acscatal.8b00886>.
54. Rinaldi R, Jastrzebski R, Clough MT, Ralph J, Kennema M, Bruijnincx PCA, Weckhuysen BM. Paving the way for lignin valorisation: recent advances in bioengineering, biorefining and catalysis. *Angew Chem Int Ed.* 2016;55:8164–215. <https://doi.org/10.1002/anie.201510351>.

55. Tejado A, Peña C, Labidi J, Echeverria JM, Mondragon I. Physico-chemical characterization of lignins from different sources for use in phenol-formaldehyde resin synthesis. *Bioresour Technol.* 2007;98:1655–63. <https://doi.org/10.1016/j.biortech.2006.05.042>.
56. Zakzeski J, Bruijnincx PCA, Jongerius AL, Weckhuysen BM. The catalytic valorization of lignin for the production of renewable chemicals. *Chem Rev.* 2010;110:3552–99. <https://doi.org/10.1021/cr900354u>.
57. Wang Y, Wang Q, He J, Zhang Y. Highly effective C-C bond cleavage of lignin model compounds. *Green Chem.* 2017;19:3135–41. <https://doi.org/10.1039/c7gc00844a>.
58. Bertella S, Luterbacher JS. Lignin functionalization for the production of novel materials. *Trends Chem.* 2020;2:440–53. <https://doi.org/10.1016/j.trechm.2020.03.001>.
59. Verboekend D, Liao Y, Schutyser W, Sels BF. Alkylphenols to phenol and olefins by zeolite catalysis: a pathway to valorize raw and fossilized lignocellulose. *Green Chem.* 2015;18:297–306. <https://doi.org/10.1039/C5GC01868D>.
60. Qu T, Zhang X, Gu X, Han L, Ji G, Chen X, Xiao W. Ball milling for biomass fractionation and pretreatment with aqueous hydroxide solutions. *ACS Sustain Chem Eng.* 2017;5:7733–42. <https://doi.org/10.1021/acssuschemeng.7b01186>.
61. Mittal A, Katahira R, Donohoe BS, Pattathil S, Kandemkavil S, Reed ML, Biddy MJ, Beckham GT. Ammonia pretreatment of corn Stover enables facile lignin extraction. *ACS Sustain Chem Eng.* 2017;5:2544–61. <https://doi.org/10.1021/acssuschemeng.6b02892>.
62. Jang SK, Lee HJ, Jung CD, Yu JH, Choi WJ, Choi IG, Kim H. High yield solvent extraction of hydrothermal and ball-milling treated lignin prior to enzymatic hydrolysis for co-valorization of lignin and cellulose in Miscanthus sacchariflorus. *Fuel.* 2020;269:117428. <https://doi.org/10.1016/j.fuel.2020.117428>.
63. Balakshin M, Capanema EA, Zhu X, Sulava I, Potthast A, Rosenau T, Rojas OJ. Spruce milled wood lignin: linear, branched or cross-linked? *Green Chem.* 2020;22:3985–4001. <https://doi.org/10.1039/D0GC00926A>.
64. Ahmed MA, Lee JH, Raja AA, Weon CJ. Effects of gamma-valerolactone assisted fractionation of ball-milled pine wood on lignin extraction and its characterization as well as its corresponding cellulose digestion. *Appl Sci.* 2020;10:1599–611. <https://doi.org/10.3390/app10051599>.
65. Sapouna I, Lawoko M. Deciphering lignin heterogeneity in ball milled softwood: unravelling the synergy between the supramolecular cell wall structure and molecular events. *Green Chem.* 2021;23:3348–64. <https://doi.org/10.1039/D0GC04319B>.
66. Biannic B, Bozell JJ. Efficient cobalt-catalyzed oxidative conversion of lignin models to benzoquinones. *Org Lett.* 2013;15:2730–3. <https://doi.org/10.1021/ol401065r>.
67. Nair V, Dhar P, Vinu R. Production of phenolics via photocatalysis of ball milled lignin-TiO₂ mixtures in aqueous suspension. *RSC Adv.* 2016;6:18204–16. <https://doi.org/10.1039/C5RA25954A>.
68. Sun C, Zheng L, Xu W, Dushkin AV, Su W. Mechanochemical cleavage of lignin models and lignin via oxidation and a subsequent base-catalyzed strategy. *Green Chem.* 2020;22:3489–94. <https://doi.org/10.1039/D0GC00372G>.
69. Kleine T, Buendia J, Bolm C. Mechanochemical degradation of lignin and wood by solvent-free grinding in a reactive medium. *Green Chem.* 2013;15:160–6. <https://doi.org/10.1039/C2GC36456E>.
70. Brittain AD, Chrisandina NJ, Cooper RE, Buchanan M, Cort JR, Olarte MV, Sievers C. Quenching of reactive intermediates during mechanochemical depolymerization of lignin. *Catal Today.* 2018;302:180–9. <https://doi.org/10.1016/j.cattod.2017.04.066>.
71. Dabral S, Wotruba H, Hernández JG, Bolm C. Mechanochemical oxidation and cleavage of lignin β-O-4 model compounds and lignin. *ACS Sustain Chem Eng.* 2018;6:3242–54. <https://doi.org/10.1021/acssuschemeng.7b03418>.
72. Peterson SC, Jackson MA, Kim S, Palmquist DE. Increasing biochar surface area: optimization of ball milling parameters. *Powder Technol.* 2012;228:115–20. <https://doi.org/10.1016/j.powtec.2012.05.005>.

73. Lyu H, Gao B, He F, Zimmerman AR, Ding C, Huang H, Tang J. Effects of ball milling on the physicochemical and sorptive properties of biochar: experimental observations and governing mechanisms. *Environ Pollut.* 2018;233:54–63. <https://doi.org/10.1016/j.envpol.2017.10.037>.
74. Huang L, Wu Q, Liu S, Yu S, Ragauskas AJ. Solvent-free production of carbon materials with developed pore structure from biomass for high-performance supercapacitors. *Ind Crop Prod.* 2020;150:112384. <https://doi.org/10.1016/j.indcrop.2020.112384>.
75. Lyu H, Gao B, He F, Ding C, Tang J, Crittenden JC. Ball-milled carbon nanomaterials for energy and environmental applications. *ACS Sustain Chem Eng.* 2017;5:9568–85. <https://doi.org/10.1021/acssuschemeng.7b02170>.
76. Xiao J, Hu R, Chen G. Micro-nano-engineered nitrogenous bone biochar developed with a ball-milling technique for high-efficiency removal of aquatic cd(II), cu(II) and Pb(II). *J Hazard Mater.* 2020;387:121980. <https://doi.org/10.1016/j.jhazmat.2019.121980>.
77. Xiao Y, Lyu H, Yang C, Zhao B, Tang J. Graphitic carbon nitride/biochar composite synthesized by a facile ball-milling method for the adsorption and photocatalytic degradation of enrofloxacin. *J Environ Sci.* 2021;103:93–107. <https://doi.org/10.1016/j.jes.2020.10.006>.
78. Xiang W, Wan Y, Zhang X, Tan Z, Gao B. Adsorption of tetracycline hydrochloride onto ball-milled biochar: governing factors and mechanisms. *Chemosphere.* 2020;255:127057. <https://doi.org/10.1016/j.chemosphere.2020.127057>.
79. Huang J, Zimmerman AR, Chen H, Gao B. Ball milled biochar effectively removes sulfamethoxazole and sulfapyridine antibiotics from water and wastewater. *Environ Pollut.* 2020;258:113809. <https://doi.org/10.1016/j.envpol.2019.113809>.
80. Zhang Y, Miao X, Xiang W, Zhang J, Cao C, Wang H, Hu X, Gao B. Ball milling biochar with ammonia hydroxide or hydrogen peroxide enhances its adsorption of phenyl volatile organic compounds (VOCs). *J Hazard Mater.* 2020;403:123540. <https://doi.org/10.1016/j.jhazmat.2020.123540>.
81. Xiang W, Zhang X, Chen K, Fang J, He F, Hu X, Tsang DCW, Ok YS, Gao B. Enhanced adsorption performance and governing mechanisms of ball-milled biochar for the removal of volatile organic compounds (VOCs). *Chem Eng J.* 2020;385:123842. <https://doi.org/10.1016/j.cej.2019.123842>.
82. Shi Q, Wang Y, Zhang X, Shen B, Wang F, Zhang Y. Hierarchically porous biochar synthesized with CaCO_3 template for efficient Hg^0 adsorption from flue gas. *Fuel Process Technol.* 2020;199:106247–54. <https://doi.org/10.1016/j.fuproc.2019.106247>.
83. Lyu H, Xia S, Tang J, Zhang Y, Gao B, Shen B. Thiol-modified biochar synthesized by a facile ball-milling method for enhanced sorption of inorganic Hg^{2+} and organic CH_3Hg^+ . *J Hazard Mater.* 2019;384:121357. <https://doi.org/10.1016/j.jhazmat.2019.121357>.
84. Yang X, Yu I, Tsang D, Budarin VL, Yong SO. Ball-milled, solvent-free Sn-functionalisation of wood waste biochar for sugar conversion in food waste valorisation. *J Clean Prod.* 2020;268:122300. <https://doi.org/10.1016/j.jclepro.2020.122300>.
85. Lyu H, Yu Z, Gao B, He F, Huang J, Tang J, Shen B. Ball-milled biochar for alternative carbon electrode. *Environ Sci Pollut Res.* 2019;26:14693–702. <https://doi.org/10.1007/s11356-019-04899-4>.
86. Xiao Y, Lyu H, Tang J, Wang K, Sun H. Effects of ball milling on the photochemistry of biochar: enrofloxacin degradation and possible mechanisms. *Chem Eng J.* 2020;384:123311. <https://doi.org/10.1016/j.cej.2019.123311>.
87. Anh TT, Chung P, Katz A. Weak-acid sites catalyze the hydrolysis of crystalline cellulose to glucose in water: importance of post-synthetic functionalization of the carbon surface. *Angew Chem Int Ed.* 2015;54:11050–3. <https://doi.org/10.1002/ange.201504865>.
88. Shrotri A, Kobayashi H, Fukuoka A. Mechanochemical synthesis of a carboxylated carbon catalyst and its application in cellulose hydrolysis. *ChemCatChem.* 2016;8:1059–64. <https://doi.org/10.1002/cctc.201501422>.
89. He J, Tang J, Zhang Z, Wang L, Liu Q, Liu X. Magnetic ball-milled FeS@biochar as persulfate activator for degradation of tetracycline. *Chem Eng J.* 2021;404:126997. <https://doi.org/10.1016/j.cej.2020.126997>.

90. Xia K, Gao Q, Jiang J, Hu J. Hierarchical porous carbons with controlled micropores and mesopores for supercapacitor electrode materials. *Carbon*. 2008;46:1718–26. <https://doi.org/10.1016/j.carbon.2008.07.018>.
91. Qu J, Wang Y, Tian X, Jiang Z, Deng F, Tao Y, Jiang Q, Wang L, Zhang Y. KOH-activated porous biochar with high specific surface area for adsorptive removal of chromium (VI) and naphthalene from water: affecting factors, mechanisms and reusability exploration. *J Hazard Mater*. 2021;401:123292. <https://doi.org/10.1016/j.jhazmat.2020.123292>.
92. He X, Li J, Meng Q, Guo Z, Liu Y. Enhanced adsorption capacity of sulfadiazine on tea waste biochar from aqueous solutions by the two-step sintering method without corrosive activator. *J Environ Chem Eng*. 2020;9:104898. <https://doi.org/10.1016/j.jece.2020.104898>.
93. Shi C, Hu L, Guo K, Li H, Zhai T. Highly porous carbon with graphene nanoplatelet microstructure derived from biomass waste for high-performance supercapacitors in universal electrolyte. *Adv Sustain Syst*. 2017;1:1600011. <https://doi.org/10.1002/adsu.201600011>.
94. Schneidermann C, Jackel N, Oswald S, Giebelter L, Presser V, Borchardt L. Solvent-free mechanochemical synthesis of nitrogen-doped nanoporous carbon for electrochemical energy storage. *ChemSusChem*. 2017;10:2416–24. <https://doi.org/10.1002/cssc.201700459>.
95. Qi J, Zhang W, Xu L. Solvent-free mechanochemical preparation of hierarchically porous carbon for supercapacitor and oxygen reduction reaction. *Chemistry*. 2018;24:18097–105. <https://doi.org/10.1002/chem.201804302>.
96. Cao L, Yu I, Tsang D, Zhang S, Sik OY, Kwon EE, Song H, Sun PC. Phosphoric acid-activated wood biochar for catalytic conversion of starch-rich food waste into glucose and 5-hydroxymethylfurfural. *Bioresour Technol*. 2018;267:242–8. <https://doi.org/10.1016/j.biortech.2018.07.048>.
97. Fiss BG, Hatherly L, Stein RS, Friščić T, Moores A. Mechanochemical phosphorylation of polymers and synthesis of flame-retardant cellulose nanocrystals. *ACS Sustain Chem Eng*. 2019;7:7951–9. <https://doi.org/10.1021/acssuschemeng.9b00764>.
98. Yan J, Quan G. Sorption behavior of dimethyl phthalate in biochar-soil composites: implications for the transport of phthalate esters in long-term biochar amended soils. *Ecotoxicol Environ Saf*. 2020;205:111169. <https://doi.org/10.1016/j.ecoenv.2020.111169>.

Chapter 11

Fundamentals of Hydrothermal Processing of Biomass-Related Molecules for Converting Organic Solid Wastes into Chemical Products



Taku Michael Aida

Abstract Organic solid wastes (OSW) are derived from biomass and related biomolecules that are the products of agricultural or chemical processing. In this chapter, an overview of methods is given for converting OSW into chemical products using either hydrothermal (water) or solvothermal (ammonia) processing. First, the physical properties of water and ammonia are discussed according to their variations with temperature and pressure. Then, the chemistry of simple carbohydrate conversions in subcritical and supercritical water as developed by the author is shown. Rapid heating techniques provide an effective methodology for hydrothermal conversion of OSW to chemicals. Biopolymers can be converted to organic acids, proteins can be converted to peptides, nutrients in OSW, or municipal waste can be recycled into microalgae cultivation systems. In the top-down approach with hydrothermal and solvothermal methods, large molecule substrates are converted to smaller size functional oligomers or heterocyclic compounds. This chapter provides some of the fundamental principles for applying hydrothermal and solvothermal methods to valorize organic solid wastes and concludes with potential research areas.

Keywords Alginate · Amino acids · Ammonia · Cellulose · Glucose · Lignin · Lipids · Microalgae · Peptides · Proteins

T. M. Aida (✉)

Faculty of Engineering, Department of Chemical Engineering, Fukuoka University, Fukuoka,
Japan

Research Institute of Composite Materials, Fukuoka University, Fukuoka, Japan
e-mail: tmaida@fukuoka-u.ac.jp

11.1 Introduction

The development of sustainable methods for chemical products is an important topic for present and future society. With the world dependent on energy for the well-being of its population, renewable energy resources have become vital for social progress. In fact, due to Covid-19, demand for low carbon and renewable energies has exceeded demand for coal in the production of primary energy since 2019 and this trend is likely to continue in the coming years with more primary energy being produced by renewables (wind, solar) [1]. Thus, production methods for chemical products are currently in the spotlight.

Present research trends for developing chemical industries based on renewable feedstocks use the concept of biorefineries within the biorefinery classification developed by the International Energy Agency (IEA) Bioenergy Task 42 [2]. For example, agricultural wastes can be converted into formic acid via fast pyrolysis, acid hydrolysis, wet oxidation, catalytic oxidation, photocatalysis, or electrocatalysis methods [3]. The formic acid thus produced can be used in chemical-related applications as catalysts, platform chemicals, or solvents, or energy-related applications in fuel cells, as H₂ carriers, or in bio-oil upgrading operations. In this chapter, the focus is on “top-down” approaches, which convert large molecules into small or smaller molecules that can be used as chemical products as opposed to the “bottom-up” approach that takes small molecules and converts them to large molecules. A related special issue on hydrothermal and solvothermal techniques for processing organic solid wastes has been published [4].

The chemistry of the reaction and solvent systems is important for converting the biomass-related wastes into the desired chemical products. Water, especially in its liquid state at high-temperature, is an effective reaction solvent for many types of biomass conversions, however, it has low-selectivity in its typical application [5]. Processing organic solid wastes (OSW) tends to create solid products especially at long reaction times when using water as a reaction solvent, the feedstock can be more suitable for producing biochars or functional biocarbon materials that can be used as adsorbents or catalysts. The processing of OSW to produce carbonaceous solids that have adsorptive or catalytic properties is discussed in other chapters of this book. In this chapter, reaction systems and methods are shown that can greatly improve the selectivity of high-temperature liquid water for converting OSW into liquid chemical products.

The arrangement of the chapter is as follows. First, the properties of water in its liquid state and supercritical state are discussed and relationships are given for using water in reaction systems that employ fast-heating of substrates to reaction conditions are shown in a brief tutorial that includes reaction systems for fast-heating of substrates with water or solvents. The chemistry of carbohydrate conversions in water at high-temperatures is described in detail. Then, applications are shown for (i) producing organic acids from alginate and related compounds, (ii) production of low molecular-weight peptides from proteins, (iii) production of bio-oil (bio crude) from lignin and lipids, (iv) recycle of nutrients from municipal sludge for microalgae

production, (v) coupling of municipal waste with hydrothermal processing for nutrient recycling, (vi) recycle of nutrients from microalgae and (vii) an overview for producing aminated products. One key point of techniques introduced in this chapter is the use of fast-heating of water (or solvent) in reaction systems so that chemical products can be obtained with high selectivity. When high selectivity is not needed, then water can be used to recycle nutrients or for making microalgae production systems efficient for bio-oil production. Studies that will be introduced in this chapter including studies conducted by the author and are given in Table 11.1.

11.2 Hydrothermal and Solvothermal Processing

According to the Merriam-Webster dictionary [18], hydrothermal is an adjective that means “of or related to hot water” which was first used in 1849. In science and engineering, hydrothermal refers to hot water in its liquid state that is at a temperature of 100 °C or higher. Similarly, solvothermal is an adjective that means “of or related to hot solvents in the liquid state”, whereas the temperature can be expected to be higher than room temperature, but typically lower than the boiling point of the solvent or solvent mixture. In the next sections, the physical properties of water will be mainly discussed to the extent necessary to show how hydrothermal processing systems are assembled and used to take advantage of the properties of water for converting OSW into chemical products. Ammonia-water mixtures can be used for aminating reaction environments in similar types of systems as those described for hydrothermal processing, which properties will also be described at the end of this section.

11.2.1 Physical Properties of Water

Figure 11.1 shows a pressure-temperature (P - T) diagram and a pressure-density-temperature (P - ρ - T) diagram of water. In the P - T diagram (Fig. 11.1), the saturated liquid state is shown by the vapor pressure curve that gives the equilibrium conditions between the liquid state and vapor state of water. The vapor pressure, which is also called the liquid-vapor curve, boiling point curve, or saturation curve, terminates at the critical point of water (374 °C) in which the liquid and vapor densities of water become equal. Water at hydrothermal conditions is commonly applied to processing organics at temperatures between 100 °C to 250 °C (P - T diagram, Fig. 11.1) due to the favorable variation of properties as discussed below. Water at hydrothermal conditions can be used at its saturation (autogenous) pressure, but practically, the pressure of the hydrothermal process is controlled, so that water is in a compressed liquid state which avoids boiling and saves energy by inhibiting vaporization. The P - ρ - T diagram shows the equilibrium states of liquid and vapor at hydrothermal conditions.

Table 11.1 List of experimental conditions of hydrothermal treatment (HT) studies introduced in this chapter

Substrates	Topic (sections)	HT-conditions	Products	Ref.
Sugars (glucose, fructose, xylose)	Carbohydrate conversion (Sect. 11.3.2)	Flow, (350–400) °C, 100 MPa, (0.1–5) s, fast heating rates	Aldehydes, organic acids, aromatic compounds	[6], [7], [8]
Sodium alginate	Chemical production (Sect. 11.4.1)	Flow, (350–400) °C, 40 MPa, (0.1–5) s, fast heating rates	Organic acids, low molecular weight alginates, ketones	[9]
		Batch, 150 °C, (30–90) min. Slow heating rates ($1.46 \text{ }^{\circ}\text{C} \cdot \text{s}^{-1}$)	Organic acids, alginate oligomers	[10]
Protein (bovine serum albumin: BSA)	Controlled depolymerization (Sect. 11.4.2)	Flow, (200–260) °C, 25 MPa, (0.1–5) s, fast heating rates ($135\text{--}180 \text{ }^{\circ}\text{C} \text{ s}^{-1}$)	Low-molecular-weight peptides (1500 Da to 8300 Da)	[11]
		Batch, 250 °C, (30–90) min. Slow heating rates ($0.25 \text{ }^{\circ}\text{C} \text{ s}^{-1}$)	Protein aggregates, peptides, amino acids, ammonia	[11]
Lignin	Depolymerization (Sect. 11.4.3)	Flow, (300 and 400) °C, 26 MPa, 60 ms, fast heating rates	Bio oil (aromatic oil)	[12]
Lipids (sunflower oil, model food wastes)	Hydrothermal liquefaction (Sect. 11.4.3)	Batch, set point temperature 600 °C, 1 min. Heating rates ($6.7 \text{ }^{\circ}\text{C} \text{ s}^{-1}$)	Bio crude	[13]
Municipal sludge	Nutrient recycle for microalgae cultivation (Sect. 11.5.1)	Two-step liquefaction, first step; batch, 225 °C, 15 min, second step; acid saccharification of solid residue in aqH_2SO_4 , slow heating	1st step: Solid (cellulose), liquid products (nitrogen and phosphorous compounds), second step: Liquid product (glucose)	[14]
Defatted microalgae	Nutrient recycle for microalgae cultivation (Sect. 11.5.2)	Batch, (175–350) °C, (10–90) min, slow heating	Liquid products (nitrogen and phosphorous compounds)	[15]
Chitin (mechanically milled)	Liquefaction of nitrogen-containing feedstocks (Sect. 11.6)	Batch, 220 °C and 400 °C, (1–20) min, slow heating	Liquid products and solid residue	[16]
Hyaluronic acid	Depolymerization for medical applications (Sect. 11.6)	Flow, (180–220) °C, 25 MPa, (0.7–18) s, fast heating rates ($417\text{--}750 \text{ }^{\circ}\text{C} \text{ s}^{-1}$)	Low-molecular-weight-hyaluronic acids	[17]
		Batch, (120–180) °C, slow heating rates ($0.6\text{--}0.7 \text{ }^{\circ}\text{C} \text{ s}^{-1}$)	Low-molecular-weight degraded hyaluronic acid	[17]

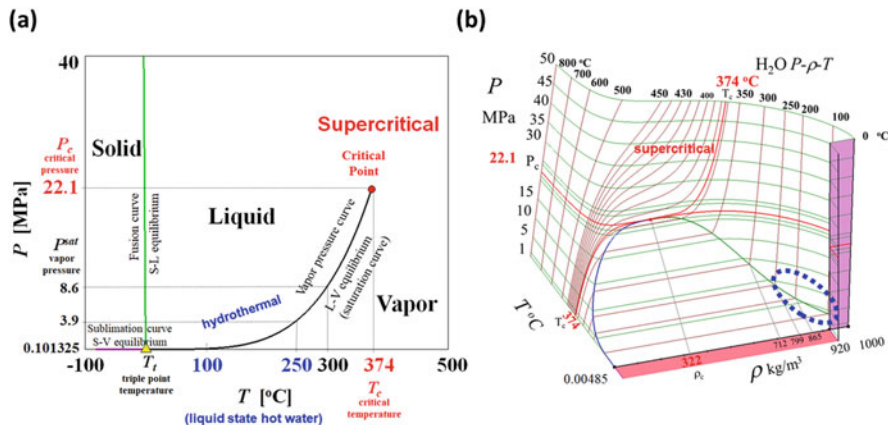


Fig. 11.1 Physical properties of water: (a) pressure-temperature (P - T) diagram and (b) pressure-density-temperature (P - ρ - T) diagram of water. Blue oval (left diagram) indicates the density region of liquid phase commonly used for hydrothermal reactions (100–250 $^{\circ}$ C). Properties of water calculated with Excel programs based on the Wagner equation as in “Introduction to Supercritical Fluids” (Smith, Inomata, Peters), Elsevier Science, 2011

Water has an extensive network of hydrogen bonds that change with conditions of temperature and pressure in many curious ways as summarized nicely on Martin Chaplin’s site [19]. As the temperature of liquid water increases, vapor pressure increases according to Fig. 11.1, but water molecules gain increased kinetic energy, and therefore, hydrogen bonds weaken, and water undergoes self-ionization as discussed below. The effect of temperature (and pressure) on the hydrogen bonds of water causes many changes in its density, relative permittivity (dielectric constant), ion product (self-ionization), viscosity, thermal conductivity, diffusivity, heat capacity, and other physical and transport properties, all of which affect the solubility and reactivity of compounds in solution or contact with water.

Figure 11.2 shows two important properties of water under hydrothermal conditions which are the dielectric constant (relative permittivity) and ion product (self-ionization product or K_w) [20, 21]. As water is heated along its saturation curve, its dielectric constant changes to values equal to those of organic solvents at 25 $^{\circ}$ C, namely, acetonitrile, methanol, and acetone for temperatures of 180 $^{\circ}$ C, 230 $^{\circ}$ C, and 300 $^{\circ}$ C, respectively. This result means that water temperature can be used to control its dielectric constant which affects the solubility of salts and ionic compounds according to the Born equation (Fig. 11.2). Furthermore, Fig. 11.2 shows the temperature dependence of the pK_w of water. Liquid water in the temperature range of 180 $^{\circ}$ C to 300 $^{\circ}$ C has a minimum in its pK_w values, which corresponds to a maximum in its self-ionization (K_w). This phenomenon suggests that although water is completely neutral under hydrothermal conditions, high concentrations of H_3O^+ and OH^- provide an effective reaction environment for promoting hydrolysis and ionic reactions. However, water under hydrothermal conditions hydrolyzes organic compounds in a highly non-selective way, therefore, proper system design and contact methods are necessary for obtaining favorable results for hydrothermal

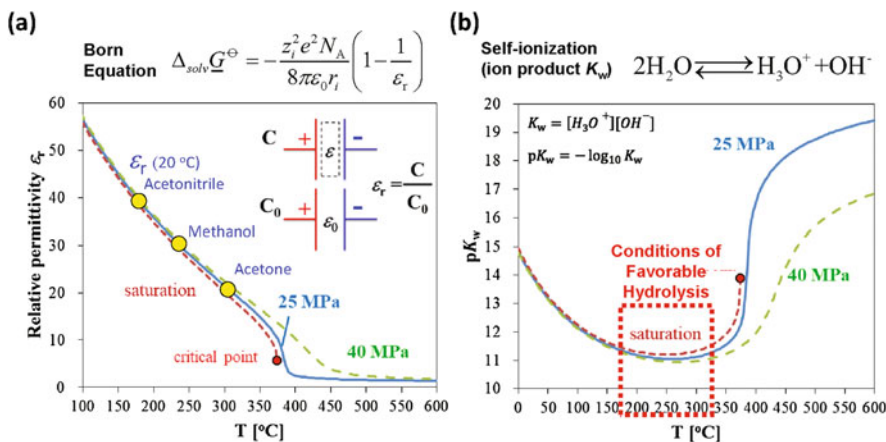


Fig. 11.2 Properties of water: (a) relative permittivity and (b) pK_w of water at hydrothermal and supercritical conditions calculated with programs in Refs. [20, 21]; N_A avogadro constant, z charge of ion, e elementary charge, ϵ_0 permittivity of free space, r_i effective radius of ion, ϵ_r dielectric constant of the solvent

processing of OSW as described in this chapter. The fundamentals of basic system design are described in the next section.

11.2.2 Physical Properties of Water and Ammonia: Variations with Temperature and Pressure

Water is a working fluid of high technological importance and because of its use in lots of physical, chemical and energy systems, there is a dedicated organization called the International Association for the Properties of Water and Steam (IAPWS) [22] that develops recommended formulations for the physical properties of water. The current president of IAPWS is Professor Masaru Nakahara of Kyoto University (Japan). Guidelines and formulations produced by the IAPWS are available for the many properties of water and steam that are implemented in numerous sites and provide convenient calculation of properties at user conditions.

In the U.S.A., the National Institute of Standards and Technology (NIST) provides properties of 75 pure fluids (water, nitrogen, carbon dioxide, ammonia, hydrocarbons, alcohols, refrigerants, etc.) through the NIST Chemistry Webbook, SRD 69 online system [23]. The NIST Chemistry Webbook can provide tabulations and simplified figures of property variations for user conditions based on IAPWS formulations that can be viewed online or exported into spreadsheet programs such as Microsoft Excel. The NIST site is widely used and cited in the scientific literature for property evaluation.

Calculation with Excel – H2Ov70.xls

		Input Field	
		Calculation Field	
53	Single Phase Region		
54	Note: U, H, S, Cp, Cv can be used		
55	on the saturation boundary		
56			
57	T,P functions		
58	V: specific volume, Wagner equ., m ³ /kg	V_TP2(T,P)	T [°C] P [Pa] Calculated Value
59	p: Density, kg/m ³	RHO_TP2(T,P)	100 1.00E+08 1.000E-03 m ³ /kg
60	f: fugacity, Pa	FUG_TP2(T,P)	100 1.10E+05 958.3530834197 kg/m ³
61	U: internal energy	U_TP2(T,P)	300 8.00E+06 6.41 MPa
62	H: Enthalpy, J/kg K	H_TP2(T,P)	100 1.00E+08 3.951E+05 J/kg
63	S: Entropy, S, J/kg K	S_TP2(T,P)	100 1.00E+08 4.951E+05 J/kg
64	Cv: constant volume heat capacity, J/kg K	CV_TP2(T,P)	100 1.00E+08 1237.5 J/kg K
65	Cp: constant pressure heat capacity, J/kg K	CP_TP2(T,P)	100 1.00E+08 3636.3 J/kg K
66	w: speed of sound, m/s	W_TP2(T,P)	100 1.00E+08 4038.5 J/kg K
67	rho,T functions		100 1.00E+08 1733.5 m/s
68	P: pressure, Wagner eqn., Pa	rho_RT2(RHO,T)	tho [kg/m ³] T [°C]
69	f: fugacity, Pa	FUG_RT2(RHO,T)	1065 425 1107.45 MPa
70	U: internal energy	U_RT2(RHO,T)	1000 25 2.389E-16 MPa
71	H: Enthalpy, H, J/kg	H_RT2(RHO,T)	1000 100 3.950E+05 J/kg
72	S: Entropy, S, J/kg K	S_RT2(RHO,T)	1000 100 4.956E+05 J/kg
			1000 100 1237.1 J/kg K

Adiabatic Mixing

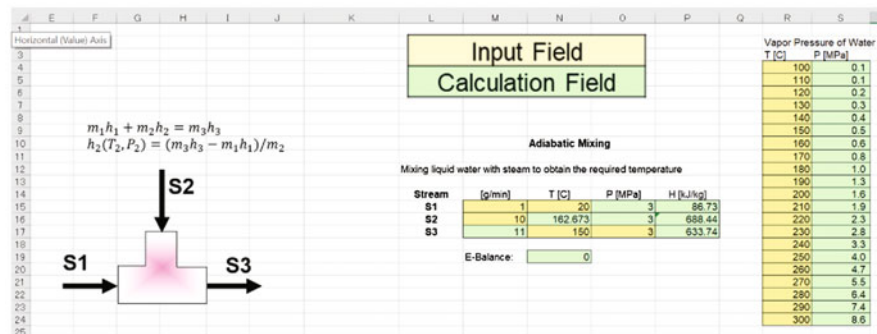


Fig. 11.3 Property functions (top) and adiabatic mixing of two streams (bottom) as a key feature for hydrothermal processing of organic compounds and materials calculated with Microsoft Excel programs in Refs. [20, 21]

The Russian National Committee (RNC) of IAPWS through Moscow Power Engineering Institute provides an online calculation source for pK_w and other properties which are implemented through a MathCad server [24]. The RNC site conveniently displays equations being used for the calculation of water properties.

Although the sites mentioned above are useful for obtaining tabulated values and reference property values, in this chapter, properties are calculated with IAPWS formulations with programs available in Refs. [20, 21], because the properties of water are available as visual basic for application (VBA) functions and can be used directly in iterations or complicated functions in a spreadsheet (Microsoft Excel) format.

Figure 11.3 shows a few of the functions for the properties of water in which density has units of kg/m³, temperature has units of °C and pressure has units of Pa. For example, a function written as = P_RT2(1065,425) in an Excel cell would return a value of 1107.45×10^6 Pa or 1107.45 MPa. These functions can be used in material and energy balance calculations to obtain adiabatic mixing temperatures

(Fig. 11.3) that are useful for design. According to the calculation shown (Fig. 11.3), Stream 1 (S1) is combined with Stream 2 (S2) under steady-flow conditions at constant pressure to generate effluent Stream (S3). Although the pressure is equal in all streams, the stream temperature and flow rates are variable according to the system design. For the case shown (Fig. 11.3), S1 (1 g/min, 20 °C) is combined with S2 (10 g/min, 162.673 °C) to produce S3 (11 g/min, 150 °C) at 3 MPa. Although the calculation is purely educational and lacks a rigorous system design, it shows that a feed (S1) may be heated theoretically *instantaneously* to the desired temperature in a thermodynamic sense by combining a cold feed with a substrate (S1) with a hot stream that is pure water (S2). Thus, Fig. 11.3 shows the basis for some types of hydrothermal processing in a continuous flow type reactor that converts substrates to desired products with high selectivity using fast heating that is described in later sections of this chapter.

There are many possible system designs used in hydrothermal processing that consist of simple pressurized autoclaves, semi-batch reactors that allow for the extractive reaction of materials, or flow systems that allow for continuous production of products. System design for a simplified flow system uses an adiabatic mixing tee as shown in Fig. 11.4. In the flow system shown (Fig. 11.4), a stream with reactants (S4, S5) is pressurized to the system pressure and mixed with a heated and pressurized water stream (S1, S2, S3) and combined in an adiabatic mixing tee as described above. However, in this case, components of the system are specified such as reactor tubing length and inner diameter so that reactor volume is known. Then, profiles of the mass flow ratios between the feed and reactants (m_5/m_6) at constant water feed temperature (T_3) and water mass flow rate (m_3) can be calculated as shown in Fig. 11.4. Assuming that the reactants are diluted in an aqueous solution, the reactor space time (τ) in units of seconds and space velocity (SV) in units of reciprocal seconds, are defined as:

$$\tau = \frac{\text{Reactor volume}}{\text{Volumetric feed rate}} = \frac{\text{Reactor volume}}{(\text{mass flow rate})/(\text{feed density})} = [\text{s}] \quad (11.1)$$

$$\begin{aligned} \text{SV} &= \frac{1}{\tau} = \frac{\text{Volumetric feed rate}}{\text{Reactor volume}} = \frac{\text{mass flow rate}}{(\text{Reactor volume})(\text{feed density})} \\ &= [\text{s}^{-1}] \end{aligned} \quad (11.2)$$

Equations (11.1) and (11.2) are used for estimating average residence times and reactor volumes that can be processed by a system.

Consider the calculation of conditions required for reacting a stream at 250 °C with fast heating. For a reactant stream with mass flow rate of 0.015 g/min (Fig. 11.4) that will be heated with water at 0.045 g/min to the reaction temperature of 250 °C, the water will need to be heated to 316.19 °C, assuming no heat gain or loss during mixing. For this case system pressure is chosen to be at any pressure higher than the vapor pressure of water at the highest temperature and was set at 30 MPa for purposes of the example. The temperature of the pure water stream (T_3) can be chosen according to any desired ratio of reactant feed (m_5) to reactor feed (m_6) as

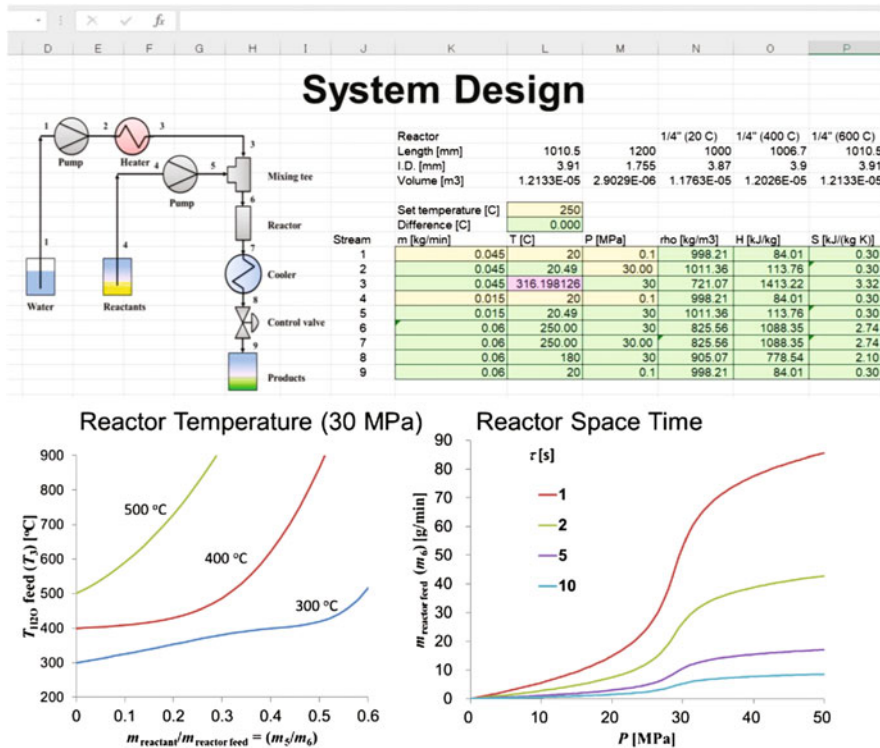


Fig. 11.4 Simplified hydrothermal processing system (top) and reactor specifications (bottom) showing reactor temperature and reactor space time (τ) according to conditions calculated with programs in Refs. [20, 21]. Note that figures and calculations shown are for illustrative purposes only

shown in Fig. 11.4, according to profiles shown for pure water stream temperatures of 300 °C, 400 °C, and 500 °C. The space time, τ , which is the time required to process one reactor volume, can be calculated at given reactor feed flow rates (m_6) according to desired operational pressures. Thus, the availability of the physical properties of water is essential for the design of hydrothermal processing systems that use fast heating techniques.

Hydrothermal and solvothermal systems that use batch processing with autoclaves generally require knowledge of pressure-density-temperature (P - ρ - T) relationships. Figure 11.5 shows the P - ρ - T properties for pure ammonia and an ammonia-water mixture calculated with the NIST reference fluid thermodynamic and transport properties (REFPROP) database [25]. Version 10.0 of REFPROP includes 147 pure fluids, 5 pseudo-pure fluids (e.g. air), and some mixtures with up to 20 components.

For batch processing, detailed physical properties (enthalpies, entropies) are used for estimating minimum energy requirements or maximum pressure in the system. For systems that use fast heating techniques, detailed properties are required in a

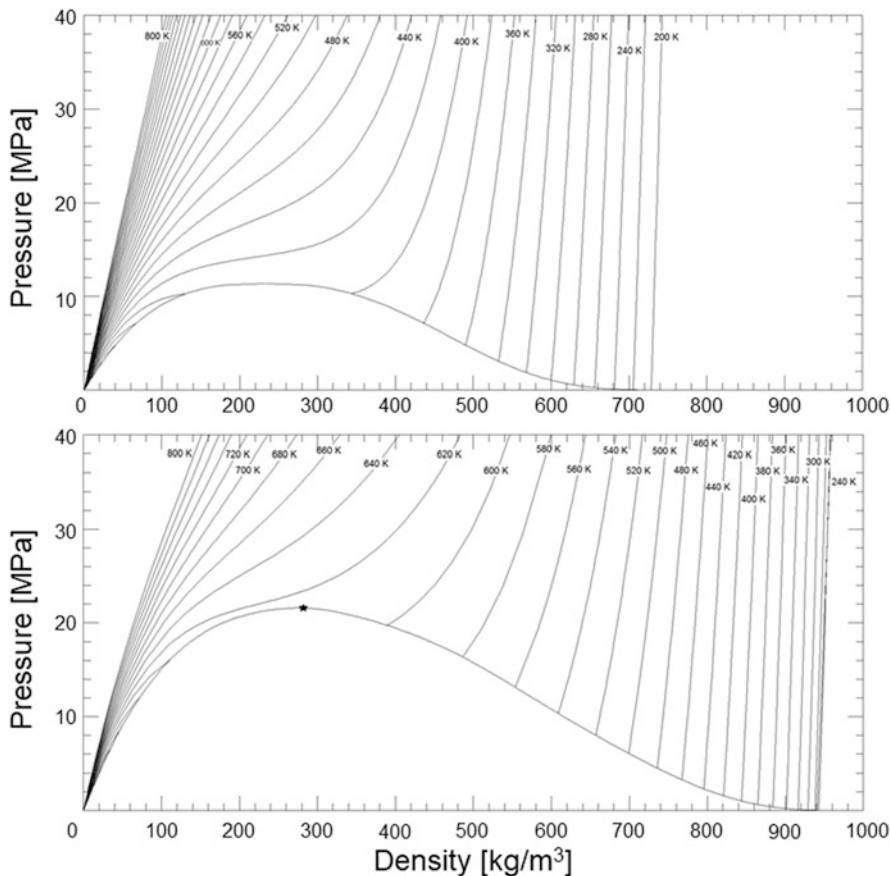


Fig. 11.5 Properties of (top) ammonia and (bottom) ammonia-water ($x_{\text{NH}_3} = 0.2$) calculated with REFPROP 10.0 (NIST). Note that isotherms are shown in units of Kelvin according to available REFPROP 10.0 options

flow sheet as given in the examples in Fig. 11.4 or REFPROP 10.0 (Fig. 11.5). In the next sections, examples are given for hydrothermal processing of organic feedstocks. Although, many solvothermal methods use alcohols to convert wastes into chemical products [26, 27] the use of ammonia-water mixtures are introduced in the last section of this chapter, because these type mixtures provide a means for both hydrothermal treatment of wastes and aminating biomolecule feedstocks, which can be used for sustainable production of nitrogen-containing compounds for pharmaceutical production.

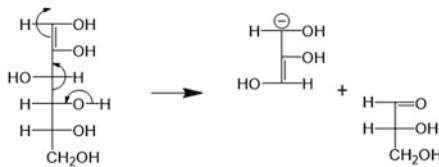
11.3 Carbohydrate Conversion Chemistry in Water at High-Temperatures

Cellulose is one of the major components of organic solid wastes derived from biomass and agricultural waste. Carbohydrates, such as D-glucose, which is the unit monomer of cellulose, are considered as one type of platform chemicals for future biomass refinery processes. For this reason, the understanding of the basic chemistry of carbohydrate reactions in aqueous solutions is important for developing successful hydrothermal processes. In the following section, the basic chemistry of carbohydrate conversions in aqueous solutions will be introduced and then extended to sub- and supercritical conditions emphasizing the product yields and their dependence on water density.

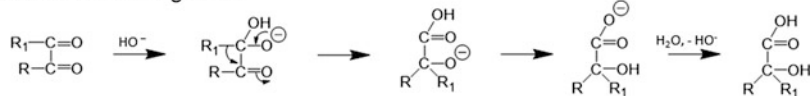
11.3.1 Reactions of D-Glucose in Aqueous Solutions

Many of the reactions of D-glucose and D-fructose that occur in aqueous solutions under acidic and basic conditions also occur in high-temperature water. The reactions of carbohydrates (monosaccharides, polysaccharides) in aqueous systems at various initial pH at or above 100 °C are reviewed extensively in the literature [28, 29]. The characteristic base-catalyzed reactions of monosaccharides in aqueous systems (Scheme 11.1) are: (i) retro-aldol reaction, a decomposition reaction; (ii) benzylic rearrangement reaction, a reaction to form carboxylic acids (saccharic acid) from aldehydes (aldose); (iii) the Lobry de Brun-Alberta van Ekenstein (LBAE) transformation, an aldose-ketose isomerization reaction; (iv) aldol addition, a nucleophilic addition of an aldehyde or ketone enolate to the carbonyl group of an aldehyde or ketone; (v) α -dicarbonyl cleavage reaction, a decomposition of α -dicarbonyl to carboxylic acid and aldehyde; and (vi) β -elimination reaction, an elimination reaction of enediol to dicarbonyl compounds. In acidic aqueous conditions, monosaccharides undergo dehydration reactions as shown in Scheme 11.2. It is well known that various aromatic products such as 5-hydroxymethylfurfural (5-HMF) can be obtained from D-fructose under acidic aqueous conditions. Other various aromatic products besides 5-HMF can also be obtained by treating D-glucose and D-fructose in aqueous acidic conditions [30]. This finding is interesting from the point of view of chemical processing since carbohydrates can provide a variety of compounds having linear or aromatic structures [31].

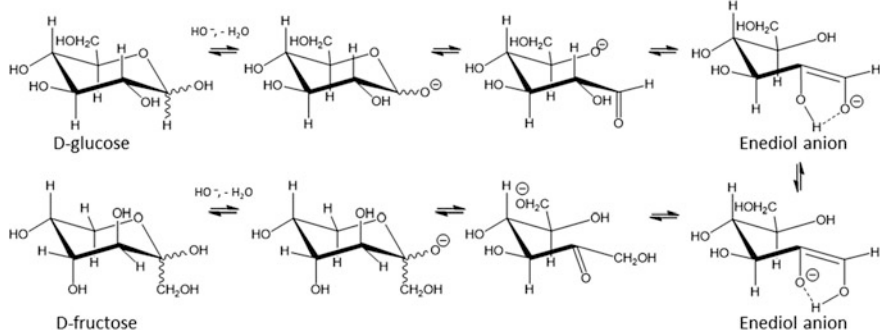
i) Retro-aldol reaction



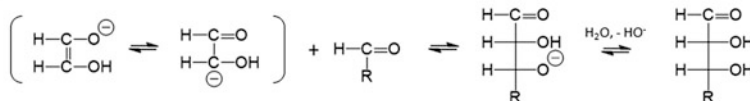
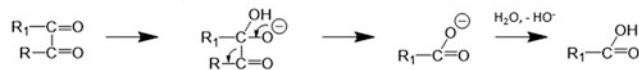
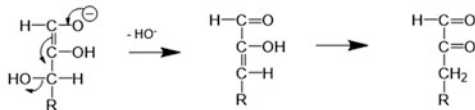
ii) Benzilic acid rearrangement



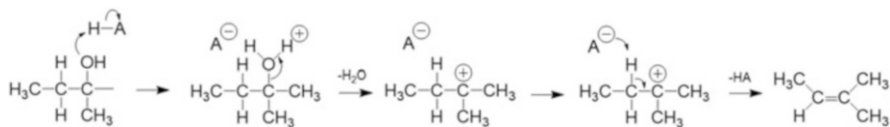
iii) The Lobry de Bruyn-Alberda van Ekenstein rearrangement



iv) Aldol addition

v) α -Dicarbonyl cleavagevi) β -Elimination

Scheme 11.1 Base catalyzed reactions of monosaccharides in aqueous solutions [28, 29]



Scheme 11.2 Mechanism of acid-catalyzed dehydration for 2-methyl-2-butanol as an example [28, 29]

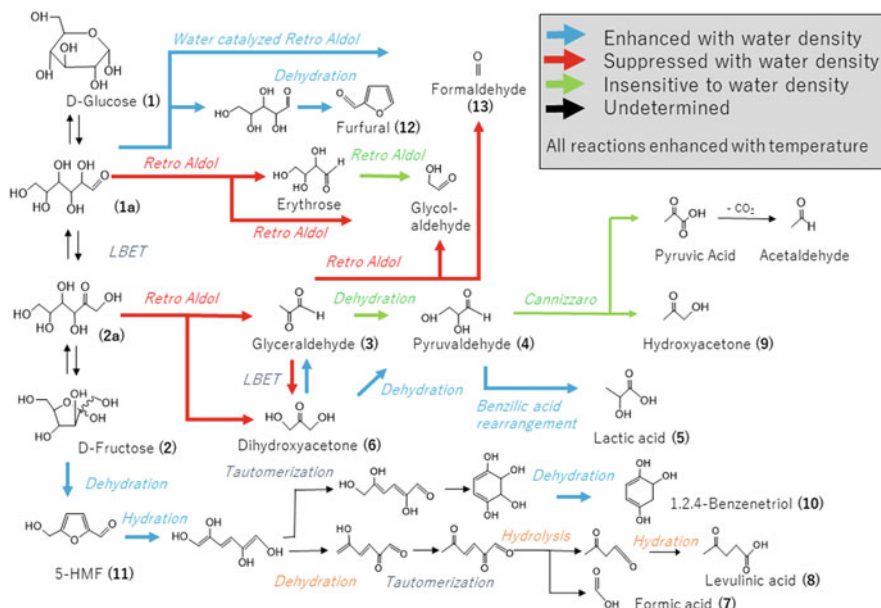


Fig. 11.6 Reaction pathways of D-glucose (1) and D-fructose (2) in high-temperature high-pressure water based on Refs. [6, 7]

11.3.2 Reaction Chemistry of Simple Saccharides in Sub- and Supercritical Water

As introduced in section 11.1, the chemical and physical properties of high-temperature water can be easily controlled by tuning the temperature and pressure, making it both a reactant and a catalyst. These properties of high-temperature water can be used to influence reaction pathways of D-glucose and D-fructose. Reactions of D-glucose and D-fructose in water at high temperatures (350 °C and 400 °C) and high pressures (40 MPa–100 MPa) at reaction times below 5 s were conducted by a continuous flow reactor to elucidate reaction pathways and reaction kinetics by the authors [6, 7]. The reaction pathways of D-glucose and D-fructose are dependent on water density at constant temperature under sub and supercritical conditions (Fig. 11.6) [6, 7]. The products obtained from the hydrothermal treatment of

D-glucose and D-fructose were furfural, 5-HMF, glycolaldehyde, glyceraldehyde, dihydroxyacetone, pyruvaldehyde, hydroxyl acetone, lactic acid, and formaldehyde. These studies showed that various reaction products from linear to cyclic hydrocarbons can be obtained in one-pot synthesis from D-glucose and D-fructose using hydrothermal treatment. In high-temperature water, higher pressures (higher water densities) favor dehydration reactions whereas moderate pressures (low water densities) favor retro-aldol reactions [32]. This trend was also the same for the reactions of pentose (D-xylose) in sub and supercritical conditions [8]. The selectivity of competitive reactions can be explained by the different roles of water molecules in the transition states of the reaction such as (i) transition states where water takes part in the transition state as in dehydration and hydration reactions and (ii) transition states where water does not take part in the transition state such as in retro-aldol reaction [6].

11.4 Reactions of Biopolymers into Chemicals

The reaction chemistry for converting biopolymers into chemicals in hydrothermal systems often relies on the chemical and physical structure of the polymer. Especially, at high-temperature conditions, chemical reactions are fast (on the order of seconds) due to the high kinetic energy. Therefore, even when the final reaction temperatures are the same, hydrothermal reactions conducted at slow and fast heating rates show large differences in product diversity and yields. Rapid heating and short reaction times are essential for improving and achieving product selectivity, especially when undesirable competing reactions exist [33]. In the following sections, the effectiveness of fast heating for hydrothermal conversion into chemicals from model organic waste compounds such as polysaccharides, proteins, lignin and lipids will be demonstrated.

11.4.1 *Conversion of Alginate into Organic Acids in High-Temperature Water Using Fast Heating Rates*

Chemical conversion of cellulose (glucose) to organic acids does not readily occur [34–41] due to structural differences of native biomass and organic acids, and for this reason, the addition of metal salts [42], base catalysts [43] and oxidation agents such as hydrogen peroxide [44–46] are required.

Alginate is a natural polymer found in sea algae. Its chemical structure consists of two hexuronic acids each containing a carboxylic acid in the structure [47]. Unlike biopolymers that do not contain carboxylic acids in their chemical structure, such as cellulose, one can obtain organic acids by simple decomposition of the alginate and preservation of the native carboxylic acid. Hydrothermal treatment of alginate at

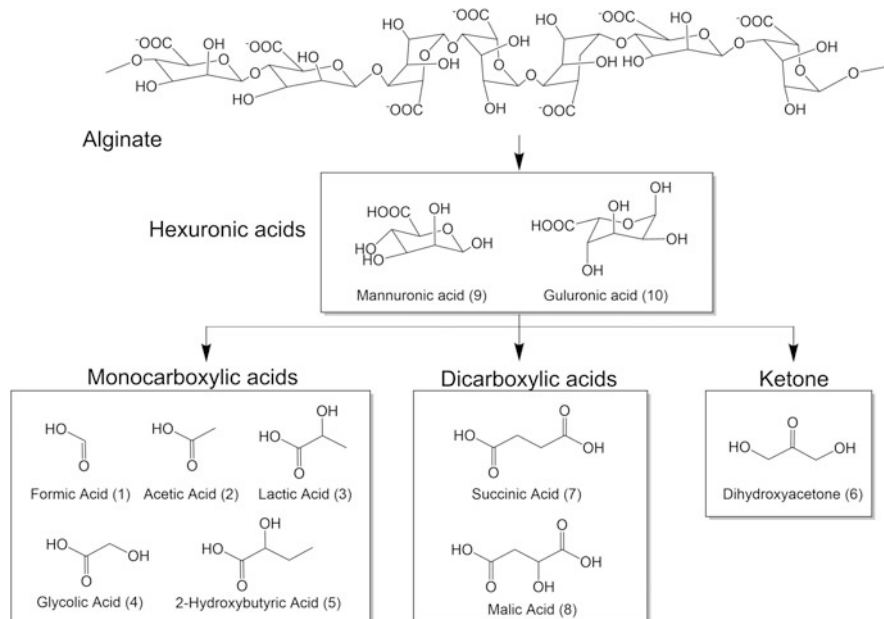


Fig. 11.7 Product distribution obtained from the hydrothermal treatment of sodium alginate and hexuronic acids in high-temperature water at temperatures at 350 °C and 400 °C. Adapted with permission from Ref. [9], Copyright © 2012, Elsevier

temperatures above 250 °C results in various organic acids such as formic acid, acetic acid, glycolic acid, lactic acid, 2-hydroxybutyric acid, succinic acid, malic acid, mannuronic acid, and guluronic acid (Fig. 11.7) [9, 10]. The maximum total yield of the organic acids was obtained when fast heating rates were applied to the hydrothermal treatment resulting in 46% at 350 °C, 40 MPa, and 0.7 s reaction time. The production of organic acids gave evidence that the carboxyl group structure of the alginate was preserved during the hydrothermal decomposition of the alginate [9]. The existence of dicarboxylic acids revealed that not only decomposition reactions but also oxidation reactions occur during the hydrothermal treatment. The vast product distribution indicates that the reaction chemistry is complicated and both acid and base-catalyzed reactions occurred during the hydrothermal treatment of alginate. Further investigation of the hydrothermal treatment of the unit hexuronic acid (mannuronic acid and guluronic acid) resulted in the production of the same organic acids, indicating the reaction from alginate to these organic acids proceeds via the formation of hexuronic acid (Fig. 11.7). These results suggest that hexuronic acids can play a role as platform chemicals for future biorefinery processes.

11.4.2 Controlled Hydrolysis of Proteins into Peptides Using Fast Heating Rates

Peptides are biopolymers that are consisted of 10–50 amino acid monomers linked by peptide bonds. Peptides obtain unique bioactivity such as, lowering blood pressure [48, 49] improving the metabolism of cholesterol [50] and enhancing skin repair [51], making them valuable chemicals for medical, food, and cosmetic industries. Currently, peptides are produced from proteins by biochemical methods using enzymes or with chemical methods using acid and base catalysts. Proteins can be converted into the desired peptides by biochemical methods, however, large amounts of enzymes are required to increase productivity, and multiple separation steps are needed to recover the expensive enzymes, which makes the process economically infeasible [52, 53]. Chemical methods using acid and base treatment can be used to convert proteins to peptides, however, the molecular weight of the product peptide is difficult to control, and undesirable neutralization steps are required for the downstream chemical processing [54, 55]. Previous studies on the decomposition of proteins under hydrothermal conditions conducted in batch reactors report protein solid aggregates and liquid products containing amino acids with low selectivity [56–59].

As proteins are high in molecular weight with a complicated chemical and physical structure, it has been reported that the hydrolysis of proteins fully depends on the local hydrophilicity and the location of the amino acid segments [60]. However, in previous research on hydrothermal treatment of a protein, bovine serum albumin (BSA), the decomposition of the protein differed greatly between fast ($135\text{ }^{\circ}\text{C s}^{-1}$ to $180\text{ }^{\circ}\text{C s}^{-1}$) and slow-heating rate ($0.25\text{ }^{\circ}\text{C s}^{-1}$) conditions [11]. In this study, the kinetic analysis showed evidence that the decomposition of BSA proceeded under a random scission mechanism only when the hydrothermal treatment was conducted at fast heating rates and not when the heating rates were slow (Fig. 11.8). At room temperature conditions, BSA takes the form of an unfolded state (unfolded-BSA) in water. However, BSA is known to aggregate around temperatures at $80\text{ }^{\circ}\text{C}$ [61]. This aggregation may have occurred significantly during the slow heating, leading to selective hydrolysis at the solid–liquid interface of the aggregated protein at elevated temperatures [62]. Shenan et al. [63] conducted investigations on hydrothermal treatment of BSA under relatively slower heating rates ($2.9\text{ }^{\circ}\text{C s}^{-1}$ to $5\text{ }^{\circ}\text{C s}^{-1}$) and higher temperatures ($350\text{ }^{\circ}\text{C}$) which gave 50% of primary and secondary amino acids and 40% NH_3 with no peptides above 5 kDa.

Hydrothermal treatment of proteins with fast-heating rates allows depolymerization of proteins to peptides with controllable molecular weights by inhibiting protein aggregation. This key technique applies not only to proteins, but also to many natural polymers so that there are wide opportunities for fast-heating of water with proteins for future food, pharmaceutical, cosmetic industries, and also for waste treatment and biomass refineries.

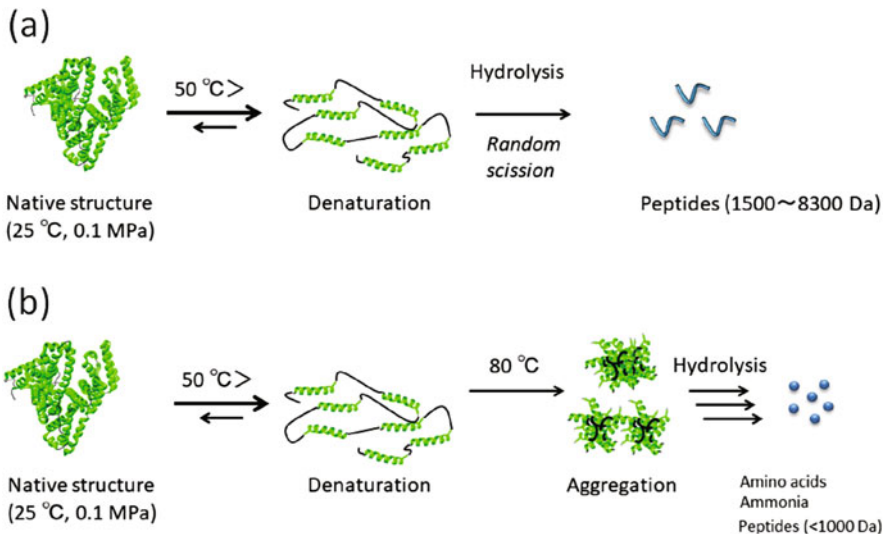


Fig. 11.8 Different decomposition mechanisms of Bovine serum albumin protein BSA in high-temperature water as a function of heating rates: (a) fast-heating-rates ($135\text{ }^{\circ}\text{C s}^{-1}$ to $180\text{ }^{\circ}\text{C s}^{-1}$), (b) slow-heating-rates ($0.25\text{ }^{\circ}\text{C} \cdot \text{s}^{-1}$). Adapted with permission from Ref. [11], Copyright © 2017, American Chemical Society

11.4.3 Reactions of Other Biopolymers (Lignin and Lipids) Under Hydrothermal and Fast Heating Rates

Biopolymers such as lignin and lipids are also major compounds found in organic solids. Lignin is one of the major biopolymers found in lignocellulosic biomass next to cellulose and hemicellulose, which can be present in amounts of (20–30) wt % depending on the type of biomass [64, 65]. Lignin is an aromatic polymer with a high molecular weight (~100 kDa) similar to phenolic resin, consisting of 3 main types of structural units, p-coumaryl alcohol, coniferyl alcohol, and sinapyl alcohol, connected to each by C-C and ether bonds [66, 67], giving a highly complex 3-D structure. Due to the highly aromatic and cross-linked chemical structure of lignin, lignin is more difficult to controllably degrade than other biopolymers such as cellulose and raw biomass (saw dust, rice hull) under hydrothermal conditions ($280\text{ }^{\circ}\text{C}$, 15 min) [68]. Thermo-chemical processes of lignin have also been under investigation such as liquefaction, gasification and combustion [64]. Hydrothermal reaction of lignin often results in low molecular weight phenolic fragments and high molecular weight crosslinked char as shown in Fig. 11.9. [69–73]. The yields of

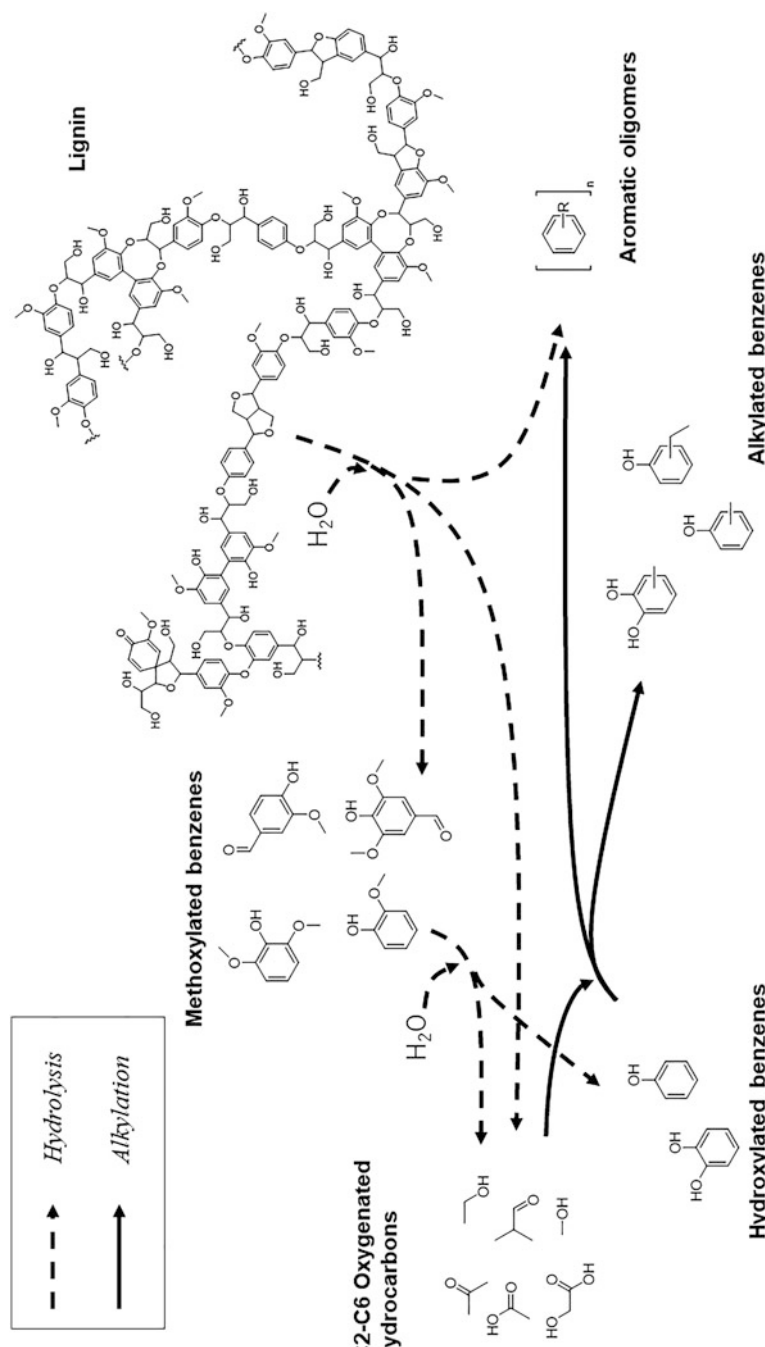


Fig. 11.9 Proposed reaction mechanism of lignin under hydrothermal conditions. Adapted with permission from Ref. [69]. Copyright © 2012 Elsevier

phenolic compounds can be controlled according to the temperature pressure and heating rate of the hydrothermal treatment [12, 74]. Fast heating hydrothermal reaction of lignin conducted at sub and supercritical water conditions using a continuous flow reactor by Abad-Fernandez et al. [12], who reported that higher oil yields were obtained at high temperatures and short reaction times (seconds) compared with low temperature and long reaction time conditions. Those authors speculated that enhancement of oil at high temperatures and short reaction times was due to enhanced fragmentation of the lignin and the reduction of secondary reactions to form char [12]. Further details on lignin conversion can be found in reviews [64, 66, 75].

Lipids are biomolecules found in biomass. The lipid content can reach up to 20–30% for microalgae [76]. Lipids consist of one tryglyceride and three fatty acid linked by a ester bonds. Lipids can be converted into biodiesel, fatty acid methyl esters (FAME), by transesterification using a catalyst. Biodiesel can be used as fuel for diesel engines directly or after simple modification. Details of these processes can be found in the literature [76–79]. Lipids can also be converted into liquid fuel via production of biocrude and hydrogenation using catalysts [80]. Biocrude is a substance obtained by often the hydrothermal liquefaction process (HTL) of microalgae and various organic solids. Hydrothermal liquefaction has an advantage for processing organic solids with high water content as no drying is required. The reaction mechanism of biocrude under hydrothermal conditions is considered to start with the fragmentation of the individual biopolymers often through the hydrolysis continued with secondary condensation reactions between the fragmentated compounds to form biocrude compounds as shown in Fig. 11.10 [81, 82]. Fast heating hydrothermal liquefaction of organic solids to obtain biocrude from feedstocks such as bacteria and yeast monocultures [83], green marine alga [84], chitin [85], microalgae [86], polysaccharides [87], sewage sludge [88], and model food wastes [13] have been reported by the group of Savage [13, 83–88], indicating that fast heating rates increase the biocrude yields compared to slow hydrothermal heating conditions often discussed by the suppression of condensation reactions to result in the formation of char. The interested reader is referred to reviews in the literature for more detailed studies on hydrothermal liquefaction processes [80, 81, 89].

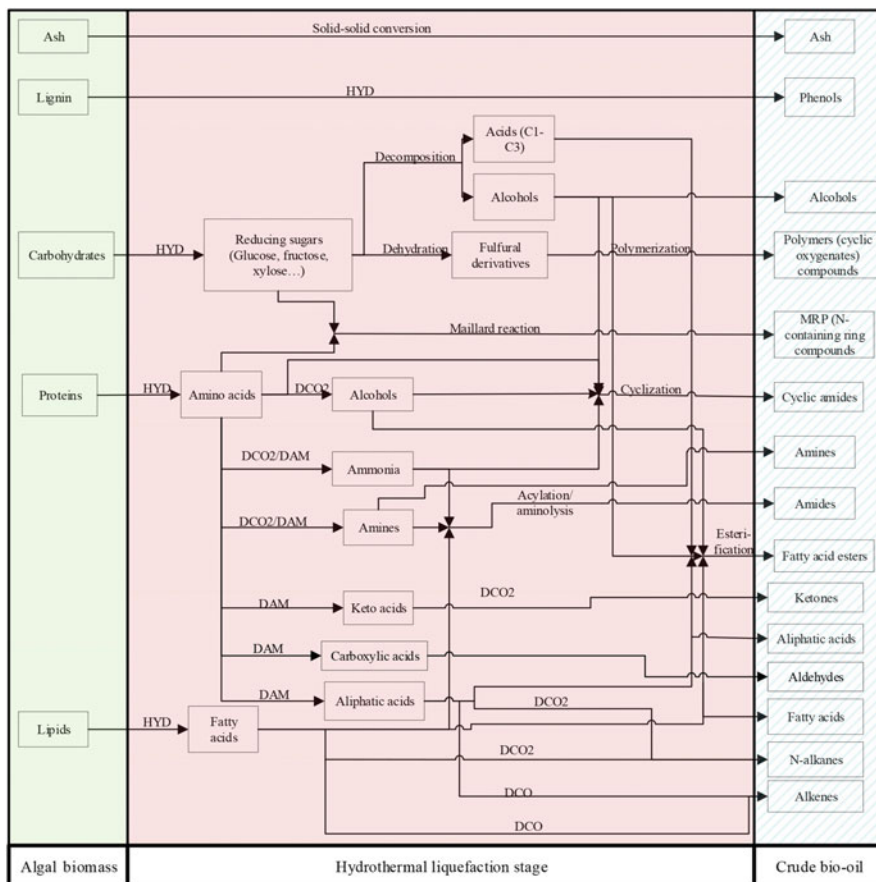


Fig. 11.10 Proposed reaction mechanism of algae to crude bio-oil (biocrude) by hydrothermal liquefaction process (DCO decarbonylation, DCO_2 decarboxylation, DAM deamination, HYD hydrolysis). Adapted with permission from Ref. [81], Copyright © 2020 American Chemical Society

11.5 Recycle Nutrients from Municipal Sludge and Defatted Microalgae for Microalgae Production

In this section, examples are introduced on hydrothermal methods for converting actual organic solid wastes such as municipal sludge and defatted microalgae into liquid nutrients for developing a sustainable microalgae cultivation process. Microalgae is a fast-growing, non-food competitive, and high lipid content biomass feedstock making it a promising source for producing chemicals and liquid fuels [76–79]. However, the mass production of bio-oil from microalgae has yet to be realized [90, 91]. One big issue is the supply of nutrients such as nitrogen and phosphorous for microalgae cultivation [90–94]. The nutrients required for microalgae cultivation will compete with agricultural commercial fertilizer and lead to a cost increase of the bio-oil and food [95, 96]. Therefore, to achieve

sustainable production of bio-oil, methods to recycle nutrients from organic solid wastes such as wastewater [97–99], microalgae [100–104], and lipid extracted (or defatted) microalgae [105] need to be considered. In the following sections, we will introduce the nutrient recovery from municipal waste and defatted algae for microalgae cultivation.

11.5.1 Coupling of Municipal Waste with Hydrothermal Processing for Nutrient Recycling

Municipal wastewater from treatment plants contains liquid and solid components that are rich in nitrogen, phosphorus, and undigested organic carbon compounds. The liquid portion of wastewater can be used as a nutrient source for cultivating autotrophic microalgae [99]. Municipal sludge, which is the solid portion of the wastewater stream, especially primary sludge, which is sludge before anaerobic digestion, is a mixture of natural polymers such as proteins and polysaccharides (cellulose) that contains nitrogen, phosphorous, and carbon in their chemical structures. However, unlike the liquid portion of wastewater, the nitrogen, phosphorous, and carbon in the municipal sludge cannot be absorbed by microalgae in solid form. As shown in the previous sections, these natural polymers, proteins, and polysaccharides can be converted into amino acids and sugars by hydrothermal methods, which then can allow them to be used as nutrients for algae cultivation. Currently, wastewater treatment facilities apply anaerobic digestion to produce biogas, and the sludge is dewatered for incineration or landfill [106, 107]. Where incineration is used as an integral part of the wastewater treatment plant, as for the case in Japan, coupling municipal waste with hydrothermal processing for nutrient recycling is promising as waste heat can also be recycled for generating the hydrothermal conditions.

An investigation for converting the solid portion of municipal sludge into nitrogen and carbon liquid nutrients that can be used for microalgae cultivation was conducted by the authors [14]. Liquid products obtained from hydrothermal treatment of municipal sludge at relatively harsh reaction conditions (275 °C, 60 min), where cellulose and proteins readily undergo decomposition were found to be insufficient as a nutrient for algae cultivation. The formation of toxic compounds (melanoidin) produced through Maillard reactions between sugars and amino acids was found to be responsible for the inhibitory effects of hydrothermal processing. The problem can be solved by applying a two-step method. A two-step hydrothermal method applied to municipal sludge allows one to obtain liquid products without the formation of melanoidin as shown in Fig. 11.11. In the first step, hydrothermal treatment is conducted at mild temperatures (225 °C, 15 min), where (i) protein decomposition occurs that forms liquid products containing nitrogen and (ii) cellulose decomposition does not occur, thus isolating the cellulose as a solid residue. In the second step, acid saccharification of the residue (cellulose content 60 wt%), is conducted to obtain a glucose solution. The liquid products obtained are

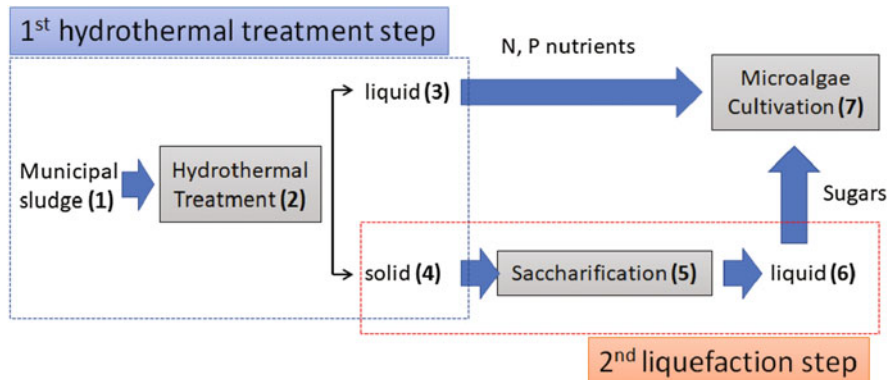


Fig. 11.11 Two-step hydrothermal method for nutrient (nitrogen, phosphorous, and glucose) recycle from municipal sludge; first step: municipal sludge (1) is treated under hydrothermal conditions (2) to separate nitrogen and phosphorous in the liquid product (3) and isolate cellulose in the solid (4), second step; acid saccharification (5) of solid (4) into liquid (6) containing glucose. By this method, production of poisonous compounds (melanoidin) for microalgae cultivation can be avoided thus making microalgae cultivation (7) from liquids (3) and (6) feasible and environmental. Adapted with permission from Ref. [14], Copyright © 2016 Elsevier

effective as nutrients for both mixotrophic microalgae (*Euglena gracilis*) and heterotrophic microalgae (*Aurantiochytrium*). However, not discussed in this paper, the choice of hydrothermal conditions where the decomposition of lignin to phenolic compounds (growth inhibiting agents) are suppressed may be key issues to consider in future studies, especially for lignocellulosic organic matter with high lignin content. The coupling of hydrothermal treatment with microalgae cultivation within a wastewater treatment process not only allows internal recycling of heat and chemicals for biofuels but also reduces the mass of the municipal sludge that is incinerated and so increases the efficiency and sustainability of the overall process.

Hydrothermal carbonization of residual biomass to produce materials with high carbon content (hydrochar) has been a topic under heavy investigation [108–111]. Hydrothermal carbonization (HTC) is similar to pyrolysis (PY) as both are conducted at high temperatures (HTC: 180 °C–250 °C, PY: >400 °C) except HTC is conducted in water or with organic material with high water content [108]. The production of hydrochar by hydrothermal carbonization of municipal sludge [94, 112] as well as processes for recovering nutrients such as nitrogen and phosphorous that can be used for agricultural purposes have also been reported [113]. The interested reader is encouraged to explore reviews on the utilization of municipal sludge with hydrothermal treatment [5, 108, 109, 114].

11.5.2 Nutrient Recycling from Microalgae with Hydrothermal Processing

Microalgae are considered to be a third-generation feedstock for biofuels [76–79]. Compared with conventional biomass feedstocks, microalgae have a fast growth

rate and high lipid content and do not compete with food. Methods to isolate not only lipids and valuable by-products from the microalgae have been reported in the literature, but the production of biofuels also have not reached industrial scale [90, 91]. Sustainability issues such as obtaining cheap nutrients arise when the production of bio-oil from microalgae on an industrial scale is analyzed. For this reason, methods for recycling nutrients from defatted microalgae have been studied [90–93]. Currently, converting defatted microalgae into gas and biocrude has been achieved through anaerobic digestion [90], catalytic hydrothermal gasification [115], hydrothermal liquefaction [116], and pyrolysis [117]. The author developed a hydrothermal method for recovering nitrogen and phosphorous nutrients from defatted microalgae for microalgae cultivation [15] (Fig. 11.12.) where hydrothermal treatment was conducted on the representative defatted microalgae (*Aurantiochytrium limacinum* SR21) at 175–350 °C for reaction times of 10–90 min. Nitrogen and phosphorous nutrients were obtained in the water-soluble fraction (WS) from the hydrothermal treatment. Depending on the condition of the hydrothermal treatment, up to 100% of the nitrogen and phosphorous in defatted microalgae was converted into compounds in the water-soluble (WS) fraction. The distribution of the nitrogen containing compounds such as proteins, amino acids and ammonia also showed to change with the hydrothermal treatment condition (Fig. 11.13). At mild hydrothermal conditions (175 °C), nitrogen in the WS fraction is likely to take the form of high molecular weight proteins while as the hydrothermal conditions get severe (350 °C), the decomposition of proteins into smaller compounds, such as amino acids and ammonia occur. The individual maximum yields of nitrogen containing compounds in WS fraction were obtained according to the hydrothermal conditions: proteins (43%), amino acids (12%) and ammonia (60%), obtained at hydrothermal treatment temperatures of 175 °C, 250 °C and 350 °C, respectively. The maximum yield (100%) of phosphorous in WS was obtained at a treatment temperature of 250 °C. The WS fraction from hydrothermal

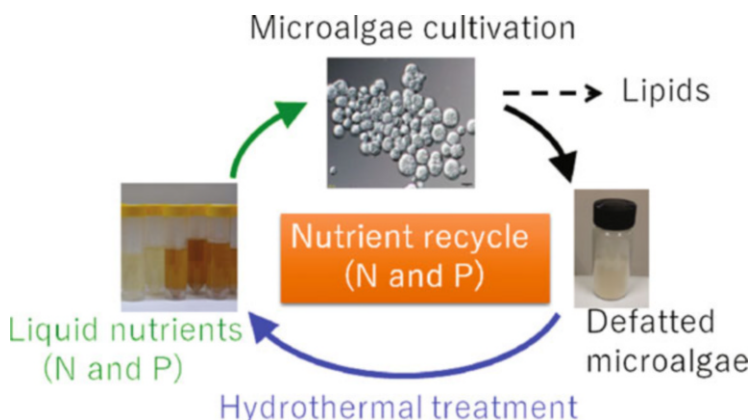


Fig. 11.12 Nutrient recycling from defatted microalgae (*Aurantiochytrium limacinum* SR21) for microalgae (*Aurantiochytrium limacinum* SR21) cultivation using hydrothermal treatment. Adapted with permission from Ref. [15], Copyright © 2017 Elsevier

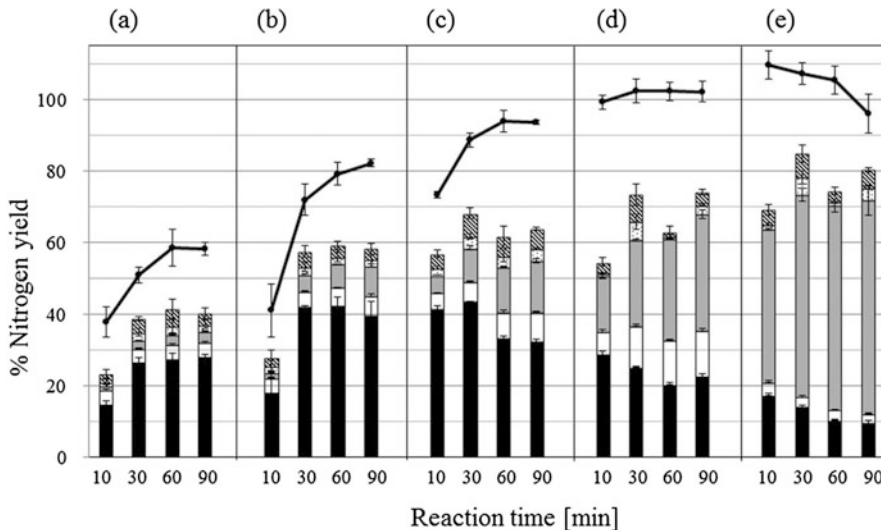


Fig. 11.13 Distribution of nitrogen-containing compounds in water-soluble fraction obtained from hydrothermal treatment of defatted microalgae (*Aurantiochytrium limacinum* SR21) as a function of temperature and treatment time: (a) 150 °C, (b) 175 °C, (c) 200 °C, (d) 250 °C, (e) 350 °C. Total nitrogen yield is given as solid lines and individual nitrogen-containing products are given as bars: black (proteins), white (amino acids), gray (ammonia), dotted (nitrites), hatched (nitrates). Adapted with permission from Ref. [15], Copyright © 2017 Elsevier

treatment of defatted microalgae is an effective nitrogen and phosphorous nutrient source for microalgae cultivation (*A. limacinum* SR21).

11.6 Top-Down Approach with Hydrothermal and Solvothermal Methods of Large Molecules into Smaller Size Functional Chemicals

The production of chemicals containing nitrogen in the chemical structure is of great importance for current and future chemical industries [118]. However, many biomass feedstocks considered for biomass refinery such as lignocellulose biomass do not have sufficient nitrogen content for producing nitrogen-containing chemicals. Strategies for converting large molecule substrates with high-temperature water, water-ammonia mixtures under hydrothermal conditions, or supercritical water - ammonia mixtures to produce aminated products are given in Fig. 11.14 [118].

One strategy is to employ an external nitrogen source in the hydrothermal treatment process. For example, when hydrothermal treatment of lignocellulosic materials with ammonia-water mixtures is conducted, pyrrole, pyridine, indole, and other heterocyclic nitrogen compounds are obtained. Another strategy is to choose a biomass feedstock containing nitrogen and to transform it into small-sized nitrogen-containing functional chemicals. For example, when chitin is used

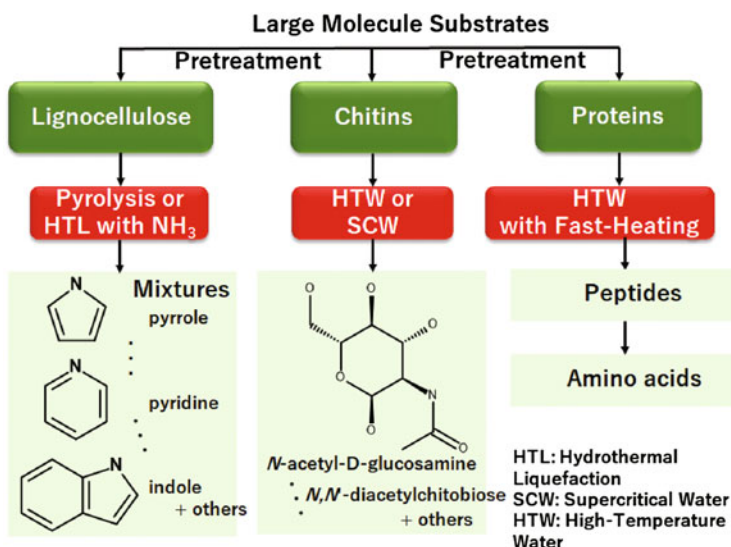


Fig. 11.14 Top-down approach with hydrothermal and solvothermal methods to convert large molecules into smaller size functional compounds. Adapted with permission from Ref. [118] Published by The Royal Society of Chemistry™

as the biomass feedstock, glucosamines can be obtained and when proteins are used, peptides are obtained as described in the above sections. Among the strategies in Fig. 11.14, HTW with fast-heating is the simplest way to modify a protein selectively.

In these top-down approaches, pretreatment methods to increase the affinity between water and biomass feedstock are important for obtaining controllable results and sufficient product selectivity. For example, in the hydrothermal decomposition of hydrophilic polymers such as chitin, hydrolysis reactions tend to be restricted to the solid-liquid interphase. In a previous study by the authors [16], pretreatment of chitin was conducted by mechanically milling resulting in reduced crystallinity and increased solubility in water. The solubility of chitin in room temperature water increased from 3% to 35% by this mechanical milling pretreatment thus allowing higher liquid product yields (73%) than that of the raw chitin (6%) [16]. In that study [16], hydrothermal treatment was conducted in batch-type reactors, where the heating rates are slow. Hydrothermal treatment of the dissolved chitin in aqueous solutions with fast heating techniques can convert these polymers efficiently and in a controllable manner to the desired chemicals. Hydrothermal treatment with ammonia-water mixtures would drastically change the reaction chemistry to produce chemical products that include highly functional nitrogen-containing chemical structures giving a promising path to N-containing compounds [119].

Table 11.2. summarizes selected studies in the literature along with those presented in this chapter. With fast-heating techniques, a wide variety of organic

Table 11.2 Selected studies that use fast-heating methods to convert substrates into liquid products

No.	Substrate	T [°C]	Reaction time	Solvent	Additive	Major products (yield)	Ref.
1.	Bacteria and yeast monocultures	276 ± 41 °C	1 min (3.6 °C s ⁻¹)	H ₂ O	—	Biocrude (50%)	[83]
2.	Casen	600	60 s	H ₂ O	—	P (21%), N (57%), water solubles (62%) biocrude (20%)	[13, 120]
3.	Cellulose	250	60 s	H ₂ O	O ₂ , NaOH	formate (46%)	[120]
4.	chitin	500	60 s	H ₂ O	—	biocrude (25%)	[85]
5.	chitin (raw)	400	1 min	H ₂ O	—	Liquid products (6%), residue (98%)	[16]
6.	chitin (milled)	400	1 min	H ₂ O	—	Liquid products (74%), residue (26%)	[16]
7.	Coconut husks	300	120 s	H ₂ O	HCl	Formic/acetic acids (50%)	[121]
8.	Corn cob	700	2.4 s	NH ₃	2%Ga/HZSM5	acetonitrile (18%)	[119]
9.	Green marine alga	600	60 s	H ₂ O	—	biocrude (66%)	[84]
10.	Hyaluronic acid	180–260	<18 s	H ₂ O	—	Low mw hyaluronic acids (<9.0 × 10 ⁵ Da)	[17]
11.	Lignin	300–400	60 ms	H ₂ O	—	Aromatic oil (45%)	[12]
12.	Macro-alga	350 °C	15 min (9.8 °C s ⁻¹)	H ₂ O	—	Biocrude (79%)	[86, 122]
13.	Microalgae	186	60 s	H ₂ O	—	biocrude (47%)	[86]
14.	polyethylene terephthalate	500	ca. s	NH ₃	γ-Al ₂ O ₃	Terephthalonitrile (52.3%)	[123]
15.	Polysaccharides	500	60 s	H ₂ O	—	biocrude (20%)	[87]
16.	Potato starch	450	60 s	H ₂ O	—	Water solubles (50%)	[13]
17.	protein (BSA)	200–260	8–18 s	H ₂ O	—	Peptides (ca. 1500–8000 Da)	[11]
18.	Sewage sludge	500	60 s	H ₂ O	—	biocrude (27%)	[88]
19.	Simulated food waste	250	60 s	H ₂ O	O ₂ , NaOH	formate (42%)	[120]
20.	Sodium alginate	350–400	0.1–5 s	H ₂ O	—	Organic acids (36–46%)	[9]
21.	Soy protein	450	90 s	H ₂ O	—	Water solubles (48%) biocrude (40%)	[124]
22.	Starch	250	60 s	H ₂ O	O ₂ , NaOH	formate (78.2%)	[120]
23.	Wheat straw	250	1–2 h	H ₂ O	CuO	Cu (90%), organic acids	[125]
24.	Wood—willow	403	22 s	H ₂ O	—	Water solubles (99%)	[126]

solid wastes can be readily and rapidly converted into less definable mixtures such as bio-crudes. On the other hand, with careful choice of feedstock, pretreatment measures, and reaction conditions that may include catalysts, fast-heating techniques can be advantageously used to produce targeted chemical products such as formate, formic acid, acetic acid, acetonitrile, uronic acids, terephthalonitrile, or low molecular weight peptides. The reader is encouraged to explore other substrates with fast-heating with water and solvothermal methods which allow selectivity control.

11.7 Conclusions

Organic solid wastes derived from biomass can be converted into chemicals using top-down methods using either hydrothermal (water) or solvothermal (ammonia, water-ammonia) processing. Controllable physical properties of water and ammonia with temperature and pressure combined with fast-heating rates change reaction chemistry and product selectivity. By using fast-heating hydrothermal techniques, one can convert organic solid wastes into a wide range of chemical products. Optimization of hydrothermal treatment methods includes choice of temperature, pressure, heating rate, and reaction time, but also depends greatly on the physical properties of the substrate. Pretreatment to increase the affinity of the substrate for water such as reducing its crystallinity and intra-molecular-hydrogen-bonding are effective methods for increasing the efficiency of the hydrothermal reactions. Here, mechanochemical methods have been applied as a pretreatment method to reduce substrate crystallinity or to introduce additives, nitrogen sources, or catalysts into the feedstocks. The addition of a nitrogen source such as ammonia to the hydrothermal environment allows the further introduction of nitrogen into the product chemical. Further understanding of fundamental principles for applying hydrothermal and solvothermal methods to various organic solid wastes will give opportunities for research and development for future biorefineries. These techniques can also be applied for producing advanced materials for advanced medical and pharmaceutical applications.

References

1. (IEA) IEA. Global energy review: the impacts of the COVID 19 crisis on global demand and CO₂ emissions. 2020 [cited 2021 June 24]; <https://www.iea.org/reports/global-energy-review-2020>.
2. Cherubini F, Jungmeier G, Wellisch M, Willke T, Skiadas I, Van Ree R, de Jong E. Toward a common classification approach for biorefinery systems. Biofuels Bioprod Biorefining Biofpr. 2009;3(5):534–46. <https://doi.org/10.1002/bbb.172>.
3. Shen F, Smith RL Jr, Li J, Guo H, Zhang X, Qi X. Critical assessment of reaction pathways for conversion of agricultural waste biomass into formic acid. Green Chem. 2021; <https://doi.org/10.1039/D0GC04263C>.

4. Fang Z, Smith RL, Li H. Special issue on hydrothermal and solvothermal approaches toward bio-products preface. *J Supercrit Fluids.* 2020;165(5):8076–88. <https://doi.org/10.1016/j.supflu.2020.104975>.
5. Leng LJ, Zhang WJ, Leng SQ, Chen J, Yang LH, Li HL, Jiang SJ, Huang HJ. Bioenergy recovery from wastewater produced by hydrothermal processing biomass: progress, challenges, and opportunities. *Sci Total Environ.* 2020;748 <https://doi.org/10.1016/j.scitotenv.2020.142383>.
6. Aida TM, Sato Y, Watanabe M, Tajima K, Nonaka T, Hattori H, Arai K. Dehydration of D-glucose in high temperature water at pressures up to 80 MPa. *J Supercrit Fluids.* 2007;40(3): 381–8. <https://doi.org/10.1016/j.supflu.2006.07.027>.
7. Aida TM, Tajima K, Watanabe M, Saito Y, Kuroda K, Nonaka T, Hattori H, Smith RL, Arai K. Reactions of D-fructose in water at temperatures up to 400 °C and pressures up to 100 MPa. *J Supercrit Fluids.* 2007; <https://doi.org/10.1016/j.supflu.2006.12.017>.
8. Aida TM, Shiraishi N, Kubo M, Watanabe M, Smith RL. Reaction kinetics of D-xylose in sub- and supercritical water. *J Supercrit Fluids.* 2010;55(1):208–16. <https://doi.org/10.1016/j.supflu.2010.08.013>.
9. Aida TM, Yamagata T, Abe C, Kawanami H, Watanabe M, Smith RL. Production of organic acids from alginates in high temperature water. *J Supercrit Fluids.* 2012;65:39–44. <https://doi.org/10.1016/j.supflu.2012.02.021>.
10. Aida TM, Yamagata T, Watanabe M, Smith RL. Depolymerization of sodium alginate under hydrothermal conditions. *Carbohydr Polym.* 2010;80(1):296–302. <https://doi.org/10.1016/j.carbpol.2009.11.032>.
11. Aida TM, Oshima M, Smith RL. Controlled conversion of proteins into high-molecular-weight peptides without additives with high-temperature water and fast heating rates. *ACS Sustain Chem Eng.* 2017;5(9):7709–15. <https://doi.org/10.1021/acssuschemeng.7b01146>.
12. Abad-Fernandez N, Perez E, Martin A, Cocero MJ. Kraft lignin depolymerisation in sub- and supercritical water using ultrafast continuous reactors. Optimization and reaction kinetics. *J Supercrit Fluids.* 2020;165 <https://doi.org/10.1016/j.supflu.2020.104940>.
13. Gollakota A, Savage PE. Hydrothermal liquefaction of model food waste biomolecules and ternary mixtures under isothermal and fast conditions. *ACS Sustain Chem Eng.* 2018;6(7): 9018–27. <https://doi.org/10.1021/acssuschemeng.8b01368>.
14. Aida TM, Nonaka T, Fukuda S, Kujiraoka H, Kumagai Y, Maruta R, Ota M, Suzuki I, Watanabe MM, Inomata H, Smith RL. Nutrient recovery from municipal sludge for microalgae cultivation with two-step hydrothermal liquefaction. *Algal Res Biomass Biofuels Bioproducts.* 2016;18:61–8. <https://doi.org/10.1016/j.algal.2016.06.009>.
15. Aida TM, Maruta R, Tanabe Y, Oshima M, Nonaka T, Kujiraoka H, Kumagai Y, Ota M, Suzuki I, Watanabe MM, Inomata H, Smith RL. Nutrient recycle from defatted microalgae (aurantiochytrium) with hydrothermal treatment for microalgae cultivation. *Bioresour Technol.* 2017;228:186–92. <https://doi.org/10.1016/j.biortech.2016.12.078>.
16. Aida TM, Oshima K, Abe C, Maruta R, Iguchi M, Watanabe M, Smith RL. Dissolution of mechanically milled chitin in high temperature water. *Carbohydr Polym.* 2014;106:172–8. <https://doi.org/10.1016/j.carbpol.2014.02.009>.
17. Aida TM, Oshima M, Sharmin T, Mishima K, Smith RL. Controlled conversion of sodium hyaluronate into low-molecular-weight polymers without additives using high-temperature water and fast-heating-rates. *J Supercrit Fluids.* 2020;155. <https://doi.org/10.1016/j.supflu.2019.104638>.
18. Merriam-Webster. “Hydrothermal.” *Merriam-Webster.com* Dictionary. 2021 [cited 2021 Jan. 31]; <https://www.merriam-webster.com/dictionary/hydrothermal>
19. Chaplin M. Water structure and science. 2003 [cited 2021 June 24]; <https://web.archive.org/web/20201210040133/http://www1.lsbu.ac.uk/water/>
20. Smith RL, Inomata H, Peters C. Website for Smith, inomata, peters: introduction to supercritical fluids: a spreadsheet-based approach. [cited 2021 June 21]; <https://booksite.elsevier.com/9780444522153/>

21. Smith RL, Inomata H, Peters C. Introduction to Supercritical FLuids: a spreadsheet-based approach, vol. 4. 1st ed. Elsevier Science; 2013.
22. The International Association for the Properties of Water and Steam. January 4, 2021 [cited 2021 June 24]; <http://www.iapws.org/index.html>
23. NIST Chemistry WebBook. Thermophysical properties of fluid systems. National Institute of Standards and Technology. 2018 [cited 2021 June 24]; <https://webbook.nist.gov/chemistry/fluid/>.
24. Alexandrov AA, Orlov KA, Ochkov VF. Thermophysical properties of thermal power engineering working substances. 2012 [cited 2021 June 24]; <http://twt.mpei.ac.ru/rbtpp/eng/>; <http://twt.mpei.ac.ru/MCS/Worksheets/WSP/KwTPo.xmcd>.
25. Thermodynamic and Transport Properties Database (REFPROP), National Institute of Standards and Technology. 2013 [cited 2021 June 24]; <https://www.nist.gov/srd/refprop>.
26. Liu M, Guo J, Gu Y, Gao J, Liu F, Yu S. Pushing the limits in alcoholysis of waste polycarbonate with DBU-based ionic liquids under metal- and solvent-free conditions. ACS Sustain Chem Eng. 2018;6(10):13114–21. <https://doi.org/10.1021/acssuschemeng.8b02650>.
27. Petrus R, Utko J, Gniłka R, Fleszar MG, Lis T, Sobota P. Solvothermal alcoholysis method for recycling high-consistency silicone rubber waste. Macromolecules. 2021;54(5):2449–65. <https://doi.org/10.1021/acs.macromol.0c02773>.
28. Brujin JM, Kieboom APG, Bekkum H, Poel PW. Reactions of monosaccharides in aqueous solutions. Sugar Technol Rev. 1986;13:21–52.
29. Theander O, Nelson DA. Aqueous, high-temperature transformation of carbohydrates relative to utilization of biomass. Adv Carbohydr Chem Biochem. 1988;46:273–326. [https://doi.org/10.1016/S0065-2318\(08\)60169-9](https://doi.org/10.1016/S0065-2318(08)60169-9).
30. Popoff T, Theander O. Formation of aromatic-compounds from carbohydrates 4. Chromosomes from reaction of hexuronic acids in slightly acidic, aqueous-solution. Acta Chem Scand Ser B. 1976;30(8):705–10. [https://doi.org/10.1016/S0008-6215\(00\)85733-X](https://doi.org/10.1016/S0008-6215(00)85733-X).
31. Tajima K. Carbohydrate, an organic compound with clever tricks. Biosci Ind (written in Japanese). 1998;56(10):671–4.
32. Sasaki M, Goto K, Tajima K, Adschari T, Arai K. Rapid and selective retro-aldol condensation of glucose to glycolaldehyde in supercritical water. Green Chem. 2002;4(3):285–7. <https://doi.org/10.1039/B203968K>.
33. Wang K, Ma QL, Burns M, Sudibyo H, Sills DL, Goldfarb JL, Tester JW. Impact of feed injection and batch processing methods in hydrothermal liquefaction. J Supercrit Fluids. 2020; 164. <https://doi.org/10.1016/j.supflu.2020.104887>.
34. Brunner G. Near critical and supercritical water. Part I. Hydrolytic and hydrothermal processes. J Supercrit Fluids. 2009;47(3):373–81. <https://doi.org/10.1016/j.supflu.2008.09.002>.
35. Kruse A, Bernolle P, Dahmen N, Dinjus E, Maniam P. Hydrothermal gasification of biomass: consecutive reactions to long-living intermediates. Energy Environ Sci. 2010;3(1):136–43. <https://doi.org/10.1039/B915034J>.
36. Kruse A, Gawlik A. Biomass conversion in water at 330-410 degrees C and 30-50 MPa. Identification of key compounds for indicating different chemical reaction pathways. Ind Eng Chem Res. 2003;42(2):267–79. <https://doi.org/10.1021/ie0202773>.
37. Sasaki M, Kabayemela B, Malaluan R, Hirose S, Takeda N, Adschari T, Arai K. Cellulose hydrolysis in subcritical and supercritical water. J Supercrit Fluids. 1998;13(1–3):261–8. [https://doi.org/10.1016/S0896-8446\(98\)00060-6](https://doi.org/10.1016/S0896-8446(98)00060-6).
38. Sasaki M, Fang Z, Fukushima Y, Adschari T, Arai K. Dissolution and hydrolysis of cellulose in subcritical and supercritical water. Ind Eng Chem Res. 2000;39(8):2883–90. <https://doi.org/10.1021/ie990690j>.
39. Rogalinski T, Ingram T, Brunner G. Hydrolysis of lignocellulosic biomass in water under elevated temperatures and pressures. J Supercrit Fluids. 2008;47(1):54–63. <https://doi.org/10.1016/j.supflu.2008.05.003>.

40. Jin FM, Enomoto H. Rapid and highly selective conversion of biomass into value-added products in hydrothermal conditions: chemistry of acid/base-catalysed and oxidation reactions. *Energy Environ Sci.* 2011;4(2):382–97. <https://doi.org/10.1039/C004268D>.
41. Rinaldi R, Schuth F. Acid hydrolysis of cellulose as the entry point into biorefinery schemes. *ChemSusChem.* 2009;2(12):1096–107. <https://doi.org/10.1002/cssc.200900188>.
42. Bicker M, Endres S, Ott L, Vogel H. Catalytical conversion of carbohydrates in subcritical water: a new chemical process for lactic acid production. *J Mol Catal A Chem.* 2005;239(1–2): 151–7. <https://doi.org/10.1016/j.molcata.2005.06.017>.
43. Yan XY, Jin FM, Tohji K, Moriya T, Enomoto H. Production of lactic acid from glucose by alkaline hydrothermal reaction. *J Mater Sci.* 2007;42(24):9995–9. <https://doi.org/10.1007/s10853-007-2012-0>.
44. Klingler D, Vogel H. Influence of process parameters on the hydrothermal decomposition and oxidation of glucose in sub- and supercritical water. *J Supercrit Fluids.* 2010;55(1):259–70. <https://doi.org/10.1016/j.supflu.2010.06.004>.
45. Calvo L, Vallejo D. Formation of organic acids during the hydrolysis and oxidation of several wastes in sub- and supercritical water. *Ind Eng Chem Res.* 2002;41(25):6503–9. <https://doi.org/10.1021/ie020441m>.
46. Jin FM, Yun J, Li GM, Kishita A, Tohji K, Enomoto H. Hydrothermal conversion of carbohydrate biomass into formic acid at mild temperatures. *Green Chem.* 2008;10(6): 612–5. <https://doi.org/10.1039/B802076K>.
47. Draget KI, Smidsrød O, Skjak-Braek G. Biopolymers. In: Steinbüchel A, editor. Polysaccharides II: polysaccharides from Eukaryotes. Weinheim: Wiley-VCH Verlag GmbH; 2002. p. 215–45.
48. Larche M, Wraith DC. Peptide-based therapeutic vaccines for allergic and autoimmune diseases. *Nat Med.* 2005;11:S69. <https://doi.org/10.1038/nm1226>.
49. Fosgerau K, Hoffmann T. Peptide therapeutics: current status and future directions. *Drug Discov Today.* 2015;20:122. <https://doi.org/10.1016/j.drudis.2014.10.003>.
50. Adler-Abramovich L, Marco P, Arnon ZA, Creasey RCG, Michaels TCT, Levin A, Scurr DJ, Roberts CJ, Knowles TPJ, Tendler SJB, Gazit E. Controlling the physical dimensions of peptide nanotubes by supramolecular polymer coassembly. *ACS Nano.* 2016;10:7436. <https://doi.org/10.1021/acsnano.6b01587>.
51. Burgess NC, Sharp TH, Thomas F, Wood CW, Thomson AR, Zaccai NR, Brady RL, Serpell LC, Woolfson DN. Modular design of self-assembling peptide-based nanotubes. *J Am Chem Soc.* 2015;137:10554. <https://doi.org/10.1021/jacs.5b03973>.
52. Sarmadi BH, Ismail A. Antioxidative peptides from food proteins: a review. *Peptides.* 2010;31:1949. <https://doi.org/10.1016/j.peptides.2010.06.020>.
53. Liang X, Qi SH, Nong XH, Huang ZH. Antifungal and antiviral cyclic peptides from the deep-sea-derived fungus simplicillium obclavatum EIODSF 020. *J Agric Food Chem.* 2017;65(25): 5114. <https://doi.org/10.1021/acs.jafc.7b01238>.
54. Voloshchuk N, Chen L, Li Q, Liang JF. Peptide oligomers from ultra-short peptides using sortase. *Biochem Biophys Rep.* 2017;10:1. <https://doi.org/10.1016/j.bbrep.2017.02.005>.
55. Thayer AM. Making peptides at large scale. *Chem Eng News.* 2011;89:21. <https://doi.org/10.1021/cen-v089n022.p021>.
56. Tavakoli O, Yoshida H. Conversion of scallop viscera wastes to valuable compounds using sub-critical water. *Green Chem.* 2006;8(1):100–6. <https://doi.org/10.1039/b507441j>.
57. Sunphorka S, Chavasiri W, Oshima Y, Ngamprasertsith S. Kinetic studies on rice bran protein hydrolysis in subcritical water. *J Supercrit Fluids.* 2012;65:54. <https://doi.org/10.1016/j.supflu.2012.02.017>.
58. Zhu X, Zhu C, Zhao L, Cheng H. Amino acids production from fish proteins hydrolysis in subcritical water. *Chin J Chem Eng.* 2008;16(3):456–60. [https://doi.org/10.1016/s1004-9541\(08\)60105-6](https://doi.org/10.1016/s1004-9541(08)60105-6).

59. Zhu G, Zhu X, Fan Q, Wan X. Kinetics of amino acid production from bean dregs by hydrolysis in sub-critical water. *Amino Acids.* 2011;40(4):1107–13. <https://doi.org/10.1007/s00726-010-0734-9>.
60. Sereewatthanawut I, Prapintip S, Watchiraruji K, Goto M, Sasaki M, Shotipruk A. Extraction of protein and amino acids from deoiled rice bran by subcritical water hydrolysis. *Bioresour Technol.* 2008;99(3):555–61. <https://doi.org/10.1016/j.biortech.2006.12.030>.
61. Sato N, Quitain AT, Kang K, Daimon H, Fujie K. Reaction kinetics of amino acid decomposition in high-temperature and high-pressure water. *Ind Eng Chem Res.* 2004;43(13):3217–22. <https://doi.org/10.1021/ie020733n>.
62. Marcket I, Alvarez C, Paredes B, Diaz M. Inert and oxidative subcritical water hydrolysis of insoluble egg yolk granular protein, functional properties, and comparison to enzymatic hydrolysis. *J Agric Food Chem.* 2014;62(32):8179–86. <https://doi.org/10.1021/jf405575c>.
63. Sheehan JD, Savage PE. Molecular and lumped products from hydrothermal liquefaction of bovine serum albumin. *ACS Sustain Chem Eng.* 2017;5(11):10967–75. <https://doi.org/10.1021/acssuschemeng.7b02854>.
64. Fang Z, Smith RL Jr. Production of biofuels and chemicals from lignin. Springer; 2016.
65. Carrier M, Loppinet-Serani A, Denux D, Lasnier J-M, Ham-Pichavant F, Cansell F, Aymonier C. Thermogravimetric analysis as a new method to determine the lignocellulosic composition of biomass. *Biomass Bioenergy.* 2011;35(1):298–307. <https://doi.org/10.1016/j.biombioe.2010.08.067>.
66. Kang SM, Li XL, Fan J, Chang J. Hydrothermal conversion of lignin: a review. *Renew Sustain Energy Rev.* 2013;27:546–58. <https://doi.org/10.1016/j.rser.2013.07.013>.
67. Domínguez JC, Santos TM, Rigual V, Oliet M, Alonso MV, Rodriguez F. Thermal stability, degradation kinetics, and molecular weight of organosolv lignins from *Pinus radiata*. *Ind Crop Prod.* 2018;111:889–98. <https://doi.org/10.1016/j.indcrop.2017.10.059>.
68. Karagoz S, Bhaskar T, Muto A, Sakata Y. Comparative studies of oil compositions produced from sawdust, rice husk, lignin and cellulose by hydrothermal treatment. *Fuel.* 2005;84(7–8): 875–84. <https://doi.org/10.1016/j.fuel.2005.01.004>.
69. Barbier J, Charon N, Dupassieux N, Loppinet-Serani A, Mahe L, Ponthus J, Courtiade M, Ducrozet A, Quoineaud AA, Cansell F. Hydrothermal conversion of lignin compounds. A detailed study of fragmentation and condensation reaction pathways. *Biomass Bioenergy.* 2012;46:479–91. <https://doi.org/10.1016/j.biombioe.2012.07.011>.
70. Tymchyshyn M, Xu CB. Liquefaction of bio-mass in hot-compressed water for the production of phenolic compounds. *Bioresour Technol.* 2010;101(7):2483–90. <https://doi.org/10.1016/j.biortech.2009.11.091>.
71. Kang SM, Li XL, Fan J, Chang J. Classified separation of lignin hydrothermal liquefied products. *Ind Eng Chem Res.* 2011;50(19):11288–96. <https://doi.org/10.1021/ie2011356>.
72. Saisu M, Sato T, Watanabe M, Adschariri T, Arai K. Conversion of lignin with supercritical water–phenol mixtures. *Energy Fuel.* 2003;17(4):922–8. <https://doi.org/10.1021/ef0202844>.
73. Wahyudiono SM, Goto M. Recovery of phenolic compounds through the decomposition of lignin in near and supercritical water. *Chem Eng Process Process Intensif.* 2008;47(9): 1609–19. <https://doi.org/10.1016/j.cep.2007.09.001>.
74. Zhang B, von Keitz M, Valentas K. Thermochemical liquefaction of high-diversity grassland perennials. *J Anal Appl Pyrolysis.* 2009;84(1):18–24. <https://doi.org/10.1016/j.jaat.2008.09.005>.
75. Lappalainen J, Baudouin D, Hornung U, Schuler J, Melin K, Bjelic S, Vogel F, Konttinen J, Joronen T. Sub- and supercritical water liquefaction of Kraft lignin and black liquor derived lignin. *Energies.* 2020;13(13) <https://doi.org/10.3390/en13133309>.
76. Chisti Y. Biodiesel from microalgae. *Biotechnol Adv.* 2007;25(3):294–306. <https://doi.org/10.1016/j.biotechadv.2007.02.001>.
77. Brennan L, Owende P. Biofuels from microalgae—a review of technologies for production, processing, and extractions of biofuels and co-products. *Renew Sustain Energy Rev.* 2010;14 (2):557–77. <https://doi.org/10.1016/j.rser.2009.10.009>.

78. Mata TM, Martins AA, Caetano NS. Microalgae for biodiesel production and other applications: a review. *Renew Sustain Energy Rev.* 2010;14(1):217–32. <https://doi.org/10.1016/j.rser.2009.07.020>.
79. Foley PM, Beach ES, Zimmerman JB. Algae as a source of renewable chemicals: opportunities and challenges. *Green Chem.* 2011;13(6):1399–405. <https://doi.org/10.1039/C1GC00015B>.
80. López Barreiro D, Prins W, Ronsse F, Brilman W. Hydrothermal liquefaction (HTL) of microalgae for biofuel production: state of the art review and future prospects. *Biomass Bioenergy.* 2013;53:113–27. <https://doi.org/10.1016/j.biombioe.2012.12.029>.
81. Djandja OS, Wang ZC, Chen L, Qin L, Wang F, Xu YP, Duan PG. Progress in hydrothermal liquefaction of algal biomass and hydrothermal upgrading of the subsequent crude bio-oil: a mini review. *Energy Fuel.* 2020;34(10):11723–51. <https://doi.org/10.1021/acs.energyfuels.0c01973>.
82. Gai C, Zhang YH, Chen WT, Zhang P, Dong YP. An investigation of reaction pathways of hydrothermal liquefaction using Chlorella pyrenoidosa and Spirulina platensis. *Energy Convers Manag.* 2015;96:330–9. <https://doi.org/10.1016/j.enconman.2015.02.056>.
83. Valdez PJ, Nelson MC, Faeth JL, Wang HY, Lin XN, Savage PE. Hydrothermal liquefaction of bacteria and yeast monocultures. *Energy Fuel.* 2014;28:67–75. <https://doi.org/10.1021/ef401506u>.
84. Faeth JL, Valdez PJ, Savage PE. Fast hydrothermal liquefaction of nanochloropsis sp. to produce biocrude. *Energy Fuels.* 2013;27(3):1391–8. <https://doi.org/10.1021/ef301925d>.
85. Gollakota A, Savage PE. Biocrude production from fast and isothermal hydrothermal liquefaction of chitin. *Energy Fuels.* 2019;33(11):11328–38. <https://doi.org/10.1021/acs.energyfuels.9b03209>.
86. Faeth JL, Savage PE, Jarvis JM, McKenna AM, Savage PE. Characterization of products from fast and isothermal hydrothermal liquefaction of microalgae. *AICHE J.* 2016;62(3):815–28. <https://doi.org/10.1002/aic.15147>.
87. Gollakota A, Savage PE. Fast and isothermal hydrothermal liquefaction of polysaccharide feedstocks. *ACS Sustain Chem Eng.* 2020;8(9):3762–72. <https://doi.org/10.1021/acssuschemeng.9b06873>.
88. Qian L, Wang S, Savage PE. Hydrothermal liquefaction of sewage sludge under isothermal and fast conditions. *Bioresour Technol.* 2017;232:27–34. <https://doi.org/10.1016/j.biortech.2017.02.017>.
89. Akhtar J, Amin NAS. A review on process conditions for optimum bio-oil yield in hydrothermal liquefaction of biomass. *Renew Sustain Energy Rev.* 2011;15(3):1615–24. <https://doi.org/10.1016/j.rser.2010.11.054>.
90. Borowitzka MA, Moheimani NR. Sustainable biofuels from algae. *Mitig Adapt Strateg Glob Chang.* 2013;18(1):13–25. <https://doi.org/10.1007/s11027-010-9271-9>.
91. Greenwell HC, Laurens LML, Shields RJ, Lovitt RW, Flynn KJ. Placing microalgae on the biofuels priority list: a review of the technological challenges. *J R Soc Interface.* 2010;7(46):703–26. <https://doi.org/10.1098/rsif.2009.0322>.
92. Clarens AF, Resurreccion EP, White MA, Colosi LM. Environmental life cycle comparison of algae to other bioenergy feedstocks. *Environ Sci Technol.* 2010;44(5):1813–9. <https://doi.org/10.1021/es902838n>.
93. Rosch C, Skarka J, Wegerer N. Materials flow modeling of nutrient recycling in biodiesel production from microalgae. *Bioresour Technol.* 2012;107:191–9. <https://doi.org/10.1016/j.biortech.2011.12.016>.
94. Liew WH, Hassim MH, Ng DKS. Review of evolution, technology and sustainability assessments of biofuel production. *J Clean Prod.* 2014;71:11–29. <https://doi.org/10.1016/j.jclepro.2014.01.006>.
95. Pate R, Klise G, Wu B. Resource demand implications for US algae biofuels production scale-up. *Appl Energy.* 2011;88(10):3377–88. <https://doi.org/10.1016/j.apenergy.2011.04.023>.

96. Pate R. Resource requirements for the large-scale production of algal biofuels. *Biofuels*. 2013;4(4):409–35. <https://doi.org/10.4155/bfs.13.28>.
97. Bohutskyi P, Liu K, Nasr LK, Byers N, Rosenberg JN, Oyler GA, Betenbaugh MJ, Bouwer EJ. Bioprospecting of microalgae for integrated biomass production and phytoremediation of unsterilized wastewater and anaerobic digestion centrate. *Appl Microbiol Biotechnol*. 2015;99(14):6139–54. <https://doi.org/10.1007/s00253-015-6603-4>.
98. Lundquist TJ, Woertz IC, Quinn N, Benemann JR. A realistic technology and engineering assessment of algae biofuel production. Energy Biosciences Institute; 2010.
99. Pittman JK, Dean AP, Osundeko O. The potential of sustainable algal biofuel production using wastewater resources. *Bioresour Technol*. 2011;102(1):17–25. <https://doi.org/10.1016/j.biortech.2010.06.035>.
100. Du ZY, Hu B, Shi AM, Ma XC, Cheng YL, Chen P, Liu YH, Lin XY, Ruan R. Cultivation of a microalga chlorella vulgaris using recycled aqueous phase nutrients from hydrothermal carbonization process. *Bioresour Technol*. 2012;126:354–7. <https://doi.org/10.1016/j.biortech.2012.09.062>.
101. Jena U, Vaidyanathan N, Chinnasamy S, Das KC. Evaluation of microalgae cultivation using recovered aqueous co-product from thermochemical liquefaction of algal biomass. *Bioresour Technol*. 2011;102(3):3380–7. <https://doi.org/10.1016/j.biortech.2010.09.111>.
102. Barreiro DL, Bauer M, Hornung U, Posten C, Kruse A, Prins W. Cultivation of microalgae with recovered nutrients after hydrothermal liquefaction. *Algal Res*. 2015;9:99–106. <https://doi.org/10.1016/j.algal.2015.03.007>.
103. Biller P, Ross AB, Skill SC, Lea-Langton A, Balasundaram B, Hall C, Riley R, Llewellyn CA. Nutrient recycling of aqueous phase for microalgae cultivation from the hydrothermal liquefaction process. *Algal Res Biomass Biofuels Bioproducts*. 2012;1(1):70–6. <https://doi.org/10.1016/j.algal.2012.02.002>.
104. Alba LG, Torri C, Fabbri D, Kersten SRA, Brilman DWF. Microalgae growth on the aqueous phase from hydrothermal liquefaction of the same microalgae. *Chem Eng J*. 2013;228:214–23. <https://doi.org/10.1016/j.cej.2013.04.097>.
105. Bohutskyi P, Chow S, Ketter B, Betenbaugh MJ, Bouwer EJ. Prospects for methane production and nutrient recycling from lipid extracted residues and whole nannochloropsis salina using anaerobic digestion. *Appl Energy*. 2015;154:718–31. <https://doi.org/10.1016/j.apenergy.2015.05.069>.
106. Tchobanoglou G, Burton F, Stensel HD, editors. *Wastewater engineering: treatment and reuse*. 4th ed. New York: McGraw-Hill; 2004.
107. Qi WK, Sunaba T, Norton M, Li YY. Effect of the great East Japan earthquake and tsunami on sewage facilities and subsequent recovery measures. *J Water Sustain*. 2014;4(1):27–40. <https://doi.org/10.11912/jws.4.1.13-26>.
108. Libra JA, Ro KS, Kammann C, Funke A, Berge ND, Neubauer Y, Titirici M-M, Fühner C, Bens O, Kern J, Emmerich K-H. Hydrothermal carbonization of biomass residuals: a comparative review of the chemistry, processes and applications of wet and dry pyrolysis. *Biofuels*. 2011;2(1):71–106. <https://doi.org/10.4155/bfs.10.81>.
109. Kruse A, Funke A, Titirici M-M. Hydrothermal conversion of biomass to fuels and energetic materials. *Curr Opin Chem Biol*. 2013;17(3):515–21. <https://doi.org/10.1016/j.cbpa.2013.05.004>.
110. Reza MT, Lynam JG, Uddin MH, Coronella CJ. Hydrothermal carbonization: fate of inorganics. *Biomass Bioenergy*. 2013;49:86–94. <https://doi.org/10.1016/j.biombioe.2012.12.004>.
111. Kirschhäuser F, Sahin O, Becker GC, Meffert F, Nusser M, Anderer G, Kusche S, Kläusli T, Kruse A, Brenner-Weiss G. Wastewater treatment--adsorption of organic micropollutants on activated HTC-carbon derived from sewage sludge. *Water Sci Technol*. 2016;73(3):607–16. <https://doi.org/10.2166/wst.2015.511>.
112. Langone M, Basso D. Process waters from hydrothermal carbonization of sludge: characteristics and possible valorization pathways. *Int J Environ Res Public Health*. 2020;17(18):6618. <https://doi.org/10.3390/ijerph17186618>.

113. Becker GC, Wüst D, Köhler H, Lautenbach A, Kruse A. Novel approach of phosphate-reclamation as struvite from sewage sludge by utilising hydrothermal carbonization. *J Environ Manag.* 2019;238:119–25. <https://doi.org/10.1016/j.jenvman.2019.02.121>.
114. Song B, Lin R, Lam CH, Wu H, Tsui T-H, Yu Y. Recent advances and challenges of interdisciplinary biomass valorization by integrating hydrothermal and biological techniques. *Renew Sust Energ Rev.* 2021;135:110370. <https://doi.org/10.1016/j.rser.2020.110370>.
115. Frank ED, Han J, Palou-Rivera I, Elgawainy A, Wang MQ. Methane and nitrous oxide emissions affect the life-cycle analysis of algal biofuels. *Environ Res Lett.* 2012;7(1): 014030/1–014030/10. <https://doi.org/10.1088/1748-9326/7/1/014030>.
116. Delrue F, Li-Beisson Y, Setier PA, Sahut C, Roubaud A, Froment AK, Peltier G. Comparison of various microalgae liquid biofuel production pathways based on energetic, economic and environmental criteria. *Bioresour Technol.* 2013;136:205–12. <https://doi.org/10.1016/j.biortech.2013.02.091>.
117. Wang X, Zhao B, Tang X, Yang X. Comparison of direct and indirect pyrolysis of micro-algae Isochrysis. *Bioresour Technol.* 2015;179:58–62. <https://doi.org/10.1016/j.biortech.2014.11.015>.
118. Li H, Guo HX, Fang Z, Aida TM, Smith RL. Cycloamination strategies for renewable N-heterocycles. *Green Chem.* 2020;22(3):582–611. <https://doi.org/10.1039/C9GC03655E>.
119. Xu L, Shi C, He Z, Zhang H, Chen M, Fang Z, Zhang Y. Recent advances of producing biobased N-containing compounds via thermo-chemical conversion with ammonia process. *Energy Fuels.* 2020;34(9):10441–58. <https://doi.org/10.1021/acs.energyfuels.0c01993>.
120. Yao G, Guo Y, Le Y, Jin B, He R, Zhong H, Jin F. Energy valorization of food waste: rapid conversion of typical polysaccharide components to formate. *Ind Eng Chem Res.* 2020;59(39): 17069–75. <https://doi.org/10.1021/acs.iecr.0c01073>.
121. Ding K, Le Y, Yao G, Ma Z, Jin B, Wang J, Jin F. A rapid and efficient hydrothermal conversion of coconut husk into formic acid and acetic acid. *Process Biochem.* 2018;68:131–5. <https://doi.org/10.1016/j.procbio.2018.02.021>.
122. Bach QV, Sillero MV, Tran KQ, Skjermo J. Fast hydrothermal liquefaction of a Norwegian macro-alga: screening tests. *Algal Res.* 2014;6:271–6. <https://doi.org/10.1016/j.algal.2014.05.009>.
123. Xu L, Zhang LY, Song H, Dong Q, Dong GH, Kong X, Fang Z. Catalytic fast pyrolysis of polyethylene terephthalate plastic for the selective production of terephthalonitrile under ammonia atmosphere. *Waste Manag.* 2019;92:97–106. <https://doi.org/10.1016/j.wasman.2019.05.011>.
124. Sheehan JD, Savage PE. Products, pathways, and kinetics for the fast hydrothermal liquefaction of soy protein isolate. *ACS Sustain Chem Eng.* 2016;4(12):6931–9. <https://doi.org/10.1021/acssuschemeng.6b01857>.
125. Ma Z, Hu J, Yao G, Duo J, Jin B, Jin F. Valorization of wheat straw: rapid reduction of CuO into cu and production of organic acids under mild hydrothermal conditions. *Process Saf Environ Prot.* 2018;115:79–84. <https://doi.org/10.1016/j.psep.2017.08.008>.
126. Fang Z. Noncatalytic fast hydrolysis of wood. *Bioresour Technol.* 2011;102(3):3587–90. <https://doi.org/10.1016/j.biortech.2010.10.063>.

Chapter 12

Third Generation Biorefineries Using Micro- and Macro-Algae



Rohit Saxena, Gilver Rosero-Chasoy, Elizabeth Aparicio, Abraham Lara, Araceli Loredo, Armando Robledo, Emily T. Kostas, Rosa M. Rodríguez-Jasso, and Héctor A. Ruiz

Abstract Algal biomass, which contains a range of biochemical components such as carbohydrates, lipids, and protein, has emerged as a possible alternative to traditional feedstocks for third-generation biofuel production and industrially high value-added bioproduct extraction. Micro- and macro-algae are gaining popularity as viable feedstock for biofuels such as biodiesel, biogas, bioethanol, and biohydrogen. Other high-value-added bioproducts must be extracted from algal biomass under the biorefinery concept to improve the economic feasibility of algal biofuel production. In this chapter, techniques for algal biofuel production are discussed, such as biochemical and chemical conversion routes, extraction of bioproducts, and advanced techniques in cultivation, extraction, and starch saccharification along with biofuel and bioenergy conversion schemes. Overall, micro-and macro-algae biorefineries open up new possibilities for many new products. The multiproduct biorefinery technique is expected to make micro-and macro-algal technology highly competitive and pave the way for large-scale applications.

Keywords Biorefinery · Extraction process · Biofuels · High value-added products · Biomass valorization · Bioethanol

R. Saxena · G. Rosero-Chasoy · E. Aparicio · A. Lara · A. Loredo · R. M. Rodríguez-Jasso · H. A. Ruiz (✉)

Biorefinery Group, Faculty of Chemistry Sciences, Food Research Department, Autonomous University of Coahuila, Saltillo, Coahuila, Mexico

e-mail: hector_ruiz_leza@uadec.edu.mx; <https://www.biorefinerygroup.com>

A. Robledo

Food Science and Technology Department, Universidad Autónoma Agraria Antonio Narro, Saltillo, Coahuila, Mexico

E. T. Kostas

Department of Biochemical Engineering, The Advanced Centre of Biochemical Engineering, University College London, London, UK

Nomenclature

CBP	Consolidated bioprocessing
GHG	Greenhouse gases
ORP	Open raceway pond
SHF	Separated hydrolysis and fermentation
SSCF	Simultaneous saccharification and co-fermentation
SSF	Simultaneous hydrolysis and fermentation
ppm	Part per million
dw	Dry weight
PLE	Pressurized liquid extraction
SFE	Supercritical fluid extraction

12.1 Introduction

Over the last few decades, unrestricted population growth, rapid industrialization, and economic development have resulted in an escalation of the global energy crisis and, as a result, exponential deterioration in non-renewable energy resources such as coal, natural gas, and oil. In addition to the energy crisis, the prolonged use of petroleum-based fuels has resulted in pollution and global climate change. Crude oil (34%), coal (28%), and natural gas (23%) have all contributed significantly to global energy generation [1]. Furthermore, the overabundance of plentiful non-renewable resources has resulted in excess greenhouse gases (GHG) such as CO₂, CH₄, and others, resulting in global climate health being disrupted. Global temperature has been reported to be rising at an alarming rate of 0.07 °C per year, with CO₂ levels increasing at a rate of 3 ppm per year, with the maximum level being 410 ppm [1]. Researchers are seeking alternative resources that are less destructive to the environment and economically affordable. Renewable energy options have been on the experts' radar for the past decade [2–4].

In this chapter, extraction of energy products in a usable form from natural sources is referred to as primary energy production, for example, in coal mines, crude oil fields, and hydropower facilities [5]. Aside from that, renewable energy resources are receiving much attention in developed countries. For example, the European Union has maintained its 2030 mandatory objective of 27%, which was pushed backward in 2014 to 32% in June 2018 [4, 6]. At the same time, the US is working to improve renewable energy resources.

One of the critical motivations for using renewable energy resources is to consider ecologically favorable energy sources. Environmental awareness is high for the world population at this time; it is believed that previous reliance on fossil fuels has resulted in carbon dioxide (CO₂) emissions, greenhouse gas (GHG) concerns, and pollution [4].

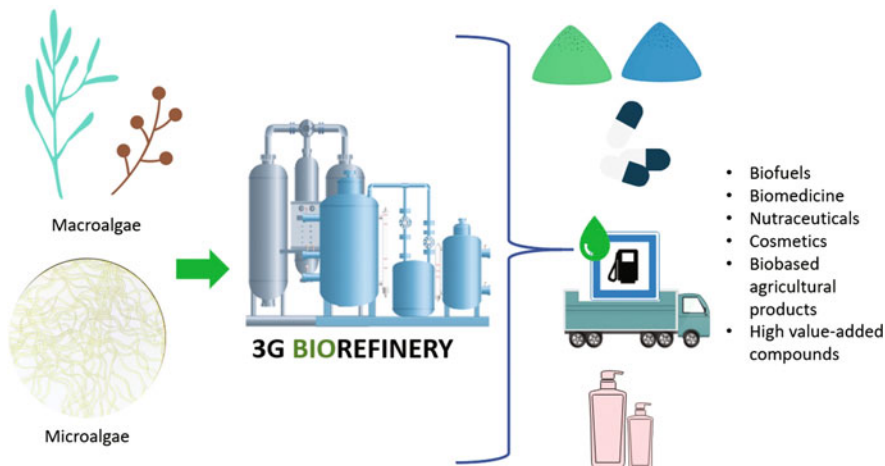


Fig. 12.1 Third generation biorefinery with biofuels and other high value-added compounds

Nowadays, research has investigated alternate sources of clean biofuels derived from renewable sources that are referred to as first-generation, second generation, and third generation. Biological biofuels are produced by biological routes like pretreatment, harvesting, and biochemical conversion processes under the biorefinery concept.

Biofuels like bioethanol, biodiesel, and biogas are considered clean and renewable. Each has massive advantages over other fuels like environmentally friendly, low toxicity, and low burn pollutant environments for replacing fossil fuels [3]. They can be produced from sugarcane, corn starch, and other cellulosic feedstocks. However, although these feedstocks are less expensive than fossil fuels, their use can influence food costs [7]. Therefore, researchers are examining alternative sources, which do not affect the food chain and agriculture.

Micro- and macro-algal biofuels are considered to be renewable and sustainable energy sources. Micro- and macro-algae are recognized as superior biomass as compared to terrestrial plants—in terms of solar energy storage, nutrient assimilation, and potential for biofuel production—due to significant advantages such as higher photosynthetic efficiency, higher biomass yield and rates, and reduced toxic gas emissions in the environment [8]. Micro- and macro-algae provide a new path to biomass production as a sustainable material for bioethanol and other high value-added bioactive compounds production under the biorefinery concept, shown in Fig. 12.1 [7, 9, 10]. For example, microalgae are tiny photosynthetic microorganisms, primarily existing as small cells of about 2–200 μm and inhabitants of freshwater, seawater, and even wastewater [11]. Microalgae efficiently convert solar light and atmospheric carbon dioxide to produce biomass by photosynthetic process [10, 12]. Microalgae are one of the favorable possibilities for eliminating CO₂ from the atmosphere by CO₂ bio-fixation. Microalgae can consume CO₂ in three ways: CO₂ from soluble carbonates, atmospheric CO₂, and CO₂ present in the

stack and discharge gases from industries. Microalgae are described as unicellular/multicellular photosynthetic microscopic cyanobacteria used to produce renewable fuels [10]. Micro- and macro-algae has significant oil content that allows biodiesel production and energy-containing polysaccharides like starch which can be degraded chemically or enzymatically that allows bioethanol production via fermentation [12].

This chapter intends to provide an overview of micro-and macro-algae biomass conversion into biofuels and other high value-added compounds in terms of the biorefinery concept. This chapter also covers cultivation, the extraction process, enzymatic hydrolysis, and fermentation strategies.

12.2 Biorefinery of Microalgae

12.2.1 *Microalgae Overview and Growth Culture in the Accumulation of Starch*

Microalgae and cyanobacteria are photosynthetic microorganisms with a cell size of 2–200 μm [12]; they can convert solar energy into chemical energy by CO_2 fixation primary carbon source [13]. There are four significant modes for microalgae cultivation: photoautotrophic, heterotrophic, mixotrophic, and photoheterotrophic cultivation [13]. Therefore, they may use another carbon source, different CO_2 , to produce a large amount of biomass, containing carbohydrates, lipids, proteins [12], high-value-added compounds such as vitamin pigments, and some organic acids [14].

Microalgae are assimilating inorganic nitrogen and phosphorus during all their growth phases. Nitrogen source and concentration have been reported as parameters that significantly affect lipid yields to the inside of the microalgae. Various nitrogen sources, such as ammonia (NH_4^+), nitrate (NO_3^-), nitrite (NO_2^-), and urea ($\text{CH}_4\text{N}_2\text{O}$), can be used for the culturing microalgae, and the choice of nitrogen source will strongly depend on the type of microalgae [15, 16]. On the other hand, the limitation of phosphorus (PO_4^{3-}) source within culture medium has negatively impacted the formation of carbohydrates and growth rate in several microalgae strains compared with other macronutrients [17]. Environmental parameters such as light intensity, nitrogen, carbon nutrient levels, salinity, temperature, and others significantly impact microalgae biomass and chemical composition. In general, microalgae growth rate and biomass production rely primarily on nitrogen availability in culture ingredients [18]. Under nitrogen-sufficient circumstances, the majority of oleaginous microalgae grow faster and produce less lipid. Instead, nitrogen loss or famine causes increased lipid accumulation in microalgae, which is most likely related to the movement of metabolic carbon from carbohydrate and protein production to lipid production. Thus, understanding the trade-off connection between

microalgae biomass, lipid, and nitrogen levels in a system during the culture phase is critical for optimizing lipid and protein synthesis, among other bioproducts [19].

Microalgae are currently contributing to the global bioeconomy by providing significant biomass for human-related uses like pharmaceuticals, cosmetics, food, and feed [20]. Microalgae biomass is considered potential biomass for biofuel production, such as bioethanol, biodiesel, biohydrogen, and biomethane. Therefore, they will play a significant role in the renewable energy sector and in the uptake of inorganic matter [21].

Microalgae are also being studied as a viable biomass feedstock for biofuel production and play a valuable role in the renewable energy sector. However, cultivating microalgae to meet only world transportation fuel demands utilizing microalgal biomass as feedstock raises various practical concerns and substantial limits, such as high land usage, high energy, water, and fertilizer consumption. The use of wastewater streams and seawater for microalgae growth may reduce the consumption of inorganic fertilizer while treatment of the wastewater occurs. They are of enormous importance due to their rich content in nutrients, which can fulfill the microalgal cyanobacterial nutrient needs. Wastewater and seawater are characterized by containing several different nutrients like carbon, nitrogen, phosphorus, and potassium (macro-nutrients) such as Mg, S, Ca, Na, Cl, Fe, Zn, Cu, Mo, Mn, B, and Co (micro-nutrients) [21]. It should be highlighted that wastewater streams limit biomass applications because they may have various pollutants present in the wastewater. Therefore, microalgae produced in wastewater can be mainly used to make biofuels rather than food or feed applications [21]. For many years, microalgae cultivation systems have been investigated. The factors more critical to microalgae growth are; illumination, photoperiod, pH, carbon and nitrogen sources concentration, and temperature [22, 23].

These factors can be monitored in open raceway pond (ORP) and controlled in closed PBRs since these devices offer suitable conditions for its investigation. The open PBRs have been developed for large-scale microalgae cultivation because they are easy to make and relatively simple to operate. These ORP generally use outdoors, which permits microalgae to CO₂ uptake from the atmosphere with a poor mass transfer rate inside the culture medium, higher risk of contamination, and a high evaporation water rate. The closed PBRs are more complex systems because these do not allow direct mass transfer between culture media and atmosphere, and its use to pilot or large scale is usually considered nonviable by the enormous consumption amount of energy, despite allowing to attain a higher yield of microalgae biomass without risk of contamination, in comparison with open PBRs. When high-value-added chemicals are manufactured, such as biopharmaceuticals, top-grade cosmetics, and human health foods, closed PBRs are widely accessible [24]. Figure 12.2 shows photobioreactor technology used for microalgae culture.

The major challenge in PBRs design and scale-up is increasing the CO₂ transfer rate in the gas-liquid interface into the microalgae suspension because microalgae cannot directly use the CO₂ bubbles injected inside PBRs as the gas aerated into solution is sparingly soluble in the culture medium. The way of dissolving CO₂ bubbles in the culture medium is through decreasing the bubble diameter, which

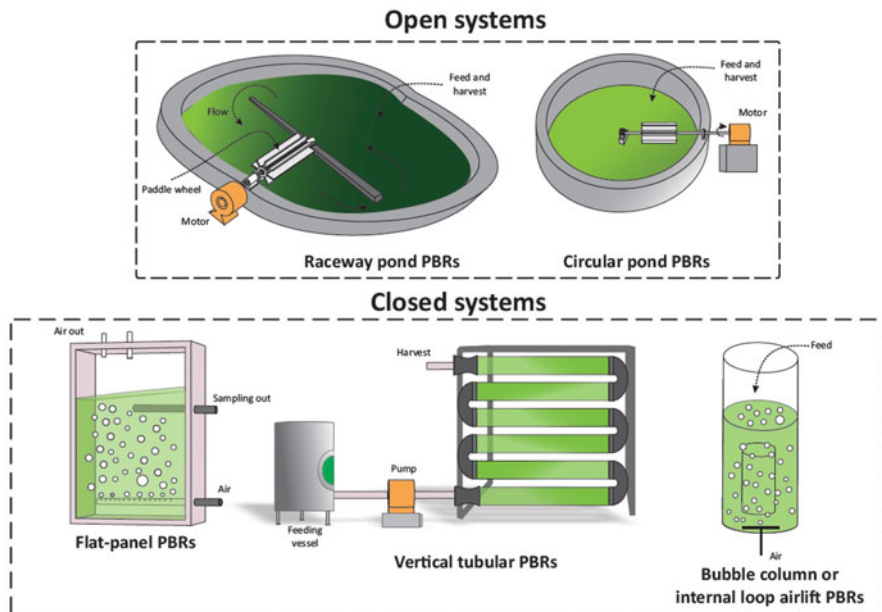


Fig. 12.2 Photobioreactors (PBRs) technology used for microalgae culture

increases the gas-liquid contacting area. It prolongs the retention time of the bubble in the microalgae suspension so that the dissolved CO₂ can be captured by the microalgae cells and converted into organic matter to form biomass through photosynthesis [25].

The culturing of some microalgae like *Chlorella*, *Dunaliella*, *Chlamydomonas*, *Scenedesmus*, and *Spirulina* in PBRs has massive carbohydrate amounts ($\geq 20\%$ of dry weight), which is excellent biomass for bioethanol production [26, 27]. Compared with conventional crops, there are various advantages to employing microalgae for bioenergy production, including: (1) the capacity to be farmed on marginal areas without causing land-use change, (2) high exponential growth rates potential to utilize CO₂ from industrial flue gas (1 kg of dry algae biomass uses about 1.83 kg of CO₂) and nutrients (mainly nitrogen and phosphorus) from wastewater, (3) semi-continuous to continuous harvesting and (4) variable lipid content in the range of 5–50% dry weight of biomass [28, 29]. The accumulation of carbohydrates, fatty acids, and pigments inside microalgae happens in the chloroplast, and this organelle is in charge of the photosynthesis process [30]. The accumulated carbohydrate by microalgae can be converted directly to ethanol under anaerobic conditions and dark [31]. Table 12.1 shows the content of carbohydrates some microalgae cultivated in PBRs, which can be used for bioethanol production.

Table 12.1 Carbohydrate content in microalgae biomass for bioethanol production

Microalgae	% (g / dry weight)	PBRs type	Cultivation	References
<i>Tribonema</i> sp.	14.5	Bubbles column	–	[32]
<i>Chlorella vulgaris</i> FSP-E	51.0	Glass vessel	2% CO ₂ /air, 28 °C, pH 6.2, agitation 300 rpm, and a light intensity 60 μmol. m ⁻² s ⁻¹	[33]
<i>Synechococcus elongatus</i> PCC7942 (transgenic cells)	90.0	Glass vessel	5% CO ₂ /air (0.2 vvm), 28 °C, and a light intensity 200 μmol. m ⁻² s ⁻¹	[34]
<i>Synechococcus</i> PCC 7002	60.0	Bubbles column	5% CO ₂ /air, pH 8.0–8.5, 28 °C, and a light intensity 100 μmol. m ⁻² s ⁻¹	[35]
<i>Synechococcus</i> sp. PCC 7002	60.0	Bubbles column	1% CO ₂ /air, 38 °C, and a light intensity 250 μmol. m ⁻² s ⁻¹	[36]
<i>Pseudochlorella</i> sp.	36	Glass vessel	Air at 0.3 vvm, 27 °C, 150 rpm, and a light intensity 60 μmol. m ⁻² s ⁻¹	[37]
<i>Chlamydomonas mexicana</i>	50			
<i>Chlamydomonas pitschmannii</i>	23			

12.3 Extraction of Starch from Microalgae

Starch is a polysaccharide that consists of numerous glucose units joined by glycosidic bonds, found naturally in green plants for energy storage. Starch content depends on plant species, environmental conditions, and biotic or abiotic factors of the aquatic ecosystem [38]. It is expected that third-generation biofuels produced from algae and aquatic plants will become carbon-neutral since they use atmospheric CO₂ for the energy acquiring process.

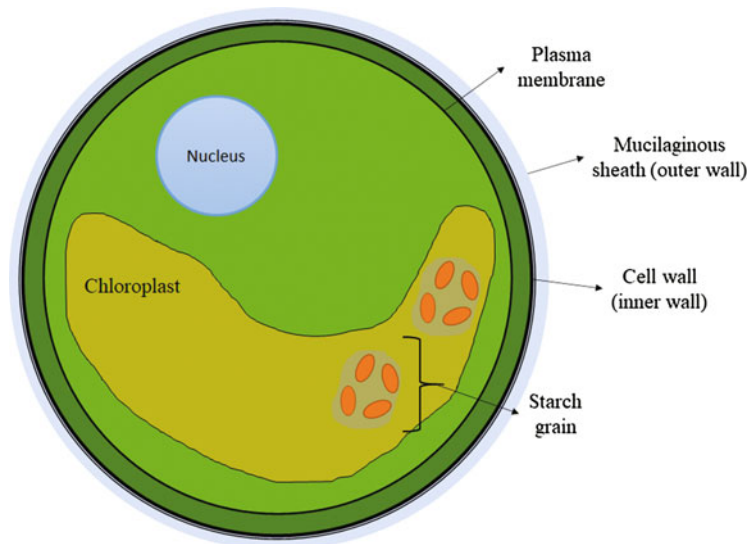
Most microalgae species contain around 37% of starch (Table 12.2); even some strains such as *Dunaliella*, *Scenedesmus*, *Spirulina*, and *Chlamydomonas* can have more than 50% starch [39].

Starch originates in the chloroplasts of microalgae as semi-crystalline granules (Fig. 12.3). Anhydrous starch granules mainly consist of two major unbranched, and large polymers such as amylose, which is a linear polysaccharide composed entirely of D-glucose units, joined by α-1,4-glycosidic linkages polymer, and amylopectin, which is a branched-chain polysaccharide consisting of glucose units linked primarily by α-1,4-glycosidic bonds, but with few α-1,6-glycosidic bonds, that are responsible for the branching [48]. Starch in the microalgae cell requires disruption of the outer cell wall composed mainly of pectin, agar, and alginates; meanwhile, the inner cell wall comprises cellulose hemicellulose glycoprotein [49].

Dilute acid/alkali processes and enzymatic hydrolysis are traditional algae cell disrupter methods; nevertheless, pressurized liquid extraction, supercritical fluid extraction, ultrasonication, bead beating, microwave, and pulse electric fields have

Table 12.2 Starch content in microalgae

Microalgae	Starch content (% weight)	References
<i>Dunaliella, Scenedesmus, Spirulina and Chlamydomonas</i>	~50	[39]
<i>Tetraselmis subcordiformis</i>	62.1	[39]
<i>Chlorococcum</i> sp.	26	[40]
<i>Chlorella vulgaris</i>	60	[41]
<i>Chlamydomonas reinhardtii</i>	49	[42]
<i>Chlorella sorokiniana</i>	40	[43]
<i>Neochloris oleoabundans</i>	27	[44]
<i>Tetraselmis subcordiformis</i>	44.1	[45]
<i>Chlorella</i> sp.	19.3–38.2%	[46]
<i>Oscillatoria</i> sp.	63.85	[47]

**Fig. 12.3** Microalgae cell basic structure for starch localization

been evaluated as novel methods to achieve algal cell hydrolysis [12, 50]. After cell wall hydrolysis, the soluble fraction needs to be separated from the solid fraction, which conserves the starch content, usually by centrifugation. Water washes and the centrifugation process should be repeated using a Percoll gradient to isolate pure starch. Figure 12.4 summarizes the starch extraction process from microalgae.

Pressurized liquid extraction (PLE): Compared to conventional procedures, PLE uses fewer solvents and delivers quicker extractions due to the fast mass transfer rate. Solvents have enhanced solubility and lower viscosity due to the higher temperatures, which helps boost mass transfer rates and penetration into the matrix.

Fig. 12.4 Process stages for starch obtention from microalgae

Microalgae biomass

Cell disruption

Centrifugation
Washing
Percoll gradient

Starch

acid/alkali
enzymatic
ultrasonication
bead beating
microwave
osmotic shock
autoclaving

Furthermore, while water is kept in its liquid state, a rise in temperature causes a significant drop in the dielectric constant (ϵ). This number is typically used to determine the polarity of a solvent. In this way, though water has a dielectric constant of around 80 at room temperature when heated to 250 °C under appropriate pressure to keep it liquid, it drops to approximately 30, equivalent to some dielectric constants organic solvents like ethanol or methanol [51].

Supercritical fluid extraction (SFE): Carbon dioxide is the most often used supercritical fluid for extracting natural sources, including microalgae. Its low critical temperature and pressure (31.1 °C and 73.8 bar) are easily attained, and it is GRAS for the food sector, inexpensive and safe. Another unique feature of this method is that supercritical CO₂ (sc-CO₂) is a very selective solvent. The most significant factors during extraction are temperature and pressure, which together govern the density of the sc-CO₂. Hence, it is the capacity to selectively remove particular compounds from the natural matrix [51].

Diluted acid/alkali hydrothermal process: This is a chemical, non-mechanical, cheap, and fast method for microalgae cell wall disruption. Nevertheless, it uses the breakdown of essential compounds and produces toxic elements that usually inhibit fermentation [52]. Acidic or alkali hydrolysis is a non-specific reaction, generally performed with concentrations between 1 and 10% w/v and temperatures of 100–160 °C [39, 50]. These chemicals limit used in more significant amounts during hydrolysis; then, pH adjustment before the fermentation process is needed that releases more salt, inhibiting yeast activity [50].

Enzymatic hydrolysis: Classified as the most efficient biological and non-mechanical pretreatment, particularly for microalgae [53], hydrolysis made by enzymes is a costly and slow procedure but environmental-friendly. This biological

hydrolysis often requires expensive pretreatment processes to enhance efficiency [52]. Apart from the pretreatment and enzyme costs, enzymatic hydrolysis provides a more specific disruption with low heating cost and no degradative effects derived from the mild temperature and pressure used [50].

Ultrasonic treatment: Ultrasonic pretreatment is a mechanical technology that produces alternating low- and high-pressure waves (20–100 MHz) in the aqueous phase, causing the formation and vigorous collapse of microbubbles [52, 54]. The microbubbles' violent failure occurs within a few microseconds inducing the occurrence of cavitation. All processes generate theoretical temperatures and pressures of up to 5000 K and 500 bar and initiate powerful hydro-mechanical shear forces and highly reactive radicals [55].

Bead beating: Another mechanical method is the bead-beating method, which involves applying glass or steel beads into a vessel where the high-speed agitating movement of beads can disrupt the algal cell wall. Bead beating is used for both disruption and extraction [56]. This disruptive mechanical method is considered an efficient technique [57].

Microwave: Microwave method is based on the perpendicular mixture of electric and magnetic waves that fluctuate at defined frequencies ranging from 0.3 to 300 GHz [58]. Microwaves use high-frequency waves to create water molecule vibrations inside microalgae biomass, increasing the humidity and pressure caused by water evaporation, causing cell wall rupture [12, 57]. Microwaves have various advantages like fast heating, uni-directional heat flow and mass, selective energy dissipation, more rapid, increase purity and yield capacity of the anticipated product [52].

Pulsed electric field lysis: In this technique, cells in a liquid media are subjected to pulses of a strong electric field ranging from 100 V/cm to 300 kV/cm within a short period of nanoseconds or milliseconds, which principally affects the formation of pores in the cell wall [12, 52]. The pores formed in the cell wall allow biochemical components to leach out from the cell. Pretreatment methods for microalgae used as feedstock for biofuels are summarized in Table 12.3.

12.4 Enzymatic Hydrolysis of Microalgae Starch

Enzymatic hydrolysis (saccharification) is the critical step for converting polysaccharides into monosaccharides that requires the action of cellulolytic enzymes sequentially and synergistically for subsequent fermentation and bioethanol production [12, 65]. Enzymatic saccharification of starch is performed at high temperatures, and it is separated into three parts: gelatinization of starch, liquefaction, and saccharification.

Gelatinization of starch and liquefaction involves breaking starch granules into a gelatinized suspension at 105 °C followed by converting oligosaccharides from gelatinized starch at 95 °C by using an α -amylase enzyme that has thermostable properties as shown in Fig. 12.5. The saccharification process converts saccharide

Table 12.3 Pretreatment processes for starch extraction from microalgae sources

Source	Pretreatment	Operational conditions	Yield (%)	References
<i>Chlorella Salina</i>	Physiochemical	Megazyme total starch analysis kit (90 °C, 30 min)	323.1 ± 32.03 (increment) 96.60 ± 2.73 (starch recovery)	[59]
<i>Chlorella sorokiniana</i> <i>Nannochloropsis gaditana</i> <i>Scenedesmus almeriensis</i>	Enzymatic	15 FPU for Celluclast 1.5 L and 15 IU for Novozyme 188 per g of DW	6.7 ^a ~1.4 ^a ~2.7 ^a	[60]
<i>Chlorella sorokiniana</i> <i>Nannochloropsis gaditana</i> <i>Scenedesmus almeriensis</i>	Enzymatic	240 α-amylase units and 750 amyloglucosidase units for Liquozyme SC DS and Spirizyme fuel	10.1 ^a ~6.0 ^a ~4.0 ^a	[60]
<i>Chlamydomonas fasciata</i>	Ultrasonic	30 W and 20 kHz for 0–40 min	93.8	[61]
<i>Scenedesmus obliquus</i>		30 W for 25 min	91.0	[50]
<i>Chlorella Salina</i>		30 W and 25 kHz for 5 min	35.7	[59]
<i>Chlorella Salina</i>	Bead beating	950 mg of glass beads (15.8 g of glass beads/1 g of biomass) at 5 min	65.4	[59]
<i>Chlorella</i> sp.	Microwave	Irradiation power of 530 W at 2450 MHz frequency, for 45 s	82 ^b	[62]
<i>Nannochloropsis oculata</i>		Irradiation power of 943 W at 2450 MHz frequency, for 5 min	~70 ^b	[63]
<i>Ulva ohnoi</i>	Pulse electric field	Field strength of 1 kV cm ⁻¹ , pulse duration of 50 µs, and pulse repetition rate of 3 Hz	59.4	[64]

^aYield % referred to a total carbohydrate^b% of cell rupture

polymer to monomers like glucose with additional disaccharides like maltose and isomaltose at significantly lower concentrations. Glucoamylase and isoamylase enzymes are added during the process to break down α-(1 → 4) glycosidic bonds as well as α-(1 → 6) glycosidic bonds at 65 °C [66–69].

Enzymatic hydrolysis efficiency depends on enzymes, substrate loading, pH, temperature, and incubation time, such as *Synechococcus* sp. PCC 7002, a marine cyanobacterium with a rich source of carbohydrates, was used for bioethanol production as feedstock when boosted accumulation was induced by nitrogen

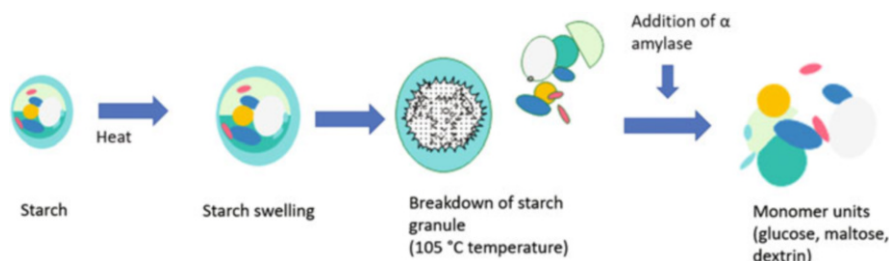


Fig. 12.5 Starch gelatinization, liquefaction, and saccharification

sources like nitrate [36, 70]. Optimizing the enzymatic hydrolysis process is essential in developing a cost-effective and efficient saccharification strategy for increased sugar concentration. The optimal enzymatic hydrolysis process conditions vary depending on the configuration of carbohydrates between the green, brown, and red algae [71]. Enzymatic saccharification structures use mild temperatures and have lesser ruin risks. Enzymes, typically amylases, cellulases, and pectinases (separately or together), are used to saccharify microalgae biomass [72].

Enzymatic hydrolysis is an eco-friendly process for the environment due to the low energy consumption and fermentable sugars produced from the feedstocks under light operational conditions, absence of corrosive problems, and excellent yields of free and limited byproducts [73]. Enzymatic hydrolysis uses mild operating conditions, gives high sugar yields, has high selectivity, and generates minimal byproducts formation [74]. Enzymatic hydrolysis has other advantages like procedure conditions with ensuing low energy requirements, high selectivity and biological specificity, and straightforward scale-up [75, 76]. However, enzymatic hydrolysis has disadvantages like the capital cost of enzymes and problematic recovery, making the process uneconomical. Enzymatic hydrolysis primary effectiveness depends on operation limits like temperature, pH, time, enzyme type and concentration, and parameter optimization for obtaining high yields and reducing capital costs [75].

Amylase enzyme is one of the most popular enzymes because it catalyzes starch to glucose precisely and effectively, as shown in Table 12.4. For example, α -amylase can randomly cut α -1-4-glycosidic bonds of amylose or amylopectin, resulting in short-chain dextrin and maltose [76, 77]. In contrast, glucoamylase can cut α -1-6-glycosidic bonds in amylopectin, which α -amylase cannot attack [76, 78]. The α -amylase and glucoamylase enzymes coordinate to complete the hydrolysis process for ethanol production from starch converted into glucose by fermentation. α -Amylases (EC 3.2.1.1) are endo-acting enzymes used to arbitrarily cut off α -1,4 glycosidic bonds present inside the starch and quickly break down the starch completely and release non-reducing ends for glucoamylase. Glucoamylases (EC 3.2.1.3) is an exo-acting enzyme that cut α -1,4 glycosidic bond and α -1,6 glycosidic bond to produce monomers sugar, the non-reducing ends that released from the starch degradation [79, 80].

Table 12.4 Bioethanol production from microalgae using amylolytic enzymes with optimal operating conditions

Algae species	Enzymes and operational condition	Concentration	Product	References
<i>Chlorella sorokiniana</i>	α -Amylase Amyloglucosidase	0.464 ± 0.013 g/g reducing sugar	Bioethanol	[83]
<i>Chlorella sorokiniana</i>	Cellulase, amylase (150 rpm, 72 h, pH 5.5–6.5)	58.78% total reducing sugar 0.504 g _{ethanol} /g _{glucose}	Bioethanol	[84]
<i>Chlorella vulgaris</i>	α -Amylase Amyloglucosidase CTec2 (50 °C, 200 rpm, 72 h)	54.5% Reducing sugar	Bioethanol	[85]
Mixed microalgae	Cellulase (50 °C, pH 4.5)	96.3% Maximum sugar yield	Bioethanol	[86]
Mixed microalgae <i>Neochloris</i> sp., <i>Scenedesmus</i> sp., <i>chlorella</i> sp.	Cellclast, β -Glucosidase, α -Amylase, Amyloglucosidase (pH 5, 60 °C, 150 rpm)	0.126 g _{ethanol} /g _{dried algae}	Bioethanol	[87]
<i>Rhizoclonium</i> sp.	Mixed enzyme Cellulase Amylase Xylanase Pectinase (45 °C, 48 h)	140.72 mg/g reducing-sugar 195.84 mg/g reducing sugar	Bioethanol	[71]
<i>Spirulina platensis</i>	Amylase	6.5 g/L ethanol	Bioethanol	[88]
<i>Synechococcus</i> sp.	Lysozyme (100 mg/L, 37 °C for 3 h), α -Amylase 240 U/g (85 °C for 1.5 h), Amyloglucosidase 750 U pH 5.5–6	0.27 g _{ethanol} /g _{cell dry weight}	Bioethanol	[36]
<i>Tetraselmis subcordiformis</i>	α -Amylase (AmyP) with calcium (40 °C, 2 h)	74.4% from 4% or 53% from 8% raw microalgae starch hydrolysate	Biofuel	[89]
<i>Arthrosphaera platensis</i>	Amylolytic enzyme (- α -amylase 0.3 U/L, glucoamylase 0.1 U/L) 168 h	43 g/L glucose concentration (without lysozyme or CaCl ₂) 67 g/L glucose concentration (with lysozyme or CaCl ₂)	Bioethanol	[90]

For cellulose, endo β -(1–4)-glucanase arbitrarily hydrolyzed amorphous areas of cellulose β -(1–4)-glycosidic bond and creating an innovative chain end. The exo β -(1–4)-glucanase enzyme performances on non-reducing ends of cellulose

molecule and celldextrins and redeeming cello-oligomers and cellobiose units (each unit has two β -(1-4) bonded glucose molecules). Hydrolysis is the final step to produce glucose monomers using β -glucosidase of these β -linkages of cellobiose molecules [81, 82]. Hemicellulose is like xylose, galactose, mannose, and other sugars with β -(1-4) and β -(1-3) linkages. These linkages are cut by enzymes like xylanases, α -L-arabinofuranosidase, and β -glucosidase and change into glucose monomer's sugars. Starch and glycogen have α -(1-4) D-glucosidic bonds that are hydrolyzed in a liquefaction process using α -amylase. Maltodextrin is a mixture of polymers of glucose having three or more α -(1-4)-linked D-glucose units. By the saccharification process, maltodextrin transforms into glucose oligomers by using amyloglucosidase. Saccharification process performance depends on both α -(1-4) and α -(1-6) D-glucosidic bonds [82].

Many authors have worked on enzymatic hydrolysis and its strategies on microalgae biomass. For example, Choi et al. [75] showed that hydrolysis efficiency improves to around 94% with a fermentation yield of approximately 60% for *S. cerevisiae* S288C in enzymatic hydrolysis of *Chlamydomonas reinhardtii* (initially carbohydrate content 59.7%), treated by SHF with amylases enzymes, in which α -amylase (0.005% v/w) from *Bacillus licheniformis* was used at 90 °C for 30 min, and with pH 6 to liquefaction and amyloglucosidase (0.2% v/w) from *Aspergillus niger* at 55 °C for 45 min, and pH 4.5 to saccharification [75].

Ho et al. [33] used a mixture of enzymes that contained endoglucanase (0.65 U mL⁻¹), β -glucosidase (1.50 U mL⁻¹), and amylase (0.09 U mL⁻¹) for enzymatic hydrolysis on *C. vulgaris* biomass. This biomass had initial carbohydrates 51% and glucose 93.1%. Feedstock and enzyme ratio was 10 g mL⁻¹, at 200 rpm for shaking on 45 °C with 20 g L⁻¹ and reported results as 0:461 g_{glucose}/g_{algae} dw (~97%) after 48 h. Furthermore, those authors compared results with dilute acid hydrolysis biomass performed at 1% H₂SO₄, 121 °C, 20 min, and 50 g/L of biomass. Lastly, 23.6 g/L (~100%) glucose concentration yields a similar yield by enzymatic hydrolysis [33].

Kim et al. [91] studied two enzymes separately for analyzed the enzymatic hydrolysis effect of microalgae, 1% (w/v): cellulase (Celluclast 1.5 L) and pectinase (Pectinex SP-L). The activities of these enzymes were 0:122 FPU/mg of protein and 240 UI/mg of protein. These enzymes were added (1.88 mg protein/g) on *C. vulgaris* biomass (22.4% of total carbohydrates) for bioethanol production, at 50 °C, 200 rpm, pH 4.8, 72 h. After enzymatic hydrolysis, sugar released from cellulase and pectinase 10% and 45%, respectively, liberating 0:1 g glucose/g algae dw. Various methods for cell lysis applied on *C. vulgaris* with bead beating combined with pectinase enzyme that extracts from *Aspergillus aculeatus*. After that, sugar extraction improved between 45% to 70%, and 89% ensuing fermentation yield after 12 h with *S. cerevisiae* KCTC 7906. The pectinase enzyme seems more practical than cellulases, amylases, and xylanases [91].

Moller et al. [36] reported *Synechococcus* sp. PCC 7002 biomass for enzymatic hydrolysis. They used 3 g/L of biomass concentration to afford 60% carbohydrate content efficiency for enzymatic hydrolysis and achieved 80% sugars with hydrolyzed after enzymatic treatment. These enzymes are lysozyme and α -glucanases

Liquozyme SC DS, and Spirizyme for biofuel. Ethanol yields reached 86% of the theoretical maximum rate with the help of *S. cerevisiae* [36].

Mahdy et al. [92] used urban wastewater to cultivate *C. vulgaris* have carbohydrate 39.6% and protein 33.3%. They used two enzymes separately, like 2.5 L alcalase (0:585 AU/g dw), and viscozyme (36:3 FBG/g dw), to solubilize protein-carbohydrate. These two enzymes alcalase with pH 8 (3.2% w/v), and 5.5% viscozyme, were carried out in enzymatic hydrolysis at 50 °C, for 3 h, in which pH was maintained during the process. The authors reported that the hydrolysis efficiency of organic matter was 54.7% for proteins (alcalase) and 28.4% for carbohydrates (Viscozyme) [92].

12.5 Conversion of Microalgae starch into Monomers for Ethanol

Starch is the principal polysaccharide formed in microalgae and can be converted into bioethanol using enzymes and microorganisms. Enzymes such as α -amylase and glucoamylase break the glycosidic bonds present in starch, then *S. cerevisiae* yeast is used in fermentation to reduce sugars [46]. Fermentation is a metabolic process, principally converting monosaccharide sugars into bioethanol and other value-added products using fermentative microorganisms [82, 93]. In the fermentation process, yeast and bacteria are commonly used as fermentative microorganisms. Some fermentative organisms play an essential role in fermentation, like *S. cerevisiae*, *Z. mobilis*, *E. coli*, *P. stipitis*, *Kluyveromyces fragilis*, *K. marxianus*, and *Klebsiella oxytoca*; the result is microalgal photosynthesis and intracellular anaerobic fermentation-derived bioethanol [93]. *Saccharomyces* and *Zymomonas* fermentative microorganisms are frequently used for bioethanol production, such as molasses, starch-based substrate (like algae), sweet sorghum cane extract, lignocellulose, and other wastes. *Z. mobilis* is a natural ethanologenic microorganism that has many advantageous properties, such as higher ethanol tolerance efficiency up to 16% and ethanol yield in a varied pH between 3.5 and 7.5. *Z. mobilis* does not need controlled aeration during fermentation time, which reduces the product capital cost. *Z. mobilis* is an appropriate industrial microbial biocatalyst used for the commercial production of bioproducts through metabolic engineering [94]. *Zymomonas* is a gram-negative bacteria with several advantages, including a higher specific rate of sugar uptake, a higher ethanol yield, lower biomass production, and the absence of the need for controlled oxygen addition during fermentation [95], and it is used for bioethanol production from starch and glycogen in fermentation [70, 96]. Theoretically, ethanol yields (0.49 to 0.50) g/g, or ethanol yields of up to 97% of theoretical values, can be obtained [97].

S. cerevisiae may play a critical role in the industrial biotechnology sector to develop a green replacement for petrochemical products due to its outstanding productivity to convert monomer sugars like glucose into ethanol and its high

tolerance. In addition, *Saccharomyces* is generally recognized as a harmless microorganism according to generally recognized as safe (GRAS) criteria. While growing, it produces flocs in the fermentation media that quickly settle down and separate. *S. cerevisiae* has a higher tolerance for alcohol, higher glucose uptake, and higher bioethanol yield than *Zymomonas* microorganism [70, 98]. Theoretically, 1 kg of glucose and xylose produce 0.51 kg ethanol with 0.49 kg of CO₂ [82, 93, 99].

One of the main complications of effective fermentation is the incapability of commonly used microorganisms that convert pentose sugars into bioethanol. Therefore, economic bioethanol production must use all potential feedstocks (i.e., cellulose and hemicellulose). Naturally occurring microorganisms that convert primary pentose sugar from hemicellulose like xylose into bioethanol exist, for example, specific bacteria, fungi, and yeasts [74]. Fermentation processes are represented by the following strategies [74, 93, 100]:

1. Separated hydrolysis and fermentation (SHF)
2. Simultaneous hydrolysis and fermentation (SSF)
3. Simultaneous saccharification and co-fermentation (SSCF)
4. Consolidated bioprocessing (CBP)

SSF and SHF are primarily used to produce bioethanol from microalgae using different fermentation strategies with various fermentative microorganisms (Table 12.5). The total valuation of the fermentation process is usually based on cell growth, consumption of reducing sugar, and bioethanol production. Environmental and operational factors greatly influence bioethanol production from algal biomass, like (i) nutrient levels; (ii) alkalinity; (iii) concentration of toxic substances; (iv) temperature; and (v) optimum pH of the fermenting microorganism [74].

12.5.1 Separated Hydrolysis and Fermentation (SHF)

Enzymatic saccharification of starchy biomass is carried out first in a SHF process at the optimum temperature using a saccharifying enzyme. The saccharified solution is then fermented using suitable microorganisms [93]. These advantages of SHF are the low capital cost of chemicals, short residence time, and simple equipment systems, which inspire its large-scale processing [93, 100]. The SHF process is usually active in research studies to enhance the operative conditions such as pH, temperature, and time of both stages, which help determine the diverse mechanisms involved in the process and the effect as displayed by several parameters and continuous fermentation with cell recycling. Nevertheless, the operation procedure of SHF has some drawbacks. When compared with SSF (Sect. 12.5.2 below), the SHF process has disadvantages such as higher capital cost due to the large mechanical setup for separation steps, and elevated enzyme concentrations and low solids loading required to achieve good ethanol yields.

Moreover, the longtime running of the process may lead to contamination of the substrate by microorganisms [108]. The main advantage of the SHF process is that

Table 12.5 Comparison of bioethanol yields from microalgae by fermentation processes with fermentative microorganisms

Microalgae species	Hydrolysis	Fermentation	Fermentative microorganism	Fermentation condition	Bioethanol yields	References
<i>Chlorococcum infusionum</i>	Chemical (NaOH)	SHF	<i>S. cerevisiae</i>	200 rpm, 72 h	0.26 g ethanol/g algae	[101]
<i>Chamydomonas reinhardtii</i> UTEX 90	Enzymatic	SSF	<i>S. cerevisiae</i> S288C	160 rpm, 30 °C, 40 h	0.235 g ethanol/g algae	[75]
<i>Chlorella vulgaris</i>	Chemical (H ₂ SO ₄)	SHF	<i>E. coli</i> SII.2526	170 rpm, 37 °C, pH 7	0.4 g ethanol/g algae	[102]
<i>Porphyridium cruentum</i>	Enzymatic	SSF	<i>S. cerevisiae</i> KCTC 7906	37 °C, 9 h, pH 4.8	2.77 mg/mL (seawater) and 2.98 mg/mL (freshwater)	[103]
<i>Scenedesmus obliquus</i> CNW-N	Chemical (H ₂ SO ₄)	SHF	<i>Z. mobilis</i> ATCC29191	30 °C within 4 h, pH 6	8.55 g/L	[33]
<i>Chlamydomonas fasciata</i>	Enzymatic	SSF	<i>S. cerevisiae</i>	100 rpm, 40 °C, 30 h	0.194 g ethanol/g algae	[61]
<i>C. vulgaris</i>	Enzymatic	SHF	<i>Z. mobilis</i>	30 °C in desktop fermentation	0.178 g ethanol/g algae	[33]
<i>C. vulgaris</i>	Enzymatic	SSF	<i>Z. mobilis</i>	30 °C in desktop fermentation	0.214 g ethanol/g algae	[33]
<i>C. vulgaris</i>	Chemical (H ₂ SO ₄)	SHF	<i>Z. mobilis</i>	30 °C in desktop fermentation	0.233 g ethanol/g algae	[33]
<i>Scenedesmus abundans</i>	Enzymatic	SHF	<i>S. cerevisiae</i>	200 rpm, 30 °C for 48 h	0.103 g ethanol/g dry weight algae	[104]
<i>Chlorella sorokiniana</i>	Enzymatic	SSF	<i>S. cerevisiae</i>	150 rpm, 72 h, pH 5.5–6.5	0.292 g ethanol/g algae	[84]
<i>Spirulina platensis</i> LEB 18	Enzymatic	SSF	<i>S. cerevisiae</i>	60 h	73 g/L	[105]
<i>Chlorella</i> sp.	Enzymatic	SHF/SSF	<i>S. cerevisiae</i>	30 °C, 20 h	0.40–0.16 g/g	[23]
<i>Chlorococcum</i> sp.	Enzymatic	SHF	<i>S. cerevisiae</i>	50 h	0.48 g/g	[101]
<i>T. suecica</i>	Chemical (NaOH)	SHF	<i>S. cerevisiae</i>	30 °C, 48 h	0.073 g/g	[106]
<i>Chlamydomonas Mexicana</i>	Combined (sonication and enzymatic)	SSF SHF	Yeast cells	30 °C, pH 5 50 °C, pH 5, 24 h	10.5 g/L 8.48 g/L	[107]

enzymatic hydrolysis and fermentation work at their optimum conditions. However, the operational disadvantage of the SHF process is an accumulation of sugars that inhibit enzyme activity [100, 109].

12.5.2 Simultaneous Saccharification and Fermentation (SSF)

SSF process uses both saccharification (enzyme hydrolysis) and fermentation processes in a single reactor or vessel, unlike SHF. In this process, feedstocks, enzymes, and yeast are added in an organized and orderly way to release fermentable (monomer) sugars, and then monomer sugars are converted into bioethanol [93, 100]. SSF is an effective process over the dilute acid or high-temperature water pretreated biomass, providing more exposure to the hydrolase enzymes. Saccharides are converted into fermentable sugars using cellulases and xylanases enzymes in SSF [93, 110]. SSF process required compatible conditions with similar pH, temperature, and optimum substrate concentration [93, 111].

Many studies specify that SSF provides better processing than other methods due to reduction in capital cost, due to the requirement of a small number of enzymes, processing time, lower risk of contamination, minor inhibitory effects, and higher production of ethanol [93, 99, 108, 112, 113].

12.5.3 Simultaneous Saccharification and Co-Fermentation (SSCF)

Fermentative microorganisms like *Saccharomyces cerevisiae* are used in fermentation for bioethanol production. Still, these fermentative microorganisms are not able to convert carbohydrates like pentose sugars into bioethanol under mild conditions, which leads to impurities in biomass and decreases bioethanol production. Genetically engineered yeasts can be used to convert leftover pentose sugars into bioethanol. Genetically modified yeasts and cellulase enzyme complex are used in the same vessel or equipment for ethanol production from feedstock in SSCF. SSCF process is usually the same as the SSF process [114]. SSCF process has many advantages like eliminating end products of enzymatic saccharification that inhibit cellulases or β -glucosidases enzymes and higher yield of ethanol and efficiency than separate hydrolysis and fermentation (SHF), and reduced capital cost [115].

SSCF is a capable process for bioethanol production from both pentose sugars (hemicellulose) and hexose sugars (cellulose) in which saccharification and fermentation coincide in a single vessel and reactor [74, 93]. SSCF is a recommended process when a significant contribution of the pentoses sugars (C5) originates after hydrolysis. Genetically modified microorganisms like *S. cerevisiae* and *Z. mobilis*

are primarily used in the SSCF to break down glucose and xylose. To reach the higher ethanol yield route, Peralta-Ruiz et al. [116] did the handling of simulated technological paths by ASPEN PLUS 7.1 software which was based on experimental information; simulation results showed the advancement of ethanol yield by 23.6% in the SSCF pathway, 20.1% enhancement by SSF pathway as well as 18.5% advancement by the SHF pathway also. Therefore, SSCF can achieve the hydrolysis and co-fermentation of pentose and hexose sugars in the same vessel or reactor without restrictive ethanol made from cellulosic biomass [93, 117]. SSCF process can break down glucose and pentoses in the same vessel or reactor. Simultaneously, SSF is separated from pentoses in fermentation, but both approaches have a quick enzymatic hydrolysis process, low capital cost, and higher ethanol yield than SHF [93, 118].

12.5.4 Consolidated Bioprocessing (CBP)

CBP integrates hydrolysis (saccharification) and fermentation of feedstock to the desired bioproduct, requiring fewer energy inputs and fewer equipment requirements than the conventional multi-step fermentation process [119]. Microorganisms, which have been modified to enhance the production of ethanol as well as tolerance of ethanol. Instead of this, there is no single commercially available consolidated bioprocessing (CBP) organism reported. One single genetically engineered microorganism is used for hydrolysis and fermentation steps in the biological approach to CBP. A consortium consists of an enzyme-producing strain that can hydrolyze the biomass and another two different strains that can ferment C5 and C6 sugars into ethanol. Brethauer and Studer [120] proposed a model utilizing *Trichoderma reesei*, which necessitates aerobic conditions for resourceful enzyme secretions; *Saccharomyces cerevisiae* breakdown hexoses sugar to ethanol. *Scheffersomyces stipitis* is one of the best natural yeasts that uses pentose sugars and capably produces ethanol under microaerophilic conditions. In a biofilm membrane reactor, all of these microbes convert lignocellulosic biomass into ethanol, and the approach seems reasonable. Still, the primary obstacle of CBP is controlling the consortium. It is also challenging to find microorganisms with identical fermentation conditions [100], potentially reducing capital costs and increasing process efficiency. However, microorganisms producing enzymes for hydrolysis of biomass and fermentation of released sugars are still in the early stage of development [121].

12.6 Macroalgae Biorefinery

Macroalgae can constitute the raw materials for third-generation biorefineries as these are composed of fermentable carbohydrates and have the advantage of not having lignin in their structure. This section will review the chemical and structural characteristics of macroalgae that can be used in a biorefinery.

According to their photosynthetic pigment, macroalgae, also known as “seaweed,” are photosynthetic aquatic organisms divided into red, green, and brown varieties. Thus, these are *Chlorophyta* (green algae), *Rhodophyta* (red algae), and *Phaeophyta* (brown algae). Macroalgae do not compete for space in farmed areas since they are aquatic plants. Water makes up 90–85% of its content, in addition to collecting CO₂ from the atmosphere [122, 123].

Macroalgae have structures similar to land plants since they have leaves, stems, and some roots, as shown in Fig. 12.6, and are listed as:

- The Thallus: which is a body-like structure that can perform photosynthesis.
- Lamina or blades: lamina is a leaf-like structure, having great property to absorb sunlight, and it is one of the keys of photosynthetic systems.
- Stripe: it a stem-like structure that provides support and exists only in some species. It can be long and challenging that transports sugars from the blades and acts as an attachment.
- Floats: floating structures filled with a kind of gas that is located on the lamina and stipe. They hold mainly carbon monoxide, and the primary function is to maintain the edges in shallow waters where light is easily captured.
- Holdfast: it is a root-like structure that assists in holding the plant on the surface of rocks and does not penetrate in the sand. It does not support gathering nutrients from the surroundings.
- Frond, commonly referred to as the combination of the blade and stipe [124]

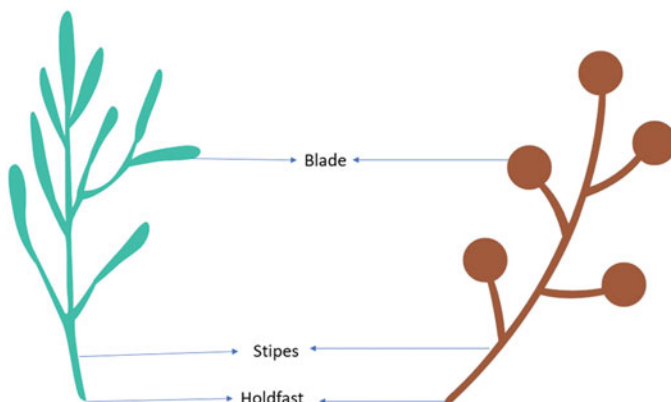


Fig. 12.6 Morphology characteristics of macroalgae

The required components for growth are frequently available in the coastal environment; therefore, seaweed production does not require arable land or fertilizer. Furthermore, macroalgae biomass outputs can be higher than most terrestrial crops throughout a growing season [125]. In this regard, using seaweed biomass to make biofuels seems to be a potential approach for supplementing and securing energy supply while also reducing reliance on fossil fuels, which is in line with the EU's goal [8].

Macroalgae are extremely important, since they can control pollution, eutrophication, and increase biomass in water bodies due to increased nutrients such as nitrogen and phosphorus. They also have characteristics that make them good candidates for application in the biorefinery. Macroalgae have higher efficiency in photon conversion than terrestrial plants and accumulate large amounts of carbohydrate biomass from inexpensive nutrient sources. Because they are buoyant, they do not produce structural polysaccharides like hemicellulose and lignin, so the process for ethanol production, in the pretreatment part, is much more straightforward [26]. Biomass production from red algae produces more energy than other biomass sources. Like terrestrial plants, macroalgae contain high value-added chemicals like carbohydrates, lipids, proteins, and other compounds, such as chlorophyll or carotenoid pigments. Carbohydrates are divided into polysaccharides and monosaccharides. These carbohydrates are in the cell walls and are generally alginates, agar, carrageenan, cellulose, fucoidan, and hemicellulose [124]. Macroalgae have advantages over terrestrial plants because several of these carbohydrates are different from glucose polysaccharides. These compounds can be used in various processes, almost always stabilizing thickening or gelling agents [126]. Also, macroalgae contain sulfur carbohydrates (sulfated carbohydrates) such as fucoidan, which has immuno-modulatory and anti-inflammatory activities, lower blood lipid levels, and anticoagulant, antithrombotic antivirus antitumor, and antioxidant activity and activity against hepatopathy and renal disease, among others [127]. In the same way, mannitol, sugar alcohol, has hydrating and antioxidant activity and has a sweet taste, so it is used as a sweetener and reduces the crystallization of sugars.

Red algae, also called Rhodophyta, have agar and carrageenans in their cell wall, composed of sulfated galactan [128]. Green algae or Chlorophyta have three heteropolysaccharides in their cell wall: glucuronoxylorhamnans, glucuronoxylorhamnogalactans, or xyloarabinogalactans. Finally, the brown algae or Phaeophyta's cell wall comprises alginate, a uronide polymer comprising manuronate and guluronate residues, and laminarin, a pillar of β -1,3-linked glucose moieties with β -1,6-linked branches [129].

As can be inferred, the composition of the different types of algae varies. Of the 10–15% of the dry matter that makes up algae, 60–65% is carbohydrates, and like all plants, this composition is influenced by the growing conditions and the climate [26]. In general, the carbohydrate composition is as follows:

- Green algae. Polysaccharides: mannan, ulvan, starch, cellulose. Monosaccharides: glucose, mannose, uronic acid.

- Red algae. Polysaccharides: carrageenan, agar, cellulose, lignin. Monosaccharides: glucose, galactose, agarose,
- Brown algae. Polysaccharides: laminarin, mannoside, alginate, glucan, cellulose. Monosaccharides: glucose, galactose, uronic acid.

Compared to other compounds, brown and red algae have less lipid content than green algae. In contrast, green algae species have higher cellulose content than red and brown algae and may contain starch. Furthermore, macroalgae have a higher range of alkali metals and halogen content [122].

Enzymatic hydrolysis research is focused on producing high-value products from seaweed biomass since the product yields could be more profitable in focused markets than biofuels. Seaweed is known to contain a wide array of naturally occurring bioactive compounds; carotenoids, fatty acids, phycocolloids, sterols, and an extensive range of secondary metabolites [130]. Compared with terrestrial biomass sources, algal biomass is composed mainly of lipids and proteins and has a faster growth rate, thus increasing photosynthetic efficiency [131]. This hydrolysis could imply a reliable source for biofuels and high added-value products. Table 12.6 lists some of the research reported for producing higher value-added compounds from seaweed biomass.

Considering the growing markets worldwide, such as the surge in some populational sectors demanding healthy products for consumption and some species of seaweed have been consumed historically in Asian cultures for millennia [132], opportunities exist for using edible seaweed biomass food formulations. Several studies propose the implementation of bioactive extracts in meat and meat derived products since the current overview of meat have been dwindling and is no longer considered essential in the human diet; polysaccharides, protein, omega-3 fatty acids, carotenoids, phenolic compounds, vitamins, and minerals could transform meat into a functional food since some formulations can improve the “bad” nutritional aspects but the most significant drawback encountered is the organoleptic modification of the meat, that impact negatively in consumer acceptance [133].

Biologically active compounds could become the backbone of some biorefinery processes. *Laminaria japonica* is a reliable source of alginic oligosaccharides that possesses a wide assortment of exploitable qualities: antioxidant, prebiotic activity, cytokine-inducing activity in mononuclear blood cells, and plant rooting enhancers, which are usually obtained with environmentally harsh procedures. It has been confirmed that a combination of commercial cellulases for the saccharification process and an engineered yeast (*Yarrowia lipolytica*) obtain a yield of 91.7% [16] and an oligosaccharide purity of 92.6%, with the added benefits of being an environmentally friendly procedure. Bioactive peptides with pharmaceutical activities are also obtainable since seaweed can be utilized as another alternative protein source, peptides are a given, and some peptides available from macroalgae present antioxidant, antihypertensive, anti-inflammatory, and antidiabetic activities, this, however, is limited to the variation of the protein content influenced by several factors, and the obtention can be difficult since the complex constitution of seaweed hinders the obtention of bioactive peptides. Also, there is a lack of proteomic studies to reduce the scope of peptide utilization and identification [134].

Table 12.6 High value-added bioproducts obtainable from macroalgal biomass using specific enzymes

Algae	Enzyme utilized/ methodology	Bioprodut obtained	Purposed outlook	References
<i>Hizikia fusiforme</i>	Commercial cellulases	Fucoidan	Antioxidant for food or cosmetic application	[136]
<i>Sargassum horneri</i>	Recombinant fucoidanase FFA1	Fucoidan	Anticancer and radiosensitizer action	[137]
<i>Macrocytis pyrifera</i>	Commercial cellulases	Bioactive proteins	Antioxidant, potential antihypertensive	[138]
<i>Chondracanthus chamussoi</i>	Commercial cellulases	Bioactive proteins	Antioxidant	[138]
<i>Palmaria palmata</i>	Cellulases/ alkaline extraction	Protein	Protein-rich feed for poultry or fish	[139]
<i>Laminaria japonica</i>	Alginate lyase/ thermo—acid pretreatment	Low-molecular-weight polysaccharides rich in uronic acid	Anti-obesity agent	[140]
<i>Sargassum fulvellum</i>	Commercial cellulases	Bioactive carbohydrates	Antioxidant	[141]
<i>Porphyra dioica</i>	Prolyve®1000 and Flavourzyme®	Bioactive proteins	Antioxidant	[142]
<i>Gracilaria lemaneiformis</i>	H ₂ O ₂ -assisted enzymatic method	Sulfated rich agar	Improved gel strength	[143]
<i>Laminaria japonica</i>	Cellulase and recombinant alginate lyase	Alginate oligosaccharides	Prebiotic, immunomodulating, antioxidant and plant rooting agent	[16]

Macroalgal biomass is predominantly used for high value-added byproducts and food production around the world. The biorefinery approximation for biofuels, bioactive compounds, and biomaterials production is currently under development [135]. The number of algal fuel producer companies is increasing globally, and there is undeniable potential for the utilization of enzymes for the marine biomass transformation industry.

12.6.1 Enzymatic Hydrolysis of Macroalgal Biomass

The more widespread utilization of enzymes in biorefinery is the hydrolysis of the structural polysaccharides to promote a more effective saccharification process to

widen the availability of assimilable sugars for posteriors biotransformation via microorganism's metabolism. Since the financial implications regarding the cost of the whole saccharification process do not allow the sole utilization of enzymes [7, 144], some methodologies have been coupled to synergize and lower the targeted production costs of biofuel or high added value products. All costs can provide seaweed biomass even in countries with cold weather; Nordic countries have limited light levels and low temperatures that hinder first-generation biofuels, but the vast coastlines are rich in marine biomass. For example, *Saccharina latissima* known for its high carbohydrate content, is widely available in the warm cost and studies to have been made for its utilization in methane production; an enzyme complex of β -1-3/1-4-glucanase, cellulase, xylanase, β -glucosidase, β -xylosidase, α -L-arabinofuranosidase was utilized to improve the reducing sugar release of alkaline treated pulp for anaerobic digestion. Enzymatic hydrolysis of macroalgal biomass can potentially harness 1760 m³ per hectare of the productive seafloor for *S. latissima* [145].

Industries revolving around marine biomass residues can be a good source for biofuels and high added-value products. An estimated 57,500 tons of carrageenan are annually produced, and as long the hydrocolloid industry is growing, its waste will increment accordingly. The waste obtained from the carrageenan extraction of *Kappaphycus alvarezii* can be transformed with an acid pretreatment and later enzymatically hydrolyzed to enhance the saccharification of galactose and glucose 13.8 g/L of ethanol yield after a fermentation process utilizing a modified *Saccharomyces cerevisiae* (ATCC 200062) [146]. Agar is another phycocolloid obtained from red algae, and the agar extraction industry for *Gelidium* and *Gracilaria* seaweeds produces around 100,000 tons of carbohydrate-rich residues each year; this residue still has potential for the extraction of valuable compounds, according to a study [147] that hydrolyzed the residues using a sulfamic acid pretreatment and enzymatic hydrolysis.

12.6.2 Conversion of Sugars into Ethanol from Macroalgae

Bioethanol can be produced from macroalgae by converting sugars released in the enzymatic saccharification process [148] by fermentation using various microorganisms [149], as shown in Table 12.7. Fermentation is a process in which alcohol and CO₂ (carbon dioxide) are converted from glucose; stoichiometrically, 1 g of glucose produces 0.51 g of ethanol along with 0.49 g of CO₂ after fermentation. Bioethanol yields are highly dependent on temperature, pH level, growth rate, alcohol tolerance, osmotic resistance, and genetic stability of the fermenting microorganism. Among the organisms that can be employed in bioethanol production, the mainly used *Saccharomyces cerevisiae*, *Pichia angophorae*, *Pichia stipitis* [150, 151], *Kluyveromyces marxianus* [152], *Zymomonas mobilis* [153], among others shown in Table 12.6.

Table 12.7 Ethanol yields from macroalgae biomass according to fermentation strategy and microorganism strain

Macroalgae biomass	Fermentation strategy	Strain	Ethanol concentration (g/L)	Ethanol yield (%)	References
<i>Sargassum</i> spp.	PSSF	<i>S. cerevisiae</i> PE-2	18.14 ± 1.11	76.23 ± 4.68	[160]
<i>Saccharina japonica</i>	SSF	Thermotolerant <i>S. cerevisiae</i> DK 410362	6.65	67.41	[161]
<i>Laminaria digitata</i>	SHF	Commercial yeast <i>S. cerevisiae</i>	20.7	70.6	[162]
<i>Gelidium amansii</i>	SHF	<i>S. cerevisiae</i> KCTC 7906	3.33	74.7	[163]
<i>Gelidium amansii</i>	SSF	<i>S. cerevisiae</i> KCTC 7906	3.78	84.9	[163]
<i>Gelidium amansii</i>	SSF	<i>S. cerevisiae</i> KCTC 7906	25.7	76.9	[163]
<i>Ulva rigida</i>	SHF	Adapted <i>Pachysolen tannophilus</i>	11.92	72.35	[158]
<i>Sargassum muticum</i>	SSF	<i>S. cerevisiae</i> CEN.PK 1137D	11.32	94.4	[164]
<i>Sargassum muticum</i>	SSF	<i>S. cerevisiae</i> PE-2	12.23	81	[164]
<i>Sargassum muticum</i> ^a	SSF	<i>S. cerevisiae</i> PE-2	14.10	81	[164]
<i>Rhizoclonium</i> sp.	SHF	Immobilized <i>S. cerevisiae</i> TISTR 5020	65.43 ± 18.13	—	[165]
<i>Laminaria digitata</i>	SHF	<i>S. cerevisiae</i> NCYC 2592	3.2	94.4	[166]

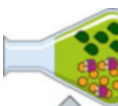
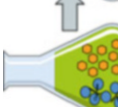
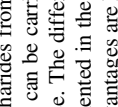
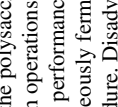
^aUsing hydrolysate from pretreatment as reaction medium

K. marxianus is a species of yeast that is thermotolerant with proficiency to ferment an extensive range of substrates. Some advantages involve the consumption of several sugars at elevated temperatures and weak glucose repression. *K. marxianus* can work at temperatures up to 47 °C with a solid affinity for xylose [152] and possesses high growth rates and less tendency to ferment when exposed to excess sugars [154]. *Z. mobilis* is a bacterium facultatively anaerobic and nonsporulating ethanologenic that converts sugars to ethanol through the Entner-Doudoroff pathway; this microorganism accumulates less biomass during fermentation more sugar can be converted to ethanol, increasing its observed yield. *Z. mobilis* metabolizes glucose, fructose, and sucrose. It can endure high sugar concentrations [155]. *P. stipitis*, also known as *Scheffersomyces stipites*, is a homo-thallic yeast that can ferment pentose sugar like xylose. The fermentation starting is not dependent on sugar concentration. However, it is regulated by a decrease in oxygen availability. It possesses a greater respiratory capacity owing to the existence of an alternate respiration system. It also includes the enzyme dihydroorotate dehydrogenase, which grants the ability to grow anaerobically [152]. *Pichia angophorae* showed that fermentation could occur with hydrolysates containing laminarin and mannitol present in brown macroalgae [151]. Other microorganisms have been used, like the marine yeast *Meyerozyma guilliermondii*, which can be a candidate for the marine bases substrates [156], non-adapted *Pachysolen tannophilus*, and the marine fungus *Cladosporium sphaerospermum* have also been studied on macroalgae feedstock for bioethanol production [157, 158]. However, *Saccharomyces cerevisiae* are the most employed microorganisms mainly due to their effectiveness, resistance to high ethanol and inhibitor concentrations, and high osmotic resistance [150, 151]. *S. cerevisiae* is the most exploited yeast in industrial for bioethanol production [157]. Besides that, *S. cerevisiae* has an exceptional function in high sugar concentrations that merge passive sugar transport with high glucose flux through glycolysis to ethanol production, despite the presence of oxygen, thereby having a strong positive Crabtree effect. These are an excellent advantage in the extensive industrial configuration where anaerobiosis has an additional level of difficulty, namely removing available oxygen in a closed batch bioreactor or fed-batch bioreactor using setting at the time of fermentation and avoiding the integration of ethanol at the final step of fermentation [159].

Another critical parameter is the fermentation strategy chosen. The primary users are SHF, Separate Hydrolysis and Co-Fermentation (SHCF), SSF, Simultaneous Saccharification and Co-Fermentation (SSCF), and Pre-Simultaneous Saccharification and Fermentation (PSSF), for bioethanol production based on first and second-generation. Table 12.8 shows all strategies in detail.

Studies have been reported for bioethanol production from macroalgae. Tan et al. [171], used *Saccharomyces cerevisiae* PE-2 under SSF strategy and reached 12.23 and 14.19 g/L of ethanol concentration employing water and hydrolysate from hydrothermal pretreatment as a medium, respectively, obtaining a conversion yield of 81%. Hou et al. [162] used *Laminaria digitata* as a feedstock for bioethanol production under SSF and SHF strategies using *S. cerevisiae* (Quick Yeast, Doves Farm Foods Ltd.), their results were 14.7 ± 0.3 g/L of ethanol equivalent to a

Table 12.8 Main strategies used in bioethanol production from macroalgae

Strategy	Schematic representation	Description	References
SHF		SHF is a process where hydrolysis of the polysaccharides from macroalgae and fermentation of hexoses are performed separately. Both operations can be carried out at optimal conditions (pH, temperature), thus maximizing general performance. The difference between SHF and SHCF is that pentoses and hexoses are simultaneously fermented in the second step. Advantages are that conditions are adequate for each procedure. Disadvantages are long process times, use of enzymes and microorganisms capable of assimilating pentoses, which entails increasing overall cost of the process	[167, 168]
SHCF			
SSF		SSF combines enzymatic hydrolysis of macroalgae and fermentation of the hexoses in a single stage. The process is faster, but inhibitors from pretreatment could affect with more intensity on yeast microorganisms. An in the above strategies, the difference between SSF and SSCF is that the second considers enzymes and microorganisms for hexoses and pentoses. SSF process has several advantages such as less enzyme requirement, low-risk contamination. Simultaneous approach is usually preferred over approaches that work separately due to the faster ethanol production rate resulting in the rapid metabolism by yeast of the sugars released. However, the difference between the optimal temperatures of hydrolysis and fermentation (50 °C for enzymatic hydrolysis and 30–35 °C for fermentation) comprises the primary deficiency	[169–171]
SSCF			
PSSF		PSSF consists of the first stage of enzymatic hydrolysis, generally between 4 and 24 h, at the optimal conditions of the enzymes, followed by the addition of the fermenting microorganism(s) to start the fermentation stage at the optimal conditions. This process allows the reduction of viscosity in the slurry, improving the mass transfer in the conversion to ethanol, thereby increasing the ethanol yields	[172, 173]

conversion yield of 50.5% under SSF strategy, and 20.7 ± 0.5 g/L of ethanol equivalent to a conversion yield of 70.6 ± 1.8 under SHF strategy. They concluded that the lesser ethanol produced is due to the low efficiency in the enzymatic hydrolysis stage (enzymes work at optimal conditions at 50 °C, and the experiment was carried out at 32 °C. Kim et al. [163] investigated bioethanol production from autoclave treated *Gelidium amansii* as biomass. The research study states that the comparative analysis of SHF and SSF for 2% (w/v) supports the SSF process for the highest bioethanol conversion yield corresponding to 90.7% with 3.33 mg/mL and 84.9% with 3.78 mg/mL, respectively. On proceeding for the SSF process at 15%, solid loading (w/v) gives a satisfactory result with an increment in bioethanol concentration 25.07 mg/mL with 76.9% conversion yield. Lee et al. [161] worked with thermotolerant yeast *S. cerevisiae* DK 410362 under SSF strategy, scaling from 3 to 6% (w/v) of solid loading. They achieved 3.84 and 6.65 g/L of maximum ethanol concentration for 3 and 6%, reaching 78.41 and 67.39% ethanol yield, respectively. Another study, El Harchi et al. [158], adapted *Pachysolen tannophilus* to ferment *Ulva rigida* biomass under SHF strategy; they reached 11.92 g/L of ethanol concentration 72.35% conversion yield.

The studies highlight that sugars from macroalgae could be a potential feedstock for bioethanol production. However, additional research is needed to achieve an eco-friendly and economically viable process. Further, more studies are required to fully comprehend the antiviral action mechanisms of algal chemicals and reap the benefits of their utilization as functional additives in the pharmaceutical and food sectors.

12.7 Conclusions and Future Outlook

Micro- and macro-algae biomass can produce novel bioproducts and are used as an indigenous biological source serving as a bridge between the environment and changing climatic conditions by creating eco-friendly energy products with extensive food, medicine, bioenergy, and cosmetics industries in terms of biorefinery. Micro- and macro-algae biofuel production under the biorefinery strategy is expected to significantly enhance algae biofuels' overall cost-effectiveness. However, integrating diverse biomass conversion methods in a whole algal biorefinery operation remains a fundamental problem. Before industrial use of algal technology and the commercialization of microalgal biofuels becomes realized, considerable technological breakthroughs and increased biomass production are required. In terms of biorefinery, technical advancements in extraction technique and enzymatic saccharification are necessary to improve the cost-effectiveness of end products such as micro-and macro-algae biofuels. Nonetheless, algal biorefinery processes can be implemented in the near future if the expense of biofuels is compensated by revenue from bioproducts for the circular bioeconomy.

Acknowledgments This work was financially supported by the Innovation Incentive Program (PEI)—Mexican Science and Technology Council (SEP-CONACYT) with the Project (Ref. PEI-251186), titled: Study of the variation temporary space of Fucoidan from Sargassum SP. Rohit Saxena is grateful to the National Council for Science and Technology (CONACYT, Mexico) for supporting his Ph.D. Fellowship.

References

1. Makut BB. Algal biofuel: emergent applications in next-generation biofuel technology. *Liq Biofuels Fundam Charact Appl.* 2021;119–44. <https://doi.org/10.1002/9781119793038.ch4>.
2. Aguilar-Reynosa A, Romani A, Rodriguez-Jasso RM, Aguilar CN, Garrote G, Ruiz HA. Microwave heating processing as alternative of pretreatment in second-generation biorefinery: an overview. *Energy Convers Manag.* 2017;136:50–65. <https://doi.org/10.1016/j.enconman.2017.01.004>.
3. Aguilar DL, Rodríguez-Jasso RM, Zanuso E, de Rodríguez DJ, Amaya-Delgado L, Sanchez A, Ruiz HA. Scale-up and evaluation of hydrothermal pretreatment in isothermal and non-isothermal regimen for bioethanol production using agave bagasse. *Bioresour Technol.* 2018;263:112–9. <https://doi.org/10.1016/j.biortech.2018.04.100>.
4. Jabeen S, Malik S, Khan S, Khan N, Qureshi MI, Saad MSM. A comparative systematic literature review and bibliometric analysis on sustainability of renewable energy sources. *Int J Energy Econ Policy.* 2021;11:270–80. <https://doi.org/10.32479/ijep.10759>.
5. BP. Statistical review of world energy. 69th ed; 2020. <https://www.bp.com/content/dam/bp/business-sites/en/global/corporate/pdfs/energy-economics/statistical-review/bp-stats-review-2020-full-report.pdf>
6. Gielen D, Boshell F, Saygin D, Bazilian MD, Wagner N, Gorini R. The role of renewable energy in the global energy transformation. *Energy Strateg Rev.* 2019;24:38–50. <https://doi.org/10.1016/j.esr.2019.01.006>.
7. Ruiz HA, Rodríguez-Jasso RM, Fernandes BD, Vicente AA, Teixeira JA. Hydrothermal processing, as an alternative for upgrading agriculture residues and marine biomass according to the biorefinery concept: a review. *Renew Sust Energ Rev.* 2013;21:35–51. <https://doi.org/10.1016/j.rser.2012.11.069>.
8. Alvarado-Morales M, Boldrin A, Karakashev DB, Holdt SL, Angelidaki I, Astrup T. Life cycle assessment of biofuel production from brown seaweed in Nordic conditions. *Bioresour Technol.* 2013;129:92–9. <https://doi.org/10.1016/j.biortech.2012.11.029>.
9. Ruiz HA, Thomsen MH, Trajano HL. Hydrothermal processing in biorefineries. 1st ed. Cham: Springer International Publishing; 2017. <https://doi.org/10.1007/978-3-319-56457-9>.
10. Rosero-Chasoy G, Rodríguez-Jasso RM, Aguilar CN, Buitrón G, Chairez I, Ruiz HA. Microbial co-culturing strategies for the production high value compounds, a reliable framework towards sustainable biorefinery implementation – an overview. *Bioresour Technol.* 2021; <https://doi.org/10.1016/j.biortech.2020.124458>.
11. Veillette M, Chamoumi M, Nikiema J, Faucheu N, Heitz M. Production of biodiesel from microalgae. *Adv Chem Eng.* 2012; <https://doi.org/10.5772/31368>.
12. Velazquez-Lucio J, Rodríguez-Jasso RM, Colla LM, Sáenz-Galindo A, Cervantes-Cisneros DE, Aguilar CN, Fernandes BD, Ruiz HA (2018) Microalgal biomass pretreatment for bioethanol production: a review. *Biofuel res J* 5:780–791. DOI: <https://doi.org/10.18331/BRJ2018.5.1.5>.
13. Chen CY, Yeh KL, Aisyah R, Lee DJ, Chang JS. Cultivation, photobioreactor design and harvesting of microalgae for biodiesel production: a critical review. *Bioresour Technol.* 2011;102:71–81. <https://doi.org/10.1016/j.biortech.2010.06.159>.

14. Chew KW, Yap JY, Show PL, Suan NH, Juan JC, Ling TC, Lee DJ, Chang JS. Microalgae biorefinery: high value products perspectives. *Bioresour Technol.* 2017;229:53–62. <https://doi.org/10.1016/j.biortech.2017.01.006>.
15. Cho S-J, Lee D-H, Luong TT, Park S-R, Oh Y-K, Lee T-H. Effects of carbon and nitrogen sources on fatty acid contents and composition in the green microalga, *Chlorella* sp. 227. *J Microbiol Biotechnol.* 2011;21:1073–80. <https://doi.org/10.4014/jmb.1103.03038>.
16. Li SY, Wang ZP, Wang LN, Peng JX, Wang YN, Han YT, Zhao SF. Combined enzymatic hydrolysis and selective fermentation for green production of alginic oligosaccharides from *Laminaria japonica*. *Bioresour Technol.* 2019;281:84–9. <https://doi.org/10.1016/j.biortech.2019.02.056>.
17. James I, Yoon LW, Chow YH. Effect of phosphorus-limited nutrients on growth and glucose production from microalgae. In AIP Conf proceedings [AIP Publishing proceedings of the international engineering research conference - 12th eureka 2019 - Selangor Darul Ehsan, Malaysia (3–4 July 2019)] (Vol. 2137, No. 1, p. 020005). AIP Publishing LLC; 2019. <https://doi.org/10.1063/1.5120981>.
18. Zaparoli M, Zienniczak FG, Mantovani L, Costa JAV, Colla LM. Cellular stress conditions as a strategy to increase carbohydrate productivity in *Spirulina platensis*. *Bioenergy Res.* 2020;13:1221–34. <https://doi.org/10.1007/s12155-020-10133-8>.
19. He Y, Chen L, Zhou Y, Chen H, Zhou X, Cai F, Huang J, Wang M, Chen B, Guo Z. Analysis and model delineation of marine microalgae growth and lipid accumulation in flat-plate photobioreactor. *Biochem Eng J.* 2016;111:108–16. <https://doi.org/10.1016/j.bej.2016.03.014>.
20. Fernández FGA, Reis A, Wijffels RH, Barbosa M, Verdelho V, Llamas B. The role of microalgae in the bioeconomy. *New Biotechnol.* 2021;61:99–107. <https://doi.org/10.1016/j.nbt.2020.11.011>.
21. Markou G, Vandamme D, Muylaert K. Microalgal and cyanobacterial cultivation: the supply of nutrients. *Water Res.* 2014;65:186–202. <https://doi.org/10.1016/j.watres.2014.07.025>.
22. Guschina IA, Harwood JL. Algal lipids and their metabolism. In: Borowitzka MA, Moheimani NR, editors. *Algae for biofuels and energy*. Dordrecht: Springer; 2013. p. 17–36. https://doi.org/10.1007/978-94-007-5479-9_2.
23. Lee OK, Oh YK, Lee EY. Bioethanol production from carbohydrate-enriched residual biomass obtained after lipid extraction of *Chlorella* sp. KR-1. *Bioresour Technol.* 2015;196:22–7. <https://doi.org/10.1016/j.biortech.2015.07.040>.
24. SundarRajan PS, Gopinath KP, Greetham D, Antonysamy AJ. A review on cleaner production of biofuel feedstock from integrated CO₂ sequestration and wastewater treatment system. *J Clean Prod.* 2019;210:445–58. <https://doi.org/10.1016/j.jclepro.2018.11.010>.
25. Fu J, Huang Y, Liao Q, Xia A, Fu Q, Zhu X. Photo-bioreactor design for microalgae: a review from the aspect of CO₂ transfer and conversion. *Bioresour Technol.* 2019;292:121947. <https://doi.org/10.1016/j.biortech.2019.121947>.
26. John RP, Anisha GS, Nampoothiri KM, Pandey A. Micro and macroalgal biomass: a renewable source for bioethanol. *Bioresour Technol.* 2011;102:186–93. <https://doi.org/10.1016/j.biortech.2010.06.139>.
27. Craggs RJ, Lundquist TJ, Benemann JR. Wastewater treatment and algal biofuel production. In: *Algae for biofuels and energy*. Springer; 2013. p. 153–63. https://doi.org/10.1007/978-94-007-5479-9_9.
28. Jez S, Spinelli D, Fierro A, Dibenedetto A, Aresta M, Busi E, Basosi R. Comparative life cycle assessment study on environmental impact of oil production from micro-algae and terrestrial oilseed crops. *Bioresour Technol.* 2017; <https://doi.org/10.1016/j.biortech.2017.05.027>.
29. Chisti Y. Biodiesel from microalgae. *Biotechnol Adv.* 2007;25:294–306. <https://doi.org/10.1016/j.biotechadv.2007.02.001>.
30. Rasala BA, Gimbel JA, Tran M, Hannon MJ, Joseph Miyake-Stoner S, Specht EA, Mayfield SP. Genetic engineering to improve algal biofuels production. In: *Algae for biofuels and*

- energy. Netherlands: Springer; 2013. p. 99–113. https://doi.org/10.1007/978-94-007-5479-9_6.
31. John RP, Bhunia P, Yan S, Tyagi RD, Surampalli RY. Microalgal ethanol production: a new avenue for sustainable biofuel production. *Bioenergy Biofuel Biowastes Biomass*. 2010;377–88. <https://doi.org/10.1061/9780784410899.ch16>.
 32. Wang H, Ji C, Bi S, Zhou P, Chen L, Liu T. Joint production of biodiesel and bioethanol from filamentous oleaginous microalgae *Tribonema* sp. *Bioresour Technol*. 2014;172:169–73. <https://doi.org/10.1016/j.biortech.2014.09.032>.
 33. Ho S-H, Huang S-W, Chen C-Y, Hasunuma T, Kondo A, Chang J-S. Bioethanol production using carbohydrate-rich microalgae biomass as feedstock. *Bioresour Technol*. 2013;135:191–8. <https://doi.org/10.1016/j.biortech.2012.10.015>.
 34. Chow T-J, Su H-Y, Tsai T-Y, Chou H-H, Lee T-M, Chang J-S. Using recombinant cyanobacterium (*Synechococcus elongatus*) with increased carbohydrate productivity as feedstock for bioethanol production via separate hydrolysis and fermentation process. *Bioresour Technol*. 2015;184:33–41. <https://doi.org/10.1016/j.biortech.2014.10.065>.
 35. Silva CEDF, Sforza E, Bertucco A. Effects of pH and carbon source on *Synechococcus* PCC 7002 cultivation: biomass and carbohydrate production with different strategies for pH control. *Appl Biochem Biotechnol*. 2017;181:682–98. <https://doi.org/10.1007/s12010-016-2241-2>.
 36. Möllers KB, Cannella D, Jørgensen H, Frigaard NU. Cyanobacterial biomass as carbohydrate and nutrient feedstock for bioethanol production by yeast fermentation. *Biotechnol Biofuels*. 2014;7:1–11. <https://doi.org/10.1186/1754-6834-7-64>.
 37. Ha GS, El-Dalatony MM, Kurade MB, Salama ES, Basak B, Kang D, Roh HS, Lim H, Jeon BH. Energy-efficient pretreatments for the enhanced conversion of microalgal biomass to biofuels. *Bioresour Technol*. 2020;309:123333. <https://doi.org/10.1016/j.biortech.2020.123333>.
 38. Thalmann M, Santelia D. Starch as a determinant of plant fitness under abiotic stress. *New Phytol*. 2017;214:943–51. <https://doi.org/10.1111/nph.14491>.
 39. Rehman ZU, Anal AK. Enhanced lipid and starch productivity of microalga (*Chlorococcum* sp. TISTR 8583) with nitrogen limitation following effective pretreatments for biofuel production. *Biotechnol Rep*. 2019;21:e00298. <https://doi.org/10.1016/j.btre.2018.e00298>.
 40. Rodjaroen S, Juntawong N, Mahakhant A, Miyamoto K. High biomass production and starch accumulation in native green algal strains and cyanobacterial strains of Thailand. *Nat Sci*. 2007;41. <https://li01.tci-thaijo.org/index.php/anres/article/view/24428>
 41. Brányiková I, Maršálková B, Doučha J, Brányík T, Bišová K, Zachleder V, Vítová M. Microalgae—novel highly efficient starch producers. *Biotechnol Bioeng*. 2011;108:766–76. <https://doi.org/10.1002/bit.23016>.
 42. Mathiot C, Ponge P, Gallard B, Sassi JF, Delrue F, Le Moigne N. Microalgae starch-based bioplastics: screening of ten strains and plasticization of unfractionated microalgae by extrusion. *Carbohydr Polym*. 2019;208:142–51. <https://doi.org/10.1016/j.carbpol.2018.12.057>.
 43. Gifuni I, Olivieri G, Krauss IR, D'Errico G, Pollio A, Marzocchella A. Microalgae as new sources of starch: isolation and characterization of microalgal starch granules. *Chem Eng Trans*. 2017;57:1423–8. <https://doi.org/10.3303/CET1757238>.
 44. Suarez Ruiz CA, Baca SZ, van den Broek LAM, van den Berg C, Wijffels RH, Eppink MHM. Selective fractionation of free glucose and starch from microalgae using aqueous two-phase systems. *Algal Res*. 2020; <https://doi.org/10.1016/j.algal.2020.101801>.
 45. Yao CH, Ai JN, Cao XP, Xue S. Characterization of cell growth and starch production in the marine green microalga *Tetraselmis subcordiformis* under extracellular phosphorus-deprived and sequentially phosphorus-replete conditions. *Appl Microbiol Biotechnol*. 2013;97:6099–110. <https://doi.org/10.1007/s00253-013-4983-x>.
 46. Singh S, Chakravarty I, Pandey KD, Kundu S. Development of a process model for simultaneous saccharification and fermentation (SSF) of algal starch to third-generation bioethanol. *Biofuels*. 2020;11(7):847–55. <https://doi.org/10.1080/17597269.2018.1426162>.

47. Kallarakkal KP, Muthukumar K, Alagarsamy A, Pugazhendhi A, Naina Mohamed S. Enhancement of biobutanol production using mixotrophic culture of *Oscillatoria* sp. in cheese whey water. *Fuel*. 2021;284:119008. <https://doi.org/10.1016/j.fuel.2020.119008>.
48. Viola R, Nyvall P, Pedersén M. The unique features of starch metabolism in red algae. *Proc R Soc B Biol Sci*. 2001;268:1417–22. <https://doi.org/10.1098/rspb.2001.1644>.
49. Chen C, Zhao X, Yen H, Ho S, Cheng C. Microalgae-based carbohydrates for biofuel production. *Biochem Eng J*. 2013;78:1–10. <https://doi.org/10.1016/j.bej.2013.03.006>.
50. de Farias Silva CE, Meneghelli D, de Souza Abud AK, Bertucco A. Pretreatment of microalgal biomass to improve the enzymatic hydrolysis of carbohydrates by ultrasonication: yield vs energy consumption. *J King Saud Univ Sci*. 2020;32:606–13. <https://doi.org/10.1016/j.jksus.2018.09.007>.
51. Gallego R, Montero L, Cifuentes A, Ibáñez E, Herrero M. Green extraction of bioactive compounds from microalgae. *J Anal Test*. 2018;2:109–23. <https://doi.org/10.1007/s41664-018-0061-9>.
52. Alam MA, Xu JL, Wang Z. Microalgae biotechnology for food, health and high value products. *Microalgae Biotechnol Food Heal High Value Prod*. 2020; <https://doi.org/10.1007/978-981-15-0169-2>.
53. Zabed HM, Akter S, Yun J, Zhang G, Awad FN, Qi X, Sahu JN. Recent advances in biological pretreatment of microalgae and lignocellulosic biomass for biofuel production. *Renew Sust Energ Rev*. 2019;105:105–28. <https://doi.org/10.1016/j.rser.2019.01.048>.
54. Kim MS, Cha J, Kim DH. Fermentative biohydrogen production from solid wastes, 1st ed. *Biohydrogen*. 2013; <https://doi.org/10.1016/B978-0-444-59555-3.00011-8>.
55. Guangyin Z, Youcui Z. Harvest of bioenergy from sewage sludge by anaerobic digestion. *Pollut Control Resour Recover*. 2017; <https://doi.org/10.1016/b978-0-12-811639-5.00005-x>.
56. Mohan SV, Devi MP, Subhash GV, Chandra R. Algae oils as fuels. In: *Biofuels from algae*. Elsevier; 2014. p. 155–87. <https://doi.org/10.1016/B978-0-444-59558-4.00008-5>.
57. Lari Z, Ahmadzadeh H, Hosseini M. Cell wall disruption: a critical upstream process for biofuel production. *Adv Feed Convers Technol Altern Fuels Bioprod New Technol Challenges Oppor*. 2019; <https://doi.org/10.1016/B978-0-12-817937-6.00002-3>.
58. Chan CH, Yusoff R, Ngoh GC, Kung FWL. Microwave-assisted extractions of active ingredients from plants. *J Chromatogr A*. 2011;1218:6213–25. <https://doi.org/10.1016/j.chroma.2011.07.040>.
59. Wong PY, Lai YH, Puspanadan S, Ramli RN, Lim V, Lee CK. Extraction of starch from marine microalgae, *Chlorella salina*: efficiency and recovery. *Int J Environ Res*. 2019;13:283–93. <https://doi.org/10.1007/s41742-019-00173-0>.
60. Hernández D, Riaño B, Coca M, García-González MC. Saccharification of carbohydrates in microalgal biomass by physical, chemical and enzymatic pre-treatments as a previous step for bioethanol production. *Chem Eng J*. 2015;262:939–45. <https://doi.org/10.1016/j.cej.2014.10.049>.
61. Asada C, Doi K, Sasaki C, Nakamura Y. Efficient extraction of starch from microalgae using ultrasonic homogenizer and its conversion into ethanol by simultaneous saccharification and fermentation. *Nat Resour*. 2012;03:175–9. <https://doi.org/10.4236/nr.2012.34023>.
62. Ma YA, Cheng YM, Huang JW, Jen JF, Huang YS, Yu CC. Effects of ultrasonic and microwave pretreatments on lipid extraction of microalgae. *Bioprocess Biosyst Eng*. 2014;37:1543–9. <https://doi.org/10.1007/s00449-014-1126-4>.
63. Ali M, Watson IA. Microwave thermolysis and lipid recovery from dried microalgae powder for biodiesel production. *Energ Technol*. 2016;4:319–30. <https://doi.org/10.1002/ente.201500242>.
64. Prabhu MS, Levkov K, Livney YD, Israel A, Golberg A. High-voltage pulsed electric field preprocessing enhances extraction of starch, proteins, and ash from marine macroalgae *Ulva ohnoi*. *ACS Sustain Chem Eng*. 2019;7:17453–63. <https://doi.org/10.1021/acssuschemeng.9b04669>.

65. Sulfahri MS, Langford A, Tassakka ACMAR. Ozonolysis as an effective pretreatment strategy for bioethanol production from marine algae. *Bioenergy Res.* 2020; <https://doi.org/10.1007/s12155-020-10131-w>.
66. Kearsley MW, Dziedzic SZ. Handbook of starch hydrolysis products and their derivatives. Dordrecht: Springer; 1995.
67. Kulp K. Handbook of cereal science and technology, revised and expanded. New York, NY: CRC Press; 2000.
68. Ratnayake WS, Jackson DS. Starch gelatinization. *Adv Food Nutr Res.* 2008;55:221–68. [https://doi.org/10.1016/S1043-4526\(08\)00405-1](https://doi.org/10.1016/S1043-4526(08)00405-1).
69. Al Abdallah Q, Nixon BT, Fortwendel JR. The enzymatic conversion of major algal and cyanobacterial carbohydrates to bioethanol. *Front Energy Res.* 2016;4:36. <https://doi.org/10.3389/fenrg.2016.00036>.
70. Lakatos GE, Ranglová K, Manoel JC, Grivalský T, Kopecký J, Masojídek J. Bioethanol production from microalgae polysaccharides. *Folia Microbiol (Praha)*. 2019; <https://doi.org/10.1007/s12223-019-00732-0>.
71. Sharma P, Sharma N, Sharma N. Optimization of enzymatic hydrolysis conditions for saccharification of carbohydrates in algal biomass: an integral walk for bioethanol production-121. *Pharma Innov.* 2019;8:461–6. <http://www.thepharmajournal.com/index.html>
72. de Farias Silva CE, Bertucco A. Bioethanol from microalgal biomass: a promising approach in biorefinery. *Braz Arch Biol Technol.* 2019;62:1–14. <https://doi.org/10.1590/1678-4324-2019160816>.
73. Córdova O, Santis J, Ruiz-Fillipi G, Zuñiga ME, Fermoso FG, Chamy R. Microalgae digestive pretreatment for increasing biogas production. *Renew Sust Energ Rev.* 2018;82:2806–13. <https://doi.org/10.1016/j.rser.2017.10.005>.
74. Harun R, Yip JWS, Thiruvenkadam S, Ghani WA, Cherrington T, Danquah MK. Algal biomass conversion to bioethanol—a step-by-step assessment. *Biotechnol J.* 2014;9:73–86. <https://doi.org/10.1002/biot.201200353>.
75. Choi SP, Nguyen MT, Sim SJ. Enzymatic pretreatment of *Chlamydomonas reinhardtii* biomass for ethanol production. *Bioresour Technol.* 2010;101:5330–6. <https://doi.org/10.1016/j.biortech.2010.02.026>.
76. Zhang C, Kang X, Wang F, Tian Y, Liu T, Su Y, Qian T, Zhang Y. Valorization of food waste for cost-effective reducing sugar recovery in a two-stage enzymatic hydrolysis platform. *Energy.* 2020;208:118379. <https://doi.org/10.1016/j.energy.2020.118379>.
77. Faraj A, Vasanthan T, Hoover R. The influence of α -amylase-hydrolysed barley starch fractions on the viscosity of low and high purity barley β -glucan concentrates. *Food Chem.* 2006;96:56–65. <https://doi.org/10.1016/j.foodchem.2005.01.056>.
78. Dura A, Blaszcak W, Rosell CM. Functionality of porous starch obtained by amylase or amyloglucosidase treatments. *Carbohydr Polym.* 2014;101:837–45. <https://doi.org/10.1016/j.carbpol.2013.10.013>.
79. Antranikian G, Bertoldo C. Starch-hydrolyzing enzymes from thermophilic archaea and bacteria. *Curr Opin Chem Biol.* 2002;151–60. [https://doi.org/10.1016/S1367-5931\(02\)00311-3](https://doi.org/10.1016/S1367-5931(02)00311-3).
80. Cripwell RA, Favaro L, Viljoen-Bloom M, van Zyl WH. Consolidated bioprocessing of raw starch to ethanol by *Saccharomyces cerevisiae*: achievements and challenges. *Biotechnol Adv.* 2020;42:107579. <https://doi.org/10.1016/j.biotechadv.2020.107579>.
81. Lam MK, Lee KT. Bioethanol production from microalgae. *Handb Mar Microalgae Biotechnol Adv.* 2015; <https://doi.org/10.1016/B978-0-12-800776-1.00012-1>.
82. Martín-Juárez J, Markou G, Muylaert K, Lorenzo-Hernando A, Bolado S. Breakthroughs in bioalcohol production from microalgae: solving the hurdles. In: Microalgae-based biofuels bioprod from feed Cultiv to end-products; 2017. p. 183–207. <https://doi.org/10.1016/B978-0-08-101023-5.00008-X>.

83. Constantino A, Rodrigues B, Leon R, Barros R, Raposo S. Alternative chemo-enzymatic hydrolysis strategy applied to different microalgae species for bioethanol production. *Algal Res.* 2021;56:102329. <https://doi.org/10.1016/j.algal.2021.102329>.
84. Tatel NJ, Madrazo C. Bioethanol production from microalgae *Chlorella sorokiniana* via simultaneous saccharification and fermentation. *IOP Conf Ser Mater Sci Eng.* 2020; <https://doi.org/10.1088/1757-899X/778/1/012039>.
85. Ma Y, Wang P, Wang Y, Liu S, Wang Q, Wang Y. Fermentable sugar production from wet microalgae residual after biodiesel production assisted by radio frequency heating. *Renew Energy.* 2020;155:827–36. <https://doi.org/10.1016/j.renene.2020.03.176>.
86. Shokrkar H, Ebrahimi S, Zamani M. Extraction of sugars from mixed microalgae culture using enzymatic hydrolysis: experimental study and modeling. *Chem Eng Commun.* 2017;204: 1246–57. <https://doi.org/10.1080/00986445.2017.1356291>.
87. Shokrkar H, Ebrahimi S. Synergism of cellulases and amylolytic enzymes in the hydrolysis of microalgal carbohydrates. *Biofuels Bioprod Biorefin.* 2018;12:749–55. <https://doi.org/10.1002/bbb.1886>.
88. Aikawa S, Joseph A, Yamada R, Izumi Y, Yamagishi T, Matsuda F, Kawai H, Chang JS, Hasunuma T, Kondo A. Direct conversion of *spirulina* to ethanol without pretreatment or enzymatic hydrolysis processes. *Energy Environ Sci.* 2013;6:1844–9. <https://doi.org/10.1039/C3EE40305J>.
89. Peng H, Zhai L, Xu S, Xu P, He C, Xiao Y, Gao Y. Efficient hydrolysis of raw microalgae starch by an α-amylase (AmyP) of glycoside hydrolase subfamily GH13-37. *J Agric Food Chem.* 2018;66:12748–55. <https://doi.org/10.1021/acs.jafc.8b03524>.
90. Aikawa S, Inokuma K, Wakai S, Sasaki K, Ogino C, Chang JS, Hasunuma T, Kondo A. Direct and highly productive conversion of cyanobacteria *Arthrospira platensis* to ethanol with CaCl₂ addition. *Biotechnol Biofuels.* 2018;11:1–9. <https://doi.org/10.1186/s13068-018-1050-y>.
91. Kim KH, Choi IS, Kim HM, Wi SG, Bae HJ. Bioethanol production from the nutrient stress-induced microalga *Chlorella vulgaris* by enzymatic hydrolysis and immobilized yeast fermentation. *Bioresour Technol.* 2014;153:47–54. <https://doi.org/10.1016/j.biortech.2013.11.059>.
92. Mahdy A, Ballesteros M, González-Fernández C. Enzymatic pretreatment of *Chlorella vulgaris* for biogas production: influence of urban wastewater as a sole nutrient source on macromolecular profile and biocatalyst efficiency. *Bioresour Technol.* 2016;199:319–25. <https://doi.org/10.1016/j.biortech.2015.08.080>.
93. Phwan CK, Ong HC, Chen W-H, Ling TC, Ng EP, Show PL. Overview: comparison of pretreatment technologies and fermentation processes of bioethanol from microalgae. *Energy Convers Manag.* 2018;173:81–94. <https://doi.org/10.1016/j.enconman.2018.07.054>.
94. Onay M. Bioethanol production via different saccharification strategies from *H. tetrachotoma* ME03 grown at various concentrations of municipal wastewater in a flat-photobioreactor. *Fuel.* 2019;239:1315–23. <https://doi.org/10.1016/j.fuel.2018.11.126>.
95. He MX, Wu B, Qin H, et al. *Zymomonas mobilis*: a novel platform for future biorefineries. *Biotechnol Biofuels.* 2014;7:1–15. <https://doi.org/10.1186/1754-6834-7-101>.
96. Ajit A, Sulaiman AZ, Chisti Y. Production of bioethanol by *Zymomonas mobilis* in high-gravity extractive fermentations. *Food Bioprod Process.* 2017;102:123–35. <https://doi.org/10.1016/j.fbp.2016.12.006>.
97. Fu N, Peiris P, Markham J, Bavor J. A novel co-culture process with *Zymomonas mobilis* and *Pichia stipitis* for efficient ethanol production on glucose/xylose mixtures. *Enzym Microb Technol.* 2009;45:210–7. <https://doi.org/10.1016/j.enzmicrotec.2009.04.006>.
98. Yang S, Pan C, Tschaplinski TJ, Hurst GB, Engle NL, Zhou W, Dam P, Xu Y, Rodriguez M Jr, Dice L. Systems biology analysis of *Zymomonas mobilis* ZM4 ethanol stress responses. *PLoS One.* 2013;8:e68886. <https://doi.org/10.1371/journal.pone.0101305>.

99. Aditiya HB, Mahlia TMI, Chong WT, Nur H, Sebayang AH. Second generation bioethanol production: a critical review. *Renew Sust Energ Rev.* 2016;66:631–53. <https://doi.org/10.1016/j.rser.2016.07.015>.
100. Alia KB, Rasul I, Azeem F, Hussain S, Siddique MH, Muzammil S, Riaz M, Bari A, Liaqat S, Nadeem H. Microbial production of ethanol. In: *Microb Fuel Cells Mater Appl Mater Res.* Pennsylvania: Forum LLC; 2019. p. 307–34. <https://doi.org/10.21741/9781644900116-12>.
101. Harun R, Jason WSY, Cherrington T, Danquah MK. Exploring alkaline pre-treatment of microalgal biomass for bioethanol production. *Appl Energy.* 2011;88:3464–7. <https://doi.org/10.1016/j.apenergy.2010.10.048>.
102. Lee S, Oh Y, Kim D, Kwon D, Lee C, Lee J. Converting carbohydrates extracted from marine algae into ethanol using various ethanolic *Escherichia coli* strains. *Appl Biochem Biotechnol.* 2011;164:878–88. <https://doi.org/10.1007/s12010-011-9181-7>.
103. Kim HM, Oh CH, Bae HJ. Comparison of red microalgae (*Porphyridium cruentum*) culture conditions for bioethanol production. *Bioresour Technol.* 2017;233:44–50. <https://doi.org/10.1016/j.biortech.2017.02.040>.
104. Guo H, Daroch M, Liu L, Qiu G, Geng S, Wang G. Biochemical features and bioethanol production of microalgae from coastal waters of Pearl River Delta. *Bioresour Technol.* 2013;127:422–8. <https://doi.org/10.1016/j.biortech.2012.10.006>.
105. Luiza Astolfi A, Rempel A, Cavanhi VAF, Alves M, Deamici KM, Colla LM, Costa JAV. Simultaneous saccharification and fermentation of spirulina sp. and corn starch for the production of bioethanol and obtaining biopeptides with high antioxidant activity. *Bioresour Technol.* 2020;301:122698. <https://doi.org/10.1016/j.biortech.2019.122698>.
106. Reymu Z, Özçimen D. Batch cultivation of marine microalgae *Nannochloropsis oculata* and *Tetraselmis suecica* in treated municipal wastewater toward bioethanol production. *J Clean Prod.* 2017;150:40–6. <https://doi.org/10.1016/j.jclepro.2017.02.189>.
107. El-Dalatony MM, Kurade MB, Abou-Shanab RAI, Kim H, Salama E-S, Jeon B-H. Long-term production of bioethanol in repeated-batch fermentation of microalgal biomass using immobilized *Saccharomyces cerevisiae*. *Bioresour Technol.* 2016;219:98–105. <https://doi.org/10.1016/j.biortech.2016.07.113>.
108. Sirajunnisa AR, Surendhiran D. Algae—a quintessential and positive resource of bioethanol production: a comprehensive review. *Renew Sust Energ Rev.* 2016;66:248–67. <https://doi.org/10.1016/j.rser.2016.07.024>.
109. Rastogi M, Shrivastava S. Recent advances in second generation bioethanol production: an insight to pretreatment, saccharification and fermentation processes. *Renew Sust Energ Rev.* 2017;80:330–40. <https://doi.org/10.1016/j.rser.2017.05.225>.
110. Balat M. Production of bioethanol from lignocellulosic materials via the biochemical pathway: a review. *Energy Convers Manag.* 2011;52:858–75. <https://doi.org/10.1016/j.enconman.2010.08.013>.
111. Ballesteros M, Oliva JM, Negro MJ, Manzanares P, Ballesteros I. Ethanol from lignocellulosic materials by a simultaneous saccharification and fermentation process (SFS) with *Kluyveromyces marxianus* CECT 10875. *Process Biochem.* 2004;39:1843–8. <https://doi.org/10.1016/j.procbio.2003.09.011>.
112. Dahnum D, Tasum SO, Tri wahyuni E, Nurdin M, Abimanyu H. Comparison of SHF and SSF processes using enzyme and dry yeast for optimization of bioethanol production from empty fruit bunch. *Energy Procedia.* 2015;68:107–16. <https://doi.org/10.1016/j.egypro.2015.03.238>.
113. Jambo SA, Abdulla R, Mohd Azhar SH, Marbawi H, Gansau JA, Ravindra P. A review on third generation bioethanol feedstock. *Renew Sust Energ Rev.* 2016;65:756–69. <https://doi.org/10.1016/j.rser.2016.07.064>.
114. Adiloğlu S, Fajardo S, García-Galvan RF, Barranco V, Galvan JC, Batlle SF. We are IntechOpen , the world ' s leading publisher of open access books built by scientists , for scientists TOP 1%. Intech i. 2016;13. <https://doi.org/10.5772/57353>.
115. Koppram R, Nielsen F, Albers E, Lambert A, Wänström S, Welin L, Zacchi G, Olsson L. Simultaneous saccharification and co-fermentation for bioethanol production using corn-cobs at lab, PDU and demo scales. *Biotechnol Biofuels.* 2013;6:2–11. <https://doi.org/10.1186/1754-6834-6-2>.

116. Peralta-Ruiz Y, Pardo Y, González-Delgado Á, Kafarov V. Simulation of bioethanol production process from residual microalgae biomass. In: Computer aided chemical engineering. Elsevier; 2012. p. 1048–52. <https://doi.org/10.1016/B978-0-444-59520-1.50068-3>.
117. Li K, Liu S, Liu X. An overview of algae bioethanol production. *Int J Energy Res.* 2014;38: 965–77. <https://doi.org/10.1002/er.3164>.
118. Azhar SHM, Abdulla R, Jambo SA, Marbawi H, Gansau JA, Faik AAM, Rodrigues KF. Yeasts in sustainable bioethanol production: a review. *Biochem Biophys Rep.* 2017;10: 52–61. <https://doi.org/10.1016/j.bbrep.2017.03.003>.
119. Kumar G, Shobana S, Nagarajan D, Lee DJ, Lee KS, Lin CY, Chen CY, Chang JS. Biomass based hydrogen production by dark fermentation — recent trends and opportunities for greener processes. *Curr Opin Biotechnol.* 2018;50:136–45. <https://doi.org/10.1016/j.copbio.2017.12.024>.
120. Brethauer S, Studer MH. Consolidated bioprocessing of lignocellulose by a microbial consortium. *Energy Environ Sci.* 2014;7:1446–53. <https://doi.org/10.1039/C3EE41753K>.
121. Devarapalli M, Atiyeh HK. A review of conversion processes for bioethanol production with a focus on syngas fermentation. *Biofuel Res J.* 2015;2:268–80. <https://doi.org/10.18331/BRJ2015.2.3.5>.
122. Chen H, Zhou D, Luo G, Zhang S, Chen J. Macroalgae for biofuels production: Progress and perspectives. *Renew Sust Energ Rev.* 2015;47:427–37. <https://doi.org/10.1016/j.rser.2015.03.086>.
123. Lara A, Rodríguez-Jasso RM, Loredo-Treviño A, Aguilar CN, Meyer AS, Ruiz HA. Enzymes in the third generation biorefinery for macroalgae biomass. *Biomass Biofuels Biochem.* 2020;:363, 96. <https://doi.org/10.1016/b978-0-12-819820-9.00017-x>.
124. Aparicio E, Rodríguez-Jasso RM, Lara A, Loredo-Treviño A, Aguilar CN, Kostas ET, Ruiz HA. Biofuels production of third generation biorefinery from macroalgal biomass in the Mexican context: an overview. *Sustain Seaweed Technol.* 2020:393–446. <https://doi.org/10.1016/B978-0-12-817943-7.00015-9>.
125. Aitken D, Bulboa C, Godoy-Faundez A, Turrión-Gómez JL, Antizar-Ladislao B. Life cycle assessment of macroalgae cultivation and processing for biofuel production. *J Clean Prod.* 2014;75:45–56. <https://doi.org/10.1016/j.jclepro.2014.03.080>.
126. Pereira L, Amado AM, Critchley AT, van de Velde F, Ribeiro-Claro PJA. Identification of selected seaweed polysaccharides (phycocolloids) by vibrational spectroscopy (FTIR-ATR and FT-Raman). *Food Hydrocoll.* 2009;23:1903–9. <https://doi.org/10.1016/j.foodhyd.2008.11.014>.
127. Li B, Lu F, Wei X, Zhao R. Fucoidan: structure and bioactivity. *Molecules.* 2008;13:1671–95. <https://doi.org/10.3390/molecules13081671>.
128. Cervantes-Cisneros DE, Arguello-Esparza D, Cabello-Galindo A, Picazo B, Aguilar CN, Ruiz HA, Rodríguez-Jasso RM. Hydrothermal processes for extraction of macroalgae high value-added compounds. In: Hydrothermal process. Biorefineries. Springer; 2017. p. 461–81. https://doi.org/10.1007/978-3-319-56457-9_20.
129. Rodrigues D, Freitas AC, Pereira L, Rocha-Santos TAP, Vasconcelos MW, Roriz M, Rodríguez-Alcalá LM, Gomes AMP, Duarte AC. Chemical composition of red, brown and green macroalgae from Buarcos bay in central west coast of Portugal. *Food Chem.* 2015;183: 197–207. <https://doi.org/10.1016/j.foodchem.2015.03.057>.
130. Gnanavel V, Roopan SM, Rajeshkumar S. Aquaculture: an overview of chemical ecology of seaweeds (food species) in natural products. *Aquaculture.* 2019;507:1–6. <https://doi.org/10.1016/j.aquaculture.2019.04.004>.
131. Kumar M, Sun Y, Rathour R, Pandey A, Thakur IS, Tsang DCW. Algae as potential feedstock for the production of biofuels and value-added products: opportunities and challenges. *Sci Total Environ.* 2020;716:137116. <https://doi.org/10.1016/j.scitotenv.2020.137116>.
132. Mouritsen OG, Rhätigan P, Pérez-Lloréns JL. World cuisine of seaweeds: science meets gastronomy. *Int J Gastron Food Sci.* 2018;14:55–65. <https://doi.org/10.1016/j.ijgfs.2018.09.002>.

133. Gullón B, Gagaoua M, Barba FJ, Gullón P, Zhang W, Lorenzo JM. Seaweeds as promising resource of bioactive compounds: overview of novel extraction strategies and design of tailored meat products. *Trends Food Sci Technol.* 2020;100:1–18. <https://doi.org/10.1016/j.tifs.2020.03.039>.
134. Cermeño M, Kleekayai T, Amigo-Benavent M, Harnedy-Rothwell P, FitzGerald RJ. Current knowledge on the extraction, purification, identification, and validation of bioactive peptides from seaweed. *Electrophoresis.* 2020;41(20):1694–717. <https://doi.org/10.1002/elps.202000153>.
135. Maneein S, Milledge JJ, Nielsen BV, Harvey PJ. A review of seaweed pre-treatment methods for enhanced biofuel production by anaerobic digestion or fermentation. *Fermentation.* 2018;4:100. <https://doi.org/10.3390/fermentation4040100>.
136. Wang L, Jayawardena TU, Yang H, Lee HG, Kang M, Sanjeeva KKA, Oh JY, Jeon Y. Isolation, Characterization, and antioxidant activity evaluation of a fucoidan from an enzymatic digest of the edible seaweed, *hizikia fusiforme*; 2020. <https://doi.org/10.3390/antiox9050363>.
137. Rasin AB, Silchenko AS, Kusaykin MI, Malyarenko OS, Zueva AO, Kalinovsky AI, Airong J, Surits VV, Ermakova SP. Enzymatic transformation and anti-tumor activity of *Sargassum horneri* fucoidan. *Carbohydr Polym.* 2020;246:116635. <https://doi.org/10.1016/j.carbpol.2020.116635>.
138. Vásquez V, Martínez R, Bernal C. Enzyme-assisted extraction of proteins from the seaweeds *Macrocystis pyrifera* and *Chondracanthus chamaissoi*: characterization of the extracts and their bioactive potential. *J Appl Phycol.* 2019;31:1999–2010. <https://doi.org/10.1007/s10811-018-1712-y>.
139. Naseri A, Marinho GS, Holdt SL, Bartela JM, Jacobsen C. Enzyme-assisted extraction and characterization of protein from red seaweed *Palmaria palmata*. *Algal Res.* 2020;47:101849. <https://doi.org/10.1016/j.algal.2020.101849>.
140. Li N, Fu X, Xiao M, Wei X, Yang M, Liu Z, Mou H. Enzymatic preparation of a low-molecular-weight polysaccharide rich in uronic acid from the seaweed: *Laminaria japonica* and evaluation of its hypolipidemic effect in mice. *Food Funct.* 2020;11:2395–405. <https://doi.org/10.1039/C9FO02994J>.
141. Wang L, Oh JY, Hwang J, Ko JY, Jeon YJ, Ryu B. In vitro and in vivo antioxidant activities of polysaccharides isolated from celluclast-assisted extract of an edible brown seaweed, *Sargassum fulvellum*. *Antioxidants.* 2019; <https://doi.org/10.3390/antiox8100493>.
142. Pimentel FB, Cermeño M, Kleekayai T, Harnedy-Rothwell PA, Fernandes E, Alves RC, Beatriz PPOM, FitzGerald RJ. Enzymatic modification of *Porphyra dioica*-derived proteins to improve their antioxidant potential. *Molecules.* 2020; <https://doi.org/10.3390/molecules25122838>.
143. Chen H, Xiao Q, Weng H, Zhang Y, Yang Q, Xiao A. Extraction of sulfated agar from *Gracilaria lemaneiformis* using hydrogen peroxide-assisted enzymatic method. *Carbohydr Polym.* 2020;232:115790. <https://doi.org/10.1016/j.carbpol.2019.115790>.
144. Ruiz HA, Conrad M, Sun S-N, Sanchez A, Rocha GJM, Romaní A, Castro E, Torres A, Rodríguez-Jasso RM, Andrade LP. Engineering aspects of hydrothermal pretreatment: from batch to continuous operation, scale-up and pilot reactor under biorefinery concept. *Bioresour Technol.* 2020;299:122685. <https://doi.org/10.1016/j.biortech.2019.122685>.
145. Lamb JJ, Hjelme DR, Lien KM. Carbohydrate yield and biomethane potential from enzymatically hydrolysed *Saccharina latissima* and its industrial potential. *Adv Microbiol.* 2019;09: 359–71. <https://doi.org/10.4236/aim.2019.94021>.
146. Meinita MDN, Marhaeni B, Jeong GT, Hong YK. Sequential acid and enzymatic hydrolysis of carrageenan solid waste for bioethanol production: a biorefinery approach. *J Appl Phycol.* 2019;31:2507–15. <https://doi.org/10.1007/s10811-019-1755-8>.
147. Túma S, Izaguirre JK, Bondar M, Marques MM, Fernandes P, da Fonseca MMR, Cesário MT. Upgrading end-of-line residues of the red seaweed *Gelidium sesquipedale* to polyhydroxyalkanoates using *Halomonas boliviensis*. *Biotechnol Rep.* 2020; <https://doi.org/10.1016/j.btre.2020.e00491>.

148. Ra CH, Kim SK. Bioethanol production from macroalgae and microbes. In: Mar Bioenergy Trends Dev. CRC Press; 2015. p. 257–71. <https://doi.org/10.1201/b18494-19>.
149. Taherzadeh MJ, Karimi K. Fermentation inhibitors in ethanol processes and different strategies to reduce their effects, 1st ed. Biofuels. 2011; <https://doi.org/10.1016/B978-0-12-385099-7.00012-7>.
150. Özçimen D, Inan B. An overview of bioethanol production from algae. Biofuels Status Perspect. 2015; <https://doi.org/10.5772/59305>.
151. Dave N, Selvaraj R, Varadavenkatesan T, Vinayagam R. A critical review on production of bioethanol from macroalgal biomass. Algal Res. 2019;42:101606. <https://doi.org/10.1016/j.algal.2019.101606>.
152. Obata O, Akunna J, Bockhorn H, Walker G. Ethanol production from brown seaweed using non-conventional yeasts. Bioethanol. 2016;2(1):134–45. <https://doi.org/10.1515/bioeth-2016-0010>.
153. Rasul I, Azeem F, Hussain S, Siddique MH. Microbial production of ethanol. 2019: 307–334. <https://doi.org/10.21741/9781644900116-12>
154. Láinez M, Ruiz HA, Arellano-Plaza M, Martínez-Hernández S. Bioethanol production from enzymatic hydrolysates of Agave salmiana leaves comparing *S. cerevisiae* and *K. marxianus*. Renew Energy. 2019;138:1127–33. <https://doi.org/10.1016/j.renene.2019.02.058>.
155. Xia J, Yang Y, Liu CG, Yang S, Bai FW. Engineering *Zymomonas mobilis* for robust cellulosic ethanol production. Trends Biotechnol. 2019;37:960–72. <https://doi.org/10.1016/j.tibtech.2019.02.002>.
156. Sudhakar MP, Jegatheesan A, Poonam C, Perumal K, Arunkumar K. Biosaccharification and ethanol production from spent seaweed biomass using marine bacteria and yeast. Renew Energy. 2017;105:133–9. <https://doi.org/10.1016/j.renene.2016.12.055>.
157. Trivedi N, Reddy CRK, Radulovich R, Jha B. Solid state fermentation (SSF)-derived cellulase for saccharification of the green seaweed *Ulva* for bioethanol production. Algal Res. 2015;9: 48–54. <https://doi.org/10.1016/j.algal.2015.02.025>.
158. El Harchi M, Kachkach FZF, El Mtili N. Optimization of thermal acid hydrolysis for bioethanol production from *Ulva rigida* with yeast *Pachysolen tannophilus*. South Afr J Bot. 2018;115:161–9. <https://doi.org/10.1016/j.sajb.2018.01.021>.
159. Favaro L, Jansen T, van Zyl WH. Exploring industrial and natural *Saccharomyces cerevisiae* strains for the bio-based economy from biomass: the case of bioethanol. Crit Rev Biotechnol. 2019;39:800–16. <https://doi.org/10.1080/07388551.2019.1619157>.
160. Aparicio E, Rodríguez-Jasso RM, Pinales-Márquez CD, Loredo-Treviño A, Robledo-Olivo A, Aguilar CN, Kostas ET, Ruiz HA. High-pressure technology for *Sargassum* spp biomass pretreatment and fractionation in the third generation of bioethanol production. Bioresour Technol. 2021;329:124935. <https://doi.org/10.1016/j.biortech.2021.124935>.
161. Lee JY, Li P, Lee J, Ryu HJ, Oh KK. Ethanol production from *Saccharina japonica* using an optimized extremely low acid pretreatment followed by simultaneous saccharification and fermentation. Bioresour Technol. 2013;127:119–25. <https://doi.org/10.1016/j.biortech.2012.09.122>.
162. Hou X, Hansen JH, Bjerre AB. Integrated bioethanol and protein production from brown seaweed *Laminaria digitata*. Bioresour Technol. 2015;197:310–7. <https://doi.org/10.1016/j.biortech.2015.08.091>.
163. Kim HM, Wi SG, Jung S, Song Y, Bae HJ. Efficient approach for bioethanol production from red seaweed *Gelidium amansii*. Bioresour Technol. 2015;175:128–34. <https://doi.org/10.1016/j.biortech.2014.10.050>.
164. del Río PG, Domínguez E, Domínguez VD, Romaní A, Domingues L, Garrote G. Third generation bioethanol from invasive macroalgae *Sargassum muticum* using autohydrolysis pretreatment as first step of a biorefinery. Renew Energy. 2019;141:728–35. <https://doi.org/10.1016/j.renene.2019.03.083>.

165. Khammee P, Ramaraj R, Whangchai N, Bhuyar P, Unpaprom Y. The immobilization of yeast for fermentation of macroalgae *Rhizoclonium* sp. for efficient conversion into bioethanol. *Biomass Convers Biorefinery*. 2021;11:827–35. <https://doi.org/10.1007/s13399-020-00786-y>.
166. Kostas ET, White DA, Cook DJ. Bioethanol production from UK seaweeds: investigating variable pre-treatment and enzyme hydrolysis parameters. *Bioenergy Res.* 2020;13:271–85. <https://doi.org/10.1007/s12155-019-10054-1>.
167. Silveira MHL, Vanelli BA, Chandel AK. Second generation ethanol production: potential biomass feedstock, biomass deconstruction, and chemical platforms for process valorization. In: *Advances in sugarcane biorefinery*. Elsevier; 2018. p. 135–52. <https://doi.org/10.1016/B978-0-12-804534-3.00006-9>.
168. Ravanal MC, Camus C, Buschmann AH, Gimpel J, Olivera-Nappa Á, Salazar O, Lienqueo ME. Production of bioethanol from brown algae. In: *Advances in feedstock conversion technologies for alternative fuels and bioproducts*. Elsevier; 2019. p. 69–88. <https://doi.org/10.1016/B978-0-12-817937-6.00004-7>.
169. Aguilar-Reynosa A, Romaní A, Rodríguez-Jasso RM, Aguilar CN, Garrote G, Ruiz HA. Comparison of microwave and conduction-convection heating autohydrolysis pretreatment for bioethanol production. *Bioresour Technol.* 2017;243:273–83. <https://doi.org/10.1016/j.biortech.2017.06.096>.
170. Ramachandra TV, Hebbale D. Bioethanol from macroalgae: prospects and challenges. *Renew Sust Energ Rev.* 2020;117:109479. <https://doi.org/10.1016/j.rser.2019.109479>.
171. Tan IS, Lam MK, Foo HCY, Lim S, Lee KT. Advances of macroalgae biomass for the third generation of bioethanol production. *Chin J Chem Eng.* 2020;28:502–17. <https://doi.org/10.1016/j.cjche.2019.05.012>.
172. Cavallaglio G, Gelosia M, Ingles D, Pompili E, D'Antonio S, Cotana F. Response surface methodology for the optimization of cellulosic ethanol production from *Phragmites australis* through pre-saccharification and simultaneous saccharification and fermentation. *Ind Crop Prod.* 2016;83:431–7. <https://doi.org/10.1016/j.indcrop.2015.12.089>.
173. Fernandes-Klajn F, Romero-García JM, Díaz MJ, Castro E. Comparison of fermentation strategies for ethanol production from olive tree pruning biomass. *Ind Crop Prod.* 2018;122: 98–106. <https://doi.org/10.1016/j.indcrop.2018.05.063>.

Part V

Techno-Economic Analysis

Chapter 13

Prospects and Perspectives for Producing Biodiesel, Bioethanol and Bio-Chemicals from Fruit Waste: Case Studies in Brazil and Serbia



Danijela Stanisić, Marija Tasić, Olivera Stamenković, and Ljubica Tasić

Abstract Fruits are some of the most valuable agro-industrial products with high nutritional value and considered very healthy food. Nevertheless, fruit residues resulting from fruit processing represent organic waste and can make up almost 1/2–3/4 of the entire year of fruit agribusiness production. These semi-solid fruit residues are being landfilled at an alarming rate and can even become dangerous organic wastes that might cause pathogen proliferation and disturb environmental microbiota. In developing countries, fruit waste is even greater because of low or no investment in refrigerated transport and cold storage facilities after harvest of the fresh fruit. Therefore, there is a strong appeal in reusing this waste and adding-in higher value to the fruit residues such as manufacture of nutritive supplements, biochemicals and biofuels. In the area of biofuel research, by far the bioethanol production from the fruit residues is an interesting topic to discuss and explore, as well as biodiesel production, which depend on chemical composition and characteristics of different types of fruit biomass. Some fruit derived biopolymers such as pectin, lignin, hemicelluloses and cellulose based polymers are very valuable commodities already explored. But some fine chemical products such as pigments, fragrances, essential oils, organic molecules, and many bioactive substances can be obtained from fruit residues and even if not the greatest in quantity, for sure may add-in great value into fruit agri-business. Brazil is one of the top-five world fruit producers and leading the world market of orange fruit production, which is one of the biomasses taken as an example for biochemicals and bioethanol production. On the other side, fruit residues in Serbia can become valuable resources for biodiesel and other commodities production. This chapter brings some important and updated

D. Stanisić · L. Tasić (✉)

Department of Organic Chemistry, Institute of Chemistry, University of Campinas, Campinas, SP, Brazil

e-mail: ljubica@unicamp.br

M. Tasić · O. Stamenković

Faculty of Technology, University of Nis, Leskovac, Serbia

state-of-the-art processes for exploring fruit waste for biofuel and biochemicals production in the laboratory scale and prospection about bioeconomy for industrial exploitation. Finally, the brief discussion on liquid and solid residues generated in some of the proposed processes are disclosed.

Keywords Fruit waste · Biopolymers · Active ingredients · Flavones · Pigments · Biofuels

13.1 Introduction

Fruit waste generation can occur in any stage of food production and supply chain. One-third of produced food each year is wasted, according to The United Nation Food and Agriculture Organization [1]. In the EU, approximately 88 million metric tones of food waste are generated, which is 20% of produced food annually [1, 2]. Industrial food waste produced in large amounts, generates great loss of valuable materials, and raises serious management problems, both from the environmental and economical point of view. Many of these residues, however, have the potential to be reused in other production systems, through e.g., bio-refineries [3]. Some of the contributing factors for augmented food waste are irrational purchase planning and preparation non-sufficient meal planning and shopping promotions, misunderstanding of data value, “use by” and “best before” labels, portion size in canteens and restaurants, stock and supplies management issues, product and packaging damage, inadequate transport and storage, overproduction or demand lack. All these factors could be a problem in all stages of the food chain [4].

During the period from 1960 to 1990, Brazil experienced expansion and development in agriculture through adoption of modern and innovative production techniques, investment in research and development and innovation in the agricultural sector. Nowadays, Brazil is one of the top five producers and exporters in the agricultural industry and in the third place in fruit production. Food waste and post-harvest losses issues have been more and more present in the media since 2015. Social inequality, combined with high unemployment and the large differences in purchasing power in Brazil, increases the risks of accessibility to food [5].

Agro-waste processing nowadays covers several practical techniques for food waste treatment, such as anaerobic digestion, vermicification, pyrolysis. Anaerobic digestion is a microbial process where biomass is converted in biogas and nutrient-rich fertilizers. Vermification is an eco-friendly and low-cost technique that employs microbes and earthworms to break down organics, and forms little or no sludge, uses little to no electricity, and is odor free. Lignocellulosic wastes are transformed through pyrolysis to the biochar. Biochar is known to be useful in water restricted areas and on infertile soil [6].

Agro-waste material increases tremendously, and the recovery of waste makes it possible to benefit from low-cost reinforcements and protect the environment. Agro-waste residues are a significant resource and low cost, environmentally friendly,

renewable, and readily available materials for various utilizations. The crop waste is abundant in natural fibers. The agriculture waste fibers can be obtained from rice straw, orange peel, cotton stalk, banana peel, pineapple leaf, soy pods, flax, hemp, potato peel, rice husk, garlic straw, grape skin, among others. Agro-waste biomass products can be used in multitude applications like the textile industry, composites, paper, furniture, constructions and medical fields [4].

Brazil, according to FAOSTAT metadata, annually produces around 17 million tons of oranges, making them leader in the World production of citrus fruit (for 2019 citrus fruit production was ~79 millions of tonnes), 6 million tonnes of bananas, 2.4 million of tonnes of pineapple, 2.3 million tonnes of watermelon, 2 million tonnes of mangoes and around 1.5 million tonnes of grape [7].

13.2 Fruit Waste Biorefinery Circular Economy

Modern industrial development is toward implementation of the circular economy model to foster sustainability.

For sustainable development of natural resources, all linear and extractive production models should be substituted with the circular economy model. This means that all industrial waste should be used as a source for obtaining value-added products. Figure 13.1 shows the perspective of winemaking biorefineries based on the circular economy model.

The whole process includes producing wines, grape liquor, biofuels, bio-active compounds, cattle feed, heat, and ashes that can be used to produce construction materials. Alternatively, wine shoots can be used for composting.

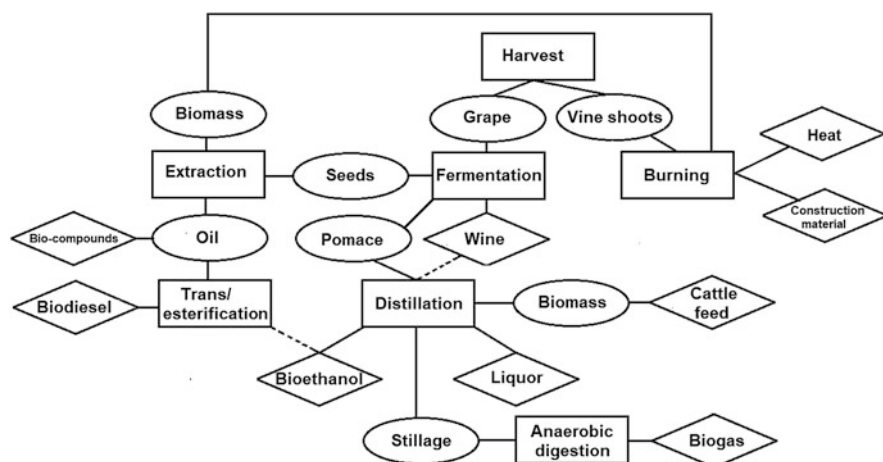


Fig. 13.1 Grape biorefinery circular economy model

Including biofuels production in the existing winemaking process contributes to reduce emissions of greenhouse gasses responsible for climate change. The proposed advanced process will provide sustainable production and valorization of wastes.

13.3 Biofuels

Simultaneously with the increased fruit production and use, the fruit waste generated by the fruit processing industry increased. The fruit residues are usually discarded as industrial waste. However, they can be exploited as oil and sugar sources and, based on their physico-chemical characteristics, used for biodiesel (methyl or ethyl esters of fatty acids) and bioethanol production. According to the global fruit production data in the last decade [7], the widely grown fruits in Serbia and Europe are apples, plums, watermelons, and grapes. Bioethanol, biogas, and biodiesel, alternatives to fossil fuels, can be produced from waste biomass. The production from waste biomass gives an inexpensive and alternative to the harsh chemicals used during industrial processes, and the possibility of controlling pollution from the waste discarded to the environment. The bioethanol, biodiesel and biogas can be utilized in the further production of industrially important chemicals, as solvents and building blocks of new chemicals [8]. In the '90., Grohmann and colleagues explored sugars from citrus waste and performed hydrolysis, which led to fermentation with *Saccharomyces cerevisiae* (*S. cerevisiae*) and *Escherichia coli* (*E. coli*) to produce ethanol [9, 10]. Prior to any hydrolysis it is necessary to remove d-limonene and/or any other essential oils that can inhibit the fermentation process [11]. Two main techniques, simultaneous saccharification and fermentation, and further hydroxylation and fermentation, combine enzymatic and microbial fermentation in one single step, simplifying ethanol production. Production costs are reduced and involve less investments, which significantly increase interest in processing agro-waste materials [8].

13.3.1 Apple Waste Processing

Over 87.2 million tonnes of apples are produced annually in the World [12]. Approximately 26% of the total apple production is used for processing purposes [13]. Apple processing generates liquid (waste waters, 60–70%) and solid (apple pomace, 30–40%) wastes [14]. Since both contain high biological oxygen demand values (highly biodegradable), disposing of them brings environmental problems [15]. Currently, wastewater is disposed of into landfills or used for feed production. There is no evidence that wastewater can be used for bioethanol production, most likely due to the low nitrogen and phosphorus [15]. Apple pomace, a waste of juice extraction, is disposed of in landfills, although it has high residual acidity

[15]. Occasionally, it is spread on land or used as bioethanol feedstock. Apple pomace usually contains cellulose, hemicellulose, lignin, and some amounts of reducing sugars [16]. However, compared to other agricultural wastes, apple pomace is rich in pectin and has a markedly less lignin portion [17]. Therefore, the enzymatic hydrolysis of cellulose and hemicellulose is more efficient [14]. Since pomace is waste during mechanical apple pressing, it contains rice husks, too (10% of the pomace's total weight) commonly used as a pressing aid in the industry [18]. Acid hydrolysis and enzymatic saccharification were the most common pretreatment methods for the release of fermentable sugars from the lignocellulosic structure of apple pomace (Table 13.1). Microwaves cause swelling of the fiber and increase surface area leading to better enzymatic binding and hydrolysis [19].

As can be seen from data shown in Table 13.1, the average submersed ethanol yield was about 0.4 g/g. Higher ethanol yields were related to higher sugar content and supplement addition (i.e., soluble soy protein). Although *S. cerevisiae* was the most common production microorganisms, higher ethanol yields were obtained by *Pichia stipitis* (*P. stipitis*) or *Kluyveromyces thermotolerans* (*K. thermotolerans*). Both *P. stipitis* and *K. thermotolerans* are pentose fermentative yeasts. While *P. stipitis* utilize cellobiose and maltose, *K. thermotolerans* can utilize maltose [20] and xylose [19]. Both strains consume sugars slower than *S. cerevisiae*, so they have a longer fermentation time [21]. Working temperature mainly did not exceed 30 °C independently on type of fermentation—solid or submerged state. Comparing submersed and solid-state fermentation of apple pomace (Table 13.1) was not possible due to different ethanol fermentation results.

One study reports that the submersed fermentation efficiency of 76.9% is higher than the range of 70–94% and 72.6–90% in a solid-state fermentation system [18]. Moisture and mixing rate are determining factors for solid fermentation [26]. By increasing the moisture and mixing rate, ethanol productivity rises as well as the fermentation time. The highest ethanol yield (16.09 v/w) in solid-state fermentation was achieved with co-cultures of *S. cerevisiae* (ethanol producer), *Aspergillus foetidus* (*A. foetidus*, pectinase producer), *Fusarium oxysporum* (*F. oxysporum*, cellulose producer). Fermenting microorganisms should utilize most of the apple pomace sugars and therefore provide high ethanol production rates. That means to be able to produce both cellulase for degradation of cellulose and to ferment sugars to ethanol.

Since all research (Table 13.1) was conducted at a laboratory scale, bioethanol was usually separated via a rotary vacuum evaporator at 78 °C, with usual minor losses. Ethanol concentration depends on apple variety, processing conditions, including the amount of press aid used [17]. However, a minimum concentration of 4% v/w is required for economic ethanol production [24]. Ethanol must be further treated in the distillation columns, which requires about 79% of the available energy [17]. For occurring submerged fermentation, a four-to-five-part dilution of the pomace is necessary, making ethanol concentration too low. To the best of authors' knowledge, just one study was performed about bioethanol apple pomace production's economic feasibility. Since costs of apple pomace are negligible, the reported ethanol price (during the 1996 year) was 0.16 US\$/L [27]. This price could be lower

Table 13.1 Apple pomace bioethanol production processes

Apple pomace	Pretreatment	Type, volume of reactor, mL/agitation intensity, rpm	Fermentation microflora/inoculum size	Operating conditions				Maximum yield, g/g	Ref.
				Time, h	pH	Carbohydrate, %	Temperature, °C		
Fresh	Homogenization, acid hydrolysis, polyphenol oxidation, enzymatic saccharification	Fermentation bucket, 6250/stationary	<i>S. cerevisiae</i>	168	4	10.2	25	0.39	[18]
	Acid hydrolysis, autoclaving	Erlenmeyer flasks, 50/170	<i>T. harzianum</i> A10	144	4.5	31	30	1.67 ^a	[22]
	Sun dried, grounded, microwave, enzymatic saccharification	Erlenmeyer flask	<i>S. cerevisiae</i> MTCC 3089/10%; <i>P. stipitis</i> NCIM 3498/10% ^c	36	5.6	27.50 ^b	—	0.30	[19]
	Enzymatic saccharification	Minifors reactor, 1000/10 g/L	<i>S. cerevisiae</i>	24	—	14 ^d	37	0.281	[24]
	Dried, homogenized, acid hydrolysis, enzymatic saccharification, autoclaving, add-in nutrition	Erlenmeyer flask, 250/100	<i>P. stipitis</i> , 5%	72	5	33.42 ^a	30	0.44	[25]
	Dried, grounded, acid hydrolysis	Erlenmeyer flask, 100/150	<i>K. thermotolerans</i> DSM 3434, 3%	72	5	59.78	30	0.444	[20]
	Dried, acid hydrolysis, enzymatic saccharification, soluble soy protein	Erlenmeyer flask, 250	<i>S. cerevisiae</i> , 5%	72	4.8	20 ^d	30	0.47	[21]
None		Mason jars, 1893	<i>S. cerevisiae</i> Montrachet 5220/0.005%	24	3.4	120 ^b	30	0.043	[17]
None		Stainless steel bioreactor, 40,000/20	<i>S. cerevisiae</i> 24,702/25 × 10 ⁵	47	3.4	48	30	0.37	[26]

	None	Glass containers/mildly shaken	<i>S. cerevisiae</i> (UCD 595)/ 5%	96	4.2	49	25	4.5 ^e	[27]
	None	Round bottom flasks/1000	<i>S. cerevisiae</i> MTCC 173, <i>A. foetidus</i> MTCC 151, <i>F. oxysporum</i> MTCC 1755	72	–	3.21 ^f	30	16.09 ^e	[28]
Dried, grounded, autoclaving	Conical flask	<i>S. cerevisiae</i> MTCC 173, 1% <i>Actinomyces</i> APW-12 1%	72	6	–	30	8 ^e	[16]	
Peels	Acid hydrolysis, autoclaving	Erlenmeyer flasks, 50/200	<i>T. harzianum</i> NRRL 31396; 1 × 10 ⁷ spore/mL; <i>A. sojae</i> ATCC 20235, 1 × 10 ⁷ spore/mL; <i>S. cerevisiae</i> NRRL Y-139	120	5	6.25	30	0.945	[23]

^ag/L^bmg/g^cImmobilized co-culture of yeast cells^dDry pomace wt %^eV/W^f% of the whole slurry of apple pomace

if revenues by selling residual fermentation waste as animal feed could be included [27].

13.3.2 Plum Waste Processing

The world plum production in 2019 was 13 million tonnes, from which 559 thousand tonnes were produced in Serbia, so Serbia ranks third in plum production [7]. Based on the plum production data in 2019 and the plums stones' average content of 4.3% [29], the stone's amount is estimated to be 559 and 24 thousand tonnes for the World and Serbia, respectively. About 19% of plum stones are plum kernels [29]. The oil content in plum kernels is in the range of 32% [30] to 45.9% [31]. Plum kernel oil is rich in unsaturated fatty acids, and the main is oleic acid, which contents range from 62.0% [31] to 77.0% [32], followed by linoleic acid in amounts from 15.9% [33] to 29.6% [31].

The plum is an important feedstock in the food processing industry for obtaining jams, marmalades, and prunes from plum flesh and skin, while plum stones remain as waste. Amounts of plum stones and kernels are significant for obtaining the value-added products, which could ensure environmental and economic benefits. So far, plum kernels are used as: (i) lignocellulosic activated carbon adsorbent precursor for commercial dyes and Pb²⁺ [34] and NO₂ [35] and (ii) raw material for obtaining the pyrolysis oil [36]. Depending on the plum variety, kernels are rich in tocopherols, especially γ - and α -tocopherol, and could be exploited to extract and prepare various products [37]. Plum kernels could also be used to obtain the peptides with antioxidant and antihypertensive activity [38]. Plum kernel oil is a considerable source of carotenes, phenolic compounds, and significant raw material in food and cosmetic industries [39]. Nowadays, plum kernel oil is considered as feedstock for biodiesel production due to its favorable fatty acid composition. However, only two studies are dealing with the use of plum kernel oil in biodiesel production.

Górnáš et al. [29] investigated the properties of plum kernel biodiesel using the experimental data of oil fatty acid composition and empirical correlations for calculating physicochemical properties of biodiesel (the kinematic viscosity, cetane number, higher heating value, density, iodine value, cold filter plugging point, and oxidation stability). Calculated biodiesel properties of 21 plum varieties were in the range of European biodiesel standard EN14214 except for oxidation stability. Such behavior can be attributed to the natural antioxidants (tocochromanols and carotenoids) in the oil, whose amounts were not included in the calculations [40]. Kostić et al. [32] reported the use of plum kernel oil as feedstock for biodiesel production. Due to the high free fatty acids (FFA) content (15.8%) in the oil, the biodiesel was produced via a two-step process. The first step included H₂SO₄ catalyzed esterification of FFA, which was investigated at various reaction conditions (methanol:oil molar ratio in the range 1.8:1–10.2:1, H₂SO₄ amount 0.66–2.34%, based on the oil mass, and temperature, 33.2 °C to 66.8 °C, to find the optimal one for achieving the lowest acid value of the oil. The esterified oil (acid value of 0.47 mg KOH/g) was

processed to the base-catalyzed methanolysis (second step) in the presence of CaO as a catalyst (5% based on the oil mass), at methanol:oil molar ratio of 9:1 and at 60 °C. The properties of purified biodiesel were within the biodiesel standard EN14214 specifications.

13.3.3 *Grape Pomace Processing*

Total world production of grapes in 2019 was 77 million tonnes, and the leading producers were China, Italy, USA, Spain, and France. Grape is the third most-produced fruit in Serbia, with 164 thousand tonnes annual production in 2019 [7]. Grapes are the source of various processed products, such as wine, juice, sweet spreads, grape seed extracts, and vinegar. About 50% of this quantity is used in the wine industry, and almost 25% of this grape weight represents waste [41], where 75% makes wastewaters [42]. The wine solid waste mainly consists of pomace (20%, [43]). According to the estimations, 1 kg of grape pomace is generated for each 6 L of wine [44]. Winery waste contributes to pollution via low pH, high phytotoxic content, and biologically non-degradable antibacterial phenolic substances [45]. Irrigation with pretreated winery wastewaters and anaerobic digestion are used as dominant waste-water treatment methods [46]. In contrast, no reports were found about wastewater implementation for bioethanol production. The known possibilities for waste pomace utilization include composting, the production of steam or electricity, as cattle feed, methane or ethanol fermentation, and extraction to obtain various bio-compounds.

The main components of grape pomace are grape skins, pulp, seeds, and stems. Grape pomace is composed of neutral polysaccharides, acid pectic substances, insoluble proanthocyanidins, lignin, structural proteins, and phenols [47]. Grapeseed is another waste of wine production that is obtained after pressing the juice. Seeds present 2–5% of fresh grapes, while their grape pomace amount is 38–52% [48]. Grape pomace is nontoxic, but both high production volumes and organic matter content make it a serious environmental problem. On the other hand, grape pomace has been proposed for producing bioethanol, biodiesel, fertilizer, animal feed, and polyphenols [49]. Generally, grape pomace is produced seasonally and therefore needs storage. A common way to facilitate its storage is drying. However, drying increases costs and brings the risk of accidental or spontaneous combustion and demands rehydration since fermentation occurs in aqueous conditions. The alternative technique is ensilage via lactic acid fermentation [49]. Since ensilage increases production costs, it is better not to store but to use the pomace immediately.

Some authors showed that stalks [50, 51] or skin [52] could be separated from pomace and used in bioethanol production. It is known that grape pomace can be used for grape spirit (pomace brandy) production. However, spirit production can utilize only one part of grape pomace, soluble sugars. A large part of insoluble sugars (complex lignocellulosic forms) remains unused. Therefore, it is evident that grape

pomace as a feedstock for bioethanol production gives a greater opportunity to utilize it wastefully.

Grape pomace fermentation can be conducted in a direct (solid-state) or indirect (with previous hydrolysis, submersed state) manner. A review and schematic processes of grape pomace bioethanol production are shown in Table 13.2 and Fig. 13.3, respectively. White and red grape pomaces reported in Table 13.2 were waste from white and red grape wine making processes, respectively. White grape pomace comes out as waste from mechanical pressing, while red grape pomace passes pressing and fermentation to give aroma to red wine (Fig. 13.2). The recovery of the residual ethanol in the grape pomace must be made before further bioethanol production. Acid hydrolysis, enzymatic saccharification, pH adjusting, nutrient supplementation, and autoclaving were common pretreatment methods of grape pomace before submerged fermentation. Using *Kluyveromyces marxianus* (*K. marxianus*) Y885 can reduce pretreatment steps since this strain can simultaneously hydrolyze cell wall's sugars and ferment substrate to ethanol [53]. As shown (Table 13.2), white grapes contain more residual sugars than red grapes and therefore provide more ethanol. It is because water-soluble carbohydrates were enriched with released sugars from cell wall components. However, Corbin et al. [54] reported that the white grape pomace bioethanol process could run profitably even if only water-soluble carbohydrates are used as feedstock. Untouched cell wall fraction may be used as animal feed, fertilizer, or a source of polyphenol.

Compared to submersed, yields in ethanol production are greater in solid-state fermentation (Table 13.2). Furthermore, in solid-state fermentation, there was no need for pH adjusting, supplementary nutrition, or higher energy demand for maintaining higher operation temperatures than 28 °C. One of the advantages of solid-state grape pomace fermentation is the reduction of mass residues to be disposed of Rodríguez et al. [55] showed that at 96 h, the final dried weight was 18% lower regarding initial dried grape pomace weight.

Grapes would not be the first-choice raw material for ethanol production in Europe since the net energy output derived from them is up to 50% lower than wheat, sugar beet, sweet sorghum, or Jerusalem artichoke [57]. Kavargiris et al. [58] reported that higher grape yields, lower chemical inputs, mechanization, and maximization of ethanol yields could improve grapes ethanol's production energy and financial balances. If the grape pomace bioethanol reaches high industrial commercialization, E20 blend (blend of grape pomace ethanol of 20% and oxygen-free gasoline) can reduce SI engines exhaust emissions (CO, NO_x, HC, and CO₂) during cold operating conditions [59]. Furthermore, fuel consumption using E20 blend or commercial gasoline are almost the same.

Grape seeds consist of fiber, oil, protein, sugar, complex phenol, and minerals. The oil content in grape seeds is about 6–20% depending on the fruit variety [60, 61]. Grapeseed oil is rich in unsaturated fatty acid (82.9–90.13%), from which linoleic acid is dominant, with the amount varying from 53.62% [62] to 75.10% [48], followed by oleic acid which content is from 14.50% [48] to 30.63% [62].

Table 13.2 Grape pomace bioethanol production processes

Grape pomace	Type, volume of reactor, mL / agitation intensity, rpm	Fermentation microflora/ inoculum size	Operating conditions				Maximum yield, g/g	Temperature, °C	Ref.
			Time, h	pH	Carbohydrate, %				
White ^a	Erlenmeyer flasks/ stationary	<i>K. marxianus</i> Y885	72	–	~7.5 ^b				[53]
–	Mason jars/1600/ stationary	Natural yeast flora ^c	48	3.6	13.7	25	0.54		[56]
Ensilage, acid hydrolysis, enzymatic saccharification ^d , pH adjusting, add-in nutrition, autoclaving	Fermenters/250/ 140	<i>E. coli</i> KO11 ^e / 0.5 ^f	24	7	49.1	37	0.29		[49]
Red ^g	Fermenters/250/ 140	<i>E. coli</i> KO11 ^e / 0.5 ^f	24	7	49.1	37	0.29		
	Fermenters/250/ 140	<i>E. coli</i> KO11 ^e / 0.5 ^f	24	7	2.7	30	0.11		
Autoclaving	Petri dishes/ stationary	<i>S. cerevisiae</i> PM-16/10 ^{8h}	48	4.5	16.5	28	0.42		[55]

^aWhite wine production
^bg/L^cFlora: *S. cerevisiae*, *K. apiculate*, *C. stellata*, *C. collulososa*, *C. pulcherrima* and *H. anomala*^dSimultaneous saccharification and fermentation^eGenetically engineered
mg cells/g dry pomace^gRed wine production^hCells/g dry matter

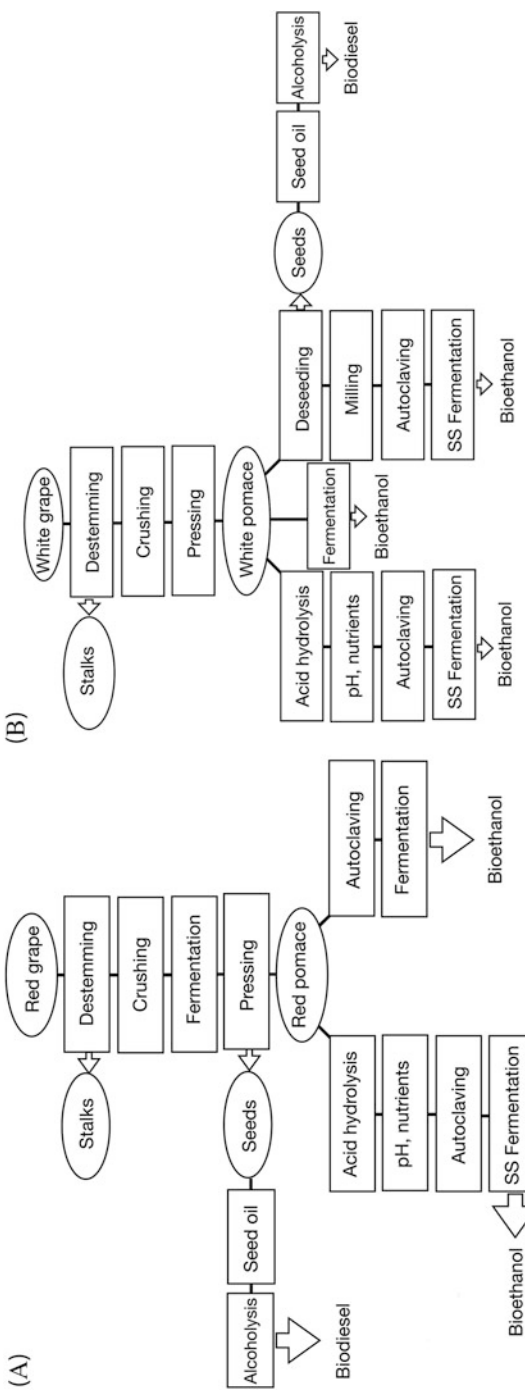


Fig. 13.2 Grape pomace biofuel production from: (a) red grapes or (b) white grapes

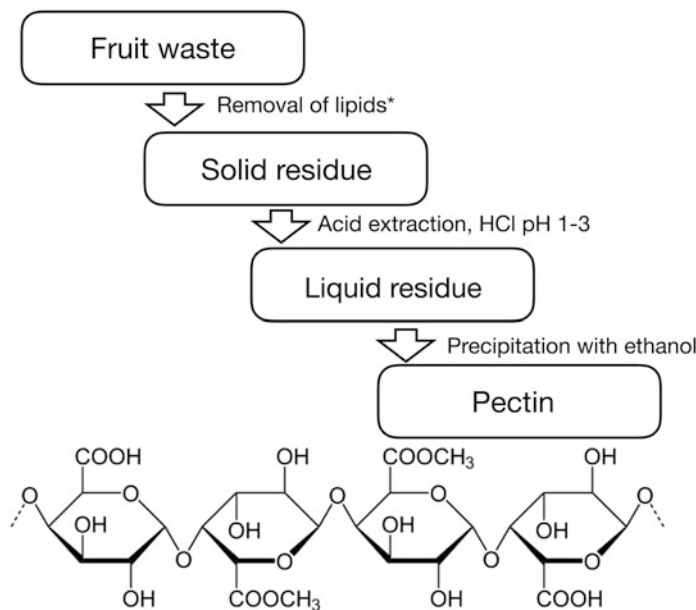


Fig. 13.3 Pectin extraction from the fruit residues

As grapeseed oil is rich in linoleic acid, vitamin E, phytosterols, and hydrophilic phenols, it can be a valuable raw material for the pharmaceutic, food, and cosmetic industry [61]. Nowadays, grapeseed oil has been considered as feedstock for biodiesel production, and various processes for alkyl esters synthesis have been investigated: conventional homogeneous base-catalyzed alcoholysis [62–67], enzyme-catalyzed process [60], and *in situ* biodiesel production processes [63, 64]. Grapeseed oil ethyl esters have been intensively studied due to their advantages: completely renewable fuel due to the possibility for using bioethanol obtained from winery wastes, higher specific energy and cetane number, better lubricity, and cold flow properties. Generally, the objectives of the investigations of grapeseed biodiesel production are optimizing the alcoholysis reaction conditions for achieving the highest alkyl esters yield and determination of biodiesel fuel properties.

The process operating conditions, including reaction temperature, methanol amount, catalyst concentration, and reaction time, were optimized using central composite rotatable design [66], Taguchi method, artificial neural network, and adaptive neuro-fuzzy inference system [67]. In some cases, grapeseed oil was pretreated to make it suitable for biodiesel production via direct base-catalyzed alcoholysis. The pretreatment methods include dewaxing [62], acid conditioning, deacidification, and drying [64] of the grapeseed oil. As a result, FFA contents, water, and phosphorus are reduced, allowing the production of good quality biodiesel.

The biodiesel production from grapeseed oil via enzyme-catalyzed alcoholysis was also studied [59]. The enzyme-catalyzed process is a relatively new biodiesel production method, considered environmentally friendly and economically favorable. Grapeseed oil methanolysis was studied in the presence of lipase from *Thermomyces lanuginosus* physically immobilized on magnetic nanoparticles of $\text{Fe}_3\text{O}_4/\text{Ag}$ coated by tartaric acid [59]. The process was performed at 45 °C, at overall methanol:oil molar ratio 6:1 (methanol addition in three steps), and enzyme amount of 10% to oil mass. The achieved esters yield was 94% in 24 h of reaction that is significantly higher than using free lipase (77%).

Due to efficient enzyme removal in a magnetic field, the esters phase separation and purification were much simpler than the homogeneous base-catalyzed process.

The direct biodiesel production from the grapeseed, known as *in situ* process, was also studied [63, 64]. The main advantage of this process is eliminating extraction, and possible purification of the oil that could decrease the overall process cost. The methyl esters' content and oil yield depended on the used catalyst. The highest methyl ester content (95.5%) and oil yield (10%) were achieved in the presence of KOH as a catalyst. When NaOH and CH_3OK were used, the efficacy of the process was significantly lower [64]. The oxidation stability of the obtained biodiesel did not depend on catalyst type, and in all cases, it was high (20–28 h). This behavior could be attributed to the methanol extraction of natural antioxidants from the seeds. Donoso et al. [63] compared the oxidation stability of methyl and ethyl ester obtained by alcoholysis catalyzed by CH_3ONa and $\text{CH}_3\text{CH}_2\text{ONa}$, respectively, in *in situ* and in the conventional process. Conventionally obtained methyl esters had higher oxidation stability than ethyl esters because of the higher antioxidant extraction capacity of methanol. However, the oxidation stability of both ester types is much below the standard limit. *In situ* obtained esters had higher oxidation stability, which was increased by seed soaking in alcohol for 24 h.

Grapeseed oil biodiesel properties are, generally, within biodiesel standard specification (EN 14214 or ASTM D6751) except for iodine value [65] and oxidation stability [62–65, 67]. Both properties are the consequence of high unsaturation degree levels and the absence of antioxidant compounds. The biodiesel properties could be improved by using the oil extracted with the hexane-methanol mixture, performing the biodiesel production via *in situ* processes, or adding additives and antioxidants to biodiesel.

13.3.4 Watermelon Waste Processing

Watermelon is a popular crop with many varieties grown all over the World. However, there are differences between the varieties which are grown in different regions. Also, various taxonomic classifications have been used in the scientific literature, as reported by Jarret and Levy [68]. The total watermelon production in 2019 was 100 million tonnes, from which 2.28 million tonnes are produced in Brazil and 163 thousand tonnes in Serbia [7]. Watermelon content of flesh, ring, and seeds

is 68%, 30%, and 2%, respectively [69]. Watermelon is cultivated for its juicy and sweet fruit that contains about 92% water, 7.5% total carbohydrates, 0.6% proteins, low fats, and significant amounts of vitamins C and A [70]. Watermelon can be used for obtaining jam, oil, proteins, sugars, xylanase, polygalacturonase, cutin, lycopene, and L-citrulline, an adsorbent for the removal of heavy metals, pesticides, and animal feed [69]. Watermelon is also a valuable feedstock for biofuel (bioethanol, biodiesel, and hydrocarbons) production because ~1/5 of annual watermelon production is refused from the fruit market and remains in the field. Additionally, the large amount of waste stream, rich in sugars, is produced during lycopene and L-citrulline extraction. Based on previously published papers, there are three types of watermelon waste: (i) crop with surface blemishes or misshapen (20%, [71]), (ii) watermelon rind [72], and (iii) watermelon lycopene free juice [71]. More than 90% of these watermelon wastes are left on fields and cause environmental problems [69].

If only watermelon peels are used, pretreatment (usually acid-hydrolysis) must be performed to yield 0.37 g/g of ethanol using *Metschnikowia cibodasensis* (*M. Cibodasensis*) Y34 yeasts [73]. The combination of two microorganisms (*Zymomonas mobilis* (*Z. mobilis*) and *S. cerevisiae*) in simultaneous saccharification and fermentation of watermelon rind provides 5.86% (v/v) of ethanol [72]. The laboratory cellulolytic bacterium isolates are also tested for waste watermelon bioethanol production. These bacterium isolates are batch cultivated in aqueous extract of watermelon rinds and sugarcane bagasse and can yield 7.4% (v/v) ethanol for 6-days fermentation [74]. Fermentation of watermelon waste crops may be performed in the shortest time of 30 h, shaken at 120 rpm with the yeast amount of 5 g [75]. Under these conditions is obtained the highest ethanol yield of 0.355 g/g. In contrast, deseeded watermelon crops enriched with nitrogen provide a higher ethanol yield of 0.467 g/g at 30 °C in medium with *S. cerevisiae* [76]. *Z. mobilis* is tested to utilize hydrolyzed watermelon waste crops and produces 27.62% (v/v) of ethanol [77].

Watermelon contains about 300–500 seeds per fruit, used as cheap animal feed or simply rejected as waste. Muhammad et al. [78] reported that *Citrullus lanatus* fruit grown in Malaysia (with an average mass of 425.49 g) contains 330.6 seeds (65.652 g) on average, which corresponds to 15.4% of fruit mass. The average fruit skin and fruit flesh were 39.318 g and 320.52 g, respectively. Based on the fruit production per hectare, it was estimated that about 2.3 tons of seeds (with about 1000 L of oil) could be produced [78]. The watermelon seeds are rich in oil and proteins and can prevent cancers, cardiovascular and gastroenterological diseases, and diabetes [79–81]. The watermelon seeds' oil content is 41.32% [82] to about 50% [83, 84]. Primary fatty acids in the watermelon seed oil are unsaturated, and the most abundant is linoleic acid, present in an amount from 56.9% [69] to 68.3% [84], followed by oleic acid in an amount from 13.25% [84] to 15.2% [85]. Palmitic and stearic acids are the main saturated fatty acids in the watermelon seed oil [79, 84–86]. The remaining waste after the oil extraction from seeds is rich in proteins (about 20%) and can be used as a meat substitute, for protein production, or as livestock feed. Recently, the watermelon seed oil is investigated as feedstock for biodiesel

production. An overview of the biodiesel production from watermelon seed oil is shown in Table 13.3. The investigations have been directed towards the biodiesel properties, fuel performances of biodiesel-diesel blends, and optimization of the reaction conditions. The homogeneous base catalysts have been mostly used for biodiesel production from watermelon seed oil, whereby the alkali hydroxides are predominant. Although the catalytic activity of NaOH was higher compared to KOH, NaOCH₃, KOCH₃ at the same concentration, the slightly higher biodiesel yield was achieved in the presence of methoxides due to the absence of side saponification reaction. However, hygroscopicity and the high price of methoxides limited their use in biodiesel production [87]. According to literature searches made by the authors, only Rao et al. [88] used heterogeneous magnesium carbonate (MgCO₃) catalyst in biodiesel production from watermelon seed oil. The high biodiesel yield was achieved under mild reaction conditions (Table 13.3) with avoiding the problems in esters purification that is characteristic for homogeneous catalysts. Recently, ionic liquids have been considered as prospective catalysts for biodiesel production from oils having FFA content >1% due to their low corrosivity, easy separation from reaction mixture, reusing ability, and simple esters purification without wastewater formation. Elsheikh [89] used four different pyrazolium based ionic liquid: 2-(3-sulfopropyl) pyrazolium hydrogensulfate (SPPHSO₄), 2-(4-sulfonylbutyl) pyrazolium hydrogensulfate (SBPHSO₄), 1-methyl-2-(3-sulfopropyl) pyrazolium hydrogensulfate (MSPPHSO₄) and 1-methyl-2-(4-sulfonylbutyl) pyrazolium hydrogensulfate (MSBPHSO₄) as catalysts in methanolysis of oil having FFA content of 3.18%. The highest catalytic activity was seen for SBPHSO₄ which was attributed to its high acidity. Additionally, SBPHSO₄ was recovered by separation and reused in seven methanolysis cycles without significant loss in catalytic activity. Methanolysis in the presence of ionic liquids, compared to base catalyzed process, is performed at higher methanol amount, catalyst concentration and reaction temperature (Table 13.3).

Two-step processes that include acid catalyzed FFA esterification and base-catalyzed methanolysis of esterified oil were applied for biodiesel production from acidic watermelon oil [90, 91]. The FFA esterification of oils with an acid value of 6.16 mg KOH/g was conducted in the presence of ionic liquids as a catalyst: 1-methyl-3-(4-sulfonylbutyl)-imidazolium hydrogensulfate, 1-methyl-2-(4-sulfonylbutyl)-pyrazolium hydrogensulfate [80], 1,3-disulfonic acid imidazolium hydrogensulfate and 3-methyl-1-sulfonic acid imidazolium hydrogensulfate [92]. Base catalyzed methanolysis was carried out in the presence of KOH as catalyzed. The ionic liquids showed high catalytic activity and achieved FFA conversion was above 95%. The esterified oil having an acid value of 0.46 mg KOH/g [90] and 0.29 ± 0.021 mg KOH/g [92] was subjected to KOH catalyzed methanolysis, whereby methyl esters purity >98% was achieved.

The reported fuel properties of produced biodiesel are within the standard ASTM D6751 or EN 14214 specification [90, 92] except for oxidation stability [93, 94] and cold flow properties [88]. Blend B10 of conventional diesel with watermelon seed oil biodiesel had similar fuel and combustion performances as diesel and improved emission characteristics. Namely, the emission of hydrocarbons, CO₂ and O₂ were

Table 13.3 Watermelon seed oil methanolysis at laboratory scale.

Variety of watermelon	Alcohol: oil molar ratio	Catalyst/loading, %	Optimal conditions			Remark/objective of study	Ref.
			Temperature, °C	Reaction conditions	Maximum yield, %/time		
<i>C. lanatus</i>	3:1–10:1	NaOH/0.5–3.5% of oil	50–60	750 rpm, 6:1, 1.5%, 60 °C	95/3 h	Reaction optimization, esters properties	[95]
<i>C. vulgaris</i>	5:1	NaOH/0.13–0.18	60	0.13	70/2 h	Ester's synthesis and properties	[83]
3:1–7:1	MgCO ₃ /1.25–2.25%	50	4:1, 1.5%	80/75 min	Reaction optimization and esters properties	[88]	
3:5 mL/mL	NaOH /0.016–0.02 g catalyst/mL oil	60	—	—/1 h	Performances and emission characteristics of blends	[96]	
—	3:1–21:1	SPBHSO ₄ , SBPHSO ₄ , MSPBHSO ₄ , MSBPHSO ₄ / 4.8–5.8% of oil	120–200	15:1; SBPHSO ₄ , 5.2%, 170 °C	89.5/6 h	Reaction optimization	[89]
<i>C. colocynthis</i>	6:1–10:1	KOH/0.5–1.25% of oil	50–70	8:1, 0.75%, 60 °C	95/1.5 h	Reaction optimization	[97]
3:1–12:1	NaOH, KOH, NaOCH ₃ , KOCH ₃ /0.6–1.5% of oil	35–80	6:1, NaOH, 1%, 60 °C	97.8/1 h	Reaction optimization	[87]	
6:1	NaOCH ₃ , /1% of oil	60	—	82/—	Ester's properties	[93]	
I step: 3:1–2:1	MSIMHSO ₄ , DSIMHSO ₄ /3–5% of oil	100–170	12:1, DSIMHSO ₄ , 3.6%, 150 °C	95.5% FFA conversion/ 105 min	Optimization of esterification reaction, esters properties	[92]	
II step: 6:1	KOH/1% of oil	60	—	98.2%/50 min			
I step: 3:1–2:1	MSBIMHSO ₄ , MSBPHSO ₄ / 3.0–4.8% of oil	100–180	12:1, MSBIMHSO ₄ , 3.8%, 130 °C	96.7% FFA conversion/3 h	Optimization of esterification reaction, esters properties	[90]	
II step: 6:1	KOH/1% of oil	60	—	98.8%/50 min			

aFAME content in the biodiesel. SPBHSO₄–2-(3-sulfopropyl) pyrazolium hydrogen sulfate, SBPHSO₄–2-(4-sulfobutyl) pyrazolium hydrogen sulfate, MSPBHSO₄–1-methyl-2-(3-sulfopropyl) pyrazolium hydrogen sulfate, MSBIMHSO₄–1-methyl-2-(3-sulfopropyl) pyrazolium hydrogen sulfate, DSIMHSO₄–1,3-disulfonic acid imidazolium hydrogen sulfate, MSBIMHSO₄–1-methyl-3-(4-sulfobutyl)-imidazolium hydrogen sulfate

lower than diesel, while CO and NO_x emissions were the lowest for the B10 blend compared to B20 and B30 [94]. Therefore, the watermelon seed oil is a promising feedstock for biodiesel production, especially in regions where the watermelon is cultivated in high amounts.

13.4 Fruit Waste Biochemicals

Brazil, as a World leader in fruit production (50% of world production of sweet oranges), produces around 17–20 million tonnes of oranges (*Citrus sinensis*), annually with 13–15 million tonnes of this total being obtained in state of São Paulo according to [CitrusBr.com](#). Only half of the fruits are used in the process for obtaining juice, thus the citrus juice industry generates about eight to ten million tonnes of waste that is underutilized [98]. After the juice extraction, citrus fruit is still extraordinarily rich in many different materials as: sugars, vitamins, lipids and waxes, proteins, polysaccharides, bioflavonoids. Orange waste shows high moisture contents, around 80% [99]. The common citrus waste presents high sugar and pectin content (15–30%, on dry basis, low lignin content - up to 4.5%, on dry basis), and high cellulose content (18%, on dry basis), hemicellulose (10.5%), lipids (1.95%), proteins (6.50%), soluble sugar content (16.5%) [9]. An efficient process for limonene, carotenoids, hesperidin, pectin, soda lignin, and cellulose extraction from industrial orange peel waste that could be applied for any agro-industrial bagasse is presented in literature [99–102].

The world production of mangoes, mangosteens, and guavas is over 55 million tonnes for 2019 according to FAOSTAT [7]. Brazil aggregates around 2.4 million tonnes of world production, which is around 4.4%. Mango waste contains 40% of fruit weight, consisting of peel and seed (internal kernel and husk) [103]. The most profitable mango waste treatment scheme is generation of pectin and oil seed [2, 103]. After the pulp is separated from peel and seed, it is transformed into juice, jellies, and jams. The husk is utilized for cellulose production and the kernel, oily core is used for mango oil production. Mango kernel oil is widely used in the cosmetic industry as a substitute for cocoa oil [103–105]. Mango kernel contains about 9–13% of lipids per dry basis, where 94% account for neutral lipids, 4% are phospholipids, and 2% glycolipids [2]. Mango fruit is also rich in carotenoids, there is an intense orange colour. Through the process of ripening, mango's peel changes colour from green to intense orange, due to the difference in carotene content, adding important assessment to the consumer selectivity and nutritional value of the fruit [106].

13.4.1 Essential Oils and Limonene

Essential oils are volatile compounds responsible for aromas in various plants and/or their parts, and they have been used since ancient times [107]. Common processes for extraction of essential oils are different versions of cold pressing, hydro-distillation, and extraction with organic solvents, usually followed by purification stages that include centrifugation and additional distillation [108]. Quality of essential oils depends on their main components, chemically classified into terpenes, oxyterpenes, and other organic substances - alcohols, aldehydes, ketones, acids, esters. The cyclic monoterpene ($C_{10}H_{16}$), limonene is present in two optical isomers: d-limonene, which gives major fragrance to orange and l-limonene, which fragrance is similar to the turpentine. The higher limonene extraction yield, by Battista and colleagues [109] was obtained using non-polar solvent *n*-hexane (1.31% w/w), and diethyl-ether (0.77% w/w) at 85 °C and in 3:1 (w/v) for orange: *n*-hexane proportion [109]. Steam hydrolyzation processes obtain around 1.5% of d-limonene from fresh orange peel. The essential oils are usually removed, before further fruit waste fermentation, because they act as yeast inhibitors [99].

The new era of green chemistry extraction reduces energy consumption and provides a natural safe, ecologically friendly, and economically acceptable process [110]. Supercritical extraction optimal conditions were 30 MPa and temperature of 40 °C, with the extraction yield of 3.13 g per 100 g of peel and limonene content 51.7% [111]. A biorefinery concept considers extraction and isolation of two or more products from fruit residues in a row. Hilali et al. [110] employed a solar hydro-distillation process for extraction of essential oils from orange peel, in a continuous process. For example, the same peel was used for extraction of polyphenols, naruritin, and hesperidin, which will be commented on in a section of bioflavonoids. The essential oil yield was around 1.03% for solar method and for conventional was around 1.05% [110].

13.4.2 Carotenoids

Carotenoids are mostly C_{40} terpenoids, a class of compounds that take part in various biological processes in plants, such as photo-protection, photosynthesis, development, and photomorphogenesis [112]. Carotenoids belong to group of tetraterpenes and can be classified into two groups: carotenes (alpha-carotene, beta-carotene, lycopene) and xanthophylls (zeaxanthin, lutein and beta-cryptoxanthin) [113]. They are the important precursors of vitamin A [114]. The conventional methods for carotenoids extraction are maceration, hydrolyzation, and more utilized Soxhlet extraction. Ultrasonication, microwave, and high shear dispersion are some of the new techniques implemented in carotenoid extraction. Baria et al., [109] tested above mentioned techniques for extraction. The highest carotenoid content was with high shear dispersion at 20,000 rpm [115]. Alternative for the organic solvent

extraction is use of the new green solvent as d-limonene application for recovery of carotenoids. Recently, the demand for greener biodegradable and non-dangerous solvents is a principal concern. Compared with other solvents, d-limonene is recognized as a safe solvent by the US Food and Drug Administration. Solvent free microwave extraction and steam distillation compared, obtained 4.02% and 4.16% of carotenoids from orange peel [114].

13.4.3 Bioflavonoids: Phenolic Compounds

Waste from peel and fruit pomace such as apple, grape, orange, banana, mango, pineapple, and pomegranate are low-cost sources of antioxidant molecules [116]. The major phenolic compound in oranges is hesperidin [100, 101], while in mango are found mangiferin, and quercetin 3-O-galactoside [103]. Flavonols (quercetin, rutin, kaempferol, myricetin, piceatannol), flavan-3-ol (epicatechin, catechin, procyanidin B1 and B2, catechin-O-gallate), glutathione, and phenolic acids (ferulic, caffeic, caftaric, gallic, fertaric and coumaric acid) are some of the main products of grape waste processing [117]. Hesperidin is a secondary plant metabolite and one of the principal bioflavonoids in citrus fruits, orange, lemon, and tangerine. This flavanone and its aglycone form, hesperetin, are present in relatively high quantities (1–2%) specifically in sweet oranges (*C. sinensis*) [100, 101]. Many different bioactive properties of bioflavonoids are reported, such as antioxidant, anti-inflammatory, hypo-lipidemic, vaso-protective, and anti-cancerogenic [100]. The bioflavonoids are secondary metabolites of plants and represent a great portion of polyphenols found in semen, cortex, roots, fruits, leaves and flowers of various species. Hesperidin can be present in high quantities – up to 14% (w/w) of immature orange fruit. It is proposed, after different *in vitro* studies, that hesperidin plays a role in plant defense, and acts as an antioxidant. Many different procedures are already described in literature and used for extraction of hesperidin from various starting materials, including maceration [118], Soxhlet extraction [99, 102], alkaline extraction [100, 119], extraction assisted with ultrasound [120], high hydrostatic pressure, microwave assisted extraction [121], extraction by an enzymatic process, and supercritical fluids extraction [111]. New and green methods, without using organic solvents and with low energy consumption, were implemented for extraction of hesperidin from fresh orange bagasse, with yield up to 1.5% [100–102]. Hesperidin extracted in this manner is safe and biocompatible for various applications [100]. Combination of two techniques, supercritical fluid extraction and ultrasound assisted extraction were implemented for combined extraction of hesperidin and limonene. Optimization of the two methods obtained limonene (purity grade up to 89%) around 3.23% and hesperidin 23.0 µg/mL. Ultrasound assisted extraction optimal conditions for hesperidin were temperature 68 °C, time 45 min, solvent-solid ratio 41 mL/g, and ethanol:water ratio 61% (v/v), with the predicted hesperidin content being 23.2 µg/mL [111]. Hesperidin and naruritin, known as bioflavonoids, or polyphenol glycoside, were isolated in the solar-distillation process. The highest

reported yield of hesperidin in such a method was around 1.95% and for narirutin from the same peel, was around 0.3%. Further, the same peel was used for pectin extraction, obtaining around 8.3% of product, compared with the conventional method, which obtained 12.08% of pectin [110]. Traditional, volatile organic solvents extraction are nowadays substituted with new green alternative methods, choline-chloride based deep eutectic solvents. One of these methods is deep eutectic solvents extraction in combination with heating, mechano-chemical extraction and microwave extraction [122]. Polarity of solvents plays an important role in bioactive compound extractions, as optimization of the process condition in purpose to obtain high yields from citrus. Choline chloride/levulinic acid/N-methyl urea showed the highest extraction yield of total flavonoids, with a yield of 1.88% of polymethoxylated polyphenols [123]. Extraction of flavonoids from grapefruit peel with deep eutectic solvents (DES) (lactic acid/glucose) and aqueous glycerol, combined with high-voltage electrical discharges, were proposed by El Kantar and authors [124]. Concentration of naringin extracted in this study, was for water extraction 0.58%, for 50% ethanol/water (v/v) was 2.09%, for 20% aqueous glycerol (w/v) was 1.96%, and finally for DES-6 (lactic acid: glucose, w/w) was 1.86% [124]. Efficient extraction method using DES as an extraction solvent was developed for isolation of four major active compounds narirutin, naringin, hesperidin, and neohesperidin from bitter orange (*Aurantii fructus*). A series of DESs were prepared and investigated by mixing betaine or choline chloride with different hydrogen-bond donors, and betaine/ethanediol was found to be the most suitable solvent. The best extraction yields were investigated, considering extraction efficiency, water content in DES, such as hydrogen-bond acceptor/hydrogen-bond donor ratio, solid/liquid ratio, extraction temperature, and extraction time. The optimal conditions were 40% of water in betaine/ethanediol (1:4, v/v) at 60 °C for heated extraction of 30 min and solid/liquid ratio 1:100 g/mL. The extraction yields of narirutin were 8.4 mg/g, naringin 83.98 mg/g, hesperidin 3.03 mg/g, and neohesperidin 35.94 mg/g. The present study showed that DES could be promising eco-friendly, and efficient solvents for extraction of the bioactive ingredients from traditional Chinese medicine [125]. Ultrasound alcohol assisted DES liquid phase microextraction was employed for quercetin extraction from wine. The method was validated and investigated by repeatability, reproducibility, and recovery assays, as well as, by comparing the obtained results for real samples with the reference method. The recommended process was successfully applied for the pre-concentration, extraction, and quantification of quercetin in wine and food samples [126].

13.4.4 Pectin

The main insoluble carbohydrate in orange, apple, apricot, peach, grapefruit, and other fruit pulp is pectin, a hydrocolloid present in the primary wall and intercellular layers (upper lamella) of the upper plants. This polysaccharide provides flexibility to the solid structure contributing to cell adhesion [127]. It is composed from around

65% of galacturonic acid connected by α -1,4-glycosidic bonds forming the homogalacturonan chain [128]. Pectin is a heterogeneous polysaccharide composed of a main chain of galacturonic acid interspersed by methoxy galacturonic acid, which has in its side chain branches containing pentoses and hexoses, such as galactose, xylose, arabinose. A major part of pectin complex structure is a homogalacturonan component, accounting for around 65–75% of pectin, made from linear polymer of α -1,4-galacturonic acid. The rest belongs to rhamnogalacturonan I, which is composed of repeating galacturonic acid and rhamnose units, partially methyl-esterified and/or acetylated. Therefore, pectin is classified into two major groups: highly methoxylated pectin (> 50% of esterification degree) and low methoxylated pectin (< 50% of esterification degree) [129]. Around 2–10% of pectin is rhamnogalacturonan II [130]. Being present in high amounts in the cell wall of plants, it forms skeletal tissue, which makes the plant chemically stable and physically strong. In addition to being abundant in the albedo, the white part of the orange that stands between the peel and the fruit pulp. The citrus waste has around 20–42% of pectin, which differs according to the variety of the oranges. The extracted pectin can be implemented in different products. Pectin is used in its polymer form, especially in the food industry as thickener for juices, drinks, and jellies production. The extraction of pectin before orange waste hydrolysis is achieved by heating the residue with water in ratio 1: 2 (w/v) with 0.05% hydrochloric acid at 100 °C for 1 hour (Fig. 13.3). The liquid is filtered and is further cooled, and the solid is a residue of extraction. The other liquid portion is joined first, and there is added an ethanol solution (95%) acidified with 0.05% hydrochloric acid, using doubled ethanol volume. Filtered and washed with 65% ethanol and acidified, the solid is put to dry in an oven at 40 °C [131, 132]. Pectin and other bio components from waste can be obtained as illustrated in Fig. 13.3. Process takes four consecutive steps, and the second step in this process results in a solid residue that can be used for lignin and cellulose production.

The structural and functional properties of pectin may be influenced by type of the extraction greatly [133]. For example, acid extraction, and hot water extractions of pectin gave products with high homogalacturonan (Gal acid) content, homogalacturonan units >65%. Alkaline treatment can lead to pectin degradation, affecting homogalacturonan stability. Alkaline extracted pectin usually shows a high quantity of rhamnogalacturonan oligomers branched fraction [134]. Kaya and colleagues [135] compared nitric acid and oxalic acid pectin extraction from orange, lemon lime and grapefruit, through several conditions. The extraction yields varied from 16.7 to 33.6% depending on the extraction condition and peel source, therefore the lowest yield was for orange and the highest for the lime peel [135]. Ohmic heating or Joule heating is an alternative uniform heating method applied to pectin extraction. Ohmic heating occurs due to alternating electrical current passing through the food, with heating effects caused due to the electrical resistance of food. This type of extraction increased the yield of pectin more than conventional heating. The maximum yield of pectin was 14.32% applying the highest voltage gradient 15 V/cm (per dry orange mass). All pectins, extracted in this manner, had high esterification degrees and the emulsification stability were extremely high

[136]. One other alternative method for pectin extraction is sonication. Patience et al. [137] obtained 11% of pectin from orange dry peel, with continuous ultrasonic irradiation at 0.24 w/mL [137]. Ultrasound extraction generally decreases time of process and improves pectin yield [129]. One of the alternative methods for pectin extraction was applied by Jin et al., [138]. The array-induced voltage of 1000 V, at 0 °C phase difference and 3 x 3 in-phase voltage array led to 10.34% of pectin from grapefruit fruit. The impact of used voltage, the physicochemical properties, as yield and kinetics were investigated. The yield was increased following the increment of the electrical field [138].

Therefore, pectin is industrially produced from fruit. Almost all industrial processes use acid-based treatment at high temperature applied for a short time to avoid pectin hydrolysis, followed by an alcoholic purification step. Most of the processes use HCl (1–3%), for the extraction and different alcohol to water ratio for precipitation, and lately are followed by ultrasonication to shorten time of process and increase efficacy of the pectin isolation [139]. Besides, pectin extraction can be more effective if used chelating agents (EDTA), which interact with bivalent ions and increase pectin solubility in hot acid solutions (pH = 1–3), consequently, the pectin yields are higher. It is also important to evaluate if fruit waste is rich in carotenoids, other lipids and soluble pigments, which must be removed before pectin can be extracted and purified. In this case, fruit waste is pretreated with ethanol and acetone, until whitened with ethanol (95%) and then dried in acetone to so called - alcohol insoluble residue (AIR). This residue is treated for isolation of different types of pectin [140].

13.4.5 Lignin

Lignin is an aromatic biopolymer constructed through natural polymerisation of sinapyl alcohol, *p*-coumaryl alcohol, and coniferyl alcohol. Its structure ledge is made of guaiacyl, syringyl, and *p*-hydroxyphenyl units [141, 142]. The exact percentage of monomers can vary and is specific for each type of the plant. The process of isolation may also have significant influences on the lignin final composition. Residual carbohydrates, such as arabinan, xylan, galactan, mannan and glucan are found to be covalently bonded to lignin compounds, and their contents can vary from 0.2–2.4%. The principal role of lignin in plants is to provide the structural integrity, microbial decay resistance and water-impermeability [143]. The lignin can be used in the dispersant formulation [144], or as an adhesive, also as an antioxidant in small concentrations in dyes, paints, UV-light adsorbents, phenolic resins, and fuels [141, 145]. Few studies have been published on lignin extracted from oranges. Barros and collaborators (2018) [142] isolated the soda lignin with 1.5% yield based on dry orange bagasse mass. After removal of essential oils and bioflavonoids, orange peel was subjected to pectin removal, and subsequent lignin extraction (Fig. 13.4). Residues from each step can be used for other valuable commodities production.

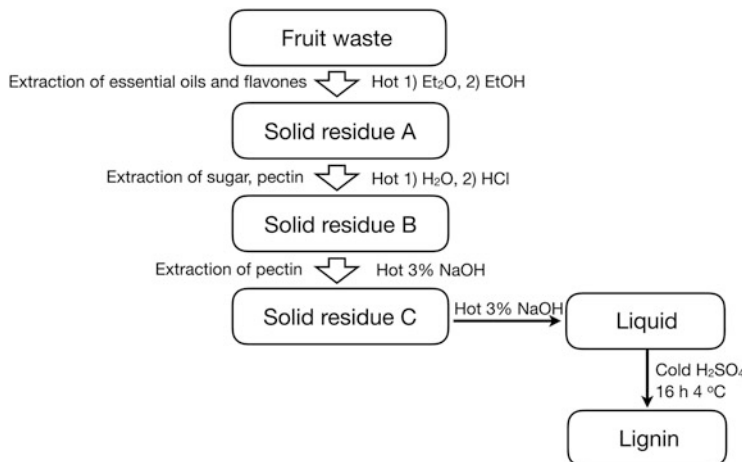


Fig. 13.4 Lignin is obtained from fruit waste in sequential extraction processes

Alkali soluble lignin was isolated with 0.3% NaOH solution and precipitated with H₂SO₄. The low content was expected having seen that bagasse material is usually poor in lignans, when compared to the woody materials [142]. Lignin can be obtained from other fruit or agro-waste materials using different processes, which share some common features as in chemical, physical, biological, or mixed methods. Chemical methods use base (NaOH, KOH) or acid (H₂SO₄, HCl, H₃PO₄), and high temperatures. Presence of alkali in lignin extraction in synergism with high temperature activates the surface area and microporosity of source material [146]. Soda and Kraft pulping are two alkaline methods, applying sodium sulfide and sodium hydroxide [141]. Kraft lignin production is a global pulping process with about 90% of total production capacity [143].

The highest content of lignin is successfully isolated from organo-solvent lignins, then alkaline lignin which can also contain more residual sugars. Arabinan and manan can be found present in straw and spruce lignin, and xylan is present in all lignins [141]. When applied to increased concentrations of HCl (20%), increased lignin yields were obtained (15.6%), from oil palm residues. The concentration of methoxyl content increased with increment of HCl concentration in the extraction solution. Hydayati and colleagues identified 34 compounds from lignin extraction, by GC-MS [145]. Two organic-solvent processes including sulfuric acid/ethanol and formic acid/acetic acid solvent mixtures, from banana biomass residues were compared. Sulfuric acid/ethanol showed higher extraction yield and better purity of lignin. The banana rachis straw was first soaked in a mixture of formic acid/acetic acid solvents for 30 min (solid to liquid ratio 1/25 w/v), and then the mixture was heated up to 107 °C for 3 h. The extraction was stopped, and the pulp was directly filtered in a vacuum filter (vacuum pore >100 um). Further, the pulp was washed with hot water, washes were collected and diluted with distilled water to pH around

2 for lignin precipitation. The process with sulfuric acid/ethanol/water in ratio 5.4/92/2.6% v/v/v, was performed in the microwave. Microwave extraction was carried out in an 80 mL reactor at 1200 W power. The reaction duration was 10 min at temperature plateau (161 °C), after which reaction was stopped. After cooling for about 10 min the mixture was filtered and diluted with water to the pH value of around 2.0 for lignin precipitation. The yield of lignin extracted with formic/acetic acid was 45.3%, and for sulfuric acid/ethanol was 58.7% [147].

13.4.6 Cellulose and Nanocellulose

Cellulose is a linear semi-crystalline homopolymer, based on 1,4-beta glycosidic linkage of the D-glucose monomers [148]. In plants, two glucose monomer units are around 1 nm, united in long chains, fibrils can reach up 10–20 nm or more in width. Several parallel fibrils organized in microfibrils, which are united with resinous mass, lignin, make up the biggest part of extracellular biomass. Plants like kenaf, giant reed, cotton, stalks, miscanthus, switchgrass, olive tree, and almond tree are considered softwood and have high content of cellulose and moderate quantities of lignin. Compared to the softwood biomass, agri-food waste has moderate to high content of cellulose material, and exceptionally low content of lignin. Therefore, cellulose isolation is faster, easier, and less expensive than from soft and hard wood materials. Lignocellulosic biomass requires elimination of non-cellulosic parts of plants such as tannins, fat, free sugars, flavonoids, resins, terpenes, waxes, and fatty acids. Such pretreatment processes can be performed using different physical, biological and chemical methods, or combining all at once [149]. These methods allow separation and isolation of pure raw cellulose from bulk, breaking the linkage between hemicellulose, lignin, and cellulose [150]. There are two main segments of cellulose isolation, mechanical (physical), and chemical processes. The use of mechanical force is represented in the wood industry, where the content of the lignin in the tree is exceedingly high and it is necessary to use great force to separate the lignocellulosic fibers and isolate cellulose. Chemical processes can be divided in isolation with chemical solvents and enzymatic extraction, with the around 18% yield calculated per dry orange bagasse [131, 148, 151–154]. In the last 20 to 30 years, the interest in cellulose nanofibers and nanocellulose whiskers has increased demand for cellulose production [149, 155]. There are different sources of cellulose, and since the extraction is much more efficient and easier from soft biomass, corn husk, coffee residues, sugarcane bagasse, orange bagasse, and other fruit and vegetables are more used for cellulose extraction [156]. Mariño and colleagues [156] compared cellulose yield and their crystallinity, isolated from orange bagasse, sugarcane straw, coffee residues and orange bagasse. All four biomasses, corn, coffee, orange, and sugarcane were subjected to alkaline hydrolysis with 4% NaOH solution in autoclave at 120 °C for 20 min. Further, the cellulose was bleached with a solution of sodium chlorite at 120 °C for 20 min. The obtained yield was 10.8% for orange bagasse, 38.5% for corn husk, 24% for sugarcane and 33% for

coffee residues. The highest crystallinity value was obtained for corn husk, (crystallinity index ~0.75), for orange bagasse was ~0.72, for sugarcane ~0.69 and for coffee residues ~0.65 [156]. Corn straw, bamboo and rice straw were used for four to six step extractions of cellulose nanofibers with 3% KOH at 90 °C (1 h). First step was for hemicellulose separation, and consequently the biomass was treated with acidified NaCl and further with 8% KOH at 90 °C for 1 h. The yield was in a range from 13 to 18%, depending on the raw materials [157]. The autoclaving processes with alkaline solutions apparently are more efficient methods for cellulose extraction from crop and agro-industrial waste. Mantovan et al., [158] tested 3 different chemical biomass treatments (sodium hydroxide, peracetic acid, peroxide alkaline) for cellulose extraction from orange bagasse, combining them with autoclave (30 min, 121 °C, 1 bar) and ultrasound (50% power output, 1 h, 25–60 °C). Hypochlorite can be substituted by peracetic acid that is an efficient bleaching agent also. Ultrasound was less efficient in removing hemicellulose and lignin from orange bagasse, compared to autoclave. Despite the high temperature and ultrasound power, all samples demonstrated characteristic infrared bands of hemicellulose, lignin and pectin presence, probably due to the short process time [158]. Banana peel is also widely used for cellulose extraction. Chemical process, alkaline treatment with 5% KOH and bleaching with NaClO₂ 1% followed by acid hydrolysis with 0.1, 1, or 10% and mechanical (high pressure homogenizer) treatments can be utilized. The unripe banana peel was first pretreated with potassium metabisulfite (1% w/v) and after 24 h dried in an air convection oven at 60 °C. Acid hydrolysis with sulfuric acid is used to remove amorphous cellulose and increase the crystallinity. The yield of cellulose nanofibers varied from 27.1% up to 71.2%, depending on the acid concentration [159]. The five repeated cycles microwave method combined with ball milling was used to obtain cellulose fibers from banana, after Soxhlet extraction. Ball milling is an old method used in modern acid treatments of cellulose fiber for removal of amorphous parts. The final step was bleaching with 5% H₂O₂ for 30 min at 70 °C, resulting in 55.5% of microcellulose fiber from residual banana peel [160]. Enzymatic processes are employed in fermentation of lignocellulosic biomass generally after pretreatments by alkali, acids, organic solvents and autohydrolysis. The enzymes are mostly used to disrupt the linkage between the glucose in cellulose and obtain bioethanol [161]. Some natural polymers, macromolecules (lignin), and polysaccharides, such as pectin and cellulose [162], extractions are mentioned in Table 13.4.

13.5 Conclusions and Future Outlook

Nowadays, the world's industrialization and the growth of the food industry are reaching a crucial point for handling the extremely high quantities of fruit waste biomass being generated, so that an extreme measure for waste and wastewater management must be taken, as soon as possible. We must reduce, recycle, and reuse

Table 13.4 Extraction of natural polysaccharides and polymer from fruit residues

Product	Source	Type of process	Solvent	Temperature, °C	Maximum yield, %	Time	Ref.
Pectin	Orange peel	Solar-hydro distillation	Water	75	12.08	5 h	[110]
		Chemical	HCl 0.05%	100	–	1 h	[130, [133]
		Ohmic heating		50–90	14.32	5–30 (min)	[136]
	Ultrasound	Distilled water		11.0	1 h		[137]
	Ultrasound	HCl 0.5 mol L ⁻¹		70	26.74	10–60 min	[140]
	Orange lemon & grapefruit peel	Chemical	HNO ₃ ; C ₂ H ₂ O ₄	70–85	33.6	2–7 (h)	[135]
Grapefruit peels		Array-induced	HCl 0.5 mol L ⁻¹	65	10.34	0.5 h	[139]
	Microwave		HCl; EDTA		38.48	12 min	[140]
	Chemical		NaOH 0.3% H ₂ SO ₄	100	0.34	45 min	[142]
	Chemical		HCl		15.61		[145]
	Chemical/microwave		H ₂ SO ₄ /EtOH & HCOOH/CH ₃ COOH	107/161	58.7	3 h	[147]
	Coffee residue; Sugarcane bagasse	Chemical/autoclave	NaOH 4%	120	40.6	20 min	[156]
Lignin	Orange peel	Chemical	KOH 3–8%	90	–	1 h	[157]
	Oil palm residue	Chemical	NaOH, NaClO ₂	121	71.1	0.5 h	[158]
	Banana residue	Chemical	KOH 5%, NaClO ₂ 1%	60	71.51	24 min	[159]
		Chemical/micro-wave/mechanical	Distilled water/H ₂ O ₂ 5%	70	64.67	0.5 h	[160]
	Sugarcane bagasse	Chemical/reactor	NaOH 4%; H ₂ O ₂	200	–	0.5 h	[162]

waste; and some of the best options for waste treatment are the production of biodiesel, bioethanol, and bio-chemicals. Some strategies adopted for the fruit waste treatment were shown in this chapter, and cite reuse of the waste as biomass, which can bring a gain in energy recovery, and diminish or sometimes avoid, disposal of organic waste. When dealing with different types of fruit waste, it is very important to analyze and evaluate their chemical composition, to propose ecologically correct, viable, cost-effective ways to produce cleaner commodities that pollute less. For example, we have summarised processes that are used for bioethanol, biodiesel, and some commodities, such as, pectin, lignin, cellulose, or bioactives - essential oil, other lipids, flavones.

Fruit waste biomasses explored in two continents (Europe, and South America), and obtained in different climates, were discussed. The case studies were selected and disclosed because of the two factors: (1) the climates found in Serbia, which is continental, and Brazil, tropical, can be found in many other countries, therefore, typical fruits for such climates are omnipresent in the World, as well, (2) the fruit waste reuse and recycling shown for the top four fruit residues are applicable for any other fruit waste. It was shown that fruit seeds can be a great option for biodiesel production, but other lipids and fine chemicals can be obtained from such biomass. If rich in sugars and easily hydrolyzable polysaccharides, waste can be used for bioethanol production. On the other hand, biopolymers, such as pectin, lignin, cellulose, and others, some not covered herein, can be isolated, purified, and obtained in processes that explore extraction and are very interesting options for biomass utilization. Other appealing alternatives count on fine chemical production from waste, such as bioflavonoids isolated and purified from citrus waste that can be further explored as pharmaceuticals and nutraceuticals. Anyway, the future processes must take into account those value-added products that can be produced from the same starting material - fruit waste, and propose a cleaner, low-cost scale-up of many, still concepts that prove laboratory-scale, options for sequential treatment of fruit waste. It could be seen that many different strategies can be employed for fruit waste treatments, and many are adaptable for different purposes and types of waste. Different types of new residues are being produced in described processes, yet there is scarce data on what should be done to their treatment and/or disposal.

Acknowledgments This work was financially supported by Republic of Serbia - Ministry of Education, Science and Technological Development, Program for financing scientific research work, number 451-03-9/2021-14/200133 (assigned to the Faculty of Technology, Leskovac, University of Niš, researchers' group III 45001). We acknowledge grant #5417 from FUNCAMP, foundation that supports University of Campinas, and INCTBio (grants #2014/50867-3 from FAPESP, and #465389/2014-7 from CNPq).

References

1. Mak TMW, Xiong X, Tsang DCW, Yu IKM, Poon CS. Sustainable food waste management towards circular bioeconomy: policy review, limitations and opportunities. *Biores Techn.* 2020;297:122497. <https://doi.org/10.1016/j.biortech.2019.122497>.
2. Zuin VG, Segatto ML, Zanotti K. Toward a green and sustainable fruit waste valorisation model in Brazil: optimisation of homogenizer-assisted extraction of bioactive compounds from mango waste using a response surface methodology. *Pure Appl Chem.* 2020;92(4): 617–29. <https://doi.org/10.1515/pac-2019-1001>.
3. Mirabella N, Castellani V, Sala S. Current options for the valorization of food manufacturing waste: a review. *J Clean Prod.* 2014;65:28–41. <https://doi.org/10.1016/j.jclepro.2013.10.051>.
4. Stenmarck Å, Jensen C, Quested T, Moates G. Estimates of European food waste levels fusions reducing food waste through social innovation. Stockholm: IVL Swedish Environmental Research Institute; 2016.
5. Henz GP, Porpino G. Food losses and waste: How Brazil is facing this global challenge? *Hortic Bras.* 2017;35:472–82. <https://doi.org/10.1590/S0102-053620170402>.
6. van der Velden R, da Fonseca-Zang W, Zang J, Clyde-Smith D, Leandro WM, Parikh P, Borron A, Campos AC. Closed-loop organic waste management systems for family farmers in Brazil. *Environ Technol.* 2021;11:1–18. <https://doi.org/10.1080/09593330.2021.1871660>.
7. FAOSTAT. 2019. Altendorf, S. 2019. Major tropical fruits market review 2018. Rome, FAO. <http://www.fao.org/publications/card/en/c/CA5692EN>; Top 20 Commodities Production in Brazil. http://www.fao.org/faostat/en/#rankings/commodities_by_country. Accessed 19 July 2021
8. Mahato N, Sharma K, Sinha M, Dhyani A, Pathak B, Jang H, Park S, Pashikanti S, Cho S. Biotransformation of citrus waste-I: production of biofuel and valuable compounds by fermentation. *Process.* 2021;9:220. <https://doi.org/10.3390/pr9020220>.
9. Grohmann K, Baldwin EA, Buslig BS. Production of ethanol from enzymatically hydrolyzed orange peel by the yeast *Saccharomyces cerevisiae*. *App Biochem Biotech.* 1994;45(46): 315–27. <https://doi.org/10.1007/BF02941808>.
10. Grohmann K, Cameron RG, Buslig BS. Fermentation of sugars in orange peel hydrolysates to ethanol by recombinant *Escherichia coli* K011. *Appl Biochem Biotechnol.* 1995;51(52): 423–35. <https://doi.org/10.1007/BF02941717>.
11. Wilkins MR, Widmer WW, Grohmann K. Simultaneous saccharification and fermentation of citrus peel waste by *Saccharomyces cerevisiae* to produce ethanol. *Process Biochem.* 2007;42: 1614–9. <https://doi.org/10.1016/j.procbio.2007.09.006>.
12. FAOSTAT. 2019. Top 20 Commodities Production in Serbia. http://www.fao.org/faostat/en/#rankings/commodities_by_country; Country Report on the State of Plant Genetic Resources for Food and Agriculture. Republic of Serbia. <http://www.fao.org/3/i1500e/Serbia.pdf>. Accessed 19 July 2021
13. Bhushan S, Kalia K, Sharma M, Singh B, Ahuja PS. Processing of apple pomace for bioactive molecules. *Crit Rev Biotechnol.* 2008;28:285–96. <https://doi.org/10.1080/07388550802368895>.
14. Dhillon GS, Kaur S, Brar SK. Perspective of apple processing wastes as low-cost substrates for bioproduction of high value products: a review. *Renew Sustain Energy Rev.* 2013;27:789–805. <https://doi.org/10.1016/j.rser.2013.06.046>.
15. Hang YD, Walter RH. Treatment and utilization of apple-processing wastes. In: Processed apple products. New York: Springer; 1989.
16. Kumar D, Surya K, Verma R. Bioethanol production from apple pomace using co-cultures with *Saccharomyces cerevisiae* in solid-state fermentation. *J Microbiol Biotechnol Food Sci.* 2020;9:742–5. <https://doi.org/10.15414/jmbfs.2020.9.4.742-745>.
17. Hang YD, Lee CY, Woodams EE. A solid state fermentation system for production of ethanol from apple pomace. *J Food Sci.* 1982;47:1851–2. <https://doi.org/10.1007/BF00933494>.

18. Parmar I, Rupasinghe HPV. Bio-conversion of apple pomace into ethanol and acetic acid: Enzymatic hydrolysis and fermentation. *Bioresour Technol.* 2013;130:613–20. <https://doi.org/10.1016/j.biortech.2012.12.084>.
19. Pathania S, Sharma N, Handa S. Immobilization of co-culture of *Saccharomyces cerevisiae* and *Scheffersomyces stipitis* in sodium alginate for bioethanol production using hydrolysate of apple pomace under separate hydrolysis and fermentation. *Biocatal Biotransform.* 2017;35: 450–9. <https://doi.org/10.1080/10242422.2017.1368497>.
20. Molinuevo-Salces B, Riaño B, Hijosa-Valsero M, González-García I, Paniagua-García AI, Hernández D, Garita-Cambronero J, Díez-Antolínez R, García-González MC. Valorization of apple pomaces for biofuel production: a biorefinery approach. *Biomass Bioenergy.* 2020;142: 105785. <https://doi.org/10.1016/j.biombioe.2020.105785>.
21. Demiray E, Kut A, Ertuğrul Karatay S, Dönmez G. Usage of soluble soy protein on enzymatically hydrolysis of apple pomace for cost-efficient bioethanol production. *Fuel.* 2021;289: 119785. <https://doi.org/10.1016/j.fuel.2020.119785>.
22. Ucuncu C, Tari C, Demir H, Buyukkileci AO, Ozen B. Dilute-acid hydrolysis of apple, orange, apricot, and peach pomaces as potential candidates for bioethanol production. *J Biobased Mater Bioenergy.* 2013;7:376–89. <https://doi.org/10.1166/jbmb.2013.1361>.
23. Evcan E, Tari C. Production of bioethanol from apple pomace by using cocultures: conversion of agro-industrial waste to value added product. *Energy.* 2015;88:775–82. <https://doi.org/10.1016/j.energy.2015.05.090>.
24. Kaiser D, Bertau M. Enzymatic hydrolysis and fermentation of apple pomace. *Chemie Ing Tech.* 2020;92:1772–9. <https://doi.org/10.1002/cite.202000139>.
25. Kut A, Demiray E, Ertuğrul Karatay S, Dönmez G. Second generation bioethanol production from hemicellulolytic hydrolysate of apple pomace by *Pichia stipitis*. *Energ Source Part A.* 2020; <https://doi.org/10.1080/15567036.2020.1838000>.
26. Ngadi MO, Correia LR. Kinetics of solid-state ethanol fermentation from apple pomace. *J Food Eng.* 1992;17:97–116. [https://doi.org/10.1016/0260-8774\(92\)90055-B](https://doi.org/10.1016/0260-8774(92)90055-B).
27. Joshi VK, Sandhu DK. Preparation and evaluation of an animal feed byproduct produced by solid-state fermentation of apple pomace. *Bioresour Technol.* 1996;56:251–25510. [https://doi.org/10.1016/0960-8524\(96\)00040-5](https://doi.org/10.1016/0960-8524(96)00040-5).
28. Chatanta D, Attri C, Gopal K, Devi M, Gupta G, Bhalla T. Bioethanol production from apple pomace left after juice extraction. *Internet J Microbiol.* 2007;5:1–5. <https://doi.org/10.5580/3a8>.
29. Górnáś P, Rudzińska M, Soliven A. Industrial by-products of plum *Prunus domestica* L. and *Prunus cerasifera* Ehrh. as potential biodiesel feedstock: impact of variety. *Ind Crops Prod.* 2017;100:77–84. <https://doi.org/10.1016/j.indcrop.2017.02.014>.
30. Minar MMH. Studies on non-traditional oils: I. Detailed studies on different lipid profiles of some *Rosaceae* kernel oils. *Grasas Aceites.* 1999;50:379–84. <https://doi.org/10.3989/gya.1999>.
31. Kamel BS, Kakuda Y. Characterization of the seed oil and meal from apricot, cherry, nectarine, peach and plum. *J Am Oil Chem Soc.* 1992;69:492–4. <https://doi.org/10.1007/BF02540957>.
32. Kostić MD, Veličković AV, Joković NM, Stamenković OS, Veljković VB. Optimization and kinetic modeling of esterification of the oil obtained from waste plum stones as a pretreatment step in biodiesel production. *Waste Manag.* 2016;48:619–29. <https://doi.org/10.1016/j.wasman.2015.11.052>.
33. Kiralan M, Kayahan M, Kiralan SS, Ramadan MF. Effect of thermal and photo oxidation on the stability of cold-pressed plum and apricot kernel oils. *Eur Food Res Technol.* 2018;244: 31–42. <https://doi.org/10.1007/s00217-017-2932-0>.
34. Treviño-Cordero H, Juárez-Aguilar LG, Mendoza-Castillo DI, Hernández-Montoya V, Bonilla-Petriciolet A, Montes-Morán MA. Synthesis and adsorption properties of activated carbons from biomass of *Prunus domestica* and *Jacaranda mimosifolia* for the removal of

- heavy metals and dyes from water. *Ind Crops Prod.* 2013;42:315–23. <https://doi.org/10.1016/j.indcrop.2012.05.029>.
- 35. Nowicki P, Skrzypczak M, Pietrzak R. Effect of activation method on the physicochemical properties and NO₂ removal abilities of sorbents obtained from plum stones (*Prunus domestica*). *Chem Eng J.* 2010;162:723–9. <https://doi.org/10.1016/j.cej.2010.06.040>.
 - 36. Islam MN, Joardder MUH, Hoque SMN, Uddin MS. A comparative study on pyrolysis for liquid oil from different biomass solid wastes. *Procedia Eng.* 2013;56:643–9. <https://doi.org/10.1016/j.proeng.2013.03.172>.
 - 37. Górnáš P, Mišina I, Grāvīte I, Lācis G, Radenkovs V, Olšteine A, Segliņa D, Kaufmane E, Rubauskis E. Composition of tocochromanols in the kernels recovered from plum pits: the impact of the varieties and species on the potential utility value for industrial application. *Eur Food Res Technol.* 2015;241:513–20. <https://doi.org/10.1007/s00217-015-2480-4>.
 - 38. González-García E, Marina ML, García MC. Plum (*Prunus Domestica* L.) by-product as a new and cheap source of bioactive peptides: extraction method and peptides characterization. *J Funct Foods.* 2014;11:428–37. <https://doi.org/10.1016/j.jff.2014.10.020>.
 - 39. Popa VM, Bele C, Poiana MA, Dumbrava D, Raba DN, Jianu C. Evaluation of bioactive compounds and of antioxidant properties in some oils obtained from food industry by-products. *Romanian Biotechnol Lett.* 2011;16:6234–41. <https://doi.org/10.25083/rbl.2011.6234>.
 - 40. Górnáš P, Rudzińska M. Seeds recovered from industry by-products of nine fruit species with a high potential utility as a source of unconventional oil for biodiesel and cosmetic and pharmaceutical sectors. *Ind Crops Prod.* 2016;83:329–38. <https://doi.org/10.1016/j.indcrop.2016.01.021>.
 - 41. Spigno G, Marinoni L, Garrido GD. State of the art in grape processing by-products. In: *Handbook of grape processing by-products: sustainable solutions*. 1st ed. Amsterdam: Elsevier Academic Press; 2017.
 - 42. Cerón-García MC, Macías-Sánchez MD, Sánchez-Miróna A, García-Camacho F, Molina-Grima E. A process for biodiesel production involving the heterotrophic fermentation of *Chlorella protothecoides* with glycerol as the carbon source. *Appl Energy.* 2013;103:341–9. <https://doi.org/10.1016/j.apenergy.2012.09.054>.
 - 43. Van Dyk JS, Gama R, Morrison D, Swart S, Pletschke BI. Food processing waste: problems, current management and prospects for utilisation of the lignocellulose component through enzyme synergistic degradation. *Renew Sustain Energy Rev.* 2013;26:521–31. <https://doi.org/10.1016/j.rser.2013.06.016>.
 - 44. Mendes JAS, Prozil SO, Evtuguin DV, Lopes LPC. Towards comprehensive utilization of winemaking residues: Characterization of grape skins from red grape pomaces of variety Touriga Nacional. *Ind Crops Prod.* 2013;43:25–32. <https://doi.org/10.1016/j.indcrop.2012.06.047>.
 - 45. Mamma D, Topakas E, Vafiadi C, Christakopoulos P. Biotechnological potential of fruit processing industry residues. In: *Biotechnology for agro-industrial residues utilisation: utilisation of agro-residues*. Amsterdam: Springer; 2009.
 - 46. Howell CL, Myburgh PA. Management of winery wastewater by re-using it for crop irrigation - a review. *S Afr J Enol Vitic.* 2018;39:116–31. <https://doi.org/10.21548/39-2-3171>.
 - 47. Dávila I, Robles E, Egüés I, Labidi J, Gullón P. The biorefinery concept for the industrial valorization of grape processing by-products. In: *Handbook of grape processing by-products: sustainable solutions*. London: Elsevier Academic Press; 2017.
 - 48. Sarno M, Iuliano M. Enzymatic production of biodiesel from grapeseed oil. *Chem Eng Trans.* 2020;80:301–6. <https://doi.org/10.1021/ef500131s>.
 - 49. Zheng Y, Lee C, Yu C, Cheng YS, Simmons CW, Zhang R, Jenkins BM, Vandergheynst JS. Ensilage and bioconversion of grape pomace into fuel ethanol. *J Agric Food Chem.* 2012;60:11128–34. <https://doi.org/10.1021/jf303509v>.
 - 50. Egüés I, Serrano L, Amendola D, De Faveri DM, Spigno G, Labidi J. Fermentable sugars recovery from grape stalks for bioethanol production. *Renew Energy.* 2013;60:553–8. <https://doi.org/10.1016/j.renene.2013.06.006>.

51. Spigno G, Moncalvo A, De Faveri DM, Silva A. Valorisation of stalks from different grape cultivars for sugars recovery. *Chem Eng Trans.* 2014;37:745–50. <https://doi.org/10.3390/chemengineering2010007>.
52. Mendes JAS, Xavier AMRB, Evtuguin DV, Lopes LPC. Integrated utilization of grape skins from white grape pomaces. *Ind Crops Prod.* 2013;49:286–91. <https://doi.org/10.1016/j.indcrop.2013.05.003>.
53. Williams DL, Schückel J, Vivier MA, Buffetto F, Zietsman AJJ. Grape pomace fermentation and cell wall degradation by *Kluyveromyces marxianus* Y885. *Biochem Eng J.* 2019;150: 107282. <https://doi.org/10.1016/j.bej.2019.107282>.
54. Corbin KR, Hsieh YSY, Betts NS, Byrt CS, Henderson M, Stork J, DeBolt S, Fincher GB, Burton RA. Grape marc as a source of carbohydrates for bioethanol: chemical composition, pre-treatment and saccharification. *Bioresour Technol.* 2015;193:76–83. <https://doi.org/10.1016/j.biortech.2015.06.030>.
55. Rodríguez LA, Toro ME, Vazquez F, Correa-Daneri ML, Gouiric SC, Vallejo MD. Bioethanol production from grape and sugar beet pomaces by solid-state fermentation. *Int J Hydrogen Energy.* 2010;35:5914–7. <https://doi.org/10.1016/j.ijhydene.2009.12.112>.
56. Hang YD, Lee CY, Woodams EE. Solid-state fermentation of grape pomace for ethanol production. *Biotechnol Lett.* 1986;8:53–6. <https://doi.org/10.1007/BF01044402>.
57. Bilal A, Vivek Y, Ashish Y, Mati UR, Wang ZY, Zhi L, Xiping W. Integrated biorefinery approach to valorize winery waste: a review from waste to energy perspectives. *Sci Total Environ.* 2020;719:137315. <https://doi.org/10.1016/j.scitotenv.2020.137315>.
58. Kavargiris SE, Mamolos AP, Tsatsarelis CA, Nikolaidou AE, Kalburutji KL. Energy resources utilization in organic and conventional vineyards: energy flow, greenhouse gas emissions and biofuel production. *Biomass Bioenergy.* 2009;33:1239–50. <https://doi.org/10.1016/j.biombioe.2009.05.006>.
59. Iodice P, Langella G, Amoresano A. Ethanol in gasoline fuel blends: effect on fuel consumption and engine out emissions of SI engines in cold operating conditions. *Appl Therm Eng.* 2018;130:1081–9. <https://doi.org/10.3390/en14134034>.
60. Dabetic NM, Todorovic VM, Djuricic ID, Antic Stankovic JA, Basic ZN, Vujovic DS, Sobajic SS. Grape seed oil characterization: a novel approach for oil quality assessment. *Eur J Lipid Sci Technol.* 2020;122:1–10. <https://doi.org/10.1002/ejlt.201900447>.
61. Martin ME, Grao-Cruces E, Millan-Linares MC, Montserrat-De la Paz S. Grape (*Vitis vinifera* L.) seed oil: a functional food from the winemaking industry. *Foods.* 2020;9:1–20. <https://doi.org/10.3390/foods9101360>.
62. Bolonio D, García-Martínez MJ, Ortega MF, Lapuerta M, Rodríguez-Fernández J, Canoira L. Fatty acid ethyl esters (FAEEs) obtained from grapeseed oil: a fully renewable biofuel. *Renew Energy.* 2019;132:278–83. <https://doi.org/10.1016/j.renene.2018.08.010>.
63. Donoso D, Bolonio D, Lapuerta M, Canoira L. Oxidation stability: the bottleneck for the development of a fully renewable biofuel from wine industry waste. *ACS Omega.* 2020;5: 16645–53. <https://doi.org/10.1021/acsomega.0c01496>.
64. Fernández CM, Ramos MJ, Pérez Á, Rodríguez JF. Production of biodiesel from winery waste: extraction, refining and transesterification of grape seed oil. *Bioresour Technol.* 2010;101:7019–24. <https://doi.org/10.1016/j.biortech.2010.04.014>.
65. Ramos MJ, Fernández CM, Casas A, Rodríguez L, Pérez Á. Influence of fatty acid composition of raw materials on biodiesel properties. *Bioresour Technol.* 2009;100:261–8. <https://doi.org/10.1016/j.biortech.2008.06.039>.
66. Hariram V, Bose A, Seralathan S. Dataset on optimized biodiesel production from seeds of *Vitis vinifera* using ANN, RSM and ANFIS. *Data Br.* 2019;25:104298. <https://doi.org/10.1016/j.dib.2019.104298>.
67. Singh G, Mohapatra SK, Ragit S, Kundu K. Optimization of biodiesel production from grape seed oil using Taguchi's orthogonal array. *Energy Sour Part A Rec Util Environ Eff.* 2018;40: 2144–53. <https://doi.org/10.1080/15567036.2018.1495778>.

68. Jarret RL, Levy IJ. Oil and fatty acid contents in seed of *Citrullus lanatus* Schrad. J Agric Food Chem. 2012;60:5199–204. <https://doi.org/10.1021/jf300046f>.
69. Ratnakaram VN, Prakasa Rao CG, Sree S. Simultaneous saccharification and fermentation of watermelon waste for ethanol production. In: Emerging technologies for agriculture and environment, lecture notes on multidisciplinary industrial engineering. Singapore: Springer; 2020.
70. Watermelon, raw Nutrition Facts & Calories. <https://nutritiondata.self.com/facts/fruits-and-fruit-juices/2072/2>. Accessed 18 Feb 2021
71. Fish WW, Bruton BD, Russo VM. Watermelon juice: A promising feedstock supplement, diluent, and nitrogen supplement for ethanol biofuel production. Biotechnol Biofuels. 2009;2: 18. <https://doi.org/10.1186/1754-6834-2-18>.
72. Alex S, Saira A, Nair DS, Soni K, Sreekantan L, Rajmohan K, Reghunath B. Bioethanol production from watermelon rind by fermentation using *Saccharomyces cerevisiae* and *Zymomonas mobilis*. Indian J Biotechnol. 2017;16:663–6. <http://nopr.niscair.res.in/handle/123456789/44362>
73. Chaudhary A, Akram AM, Ahmad Q-U-A, Minahal Q, Ara C, Andleeb S, Iqtedar M, Ali Q. RSM-Based fermentative ethanologenic employing acid hydrolyzate watermelon peels. Plant Cell Biotechnol Mol Biol. 2020;29:63–77. <https://www.ikppress.org/index.php/PCBMB/article/view/5667>
74. Borja R, Fernández-Rodríguez MJ. Energy recovery as added value from food and agricultural solid wastes. In: Current developments in biotechnology and bioengineering - strategic perspectives in solid waste and wastewater management. Amsterdam: Elsevier; 2021.
75. Jahanbakhshi A, Salehi R. Processing watermelon waste using *Saccharomyces cerevisiae* yeast and the fermentation method for bioethanol production. J Food Process Eng. 2019;42: e13283. <https://doi.org/10.1111/jfpe.13283>.
76. Ünal MÜ, Chowdhury G, Şener A. Effect of temperature and nitrogen supplementation on bioethanol production from waste bread, watermelon and muskmelon by *Saccharomyces cerevisiae*. Biofuels. 2020; <https://doi.org/10.1080/17597269.2020.1724440>.
77. Rueda OD, Angulo A, Mafla E, Bangeppagari M, Rueda BB, Gangireddygari VS, Naga RM, Bugude R. Comparative study of native microorganisms isolated from watermelon (*Citrullus lanatus*) waste and commercial microorganism (*Clostridium thermocellum*) used for bioethanol production. Afr J Biotechnol. 2017;16:380–7. <https://doi.org/10.5897/AJB2016.15643>.
78. Muhammad BY, Mariah AN, Bin OJ, Yahya A, Bashar ZU. Egusi melon (*Citrullus lanatus*) crop - Malaysian new oil/energy source: production, processing and prospects. Aust J Crop Sci. 2013;7:2101–7. <https://doi.org/10.3316/informit.801257585594331>.
79. Oluba O, Ogunlowo Y, Ojieh G, Adebiyi KE. Physicochemical properties and fatty acids composition of Egusi seeds. J Biol Sci. 2008;8:814–7. <https://doi.org/10.7324/JAPS.2015.50309>.
80. Sani UM. Phytochemical screening and antidiabetic effect of extracts of the seeds of *Citrullus lanatus* in alloxan-induced diabetic albino mice. J Appl Pharm Sci. 2015;5:51–4.
81. Tabiri B. Watermelon seeds as food: nutrient composition, phytochemicals and antioxidant activity. Int J Nutr Food Sci. 2016;5:139. <https://doi.org/10.11648/J.IJNFS.20160502.18>.
82. Duduyemi O, Adebajo SA, Kehinde O. Extraction and determination of physico-chemical properties of watermelon seed oil (*Citrullus Lanatus* L) for relevant uses. Int J Sci Technol Res. 2013;2:66–8. [https://doi.org/10.5402/2012/621518\(2012\)](https://doi.org/10.5402/2012/621518(2012)).
83. Efavi JK, Kanbogtah D, Apalangya V, Nyankson E, Tiburu EK, Dodoo-Arhin D, Onwona-Agyeman B, Yaya A. The effect of NaOH catalyst concentration and extraction time on the yield and properties of *Citrullus vulgaris* seed oil as a potential biodiesel feed stock. S Afr J Chem Eng. 2018;25:98–102. <https://doi.org/10.1016/j.jpecs.2017.03.002>.
84. Baboli ZM, Safe Kordi AA. Characteristics and composition of watermelon seed oil and solvent extraction parameters effects. J Am Oil Chem Soc. 2010;87:667–71. <https://doi.org/10.1007/s11746-010-1546-5>.

85. Dumitru MG, Tutunea D. Extraction and determination of physico-chemical properties of oil from watermelon seeds (*Citrullus lanatus* L) to use in internal combustion engines. Rev Chim. 2017;68:2676–81. <https://doi.org/10.37358/RC.17.11.5952>.
86. Milovanovic M, Picuric-Jovanovic K. Characteristics and composition of melon seed oil. J Agric Sci Belgrade. 2005;50:41–7. <https://doi.org/10.2298/JAS0501041M>.
87. Elsheikh YA, Man Z, Bustam MA, Akhtar FH, Yusup S, Muhammad A. Preparation and characterisation of *Citrulus colocynthis* oil biodiesel: Optimisation of alkali-catalysed transesterification. Can J Chem Eng. 2014;92:435–40. <https://doi.org/10.1002/cje.21846>.
88. Rao YR, Varala R, Reddy JN, Santhoshi PS, Kondhare D, Deshmukh S, Zubaidha PK. Evaluation of watermelon seed oil as an alternative feedstock for the production of biodiesel in the presence of crystalline manganese carbonate. Int J Altern Fuels. 2013;14: 378–81. <https://doi.org/10.12817/18.2013.14.12.27702205>.
89. Elsheikh YA. Optimization of novel pyrazolium ionic liquid catalysts for transesterification of bitter apple oil. Process Saf Environ Prot. 2014;92:828–34. <https://doi.org/10.1007/s11356-020-09054-y>.
90. Elsheikh YA. Preparation of *Citrullus colocynthis* biodiesel via dual-step catalyzed process using functionalized imidazolium and pyrazolium ionic liquids for esterification step. Ind Crops Prod. 2013;49:822–9. <https://doi.org/10.1016/j.indcrop.2013.06.041>.
91. Elsheikh YA, Akhtar FH, Muhammad A. Kinetics of *Citrulus colocynthis* oil transesterification. J Chem Soc Pak. 2014;36:243–9. <https://doi.org/10.1155/2014/540765>.
92. Ali Elsheikh Y, Hassan Akhtar F. Biodiesel from citrullus colocynthis oil: Sulfonic-ionic liquid-catalyzed esterification of a two-step process. Sci World J. 2014;2014:540765. <https://doi.org/10.1155/2014/540765>.
93. Giwa S, Abdullah LC, Adam NM. Investigating “egusi” (*Citrullus colocynthis* L.) seed oil as potential biodiesel feedstock. Energies. 2010;3:607–18. <https://doi.org/10.3390/en3040607>.
94. Giwa SO, Chuah LA, Adam NM. Fuel properties and rheological behavior of biodiesel from egusi (*Cocoynthis citrullus* L.) seed kernel oil. Fuel Process Technol. 2014;122:42–8. <https://doi.org/10.1016/j.fuproc.2014.01.014>.
95. Orbih A, Obahiagbon K, Amenaghawon N. Production of biodiesel from watermelon seed (*Citrullus lanatus*) oil via alkali catalysed transesterification. Niger Res J Eng Environ Sci. 2019;4:593–603. <https://doi.org/10.11648/j.jeece.20200502.11>.
96. Xavier J. Performance and emission characteristics of diesel engine using watermelon seed oil methyl ester. J Biol Sci. 2020;20:88–93. <https://doi.org/10.3923/jbs.2020.88.93>.
97. Chavan SB, Kumbhar RR, Sharma YC. Transesterification of *Citrullus colocynthis* (Thumba) oil: optimization for biodiesel production. Adv Appl Sci Res. 2014;5:10–20. <https://www.imedpub.com/abstract/transesterification-of-citrullus-colocynthis-thumba-oiloptimization-for-biodiesel-production-14158.html>
98. Zema DA, Calabró PS, Folino A, Tamburino V, Zappia G, Zimbone SM. Valorisation of citrus processing waste: a review. Waste Manag. 2018;80:252–73. <https://doi.org/10.1016/j.wasman.2018.09.024>.
99. Awan AT, Tsukamoto J, Tasic L. Orange waste as a biomass for 2G-ethanol production using low cost enzymes and co-culture fermentation. RSC Adv. 2013;3:25071–8. <https://doi.org/10.1039/C3RA43722A>.
100. Stanisic D, Liu LHB, dos Santos RV, Costa AF, Durán N, Tasic L. New sustainable process for hesperidin isolation and anti-ageing effects of hesperidin nanocrystals. Molecules. 2020;25:4534. <https://doi.org/10.3390/molecules25194534>.
101. Tasic L, Mandic B, Barros CHN, Cypriano DZ, Stanisic D, Schultz LG, Silva LL, Mariño MAM, Queiroz VL. Exploring bioactivity of hesperidin, naturally occurring flavanone glycoside, isolated from the oranges. In: Citrus fruits: production, consumption and health benefits. 1st ed. New York: Nova Scientific; 2016.
102. Tsukamoto J, Durán N, Tasic L. Nanocellulose and bioethanol production from orange waste using isolated microorganisms. J Braz Chem Soc. 2013;24:1537–43. <https://doi.org/10.5935/0103-5053.20130195>.

103. Arora A, Banerjee J, Vijayaraghavan R, MacFarlane D, Patti AF. Process design and techno-economic analysis of an integrated mango processing waste biorefinery. *Ind Crops Prod.* 2018;116:24–34. <https://doi.org/10.1016/j.indcrop.2018.02.061>.
104. Jahurul MHA, Zaidul ISM, Norulaini NAN, Sahena F, Abedin MZ, Mohamed A, Mohd Omar AK. Hard cocoa butter replacers from mango seed fat and palm stearin. *Food Chem.* 2014;154: 323–9. <https://doi.org/10.1016/j.foodchem.2013.11.098>.
105. Wu M, Kashiwagi A, Henmi A, Okada Y, Tachibana S, Nomura M. Evaluation of the fatty acid composition of the seeds of *Mangifera indica* L. and their application. *J Oleo Sci.* 2015;64: 479. <https://doi.org/10.5650/jos.ess14238>.
106. Liang M, Su X, Yang Z, Deng H, Yang Z, Liang R, Huang J. Carotenoid composition and expression of carotenogenic genes in the peel and pulp of commercial mango fruit cultivars. *Sci Hortic.* 2020;263:109072. <https://doi.org/10.3390/app11094249>.
107. Lago S, Rodríguez H, Arce A, Soto A. Improved concentration of citrus essential oil by solvent extraction with acetate ionic liquids. *Fluid Phase Equilibria.* 2014;361:37–44. <https://doi.org/10.1016/j.fluid.2013.10.036>.
108. Zhang QW, Lin LG, Ye WC. Techniques for extraction and isolation of natural products: a comprehensive review. *Chin Med.* 2018;13:20. <https://doi.org/10.1186/s13020-018-0177-x>.
109. Battista F, Remelli G, Zanzoni S, Bolzonella D. Valorization of residual orange peels: limonene recovery, volatile fatty acids, and biogas production. *ACS Sustainable Chem Eng.* 2020;8:6834–43. <https://doi.org/10.1021/acssuschemeng.0c01735>.
110. Hilali S, Fabiano-Tixier AS, Ruiz K, Hejjaj A, Nouh FA, Idlimam A, Bily A, Mandi L, Chemat F. Green extraction of essential oils, polyphenols, and pectins from orange peel employing solar energy: toward a zero-waste biorefinery. *ACS Sustainable Chem Eng.* 2019;7:11815–22. <https://doi.org/10.1021/acssuschemeng.9b02281>.
111. Jokić S, Molnar M, Cikoš AM, Jakovljević M, Šafranko S, Jerković I. Separation of selected bioactive compounds from orange peel using the sequence of supercritical CO₂ extraction and ultrasound solvent extraction: optimization of limonene and hesperidin content. *Sep Sci Technol.* 2019;55:2799–811. <https://doi.org/10.1080/01496395.2019.1647245>.
112. Nisar N, Li L, Lu S, Khin NC, Pogson BJ. Carotenoid metabolism in plants. *Mol Plant.* 2015;8:68–82. <https://doi.org/10.1016/j.molp.2014.12.007>.
113. Lizárraga-Velázquez CE, Leyva-López N, Hernández C, Gutiérrez-Grijalva EP, Salazar-Leyva JA, Osuna-Ruiz I, Martínez-Montaña E, Arrizon J, Guerrero A, Benítez-Herández A, Ávalos-Soriano A. Antioxidant molecules from plant waste: extraction techniques and biological properties. *Processes.* 2020;8:1566. <https://doi.org/10.3390/pr8121566>.
114. Boukroufa M, Boutekedjiret C, Chemat F. Development of a green procedure of citrus fruits waste processing to recover carotenoids. *Resour Effic Technol.* 2017;3:252–62. <https://doi.org/10.1016/j.reffit.2017.08.007>.
115. Baria B, Upadhyay N, Singh AK, Malhotra RK. Optimization of ‘green’ extraction of carotenoids from mango pulp using split plot design and its characterization. *LWT.* 2019;104:186–94. <https://doi.org/10.1016/j.lwt.2019.01.044>.
116. Colantuono A, Ferracane R, Vitaglione P. In vitro bioaccessibility and functional properties of polyphenols from pomegranate peels and pomegranate peels-enriched cookies. *Food Funct.* 2016;7:4247–58. <https://doi.org/10.1039/c6fo00942e>.
117. Fia G, Bucalossi G, Gori C, Borghini F, Zanoni B. Recovery of bioactive compounds from unripe red grapes (cv. Sangiovese) through a green extraction. *Foods.* 2020;9:566. <https://doi.org/10.3390/foods9050566>.
118. Ikan R. Isolation of hesperidin from orange peels. In: Natural products: a laboratory guide. 2nd ed. San Diego, CA: Academic Press; 1991.
119. Dugo G, Di Giacomo A. Citrus: the genus citrus. 1st ed. London: Taylor & Francis; 2002.
120. Londoño-Londoño J, Rodrigues de Lima V, Lara O, Gil L, Crecsynski Pasa TB, Arango GJ, Ramirez Pineda J. Clean recovery of antioxidant flavonoids from citrus peel: optimizing an aqueous ultrasound-assisted extraction method. *Food Chem.* 2010;119:81–7. <https://doi.org/10.1016/j.foodchem.2009.05.075>.

121. M'hiri N, Ioannou I, Mihoubi Boudhriou N, Ghoul M. Effect of different operating conditions on the extraction of phenolic compounds in orange peel. *Food Bioprod Process.* 2015;96:161–70. <https://doi.org/10.1016/j.fbp.2015.07.010>.
122. Cao D, Liu Q, Jing W, Tian H, Yan H, Bi W, Jiang Y, Chen DDY. Insight into the deep eutectic solvent extraction mechanism of flavonoids from natural plants. *ACS Sustainable Chem Eng.* 2019;8:19169–77. <https://doi.org/10.1021/acssuschemeng.0c08146>.
123. Xu M, Ran L, Chen N, Fan X, Ren D, Yi L. Polarity-dependent extraction of flavonoids from citrus peel waste using a tailor-made deep eutectic solvent. *Food Chem.* 2019;297:124970. <https://doi.org/10.1016/j.foodchem.2019.124970>.
124. El Kantar S, Rajha HN, Bousselata N, Vorobiev E, Maroun RG, Louka N. Green extraction of polyphenols from grapefruit peels using high voltage electrical discharges, deep eutectic solvents and aqueous glycerol. *Food Chem.* 2019;295:165–71. <https://doi.org/10.1016/j.foodchem.2019.05.111>.
125. Liu Y, Zhang H, Yu H, Guo H, Chen D. Deep eutectic solvent as a green solvent for enhanced extraction of narirutin, naringin, hesperidin and neohesperidin from *Aurantii Fructus*. *Phytochem Anal.* 2018;30:156–63. <https://doi.org/10.1002/pca.2801>.
126. Altunay N, Elik A, Unal Y, Kaya S. Optimization of an ultrasound-assisted alcohol-based deep eutectic solvent dispersive liquid-phase microextraction for separation and preconcentration of quercetin in wine and food samples with response surface methodology. *J Separat Sci.* 2021;44:1998–2005. <https://doi.org/10.1002/jssc.202100048>.
127. Hosseini SS, Khodaiyan F, Yarmand MS. Aqueous extraction of pectin from sour orange peel and its preliminary physicochemical properties. *Int J Biol Macromol.* 2016;82:920–6. <https://doi.org/10.1016/j.ijbiomac.2015.11.007>.
128. Tamaki Y, Konishi T, Tako M. Isolation and characterization of pectin from peel of *Citrus tankan*. *Biosci Biotechnol Biochem.* 2008;72(3):896–9. <https://doi.org/10.1271/bbb.70706>.
129. Marić M, Grassino AN, Zhu Z, Barba FJ, Brnčić M, Brnčić SR. An overview of the traditional and innovative approaches for pectin extraction from plant food wastes and by-products: Ultrasound-, microwaves-, and enzyme-assisted extraction. *Trends Food Sci Technol.* 2018;76:28–37. <https://doi.org/10.1016/j.tifs.2018.03.022>.
130. Mao G, Wu D, Wei C, Tao W, Ye X, Linhardt RJ, Orfila C, Chen S. Reconsidering conventional and innovative methods for pectin extraction from fruit and vegetable waste: Targeting rhamnogalacturonan I. *Trends Food Sci Technol.* 2019;94:65–78. <https://doi.org/10.1016/j.tifs.2019.11.001>.
131. Albuquerque PBS, Coelho LCBB, Teixeira JA, Carneiro-da-Cunha MG. Approaches in biotechnological applications of natural polymers. *AIMS Mol Sci.* 2016;3:386–425. <https://doi.org/10.3934/molsci.2016.3.386>.
132. Rinaudo M. Main properties and current applications of some polysaccharides as biomaterials. *Polym Int.* 2008;57:397–430. <https://doi.org/10.1002/pi.2378>.
133. Ma S, Yu S, Zheng X, Wang X, Bao Q, Guo X. Extraction, characterization and spontaneous emulsifying properties of pectin from sugar beet pulp. *Carbohydrate Polymers.* 2013;98:750–3. <https://doi.org/10.1016/j.carbpol.2013.06.042>.
134. Yeoh S, Shi J, Langrish TAG. Comparisons between different techniques for water-based extraction of pectin from orange peels. *Desalination.* 2008;218:229–37. <https://doi.org/10.1016/j.desal.2007.02.018>.
135. Kaya M, Sousa AG, Crépeau MJ, Sørensen SO, Ralet MC. Characterization of citrus pectin samples extracted under different conditions: influence of acid type and pH of extraction. *Ann Bot.* 2014;114:1319–26. <https://doi.org/10.1093/aob/mcu150>.
136. Saberian H, Hamidi-Esfahani Z, Gavighi HA, Barzegar M. Optimization of pectin extraction from orange juice waste assisted by ohmic heating. *Chem Eng Process.* 2017;117:154–61. <https://doi.org/10.1016/j.cep.2017.03.025>.
137. Patience NA, Schieppati D, Boffito DC. Continuous and pulsed ultrasound pectin extraction from novel orange peels. *Ultrason Sonochem.* 2021;73:105480. <https://doi.org/10.1016/j.ultsonch.2021.105480>.

138. Jin Y, Yang N. Array-induced voltages assisted extraction of pectin from grapefruit (*Citrus paradisi* Macf.) peel and its characterization. *Int J Biol Macromol.* 2020;152:1205–12. <https://doi.org/10.1016/j.ijbiomac.2019.10.215>.
139. Xu Y, Zhang L, Bailina Y, Ge Z, Ding T, Ye X, Liu D. Effects of ultrasound and/or heating on the extraction of pectin from grapefruit peel. *J Food Eng.* 2014;126:72–81. <https://doi.org/10.1016/j.jfoodeng.2013.11.004>.
140. You Q, Wan M, Fang X, Yin X, Luo C, Zhang X. Optimisation of intermittent microwave extraction method for the determination of pectin from pomelo peels. *Mater Res Express.* 2019;6:065405. <https://doi.org/10.18697/ajfand.90.17940>.
141. Constant S, Wienk HLJ, Frissen AE, de Peinder P, Boelens R, van Es DS, Grisel RJH, Weckhuysen BM, Huijgen WJJ, Gosselink RJA, Bruijnincx PCA. New insights into the structure and composition of technical lignins: A comparative characterization study. *Green Chem.* 2016;18:2651–65. <https://doi.org/10.1039/C5GC03043A>.
142. Barros CHN, Stanisic D, Morais BF, Tasic L. Soda lignin from *Citrus sinensis* bagasse: extraction, NMR characterization and application in bio-based synthesis of silver nanoparticles. *Energy Ecol Environ.* 2018;1:1–8. <https://doi.org/10.1007/s40974-017-0078-3>.
143. Azadi P, Inderwildi OR, Farnood R, King DA. Liquids fuels, hydrogen and chemicals from lignin: a critical review. *Renew Sust Energy Rev.* 2013;21:506–23. <https://doi.org/10.1016/j.rser.2012.12.022>.
144. Rajesh Banu J, Kavitha S, Yukesh Kannah R, Poornima Devi T, Gunasekaran M, Kim SH, Kumar G. A review on biopolymer production via lignin valorisation. *Bioresour Technol.* 2019;290:121790. <https://doi.org/10.1016/j.biortech.2019.121790>.
145. Hidayati S, Satyajaya W, Fudholi A. Lignin isolation from black liquor from oil palm empty fruit bunch using acid. *J Mater Res Technol.* 2020;9:11381–91. <https://doi.org/10.1016/j.jmrt.2020.08.023>.
146. Lobato-Peralta DR, Duque-Brito E, Villafán-Vidales HI, Longoria A, Sebastian PJ, Cuentas-Gallegos AK, Arancibia-Bulnes CA, Okoye PU. A review on trends in lignin extraction and valorization of lignocellulosic biomass for energy applications. *J Clean Prod.* 2021;293: 126123. <https://doi.org/10.1016/j.jclepro.2021.126123>.
147. Florian TDM, Villani N, Aguedo M, Jacquet N, Thomas HG, Gerin P, Magali D, Richel A. Chemical composition analysis and structural features of banana rachis lignin extracted by two organosolv methods. *Ind Crop Prod.* 2019;132:269–74. <https://doi.org/10.1016/j.indcrop.2019.02.022>.
148. Mariño MAM, Silva LL, Durán N, Tasic L. Enhanced materials from nature: Nanocellulose from citrus waste. *Molecules.* 2015;20:5908–23. <https://doi.org/10.3390/molecules20045908>.
149. Trache D, Tarchoun AF, Derradji M, Hamidon TS, Masruchin N, Brosse N, Hussin MH. Nanocellulose: from fundamentals to advanced applications. *Front Chem.* 2020;8:392. <https://doi.org/10.3389/fchem.2020.00392>.
150. Kargarzadeh H, Ahmad I, Thomas S, Dufresne A. Handbook of nanocellulose and cellulose nanocomposites. Weinheim: John Wiley & Sons; 2017.
151. Dufresne A. Nanocellulose: a new ageless bionanomaterial. *Mater Today.* 2013;16:220–7. <https://doi.org/10.1016/j.matod.2013.06.004>.
152. Mariño MA, Rezende CA, Tasic L. A multistep mild process for preparation of nanocellulose from orange bagasse. *Cellulose.* 2018;25:5739–50. <https://doi.org/10.1007/s10570-018-1977-y>.
153. Cypriano DZ, da Silva LL, Tasic L. High value-added products from the orange juice industry waste. *Waste Management.* 2018;79:71–8. <https://doi.org/10.1016/j.wasman.2018.07.028>.
154. Rajinipriya M, Nagalakshmaiah M, Robert M, Elkoun S. Importance of agricultural and industrial waste in the field of nanocellulose and recent industrial developments of wood based nanocellulose: a review. *ACS Sustain Chem Eng.* 2018;6:2807–28. <https://doi.org/10.1021/acssuschemeng.7b03437>.

155. Xie H, Du H, Yang X, Si C. Recent strategies in preparation of cellulose nanocrystals and cellulose nanofibrils derived from raw cellulose materials. *Int J Polym Sci.* 2018;2018:7923068. <https://doi.org/10.1155/2018/7923068>.
156. Marinó MA, Cypriano D, Tasic L (2021) Agroindustry residues as a source for cellulose nanofibers production. *J Braz Chem Soc* 32:878–888 doi: 10.21577/0103-5053.20200239
157. Chen W, Li Q, Cao J, Liu Y, Li J, Zhang J, Luo S, Yu H. Revealing the structures of cellulose nanofiber bundles obtained by mechanical nanofibrillation via TEM observation. *Carbohydrate Polymers.* 2015;117:950–6. <https://doi.org/10.1016/j.carbpol.2014.10.024>.
158. Mantovan J, Giraldo GAG, Marim BM, Kishima JOF, Mali S. Valorization of orange bagasse through one-step physical and chemical combined processes to obtain a cellulose rich material. *J Sci Food Agric.* 2020;101:2362–70. <https://doi.org/10.1002/jsfa.10859>.
159. Tibolla H, Pelissari FM, Martins JT, Vicente AA, Menegalli FC. Cellulose nanofibers produced from banana peel by chemical and mechanical treatments: characterization and cytotoxicity assessment. *Food Hydrocolloids.* 2018;75:192–201. <https://doi.org/10.1016/j.foodhyd.2017.08.027>.
160. Harini K, Ramya K, Sukumar M. Extraction of nanocellulose fibers from the banana peel and bract for production of acetyl and lauroyl cellulose. *Carbohydr Polym.* 2018;201:329–229. <https://doi.org/10.1016/j.carbpol.2018.08.081>.
161. da Silva GF, Mathias SL, de Menezes AJ, Vicente JGP, Delforno TP, Varesche MBA, Duarte ICS. Orange bagasse pellets as a carbon source for biobutanol production. *Curr Microbiol.* 2020;77:4053–62. <https://doi.org/10.1007/s00284-020-02245-3>.
162. Feng YH, Cheng TY, Yang WG, Ma PT, He HZ, Yin XC, Yu XX. Characteristics and environmentally friendly extraction of cellulose nanofibrils from sugarcane bagasse. *Ind Crop Prod.* 2018;111:285–91. <https://doi.org/10.1016/j.indcrop.2017.10.041>.

Chapter 14

Sustainable Recycling and Valorization of Organic Solid Wastes for Fuels and Fertilizers



Lijun Wang, Bahare Salehi, and Bo Zhang

Abstract Recycle and valorization of organic solid wastes can produce fuels, fertilizers and reduce their disposal costs and negative environmental impacts. Municipal solid wastes (MSW) are traditionally dumped in landfills and some MSW components are incinerated to reduce their landfilling volume and recover part of their energy. Composting is widely used to convert biodegradable wastes such as animal manure and food wastes into a compost as a fertilizer. Those traditional technologies have low energy recovery efficiency and low reduction of negative environmental impacts of the wastes due to leachate and emissions generated during those processes. Pyrolysis, gasification, anaerobic digestion (AD) are three advanced technologies with higher recovery efficiencies of energy and materials, and lower environmental emissions that are widely studied to convert organic solid wastes into energy and fertilizer products. However, more studies are needed to improve the economics and environmental impact of those advanced processes by increasing conversion efficiency and the quality of the products, and minimize the negative impacts of hazardous materials in the wastes. Various methods and nanomaterials have been studied to improve the process conversion efficiency and environmental sustainability, and the quality of products for recycling and valorizing various wastes.

Keywords Municipal solid wastes · Agricultural wastes · Circular economy · Environmental sustainability · Anaerobic digestion · Pyrolysis · Gasification · Incineration · Composting

L. Wang (✉) · B. Zhang

Department of Natural Resources and Environmental Design, North Carolina Agricultural and Technical State University, Greensboro, NC, USA
e-mail: lwang@ncat.edu

B. Salehi

Department of Nanoengineering, North Carolina Agricultural and Technical State University, Greensboro, NC, USA

14.1 Introduction

Global population growth is increasing society's dependence on fossil fuels which causes many environmental issues such as global warming, air and water pollution, and the depletion of these resources. Therefore, there is an increasing demand for sustainable clean energy resources [1]. On the other hand, population growth increases production of industrial, municipal, and agricultural wastes which must be treated and managed due to their associated issues of disposal cost and land use, human and ecological health, and soil, water, and air pollution. Solid wastes can be categorized as biodegradable (bio-wastes) and non-biodegradable wastes [2]. Bio-wastes include manure, crop residues, forest residues, food wastes, and a large portion of municipal solid waste (MSW). The large variation in the physical and chemical properties of solid wastes affects their valorization and profit [2].

Waste management generally follows three principles including (1) identification and evaluation of waste types and quantities, (2) reduction of waste production and (3) reuse and recycle of wastes into value-added products [3]. Waste characteristics such as content of water, biodegradable organic compounds, carbohydrates, and lipids, heating value, particle size, and potential contaminants affect the selection of waste management methods. The water content of wastes plays a key role in the selection of a management approach. Wet wastes such as animal manure are more suitable for biochemical conversion techniques such as anaerobic digestion (AD), composting, and fermentation, whereas the dry wastes are more suitable for thermochemical processes such as incineration, pyrolysis, and gasification. As the water content of wastes can also affect handling and transportation costs, those wastes may have to be treated onsite at a specific scale corresponding to the available amount of the wastes. Furthermore, some technologies can only be used to treat a specific type of wastes. Fermentation and transesterification require wastes with high carbohydrate content and high lipid content, respectively [4]. The main challenges in waste management include minimization of emissions, recovery of fertilizer nutrients, production of high-quality products and closed material recycling loop with free wastes [2]. The wastes can be considered as secondary raw materials to produce industrial products, compared to non-renewable sources [5, 6]. This chapter reviews advantages and disadvantages of waste management technologies in terms of waste reduction, stabilization, material recycling, energy recycling, and GHG reduction. We also discuss methods and nanomaterials that have been studied to improve process conversion efficiency and environmental sustainability, and the quality of products for recycling and valorizing different wastes using three advanced technologies, namely, pyrolysis, gasification, and anaerobic digestion.

14.2 Organic Solid Wastes

MSW and agricultural wastes are two major sources of organic solid wastes that have been used for the production of fuels and fertilizers. It is estimated that global agricultural waste production is more than four and a half times that of MSW. On average, each person around the world generates 3.35 kg of agricultural wastes per day, compared with 0.74 kg of MSW per day. Agricultural wastes are usually managed separately from MSW and a large portion of agricultural wastes are used as inputs for agricultural production activities [7].

14.2.1 Municipal Solid Waste

MSW consists of all organic and non-organic refuses including wet wastes such as kitchen wastes, food wastes, crop straws, garden trimmings and sawdust, and dry wastes such as glass, plastics, metals and ash [8]. Figure 14.1 shows the amounts of MSW generated by region around the world in 2016 [7]. The total annual amount of MSW is estimated to reach 2.2 billion tons globally by 2025 [9]. The quantity and quality of MSW generated depend on the economical, demographic, educational and social status of a region [10, 11]. The United States produced about 258 million tons in 2014 [8, 9]. China collected 191 million tons of MSW in 2015 [12].

The composition of MSW is affected by geographic locations, the areas of collection (such as rural, urban, industrial or commercial areas), seasons, and

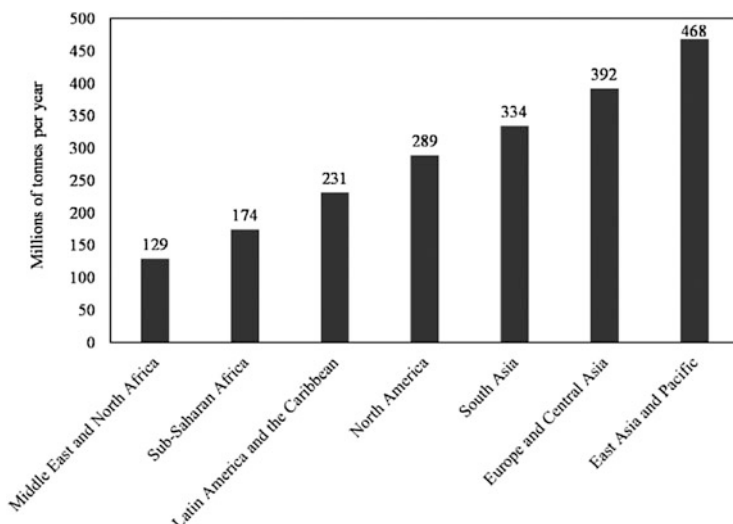


Fig. 14.1 Global municipal solid waste (MSW) generation by region in 2016, reprinted with permission from reference [7]. Copyright @ 2018, The World Bank

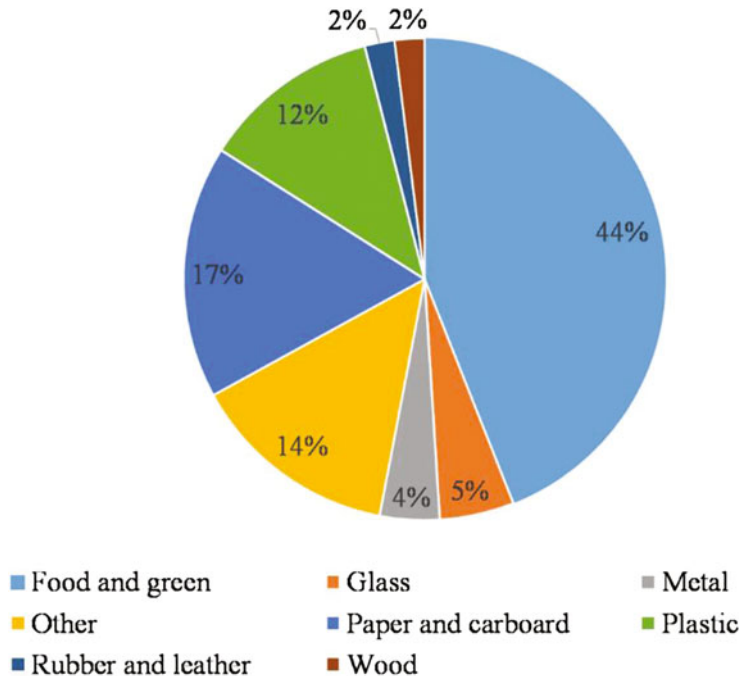


Fig. 14.2 Global municipal solid waste (MSW) composition, reprinted with permission from reference [7]. Copyright @ 2018, The World Bank

recycling levels [13, 14]. Figure 14.2 shows the average composition of MSW around the world. On average, food and green wastes makes up 44% and dry recyclables including plastics, paper, cardboard, metal, and glass are another 38%. MSW around the world contains 70% to 80% organic compounds on average including 44% food and green wastes, 2% wood, 17% paper and cardboard, 12% plastics, and 2% rubber and leather [7]. MSW in China consists of 58.8% food and green waste, 8.5% paper, 12% plastic and rubber, 3.2% fabric and leather, 5% glass, 4.6% metal, 3.9% ceramic, and 7.9% ash. MSW in Europe consists of 32% food and green waste, 29% paper and board, 8% plastics, 11% glass, 5% metals, 2% textile and 13% other materials [8]. MSW in the USA contains 27% paper, 15% food wastes, 14% yard trimmings, 13% plastics, 9% leather, rubber and textiles, 9% metals, 6% wood waste, 4% glass and 3% of other materials [12].

MSW usually contains a large amount of moisture due to the presence of food and yard wastes. Improper management and treatment of MSW may produce large amounts of leachates containing toxic materials like heavy metals, odors and greenhouse gases causing pollution of soil, water and air [10, 15]. Furthermore, high moisture content and low energy content of MSW result in a low energy recovery rate if the MSW is used as a feedstock in thermochemical conversion processes such as incineration [12]. Large portions of MSW such as food wastes are easily biodegradable and converted to landfill gas (LFG) in a landfill [12]. Besides

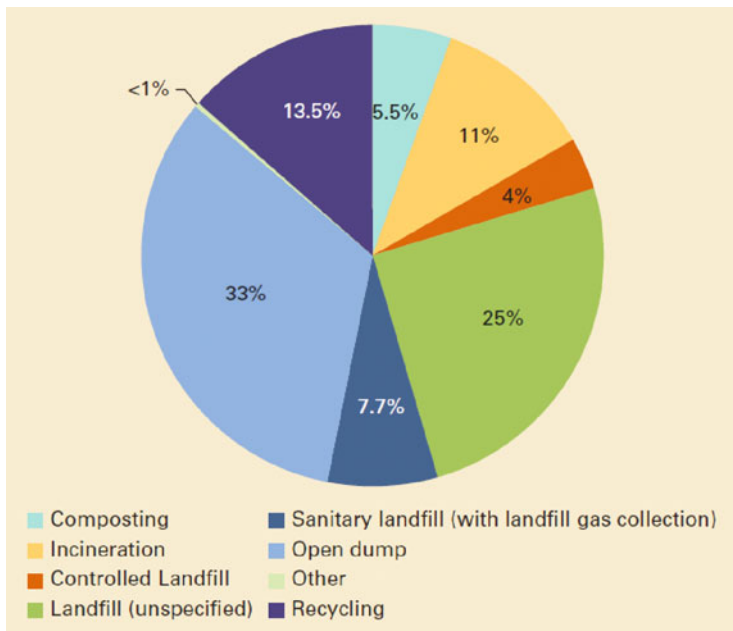


Fig. 14.3 Global municipal solid waste (MSW) treatment and disposal, reprinted with permission from reference [7]. Copyright @ 2018, The World Bank

the negative environmental impact, improper MSW management results in a loss of resources [16]. Appropriate MSW classification and treatment can minimize the negative environmental impact of MSW, but also convert MSW into energy and other value-added products to reduce the use of fossil-based fuels and products. It is recommended to classify raw MSW as an available resource. Different countries have different waste classification methods. Both environmental and economic factors should be considered in the MSW classification [17]. MSW is commonly classified into three groups including i) biodegradable fraction of food waste and green waste, ii) high calorific value components (HCVCs) of plastic, fabric, and paper, and iii) residual fraction of metal, glass, ceramic, and ash. Biological processes such as AD can be used to convert the biodegradable fraction of MSW while the HCVCs can be treated by thermochemical processes such as incineration and pyrolysis to achieve high conversion efficiency [12].

Figure 14.3. shows the current global MSW treatment and disposal methods. Almost 40% of MSW around the world is disposed of in landfills including controlled landfills, sanitary landfills, and other unspecified landfills and another 33% of MSW is dumped in open fields. Only 13.5%, 5.5%, and 11% of MSW undergo recycling, composting, and incineration [7]. Among the 258 million tons of MSW generated in the USA in 2014, 34.6 wt % was recycled and composted, and 12.8 wt % was combusted with energy recovery, and more than 50 wt% was landfilled [8, 9]. A dominant portion or 63.7% of the 191 million tons of MSW collected in

China in 2015 was landfilled, another 34.3% was incinerated, and 2% was treated in biological processes [12].

14.2.2 Agricultural Wastes

Agricultural production has increased more than three times over the last 50 years due to accelerated growth of population. Agriculture produces an average of 23.7 million tons of foods worldwide each day. Agricultural production generates large amounts of organic wastes including animal manure, crop residues, and food processing wastes. Agriculture is responsible for 21% of greenhouse gases emissions [18].

Animal manure. Rapid population growth has increased the demand for animal products [19], which has resulted in the production of large quantities of animal wastes. The estimated amount of animal manure produced in 12 major livestock-producing countries is 9 billion tons each year. In the USA, the amount of manure produced by top three livestock animals, cattle, pigs, and chickens were 1166, 91, and 164 million tons per year, respectively [20]. The amount of manure produced in Canada was estimated at 51 million tons that consisted of 49.181 million tons of water and 2.589 million tons of solid materials including 1.761 million tons of organic matter, 143,000 tons of nitrogen, 46,000 tons of phosphorous, 93,000 tons of potassium, and 545,000 tons of other solids [21]. As shown in Table 14.1 and Table 14.2, there are large variations in quantities and composition for different types of animal manure due to variations in the physiology and anatomy of different animals, body weight, diets, and geographical locations [22, 23].

Animal wastes endanger environment, human health, and animal health due to the potential presence of microbial flora and pathogens. Furthermore, landfilling of those wastes causes gaseous and leachate emissions [19]. The decomposition of organic wastes generates unpleasant odors and releases chemical pollutants into the atmosphere. Moreover, the direct use of extra amounts of animal manure as a fertilizer can accumulate fertilizer nutrients in soil, which leach into surface water and ground-water [19]. However, animal manure can be used to produce value-added products such as (i) fertilizer and soil conditioner, (ii) biofuels and biopower, and (iii) irrigation water [21].

Crop residues. Crop residues are another type of abundant waste from agricultural production. The estimated annual production of crop residues around the world

Table 14.1 Daily feces and urine production for several kinds of livestock. Reprinted with permission from reference [22]. Copyright @ 2018, Elsevier

	Beef cattle	Dairy cows	Fattening pigs	Layers	Broilers
Solid (kg/head/day)	13.28	29.70	1.29	0.132	0.139
Slurry (kg/head/day)	8.52	14.07	2.93	—	—
Total (kg/head/day)	21.80	42.77	4.22	0.132	0.139

Table 14.2 Average elemental composition of fresh manure. Reprinted with permission from reference [23]. Copyright @ 2015, Elsevier

Compositions		Type of manure				
		Pig	Dairy	Beef	Layers	Broiler
Proximate analysis (%)	Moisture content	71.99	75.59	75.66	72.26	63.88
	Volatile matter	66.12	60.60	64.58	62.56	62.47
	Fixed carbon	10.54	11.73	13.73	6.48	10.45
	Ash	24.18	28.20	22.64	32.44	27.76
Ultimate analysis (%)	C	37.74	34.42	37.64	33.02	33.62
	H	5.62	4.91	5.26	4.81	5.06
	O	28.90	30.44	31.90	25.74	30.75
	N	2.79	1.92	2.16	3.39	3.70
	S	0.63	0.65	0.59	0.81	0.89
Mineral element (g/kg)	P	19.86	6.00	6.07	12.83	11.07
	K	15.35	9.39	12.04	23.86	23.35
	Na	2.56	2.29	3.33	3.08	3.90
	Ca	18.44	16.01	12.40	45.17	23.46
	Mg	12.08	8.59	6.54	10.47	7.88
	Fe	3.61	4.04	3.23	2.95	3.68
	Cu	0.66	0.066	0.056	0.082	0.088
	Zn	1.39	0.16	0.13	0.35	0.32

was about 3.8 billion tons in 2011 [24, 25]. About 111 million dry tons of primary crop residues are generated in the USA each year with more than 76% of them being corn stover, and the remaining 24% being wheat and other grains (USDOE, 2011). A number of studies have shown that the sustainable removal rate of crop residues varies between 30% and 70% [26]. The total amount of biomass available for sustainable removal in 25 EU member countries in 2020 was estimated to be 235 million tons including 39 million tons from forestry, 96 million tons from agriculture, and 100 million tons from other wastes [27, 28]. Crop residues are usually burnt or used as animal feed [29]. Crop residues have been considered as an important global renewable resource of biomass for biofuel production [24].

Food processing wastes. It is estimated that more than 50% of food materials, or globally over 1.3 billion tons of foods per year for human consumption, are wasted before and after reaching the customer. Food waste is a complex of lipids, carbohydrates, amino acids, phosphates, vitamins and carbonaceous and can be divided into organic crop residues, catering waste and derivatives including used cooking oils, animal by-products, and mixed domestic food waste. In contrast to other types of waste streams, food wastes undergo biological degradation during handling, resulting in decreased nutrient and energy recovery potential and increased pollutant emissions. Therefore, food wastes are more affected by local conditions and process timing than other types of wastes [30].

Agricultural wastes cause environmental pollution, public health issues, and loss of valuable resources. Sustainable and intensive agricultural production demands

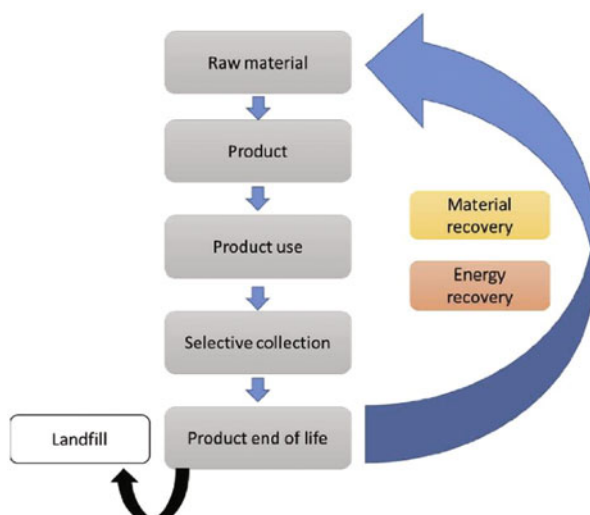
sustainable management of agricultural wastes. Animal manure is typically applied to soil as a fertilizer. However, traditional manure management increases global climate change due to emission of methane and nitrous oxides. Runoff of N and P in manure can impair ground and surface water [20]. Innovative conversion technologies for the valorization of agricultural wastes are crucial in the circular economy for transition to sustainable agriculture [31]. Agricultural wastes have been considered as main feedstocks for production of biofuels and biochemicals [32, 33]. AD is an effective technology for converting manure and other wet agricultural wastes to biogas (a gaseous mixture of CH₄ and CO₂) as an alternative to natural gas and digestate as organic fertilizers [34]. Thermochemical technologies of pyrolysis and gasification have been studied to convert dry agricultural wastes into heat, power and biofuels [33, 35].

14.3 Recycle and Valorization of Organic Solid Wastes for Circular Economy and Environmental Sustainability

14.3.1 Circular Economy and Environmental Sustainability Via Recycling and Valorizing Wastes

Conversion of wastes to energy is a typical way to solve two problems at once, reducing fossil fuel consumption and disposing of the wastes [36]. Conversion of waste materials into a wide range of valuable products such as foods, feeds, bioproducts and bioenergy provides both economic and environmental benefits

Fig. 14.4 Schematic view of circular economy (CE). Reprinted with permission from reference [5]. Copyright @ 2019, Elsevier



[37, 38]. From the economic viewpoint, it can change the linear economy into a circular economy (CE) by closing the loop of economic value chains as shown in Fig. 14.4, which can save resources and promote environmental sustainability [5].

Reusing or recycling waste materials extends their usability by creating new products in a sustainable manner [5, 39]. It is estimated that the transformation to a circular economy can bring net savings around EUR 600 billion to the manufacturing sector in the EU. Valorization of wastes to energy and products not only decreases the dependency on fossil fuels, but also protects the environment by decreasing GHG emission and consequent climate change, and the land used for the disposal of wastes [36, 37]. Implementation of integrated waste management strategies to reduce the amount of wastes treated by conventional technologies such as landfilling and incineration can significantly reduce their GWP and other negative environmental impacts. Waste management is significantly affected by the technological development, socio-economic and environmental factors. A waste management plan should take into account all environmental, economic and social factors for selecting the most appropriate waste practice in a region. The main criteria for selection of the waste treatment method are long-term sustainability, eco-friendliness, economics and efficiency. In addition, the volume of final residues which still impose an extra burden on the environment and their potential use such as construction materials must be considered [40].

Nitrogen (N), phosphorus (P) and potassium (K) are primary macronutrients that are vital to support plant growth. The increase in world population sharply increased demand for fertilizers that are needed to secure the supply of foods. P and K fertilizers are achieved via mining phosphate rock reservoirs and potash reserves. N fertilizer is chemically produced through a Haber-Bosch process. Although N is considered as a renewable nutrient element in air, the Haber-Bosch process consumes a significant amount of energy for nitrogen fixation, which is around 1–2% of world's total energy consumption [38]. With the current mining rate of phosphorus, P reserves may be exhausted in near future. Potassium is a nutrient element with finite reserves in the earth. Besides recovery of energy from wastes, fertilizer nutrients of N, P, and K can be recovered from the waste streams with significant amounts of N, P, and K such as food wastes, manure, and sewage [5]. There are significant amounts of NPK in organic solid wastes that can be recovered and reused as fertilizers in a sustainable and economic manner. Approximately, 15% and 19% of agricultural nitrogen inputs end up in wastewater and animal manure, respectively, which make them to be good sources for nitrogen recovery. MSW and agricultural wastes contained about 15% and 40% of total mined phosphorus, which make them to be good sources for phosphorus recovery. More than 90% of potassium in agricultural production ends up in animal wastes. These macronutrient elements can be present in the wastes in various forms. For example, P is in the form of free phosphate, polyphosphate, ATP, DNA/RNA and phospholipids. K can be in the form of free potassium ion, while N can be in the form of ammonia/ammonium, nitrate/nitrite, amino acids, DNA/RNA and chlorophyll, respectively [38].

14.3.2 Traditional Technologies for Treatment of Organic Solid Wastes

Landfilling, composting, and incineration are three major commercial technologies for treatment of organic solid wastes. Landfilling and composting are biological processes that decompose organic wastes in the absence and in the presence of air, respectively. Landfilling produces methane-rich landfill gas (LFG), which can be recovered as an energy product. Composting converts biodegradable wastes into a compost as a fertilizer. Incineration is a thermochemical process to burn organic wastes to generate heat and power.

Landfilling. Landfilling is the primary method for MSW management around the world. In Europe, 23% of the MSW was landfilled in 2017 [41]. Figure 14.5 shows a schematic view for landfilling with and without landfill gas (LFG) energy recovery [12]. Landfilling performance is evaluated by LFG collection and oxidation efficiency at the surface of a landfill over time. In a well-controlled sanitary landfill, LFG collection efficiency increases from 40% of the total amount of LFG produced in the first year to around 80% in years 2–25 following initial establishment. Surface oxidation increases from 15% of the LFG produced in years 1–9 to 20% of the LFG produced after 10 years. LFG can be recovered to generate electricity at an energy

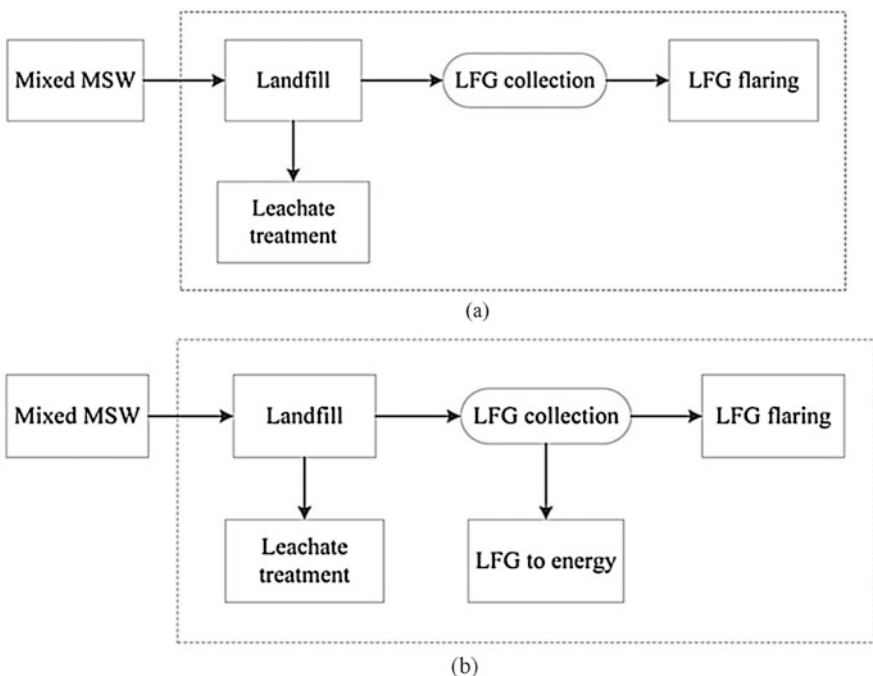


Fig. 14.5 Schematic view of landfilling wastes. Reprinted with permission from reference [12]. Copyright @ 2017, Elsevier

recovery rate up to 30% or 2234 MJ LFG energy per ton of MSW with a higher heating value of 6216 MJ/t. However, the amount of LFG energy that can be recovered from MSW with high content of food wastes and moisture content is significantly lower [12]. Therefore, as LFG collection efficiency is usually low, landfilling is not an efficient approach to reduce the GWP of MSW, particularly for wastes having high moisture content. Operation of a landfill consumes energy. It has been reported that it requires about 66 MJ diesel energy and 54 MJ electricity to treat the leachate from each ton of MSW in a landfill [12].

Incineration. Direct burning or incineration is an ancient method to treat organic solid wastes [42]. Incineration converts dry organic materials into gaseous oxides by exposing them to high-temperatures which produces heat and ash. Incineration is the most widespread waste-to-energy technology used around the world [43]. Half of MSW was incinerated in China in 2020 [12] and an average of 29% of MSW was incinerated in Europe in 2017 [44]. During incineration, almost all organic materials in the wastes are transformed into gaseous oxides such as CO₂ and only a small portion of mineral elements remains in the ash [42]. As the ashes from the incineration of MSW contains heavy metals and dioxins, they are considered as hazardous wastes and are usually disposed of in special landfills [43]. The ash from the incineration of agricultural wastes contains recoverable P and K, which can be used in fertilizers [38]. Incineration can significantly reduce the volume of wastes and destroy any pathogenic organisms. Grate-fired furnaces are widely used to incinerate MSW [43]. For example, it has been reported that incineration of one ton of MSW with an average moisture content of 32.5% produced 20.1 kg of fly ash and 181.6 kg of bottom ash and the overall thermal efficiency of a boiler connected to an incineration furnace was 81.2% [12]. Heat in the flue gas from incineration can be used to dry MSW to further increase the overall energy recovery efficiency [30].

Composting. Composting is an aerobic digestion process to transform organic solid wastes into a compost in the presence of oxygen through oxidation of long-chain organic materials to short-chain products by aerobic microbes, while producing a mixture of gases including CO₂, NH₃ and a small amount of methane [38]. Properly prepared composts normally have 11–14% water content, 90% dry matter, and a C/N ratio of 15–30, which can be affected by the type of feedstocks and composting time. During composting, microorganisms generate heat, which not only promotes physical degradation, but also deactivates plant pathogens and weed seeds present in the wastes. The produced composts have higher pH and lower electrical conductivity than the original wastes due to the removal of volatile organic acids and salts [42]. Aerobic digestion during composting can reduce around 50–75% of the biodegradable compounds in wastes. The generated heat and air injection during composting increase water vaporization and volatilization.

14.3.3 Advanced Technologies for Valorization of Organic Solid Wastes

Both advanced thermochemical processes such as pyrolysis and gasification, and biological processes such as AD have been studied to convert organic solid wastes to fuels and fertilizers. Pyrolysis and gasification, which are alternative thermochemical processes to conventional incineration, can convert organic wastes to chemicals and fuels by reducing the amounts of nitrogen oxides and sulfur oxides emitted to the atmosphere. Furthermore, the solid residue of biochar produced by pyrolysis and gasification is more valuable than the ash from incineration. AD is an alternative biological process for converting biodegradable wastes into biogas as a fuel and digestate as a fertilizer.

Pyrolysis. Pyrolysis is a non-oxidative thermochemical process for decomposing organic materials in the absence of oxygen or in an atmosphere of inert gas at an elevated temperature [8, 38]. Pyrolysis produces three main products: non-condensable syngas, liquid oil, and solid char [38] with yields that depend on the type of feedstock and the operating parameters of temperature, heating rate, and residence time [8, 45, 46]. The main economic advantage of pyrolysis over incineration is that pyrolysis produces high-quality products of oil, syngas and char instead of heat [46]. Pyrolysis is operated at lower temperatures than incineration [8] and is typically conducted at (500 to 550) °C for producing oil as the main product as higher temperatures increase the yield of syngas. In pyrolysis, the residence time varies between few seconds to 2 h. The increase of residence time can increase syngas yield due to tar cracking, and improve the oil quality by reducing its water content and waxy compounds. High heating rates used in flash or fast pyrolysis can increase oil and gas yields and decrease char yield [46]. Pyrolysis is the main approach for producing char with almost all inorganic compounds in the original waste and a considerable fraction of heavy oil compounds dispersed through the solid porous structure. Biochar can be used as a solid fuel, because it has a heating value close to that of coal. Biochar can be upgraded into activated carbon. Biochar contains significant amounts of carbon, nitrogen, phosphorus and potassium, which can be used as fertilizers and soil conditioners by increasing nutrient and water retention in soil, and supporting microorganisms [38].

Gasification. Gasification is the partial oxidation of feedstocks in the presence of an oxidant such as air or pure oxygen at amounts lower than those needed for stoichiometric combustion [47, 48]. Air, pure oxygen, steam and carbon dioxide have been used as gasifying agents that can facilitate the conversion of carbonaceous compounds into gases through endothermic and exothermic reactions [49]. The required heat during gasification can be supplied by oxidation reactions if air or pure oxygen is used as the gasifying agent. However, external supply of heat is required if steam or carbon dioxide is used as the gasifying agent [49]. As shown in Fig. 14.6, gasification can convert the carbonaceous compounds in wastes into the main product of syngas which can be further utilized for power generation or synthesis of various fuels and chemicals [49].

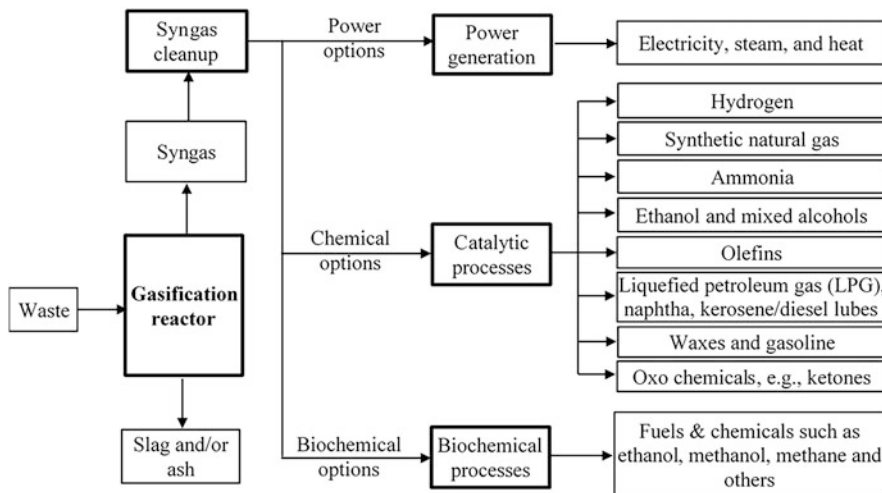


Fig. 14.6 Conversion of waste materials to energy via gasification. Reprinted with permission from reference [49]. Copyright @ 2018, IntechOpen

It has been reported that the electricity efficiency based on gasification is above 27% which is higher than incineration efficiency of 15–20% [9]. Gasification occurs at much higher temperatures (*ca.* 1000 °C) than pyrolysis (*ca.* 500 °C) [48, 50]. During gasification, nitrogen-containing compounds in the wastes are transformed into a volatile phase and inorganic phosphorus and potassium can be recovered from the ash [38]. The main economic benefit of gasification of organic wastes is that it can convert wastes into syngas for on-site electricity and heat generation, and subsequent synthesis of chemicals and fuels [49]. Gasification can also significantly reduce the volume of wastes (up to 90% reduction) to minimize land requirements and costs for waste disposal. Like pyrolysis, gasification can achieve much higher conversion rates and efficiencies than biochemical methods, decompose organic contaminations such as halogenated hydrocarbons, destroy any pathogens, concentrate inorganic elements in ash, and significantly reduce GHG emissions compared with landfilling.

Anaerobic digestion. AD is the degradation of organic materials (Fig. 14.7) by microorganisms in the absence of oxygen for the purpose of producing biogas, which is a mixture of mainly CH₄ and CO₂ as an energy product and digestate residues as a fertilizer product or soil amendment [42, 51]. AD of agricultural wastes can decrease dependency on chemical fertilizers and fossil energy in the agricultural industry [52].

Biogas contains 60–70% methane with the balance being 30–40% carbon dioxide and is the main product of AD. Besides production of biogas, AD can significantly reduce the volume of wastes, transform organic nitrogen-containing compounds into a recoverable form, and produce digestate with concentrated NH₄⁺ and K⁺ species that can be recovered as fertilizers [38, 47]. The destination of phosphorus in AD is significantly affected by other chemicals such as calcium, magnesium, and iron

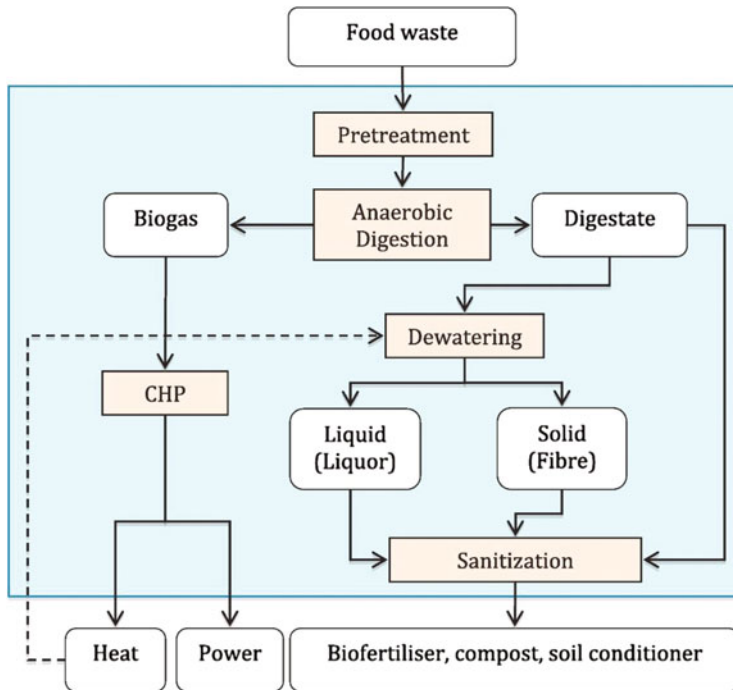


Fig. 14.7 Schematic diagram of anaerobic digestion (AD) process. Reprinted with permission from reference [42]. Copyright @ 2018, Elsevier

which can precipitate phosphorus in the effluent [38]. It has been reported that AD of one ton of waste consumes 50 kWh electricity and that biogas can be used to generate electricity at an overall efficiency of 35%. An increasing number of studies on AD-based biorefineries are being conducted to improve the efficiency of feedstock utilization and nutrient recovery, thus AD is becoming a promising method to recycle organic wastes [37].

14.4 Environmental Impact of Technologies for Recycling and Valorizing Organic Solid Wastes

14.4.1 Life Cycle Assessment of Environmental Sustainability of Wastes Management

Life cycle assessment (LCA) is a widely used tool to assess the environmental impact of the entire use of a product, process or service. LCA includes four steps: scope and goal, inventory data, impact assessment, and interpretation by ISO

standards 14,041–14,045. Major environmental indicators for LCA according to the Centrum voor Milieukunde Leiden (CML) method include global warming potential (GWP), acidification potential (AP), eutrophication potential (EP), aquatic depletion, photochemical ozone formation to human health (POFH) [53]. GWP is evaluated by the emissions of methane (CH_4), nitrogen monoxide (N_2O) and carbon dioxide (CO_2). The total GWP can be computed in terms of CO_2 as an equivalent substance. The AP is defined as the acidifying substances in the emissions including SO_2 , NO_x and NH_3 , which lower soil and water pH. AP can be measured in terms of equivalent SO_2 emissions (kg SO_2 eq). EP is referred to as the increase in the rate of inorganic matter in the ecosystem including NH_3 , NO_x and PO_4^{3-} and is mainly measured in terms of PO_4^{3-} [45]. Aquatic depletion is the impact of waste residues on marine and fresh aquatic categories. Vanadium, copper, selenium, nickel, zinc, antimony and metallic substances are the main concerns in aquatic depletion [40]. POFH is caused by NO_x , SO_2 , HCl and HF [50]. LCA has been used to compare the environmental impact of technologies used for treating and valorizing organic solid wastes [45, 54–56].

14.4.2 Comparison of Environmental Sustainability of Various Waste Treatment Technologies

Landfilling. One of the environmental issues associated with landfilling of wastes is the leachate. It has been reported that one ton of MSW generates around 500 L of leachate through landfilling which contains 2–4% biological source carbon (BSC). Several approaches have been used to treat leachate, which includes upflow anaerobic sludge blanket (UASB), membrane bioreactor (MBR), nanofiltration, and reverse osmosis. It is estimated that 1.68 kg diesel and 30 kWh electricity are required to treat one ton of typical leachate in a landfill [12]. Furthermore, the high moisture content of MSW reduces LFG collection efficiency, which may cause around 10% of BSC to be released into the atmosphere as methane. Another environmental issue associated with landfilling of MSW is that fossil-based carbon in MSW such as plastics cannot be decomposed in landfills, which thus reduces overall waste reduction efficiency. The environmental impact of landfills are affected by waste composition, LFG treatment and climatic conditions. The GHG emissions for 1 ton of MSW in landfills in Europe was reported to be (124–841) kg CO_2 eq. [41]. Another study showed that net GHG emissions from each ton of MSW in a landfill was 192.2 kg CO_2 -eq without LFG recovery, and 116.7 kg CO_2 -eq with LFG recovery. The increase of biodegradable waste fraction in MSW increases LFG generation, which increases the GHG emissions [12]. Besides GHG emissions, landfills have environmental impact in factors such as human toxicity, ecotoxicity, terrestrial and aquatic toxicity, eutrophication and land use, all of which must be assessed.

Incineration. During incineration, moisture in MSW is removed and almost all organic compounds are decomposed to a mineralized form (i.e., CO₂) at high-temperatures. For example, during incineration it has been reported that 97.8% of organic compounds can be decomposed and mineralized and 79.2% of inorganic matter is reduced, while the remaining portions of organics and inorganics become fly and bottom ash [12]. The ashes are considered as hazardous waste due to their content of heavy metals and dioxins. Useful metal compounds such as iron and aluminum can be extracted from the ashes that are usually landfilled, but increasing efforts have been made to use the ashes as construction materials after extraction of metals and stabilization of the residual waste [43].

Incineration can significantly reduce and stabilize organic solid wastes while producing heat and power to minimize GHG emissions. Research has shown that incineration of 1 kg of horticulture waste with 40% leaf could recover 4.57 MJ energy in heat and reduce 0.28 kg CO₂ eq emissions from the credit of thermal energy generated [47]. However, energy recovery efficiency from incineration of wastes with a high moisture content is very low [12]. Incineration generates a large amount of flue gas with CO₂ diluted by nitrogen gas from the air used in the process. Compared to the advanced thermochemical conversion technologies of pyrolysis and gasification, incineration has the highest GWP because the flue gas containing CO₂ is directly released into the atmosphere [30]. In general, incineration has higher environmental burden in AP, EP, GWP, human toxicity and aquatic toxicity than pyrolysis or gasification, but less AP and EP than composting and AD [40] [30]. It has been estimated that incineration of one ton of MSW releases 1600 g nitrogen oxide, 42 g sulfur dioxide, 58 g hydrogen chloride, 1 g hydrogen fluoride, 8 g VOCs, 0.05 g cadmium, 0.05 g nickel, 0.005 g arsenic, 0.05 g mercury, 4×10^{-7} g dioxins and furans, 0.0001 g polychlorinated biphenyls and 1 ton carbon dioxide [57]. Furthermore, the environmental impact of the bottom ash generated by incineration should be considered. Studies show that phasing-out incineration could reduce its environmental impact of GWP, AP, EP, POFH and human toxicity cancer if the biodegradable wastes can be separated and treated by a biological process such as AD and composted to mitigate the potential increase in landfill rate [44]. Paper, plastic, and glass in MSW can be recycled as well to mitigate the potential increase in landfill rate.

Pyrolysis. Among the technologies of landfilling, incineration, AD, and pyrolysis for treatment of 1 kg of MSW, pyrolysis has the lowest GWP (1.194 kg CO₂ eq) which is 36.8% of AD, 18% of incineration and 21.8% of landfill values. Furthermore, AP and EP of pyrolysis were only 4.80% and 0.08% of AD, 4.56% and 0.08% of incineration, and 4.79% and 0.07% of landfilling, respectively [45]. The GHG emission of pyrolysis was found to be highly affected by bio-oil yield and a 15% variation of bio-oil yield from baseline values can change GWP from -5.6% to 9.9% [45]. Pyrolysis can decrease the required area for landfilling MSW [45]. The main environmental advantages of pyrolysis over incineration is that pyrolysis generates lower emissions by converting most of the carbon in waste into energy products and char. Pyrolysis of wastes with a high protein content such as food wastes and animal manure releases nitrogen in the three main products, which is

desirable in biochar as a fertilizer, but undesirable in bio-oil and syngas as fuels. Furthermore, the application of char from wastes must be evaluated carefully for any significant negative impact on environment and human health, because waste-derived char may contain significant amounts of heavy metals and other hazardous elements depending on the kind of wastes.

Gasification. In comparison with the conventional incineration, gasification provides easier and cheaper control of air pollution by using a limited amount of air or other oxidizing agents to convert organic wastes into syngas mainly CO, CO₂, CH₄, and H₂. Unlike incineration, gasification does not release flue gas into the atmosphere [40]. Gasification using steam, carbon dioxide and metal oxides as oxygen carriers instead of air can avoid the large amount of nitrogen in syngas, which can increase the syngas heating value [49]. The composition of syngas and the emission of gasification are significantly affected by feedstocks and gasification technology as shown in Table 14.3 [48].

Gasification of 1 kg of horticulture waste with 40% leaf waste in a downdraft gasifier with 89.7% carbon conversion efficiency recovers 10.2 MJ energy and decreases 1.46 kg CO₂-eq. emissions due to the credits of recovered energy and carbon-neutral source of biomass [47]. It has been reported that gasification of wastes had a 28–83% decrease in AP, EP, PPOFH, and NO_x generation, compared with incineration. Furthermore, syngas, which has a much smaller volume than flue gas from incineration of the same amount of wastes, can be purified by removing its acid gases to further reduce the emissions for downstream combustion of syngas [50]. Combustion of syngas from gasification has lower emissions than combustion of bio-oil and char from pyrolysis [50]. Furthermore, syngas from gasification can be used in a gas turbine to generate electricity, which has higher energy recovery efficiency and lower emissions than electricity generated by a steam turbine using heat from incineration [40, 50]. However, gasification of wastes needs to be improved to meet safety and health requirements. The yield and composition of bottom and fly ash are affected by feedstock composition and gasification technology [49]. More attention must be paid to the toxic impact of the bottom and fly ash. It should be noted that both gasification and pyrolysis have high energy demand in the steps of waste pretreatment, syngas cleaning, and endothermic pyrolysis reactions.

Composting. Composting of organic wastes can decrease GHG emissions over that of landfilling, by stabilizing the biodegradable fraction of the wastes and minimizing methane generation [12]. Emissions from composts contain carbon and nitrogen compounds and the amounts of emissions depend on water content, oxygen exposure, C/N ratio, and type of feedstocks. The emissions come from composting treatment and later use as fertilizer. N₂O and CH₄ emissions from composting have significant impact on the overall GWP of composting, while NH₃ emissions contribute to acidification and eutrophication. Moreover, leachate and related emissions from composting can often be assumed to be negligible [30]. Emissions of N₂O, CH₄, and NH₃ in an air-controlled composting plant can be treated by biofilters to minimize their environmental impact. Composting of one ton of waste consumes approximately 15.6 kWh electricity for the composting operation and treatment of leachate and gases. One study shows that the net GHG

Table 14.3 Certified emissions from MSW gasification plants. Adopted with permission from reference [48]. Copyright @ 2012, Elsevier

Company plant	JFE/ Thermoselect, Japan	Ebara TwinRec, Japan	Mitsui R21, Japan	Plasco En., Canada
Type of gasifier	Down draft, oxygen enriched air, high temp (1200 °C)	Internally circulating fluidized bed, air	Rotary kiln, air, low temp (900 °C)	Plasma, high temp
Waste capacity (tons/day)	200	300	420	400
Power production (MW _e)	2.3	8	5.5	8.7
Emissions (mg/m ³) at normal condition)	Particulate 10.1 HCl <8.9 NO _x 22.3 SO _x <15.6 Hg –	<3.4 10.1 8.3 – – –	<1 <2 29 <2.9 <0.005 –	<0.71 0.24 39.9 59.1 18.5 – 0.0026
Dioxins/furans (ng-TEQ/m ³)	0.032	0.018	0.00051	0.0008 0.0001 0.0006

reduction by composting was not significant at $-32.3 \text{ kg CO}_2\text{-eq}$ per ton waste composted due to the use of electricity and trace GHGs leakage during composting that contribute to $30.3 \text{ kg CO}_2\text{-eq}$ and $26.4 \text{ kg CO}_2\text{-eq}$ for each ton of wastes composted, respectively [12]. It should be noted that GHG emissions of composting depend on waste type and composition (e.g., kitchen organics and garden waste), technology type (e.g., open systems, closed systems, home composting), efficiency of off-gas cleaning at enclosed composting systems, and the use of the compost. It is reported that the overall global warming factor (GWF) for composting varies between significant savings ($-900 \text{ kg CO}_2\text{-eq ton}^{-1}$ wet waste) and a net load ($300 \text{ kg CO}_2\text{-eq ton}^{-1}$) [58]. Material recovery from composting is practical by land application of the compost as a biofertilizer. The use of compost as a fertilizer can recover and recycle fertilizer nutrient from wastes, which can avoid emissions and energy usage for synthetic fertilizer production. The content of nitrogen, phosphorous and potassium in compost affect its value as a fertilizer and depends on N, P, and K content in the wastes. The effect of carbon sink of the compost should also be taken into account as the application of compost as organic fertilizer promotes, over time, a build-up of carbon in the soil which could prove to be a powerful sink for the carbon sequestered in the soil. The potential of carbon sequestration can vary as (133–213) $\text{kg CO}_2\text{-eq}$ per ton of mature compost [59].

Compost yield is usually very low, which means that 6–17% of wet wastes, compared with 13–35% of wet waste for digestate yield of AD [30]. Studies show that the net energy recovery rate of composting is only about 9.5% [12]. Another study shows that composting of 1 kg of horticulture waste with 40% leaf could recover 0.28 MJ energy in compost and reduce 0.1 $\text{kg CO}_2\text{-eq}$ emissions from the credit of compost as a fertilizer [47]. The emissions from carbon and nitrogen compounds in wastes during composting are a great environmental concern about composting in terms of its overall GWP, acidification, and eutrophication if the process is not properly managed. Composting needs a long period of time and the conditions need to be controlled for optimum conversion of wastes into fertilizers [30].

Anaerobic digestion. AD can convert wastes into biogas as an alternative fuel and digestate as an alternative fertilizer. Due to credits given for alternative fuels and fertilizers produced by the technology, AD has a much lower GWP than that of composting, incineration, or gasification. It has been reported that AD of 1 kg of horticulture waste with 40% leaf waste reduces GWP by 1.48 $\text{kg CO}_2\text{-eq}$ due to the recovery of 8.94 MJ including 7.83 MJ of biogas and 1.11 MJ of digestate-based fertilizer, compared with 0.1 $\text{kg CO}_2\text{-eq}$ for composting, 0.28 $\text{kg CO}_2\text{-eq}$ for incineration, and 1.46 $\text{kg CO}_2\text{-eq}$ for gasification [47]. This comparison did not take into account the energy and emissions associated with collection and transportation. In general, AD is more favorable than composting in terms of energy recovery and GWP reduction for biodegradable wastes such as food wastes, animal manure, and crop residues. However, as composting produces less methane than AD by nature, comparison of GHG emissions is usually done without release of methane from AD [47]. There is not a common agreement on the fugitive emissions of methane during AD, which may contribute a significant amount of GHG emissions. However, it has been reported that the amount of methane leakage in AD could be in the range of

0–10% of produced biogas [60]. Another study shows that fugitive emissions of CH₄ are in the range of (0–8) g/kg waste (dry weight) or (0–11) % methane production [30]. GHG emissions from AD can be reduced by increasing the decomposition rate and minimizing GHG leakage during AD [12].

It is common practice to use digestate as a biofertilizer in land applications. However, the low quality and potential environmental risk of the digestate due to the presence of harmful chemicals may limit its direct land application [12]. The value and safety of digestate and compost based fertilizers depend on the quality of wastes. AD and composting are promising methods for the conversion of door-to-door separate organic wastes, and conversion of agricultural residues into fertilizers. Table 14.4 gives the median values of main characteristics, NPK composition, and concentrations of key elements of 12 digestate samples including 6 generated by AD of pig slurry and another 6 generated by AD of cattle slurry [61]. The digestates from AD of animal manure have high fertilizing potential in terms of NH₄-N content, but their land application might be restricted due to their Cu and Zn content, salinity, biodegradability, phytotoxicity, and hygiene characteristics [61].

Summary. Table 14.5 shows a comparison of GHG emissions and environmental impact of solid waste management methods. Environmental impact of waste

Table 14.4 Average characteristics, NPK composition and key element concentration of digestate generated by anaerobic digestion of pig slurry and cattle slurry. Reprinted with permission from reference [61]. Copyright @ 2012, Elsevier

	Digestate from AD of pig slurry	Digestate from AD of cattle slurry
pH	7.91	7.42
Electrical conductivity (dS m ⁻¹)	25.0	10.9
Dry matter (g L ⁻¹)	28.9	31.4
Total organic carbon, TOC (g L ⁻¹)	8.4	13.6
Dissolved organic carbon (g L ⁻¹)	3.6	6.8
Biochemical oxygen demand (g L ⁻¹)	4.4	8.3
Total nitrogen, TN (g L ⁻¹)	3.6	1.7
NH ₄ -N (g L ⁻¹)	2.8	0.9
P (g L ⁻¹)	0.9	0.3
K (g L ⁻¹)	2.9	1.4
TOC/TN	2.2	9.0
S (mg L ⁻¹)	384	155
Ca (mg L ⁻¹)	1345	1293
Mg (mg L ⁻¹)	499	290
Na (mg L ⁻¹)	698	525
Cl (mg L ⁻¹)	1606	558
Fe (mg L ⁻¹)	103	106
Mn (mg L ⁻¹)	19.1	10.3
Zn (mg L ⁻¹)	55.8	14.4
Cu (mg L ⁻¹)	8.1	6.9
B (mg L ⁻¹)	2.9	2.6

Table 14.5 Comparison of environmental impacts of various solid waste management methods

Treatment methods	Type of wastes	Main assumptions	GHG emissions (kg CO ₂ eq/ton)	Other major environmental impacts	Reference
Landfills	MSW	Energy recovered, waste collection and source separation not included	124–841	<ul style="list-style-type: none"> • Leachate • LFG emission 	[41]
	MSW	No energy recovery, waste collection and transport included	5476		[63]
Incineration	MSW	Energy recovered, waste collection, transport, and residual disposal included	6640	<ul style="list-style-type: none"> • Hazardous fly and bottom ash • A large amount of flue gas • N₂O, HCl, and SO₂ emissions 	[63]
	Horticulture wastes	Energy recovered, waste collection and transport not included, product credits included	-281		[47]
Pyrolysis	MSW	Energy recovered, waste collection, transport, and residual disposal included	1194	<ul style="list-style-type: none"> • Hazardous fly and bottom ash 	[45]
	Corn Stover	Energy recovered, waste collection, transport, and pretreatment included	-864		[64]
Gasification	Horticulture wastes	Energy recovered, waste collection and transport not included, product credits included	-1460	<ul style="list-style-type: none"> • Hazardous fly and bottom ash 	[47]
Composting	Horticulture wastes	Energy recovered, waste collection and transport not included, product credits included	-100	<ul style="list-style-type: none"> • Low compost yield • High GHGs leakage 	
Anaerobic digestion	MSW	Energy recovered, waste collection, transport, and residual disposal included	3245	<ul style="list-style-type: none"> • Digestate treatment • Methane leakage 	[63]
	Horticulture wastes	Energy recovered, waste collection and transport not included, product credits included	-1480		[47]

treatment depends on many factors such as type and composition of the wastes, collection, transportation, local climate conditions, treatment processes, recovery efficiency of energy and materials, and residual waste treatment [62]. There is a large variation in the data of the environmental impact of solid waste management methods reported in the literature due to inconsistencies in the LCA methodology with scope definition and assumptions for the collection of inventory data, impact assessment, and interpretation. In LCA, CO₂ emissions from the conversion of organic solid wastes may come from a biogenic carbon source such as agricultural residues, food wastes, and animal manure or a fossil origin carbon source such as plastics. Biogenic CO₂ emissions are usually treated as carbon neutral (i.e., GWP of zero). Recovered energy and materials are counted as carbon credits with negative carbon emissions [62]. In general, the conversion of MSW that contains fossil carbon sources of plastics usually generates positive GHG emissions due to low energy recovery efficiencies and large amounts of residue that have to be disposed of while conversion of green wastes such as agricultural residues generates negative GHG emissions due to high energy recovery efficiencies, and low amounts of residue requiring disposal. The scope of LCA with and without the consideration of collection, transportation, pretreatment, and residual ash treatment also contributes to significant variations in the assessed environmental impact.

14.5 Challenges and Perspectives of Advanced Waste Conversion Technologies

14.5.1 Pyrolysis of Organic Solid Wastes

Pyrolysis of wastes can reduce corrosion and emissions by retaining alkali and heavy metals, sulfur and chlorine within the products. Pyrolysis operates at much lower temperatures than traditional incineration and can also reduce thermal NO_x formation. Furthermore, as pyrolysis generates a small volume of fuel gas, compared to a large volume of flue gas generated in incineration, it reduces the cost of cleaning emissions. However, Cl and S species such as HCl and SO₂ (or H₂S) may be present in the fuel gas produced by pyrolysis, which have to be removed. Liquid oil and solid char products produced by pyrolysis may contain contaminants such as heavy metals which must be removed [46]. Pyrolysis can be further developed by improving the energy recovery and product quality, reducing emissions, and minimizing the requirement of waste pretreatment [8].

The main challenge for pyrolysis of organic wastes, particularly MSW is in the control of emissions and contamination of products. During pyrolysis, Cl, N and S volatiles are generated at (230–400) °C for HCl, (300–600) °C for SO₂ and above 260 °C for NH₃, which present in gas and liquid products [46]. Mineral elements such as K, S, P, Cl, Ca, Zn, Fe, Cr, Br and Sb present in the pyrolysis oil and fuel gas, which decreases their quality and application. The amounts of those elements in

pyrolytic oil and gas depends on temperature and composition of the feedstock [46]. NaCl in wastes reacts with water. Pyrolysis of PVC at high temperatures forms HCl, which presents in the oil and gas products, leading to corrosion of processing facilities. It has been found that the toxicity equivalent (TE) of products from wastes in a rotary kiln was approximately three folds higher than that of the original waste due to the formation of less chlorinated dioxins and furans and polychlorinated dibenzodioxins (PCDD/F). These contaminants limit the applications of the pyrolytic oil. The char produced by the pyrolysis of wastes also has organic and/or inorganic contaminants which limit its applications. Therefore, pyrolysis of wastes should be improved by reducing emissions of HCl, SO₂ and NH₃ in the products, upgrading the quality of the products, and avoiding the use of wastes containing certain components. Several approaches such as gas scrubbing and catalytic conversion can be used to remove HCl, SO₂ and NH₃ in the pyrolytic products [46].

More studies are needed to improve the quality of pyrolytic products and reduce environmental pollution during the pyrolysis of organic wastes. There is a large variation in pyrolysis characteristics among the wastes. Pretreatment and separation of wastes are effective ways to control undesirable elements in the pyrolytic products [65]. Dehalogenation of plastic wastes can remove halogens prior to pyrolysis to prevent formation of HCl in oil and gas products. Separation of wastes is also an effective way to prevent contaminants from entering oil and gas products. Pyrolysis of food wastes in MSW leads to the formation of higher concentrations of Cl and S in pyrolytic oil, and low heat value due to the high moisture content of food wastes. Food wastes can be separated from MSW and processed using other methods such as composting and AD. Pyrolysis can also be combined with gasification or combustion methods to reduce overall contaminants [46]. Removal of nitrogen compounds in protein-rich wastes prior to pyrolysis can reduce the nitrogen content in the pyrolytic oil [65].

Pyrolysis of organic solid wastes affords bio-crude oil, which is considered as a promising alternative to petroleum for the production of transportation fuels and other valuable chemicals [66]. The pyrolytic oil can be catalytically upgraded using catalysts containing iron (Fe⁻) and calcium (Ca⁻) that have good performance in bromine and chlorine removal, respectively. Although the bio-oil usually has a lower sulfur content and thus fewer emissions of SO₂ than conventional fuels, it has some undesired properties, such as the high oxygen content due to oxygenated compounds (ketones, phenols, aldehydes, esters), high viscosity, and high corrosiveness. Therefore, it is necessary to upgrade the bio-oil into transportation fuel. Upgrading of bio-oil can be carried out through emulsification, esterification, catalytic cracking, solvent extraction, or hydro-deoxygenation [67, 68].

14.5.2 Gasification of Organic Solid Wastes

Gasification has been investigated to convert organic solid wastes into syngas for heat and power generation, synthesis of liquid fuels, and production of hydrogen.

Significant advances have been made in gasification technology and syngas utilization [69]. However, more research is needed to address several critical issues in gasification including ash agglomeration, syngas quality control and cleaning, and efficient syngas utilization [69]. The toxic and explosive nature of syngas increases safety concerns and necessitates reliable control equipment. Moreover, two-step conversion of organic solid wastes into energy products via gasification of the solid wastes into syngas and downstream utilization requires a complex plant with strict operational and maintenance schedules. Conditioning and cleaning syngas for downstream utilization is costly [48]. One of the main obstacles in gasification of organic wastes is instable operation due to the heterogeneity of wastes with large variation in composition, especially MSW, which requires pretreatment of the wastes prior to gasification. Furthermore, although a gas turbine has higher energy efficiencies and lower emissions than a steam turbine to generate electricity from the syngas produced by gasification, syngas from gasification of organic solid wastes cannot meet the quality requirements of a gas turbine. The main potential areas which need to be developed for gasification of organic solid wastes include (1) increasing the gasification efficiency, (2) using selected waste streams, and (3) syngas cleaning and upgrading to be used for synthesis of liquid fuels and chemicals [50].

A chemical looping gasification (CLG) process uses lattice oxygen in an oxygen carrier such as metal oxides as an oxidant agent to avoid direct contact between fuel and air [70]. CLG can increase gasification efficiency, avoid introduction of a large amount of nitrogen in air into syngas, and reduce tar and carbon dioxide in the syngas [71]. A CLG process is usually implemented as dual fluidized bed reactors to ensure high rates of heat and mass transfer via fluidization. An oxygen carrier is used as the bed material of the gasification reactor to supply oxygen and heat. The reduced oxygen carrier is then transported into the second reactor where it is oxidized with air for re-use. The overall reaction of both reactors using an oxygen carrier is exothermic that is the same as biomass gasification with pure oxygen. It has been reported that CLG of biomass with natural hematite as an oxygen carrier increases carbon conversion and gas yields by 7.45% and 11.02%, respectively, while decreasing tar content by 51.53% compared with steam gasification [72]. A number of Ni, Co, Cu and Fe-based materials have been tested as oxygen carriers. Pure metal oxides often do not satisfy all the favorable traits of an oxygen carrier and the reaction rates of pure metal oxides are reduced greatly after a few reduction and oxidation cycles [73]. Bimetallic oxygen carriers and metal oxides on novel porous supports have been studied to enhance the performance of CLG [71, 74]. Chemical looping processes with an oxygen carrier of metal oxides can be used to combust organic solid wastes and syngas, or gasify organic solid wastes [75–77]. Some metal oxides such as CaO, MgO, and BaO can be used not only as an oxygen carrier to supply oxygen for completely or partially oxides organic solid wastes, but also an adsorbent to remove H₂S, HCl, and CO₂ from the product gas [76, 78, 79].

14.5.3 Anaerobic Digestion of Organic Solid Wastes

AD produces biogas as a renewable energy product from various biodegradable wastes at different yields [80]. Biodegradability of organic wastes in AD depends on the complexity and accessibility of the organic materials, and their physical properties including particle size and porosity. Biodegradability of organic wastes can be assessed by biochemical methane potential test (BMP) [51]. Various physical, chemical and biological pretreatment methods have been studied to improve the digestibility of agricultural wastes, particularly lignocellulosic crop residues [81]. Co-digestion of manure and crop residues can increase biogas production by providing a feedstock with an optimum C/N ratio. Anaerobic co-digestion of manure and pretreated crop residues significantly increases biomethane production [82]. One of the main challenges in AD of organic solid wastes is reducing emissions of methane, carbon dioxide, ammonia and other odorous gases to the atmosphere, because this results in greenhouse gas and contributes to air pollution, and lowers the energy value of the wastes [42].

Nanomaterials have been studied as additives to improve the performance of AD, which can be classified into four categories: nanoscale zero valent metals (NZVMs) (e.g. Fe, Ni, Cu, Co, Ag, Au), metal oxide NPs (e.g. ZnO, CuO, TiO₂, MgO, NiO, Fe₂O₃), carbon based nanomaterials (e.g. graphene, diamond, nanotube and nanofibers), and multi-compound NPs [80, 83]. Nanomaterials with nano-sized structures and specific physicochemical properties can have positive and negative effects on the rate of AD through interaction with feedstock and microorganisms [83]. Studies have shown that ZnO, CuO, Mn₂O₃ and Al₂O₃ significantly reduce biogas production rate that can be attributed to the toxicity of these materials. The impact of TiO₂ and CeO₂ is completely dependent on their concentrations in the reactor and digestion time. Nano-iron oxide (Fe₃O₄) has a remarkable positive impact that can increase methane production by 234% due to the presence of non-toxic Fe³⁺ and Fe²⁺ ions. It has also been reported that addition of nano zero-valent iron (NZVI) results in a mixed effect on methane production depending on its concentration. The addition of silver or gold nanoparticles result in either a decrease or no change in biogas production rate, depending on their concentration in the reactor. Addition of micro/nano fly ash and micro/nano bottom ash has a positive impact and considerably increases biogas production, but the addition of fullerene (C60) and silica (SiO₂) nanoparticles, and single-walled carbon nanotubes had no effect on cumulative biogas production. The ZnFe nanocomposite can significantly improve methane production by up to 185%. Moreover, ZnFe with 10% carbon nanotubes (ZFCNTs) and zinc ferrite with 10% C76 fullerene (ZFC76) showed a positive effect on hydraulic retention time and enhanced methane production up to 162% and 146%, respectively [80].

Since the AD digestate is used as a fertilizer, the nutrient recovery becomes significant which can be improved by decreasing nitrogen emission and increasing the conversion of polyphosphate to orthophosphate. The digestate is usually composted prior to its land application. The loss of nitrogen to the atmosphere can

be controlled by properly designing the composting process and adjusting operating conditions such as aeration mode and rate, water content, porosity, and temperature. Decrease of the anoxic or anaerobic microenvironment and the water content can lower denitrification and consequently NO₂ emissions, and increase the N recovery potential [38].

Another challenge of AD is that it is still not common for widespread land application of composting and digestate as biofertilizer because of its low quality and environmental risk. Some countries restrict direct use of the digestate as fertilizer due to concerns on its quality and safety [12]. The chemical composition of the digestate is highly dependent on the feedstock composition. The digestate usually has higher concentrations of nitrate, ammonia, Ca and Mg than the original wastes. The quality of digestate can be improved by optimizing the AD process and pretreatment of the organic wastes. AD generates a large amount of liquid effluent with dissolved N, P, and K fertilizer compounds. Instead of direct land application of the digestate, the solid digestate can be converted into biochar that can be used to recover fertilizer nutrients in the digestion effluent to produce high-quality fertilizer and recycle the water [68, 84].

14.5.4 Perspectives of Advanced Organic Solid Wastes conversion Technologies

Advanced thermochemical conversion technologies, pyrolysis and gasification, have been studied as environmentally-friendly alternatives to traditional incineration for the recovery of energy from organic solid wastes. AD has been studied as an alternative to composting to recover both energy and fertilizer nutrients from organic solid wastes. However, selection of a waste conversion technology should consider the type of wastes, the process efficiency, and the desirable products. Table 14.6 summarizes the challenges and recommendations of advanced conversion technologies for the valorization of various organic solid wastes. In general, thermochemical processes of pyrolysis and gasification can be applied to convert dry biomass wastes, waste plastics, waste paper, and cardboard into petroleum-like oil, syngas, and char as main products. Thermochemical conversion of organic wastes faces challenges of high HCl, NH₃, and SO₂ emissions due to the presence of Cl, N and S containing compounds in the wastes, ash agglomeration due to the use of high temperatures, quality control of char, oil, and syngas products, and safety control of the explosive and toxic syngas products. More studies on pretreatment and separation of wastes, catalytic upgrading of products, and novel process development are needed for the commercialization of pyrolysis and gasification technologies to valorize organic solid wastes. The biological process of AD can be applied to convert wet biogenic wastes of agricultural residues, animal wastes, food wastes, and yard waste into biogas and fertilizers as main products. Biogenic waste usually has high moisture content and is more suitable for AD than for thermochemical

Table 14.6 Challenges and recommendations for the valorization of organic solid wastes with advanced conversion technologies

Processes	Type of wastes	Challenges	Recommendations	Reference
Pyrolysis / gasification	<ul style="list-style-type: none"> • Dry agricultural /forestry residues • Waste plastics • Waste paper and cardboards 	<ul style="list-style-type: none"> • HCl emissions from polyvinyl chloride (PVC) in MSW • NH₃ emissions from protein-containing wastes • SO₂, and • Ash agglomeration • Product quality control • Syngas safety control 	<ul style="list-style-type: none"> • Pretreatment and separation of cl, S and N containing compounds • Catalytic conversion and upgrading products • Syngas cleaning and upgrading • Novel gasification technology 	[46, 50, 65, 78]
Anaerobic digestion	<ul style="list-style-type: none"> • Wet agricultural residues • Animal wastes • Food wastes • Yard waste 	<ul style="list-style-type: none"> • Low biodegradability • Undesirable C/N ratio in the wastes • Large amounts of digestate and effluent 	<ul style="list-style-type: none"> • Pretreatment to increase digestibility • Co-digestion to adjust C/N ratio • Application of nanomaterials and additives for enhanced efficiency • Value-added processing of digestate and effluent 	[81, 84]

conversion. However, AD faces the technical barriers of low digestibility, unbalanced C/N ratio in the wastes, and generation of large amounts of solid digestate and effluent. Therefore, studies are needed to increase the digestibility of wastes via pretreatment, co-digestion, and biologically active additives, and for processing digestate and effluent.

Thermochemical conversion and AD can be used to efficiently convert different types of organic solid wastes, therefore, it is critical to separate and sort those wastes. In this case, the inorganic wastes of metals, glass, ceramic and ash should be removed from the organic solid wastes prior to conversion. Dry non-biodegradable wastes of plastic, rubber, fabric and leather can be converted by pyrolysis or gasification, while wet green biogenic wastes of food and yard wastes, agricultural residues, and animal wastes can be converted by AD. Dry biogenic wastes such as paper, cardboard, agricultural and forestry residues can also be converted by pyrolysis and gasification.

14.6 Conclusions and Future Outlook

This chapter has evaluated the advantages and disadvantages of waste management technologies in terms of waste reduction, stabilization, material recycling, energy recycling, GHG reduction, and other environmental factors. Feedstock composition

and technical conditions used in those technologies can affect efficiency, economics and environmental sustainability of each technique, and portfolio and quality of products. Landfilling, incineration, and composting are three traditional commercialized methods for treatment of organic wastes. Conversion of waste materials into a wide range of valuable products provides both economic and environmental benefits. Both advanced thermochemical processes such as pyrolysis and gasification, and biological processes such as anaerobic digestion have been studied to convert organic solid wastes to value-added products such as fuels and fertilizers. Although thermochemical methods including incineration, pyrolysis, and gasification have faster conversion rates and higher waste reduction efficiencies than biochemical methods of composting and anaerobic digestion, the exhaust gas cleanup needs to be improved to meet safety and health requirements. Pretreatment and separation of wastes are effective ways to control undesirable elements in the products produced by thermochemical conversion technologies. On the other hand, biochemical approaches, specifically anaerobic digestion, have better nutrient recovery and can remarkably reduce emissions and energy usage for producing biogas as an energy product and digestate as a nutrient rich co-product of fertilizers. However, anaerobic digestion needs to be improved by removing some hazardous materials from the wastes, increasing biogas production efficiency, and enriching nutrient content. Nanomaterials have been studied to improve conversion efficiency and quality of products for recycling and valorizing organic wastes and are possibly practical for land application of the digestate and compost as a biofertilizer. However, low quality and potential environmental risk of the digestate and compost due to the presence of harmful chemicals may limit its direct land application. Value and safety of digestate and compost based fertilizers depend on the quality of wastes. Anaerobic digestion and composting could be promising methods for conversion of selected organic wastes such as food processing wastes and agricultural residues into fertilizers. Digestates from anaerobic digestion of animal manure have high fertilizing potential in terms of $\text{NH}_4\text{-N}$ content but their land application might be restricted by their Cu and Zn content, salinity, biodegradability, phytotoxicity, and hygiene characteristics.

Acknowledgement This publication was made possible by the grant from the U.S. Department of Agriculture-National Institute of Food and Agriculture (USDA-NIFA, award number 2020-38821-31114), U.S. Department of Energy (DE-EE0008809) and National Science Foundation (NSF, award number 1736173). Its contents are solely the responsibility of the authors and do not necessarily represent the official views of the USDA-NIFA and NSF.

References

1. Dhanya B, Mishra A, Chandel AK, Verma ML. Development of sustainable approaches for converting the organic waste to bioenergy. *Sci Total Environ.* 2020;723:138109. <https://doi.org/10.1016/j.scitotenv.2020.138109>.

2. Xu C, Nasrollahzadeh M, Selva M, Issabadi Z, Luque R. Waste-to-wealth: biowaste valorization into valuable bio (nano) materials. *Chem Soc Rev.* 2019;48:4791–822. <https://doi.org/10.1039/C8CS00543E>.
3. Kumar D, Kumar D. Sustainable management of coal preparation. Cambridge: Woodhead Publishing; 2018.
4. Ghose S, Franchetti MJ. Economic aspects of food waste-to-energy system deployment. In: Sustainable food waste-to-energy systems. Netherlands: Elsevier; 2018. p. 203–29.
5. Chojnacka K, Gorazda K, Witek-Krowiak A, Moustakas K. Recovery of fertilizer nutrients from materials—Contradictions, mistakes and future trends. *Renewable Sustainable Energy Rev.* 2019;110:485–98. <https://doi.org/10.1016/j.rser.2019.04.063>.
6. Górecka H, Górecki H, Chojnacka K, Baranska M, Michalak I, Zielinska A. New role of sulfuric acid in production of multicomponent fertilizers from renewable sources. *Am J Agric Biol Sci.* 2007;2:241–7. <https://doi.org/10.3844/ajabssp.2007.241.247>.
7. Kaza S, Yao L, Bhada-Tata P, Van Woerden F. What a waste 2.0: a global snapshot of solid waste management to 2050. Urban Development. Washington, DC: World Bank; 2018.
8. Williams PT, Gurau S. Pyrolysis of municipal solid waste. *J Inst Energy.* 1992;65:192–200.
9. Ramachandran S, Yao Z, You S, Massier T, Stimming U, Wang C-H. Life cycle assessment of a sewage sludge and woody biomass co-gasification system. *Energy.* 2017;137:369–76. <https://doi.org/10.1016/j.energy.2017.04.139>.
10. Das S, Lee S-H, Kumar P, Kim K-H, Lee SS, Bhattacharya SS. Solid waste management: scope and the challenge of sustainability. *J Cleaner Prod.* 2019;228:658–78. <https://doi.org/10.1016/j.jclepro.2019.04.323>.
11. Abdel-Shafy HI, Mansour MS. Solid waste issue: sources, composition, disposal, recycling, and valorization. *Egypt J Pet.* 2018;27:1275–90. <https://doi.org/10.1016/j.ejpe.2018.07.003>.
12. Liu Y, Xing P, Liu J. Environmental performance evaluation of different municipal solid waste management scenarios in China. *Resour Conserv Recycl.* 2017;125:98–106. <https://doi.org/10.1016/j.resconrec.2017.06.005>.
13. Al-Salem S, Evangelisti S, Lettieri P. Life cycle assessment of alternative technologies for municipal solid waste and plastic solid waste management in the Greater London area. *Chem Eng J.* 2014;244:391–402. <https://doi.org/10.1016/j.cej.2014.01.066>.
14. Yassin L, Lettieri P, Simons SJ, Germanà A. Techno-economic performance of energy-from-waste fluidized bed combustion and gasification processes in the UK context. *Chem Eng J.* 2009;146:315–27. <https://doi.org/10.1016/j.cej.2008.06.014>.
15. H-j F, Shu H-Y, Yang H-S, Chen W-C. Characteristics of landfill leachates in central Taiwan. *Sci Total Environ.* 2006;361:25–37. <https://doi.org/10.1016/j.scitotenv.2005.09.033>.
16. Bolton K, Rousta K. Solid waste management toward zero landfill: a Swedish model. In: Taherzadeh MJ, Bolton K, Wong J, Pandey A, editors. Sustainable resource recovery and zero waste approaches. Netherlands: Elsevier; 2019. p. 53–63.
17. Nie Y, Wu Y, Zhao J, Zhao J, Chen X, Maraseni T, Qian G. Is the finer the better for municipal solid waste (MSW) classification in view of recyclable constituents? A comprehensive social, economic and environmental analysis. *Waste Manage.* 2018;79:472–80. <https://doi.org/10.1016/j.wasman.2018.08.016>.
18. Duque-Acevedo M, Belmonte-Ureña LJ, Cortés-García FJ, Camacho-Ferre F. Agricultural waste: review of the evolution, approaches and perspectives on alternative uses. *Global Ecol Conserv.* 2020;22:e00902. <https://doi.org/10.1016/j.gecco.2020.e00902>.
19. Cheng D, Liu Y, Ngo HH, Guo W, Chang SW, Nguyen DD, Zhang S, Luo G, et al. A review on application of enzymatic bioprocesses in animal wastewater and manure treatment. *Bioresour Technol.* 2020;313:123683. <https://doi.org/10.1016/j.biortech.2020.123683>.
20. He Z, Pagliari PH, Waldrip HM. Applied and environmental chemistry of animal manure: a review. *Pedosphere.* 2016;26:779–816. [https://doi.org/10.1016/S1002-0160\(15\)60087-X](https://doi.org/10.1016/S1002-0160(15)60087-X).
21. Lagué C. Challenges and opportunities in livestock manure management. 2001. <https://citeserx.ist.psu.edu/viewdoc/download?doi=10.1.1.493.2066&rep=rep1&type=pdf>.

Accessed 16 July 2021

22. Qian Y, Song K, Hu T, Ying T. Environmental status of livestock and poultry sections in China under current transformation stage. *Sci Total Environ.* 2018;622-623:702–9. <https://doi.org/10.1016/j.scitotenv.2017.12.045>.
23. Shen X, Huang G, Yang Z, Han L. Compositional characteristics and energy potential of Chinese animal manure by type and as a whole. *Applied Energy.* 2015;160:108–19. <https://doi.org/10.1016/j.apenergy.2015.09.034>.
24. Dai Y, Zheng H, Jiang Z, Xing B. Comparison of different crop residue-based technologies for their energy production and air pollutant emission. *Sci Total Environ.* 2020;707:136122. <https://doi.org/10.1016/j.scitotenv.2019.136122>.
25. Lal R. World crop residues production and implications of its use as a biofuel. *Environ Int.* 2005;31:575–84. <https://doi.org/10.1016/j.envint.2004.09.005>.
26. Lemke RL, VandenBygaart AJ, Campbell CA, Lafond GP, Grant B. Crop residue removal and fertilizer N: effects on soil organic carbon in a long-term crop rotation experiment on a Udic Boroll. *Agric Ecosyst Environ.* 2010;135:42–51. <https://doi.org/10.1016/j.agee.2009.08.010>.
27. Scarlat N, Fahl F, Lugato E, Monforti-Ferrario F, Dallemand J. Integrated and spatially explicit assessment of sustainable crop residues potential in Europe. *Biomass Bioenergy.* 2019;122: 257–69. <https://doi.org/10.1016/j.biombioe.2019.01.021>.
28. Wiesenthal T, Mourelatou A. How much bioenergy can Europe produce without harming the environment? vol 7. European Environment Agency. 2006. https://www.forestryresearch.gov.uk/documents/2098/EEA_How_much_bioenergy_can_Europe_produce_without_harming_the_environment_2006.pdf. Accessed 16 July 2021
29. Alvarado M, Guzmán N, Solís N, Vega Baudrit J. Recycling and elimination of wastes obtained from agriculture by using nanotechnology: nanosensors. *Int J Biosensors Bioelectronics.* 2017;3:00084. <https://doi.org/10.15406/ijbsbe.2017.03.00084>.
30. Bernstad A, la Cour JJ. Review of comparative LCAs of food waste management systems—current status and potential improvements. *Waste manage.* 2012;32:2439–55. <https://doi.org/10.1016/j.wasman.2012.07.023>.
31. Donner M, Verniquet A, Broeze J, Kayser K, De Vries H. Critical success and risk factors for circular business models valorising agricultural waste and by-products. *Resour Conserv Recycl.* 2021;165:105236. <https://doi.org/10.1016/j.resconrec.2020.105236>.
32. Wang LJ. Production of bioenergy and bioproducts from food processing wastes: a review. *Trans ASABE.* 2013;56:217–30. <https://doi.org/10.13031/2013.42572>.
33. Wang L, Shahbazi A, Hanna MA. Characterization of corn stover, distiller grains and cattle manure for thermochemical conversion. *Biomass Bioenergy.* 2011;35:171–8. <https://doi.org/10.1016/j.biombioe.2010.08.018>.
34. Joseph G, Zhang B, Harrison SH, Graves JL, Thomas MD, Panchagavi R, Ewunekem JAJ, Wang L. Microbial community dynamics during anaerobic co-digestion of corn stover and swine manure at different solid content, carbon to nitrogen ratio and effluent volumetric percentages. *J Environ Sci Health, Part A.* 2020;55:1111–24. <https://doi.org/10.1080/10934529.2020.1771975>.
35. Wang L, Hanna MA, Weller CL, Jones DD. Technical and economical analyses of combined heat and power generation from distillers grains and corn stover in ethanol plants. *Energy Convers Manage.* 2009;50:1704–13. <https://doi.org/10.1016/j.enconman.2009.03.025>.
36. Quck A, Balasubramanian R. Life cycle assessment of energy and energy carriers from waste matter—a review. *J Cleaner Prod.* 2014;79:18–31. <https://doi.org/10.1016/j.jclepro.2014.05.082>.
37. Awasthi MK, Sarsaiya S, Patel A, Juneja A, Singh RP, Yan B, Awasthi SK, Jain A, et al. Refining biomass residues for sustainable energy and bio-products: an assessment of technology, its importance, and strategic applications in circular bio-economy. *Renewable Sustainable Energy Rev.* 2020;127:109876. <https://doi.org/10.1016/j.rser.2020.109876>.
38. Carey DE, Yang Y, McNamara PJ, Mayer BK. Recovery of agricultural nutrients from biorefineries. *Bioresour Technol.* 2016;215:186–98. <https://doi.org/10.1016/j.biortech.2016.02.093>.

39. Johansson N, Corvillec H. Waste policies gone soft: an analysis of European and Swedish waste prevention plans. *Waste Manage.* 2018;77:322–32. <https://doi.org/10.1016/j.wasman.2018.04.015>.
40. Zaman AU. Life cycle assessment of pyrolysis–gasification as an emerging municipal solid waste treatment technology. *Int J Environ Sci Technol.* 2013;10:1029–38. <https://doi.org/10.1007/s13862-013-0230-3>.
41. Sauve G, Van Acker K. The environmental impacts of municipal solid waste landfills in Europe: a life cycle assessment of proper reference cases to support decision making. *J Environ Manage.* 2020;261:110216. <https://doi.org/10.1016/j.jenvman.2020.110216>.
42. Du C, Abdullah JJ, Greetham D, Fu D, Yu M, Ren L, Li S, Lu D. Valorization of food waste into biofertiliser and its field application. *J Cleaner Prod.* 2018;187:273–84. <https://doi.org/10.1016/j.jclepro.2018.03.211>.
43. Leckner B. Process aspects in combustion and gasification Waste-to-Energy (WtE) units. *Waste Manage.* 2015;37:13–25. <https://doi.org/10.1016/j.wasman.2014.04.019>.
44. Istrate I-R, Galvez-Martos J-L, Dufour J. The impact of incineration phase-out on municipal solid waste landfilling and life cycle environmental performance: Case study of Madrid, Spain. *Sci Total Environ.* 2021;755:142537. <https://doi.org/10.1016/j.scitotenv.2020.142537>.
45. Wang H, Wang L, Shahbazi A. Life cycle assessment of fast pyrolysis of municipal solid waste in North Carolina of USA. *J Cleaner Prod.* 2015;87:511–9. <https://doi.org/10.1016/j.jclepro.2014.09.011>.
46. Chen D, Yin L, Wang H, He P. Pyrolysis technologies for municipal solid waste: A review. *Waste Manage.* 2014;34:2466–86. <https://doi.org/10.1016/j.wasman.2014.08.004>.
47. Lee JTE, Ee AWL, Tong YW. Environmental impact comparison of four options to treat the cellulosic fraction of municipal solid waste (CF-MSW) in green megacities. *Waste Manage.* 2018;78:677–85. <https://doi.org/10.1016/j.wasman.2018.06.043>.
48. Arena U. Process and technological aspects of municipal solid waste gasification. A review. *Waste Manage.* 2012;32:625–39. <https://doi.org/10.1016/j.wasman.2011.09.025>.
49. Seo Y-C, Alam MT, Yang W-S. Gasification of municipal solid waste. In: Yun Y, editor. *Gasification for low-grade feedstock.* London: IntechOpen; 2018. p. 115–41. <https://doi.org/10.5772/intechopen.73685>.
50. Dong J, Tang Y, Nzihou A, Chi Y, Weiss-Hortala E, Ni M. Life cycle assessment of pyrolysis, gasification and incineration waste-to-energy technologies: Theoretical analysis and case study of commercial plants. *Sci Total Environ.* 2018;626:744–53. <https://doi.org/10.1016/j.scitotenv.2018.01.151>.
51. Jimenez J, Lei H, Steyer J-P, Houot S, Patureau D. Methane production and fertilizing value of organic waste: Organic matter characterization for a better prediction of valorization pathways. *Bioresour Technol.* 2017;241:1012–21. <https://doi.org/10.1016/j.biortech.2017.05.176>.
52. Mavrotas G, Gakis N, Skoulaxinou S, Katsouros V, Georgopoulou E. Municipal solid waste management and energy production: consideration of external cost through multi-objective optimization and its effect on waste-to-energy solutions. *Renewable Sustainable Energy Rev.* 2015;51:1205–22. <https://doi.org/10.1016/j.rser.2015.07.029>.
53. Oers LV. CML-IA database, characterisation and normalisation factors for midpoint impact category indicators (Version 4.8). 2016. <http://www.cml.leiden.edu/software/data-cmlia.html>. Accessed 16 July 2021
54. Lee E, Oliveira DSBL, Oliveira LSBL, Jimenez E, Kim Y, Wang M, Ergas SJ, Zhang Q. Comparative environmental and economic life cycle assessment of high solids anaerobic co-digestion for biosolids and organic waste management. *Water Res.* 2020;171:115443. <https://doi.org/10.1016/j.watres.2019.115443>.
55. Iqbal A, Liu X, Chen G-H. Municipal solid waste: review of best practices in application of life cycle assessment and sustainable management techniques. *Sci Total Environ.* 2020;729:138622. <https://doi.org/10.1016/j.scitotenv.2020.138622>.

56. Zhang J, Qin Q, Li G, Tseng C-H. Sustainable municipal waste management strategies through life cycle assessment method: a review. *J Environ Manage.* 2021;287:112238. <https://doi.org/10.1016/j.jenvman.2021.112238>.
57. Gladding T, Thurgood M. Review of environmental and health effects of waste management: municipal solid waste and similar wastes. 2004. <http://oro.open.ac.uk/53447/>. Accessed 16 July 2021
58. Boldrin A, Andersen JK, Møller J, Christensen TH, Favoino E. Composting and compost utilization: accounting of greenhouse gases and global warming contributions. *Waste Manag Res.* 2009;27:800–12. <https://doi.org/10.1177/0734242x09345275>.
59. Blengini G. Applying LCA to organic waste management in Piedmont, Italy. *Management of Environmental Quality.* 2008;19:533–49. <https://doi.org/10.1108/14777830810894229>.
60. Eggleston S, Buendia L, Miwa K, Ngara T, Tanabe K. 2006 IPCC guidelines for national greenhouse gas inventories. 2006. <https://www.ipcc-nccc.iges.or.jp/public/2006gl/>. Accessed 16 July 2016
61. Alburquerque JA, de la Fuente C, Ferrer-Costa A, Carrasco L, Cegarra J, Abad M, Bernal MP. Assessment of the fertiliser potential of digestates from farm and agroindustrial residues. *Biomass Bioenergy.* 2012;40:181–9. <https://doi.org/10.1016/j.biombioe.2012.02.018>.
62. Dong J, Tang Y, Nzhou A, Chi Y. Key factors influencing the environmental performance of pyrolysis, gasification and incineration Waste-to-Energy technologies. *Energy Convers Manage.* 2019;196:497–512. <https://doi.org/10.1016/j.enconman.2019.06.016>.
63. Özeler D, Yetiş Ü, Demirer GN. Life cycle assessment of municipal solid waste management methods: ankara case study. *Environ Int.* 2006;32:405–11. <https://doi.org/10.1016/j.envint.2005.10.002>.
64. Alhazmi H, Loy ACM. A review on environmental assessment of conversion of agriculture waste to bio-energy via different thermochemical routes: current and future trends. *Bioresour Technol Rep.* 2021;14:100682. <https://doi.org/10.1016/j.biteb.2021.100682>.
65. Ansah E, Wang L, Zhang B, Shahbazi A. Catalytic pyrolysis of raw and hydrothermally carbonized Chlamydomonas debaryana microalgae for denitrogenation and production of aromatic hydrocarbons. *Fuel.* 2018;228:234–42. <https://doi.org/10.1016/j.fuel.2018.04.163>.
66. Saber M, Golzary A, Hosseinpour M, Takahashi F, Yoshikawa K. Catalytic hydrothermal liquefaction of microalgae using nanocatalyst. *Appl Energy.* 2016;183:566–76. <https://doi.org/10.1016/j.apenergy.2016.09.017>.
67. Arun J, Varshini P, Prithvinath PK, Priyadarshini V, Gopinath KP. Enrichment of bio-oil after hydrothermal liquefaction (HTL) of microalgae *C. vulgaris* grown in wastewater: Bio-char and post HTL wastewater utilization studies. *Bioresour Technol.* 2018;261:182–7. <https://doi.org/10.1016/j.biortech.2018.04.029>.
68. Nan W, Krishna CR, Kim TJ, Wang LJ, Mahajan D. Catalytic upgrading of switchgrass-derived pyrolysis oil using supported ruthenium and rhodium catalysts. *Energy Fuels.* 2014;28:4588–95. <https://doi.org/10.1021/ef500826k>.
69. Wang L, Weller CL, Jones DD, Hanna MA. Contemporary issues in thermal gasification of biomass and its application to electricity and fuel production. *Biomass Bioenergy.* 2008;32: 573–81. <https://doi.org/10.1016/j.biombioe.2007.12.007>.
70. Rydén M, Lyngfelt A, Mattisson T, Chen D, Holmen A, Bjørgum E. Novel oxygen-carrier materials for chemical-looping combustion and chemical-looping reforming; $LaxSr_{1-x}Fe_{y}Co_{1-y}O_3-\delta$ perovskites and mixed-metal oxides of NiO , Fe_2O_3 and Mn_3O_4 . *Int J Greenhouse Gas Control.* 2008;2:21–36. [https://doi.org/10.1016/S1750-5836\(07\)00107-7](https://doi.org/10.1016/S1750-5836(07)00107-7).
71. Li X, Wang L, Zhang B, Khajeh A, Shahbazi A. Iron oxide supported on silicalite-1 as a multifunctional material for biomass chemical looping gasification and syngas upgrading. *Chem Eng J.* 2020;401:125943. <https://doi.org/10.1016/j.cej.2020.125943>.
72. de Diego LF, Ortiz M, Adámez J, García-Labiano F, Abad A, Gayán P. Synthesis gas generation by chemical-looping reforming in a batch fluidized bed reactor using Ni-based oxygen carriers. *Chem Eng J.* 2008;144:289–98. <https://doi.org/10.1016/j.cej.2008.06.004>.

73. Nandy A, Loha C, Gu S, Sarkar P, Karmakar MK, Chatterjee PK. Present status and overview of Chemical Looping Combustion technology. *Renewable Sustainable Energy Rev.* 2016;59: 597–619. <https://doi.org/10.1016/j.rser.2016.01.003>.
74. Muriungi B, Wang L, Shahbazi A. Comparison of bimetallic Fe-Cu and Fe-Ca oxygen carriers for biomass gasification. *Energies.* 2020;13:2019. <https://doi.org/10.3390/en13082019>.
75. Chen P, Sun X, Gao M, Ma J, Guo Q. Transformation and migration of cadmium during chemical-looping combustion/gasification of municipal solid waste. *Chem Eng J.* 2019;365: 389–99. <https://doi.org/10.1016/j.cej.2019.02.041>.
76. Wang H, Liu G, Veksha A, Dou X, Giannis A, Lim TT, Lisak G. Iron ore modified with alkaline earth metals for the chemical looping combustion of municipal solid waste derived syngas. *J Cleaner Prod.* 2021;282:124467. <https://doi.org/10.1016/j.jclepro.2020.124467>.
77. Wang H, Dou X, Veksha A, Liu W, Giannis A, Ge L, Thye Lim T, Lisak G. Barium aluminate improved iron ore for the chemical looping combustion of syngas. *Appl Energy.* 2020;272: 115236. <https://doi.org/10.1016/j.apenergy.2020.115236>.
78. Wang H, Liu G, Veksha A, Giannis A, Lim T-T, Lisak G. Effective H₂S control during chemical looping combustion by iron ore modified with alkaline earth metal oxides. *Energy.* 2021;218:119548. <https://doi.org/10.1016/j.energy.2020.119548>.
79. Wang H, Liu G, Boon YZ, Veksha A, Giannis A, Lim TT, Lisak G. Dual-functional witherite in improving chemical looping performance of iron ore and simultaneous adsorption of HCl in syngas at high temperature. *Chem Eng J.* 2021;413:127538. <https://doi.org/10.1016/j.cej.2020.127538>.
80. Ganzoury MA, Allam NK. Impact of nanotechnology on biogas production: a mini-review. *Renewable Sustainable Energy Rev.* 2015;50:1392–404. <https://doi.org/10.1016/j.rser.2015.05.073>.
81. Bekoe D, Wang L, Zhang B, Scott Todd M, Shahbazi A. Aerobic treatment of swine manure to enhance anaerobic digestion and microalgal cultivation. *J Environ Sci Health Part B.* 2018;53: 145–51. <https://doi.org/10.1080/03601234.2017.1397454>.
82. Joseph G, Zhang B, Mahzabin Rahman Q, Wang L, Shahbazi A. Two-stage thermophilic anaerobic co-digestion of corn stover and cattle manure to enhance biomethane production. *J Environ Sci Health Part A.* 2019;54:452–60. <https://doi.org/10.1080/10934529.2019.1567156>.
83. Baniamerian H, Isfahani PG, Tsapekos P, Alvarado-Morales M, Shahrokh M, Vossoughi M, Angelidaki I. Application of nano-structured materials in anaerobic digestion: Current status and perspectives. *Chemosphere.* 2019;229:188–99. <https://doi.org/10.1016/j.chemosphere.2019.04.193>.
84. Zhang B, Joseph G, Wang L, Li X, Shahbazi A. Thermophilic anaerobic digestion of cattail and hydrothermal carbonization of the digestate for co-production of biomethane and hydrochar. *J Environ Sci Health Part A.* 2020;55:230–8. <https://doi.org/10.1080/10934529.2019.1682367>.

Index

A

- Ablative, 38, 82
Abstraction, 252, 257
Acetaldehyde, 295
Acetic acid, 14, 139, 181, 216, 290, 292, 318, 353, 364, 365, 438, 439
Acetogenesis, 14, 142, 144–145, 181, 182, 185, 195, 222
Acetone, 118, 122, 206, 209, 212, 214–216, 218, 232, 326, 328, 343, 352, 437
Acetone-butanol-ethanol (ABE), 206, 209, 211–213, 215–220, 222, 227–230, 232, 233
Acetonitrile, 343, 364, 365
Acid, 14, 84, 107, 136, 257, 284, 286, 291–298, 302, 303, 306–308, 319, 321, 323, 329, 340, 376, 418, 459
Acid catalysts, 41, 95, 213, 294, 296, 321
Acid catalyzed, 430
Acid hydrolysis, 329, 340, 386, 419–421, 424, 425, 429, 440
Acidification, 151, 160, 185, 189, 467, 469, 471
Acidities, 39, 42, 54, 57, 58, 60, 61, 84, 85, 87, 88, 91, 95, 96, 291, 418, 430
Acidogenesis, 14, 142, 144, 151, 181, 182, 186, 195, 215, 221, 222, 225
Acidogenic bacteria, 148, 151, 186
Acid sites, 87, 91–93, 96, 291
Activated carbons, ix, 39, 77, 82, 85–93, 146, 422, 464
Activating agent, 330
Activation energies, 49, 94, 95, 289, 290, 294, 295, 299, 301, 302, 305, 306
Active sites, 41, 54, 55, 64, 91, 144, 247, 260, 264, 267, 324, 332
Activities, 5, 16, 41, 76, 92, 94, 95, 102, 112, 118, 126, 166, 181, 183, 186, 194, 217, 256, 257, 259, 261, 263, 264, 269, 271, 287, 291–293, 297, 298, 306–308, 323, 329, 330, 381, 386, 390, 393, 394, 422, 430, 455
Additives, 7, 8, 78, 96, 102, 188, 267, 270, 284, 301, 364, 365, 400, 428, 477, 479
Adenosine triphosphate (ATP), 18, 145, 461
Adipic acid, 307
Adsorbent, 83, 85, 327–328, 332, 340, 422, 429, 437, 476
Advanced treatment, 4
Aerobic composting, 15–16
Aerobic fermentation, 4, 14, 20
Aglycone, 434
Agricultural, vii, 4, 8–9, 14, 15, 35, 49, 136, 160, 174–178, 188, 190, 196, 206–208, 210, 213, 217, 219, 220, 226, 227, 233, 249, 255, 269, 271, 272, 340, 349, 358, 360, 416, 419, 454, 455, 458–461, 463, 465, 472, 474, 477–480
Agricultural and forestry solid waste, 8–9
Agricultural industries, 136, 416, 465
Agricultural residue, 35, 206–208, 210, 211, 213, 217–220, 223, 226, 227, 233, 472, 474, 478–480
Agricultural waste, vii, 4, 174–178, 188, 208, 249, 255, 269, 273, 340, 349, 419, 454, 455, 458–461, 463, 465, 477

- Agriculture, 7, 15, 86, 160, 174, 176, 375, 416, 417, 458–460, 480
 Agro-industrial, 160, 162, 164, 440
 Agro-industrial bagasse, 432
 Agro-waste, 416–418, 438
 Agro-waste processing, 416
 Alcohols, 12, 17, 39, 41, 52, 94, 107, 181, 208, 249, 260, 261, 264, 287, 298, 301–302, 304, 306, 323, 344, 348, 355, 388, 393, 396, 428, 431, 433, 435, 437
 Alcoholysis, 17, 301, 304, 427, 428
 Aldehyde, 39, 41, 263, 342, 349, 433, 475
 Aldol addition reaction, 349
 Aldol condensation, 42
 Aldose, 349
 Aldose-ketose isomerization reaction, 349
 Alfa-dicarbonyl cleavage reaction, 349
 Algae, 13, 136, 271, 352, 358, 359, 378, 379, 384–387, 392–396, 400
 Algal biomass, 388, 394
 Algal cultures, 271, 274
 Alkali hydrolysis, 190, 381
 Alkaline, 54, 55, 78, 151, 158, 160, 164, 258, 269, 294, 295, 298, 319, 395, 396, 434, 436, 438, 440
 Alkaline and alkaline earth metals, 54, 55
 Alkaline earth, 78
 Alkaline extraction, 395, 434
 Alkaline pretreatment, 213, 228
 Alkalinity, 137, 139–141, 144, 148–150, 152, 159, 164, 175, 184, 388
 Almond, 49, 87, 439
 Almond tree, 439
 Aluminum, 8, 55, 122, 468
 Amino acids, 14, 140, 214, 342, 354, 359, 361, 362, 459, 461
 Aminolysis, 17, 286, 298–301
 Ammonia, ix, 17, 137, 139, 141, 149, 150, 177, 188, 261, 298, 299, 302, 342, 344–349, 361, 362, 365, 376, 461, 477, 478
 Ammonia-water, 341, 347, 348, 362, 363
 Ammonolyis, 298
 Amorphous cellulose, 208, 440
 Amylase, 181, 215, 384–386
 Anaerobes, 140, 150, 181
 Anaerobic co-digestion, 477
 Anaerobic digester, 176, 178, 183, 187, 189
 Anaerobic digestion (AD), ix, x, 14–15, 19, 136, 137, 142, 150, 158, 174–197, 208, 209, 214, 221, 222, 224, 225, 232, 233, 359, 361, 396, 416, 423, 454, 465, 466, 471–473, 477–480
 Anaerobic digestion effluent, 479
 Anaerobic digestion technologies, x
 Anaerobic fermentation, 4, 14, 20, 136–164
 Anaerobic microorganisms, 15, 136, 160, 164
 Anaerobic sludges, 151, 181, 223, 225, 231, 232, 467
 Animal husbandry, 8
 Animal manure, 8, 9, 13–15, 136, 160, 175, 454, 458, 460, 461, 468, 471, 472, 474, 480
 Animal manure waste, 8, 9
 Antennae, 255, 271
 Antioxidant, 102, 103, 107, 116–125, 272, 393–395, 422, 428, 434, 437
 Antioxidant capacity (AOC), 110, 116–126
 Apple, 418–420, 422, 434, 435
 Apple pomaces, 418–420
 Applications, ix, 7, 9, 11, 12, 17, 18, 39–42, 56, 59, 78, 86, 87, 126, 137, 152, 157–164, 174, 176, 184, 190, 247, 250, 251, 254–273, 284, 286, 302, 307, 308, 318, 319, 326, 328, 330, 332, 340, 342, 345, 365, 377, 393, 395, 417, 434, 469, 471, 472, 474, 475, 477–480
 Apricot, 435
 Aqueous, 16, 17, 41, 53, 56, 213, 255, 261, 263, 293, 294, 302, 303, 346, 349–351, 363, 382, 423, 429, 435
 Arabinan, 437, 438
 Arabinose, 9, 138, 269, 436
 Archaea, 148, 151, 183, 226, 256
 Aromas, 424, 433
 Aromatic, 37, 39, 41, 42, 44, 52, 55, 56, 58, 61, 64, 78, 84, 91–96, 249, 254, 260, 271, 273, 284, 286, 296, 298, 299, 302, 304, 307, 349, 355, 364, 437
 Aromatic biopolymer, 437
 Aromatic compounds, 42, 93, 137, 260, 342
 Aromatic hydrocarbons, 41, 52, 90, 92, 93, 95, 96, 249
 Aromatization, 42, 43, 58, 84, 85, 92, 94, 96
 Artificial neural networks, 185, 427
 Ash Content, 8, 35, 84, 95
 Aspen PlusTM, 391
Aspergillus foetidus, 419, 421
 Attapulgite, 39, 41, 56, 57, 60
 Auger, 38, 60, 61
 Auger reactors, 38, 39, 60, 61, 64
Aurantiiflora, 435
Aurantiochytrium, 360–362
 Autoclaves, 38, 178, 285, 300, 346, 347, 400, 439, 440
 Autohydrolysis, 440
 Automotive, 7, 302
 Autotrophic microalgae, 359

- B**
- Bacillus*, 142, 144, 181, 209, 223, 231, 264, 265, 297, 386
- Back-pressure, 106
- Back pressure regulator, 106
- Bacteria, 14, 15, 142, 144, 145, 148, 152, 158, 176, 181, 183, 186–188, 190, 193, 214, 215, 217, 220, 222, 224, 227, 256, 258, 297, 304, 307, 387, 388, 398, 429
- Bacteria and yeast monocultures, 357, 364
- Baeyer-Villinger MonoOxygenases (BVMOs), 262–263
- Bagasse, 8, 44, 87, 136, 160, 207, 211, 213, 320, 327, 434, 437–440
- Ball mill, 327, 329
- Bamboo, 48, 87, 94, 108, 117, 118, 121, 122, 125, 321, 322, 327, 440
- Bamboo leaves, 118
- Bamboo powder, 321, 322
- Bamboo sawdust, 94
- Banana, 177, 417, 434, 438, 440
- Banana peel, 417, 440
- Barley straw, 176, 207–211, 218, 229
- Base, 92, 137, 148, 291, 299, 325, 349, 350, 353, 354, 423, 427, 428, 430, 438
- Base catalyst, 92, 352, 354, 430
- Base nanomaterial, 252
- Batch, 83, 152, 163, 165, 179, 180, 193, 346, 347, 354, 363, 398, 429
- Batch reactor, 44, 83, 163, 165, 354
- Bed material, 296, 476
- Bentonite, 39, 41, 60
- Benzene, 56, 78, 260, 297, 303
- Benzylidic rearrangement reaction, 349
- Beta-cryptoxanthin, 433
- Beta-elimination reaction, 349
- β-glucosidase, 211, 212, 215, 385, 386, 390, 396
- Binder, 301, 327
- Biobutanol, 216, 220
- Biocatalyst, 16, 246, 254, 256, 263, 265, 387
- Bio-char, 9, 35, 37–39, 41, 84, 87, 95, 161, 321, 327–331, 340, 416, 464, 469, 478
- Biochemicals, x, 9, 14–17, 19, 136, 178, 181, 185, 206, 257, 259, 297, 354, 375, 382, 432–440, 454, 460, 465, 472, 477, 480
- Bio-components, 436
- Biocrude, 357, 358, 361, 364
- Biodegradability, 304, 477, 479
- Biodegradable waste, 174, 462, 464, 467, 468, 471, 477
- Biodegradation, vii, ix, 18, 206–209, 211, 213, 216, 221, 225, 227, 228, 233, 267, 297
- Biodiesel, 140, 249, 272, 357, 375–377, 418, 422, 423, 427–432, 440–442
- Bioenergy, 140, 340, 378, 400, 460
- Bioethanol, 136, 267, 375–379, 382, 383, 385–390, 396, 398–400, 418–420, 423–425, 427, 429, 440–442
- Bioflavonoids, 432–435, 437, 442
- Biofuel, 4, 35, 174, 257, 258, 264, 271, 273, 319, 321, 360, 375, 417, 458
- Biofuels production, 264, 418
- Biogas, 9, 11, 14, 15, 138–141, 174–197, 212–214, 226, 231, 232, 359, 375, 416, 418, 460, 464–466, 471, 472, 477, 478, 480
- Biological, ix, xii, 15, 20, 126, 151, 164, 188, 190, 192, 210, 212, 246, 257, 258, 273, 319, 375, 381, 384, 391, 400, 418, 433, 438, 439, 457–459, 462, 464, 467, 468, 478, 480
- Biological pretreatments, 176, 190, 215, 477
- Biomass, 8, 34, 77, 102, 135, 188–191, 213, 250, 255, 259, 260, 267, 268, 271, 304, 306, 308, 319–326, 328–330, 332, 340, 375, 417, 459
- Biomass composition, 35
- Biomethanation, 14–15
- Biomolecules, 348, 357
- Bio-oil, 11, 13, 35, 37–42, 44, 50, 54–61, 64, 82, 340–342, 358, 359, 361, 468, 469, 475
- Bioplastics, 224, 257
- Biopolymers, 43, 352–358, 442
- Bioprocesses, 272, 274
- Bioproducts, 377, 387, 391, 395, 400, 460
- Bioreactor design, 273
- Biorefineries, vii, x, 266, 267, 269, 274, 321, 340, 353, 365, 373–401, 417–418, 433, 466
- Bioresources, 246–274
- Biwastes, 136, 138, 140, 142, 151, 159–162, 164, 165, 247, 267, 274
- Bis(2-aminoethyl)terephthalamide (BAET), 299, 300
- Bitter orange, 435
- Bitumen additives, 301
- Boilers, 10, 40, 41, 174, 463
- Boiling point curve, 341
- Bonds, 8, 9, 16, 17, 40, 83, 92–94, 96, 144, 174, 190, 256, 257, 259, 260, 265, 270, 273, 287, 291, 343, 354, 355, 357, 379, 383–387, 435, 436
- Born equation, 343
- Bottom ash, 10, 463, 468, 473, 477

- Bound water, 37
 Bovine serum albumin (BSA), 342, 354, 355, 364
 Branching, 379
 Brazil, xii, 415–442
 Breakage, 17, 40
 Brønsted, 52
 Brønsted acid, 52
 Brunauer-Emmett-Teller Bioconversion Analysis, 85
 Bubbling, 38, 82, 83, 220
 Burning, 86, 463
 Butanol, 13, 213, 215–220, 227, 230, 233, 306
 Butanol toxicity, 219
 By-products, ix, 35, 54, 78, 136, 142, 195, 288, 295, 299, 301, 307, 361, 459
- C**
 Calcite, 39, 41
 Calcium sorbent, 58, 60
 Calorific values, 4, 7, 8, 39, 43, 44, 53, 57, 58, 60, 61, 266, 457
 CaO, 50, 51, 54–63
 Capital costs, 194, 196, 384, 387, 388, 390, 391
 Caprolactone, 262, 263, 307
 Carbohydrates, 39, 95, 138, 140, 141, 144, 160, 164, 206, 213, 214, 225, 259, 269, 319, 340, 342, 349–352, 376, 378, 379, 383, 384, 386, 387, 390, 392, 393, 395, 396, 420, 424, 425, 429, 435, 454, 459
 Carbon dioxide (CO_2), ix, 102, 174, 181, 220, 344, 374, 375, 381, 396, 464, 465, 467–469, 476, 477
 Carbonization, 86, 87, 91, 95
 Carbon monoxide, 392
 Carbon nanotubes, 255, 292, 477
 Carbon neutral resource, 9
 Carbon/nitrogen ratio (C/N), 194
 Carbon scarcity, 308
 Carboxylic acids, 39, 266, 296, 297, 349, 352
 Cardanol, 300
 Carotenes, 422, 432, 433
 Carotenoids, 105, 393, 394, 422, 432–434, 437
 Casein, 364
 Cassava bagasse, 207–209, 211, 218–220, 223, 227, 229–231
 Catalyst, ix, 11–13, 17, 18, 37, 40–43, 45, 46, 49–58, 61, 63–65, 77, 78, 83–95, 247, 263, 265–267, 285, 287, 290–299, 301, 302, 304–307, 321–324, 326–330, 332, 340, 351, 357, 365, 423, 427, 428, 430, 431, 475
 Catalytic co-pyrolysis, ix, 34–65
 Catalytic cracking, 40, 58, 325, 475
 Catalytic effect, 91–94
 Catalytic fast pyrolysis (CFP), 11
 Catalytic oxidation, 340
 Catalytic pyrolysis, 11, 40–43, 45, 49, 52–55, 58–64, 76–96
 Catalytic reactions, 92, 329
 Catalytic upgrading, 41, 478
 Catechins, 101, 107, 122, 434
 Catering industry, 5
 Cathode, 266
 Cellulobiose, 16, 138, 386, 419
 Cellodextrins, 16, 386
 Cellulases, 16, 211, 212, 215, 217, 384–386, 390, 394–396, 419
 Cellulose, 6, 35, 87, 138, 176–178, 181, 184, 189, 190, 206–208, 210, 213–215, 217, 227, 255, 257, 259, 269–271, 319–325, 329, 331, 342, 379, 385, 419
 Cellulose fibers, 207, 270, 271, 440
 Cellulose nanocrystals, 331
 Cellulose nanofibers, 439, 440
 Cell walls, 15, 102, 104, 114, 121, 125, 213, 269, 270, 324, 325, 379–382, 393, 424, 436
 Centrifugal, 39
 Ceramic, 456, 457, 479
 Cetane number, 422, 427
 Charcoal, 55
 Chars, 38, 39, 48, 52, 58, 60, 62, 63, 78, 82, 83, 86, 95, 355, 357, 464, 468, 469, 474, 475, 478
 Chemical composition, 20, 39, 43, 57, 376, 442, 478
 Chemical looping, 476
 Chemical oxygen demand, 137, 163, 191, 214
 Chemical pretreatments, 178, 189, 213–214, 319
 Chemical reactions, 11, 13, 17, 318, 352
 Chemistry, 17, 18, 246, 318, 319, 326, 340, 344, 349–353, 363, 365
 Chemolysis, 4, 17, 20
 Chitin, 17, 249, 270, 342, 357, 362–364
 Chlorophyll, 252, 253, 257, 270, 271, 393, 461
 Chromatography, 52
 Circular economy, 206, 417–418, 460–466
 Citric acid, 179
Citrullus lanatus, 429
 Citrus fruits, 417, 432, 434
 Citrus juice industry, 432
Citrus sinensis, 432
 Citrus wastes, 418, 432, 436, 442

- Climate change, 4, 308, 374, 418, 460, 461
Clostridium, 142, 144, 152, 181, 209, 215, 217, 219, 220, 227, 229, 230, 233, 297
Coals, 8, 39, 48, 86, 340, 374, 464
Cobalt, 292
Cocoa, 432
Coconut husks, 364
Co-culture, 421
Co-digestion, 160–165, 177, 178, 188, 196, 477, 479
Cofactor dependent enzymes, 261–266
Co-fermentation, 388, 390–391, 398
Coffee, 439
Coffee residues, 439, 440
Coke, 12, 13, 41, 49, 50, 54, 55, 85, 94, 329
Cold filter plugging point, 422
Cold flow, 427, 430
Cold pressing, 433
Combined heat and power (CHP), 174
Combustible, 331
Combustion, 8, 10–11, 35, 37, 39, 58, 60, 136, 137, 264, 355, 423, 430, 464, 469, 475
Commercialization, 233, 400, 424, 478
Commercial scale, x, 39, 59, 195, 274
Complexes, 4, 5, 8, 9, 11, 12, 16, 39, 40, 52, 135, 177, 181, 185, 190, 206, 211, 214, 246, 248, 252–254, 258, 259, 273, 288, 292, 293, 305, 306, 318, 319, 325, 326, 332, 355, 377, 390, 394, 396, 423, 424, 436, 459, 476
Composites, 297, 323, 327–331, 417, 427
Composting, 9, 15, 19, 213, 284, 417, 423, 454, 457, 462, 463, 468, 469, 471–473, 475, 478, 480
Composts, 16, 174, 196, 297, 462, 463, 469, 471–473, 480
Comprehensive model, 185
Compression, 17
Concerted mechanisms, 11
Concerted reaction, 11
Con-condensable, 58
Conduction, 247, 251, 274, 285, 293
Conductivity, 330, 463, 472
Coniferyl alcohol, 355, 437
Consolidated bioprocessing (CBP), 219, 227, 229, 232, 233, 388, 391
Consortia, 183, 224, 233, 391
Constant extraction rate step (CER), 114, 116, 125
Construction, 5, 7, 8, 19, 301, 417, 461, 468
Consumers, 7, 20, 136, 394, 432
Convection, 285, 440
Conventional pyrolysis, 4, 41, 44, 45, 64, 91, 469
Conventional treatment, 4
Conversion efficiency, x, 454, 457, 469, 480
Conversions, vii, ix, x, 4, 12–16, 18, 20, 48, 49, 81, 94, 135, 136, 144, 148, 164, 187, 193, 195, 196, 206, 207, 227, 246, 248, 249, 251, 252, 254, 256, 257, 260–267, 269, 273, 274, 284, 286, 288, 289, 292, 295, 298–300, 304, 305, 307, 319, 321–325, 332, 340, 342, 349–353, 357, 375, 376, 387–391, 393, 396–400, 430, 431, 454, 460, 464, 465, 471, 472, 474–480
Co-pyrolysis, 40, 44, 45, 47–49, 51–55, 57–64, 77, 94–96
Corn, 54, 87, 92, 94, 176, 207, 208, 210, 218, 230, 233, 306, 324, 375, 439, 459
Corn husk, 439, 440
Corn stover, 54, 92, 94, 176, 177, 179, 184, 190, 192, 193, 207–211, 218, 223, 229, 231, 233, 324, 459, 473
Corn straw, 180, 190, 193, 440
Correlation, 422
Corrosion, 294, 300, 474, 475
Corrosiveness, 41, 475
Cortex, 434
Co-solvent, 105–107, 110, 117–119, 121, 122, 125, 126
Cotton, 190, 206, 208, 213, 214, 417, 439
Cotton fibers, 209, 218, 228
Coumaric acid, 434
Coumaryl alcohol, 437
Cracking, 11–13, 37–39, 42, 43, 50, 52, 56, 61, 84, 85, 87, 92, 94, 96, 464
Cresol, 118
Critical point, 104, 301, 341
Critical pressure, 12, 104, 126, 301
Crop residue, 14, 15, 176, 454, 458, 459, 471, 477
Crop waste, 417
Crotonic acid, 308
Crudes, 34, 40, 264, 340, 342, 358, 374
Crushing, 189
Crystallinity, 17, 188, 189, 213, 297, 298, 319, 320, 330, 363, 365, 439, 440
Crystallinity index, 320, 440
Current density, 331
Cutinases, 297, 298
Cyclic hydrocarbons, 44, 56–58, 352
- D**
- Databases, ix, 19
Deactivation, 12, 40, 41, 77, 84, 85, 148, 251, 252, 260
Deamination reaction, 358
Decarbonylation reaction, 358

- Decarboxylation, 37, 51, 56, 58, 60, 264, 265, 296, 358
 Decarboxylation reactions, 50, 51, 58
 Dechlorination, 83, 96, 295
 Decomposition, 10, 11, 13, 15, 18, 47, 48, 50–52, 81, 94, 121, 125, 195, 206, 349, 352–355, 359–361, 363, 458, 472
 Deep eutectic solvents, 287, 290, 291, 293, 301, 302, 435
 Defatted microalgae, 342, 358–362
 Degradation, 4, 11, 13, 17, 18, 20, 40, 83, 84, 94, 95, 140, 151, 159, 160, 164, 175, 184, 189, 190, 195, 206, 213–215, 225, 256, 257, 263, 265, 270, 284, 295–297, 299, 301, 303, 305–307, 319, 325, 328, 330, 384, 419, 436, 459, 463, 465
 Dehydration, 11, 37, 50, 51, 94, 95, 319, 321, 323, 326, 332, 349, 351, 352
 Dehydrogenation, 93, 144, 181, 260, 324
 Demineralization, 225
 Demonstration scale, 59
 Densities, 39, 55, 78, 87, 104, 105, 114, 119, 121, 124, 179, 192, 210, 341, 343, 345, 349, 351, 352, 381, 422
 Deoxygenation, 40–42, 50, 54, 55, 58, 94
 Depolymerization, 17, 48, 51, 52, 56, 95, 256, 324–326, 342, 354
 Derivative thermogravimetry, 47
 Devolatilization, 38, 40, 43, 47–52, 54, 82, 91, 96
 D-fructose, 349, 351, 352
 D-glucose, 8, 349, 351, 352, 379, 386, 439
 Dicarbonyl cleavage reaction, 349
 Dielectric constant, 105, 343, 344, 381
 Diethyl terephthalate, 304
 Diffusion, 54, 55, 114, 115, 121, 125, 148, 290, 294, 327, 330
 Diffusion controlled (DC) step, 114
 Diffusivity, 104, 105, 343
 Digestates, 174, 175, 177, 460, 464, 465, 471–473, 477–480
 Digesters, 177, 183–185, 187, 193, 196
 Digestion time, 190, 477
 Dihydroxyacetone, 352
 Dilute acid, 189, 220, 228, 379, 386, 390
 Dilution, 419
 Dimers, 53, 56, 258, 259, 288–290, 299, 302
 Dimethyl terephthalate (DMT), 284, 301, 302, 304
 Dioxins, 10, 13, 45, 95, 463, 468, 470, 475
 Discarded branches, 8
 Dispose, 7
 Dissolution, 112, 114, 118, 286, 294, 296, 301
 Distillation, 125, 224, 293, 297, 419, 433
 Distributed activation energy model (DAEM), 49
 Dolomite, 39, 41, 42, 56, 57, 60, 65
 Douglas fir, 51, 320
 DPPH radical-scavenging assay, 118
 Drop-in fuels, 45, 64
 Dry basis, 6, 7, 206, 207, 432
 Drying, 37, 357, 423, 427
 Durability, 7, 76
 D-xylose, 352
 Dye, 6, 7, 257, 261
- E**
- Easetech, 19
 Easewaste, 19
 Eco-friendly, 9, 20, 319, 384, 400, 416, 435, 461
 Ecoinvent, 19
 Economic, 3, 9, 19, 20, 34, 95, 174, 196–197, 220, 222, 227, 228, 233, 293, 319, 374, 419, 422, 457, 461, 464, 480
 Economic analysis, vii, 220
 Economic benefit, 465
 Economic factors, 293, 319, 457
 Ecosystem, 7, 8, 246, 273, 379, 467
 Efficiencies, ix, 17, 40, 44, 52, 93, 95, 151, 181, 183, 186, 187, 189, 191, 246, 257, 264–266, 327, 328, 360, 365, 375, 382, 383, 386, 387, 390, 391, 393, 394, 400, 419, 435, 461–463, 465–469, 471, 474, 476, 478–480
 Electric fields, 179, 192, 379, 382, 383
 Electricity, 4, 10, 18, 39, 78, 178, 196, 197, 251, 416, 423, 462, 463, 465–467, 469, 471, 476
 Electrocatalysis, 328, 340
 Electrodes, 87, 250, 266, 327, 330–332
 Electrodialysis (ED), 224, 225
 Electromagnetic frequencies, 213
 Electromagnetic waves, 213
 Electron acceptors, 136, 251, 256, 259, 260
 Electron donors, 136, 181, 246, 251, 252, 255, 257, 258, 266, 267, 269, 274
 Electronics, 5, 7, 42, 247, 252, 274, 302
 Electron transfer, 146, 164, 246, 248, 251, 252, 254, 255, 257–259, 266, 330
 Electron transfer kinetics, 330
 Elemental Analysis, 137
 Emissions, 13, 15, 19, 35, 39, 42, 76, 174, 250, 251, 255, 260, 374, 375, 424, 430–432, 454, 458, 460, 461, 467–480

- Empirical models, 185
Enantiomers, 224, 304
Endo-glucanases, 256, 386
Ene-reductases, 265–266, 273
Energy, 4, 34, 77, 174, 206, 210, 214, 221, 225, 227, 246, 247, 251, 252, 257, 259, 261–263, 265–267, 272, 273, 284, 285, 297, 305, 306, 318, 320, 330, 332, 340, 374, 419, 454
Energy balance, 61, 345
Energy consumption, 18, 136, 320, 384, 433, 434, 461
Energy storage, 330, 375, 379
Engineering, x, xii, 136, 175, 183–184, 197, 262, 272, 273, 319, 341
Enterococci, 222
Entrained flow reactor, 38
Environmental, 4, 34, 77, 102, 152, 174, 221, 250, 255, 291, 292, 302, 304, 360, 374, 416, 454
Environmental impacts, 19, 34, 35, 225, 304, 324, 457, 461, 466–474
Environmentally friendly, 34, 35, 77, 86, 102, 126, 318–321, 375, 394, 416, 428, 478
Environmental pollution, 4, 7, 42, 174, 459, 475
Environmental sustainability, x, 454, 460–474, 480
Enzymatic, 4, 215, 284, 297, 298, 319, 321, 376, 418
Enzymatic hydrolysis, x, 4, 14, 16, 20, 189, 211, 215–217, 219–221, 228–232, 264, 269, 298, 319, 321, 376, 379, 381–388, 391, 394–396, 399, 400, 419
Enzymatic pretreatments, 190
Enzymatic processes, 319, 434, 440
Enzymatic saccharification, 382, 384, 388, 390, 396, 400, 419, 420, 424, 425
Enzyme-catalyzed, 427, 428
Enzymes, 14–16, 151, 176, 183, 186, 190, 211, 213, 215, 219, 246–249, 252, 254, 256–267, 269–274, 285, 294, 297, 298, 307, 319, 321, 332, 354, 381–388, 390, 391, 395, 396, 398–400, 427, 428, 440
Epidermal system, 102, 103
Epoxy resins, 13
Equilibrium, 105, 114, 115, 151, 264, 285, 287, 288, 290, 291, 295, 299, 341
Equivalence, 155
Escherichia coli, 217, 219, 263, 297, 305, 387, 389, 418, 425
Essential oils, 418, 433, 437, 442
Esterification, 40, 422, 430, 431, 475
Esterification degrees, 436
Ester, 39, 41, 58, 109, 262, 264, 287, 291, 302, 307, 331, 357, 418, 427, 428, 430, 431, 433, 475
Ethane, 39
Ethanol, 16, 19, 105, 107, 110, 117, 118, 121, 122, 125, 126, 139, 142, 160, 181, 211–213, 215, 216, 219, 220, 274, 294, 295, 298, 304, 306, 308, 328, 378, 381, 384, 385, 387–391, 393, 396–400, 418, 419, 423, 424, 429, 434–439
Ethanolamine, 299, 300
Ethylbenzene, 260, 261
Ethylene, 17, 77, 284–299, 301–303
Ethylene diamine, 299
Ethylene glycol, 17, 285–297, 301–303
Eugenol, 107, 109, 110
Euglena gracilis, 360
Euryarchaeota, 226
Eutrophication, 393, 467, 469, 471
Evaporation, 136, 377, 382
Evaporation model, 136, 377, 382
Exhaust gases, 10, 480
Exo-glucanase, 385
Ex situ, 11, 40, 41, 84, 88, 89, 92
Ex-situ catalytic fast pyrolysis (Ex situ CFP), 11
Extracellular polymeric substances (EPS), 6, 77
Extraction curves, 112, 114–116, 125
Extractions, ix, x, 34, 101–126, 136, 140, 220, 225, 325, 374, 376, 379–383, 386, 396, 400, 423, 428, 429, 432–440, 442, 468
Extractor, 106, 112
- F**
- Falling extraction rate step (FER), 114, 116, 125
Fast pyrolysis, 11, 38–41, 44, 45, 49, 56, 340, 464
Fatty acid esters, 58, 270, 357, 428
Fatty acid methyl esters, 357
Fatty acid photodecarboxylases (FAPs), 263–266
Fatty acids, 14, 58, 109, 136, 139, 142, 248, 249, 263–265, 268, 270, 271, 357, 378, 394, 418, 422, 424, 429, 439
Feed/inoculum ratio, 194
Feedstock, 11, 34, 78, 160, 175, 206, 208, 213, 216, 217, 226, 227, 233, 252, 266, 304, 323, 340, 375, 419, 456
Feedstock availability, 196
Fenton oxidation, 18–20
Fermentable sugar, 214, 384, 390, 419

- Fermentation, ix, x, 19, 136–152, 157–162, 164, 165, 189, 195, 206, 207, 210, 214–225, 227, 229, 232, 233, 257, 266, 304, 376, 381, 382, 384, 386–391, 396–399, 418–420, 422–425, 429, 433, 440, 454
- Fertilizer, 9, 15, 16, 19, 39, 78, 102, 174, 177, 196, 358, 377, 393, 416, 423, 424, 453–480
- Fixed bed reactor, 44, 55, 56, 60, 61, 64, 91
- Fixed carbon, 7, 35, 37, 39, 78, 80, 459
- Flame, 327, 331
- Flame-retardant, 327, 331
- Flash pyrolysis, 11, 38
- Flavan-3-ol, 434
- Flavanone, 434
- Flavone, 442
- Flavonoids, 102, 105, 107, 110, 122–124, 435, 439
- Flax, 417
- Flow, 11, 12, 19, 38, 39, 82, 83, 106, 112, 114, 118, 120, 151, 152, 156, 216, 221, 222, 342, 346, 347, 351, 357, 382, 427, 430
- Flowers, 434
- Flow reactors, 38, 156, 351, 357
- Flue gases, 10, 77, 328, 378, 463, 468, 469, 473, 474
- Fluid catalytic cracking (FCC), 40, 41
- Fluidized bed reactors, 12, 39, 40, 60, 476
- Fly ash, 10, 463, 469, 477
- Folin-Ciocalteu method, 121
- Food, 4, 102, 135, 174, 206–208, 210, 221, 224, 233, 270, 284, 342, 375, 454
- Food waste (FW), 19, 136, 159–161, 164, 165, 175, 178, 194, 206, 208–210, 212, 213, 223, 224, 226, 227, 230, 231, 233, 249, 272, 416, 457, 459
- Forestry, 8, 35, 49, 459, 479
- Formaldehyde, 352
- Formate, 17, 263, 292, 293, 364, 365
- Formic acid, 139, 340, 353, 365, 438
- Fossil fuels, 20, 34, 35, 42, 45, 77, 174, 284–308, 374, 375, 393, 418, 454, 460, 461
- Fossil sources, 332
- Foul odors, 10
- Fragmentation, 255, 357
- Fragrance, 433
- Frameworks, 20, 255
- Free energy, 288
- Free-radical, 11
- Frequency, 16, 213, 383
- Friction, 332
- Fructose, 138, 321, 342, 398
- Fruit, x, 87, 159, 208, 440–442
- Fruit pomace, 434
- Fruit pulp, 435, 436
- Fruit residues, 418, 433, 442
- Fruit seeds, 442
- Fruit waste (FW), x, 159, 165, 416–418, 432–442
- Fuels, vii, ix, 4, 8, 20, 34, 39–45, 58, 60, 61, 64, 77, 78, 84, 92, 196, 266, 284, 319, 322, 332, 340, 357, 374–377, 383, 395, 424, 427, 430, 437, 455, 457, 464, 465, 469, 471, 474–476, 480
- Functional carbon materials, 319, 327, 332
- Functional groups, 86, 91, 92, 95, 96, 136, 255, 327, 328, 330, 331
- Fundamental tissue system, 102
- Fungi, 142, 190, 215, 258, 270, 388, 398
- Furan, 41, 94–96, 195, 468, 470, 475
- Furfurals, 41, 189, 213, 321, 322, 326, 332, 352
- Furnaces, 10, 463
- Fusarium oxysporum*, 419, 421
- G**
- GaBi, 19
- Galactan, 393, 437
- Galactose, 8, 269, 386, 394, 396, 436
- Galacturonic acid, 436
- Gallic acid, 109, 121
- Garden wastes, 178, 471
- Gas, 10, 34, 35, 37, 39–41, 44, 46, 50, 53, 56, 58, 60, 62, 63, 76, 102, 140, 174, 206, 220, 225, 226, 229, 230, 250, 292, 294, 296, 298, 302, 328, 361, 374, 456
- Gas chromatograph, 38, 52
- Gas chromatography mass spectrometry (GCMS), 38, 52
- Gas discharge lamps, 250
- Gas flow, 11, 38
- Gasification, x, 4, 9, 12–13, 19, 20, 35, 39, 355, 454, 460, 464, 465, 468–471, 473, 475–476, 478–480
- Gasoline, 64, 424
- Gas products, 11, 475
- Gas purification, 15
- Gas residence time, 53
- Gas stripping, 220, 229, 230
- Gas turbine, 469, 476
- Glass, 5, 6, 78, 208, 250, 302, 379, 382, 383, 421, 455–457, 468, 479
- Global warming, 4, 306, 454, 467, 471
- Glucan, 322, 394, 437

- Glucose, 8, 14, 16, 138, 139, 141, 181, 213, 214, 230, 262, 267, 269, 273, 321, 329, 342, 352, 359, 360, 379, 383–388, 391, 393, 394, 396, 398, 435, 439, 440
- Glyceraldehyde, 352
- Glycerol, 14, 17, 140, 142, 165, 260, 264, 435
- Glycolaldehyde, 352
- Glycolysis, 17, 284–293, 301, 304, 398
- Grape, 35, 47, 49–51, 55, 56, 58, 60, 61, 64, 65, 87, 417, 423–428, 434
- Grapefruit, 435–437
- Grapefruit peels, 435
- Grape pomaces, 423–428
- Grape seed (GS), 35, 47–52, 55–65, 423, 424
- Graphene, 146, 291, 292, 477
- Graphitic carbon, 83
- Grasses, 6, 178, 208, 267, 270
- Green chemistry, 433
- Greenhouse gas (GHG), x, 19, 197, 374, 454, 461, 468, 469, 472, 477, 479
- Greenhouse gas emissions (GHG emissions), 16, 19, 34, 35, 44, 76, 174, 206, 298, 465, 467–469, 471–474
- Green marine alga, 357, 364
- Grinding, 17, 210, 213, 230, 318, 319, 321, 324
- Guaiacols, 41
- Guaiacyl, 269, 437
- Guavas, 432
- H**
- H-abstraction, 257
- Hardwood, 439
- Harvest, 207, 222, 284
- Hazards, 7, 302
- Heat, 4, 9, 10, 13, 19, 37, 39, 56, 60, 78, 83, 151, 158, 160, 174, 196, 197, 220, 251, 264, 285, 292, 343, 346, 359, 360, 382, 417, 460, 462–465, 468, 469, 475, 476
- Heat capacity, 343
- Heating, 8, 11, 35, 38, 39, 41–43, 46–49, 57, 60, 81, 91, 147, 151, 174, 175, 196, 251, 285, 297, 305, 306, 308, 340, 341, 346, 347, 352–355, 357, 358, 363–365, 382, 422, 435, 436, 454, 463, 464, 469
- Heating rates, 11, 35, 38, 39, 41, 46–49, 53, 60, 81–83, 297, 342, 352–358, 363, 365, 464
- Heating values, 8, 39, 40, 42, 43, 57, 78, 196, 422, 454, 463, 464, 469
- Heat transfer, 13, 38, 39, 60, 83, 285
- Heavy metals, 7, 16, 78, 290, 327, 429, 456, 463, 468, 469, 474
- Heavy polycyclic aromatic hydrocarbons, 37
- Hemicelluloses, 8, 9, 35, 47, 48, 51, 138, 160, 176–178, 184, 189, 190, 210, 214, 233, 249, 269, 319, 321, 324, 355, 379, 386, 388, 390, 393, 419, 432, 439, 440
- Hemp, 417
- Hesperetin, 434
- Hesperidin, 432–435
- Heteroatoms, 45, 86, 95, 329, 331, 332
- Heterocyclic compounds, 362
- Heterogeneous, 17, 47, 85, 185, 291, 293, 321, 329, 430, 436
- Heteropolysaccharides, 393
- Hexoses, 138, 141, 390, 391, 399, 436
- Hierarchical, 328
- High density polyethylene (HDPE), 42, 47, 49, 51–55, 77, 79, 80, 94
- Higher, 78
- High heating rates, 11, 464
- High heating value (HHV), 7, 8, 37, 57–59, 62, 63, 78–80, 94
- High-income, 6
- High pressure hydrodeoxygenation (HDO), 40
- High-pressure-water, 351
- High shear dispersion, 433
- High voltage electricity, 435
- Holocellulose, 87
- Homogalacturonan units, 436
- Homogeneous, 17, 92, 105, 106, 263, 266, 293, 303, 321, 332, 427, 428, 430
- Homopolymer, 439
- Hot water, 178, 302, 303, 306, 307, 341, 436, 438
- Households, 5, 6, 159, 161, 210, 272
- Husks, 432
- Hybrids, 161, 259, 263
- Hydraulic retention time (HRT), 150–152, 155–157, 187, 191, 194, 226, 477
- Hydrocarbon pool, 42
- Hydrocarbons, 12, 53, 54, 61, 77, 78, 82–84, 91–94, 96, 264, 272–273, 344, 429, 430, 465
- Hydrochar, 360
- Hydrochloric acid, 211, 231, 436
- Hydrocracking, 44, 56, 59
- Hydrocyclization, 56, 58, 59
- Hydrodeoxygenation, 44, 56, 58–60
- Hydrogen (H_2), 4, 137–152, 181, 215, 220, 250, 252, 257, 265, 287, 291, 321, 322, 332, 343, 431, 468
- Hydrogenation, 56, 94, 96, 181, 322, 324, 326, 332, 357
- Hydrogen-rich, 94

- Hydrogen transfer reaction, 42, 48, 51, 52, 54, 84
 Hydrolases, 142, 181, 269, 297
 Hydrolysates, 161, 162, 218, 220, 233, 255, 267, 385, 397, 398
 Hydrolysed, 294, 297, 303
 Hydrolysis, 13, 14, 16, 17, 142–144, 151, 157, 181, 182, 185, 186, 188, 189, 195, 214, 215, 219, 222, 229, 230, 284–286, 293–298, 302, 303, 305–307, 319–324, 326, 329, 332, 343, 354, 357, 358, 363, 380, 381, 384, 386–391, 394, 395, 398, 399, 418, 419, 424, 436, 439
 Hydrophobic extractives, 140
 Hydrothermal, 4, 41, 136, 191, 214, 226, 228, 255, 269, 319, 325, 340, 381
 Hydrothermal carbonization (HTC), 360
 Hydrothermal gasification, 12, 13, 361
 Hydrothermal liquefaction (HTL), 13, 342, 357, 358, 361
 Hydrothermal pretreatment (HTP), 191, 214, 228, 398
 Hydrothermal treatment, 4, 342, 348, 351–354, 357, 359–363, 365
 Hydroxyacetaldehyde, 41
 Hydroxyacetone, 41
 Hydroxyalkanoates, 285
 Hydroxymethylfurfural (5-HMF), 321, 322, 326, 332, 349, 352
 HZSM-5, 49, 51, 54
- I**
 Ilmenite, 39, 41, 56, 57
 Impaction, 17
 Inactivation, 257
 Incineration, 4, 9–13, 19, 20, 42, 77, 174, 359, 454, 456, 457, 461–465, 468, 469, 471, 473, 474, 478, 480
 Indispensable, 7, 184
 Indole, 362
 Industrial, ix, x, 3, 5, 7, 35, 41, 53, 59, 60, 76, 77, 83, 93, 136, 160, 164, 174, 175, 178, 189, 190, 215, 216, 220, 222, 250, 251, 257, 258, 260, 262, 265, 270, 273, 274, 319, 361, 378, 387, 398, 400, 416–418, 424, 432, 437, 440, 454, 455
 Industrial juices, 220
 Industrial revolution, 3
 Industrial-scale plants, 60
 Inert atmosphere, 11, 87
 Ingredients, 8, 376, 435
 Innovative production, 416
- Inoculation, 184
 Inoculum, 151, 184, 185, 193, 232, 420
 Inorganic compounds, 78, 464
 Inorganics, 5, 6, 8, 35, 37, 41, 77, 78, 83, 87, 208, 327, 376, 377, 465, 467, 468, 475, 479
 Inputs, 19, 147, 185, 191, 221, 225, 246, 257, 267, 332, 391, 424, 455, 461
 In-situ, 11, 40, 42, 44, 84, 220, 221, 227, 252, 255, 257, 260, 261, 263, 301, 427, 428
 In-situ catalytic fast pyrolysis (In situ CFP), 11
 Interactions, 44, 47, 48, 52–54, 85, 95, 121, 125, 184, 213, 214, 254, 292, 326–328, 477
 Intermediate pyrolysis, 11
 Internal, 54, 55, 83, 213, 328, 360, 432
 International Association for the Properties of Water and Steam (IAPWS), 344, 345
 Iodine value, 422, 428
 Ionic liquids, 189, 287, 292, 293, 296, 298, 304, 306, 307, 430
 Ion product, 343
 Irradiation, 18, 250, 251, 260, 265, 266, 383, 437
 Isolation, 272, 433, 435, 437, 439
 Isomerization, 11, 13, 84, 265, 266
 Isothermal, 47
 Itaconic acid, 260
- J**
 Jam, 429
 Jellies, 432, 436
 Joule heating, 436
 Juice extraction, 418, 432
 Juices, 255, 270, 418, 423, 429, 432, 436
- K**
 Kenaf, 439
 Ketones, 39, 41, 56, 58, 249, 261–263, 342, 349, 433, 475
 Ketonization, 42, 56, 60
 Kinetic energy, 343, 352
 Kinetic modeling, 49
 Kinetic parameters, 47, 49
 Kinetics, 13, 49, 84, 102, 184, 186, 255, 289, 290, 294, 330, 343, 437
 Kitchen discards, 5
Kluyveromyces thermotolerans, 419, 420
 Kraft, 438
 Kraft lignin, 438
 Kraft pulping, 438

L

- Laboratory scale, ix, x, 34–65, 106, 274, 419, 431, 442
Laccases, 257–259, 269, 273
Lactic acid (LA), 136, 139, 152, 159, 193, 206, 209, 211, 221–225, 231, 233, 260, 284, 304–306, 352, 353, 423, 435
Lactic acid bacterium (LAB), 222
Lactide, 304, 305
Lactobacilli, 222, 224
Lactobacillus, 144, 209, 214, 223, 231, 304
Landfilling, 10, 206, 458, 461–463, 465, 467–469, 480
Landfills, 42, 44, 76, 77, 174, 179, 192, 206, 226, 359, 418, 456, 457, 462, 463, 467, 468, 473
Leaf, 101–126, 392, 417, 468, 469, 471
Leaves, ix, 6, 101–126, 178, 297, 392, 434, 468, 469, 471
Lemon, 109, 117, 434, 436
Levoglucosan, 41, 319, 321
Levoglucosenone, 319
Lewis acid, 93, 291, 304
Life cycle assessment (LCA), ix, 19, 466–467, 474
Lifestyles, 5
Light emitting diodes (LEDs), 249, 251
Light hydrocarbons, 39, 42, 56, 58
Light sources, 18, 247–255
Lightweight, 7
Lignans, 438
Lignin, 6, 35, 87, 136, 176, 213, 257, 324, 355, 392
Lignin compounds, 437
Lignin decomposition, 47, 49
Lignin extraction, 437, 438
Lignocellulose, x, 8, 16, 160, 195, 249, 259, 267–270, 362, 387
Lignocellulosic, ix, 8, 9, 16, 34–65, 77, 87, 94–96, 160, 176–178, 188–190, 210, 213, 214, 233, 254, 257, 267, 269, 270, 324, 355, 360, 362, 391, 416, 419, 422, 423, 439, 440, 477
Lignocellulosic biomasses, ix, 9, 34–65, 78, 94–96, 189, 190, 213, 214, 257, 269, 355, 391, 439, 440
Lignocellulosic feedstocks, 176, 178
Lignocellulosic wastes, 8, 9, 416
Lime, 436
Lime peel, 436
Limonene, 107, 108, 110, 432–434
Linear low-density polyethylene (LLDPE), 77, 94
Linoleic acid, 422, 424, 427, 429
Lipase, 181, 297, 307

Lipid extracted microalgae, 359

- Lipids, 35, 37, 38, 41, 43, 44, 50, 53, 57–60, 138, 140, 142, 159, 180, 181, 249, 263, 267, 270–272, 340, 342, 352, 355–359, 361, 376–378, 393, 394, 432, 437, 442, 454, 459

Liquid biofuels, vii, 136

- Liquid fuels, ix, 76–96, 216, 357, 358, 475, 476

Liquid-liquid extraction, 225**Liquid-vapor curve**, 341**Liquid water**, 191, 340, 343**Liquor**, 230, 417**Livestock**, 9, 160, 174, 429, 458

- Long-chain fatty acids (LCFA), 136, 140, 142, 151

Low cost materials, 41

- Low cost, ix, 41, 42, 55, 57, 60, 64, 77, 87, 91–96, 136, 269, 416, 434, 442

- Low-density polyethylene (LDPE), 42, 44, 48, 49, 51, 53, 55, 77, 79, 80, 88, 89, 91–95

Low heating rates, 11, 38**Low heating value**, 41**Low-income**, 6**Lutein**, 433**Luteolin**, 107, 109, 110, 122

- Lytic Polysaccharides MonoOxygenases (LPMOs), 256, 257, 259, 270

M**Maceration**, 433, 434**Macroalgae**, 392–400**Magnesium**, 8, 430, 465**Magnesium sulfate**, *see* MgCO₃**Magnet**, 228**Magnetic**, 291–293, 297, 382, 428**Magnetic field**, 211, 213, 428**Magnetic tape**, 297**Maillard reactions**, 359**Malic acid**, 353**Maltose**, 138, 383, 384, 419**Mango**, 417, 432, 434**Mango fruit**, 432**Mango kernel**, 432**Mango's peel**, 432**Mangosteens**, 432**Mango waste**, 432**Mannan**, 393, 437**Mannose**, 8, 9, 269, 386, 393

- Manure, 9, 13–15, 136, 160, 165, 175, 177, 180, 187, 196, 454, 458–461, 468, 471, 472, 474, 477, 480

Mass balance, 114, 115, 140**Mass flow**, 346**Mass flow rate**, 114, 346

- Mass transfer, 53, 83, 104, 114, 115, 121, 140, 146, 175, 185, 301, 302, 332, 377, 380, 399, 476
- Mass transfer resistance, 294, 295, 301
- Materials, vii, ix, x, 3–9, 11, 13, 16, 19, 20, 35, 39, 41–44, 47, 48, 54–56, 60, 76–78, 83, 85, 87, 91, 93–94, 102, 105, 112, 146, 151, 158, 160, 174, 176–178, 188, 189, 191, 193, 208, 210, 213, 227, 251, 253, 255, 269, 274, 284–287, 296–299, 301, 302, 304, 306, 319, 322, 324, 327–332, 340, 345, 346, 360, 362, 365, 375, 392, 416–418, 422, 424, 427, 432, 434, 438–440, 442, 454, 456, 458–461, 463–465, 468, 471, 474, 476, 477, 479, 480
- Mathematical modelling, 114, 186
- MCM-41, 52, 54, 55, 84
- Mechanical force, 213, 318, 439
- Mechanical pretreatment, 210–213, 320, 321, 323
- Mechanism, ix, x, 35, 42, 44, 84, 252, 258, 261, 293, 304, 307, 327, 351, 354
- Mechanochemical, ix, 4, 17–18, 20, 180, 318–332, 365
- Melanoidin, 214, 359, 360
- Mesophilic organisms, 187
- Mesoporous, 51, 54, 55
- Metabolic engineering, 183, 227, 233, 254, 387
- Metabolic pathways, 183, 185, 264
- Metal, 5, 41, 78, 208, 252, 287, 323, 352, 394, 429, 455
- Metal complexes, 252–255, 274
- Metal oxide, 41, 54, 55, 93, 255, 329, 330, 332, 469, 476, 477
- Metathesis, 307
- Methane, 15, 39, 137–152, 157, 159–165, 174–176, 178–181, 183–185, 188–194, 196, 197, 206, 208–213, 221, 222, 225, 226, 231, 233, 261, 396, 423, 460, 463, 465, 467, 469, 471–473, 477
- Methanogenesis, 14, 142, 146, 147, 150, 151, 158, 160, 181, 182, 184, 185, 195, 221, 222, 231
- Methanogenic bacteria, 14, 181, 183, 186
- Methanol, 13, 17, 105, 107, 110, 117–119, 181, 296, 301, 302, 304–306, 308, 343, 381, 422, 423, 427, 428, 430
- Methanolysis, 17, 284, 301, 302, 305–307, 423, 428, 430, 431
- Methanosarcina*, 181, 184, 222
- Methoxy, 436
- Methoxyl, 438
- Methoxylated pectin, 436
- Methyl acrylate, 307
- Methylamine, 298, 299
- Methyl crotonate, 307
- Methyl lactate, 305, 306
- Metschnikowia cibodasensis*, 429
- Microalgae, 180, 263, 340, 341, 357–362, 364, 375–400
- Microalgae cultivation, 250, 342, 358–362, 376, 377
- Microbial communities, 147, 148, 181–187, 233, 249
- Microbial consortia, 183, 184, 190, 197
- Microbial fuel cells, 4, 18, 20
- Microbiological diversity, 16
- Microorganisms, ix, 14, 15, 136, 147, 148, 150–152, 157, 158, 180, 189, 206, 209, 213, 215–220, 222–224, 226, 232, 233, 250, 254, 258, 262, 267, 375, 376, 387–391, 396–399, 419, 429, 463–465, 477
- Microplastics, 7
- Microporosity, 438
- Microporous, 51, 84, 330
- Microreactor, 53
- Microscopy, 320
- Microwave-absorbers, 285
- Microwave assisted pyrolysis (MAP), 83
- Microwave power, 285, 300
- Microwaves, 38, 44, 83, 178, 189, 210, 212, 213, 285, 287, 292, 293, 296, 299, 300, 302, 305, 306, 308, 382, 420, 433, 434, 439
- Milling, 189, 318, 320–332, 363, 425, 440
- Mills, 6, 108, 163, 188, 210, 228, 229, 318
- Minerals, 35, 39–41, 60, 294, 319, 331, 394, 424, 459, 463, 474
- Miscanthus, 439
- Miscible, 40
- Mix ball milling, 332
- Mixed cultures, 215, 222–224, 226, 231
- Mixotrophic microalgae (*Euglena gracilis*), 360
- Mixtures, 15, 39, 44, 46–56, 58, 60, 61, 64, 65, 77, 79, 80, 84, 87, 92–96, 105, 106, 122, 125, 126, 160, 164, 174, 216, 219, 224, 250, 265, 266, 271, 296, 308, 325, 329, 341, 347, 348, 359, 362, 363, 365, 382, 386, 428, 430, 438, 439, 460, 463, 465
- Model simulation, 185
- Model's output, 19
- Modeling, 49, 185–186
- Modifications, 84, 85, 87, 94, 219, 224, 227, 252, 254, 255, 257, 271, 328, 357, 394

- Modular incineration, 10
Moisture, 7, 11, 16, 35, 37, 80, 174, 175, 419, 456, 468
Moisture content, 136, 175, 207, 208, 432, 456, 459, 463, 467, 468, 475, 478
Molecular model, 49
Molecular weight, 83, 84, 181, 258, 286, 288, 290, 295, 299, 301, 302, 306, 307, 325, 340, 342, 354, 355, 361, 365
Molecules, 14–16, 40, 43, 54, 56, 83, 121, 124, 136, 146, 181, 246, 250–252, 254, 256–258, 260, 262, 263, 267, 269–274, 301, 322, 328, 340–365, 382, 386, 434
Monoaromatic, 54, 56
Monomer recovery, 308
Monomer, ix, 8, 9, 14, 17, 53, 56, 77, 78, 257, 260, 284, 285, 304, 307, 308, 322, 349, 354, 383, 384, 386–391, 437, 439
Monosaccharides, 16, 138, 142, 257, 269, 321, 349, 350, 382, 387, 393, 394
Mono(2-hydroxyethyl)terephthalate (MHET), 297, 298
Moscow power Engineering Institute, 345
Multistage operation, 191, 195
Municipal sanitation, 5
Municipal sludge, 340, 342, 358–362
Municipal solid waste (MSW), vii, 4–6, 10, 11, 14, 15, 19, 47, 159, 164, 165, 174, 175, 179, 180, 192, 206, 208, 212–214, 220, 228, 232, 454–458, 461–463, 467, 468, 470, 473–476, 479
Municipal wastes, 93, 272, 341, 359–360
- N**
Nanomaterials, x, 255, 454, 477, 480
Nanoparticles, 146, 249, 255, 273, 274, 291–293, 428, 477
Nanotubes, 291, 477
Naphthalene, 94, 260, 273, 297, 303
Napier grass, 178, 179, 192
Naringin, 435
Narirutin, 435
Naruritin, 433–435
National Institute of Standards and Technology (NIST), 344
Natural fibers, 417
Near-ultraviolet wavelengths, 18
Neohesperidin, 435
Neuro-fuzzy inference system, 427
New techniques, 433
NIST reference fluid thermodynamic and transport properties (REFPROP) database, 347
Nitrates, 137, 362, 376, 384, 461, 478
Nitric acid, 294, 436
Nitrites, 137, 362, 376, 461
Nitrogen, 7, 82, 137, 177, 248, 291, 327, 342, 376, 418, 458
Nitrogen compounds, 362, 469, 471, 475
NMR, 305, 321, 331
Non-biodegradable, 8, 77, 454, 479
Non-catalytic, 11, 12, 56, 57, 60, 84, 93, 94
Non-condensable, 37, 62, 63, 83, 464
Non-condensable gases, 83
NO_x, 39, 424, 432, 467, 469, 470, 474
Nutrient recycle, 342
Nutrients, 7, 9, 15, 16, 174, 177, 178, 187, 340, 341, 358–362, 375–378, 388, 392, 393, 416, 424, 454, 458, 459, 461, 464, 466, 471, 477, 478, 480
Nutritional, 394, 432
Nutrition elements, 15
Nylons, 17, 261
- O**
Ohmic heating, 436
Oil, 34, 40, 54, 56, 78, 83, 84, 87, 88, 90, 91, 94–96, 249, 271, 272, 320, 342, 357, 364, 374, 376, 418, 422–424, 427–432, 438, 464, 474, 475, 478
Oleic acid, 264, 422, 424, 429
Oligomerization, 40, 84
Oligomers, 14, 249, 284, 286–291, 295, 296, 298, 299, 301, 302, 306, 307, 342, 386, 436
Oligosaccharides, 249, 257, 270, 321, 382, 394, 395
Olive, 264, 271, 272, 439
Olive oil, 264, 271, 272
Operating costs, 10, 12, 13, 16, 39, 55, 177, 193, 195
Optimisation (Optimization), ix, 64, 118, 164, 217, 246, 257, 265, 274, 299, 365, 384, 430, 431, 434, 435
Orange, 194, 250, 417, 432–437, 439
Orange peels, 417, 432–434, 437
Orange waste, 432, 436
Organic, vii, 4, 35, 77, 102, 136, 174, 206, 250, 292, 340, 376, 416, 458
Organic acid, 41, 144, 150, 160, 181, 213, 216, 221, 226, 271, 340, 342, 352–353, 364, 376, 463
Organic compound, 13, 18, 37, 39, 102, 137, 146, 174, 181, 343, 345, 454, 456, 468
Organic content, 7, 208, 298

- Organic fraction of municipal solid waste (FMSW), ix, 179, 192, 206, 209, 232
- Organic loading rate (OLR), 175, 180, 185, 187, 193–195, 197
- Organic sludge, vii, 4, 6–7
- Organic solid waste (OSW), vii, ix, 4–20, 135–166, 178, 210, 215, 221, 224, 340, 341, 344
- Organic solvents, 13, 102, 213, 264, 319, 325, 343, 381, 433–435, 438, 440
- Organic waste, vi, 5, 157, 161, 174, 175, 178, 182, 183, 187–191, 197, 206, 210, 214, 227, 233, 267, 274, 352, 442, 458, 462, 464–466, 469, 472, 474–480
- Organosolv, 211–213, 228
- Outer surface, 146
- Outputs, 19, 185, 214, 219, 393, 424, 440
- Oxalic acid, 296, 436
- Oxidation, 10, 12, 18, 20, 138, 146, 184, 254, 256–263, 265, 266, 271, 324–326, 329, 332, 340, 353, 420, 422, 428, 430, 462–464, 476
- Oxidation stability, 422, 428, 430
- Oxygen, 7, 39, 81, 137, 191, 214, 256, 291, 327, 387, 418, 463
- Oxygenated compounds, 41, 52, 58, 95, 297, 475
- Oxygenates, 41, 94
- Oxygen content, 15, 16, 39, 43, 44, 55, 57, 58, 60, 61, 475
- Ozonation, 18, 19
- P**
- Palm, 8, 45, 108, 163, 271, 438
- Palmitic acid, 264, 272
- Palm kernel shells, 8
- Palm oil, 163, 188
- Paper, 5–7, 84, 121, 136, 165, 208, 249, 288, 360, 417, 429, 456, 457, 468, 478, 479
- Paper and pulp industry, 9
- Paraffins, 56
- Paraffin waxes, 17
- Para-hydroxyphenyl, 269
- Particle, 11, 37–40, 60, 86, 115, 121, 176, 186–189, 210, 255, 274, 288–290, 292, 298, 319, 320, 326, 327, 330, 454, 477
- Particle size, 11, 37, 38, 176, 189, 210, 255, 288, 290, 292, 298, 319, 320, 326, 327, 454, 477
- Particulates, 137, 470
- Pathogens, 7, 16, 148, 458, 463, 465
- Pathway, 12, 56, 85, 141, 142, 144–147, 184, 219, 228–230, 232, 251, 272, 273, 284, 286, 351, 391, 398
- P*-coumaryl alcohol, 437
- Peach, 255, 435
- Pectin, 379, 419, 432, 435–438, 440, 442
- Pectinases, 211, 384–386, 419
- Pectin extraction, 427, 435–437
- Pectin hydrolysis, 437
- Pectin solubility, 437
- Peels, 207, 417, 421, 429, 432–437
- Pennisetum purpureum*, 178, 179, 192
- Pentoses, 138, 388, 390, 391, 398, 399, 419, 436
- Peptides, 340, 342, 352, 354, 363–365, 394, 422
- Performances, 40, 51, 52, 55, 58, 60, 84–86, 148, 158, 183–185, 187, 189, 193, 195, 291, 328, 330, 331, 385, 386, 399, 430, 431, 462, 475–477
- Permeabilities, 125, 220
- Permittivity, 344
- Pervaporation, 220
- pH, 15, 16, 39, 57, 59, 62, 63, 146, 148–152, 158–167, 175, 179–181, 183, 186–189, 194, 195, 197, 209, 217, 218, 223–226, 255, 258, 260, 292, 298, 327, 349, 377, 379, 383–390, 396, 399, 420, 423–425, 437–439, 463, 467, 472
- Phases, 13, 16, 17, 41, 53, 56–59, 61–63, 85, 92, 104–106, 114, 115, 119, 125, 126, 136, 140, 142–146, 150, 157–159, 164, 185, 187, 193, 214, 216, 220–222, 225, 233, 263, 288, 290, 294, 303, 343, 376, 377, 382, 428, 435, 437, 465
- Phenolic compounds, 56, 103, 105, 122, 258, 325, 355, 360, 394, 422, 434–435
- Phenolic resin, 355, 437
- Phenolics, ix, 102, 103, 112, 117, 118, 121, 124–126, 195, 258, 259, 267, 269–271, 325, 328, 355, 423, 434
- Phenols, 9, 41, 58, 63, 258, 261, 324–326, 332, 423, 424, 427, 475
- Phosphoric acid, 211, 214, 331
- Phosphoric-acid-acetone, 213, 214, 228
- Phosphorous, 342, 358–362, 458, 471
- Photobiocatalysis (PBC), 246–252, 255, 256, 261, 266–270, 272–274
- Photocatalyst, 254, 260, 262, 263
- Photocatalytic, 246, 247, 251, 260–262, 265, 267, 269, 272, 325, 328
- Photo-chemical, ix
- Photodegradation, 4, 18, 20

- Photosensitizers, 246–248, 250–255, 257, 269, 270, 272–274
Photosynthetic, 102, 250, 252, 254, 263, 264, 273, 375, 376, 392, 394
P-hydroxyphenyl units, 437
Physical pretreatments, 176, 189
Physical properties, ix, 5, 20, 104, 210, 341–348, 351, 365, 477
Physical structure, 17, 352, 354
Physicochemical, 35, 41, 42, 61, 76, 210, 422, 437, 477
Physiochemical pretreatments, 214–215
Phytosterols, ix, 105, 112, 125, 427
Pichia stipitis, 396, 419
Pigments, 77, 246–261, 267, 270, 271, 273, 274, 376, 378, 392, 393, 437
Pilot plant, ix, 33–65, 293, 298
Pine, 44, 45, 47, 48, 50, 51, 53, 59, 65, 322
Pineapple, 417, 434
Pineapple leaf, 417
Pine wood, 47
Planetary mills, 318
Plants, 7, 19, 38, 84, 101, 102, 105, 107, 110, 112, 114, 122, 160, 174, 177, 178, 226, 232, 250, 252, 254, 258, 268–270, 272, 298, 332, 359, 375, 379, 392–395, 433–437, 439, 461, 463, 469, 470, 476
Plastics, 5–8, 18, 42, 45, 48, 51, 53, 54, 56, 76–78, 80, 83, 91, 94–96, 208, 224, 273, 284, 308, 455–457, 467, 468, 474, 479
Plastic wastes, vii, ix, 8, 42–44, 46–51, 53–55, 58, 60, 76–96, 475
Plum, 418, 422
Plum kernels, 422
Plum stones, 422
Polar compounds, 53, 125, 126
Polarity, 43, 86, 105, 125, 286, 328, 381, 435
Pollutant emissions, 459
Pollutants, 11, 151, 267, 327, 331, 375, 377, 458
Polyamides, 17, 298
Polyaromatics, 92
Poly (butylene succinate) (PBS), 267, 304, 306–308
Poly (butylene terephthalate) (PBT), 284
Polycaprolactone, 304
Polycarbonate (PC), 17
Polycyclic aromatic hydrocarbons (PAHs), 44, 54
Polyesters, ix, 16, 17, 284–308
Polyethylene (PE), 7, 42, 47, 53, 77–79, 90, 93, 298, 302, 364
Poly (ethylene naphthalenate) (PEN), 284
Poly (ethylene terephthalate) (PET), 7, 77, 284
Polyhydroxyalkanoates, 284, 304
Poly (lactic acid) (PLA), 16, 304
Polymer, 8, 9, 18, 34–65, 324, 352, 382, 393, 436, 439
Polymer solid waste, vii, 4, 7–8
Polymerization, 8, 39, 40, 188, 189, 321, 332
Polymer wastes, 34–65
Polyolefins, 42, 43, 48, 53, 76, 94, 293, 308
Polyphenols, 258, 420, 423, 424, 433–435
Polypropylene (PP), 7, 42, 44, 47–49, 52, 53, 76–80, 90, 93, 94, 307
Polysaccharides, 41, 138, 142, 248, 252, 256, 257, 259, 268–270, 349, 352, 357, 359, 364, 376, 379, 382, 387, 393–395, 399, 423, 432, 435, 436, 440, 442
Polystyrene (PS), 7, 42–45, 47–53, 55, 56, 58–62, 65, 77–80, 90, 93, 246, 249, 251, 252, 260, 267, 270, 271, 273, 274
Polyurethane (PUR), 7, 42, 77
Poly (vinyl chloride) (PVC), 7, 42, 45, 77, 79, 83, 94, 95, 475, 479
Porosity, 54, 84–86, 95, 115, 477, 478
Porous carbons, 85, 328–332
Porous structures, 328, 464
Potassium, 8, 54, 137, 296, 377, 440, 458, 461, 464, 471
Potato starch, 231, 364
Power, 10, 19, 103, 105, 174, 251, 263, 265, 266, 300, 345, 383, 439, 440, 460, 462, 475
Precipitation, 224, 294, 298, 299, 305, 437, 439
Pre-exponential factor, 49, 290, 294
Press aid, 419
Pressure, 12, 35, 81, 104, 136, 179, 213, 250, 285, 365, 381, 434
Pressure-density-temperature diagram, 104
Pressure-temperature (*P-T*) diagram, 341, 343
Pretreatment, ix, 10, 39, 148, 188, 210, 269, 298, 319, 363, 375, 469
Pretreatment techniques, 188, 191, 194, 214
Primary amino acids, 354
Primary sludge, 160, 359
Process, 8, 35, 77, 101, 136, 206, 247, 284, 318, 340, 375, 417, 454
Process operations, 187, 191–195
Process variables, ix, 60, 187
Propane, 114
Propylene, 77, 307
Proteins, 137, 138, 140, 142, 150, 159, 177, 188, 214, 248, 260, 262, 264, 270, 340, 342, 352, 354, 355, 359, 361–364, 376, 377, 386, 387, 393–395, 423, 424, 429, 432, 468

- Proximate Analysis, 7, 35, 78–80, 459
 Pulp, 6, 207, 396, 423, 432, 438
 Purification, 12, 13, 264, 293, 301, 428, 430,
 433, 437
 Pyridine, 260, 362
 Pyrolysis, 4, 35–42, 45, 46, 48–63, 77, 136,
 296, 329, 361, 416, 454
 Pyrolysis oils, 84, 422, 474
 Pyrolysis reactors, 11, 49, 53
 Pyrolytic oil, 44, 54, 474, 475
 Pyroprobe-GC/MS, 52
 Pyrrole, 362
 Pyruvaldehyde, 352
- Q**
 Quality of bio-oil, 11, 40, 45, 59
 Quantification, 435
 Quantum dots (QDs), 253, 255
 Quercetin, 122, 434, 435
 Quercetin 3-O-galactoside, 434
- R**
 Radiation, 246, 250, 285, 292, 296, 300
 Rate, 3, 35, 78, 106, 136, 175, 247, 287, 318,
 342, 374, 419, 459
 Rate constant, 185
 Reaction, vi, 10, 35, 83, 136, 181, 214, 246,
 284, 318, 340, 381, 422, 464
 Reaction kinetics, 13, 84, 185, 351
 Reaction mechanism, 58, 301, 306, 356–358
 Reaction temperature, 13, 17, 41, 285, 291,
 292, 295, 304, 346, 352, 427, 430
 Reaction times, 10, 13, 17, 285, 287, 288,
 290–292, 295, 296, 299, 302, 307,
 321–323, 326, 332, 340, 351–353, 357,
 361, 365, 427
 Reactivity, 298, 343
 Reactor, ix, 11–13, 15, 35, 38–40, 44, 45, 49,
 53–56, 60, 61, 64, 81, 83, 84, 91, 151,
 152, 154–158, 163, 164, 177, 181, 184,
 185, 194, 195, 213, 217, 219, 222, 251,
 285, 288, 298, 299, 302, 346, 347, 351,
 354, 357, 363, 390, 391, 439, 476, 477
 Reactor feed, 346, 347
 Recalcitrant wastes, 187
 Recirculation, 61, 152–156, 158–160, 164, 185
 Recycle, vii, ix, 4, 5, 7–9, 14, 16–18, 20, 220,
 331, 340, 341, 358–362, 440, 454,
 460–466, 471, 478
 Recycling, vii, ix, x, 3–20, 42, 76–78, 81, 91,
 93, 174–197, 206, 233, 284, 286, 293,
 306, 308, 341, 359–362, 388, 442,
 454, 455, 457, 460–461, 466–474,
 479, 480
 Redox, 246, 247, 251, 254, 256–258, 262, 265,
 266, 269–271
 Reducing sugars (RS), 319–321, 326, 332, 385,
 388, 396, 419
 Reduction, x, 10, 18, 35, 56–58, 82, 94, 96,
 147, 177, 184, 190, 206, 210, 217, 225,
 246, 256–258, 261, 262, 265, 266, 295,
 304, 306, 330, 357, 390, 399, 424, 454,
 465, 467, 469, 471, 476, 479, 480
 Refining, 40
 Regression, 115, 185
 Relative permittivity, 343, 344
 Renewable, 4, 6, 9, 34, 35, 41, 174, 175, 216,
 246, 250, 251, 256, 266, 267, 271, 332,
 340, 374–377, 416, 427, 459, 461, 477
 Renewable energy generation, 175
 Research group using, 60
 Residence times, 11, 38, 41, 60, 64, 81, 82, 187,
 218, 223, 346, 388, 464
 Residual carbohydrates, 437
 Residues, 6, 10, 15, 35, 37, 48, 49, 84, 160, 162,
 176, 188, 190, 207, 208, 260, 269, 286,
 304, 342, 359, 364, 393, 396, 416, 424,
 436–438, 442, 454, 461, 464, 465, 467,
 474, 479
 Resource recovery, 284
 Resources, ix, 4, 6, 9, 34, 42, 77, 183, 206, 210,
 246, 270, 284, 340, 374, 417, 454, 457,
 459, 461
 Response surface analysis, 119–122
 Retention time, 150–151, 175, 187, 378
 Retro-aldol reaction, 349, 352
 Reuse, 5, 7, 20, 206, 284, 319, 440, 442, 454
 Rhamnogalacturonan II, 436
 Rice, 8, 44, 48, 49, 207, 208, 213, 214, 220,
 226, 233, 320, 328, 355, 419, 440
 Rice husk, 44, 417, 419
 Rice straw, 8, 49, 176, 177, 179, 192, 207–209,
 211, 213, 214, 218, 220, 228, 230, 233,
 320, 328, 417, 440
 Ring opening polymerisation, 300, 304, 307
 Roots, 102, 153, 160, 392, 434
 Rotary drum reactor, 210–213
 Rotary kiln, 10, 11, 82, 83, 470, 475
 Rotating cone reactor, 39
 rRNA genes, 183, 184
 Rubber, 6–8, 11, 16, 54, 208, 260, 456, 479
 Russian National Committee (RNC) of IAPWS,
 345
 Rutin, 107, 109, 122, 434

- S**
- Saccharic acid, 349
Saccharification, 16, 164, 342, 359, 360, 382, 384, 386, 388, 390–391, 394–396, 398
Saccharomyces cerevisiae, 215, 217, 219, 222, 224, 229, 273, 386–391, 396–398, 400, 418–421, 425, 429
Saturation, 265, 341
Saturation curve, 341, 343
Sawdust, 8, 44, 45, 48, 51, 52, 322, 455
SBA-15, 54, 55
Scale-up of technology, 19
Screw, 61, 82, 83, 270, 307, 319
Screw/auger reactors, 61
Seaweeds, 392–394, 396
Secondary amino acid, 354
Secondary reaction, 38, 82, 297, 357
Security, 206
Seeds, 45, 54, 271, 423, 428–432, 463
Selectivities, 13, 16, 17, 84, 90, 92, 93, 96, 266, 286, 296, 318, 323, 340, 341, 346, 352, 354, 363, 365, 384, 432
Self-ionization product, 343
Semen, 434
Semi-batch reactor, 53, 55
Separation, ix, 18, 84, 102, 105, 125, 137, 157, 158, 160, 216, 219–221, 224–225, 227, 247, 251, 254, 270, 273, 290, 293, 308, 319, 324, 325, 330, 354, 388, 428, 430, 439, 440, 473, 475, 478–480
Sepiolite, 39, 41, 56, 57, 60
Sewage, 6, 7, 15, 139, 461
Sewage sludge, 6, 13–15, 78, 87, 94–96, 136, 160, 165, 357, 364
Shaker mill, 318, 319
Shearing, 17
Shrinking, 290, 294, 299
Shrinking core model, 290, 294, 299
Sieve, 228
Silicas, 8, 52, 54, 55, 291, 477
Simulated food waste, 364
Simulations, 185, 391
Simultaneous saccharification and fermentation (SSF), 213, 217, 219, 229, 231, 232, 388–391, 397–400, 418, 425, 429
Sinapyl, 355, 437
Sinapyl alcohol, 355, 437
Single stage process, ix, 45, 64
Size reduction, 213, 327
Slag, 10
Slow pyrolysis, 11, 38
Sludge, 5–7, 48, 150–152, 159–161, 164, 165, 177, 179, 180, 183, 223, 225, 231, 359, 416
Soda lignin, 432, 437
Sodium, 8, 261, 290, 291, 295, 296, 299, 342, 353, 438, 439
Sodium alginate, 342, 353, 364
Sodium hydroxide, 192, 438, 440
Software, 19, 391
Softwood, 269, 439
Soil, 9, 15, 16, 77, 174, 327, 331, 332, 416, 454, 456, 458, 460, 464, 465, 467, 471
Soil remediation, 327, 331
Solar, 135, 255, 300, 340, 375, 376, 433
Solid catalysts, 291
Solid fuel, 464
Solid organic wastes, 175, 178, 187, 188, 190, 191
Solid retention time (SRT), 150–152, 187, 193, 194
Solid-state fermentation, 419, 424
Solid state polycondensation (SSP), 286
Solid waste, vii, 4, 47, 76, 136, 174, 206, 272, 319, 340, 423, 455
Solid waste management, 76, 175, 472–474
Solubility, 105, 112, 114, 119, 124–126, 140, 191, 210, 225, 255, 286, 290, 292, 296, 304, 343, 363, 380
Solvent, x, 13, 40, 102, 213, 261, 286, 318, 340, 380, 418, 475
Solvent density, 121, 124, 126
Solvent extraction, 41, 224, 225, 434, 475
Solvent free, 318, 329–332, 434
Solventogenesis, 215, 216, 229
Solvolytic, 17, 301–302
Solvothermal, ix, x, 255, 340–348, 362–365
Solvothermal liquefaction, 13
Sorbitol, 322–324, 326, 332
SO_x, 39, 470
Soxhlet extraction, 433, 434, 440
Soybean, 271
Soy pods, 417
Soy protein, 364, 419, 420
Space time, 346, 347
Space velocity, 346
Species, 19, 39, 93, 175, 184, 208, 215, 217, 219, 222, 224, 227, 248, 251, 252, 260, 261, 269, 304, 328, 379, 385, 389, 392, 394, 398, 434, 465, 474
Spirulina, 378–380, 385, 389
Spruce, 438
Stability, 7, 18, 39, 41, 54, 55, 118, 150, 164, 197, 246, 248, 252, 254, 255, 257–262, 266, 297, 298, 329, 331, 396, 436
Stalks, 136, 177, 190, 417, 423, 439
Starch, 138, 139, 159, 160, 164, 181, 207, 217, 229, 306, 364, 375–391, 393, 394

- Steam, 12, 13, 41, 86, 151, 174, 189, 214, 259, 285, 294, 296, 297, 302, 303, 319, 423, 433, 434, 464, 469, 476
- Steam distillation, 434
- Steam explosion, 151, 189, 192, 211, 214, 230, 319
- Steam reforming, 13, 41
- Stoichiometric combustion, 464
- Storage, 11, 40, 159, 255, 271, 416, 423
- Straw, 8, 160, 165, 178, 207, 210, 417, 438, 439, 455
- Streptococcus*, 144, 209, 223, 231
- Structures, 16, 17, 42, 43, 82, 84, 85, 87, 92, 103, 104, 107, 110, 111, 114, 118, 122, 123, 125, 144, 146, 160, 189, 247, 252–255, 262, 268, 269, 285, 292, 297, 304, 308, 319, 321, 325–328, 330, 332, 349, 352, 353, 355, 359, 362, 363, 380, 384, 392, 419, 435–437, 477
- Styrene, 53, 56, 94, 259–261, 273
- Subcritical, 12, 290
- Subcritical water, 12
- Submersed fermentation, 419
- Substrate, 9, 10, 13–17, 20, 105, 136, 137, 139–141, 147, 159, 175, 178, 181, 184, 185, 189, 191, 209, 210, 212–221, 223–227, 247–249, 252, 254, 256–268, 270–274, 320, 322–324, 332, 340, 342, 346, 362, 364, 365, 383, 387, 388, 390, 398, 424
- Succinic acid, 307, 353
- Sugar beet pulp, 190, 207, 208, 211, 213, 222, 223, 226, 231, 232
- Sugarcane, 375, 439, 440
- Sugarcane bagasse, 160, 177, 192, 193, 214, 259, 269, 429, 439
- Sugars, 8, 41, 87, 160, 206–208, 213, 217, 218, 220, 222, 223, 255, 270, 319–323, 332, 342, 359, 384–388, 390–393, 396–400, 418, 419, 423, 424, 429, 432, 439, 442
- Sulfur, 45, 54, 57, 78, 137, 393, 464, 468, 474, 475
- Sulfuric acid, 211, 213, 231, 438–440
- Sunflower, 177, 342
- Sunlight, 18, 246, 249, 250, 392
- Supercapacitors, 87, 330
- Supercritical, ix, 12, 102, 211, 285, 340, 381, 433
- Supercritical carbon dioxide (sc-CO₂), 125
- Supercritical ethanol, 302
- Supercritical fluid extraction (SFE), 379, 381, 434
- Supercritical fluids, 343, 381, 434
- Supercritical water, 12, 285, 351–352, 357, 362
- Surface area, 17, 84–87, 91, 92, 95, 115, 187–189, 213, 255, 288, 291, 292, 294, 320, 321, 327, 328, 330–332, 419, 438
- Surge, 34, 394
- Surroundings, 10, 219, 392
- Sustainability, 20, 44, 54, 267, 274, 360, 361, 417, 461
- Sustainable energy, 375
- Sustainable sources, 332
- Sweet oranges, 432, 434
- Switchgrass, 209, 210, 218, 229, 439
- Synergistic effects, 56
- Syngas, 12, 464, 465, 469, 475, 476, 478, 479
- Syntheses, 55, 144, 188, 221, 255, 265, 266, 284, 319, 321, 322, 324, 327, 352, 377, 427, 431, 464, 465, 475, 476
- Syringyl, 269, 437
- T**
- Taguchi method, 427
- Tail gas, 10
- Tangerine, 434
- Tar, 50, 52, 53, 83, 464, 476
- Techno-economic analysis (TEA), vii, 220, 227, 228
- Technology readiness level (TRL), ix, 38, 46–64
- Terephthalamides, 298–300
- Terephthalic acid, 286, 293–298, 302, 303, 307
- Termination reaction, 43
- Terpenes, ix, 112, 125, 433, 439
- Terpenoids, 249, 261, 268, 272–273, 433
- Textile industry, 7, 417
- Textile wastes, 208, 213, 226, 232
- Thermal, 10, 12, 35, 38, 41, 45, 47–49, 51, 76, 83, 84, 92, 118, 176, 188, 189, 191, 224, 285, 298, 306, 329, 343, 463, 468, 474
- Thermal conductivity, 83, 285, 343
- Thermal decomposition, 45, 49
- Thermal pretreatment, 176, 180, 189, 191
- Thermochemical, ix, 9–13, 17, 20, 35, 87, 454, 456, 457, 460, 462, 464, 468, 478–480
- Thermochemical conversion, 9, 456, 468, 478–480
- Thermo-gasification, 12, 13
- Thermogravimetric, ix, 38, 45, 46, 50, 94
- Thermogravimetric analysis (TGA), ix, 38, 45–52, 83, 94, 95, 331
- Thermomyces lanuginosus*, 428
- Thermoplastic polymers, 17
- Thermosets, 300
- Thylakoids, 248, 254, 257, 270, 271, 274
- Tires, 8, 45
- Toluene, 56, 78, 94, 260, 273, 302, 307, 328

- Torrefaction, 13
Total flavonoid content (TFC), 116–126
Total phenolic content (TPC), 103, 116–126, 325
Toxicity, 186, 188, 194, 292, 293, 375, 467, 468, 475, 477
Toxic substances, 7, 388
Transformations, ix, 11, 20, 93, 184, 222, 227, 260, 267, 273, 274, 319, 322, 326, 332, 349, 395, 461
Transition metals, 54, 252, 254, 255
Transport, 10, 39, 40, 102, 254, 306, 343, 347, 398, 416, 473
Transportation, 5, 8, 19, 20, 40, 41, 64, 78, 112, 124, 196, 377, 454, 471, 474, 475
Trap, 106, 107
Treatments, 5, 8, 10, 12, 15–19, 40, 42, 52, 76, 77, 87, 112, 150, 151, 157–161, 164, 174, 175, 177, 206, 207, 210, 230, 255, 319, 321, 323–325, 327, 328, 331, 332, 354, 359, 361, 362, 377, 382, 386, 416, 423, 432, 436, 437, 440, 442, 456, 457, 461–463, 467–474, 480
Triangle Institute (RTI), 19
Trimmers, 53, 56, 288, 299
Turbines, 469, 476
Turpentine, 433
Twin screw extruder, 307
Two-phase anaerobic digestion, ix, 137, 158, 164, 214
- U**
Ultrafiltration, 298
Ultrasonication, 210, 213, 379, 433, 437
Ultrasound, 180, 189, 192, 434, 435, 440
Ultrasound extraction, 437
Underutilized, vii, 432
Unit operations, 216, 217, 221, 227
Unspecific peroxygenases (UPOs), 259–261
Upgrading, 40, 42, 44, 45, 53–56, 58, 61, 64, 84, 196, 227, 340, 475, 476, 479
Urban, 3, 5, 165, 272, 387, 455
- V**
Valorization, ix, 9, 18, 59, 81, 96, 249, 259, 327, 332, 418, 454, 460–466, 478–480
Valuable materials, 416
Vapor pressure, 119, 121, 124, 126, 341, 343, 346
Vapor residence time, 11, 35, 38, 46, 60
Vapours (Vapors), 38, 40, 220
Vascular system, 102
Vermification, 416
Vinegar, 423
Viscosity, 40, 41, 44, 55, 95, 104, 284, 343, 380, 399, 422, 475
Vitamin A, 433
Vitamins, 146, 376, 394, 427, 429, 432, 459
Volatile compounds, 4, 433
Volatile fatty acids (VFA), 14, 142, 144, 148–152, 157, 181, 184, 185, 187, 189, 193, 210, 212, 221, 266
Volatile matter, 35, 37, 39, 78, 87, 91, 459
Volatiles, 7, 8, 38, 40, 48, 50, 52, 61, 64, 80, 84, 92, 139, 144, 152, 163, 178, 187, 190, 194, 226, 294, 297, 435, 463, 465, 474
Volumetric heating, 83
- W**
Waste, vii, 4, 35, 76, 101, 136, 174, 206, 255, 291, 340, 387, 416, 454
Waste activated sludge (WAS), 139, 160, 165, 175, 177
Waste biomass, ix, 11, 319–332, 418, 440, 442
Waste fibers, 206, 417
Waste management, x, 4, 42, 136, 206, 319, 454, 461, 479
Waste paper, 165, 478, 479
Waste plastics, 7, 8, 11, 16, 43–45, 48–53, 55, 56, 58, 65, 77–80, 85, 93–95, 478, 479
Waste tires, 8, 47, 48, 65
Waste-to-energy and chemicals (WTEC), 4
Wastewater, 6, 7, 15, 150, 157, 175, 177, 267, 271, 272, 298, 327, 359, 360, 375, 377, 378, 387, 418, 423, 430, 440, 461
Wastewater treatment, 6, 7, 150, 157, 177, 359, 360
Water, vii, 4, 37, 77, 102, 139, 174, 214, 246, 285, 323, 340, 377, 416, 454
Water content, 7, 15, 61, 82, 175, 191, 357, 360, 435, 454, 463, 464, 469, 478
Water feed, 346
Water-gas shift reaction, 56, 58
Water-impermeability, 437
Watermelon, 417, 418, 428–432
Watermelon wastes, 428–432
Wavelength, 246, 247, 250, 251, 255, 260
Waves, 210, 213, 382
Waxes, 44, 83, 91–93, 432, 439
Weeds, 6, 463
Wet oxidation, 340
Wheat straw, 8, 87, 162, 176, 177, 189, 192, 193, 210, 211, 230, 259, 269, 324, 331, 364
Wine, 417, 423–425, 435

Wood, 6, 8, 44, 47, 52, 54, 86, 87, 93, 94, 208, 211, 230, 324, 328, 439, 456
 Wool, 226, 232
 World production, 417, 423, 432
 Woven fabrics, 294, 295

X

Xanthenes, 253, 254
 Xanthophylls, 433
 X-ray diffraction (XRD), 296, 320, 325
 X-ray film, 297
 Xylan, 269, 322, 437, 438
 Xylanases, 211, 215, 385, 386, 390, 396, 429
 Xylose, 9, 138, 269, 321, 342, 386, 388, 391, 398, 419, 436

Y

Yard, 5, 175, 177, 178, 190, 196, 208, 456, 478, 479
 Yeasts, 193, 224, 381, 387–391, 394, 397–400, 419, 421, 425, 429, 433

Yield, 11, 13, 14, 37, 38, 43, 44, 53, 55–63, 82–84, 87, 90–96, 112–116, 119, 120, 138, 140, 142, 161–165, 176, 178, 184, 185, 188–194, 210, 213–221, 223–227, 232, 248, 250, 255, 257, 264–266, 271, 273, 274, 286, 288, 290–292, 295–297, 299, 302–307, 318, 320–326, 329, 332, 349, 352, 353, 355, 357, 361–364, 375–377, 382–391, 394, 396–400, 419, 420, 424, 425, 427–431, 433–440, 464, 468, 469, 471, 473, 476, 477

Z

Zeaxanthin, 433
 Zeolites, 40, 41, 43, 49, 50, 52, 54, 55, 84, 93, 94, 321, 322
 Zero-waste society, 9
 Zinc acetate, 289–291, 293–295, 299, 301, 302, 306
 Zinc chloride (ZnCl_2), 87, 93, 96, 292
 ZSM-5, 49, 51, 52, 54, 55, 84, 93, 94